

主論文

**Novel Coupling Reactions via C–H, C–C, and C–O Bond
Activation by Nickel Catalyst**

ニッケル触媒を用いた炭素–水素、炭素–炭素、炭素–酸素
結合活性化に基づく新規カップリング反応

Kei Muto

武藤 慶

2015

Preface

The studies presented in this thesis have been carried out under the direction of Professor Kenichiro Itami at Department of Chemistry, Graduate School of Science, Nagoya University between April 2010 and September 2015. The studies are concerned with development of Novel Coupling Reactions via C–H, C–C, and C–O Bond Cleavage by Nickel Catalyst.

I would like to express my sincerest gratitude to Professor Kenichiro Itami for great support, valuable suggestions and hearty encouragement throughout this work. I would like to greatly appreciate everything Associate Professor Junichiro Yamaguchi provided me during the course of this study. I appreciate to Associate Professor Yasutomo Segawa for his helpful suggestions and the measurement of X-ray crystallography. I also appreciate Associate Professor Shinya Hagihara, Lecturer Hideto Ito and Assistant Professor Kei Murakami for their insightful comments, helpful discussions, and encouragements.

I would like to express my heartfelt appreciation to Professor Aiwen Lei for giving me an opportunity to visit Wuhan University as an exchange student, great support and valuable suggestions. I would also like to thank Dr. Liqun Jin, Dr. Hua Zhang, and all members in Lei's laboratory.

I am deeply grateful to Professor Musaev G. Djamaradin for fruitful collaboration through theoretical calculation investigations.

I would like to express my gratitude to Professor Susumu Saito and Professor Shigehiro Yamaguchi for their helpful guidance and encouragement.

I must make special mention of Mr. Takuya Yamamoto for his helpful guidance and supports. I owe much inspiration to him. I must make special mention of Dr. Lingkui Meng, Mr. Kazuma Amaike, Ms. Yuko Kamada, Mr. Ryosuke Takise, Mr. Tsuyoshi Oshima, and Mr. Taito Hatakeyama for their wonderful collaborations, valuable discussions and encouragement.

I gratefully acknowledge Kanto Chemical Co., Inc. for their commercialization of Ni(dcppe)(CO)₂ complex.

I thank Mr. Toshiaki Noda, Ms. Hideko Natsume, and Mr. Hisakazu Okamoto for their excellent work on scientific glassware. This thesis cannot exist without their glassware.

I heartily thank to Dr. Masakazu Nambo, Dr. Shuichi Yanagisawa, Dr. Debashis Mandal, Dr. Kirika Ueda, Dr. Haruka Omachi, Dr. Katsuaki Kawasumi, Dr. Kazuya Yamaguchi, Dr. Eiji Yamaguchi, Dr. Kenji Mochida, Dr. Atsushi Yamaguchi, Dr. Takehisa Maekawa, Dr. Kazuhiro Hata, Dr. Petr Šenel, Dr. Venkataramana Gandikota, Dr. Jiao Jiao, Dr. Asraa Ziadi, Dr. Guillaume Povie, Mr. Shin Miyamura, Mr. Takeshi Kaneda, Ms. Hiromi Yamaguchi, Mr. Toshiki Kojima, Mr. Satoshi Tani, Ms. Sanae Matsuura, Mr. Hiroyuki Ishikawa, Mr. Kyohei Ozaki, Mr. Kazuki Kimura, Mr. Katsuma Matsui, Ms. Akiko Yagi, Ms. Hiromi Yoshida, Mr. Yuuki Ishii, Mr. Takahiro Uehara, Mr. Tomonori Kajino, Ms. Keika Hattori, Ms. Yukari Mitamura, Mr. Tetsushi Yoshidomi, Mr. Takao Fujikawa, Mr. Hiroki Kondo, Mr. Kakishi Uno, Ms. Misaho Araki, Ms. Natsumi Kubota, Mr. Yutaro Saito, Mr. Shin Suzuki, Mr. Masahiko Yoshimura, Mr. Tsuyoshi Oshima, Mr. Jun Orii, Mr. Kenta Kato, Ms. Mari Shibata, Ms. Kaho Maeda, Mr. Kiyotaka Mori, Mr. Shun Yamashita, Mr. Keishu Okada, Mr. Takahiro Kawakami, Ms. Chisa Kobayashi, Ms. Masako Fushimi, Mr. Keiichiro Murai, Ms. Manami Muraki, Mr. Shuya Yamada, Ms. Eri Ito, Mr. Kazushi Kumazawa, Mr. Yoshito Koga, Mr. Jumpei Suzuki, Ms. Wakana Hayashi, Mr. Wataru Matsuoka, Dr. Sylvia Kirchberg, Dr. Anna Junker, Dr. Christina Meyer, Dr. Shu-Hua Chou, Dr. Lilia Lohrey, Mr. Christoph Rosorius, Mr. Richard Maceiczky, Dr. Friederike Sibbel, Dr. Nils Schröder, Mr. Dominik Johannes Bergmann, Dr. Eva Koch, Mr. Artur Kokornaczyk, Dr. Chepiga Kathryn Megan, Mr. Michael Wade Wolfe McCreery, Ms. Huimin Dai, Mr. Shijian Jin, Mr. Jake Schlessinger, Ms. Rika Kato, Ms. Yui Ueyama, Mr. Satoru Kawai, Ms. Akemi Saito, Ms. Nanako Kato and all alumni of Itami group.

I am grateful to the Japan Society for the Promotion of Science (JSPS) for the research fellowship for young scientists (DC1). I also thank to Integrative Graduate Education and Research Program in Green Natural Sciences (IGER) and International Research Program for Students and Young Researchers for their financial support.

Last but not least, I would like to express my deepest appreciation to my family, especially my parents, Mr. Toshiro Muto, Mrs. Miyuki Muto, and Mr. Jun Muto for their constant assistance and encouragement.

Kei Muto

Kei Muto

Department of Chemistry
Graduate School of Science
Nagoya University

2015

Contents

List of Abbreviations	1
General Introduction	3
Chapter 1	
Nickel-Catalyzed C–H Arylation of 1,3-Azoles with Haloarenes	27
Chapter 2	
Decarbonylative Cross-Coupling of Esters and Organoborons by Nickel Catalysis	59
Chapter 3	
Nickel-Catalyzed C–H Coupling Reaction of Azoles with Phenol and Enol Derivatives	131
Chapter 4	
Mechanistic Studies of Nickel-Catalyzed C–H Arylation of Azoles with Phenol Derivatives	173
Chapter 5	
C–H Arylation and Alkenylation of Imidazoles with Nickel Catalyst	225
List of Publication	279

General Introduction

Cross-Coupling Reactions Forming Aryl–Aryl Bonds

Organic molecules having aryl–aryl (Ar–Ar) bonds often display unique biological activities as well as optoelectronic properties. Thus, arene-assembled molecules are often recognized as “privileged” structures and are frequently exploited in a wide range of pharmaceuticals and conjugated molecules for organic materials and devices. Owing to this significant potential, the development of the methodology that enables efficient biaryl construction is a topic of utmost importance in organic synthesis. The current standard method to construct biaryls is the transition metal-catalyzed cross-coupling between metalloarenes (aryl nucleophiles) and haloarenes (aryl electrophiles).^[1] For example, the Suzuki–Miyaura coupling uses palladium as the catalysts, arylboronic acids (Ar–B) as the nucleophile, and aryl halides (Ar'–Hal; Hal = halogen) as the electrophile to produce a biaryl product (Ar–Ar'). The metal-catalyzed cross-coupling reaction is quite a powerful synthetic tool to construct biaryl bonds, and is recognized as one of the most reliable methods for the synthesis of bioactive molecules and organic materials.^[2] This methodology has opened a new avenue in organic synthesis, however it still displays significant drawbacks to be solved. For example, the conventional coupling reaction requires the preparation of organometallic compounds prior to the reaction, and thus becomes a multi-step route to form the desired C–C bonds. Moreover, the reaction generates a significant amount of metal halides as environmentally toxic co-products. To overcome these issues, recent efforts are directed toward the replacement of each component in cross-coupling reactions with readily available and/or less toxic compounds (Figure 1). Thus, streamlined cross-coupling reactions have been developed by changing (1) aryl nucleophiles from metalloarenes to simple arenes (by C–H activation),^[3] and (2) aryl electrophiles from aryl halides to non-halogen-containing aryl electrophiles such as arene carboxylates (by C–C activation),^[4] phenol derivatives (by C–O activation)^[5] as well as aniline derivatives (by C–N activation).^[6] Moreover, the metal catalysts used in cross-coupling have also been directed toward inexpensive metals such as nickel, copper, cobalt, and iron from conventional but expensive metal catalysts such as palladium and rhodium. Among these first-row transition metals, nickel catalysts have received particular attention in the unconventional cross-coupling reactions.^[7]

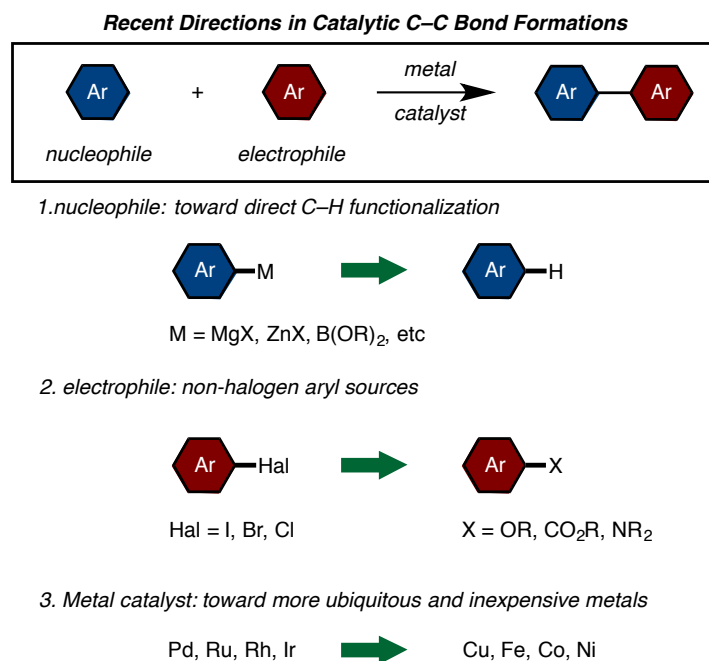


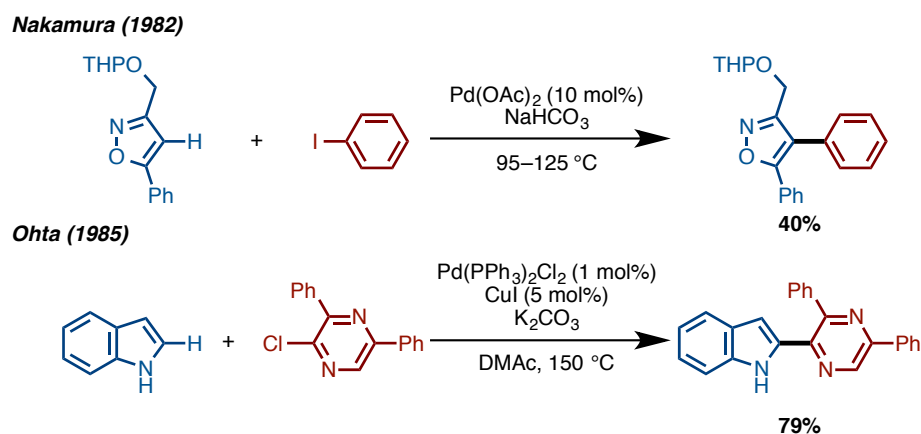
Figure 1. Recent directions in catalytic biaryl coupling reactions

Palladium has reigned as the most widely used transition metal for the cross-coupling reaction, while palladium and nickel share common chemical features. For instance, both metals belong to the d¹⁰ transition metal group, and can have oxidation numbers of 0 and +2 (it is worth noting that, in the case of nickel, oxidation numbers of +1 and +3 are also known).^[8] However, nickel is known to be more nucleophilic and is smaller in atomic radius than palladium. Therefore, oxidative addition reaction to nickel can occur readily. This facile oxidative addition enables the use of aryl electrophiles that are unreactive in palladium catalysts, such as phenol derivatives (C–O bonds). Considering its low cost and unique properties, the use of nickel should provide great opportunities to develop unconventional, but streamlined cross-coupling reactions that involve activation of inert bonds. In the general introduction of this thesis, the history of the utilization of simple arenes, arenecarboxylates, and phenol derivatives in metal-catalyzed cross-couplings is described.

Transition Metal-Catalyzed C–H Arylation of Aromatics

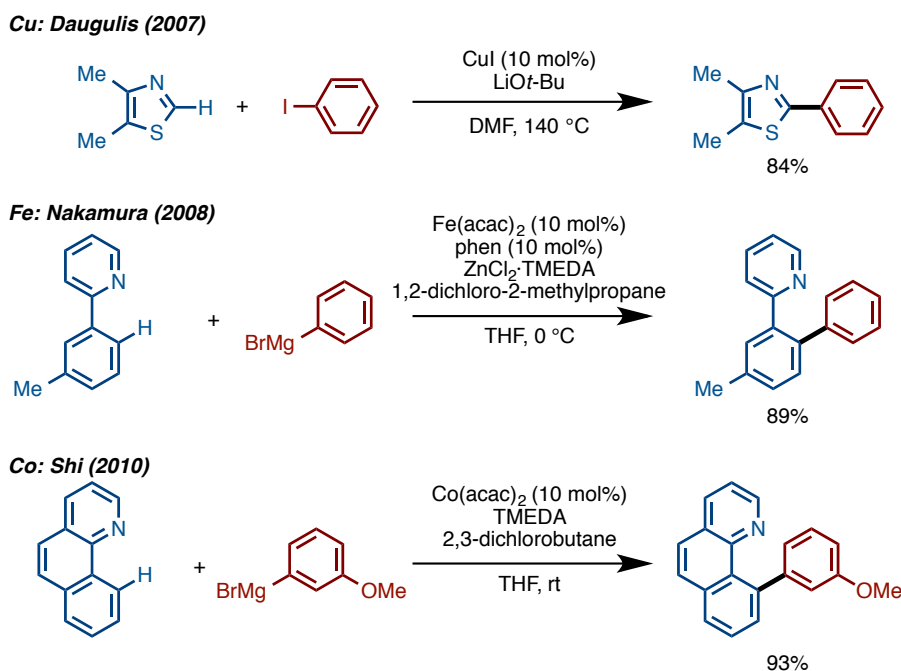
The C–H arylation of aromatic compounds allows rapid and straightforward synthesis of biaryl C–C bonds. The synthetic chemistry community started to prefer this method because the pre-functionalization of nucleophilic coupling partner such as metalloarenes

is unnecessary. As one of the pioneering works in this field, Nakamura developed a Pd-catalyzed C–H arylation of heteroarenes and haloarenes in 1982 (Scheme 1).^[9] Similarly, Ohta also reported early examples of C–H arylation of heteroarenes in 1985.^[10]



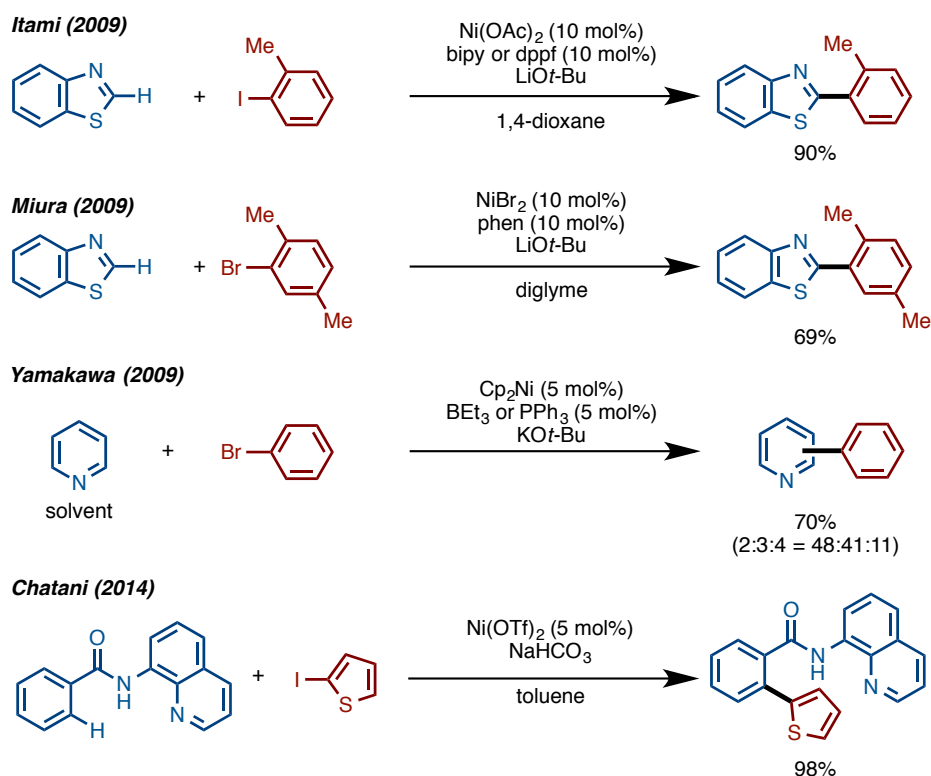
Scheme 1. Pioneering works in metal-catalyzed aromatic C–H arylation

Thereafter, the C–H arylation of a wide range of aromatics and heteroaromatics has been studied,^[3] and almost all C–H arylations have been achieved by using palladium^[11] and rhodium^[12] catalysis. Despite their utility, palladium and rhodium are expensive transition metals even when they are used in catalytic amounts. However, the recent studies in C–H arylation have elicited the capability of first-row transition metals as catalysts. To date, inexpensive transition metals such as copper,^[13] iron,^[14] cobalt,^[15] and nickel^[16] have been recognized to be effective for the direct C–H coupling of heteroarenes (Scheme 2). In 1998, Miura and co-workers discovered that CuI can facilitate the C–H arylation of heteroaromatics with haloarenes although this required a stoichiometric amount of CuI.^[13a] For the first catalytic reaction with copper, in 2007, the group of Daugulis realized a Cu-catalyzed C–H arylation of heteroarenes with iodo- and bromoarenes.^[13b] This copper-based catalytic system has broad substrate generality, as indole, 1,3-azoles, and fluorinated benzenes can be directly arylated. It was also reported by the groups of Nakamura and Shi that iron and cobalt also catalyze the C–H arylation of 2-pyridylbenzene derivatives.^[14,15]



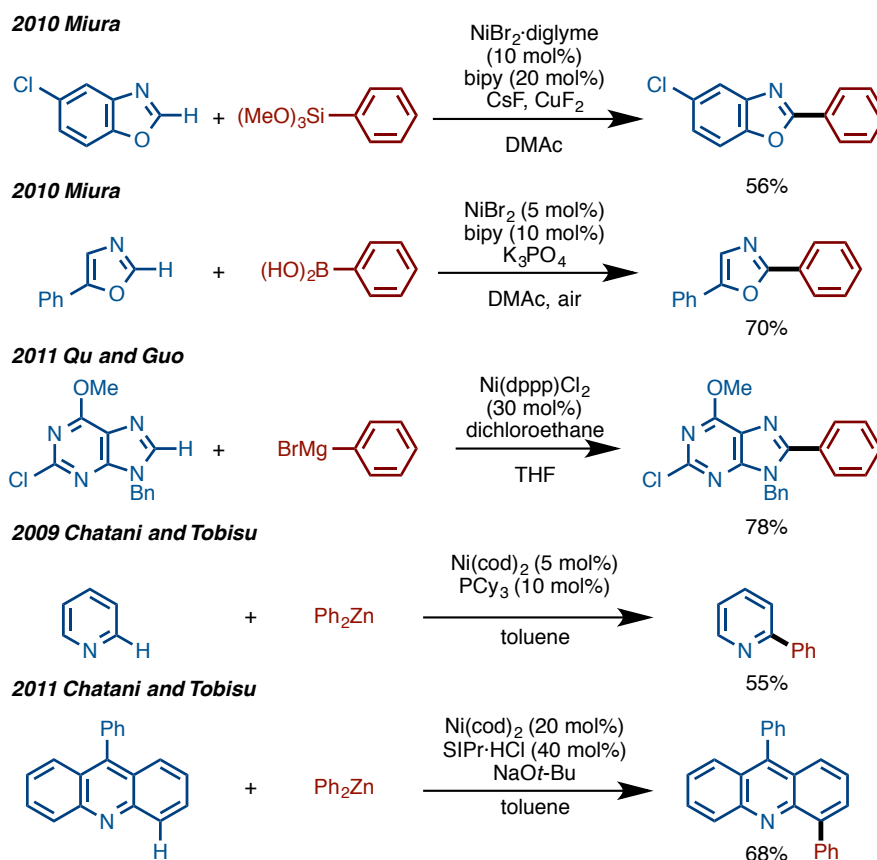
Scheme 2. Aromatic C–H arylation catalyzed by copper, iron, and cobalt

Significant advances have been seen in Ni-catalyzed C–H arylation (Scheme 3). In 2009, the groups of Itami and Miura independently reported the first example of Ni-catalyzed C–H arylation of aromatic compounds.^[16a,b] In this report, Itami and co-workers successfully developed a Ni(OAc)₂/bipy/LiOt-Bu catalyst system for the C–H arylation of 1,3-azoles with haloarenes. Furthermore, this method was applied to the rapid synthesis of bioactive compounds. In the same year, Yamakawa and co-workers reported the direct arylation of benzene, naphthalene, and pyridine with haloarenes using a (Cp)₂Ni/BET₃ (or PPh₃)/KOt-Bu catalyst system.^[16c] Because regioisomers were produced by this system, it is presumed that the cross-coupling reaction proceeds through a radical-type reaction pathway. Chatani and co-workers also developed the C–H arylation of aromatic amides containing an 8-aminoquinoline moiety as a directing group.^[16j] In this report, they proposed a Ni(II)/Ni(IV) redox catalytic cycle in the reaction mechanism.



Scheme 3. Ni-catalyzed C–H arylation using haloarenes

Ni-catalyzed oxidative C–H arylation reactions using arylmetal species as the aryl source (C–H/C–M coupling) have also been reported in recent years (Scheme 4). The first Ni-catalyzed oxidative direct arylation was disclosed by Miura and co-workers in 2010, where they developed a direct arylation of 1,3-azoles with arylsilanes in the presence of copper salts as oxidants.^[16g] This report can be regarded as an important finding not only because this is the first Ni-catalyzed oxidative C–H arylation, but also because oxidative C–H arylation with arylsilane is rare even with other transition metal catalysts. A Ni-catalyzed oxidative direct arylation of oxazoles with arylboronic acids employing air as the oxidant was also developed by the group of Miura in the same year.^[16f] An oxidative direct arylation using aryl Grignard reagents by nickel catalyst was reported by Qu, Guo and co-workers.^[16h] In 2009, Chatani and Tobisu reported a Ni-catalyzed direct arylation between azines and arylzinc species.^[16e] This reaction selectively provides C2-arylated azines. A similar organozinc-based C–H arylation of acridine at its C4 position was found to take place by a Ni(cod)₂/SIPr·HCl/NaOt-Bu catalytic system.^[16i,j]



Scheme 4. Ni-catalyzed oxidative C–H arylation

Metal-Catalyzed Cross-Coupling of Arenecarboxylates

As mentioned above, in the cross-coupling reaction, the replacement of arylmetals by simple arenes can now be achieved to some extent. Although palladium catalysts have been predominantly used in this area, recent efforts have opened opportunities for inexpensive metal catalysts such as copper, iron, cobalt, and nickel in aromatic C–H arylation reaction.

In parallel to the advances of aryl nucleophiles in cross-coupling chemistry, significant attention has been also paid to the improvement of aryl electrophiles. Recent progress in metal-catalyzed biaryl coupling with metalloarenes has enabled the use of unconventional aryl electrophiles, arene carboxylates (by C–C cleavage) and phenols (by C–O cleavage), to participate in the next generation of cross-coupling chemistry.

The utilization of arenecarboxylates ($\text{Ar-CO}_2\text{R}$), such as carboxylic acids ($\text{R} = \text{H}$), carboxylic acid anhydrides ($\text{R} = \text{COAr}$), and esters ($\text{R} = \text{alkyl or aryl}$) in the coupling reaction, is advantageous not only because their use avoids the production of

environmentally harmful halogen wastes, but also because they are abundant and readily available chemical feedstock both commercially and synthetically. With these advantages of carboxylates, recent studies in cross-coupling have successfully realized the coupling reaction of carboxylates.^[4] Mechanistically, there are two different pathways in order for carboxylates to participate in metal-catalyzed cross-coupling reactions; one proceeds in decarboxylative manner, and another proceeds in decarbonylative manner (Figure 2). In a decarboxylative coupling reaction, the carboxylic acid reacts as an aryl nucleophile to generate the biaryl with the release of CO₂ gas. On the other hand, arenecarboxylic acid anhydride and ester function as an aryl electrophile and emit CO gas after the reaction. Therefore, the use of arenecarboxylic anhydrides or esters leads to the development of a halogen-free cross-coupling reaction.

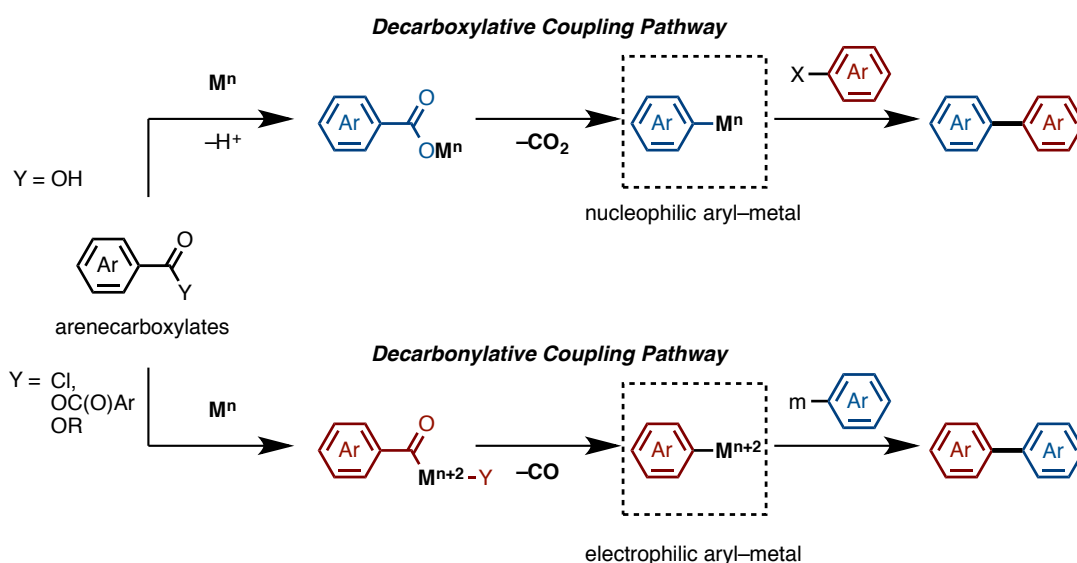
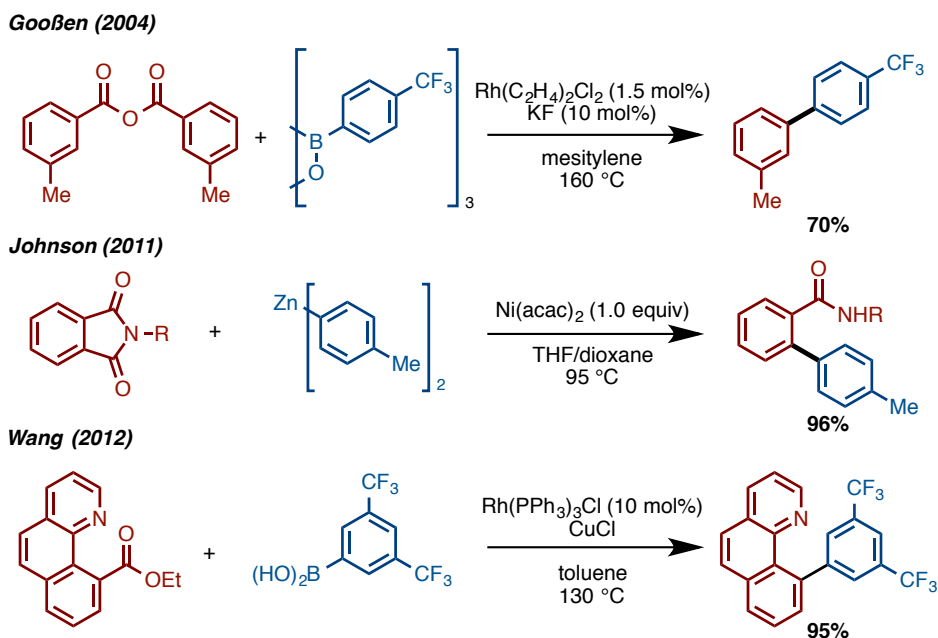


Figure 2. The decarboxylative and decarbonylative coupling pathways

A few decarbonylative cross-couplings were reported so far (Scheme 5). In 2004, Gooßen developed a decarbonylative biaryl coupling of aromatic anhydrides and aryl boroxines with a rhodium catalyst.^[17] Furthermore, it was reported that a decarbonylative cross-coupling between phthalimides and arylzincs can proceed, albeit with a stoichiometric amount of nickel salt.^[18] Then, esters were found to work as an aryl electrophile in 2012 by Wang. However, in this report, a nitrogen coordinating group on the arene substrate was required for reaction efficiency.^[19] In parallel to the

development of metal-catalyzed decarbonylative couplings, the decarboxylative cross-couplings using benzoic acid derivatives have been well established by Gooßen.^[20]



Scheme 5. Metal-catalyzed or mediated decarbonylative cross-coupling reactions

Decarbonylative coupling still shows significant room for further improvements in terms of applicable arenecarboxylates and metal catalysts. The only effective metal catalyst was an expensive rhodium. While nickel showed the potential as an appropriate metal catalyst in decarbonylative coupling, the use of stoichiometric amount of nickel should be avoided. Furthermore, although aromatic anhydrides are known to be reactive, they are sometimes unstable toward nucleophiles. When acid anhydrides are used in cross-coupling reactions, there is also a shortcoming that one half of the substrate would become chemical wastes because the anhydride cannot be generated *in situ* from the carboxylic acid side product. Therefore, it is more desirable to use aromatic esters as aryl electrophiles than arenecarboxylate anhydrides. However, cross-coupling reactions using esters (without any coordinating groups) were hitherto unknown.^[21]

Metal-Catalyzed C–M/C–O Coupling of Phenol Derivatives

In parallel with the metal-catalyzed cross-coupling using arenecarboxylates instead of halogen-based electrophiles, cross-couplings using phenol derivatives as alternatives to

conventional haloarenes have been developed. For example, cross-coupling reactions using metalloarenes as nucleophiles and phenol derivatives as electrophiles (C–M/C–O coupling) have recently been attracting attention because arenes containing C–O bonds, such as phenol and naphthol, are readily available and less expensive than their aryl halide counterparts.^[5,7a] While aryl triflates are generally inferior to aryl halides in terms of reactivity, they were found to be the first C–O-containing coupling partners because of their relatively high reactivity. Later, the coupling reaction of arylmetal species with aryl tosylates and mesylates has been reported. Through extensive efforts in recent years, Ni-catalyzed cross-coupling reactions involving less conventional electrophilic coupling partners, such as aryl esters (Ar–OCOR) or aryl ethers (Ar–OR), have become possible.^[22,23]

In 1979, Wenkert reported a Ni-catalyzed cross-coupling reaction between Grignard reagents with aryl ethers (Figure 3).^[22a] After this pioneering report, it was recognized that an oxidative addition of C–O bonds of aryl ethers to Ni(0) species can occur. Three decades later, more efficient nickel catalysis, a Ni/PCy₃ system, for the cross-coupling of Grignard reagents with aryl ethers was developed by Dankwardt.^[22d] Using this Ni/PCy₃ system, Chatani and Tobisu achieved a Ni-catalyzed cross-coupling of arylboron compounds with aryl ethers in 2008.^[23a] Concurrently, the groups of Garg and Shi also disclosed similar types of coupling reactions of arylboron compounds with aryl esters.^[23b,c,d] Afterward, aryl carbamates, carbonates, sulfamates, and even phenol salts were found to react with arylmetal reagents under the influence of Ni/PCy₃ catalyst. Very recently, a Ni/ICy (ICy: 1,3-dicyclohexylimidazol-2-ylidene) catalyst was developed as an alternative and superior catalyst to Ni/PCy₃ for a C–O bond arylation by Tobisu and Chatani.^[24] Recent progress on Ni-catalyzed C–M/C–O coupling is summarized in Figure 3.

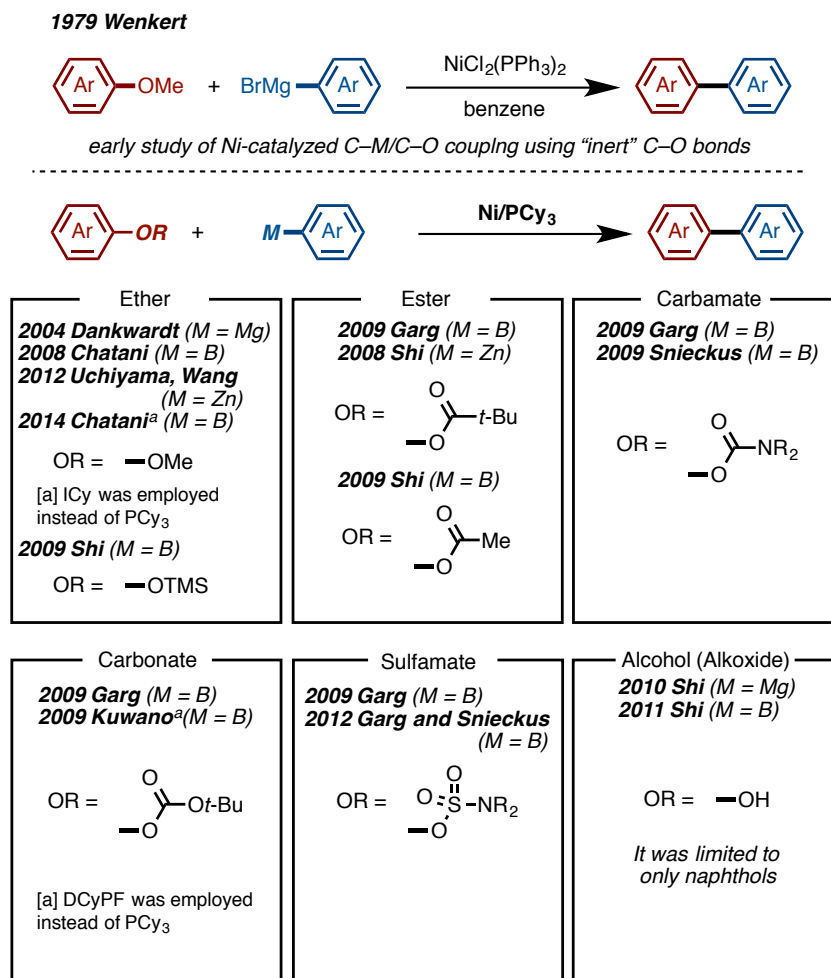
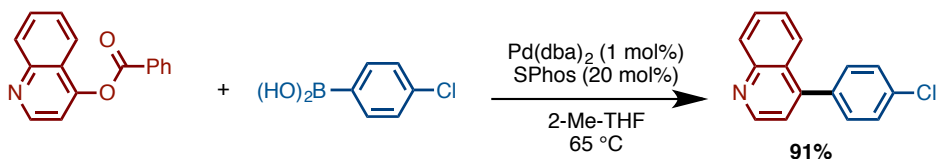


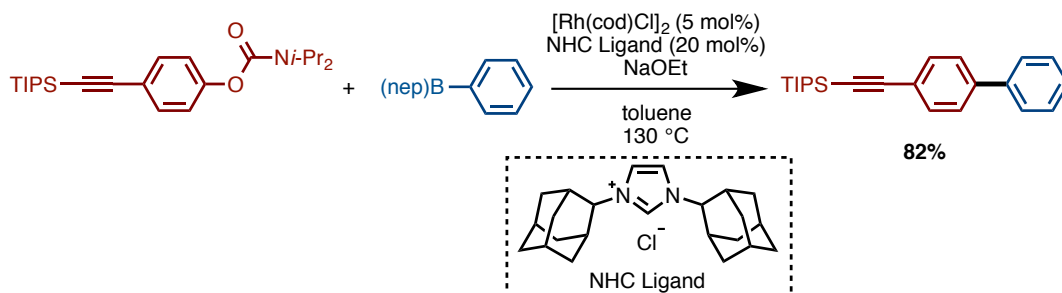
Figure 3. Pioneering works in Ni-catalyzed C–M/C–O coupling

The C–M/C–O coupling reaction catalyzed by palladium was also reported by Li.^[25] The Pd/SPhos system could catalyze the C–M/C–O coupling of aryl benzoates and aryl boron compounds, although the scope was limited to only quinolin-4-yl benzoates. In 2015, a Rh-catalyzed C–M/C–O coupling was developed by Tobisu and Chatani.^[26] A variety of aryl carbamates could couple with neopentyl arylboronic acid esters to afford biaryls (Scheme 6).

Li (2011)



Tobisu and Chatani (2014)

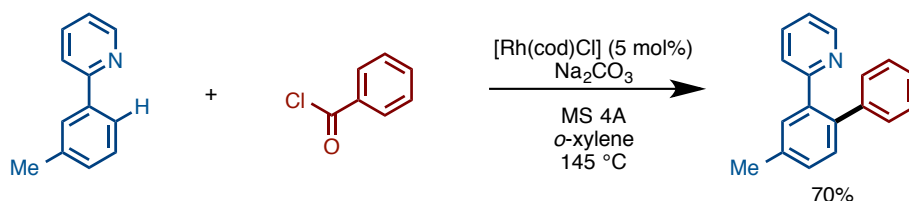


Scheme 6. Metal-catalyzed C–M/C–O coupling

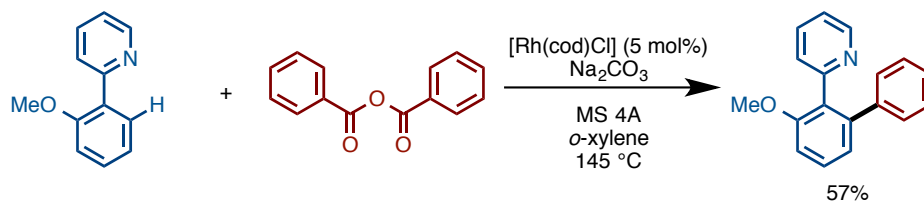
Metal-Catalyzed Decarbonylative C–H Coupling and C–H/C–O Coupling

Mentioned above are successful examples that replace *either* the electrophilic or nucleophilic aryl component with unconventional and efficient molecules. However, these can be regarded as milestones en route to truly ideal cross-coupling. It is highly desirable to replace *both* metal- and halide-based coupling components with new environmentally and economically sound compounds. Recent efforts have succeeded in developing “next-generation” couplings such as decarbonylative C–H arylation of arenes with arenecarboxylates (Scheme 7). As the first report, Rh-catalyzed decarbonylative C–H arylation of 2-phenylpyridines with aroyl chlorides was developed by Yu in 2008.^[27] Treatment of these substrates with [Rh(cod)Cl]₂ as catalyst and Na₂CO₃ as base in toluene promotes the decarbonylative C–H arylation. Although this reaction succeeded in replacing haloarenes with unconventional coupling counterparts, the halogen wastes are still generated due to the use of aroyl halides. In 2009, the same group extended the applicable scope of aryl electrophiles to benzoic anhydrides.^[28] These represent the first examples of decarbonylative C–H arylation, however, the reactive C–H bond-containing substrates were still limited to arenes bearing nitrogen-containing coordinating groups, and the catalyst consisted of the expensive metal of rhodium.

Yu (2008)



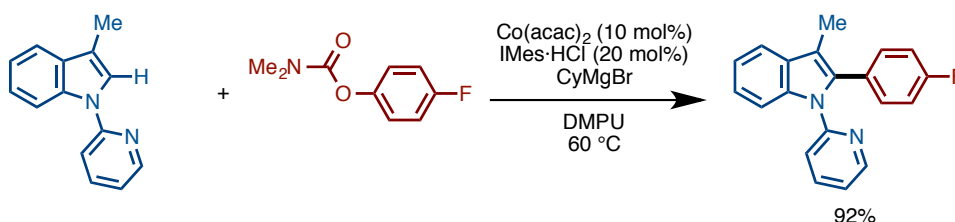
Yu (2009)



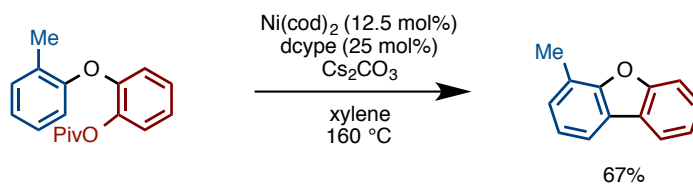
Scheme 7. Rh-catalyzed decarbonylative C–H arylation

As for a C–H/C–O coupling of arenes with phenol derivatives, reactions using sulfur-containing aryl triflates, tosylates and mesylates in the presence of palladium catalyst were already known.^[29] On the other hand, during the study of this thesis, Ackermann developed a Co-catalyzed C–H/C–O coupling of 2-pyridyl substituted arenes with aryl carbamates.^[30] Intramolecular C–H/C–O coupling with a nickel catalyst was reported in 2013.^[31] These reports achieved the replacement of all coupling participants, such as metalloarenes, haloarenes, and expensive metal catalysts with simple arenes, halogen-free aryl electrophiles, and inexpensive metal catalysts, respectively (Scheme 8).

Ackermann (2012)



Kalyani (2013)



Scheme 8. Metal-catalyzed C–H/C–O coupling

Overview of This Thesis

In this thesis, the author describes the development of streamlined synthetic methods for heterobiaryls using originally devised nickel catalysts. The developed Ni-catalyzed biaryl couplings have achieved the replacement of conventional coupling partners of metalloarenes and haloarenes with simple arenes and arenecarboxylates or phenol derivatives, respectively. Moreover, these novel methods allowed for the streamlined synthesis of various biologically active natural products and pharmaceuticals, showcasing their synthetic utility.

Chapter 1 describes the discovery of a new protocol for Ni(OAc)₂/bipy-catalyzed C–H/C–X coupling of azoles and haloarenes using Mg(*Ot*-Bu)₂ as a mild base. Compared with the previous protocol using Li*Ot*-Bu, the newly developed Mg(*Ot*-Bu)₂-based method is more effective for the reactions using electron-deficient haloarenes. Furthermore, mechanistic investigations of this Ni-catalyzed C–H arylation are discussed in detail. The synthetic utility of this newly developed methodology is demonstrated in the rapid synthesis of bioactive molecules such as febuxostat, tafamidis, and texaline (Figure 4).

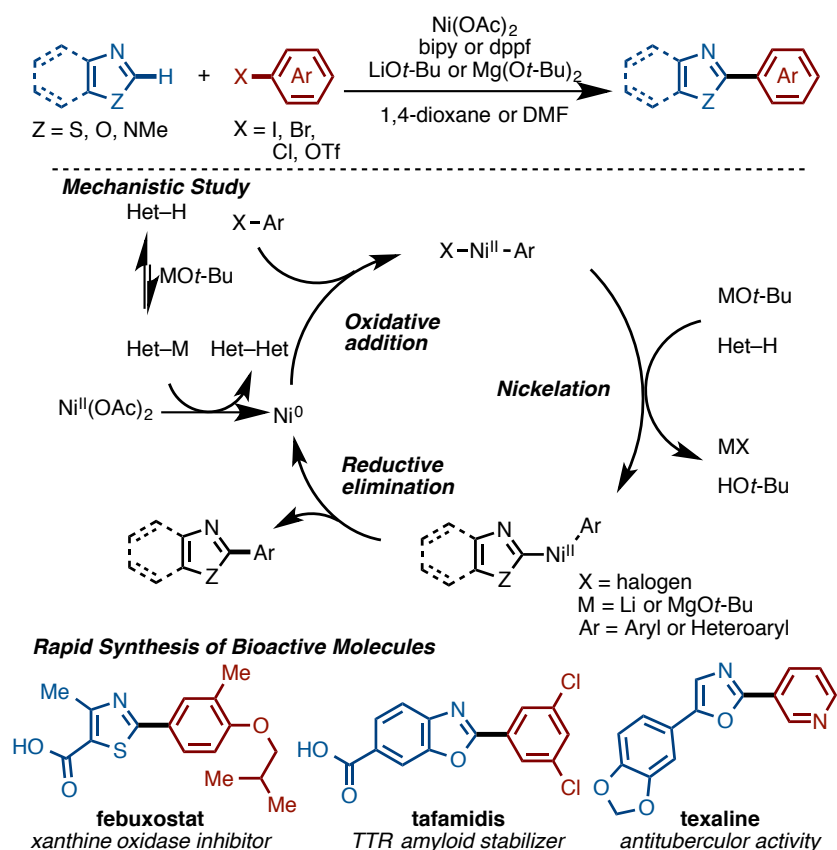


Figure 4. Ni-catalyzed C–H/C–X coupling of azoles and haloarenes

In Chapter 2, the development of decarbonylative organo-boron cross-coupling of esters by nickel catalyst is described. Under the influence of $\text{Ni}(\text{OAc})_2/\text{P}(n\text{-Bu})_3$ catalyst and Na_2CO_3 as base, phenyl esters ($\text{R-CO}_2\text{Ph}$) undergo decarbonylative coupling with boronic acids ($\text{R-B}(\text{OH})_2$). With this user-friendly and inexpensive nickel catalyst, a wide range of phenyl ester of aromatic, heteroaromatic, and aliphatic carboxylic acids can couple with boronic acids in a decarbonylative manner. One of the remarkable features of this reaction is that the reaction is selective to phenyl ester, as methyl esters are completely intact under the reaction conditions. Theoretical calculations have uncovered the key mechanistic features of this decarbonylative coupling, including the phenyl ester selectivity. The synthetic utilities of this catalytic decarbonylative reaction are demonstrated by the transformation of complex drug molecule and a range of orthogonal cross-coupling reactions (Figure 5).

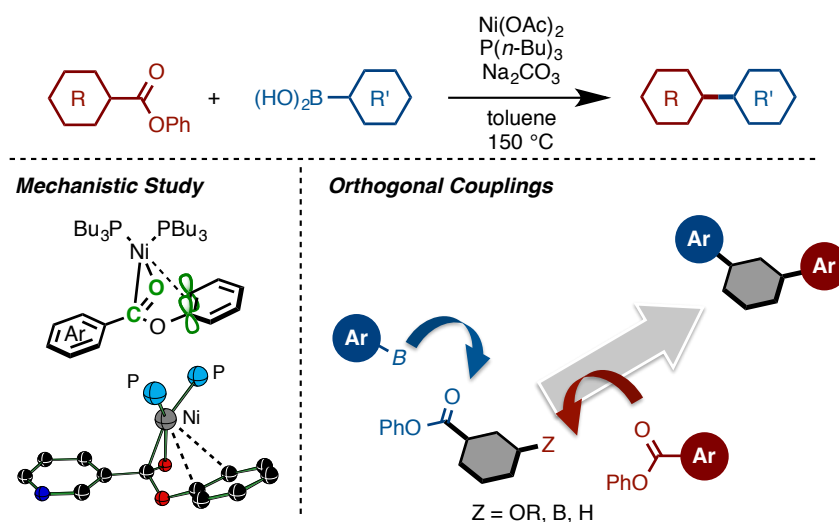


Figure 5. Decarbonylative organoboron coupling of esters by nickel catalyst

In Chapter 3, the development of the first Ni-catalyzed C–H/C–O coupling is described. In the presence of Ni(cod)₂/dcype catalyst and Cs₂CO₃ as base, 1,3-azoles and phenol derivatives can be coupled to produce the corresponding heterobiaryls. Intriguingly, this reaction displayed dramatic ligand effects, as other ligands do not deliver coupling products. Under the influence of the nickel catalyst, several kinds of phenol derivatives, such as aryl pivalates (Ar–OPiv), carbamates (Ar–OCONR₂), carbonates (Ar–OCO₂R), sulfamates (Ar–OSO₂NR₂), triflates (Ar–OTf), tosylates (Ar–OTs), and mesylates (Ar–OMs), can react efficiently. Additionally, Ni/dcype also catalyzes C–H/C–O alkenylation using enol derivatives. The synthetic utility of these reactions is demonstrated by the application to the direct arylation of naturally occurring molecules as well as the rapid and convergent synthesis of siphonazole B, a natural product (Figure 6).

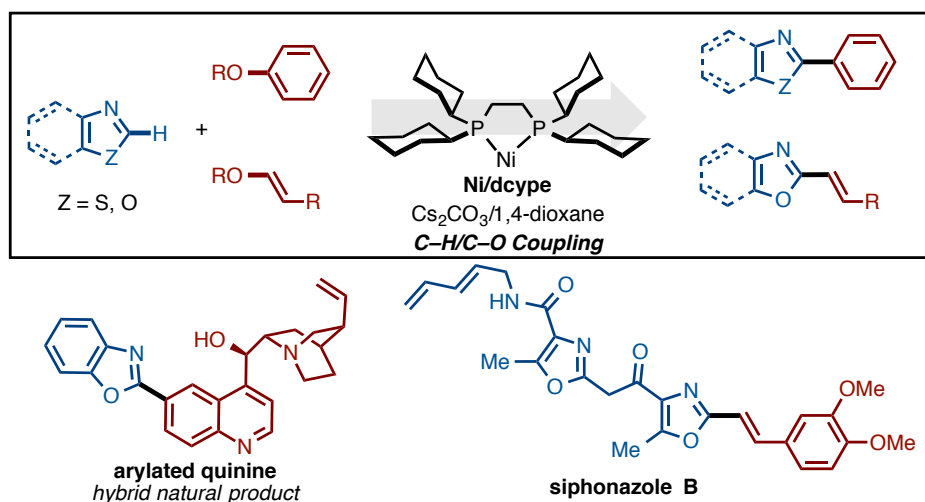


Figure 6. Ni-catalyzed C–H/C–O coupling

Chapter 4 discusses the mechanistic investigations of the Ni-catalyzed C–H/C–O coupling reaction. Depicted in Figure 7 is a plausible catalytic cycle based on a Ni(0)/Ni(II) redox catalytic cycle, occurring via: 1) oxidative addition of an aromatic C–O bond to Ni(0) species **A**, 2) C–H nickelation of an azole with Ar–Ni(II)–OR species **B**, and 3) reductive elimination of the heterobiaryl product to regenerate the Ni(0) species. Extensive studies involving the isolation of intermediate **B** and kinetic studies are discussed in detail. Furthermore, theoretical calculations were performed to gain further insight regarding the effect of base, especially in the C–H nickelation step. Through these combined experimental and computational studies, a detailed catalytic cycle and the dramatic dcype ligand effect on this reaction were unveiled (Figure 7).

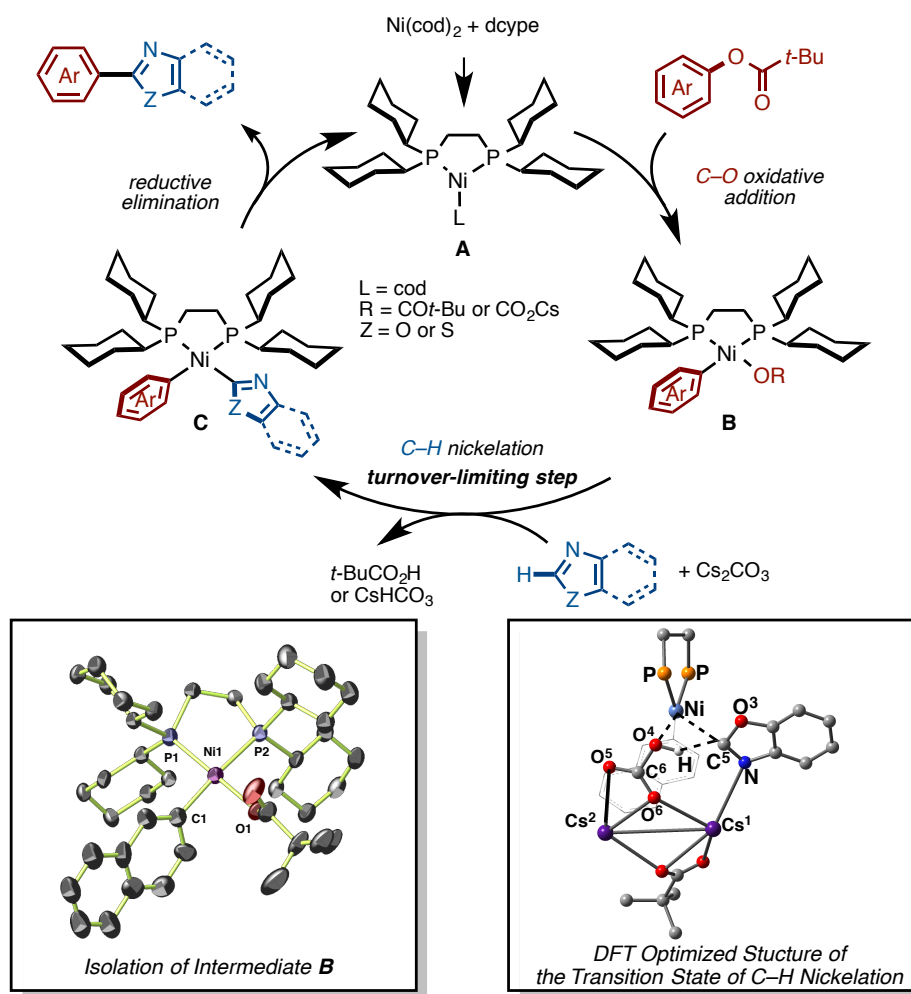


Figure 7. Mechanistic studies of Ni-catalyzed C–H/C–O coupling

Chapter 5 describes the development of Ni/dcype-catalyzed C–H coupling of imidazoles and benzimidazoles. As described in Chapters 1 and 3, imidazoles are mostly unreactive in Ni-catalyzed C–H couplings. The key to achieve C–H coupling of imidazoles was to use *t*-AmylOH as the solvent with the Ni/dcype catalyst. This new protocol enabled not only C–H/C–O arylation using phenol derivatives, but also C–H/C–O alkenylation with enol derivatives. Moreover, this new protocol (Ni/dcype catalyst in *t*-AmylOH) has much wider substrate scope than the previous reaction systems. The dramatic solvent effect is also discussed through a mechanistic study including kinetic studies and control experiments using a deuterated alcohol solvent (Figure 8).

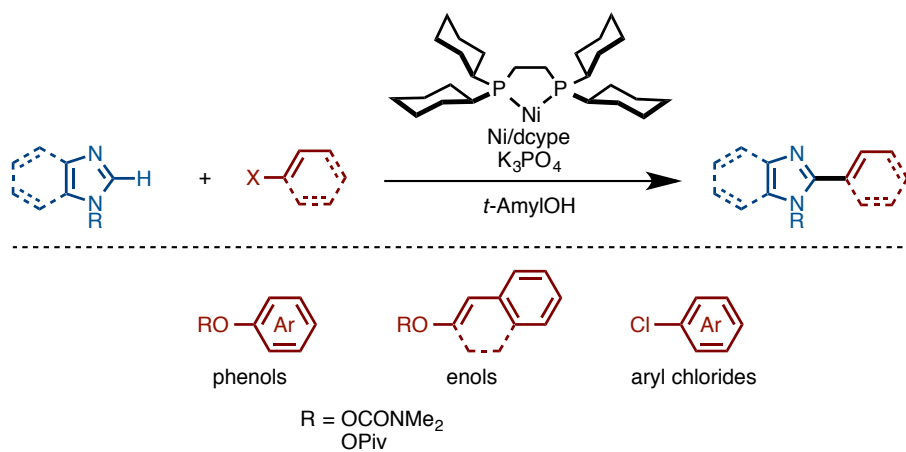


Figure 8. Ni-catalyzed C–H coupling of imidazoles

References and Notes

1. (a) *Metal-catalyzed cross-coupling reactions and more*: (Eds: de Meijere, A.; Bräse, S.; Oestreich, M.), Wiley-VCH: Weinheim, **2014**. (b) *Topics in Current Chemistry, Vol. 219, Cross-Coupling Reactions: A Practical Guide* (Ed.: Miyaura, N.), Springer, Berlin, **2002**.
2. (a) Nicolaou, K. C.; Bulger, P. G.; Sarlah, D. *Angew. Chem., Int. Ed.* **2005**, *44*, 4442. (b) Lloyd-Williams, P.; Giralt, E. *Chem. Soc. Rev.* **2001**, *30*, 145.
3. For selected reviews on catalytic C–H bond arylation of arenes, see: (a) Campeau, L.-C.; Fagnou, K. *Chem. Commun.* **2006**, 1253. (b) Daugulis, O.; Zaitsev, V. G.; Shabashov, D.; Pham, Q.-N.; Lazareva, A. *Synlett* **2006**, 3382. (c) Alberico, D.; Scott, M. E.; Lautens, M.; *Chem. Rev.* **2007**, *107*, 174. (d) Seregin, I. V.; Gevorgyan, V. *Chem. Soc. Rev.* **2007**, *36*, 1173. (e) Satoh, T.; Miura, M. *Chem. Lett.* **2007**, *36*, 200. (f) Kakiuchi, F.; Kochi, T. *Synthesis* **2008**, 3013. (g) Li, B.-J.; Yang, S.-D.; Shi, Z.-J. *Synlett* **2008**, 949. (h) Lewis, J. C.; Bergman, R. G.; Ellman, J. A. *Acc. Chem. Res.* **2008**, *41*, 1013. (i) Miura, M.; Satoh, T. in *Modern Arylation Methods* (Ed.: Ackermann, L.), Wiley-VCH, Weinheim, **2009**, pp. 335–361. (j) Chen, X.; Engle, K. M.; Wang, D.-H.; Yu, J.-Q. *Angew. Chem., Int. Ed.* **2009**, *48*, 5094. (k) Ackermann, L.; Vicente, R.; Kapdi, A. R. *Angew. Chem., Int. Ed.* **2009**, *48*, 9792. (l) Yamaguchi, J.; Yamaguchi, A. D.; Itami, K. *Angew. Chem., Int. Ed.* **2012**, *51*, 8960. (m) Wencel-Delord, J.; Glorius, F. *Nat. Chem.* **2013**, *5*, 369. (n) Segawa, Y.; Maekawa, T.; Itami, K. *Angew. Chem., Int. Ed.* **2014**, *54*, 66.
4. For recent reviews on metal-catalyzed cross-coupling reactions of carboxylates, see: (a) Gooßen, L. J.; Rodríguez, N.; Gooßen, K. *Angew. Chem., Int. Ed.* **2008**, *47*, 3100. (b) Rodríguez, N.; Gooßen, L. J. *Chem. Soc. Rev.* **2011**, *40*, 5030. (c) Dzik, W. I.; Lange, P. P.; Gooßen, L. J. *Chem. Sci.* **2012**, *3*, 2671.
5. For reviews of cross-coupling involving C–O bond activation, see: (a) Li, B.-J.; Yu, D.-G.; Sun, C.-L.; Shi, Z.-J. *Chem. Eur. J.* **2011**, *17*, 1728. (b) Rosen, B. M.; Quasdorf, K. W.; Wilson, D. A.; Zhang, N.; Resmerita, A.-M.; Garg, N. K.; Percec, V. *Chem. Rev.* **2011**, *111*, 1346. (c) Yu, D.-G.; Li, B.-J.; Shi, Z.-J. *Acc. Chem. Res.* **2010**, *43*, 1486. (d) Su, B.; Cao, Z.-C.; Shi, Z.-J. *Acc. Chem. Res.* **2015**, 150213140612002. (e) Tobisu, M.; Chatani, N. *Acc. Chem. Res.* **2015**, *48*, 1717. (f) Mesganaw, T.; Garg, N. K. *Org. Process Res. Dev.* **2013**, *17*, 29.
6. For reviews of cross-coupling involving C–N bond activation, see: (a) Roglans, A.;

- Pla-Quintana, A.; Moreno-Mañas, M. *Chem. Rev.* **2006**, *106*, 4622. (b) Mo, F.; Dong, G.; Zhang, Y.; Wang, J. *Org. Biomol. Chem.* **2013**, *11*, 1582. For selected examples of cross-coupling involving C–N bond activation, see; (c) Blakey, S. B.; MacMillan, D. W. C. *J. Am. Chem. Soc.* **2003**, *125*, 6046. (d) Uehara, T. N.; Yamaguchi, J.; Itami, K. *Asian J. Org. Chem.* **2013**, *2*, 938.
7. For recent reviews on Ni-catalyzed reactions, see: (a) Yamaguchi, J.; Muto, K.; Itami, K. *Eur. J. Org. Chem.* **2013**, 19. (b) Tasker, S. Z.; Standley, E. A.; Jamison, T. F. *Nature* **2014**, *509*, 299.
8. For recent examples on Ni(I)/Ni(III) involving reactions, see: (a) Zuo, Z.; Ahneman, D. T.; Chu, L.; Terrett, J. A.; Doyle, A. G.; MacMillan, D. W. C. *Science* **2014**, *345*, 437. (b) Tellis, J. C.; Primer, D. N.; Molander, G. A. *Science* **2014**, *345*, 433. (c) Zhang, C.-P.; Wang, H.; Klein, A.; Biewer, C.; Stirnat, K.; Yamaguchi, Y.; Xu, L.; Gomez-Benitez, V.; Vicic, D. A. *J. Am. Chem. Soc.* **2013**, *135*, 8141. (d) Schley, N. D.; Fu, G. C. *J. Am. Chem. Soc.* **2014**, *136*, 16588. (e) Mazzotti, A. R.; Campbell, M. G.; Tang, P.; Murphy, J. M.; Ritter, T. *J. Am. Chem. Soc.* **2014**, *135*, 14012. (f) McMahon, C. M.; Alexanian, E. J. *Angew. Chem., Int. Ed.* **2014**, *53*, 5974.
9. Nakamura, N.; Tajima, Y.; Sakai, K. *Heterocycles* **1982**, *17*, 235.
10. (a) Akita, Y.; Inoue, A.; Yamamoto, K.; Ohta, A.; Kurihara, T.; Shimizu, M. *Heterocycles* **1985**, *23*, 2327. (b) Akita, Y.; Itagaki, Y.; Takizawa, S.; Ohta, A. *Chem. Pharm. Bull.* **1989**, *37*, 1477. (c) Ohta, A.; Akita, Y.; Ohkuwa, T.; Chiba, M.; Fukunaga, R.; Miyafuji, A.; Nakata, T.; Tani, N.; Aoyagi, Y. *Heterocycles* **1990**, *31*, 1951.
11. For selected recent examples of Pd-catalyzed direct C–H arylations, see: (a) Lane, B. S.; Brown, M. A.; Sames, D. *J. Am. Chem. Soc.* **2005**, *127*, 8050. (b) Lafrance, M.; Fagnou, K. *J. Am. Chem. Soc.* **2006**, *128*, 16496. (c) Stuart, D. R.; Fagnou, K. *Science* **2007**, *316*, 1172. (d) Turner, G. L.; Morris, J. A.; Greaney, M. F. *Angew. Chem., Int. Ed.* **2007**, *46*, 7996. (e) Campeau, L.-C.; Bertrand-Laperle, M.; Leclerc, J.-P.; Villemure, E.; Gorelsky, S.; Fagnou, K. *J. Am. Chem. Soc.* **2008**, *130*, 3276. (f) Ackermann, L.; Althammer, A.; Fenner, S. *Angew. Chem., Int. Ed.* **2008**, *48*, 201. (g) Campeau, L.-C.; Stuart, D. R.; Leclerc, J.-P.; Bertrand-Laperle, M.; Villemure, E.; Sun, H.-Y.; Lasserre, S.; Guimond, N.; Lecavallier, M.; Fagnou, K. *J. Am. Chem. Soc.* **2009**, *131*, 3291. (h) Huang, J.; Chan, J.; Chen, Y.; Borths, C.

- J.; Baucom, K. D.; Larsen, R. D.; Faul, M. M. *J. Am. Chem. Soc.* **2010**, *132*, 3674.
- (i) Joo, J. M.; Touré, B. B.; Sames, D. *J. Org. Chem.* **2010**, *75*, 4911. (j) Ueda, K.; Yanagisawa, S.; Yamaguchi, J.; Itami, K. *Angew. Chem., Int. Ed.* **2010**, *49*, 8946.
- (k) Guo, P.; Joo, J. M.; Rakshit, S.; Sames, D. *J. Am. Chem. Soc.* **2011**, *133*, 16338.
- (l) Wang, X.; Leow, D.; Yu, J.-Q. *J. Am. Chem. Soc.* **2011**, *133*, 13864. (m) Engle, K. M.; Thuy-Boun, P. S.; Dang, M.; Yu, J.-Q. *J. Am. Chem. Soc.* **2011**, *133*, 18183.
- (n) Ye, M.; Gao, G.-L.; Edmunds, A. J. F.; Worthington, P. A.; Morris, J. A.; Yu, J.-Q. *J. Am. Chem. Soc.* **2011**, *133*, 19090. (o) Mochida, K.; Kawasumi, K.; Segawa, Y.; Itami, K. *J. Am. Chem. Soc.* **2011**, *133*, 10716. (p) Kirchberg, S.; Tani, S.; Ueda, K.; Yamaguchi, J.; Studer, A.; Itami, K. *Angew. Chem., Int. Ed.* **2011**, *50*, 2387. (q) Mandal, D.; Yamaguchi, A. D.; Yamaguchi, J.; Itami, K. *J. Am. Chem. Soc.* **2011**, *133*, 19660. (r) Kuhl, N.; Hopkinson, M. N.; Glorius, F. *Angew. Chem., Int. Ed.* **2012**, *51*, 8230. (s) Wan, L.; Dastbaravardeh, N.; Li, G.; Yu, J.-Q. *J. Am. Chem. Soc.* **2013**, *135*, 18056. (t) Ye, M.; Edmunds, A. J. F.; Morris, J. A.; Sale, D.; Zhang, Y.; Yu, J.-Q. *Chem. Sci.* **2013**, *4*, 2374. (u) Tang, D.-T. D.; Collins, K. D.; Ernst, J. B.; Glorius, F. *Angew. Chem., Int. Ed.* **2014**, *53*, 1809. (v) Tani, S.; Uehara, T. N.; Yamaguchi, J.; Itami, K. *Chem. Sci.* **2014**, *5*, 123. (w) Ozaki, K.; Kawasumi, K.; Shibata, M.; Ito, H.; Itami, K. *Nat. Commun.* **2015**, *6*, 6251.
12. For selected recent examples of Rh-catalyzed direct C–H arylations, see: (a) Lewis, J. C.; Wiedemann, S. H.; Bergman, R. G.; Ellman, J. A. *Org. Lett.* **2004**, *6*, 35. (b) Lewis, J. C.; Berman, A. M.; Bergman, R. G.; Ellman, J. A. *J. Am. Chem. Soc.* **2008**, *130*, 2493. (c) Berman, A. M.; Lewis, J. C.; Bergman, R. G.; Ellman, J. A. *J. Am. Chem. Soc.* **2008**, *130*, 14926. (d) Berman, A. M.; Bergman, R. G.; Ellman, J. A. *J. Org. Chem.* **2010**, *75*, 7863. (e) Yanagisawa, S.; Sudo, T.; Noyori, R.; Itami, K. *J. Am. Chem. Soc.* **2008**, *128*, 11748. (f) Ueda, K.; Amaike, K.; Maceiczky, R. M.; Itami, K.; Yamaguchi, J. *J. Am. Chem. Soc.* **2014**, *136*, 13226. (g) Yamaguchi, A. D.; Chepiga, K. M.; Yamaguchi, J.; Itami, K.; Davies, H. M. L. *J. Am. Chem. Soc.* **2015**, *137*, 644. (h) Kim, M.; Kwak, J.; Chang, S. *Angew. Chem., Int. Ed.* **2009**, *48*, 8935. (i) Kwak, J.; Kim, M.; Chang, S. *J. Am. Chem. Soc.* **2011**, *133*, 3780.
13. For selected recent examples of Cu-catalyzed or mediated direct C–H arylations, see: (1) Pivsa-Art, S.; Satoh, T.; Kawamura, Y.; Miura, M.; Nomura, M. *Bull. Chem. Soc. Jpn.* **1998**, *71*, 467. (b) Do, H.-Q.; Daugulis, O. *J. Am. Chem. Soc.*

- 2007**, *129*, 12404. (c) Yoshizumi, T.; Tsurugi, H.; Satoh, T.; Miura, M. *Tetrahedron Lett.* **2008**, *49*, 1598. (d) Do, H.-Q.; Khan, R. M. K.; Daugulis, O. *J. Am. Chem. Soc.* **2008**, *130*, 15185. (e) Phipps, R. J.; Grimster, N. P.; Gaunt, M. J. *J. Am. Chem. Soc.* **2008**, *130*, 8172. (f) Phipps, R. J.; Gaunt, M. J. *Science* **2009**, *323*, 1593. (g) Ban, I.; Sudo, T.; Taniguchi, T.; Itami, K. *Org. Lett.* **2008**, *10*, 3607. (h) Kitahara, M.; Umeda, N.; Hirano, K.; Satoh, T.; Miura, M. *J. Am. Chem. Soc.* **2011**, *133*, 2160. (i) Nishino, M.; Hirano, K.; Satoh, T.; Miura, M. *Angew. Chem., Int. Ed.* **2012**, *51*, 6993.
14. For recent examples of Fe-catalyzed or mediated direct C–H arylations, see: (a) Norinder, J.; Matsumoto, A.; Yoshikai, N.; Nakamura, E. *J. Am. Chem. Soc.* **2008**, *130*, 5858. (b) Yoshikai, N.; Matsumoto, A.; Norinder, J.; Nakamura, E. *Angew. Chem., Int. Ed.* **2009**, *48*, 2925. (c) Wen, J.; Qin, S.; Ma, L.-F.; Dong, L.; Zhang, J.; Liu, S.-S.; Duan, Y.-S.; Chen, S.-Y.; Hu, C.-W.; Yu, X.-Q. *Org. Lett.* **2010**, *12*, 1694. (d) Ilies, L.; Kobayashi, M.; Matsumoto, A.; Yoshikai, N.; Nakamura, E. *Adv. Synth. Catal.* **2012**, *354*, 593.
15. For recent examples of Co-catalyzed direct C–H arylations, see: (a) Li, B.; Wu, Z.-H.; Gu, Y.-F.; Sun, C.-L.; Wang, B.-Q.; Shi, Z.-J. *Angew. Chem., Int. Ed.* **2011**, *50*, 1109. (b) Gao, K.; Lee, P.-S.; Long, C.; Yoshikai, N. *Org. Lett.* **2012**, *14*, 4234. (c) Song, W.; Ackermann, L.; *Angew. Chem., Int. Ed.* **2012**, *51*, 8251.
16. For recent examples of Ni-catalyzed direct C–H arylations, see: (a) Canivet, J.; Yamaguchi, J.; Ban, I.; Itami, K. *Org. Lett.* **2009**, *11*, 1733. (b) Hachiya, H.; Hirano, K.; Satoh, T.; Miura, M. *Org. Lett.* **2009**, *11*, 1737. (c) Kobayashi, O.; Uruguchi, D.; Yamanaka, T. *Org. Lett.* **2009**, *11*, 2679. (d) Yamamoto, T.; Muto, K.; Komiyama, M.; Canivet, J.; Yamaguchi, J.; Itami, K. *Chem. Eur. J.* **2011**, *17*, 10113. For C–H/C–M coupling, see: (e) Tobisu, M.; Hyodo, I.; Chatani, N. *J. Am. Chem. Soc.* **2009**, *131*, 12070. (f) Hachiya, H.; Hirano, K.; Satoh, T.; Miura, M. *ChemCatChem* **2010**, *2*, 1403. (g) Hachiya, H.; Hirano, K.; Satoh, T.; Miura, M. *Angew. Chem., Int. Ed.* **2010**, *49*, 2202. (h) Qu, G.-R.; Xin, P.-Y.; Niu, H.-Y.; Wang, D.-C.; Ding, R.-F.; Guo, H.-M. *Chem. Commun.* **2011**, *47*, 11140. (i) Hyodo, I.; Tobisu, M.; Chatani, N. *Chem. Asian J.* **2012**, *7*, 1357. (j) Hyodo, I.; Tobisu, M.; Chatani, N. *Chem. Commun.* **2012**, *48*, 308. (k) Yokota, A.; Aihara, Y.; Chatani, N. *J. Org. Chem.* **2014**, *79*, 11922.
17. Gooßen, L. J.; Paetzold, J. *Adv. Synth. Catal.* **2004**, *346*, 1665.

18. Havlik, S. E.; Simmons, J. M.; Winton, V. J.; Johnson, J. B. *J. Org. Chem.* **2011**, *76*, 3588.
19. Wang, J.; Liu, B.; Zhao, H.; Wang, J. *Organometallics* **2012**, *31*, 8598.
20. (a) Gooßen, L. J.; Deng, G.; Levy, L. M. *Science* **2006**, *313*, 662. (b) Gooßen, L. J.; Rodríguez, N.; Linder, C. *J. Am. Chem. Soc.* **2008**, *130*, 15248.
21. An important decarbonylation reaction of esters with a Ni complex, see: Yamamoto, T.; Ishizu, J.; Kohara, T.; Komiya, S.; Yamamoto, A. *J. Am. Chem. Soc.* **1980**, *102*, 3758.
22. For Ni-catalyzed C–Mg/C–O, C–Zn/C–O biaryl coupling, see: (a) Wenkert, E.; Michelotti, E. L.; Swindell, C. S. *J. Am. Chem. Soc.* **1979**, *101*, 2246. (b) Wenkert, E.; Michelotti, E. L.; Swindell, C. S.; Tingoli, M. *J. Org. Chem.* **1984**, *49*, 4894. (c) Hayashi, T.; Katsuro, Y.; Okamoto, Y.; Kumada, M. *Tetrahedron Lett.* **1981**, *22*, 4449. (d) Dankwardt, J. W. *Angew. Chem., Int. Ed.* **2004**, *43*, 2428. (e) Macklin, T. K.; Snieckus, V. *Org. Lett.* **2005**, *7*, 2519. (f) Li, B.-J.; Li, Y.-Z.; Lu, X.-Y.; Liu, J.; Guan, B.-T.; Shi, Z.-J. *Angew. Chem., Int. Ed.* **2008**, *47*, 10124. (g) Yu, D.-G.; Li, B.-J.; Zheng, S.-F.; Guan, B.-T.; Wang, B.-Q.; Shi, Z.-J. *Angew. Chem., Int. Ed.* **2010**, *49*, 4566. (h) Wang, C.; Ozaki, T.; Takita, R.; Uchiyama, M. *Chem. Eur. J.* **2012**, *18*, 3482.
23. For Ni/PCy₃-catalyzed C–B/C–O biaryl coupling using phenol derivatives (ethers, esters, carbamates, carbonates, sulfamates, phosphates, and metal salts), see: (a) Tobisu, M.; Shimasaki, T.; Chatani, N. *Angew. Chem., Int. Ed.* **2008**, *47*, 4866. (b) Quasdorf, K. W.; Tian, X.; Garg, N. K. *J. Am. Chem. Soc.* **2008**, *130*, 14422. (c) Guan, B.-T.; Wang, Y.; Li, B.-J.; Yu, D.-G.; Shi, Z.-J. *J. Am. Chem. Soc.* **2008**, *130*, 14468. (d) Quasdorf, K. W.; Riener, M.; Petrova, K. V.; Garg, N. K. *J. Am. Chem. Soc.* **2009**, *131*, 17748. (e) Antoft-Finch, A.; Blackburn, T.; Snieckus, V. *J. Am. Chem. Soc.* **2009**, *131*, 17750. (f) Xi, L.; Li, B.-J.; Wu, Z.-H.; Lu, X.-Y.; Guan, B.-T.; Wang, B.-Q.; Zhao, K.-Q.; Shi, Z.-J. *Org. Lett.* **2010**, *12*, 884. (g) Quasdorf, K. W.; Antoft-Finch, A.; Liu, P.; Silberstein, A. L.; Komaromi, A.; Blackburn, T.; Ramgren, S. D.; Houk, K. N.; Snieckus, V.; Garg, N. K. *J. Am. Chem. Soc.* **2011**, *133*, 6352. (h) Chen, H.; Huang, Z.; Hu, X.; Tang, G.; Xu, P.; Zhao, Y.; Cheng, C.-H. *J. Org. Chem.* **2011**, *76*, 2338. (i) Yu, D.-G.; Shi, Z.-J. *Angew. Chem., Int. Ed.* **2011**, *50*, 7097. For reactions using a ferrocenyl bisphosphine ligand, see: (j) Kuwano, R.; Shimizu, R. *Chem. Lett.* **2011**, *40*, 913.

24. Tobisu, M.; Yasutome, A.; Kinuta, H.; Nakamura, K.; Chatani, N. *Org. Lett.* **2014**, *16*, 5572.
25. Li, W.; Gao, J. J.; Zhang, Y.; Tang, W.; Lee, H.; Fandrick, K. R.; Lu, B.; Senanayake, C. H. *Adv. Synth. Catal.* **2011**, *353*, 1671.
26. Nakamura, K.; Yasui, K.; Tobisu, M.; Chatani, N. *Tetrahedron* **2015**, *71*, 4484.
27. Zhao, X.; Yu, Z. *J. Am. Chem. Soc.* **2008**, *130*, 8136.
28. Jin, W.; Yu, Z.; He, W.; Ye, W.; Xiao, W.-J. *Org. Lett.* **2009**, *11*, 1317.
29. Metal-catalyzed C–H/C–O biaryl coupling of aryl tosylates, mesylates, and imidazolylcarbamates are known: Ru-catalyzed reaction using aryl tosylates: (a) Ackermann, L.; Althammer, A.; Born, R. *Angew. Chem., Int. Ed.* **2006**, *45*, 2619. (b) Ackermann, L.; Vicente, R.; Althammer, A. *Org. Lett.* **2008**, *10*, 2299. (c) Ackermann, L.; Mulzer, M. *Org. Lett.* **2008**, *10*, 5043. Pd-catalyzed reaction using aryl tosylates: (d) Ackermann, L.; Althammer, A.; Fenner, S. *Angew. Chem., Int. Ed.* **2009**, *48*, 201. (e) Ackermann, L.; Fenner, S. *Chem. Commun.* **2011**, *47*, 430. Using aryl mesylates: (f) So, C. M.; Lau, C. P.; Kwong, F. Y. *Chem. Eur. J.* **2011**, *17*, 761. Using aryl imidazolylsulfamates: (g) Ackermann, L.; Barfüsser, S.; Pospech, J. *Org. Lett.* **2010**, *12*, 724.
30. Song, W.; Ackermann, L. *Angew. Chem., Int. Ed.* **2012**, *51*, 8251.
31. Wang, J.; Ferguson, D. M.; Kalyani, D. *Tetrahedron* **2013**, *69*, 5780.

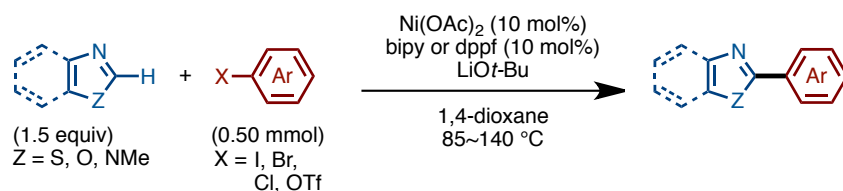
Nickel-Catalyzed C–H Arylation of 1,3-Azoles with Haloarenes

Abstract

The development of a new Ni(OAc)₂/bipy protocol for the C–H arylation of 1,3-azoles with haloarenes (C–H/C–X coupling) is described. Previously, the Itami group established that Ni(OAc)₂/bipy/Li*Ot*-Bu as a nickel catalyst system for C–H arylation of 1,3-azoles with haloarenes. In this study, a new protocol for the aromatic C–H arylation using Mg(*Ot*-Bu)₂ as a milder and less expensive base as an alternative to Li*Ot*-Bu has been developed. Furthermore, mechanistic investigations of this Ni-catalyzed C–H arylation are discussed in detail. The synthetic utility of Ni-catalyzed aromatic C–H arylation is illustrated by the synthesis of bioactive molecules such as febuxostat, tafamidis, and texaline.

1. Introduction

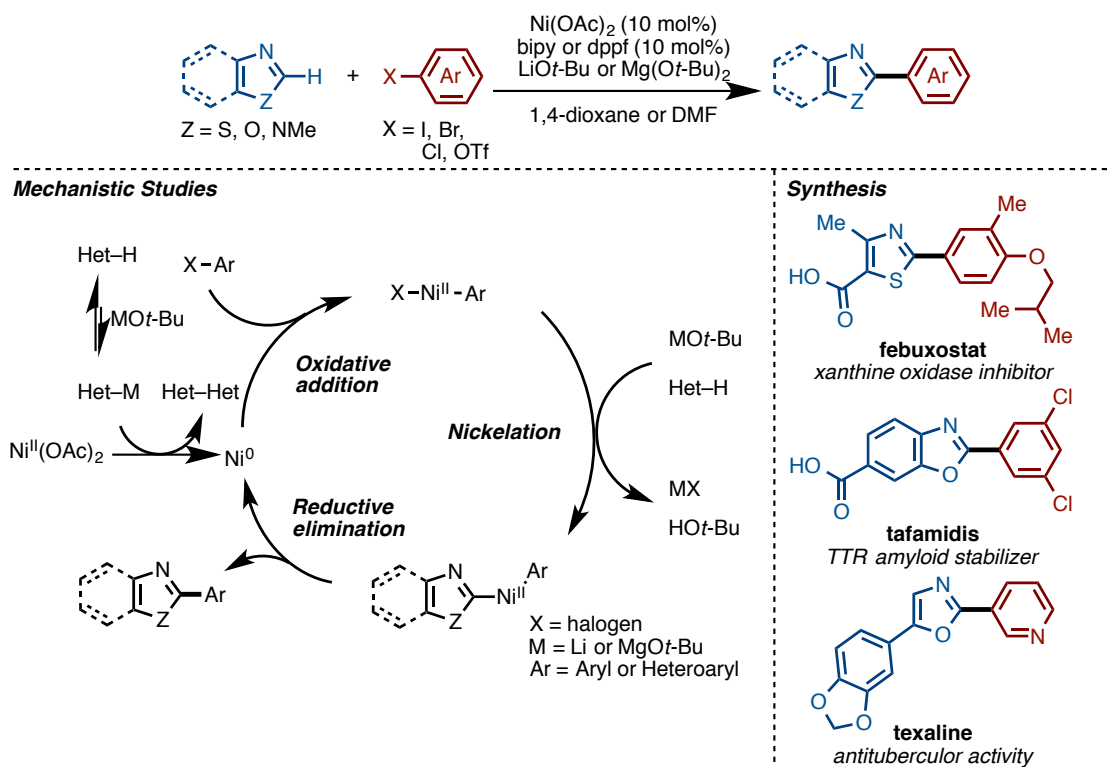
Heterobiaryl frameworks such as 2-aryl-1,3-azoles represent privileged structural motifs often found in bioactive molecules. In order to construct these skeletons, Pd-catalyzed cross-coupling of metalloarenes and haloarenes is often used. Although cross-coupling is one of the most reliable methods to synthesize a range of molecules including natural products, pharmaceutical compounds and organic materials, it requires several steps in order to prepare the metalloarenes precursors prior to the cross-coupling event.^[1] In contrast, a direct C–H bond arylation of simple heteroarenes with haloarenes can eliminate the use of pre-functionalized metalloarenes.^[2] In the past, the C–H arylation of 1,3-azoles has been reported with palladium or rhodium as a catalyst.^[3] However, there still exists room for improvement since these protocols require the use of expensive metal catalysts. Recently, inexpensive transition metal catalysts such as copper,^[4] iron,^[5] cobalt,^[6] and nickel,^[7] have seen increasing use in the laboratory. Along with this trend, the Itami group reported the first example of Ni-catalyzed C–H arylation of heteroarenes with haloarenes in 2009 (Scheme 1).^[7a] A Ni(OAc)₂/bipy system catalyzes the coupling reaction between 1,3-azoles and iodo- or bromoarenes (C–H/C–X coupling). Additionally, chloroarenes and aryl triflates also react with 1,3-azoles in the presence of Ni(OAc)₂/dppf catalyst instead of Ni(OAc)₂/bipy. Concurrently, Miura also reported a similar nickel-based catalytic reaction.^[7b] In the catalytic system, the use of LiOt-Bu in 1,4-dioxane was essential but other bases were totally ineffective. However, the strong basicity of LiOt-Bu was drawback when applying to the synthesis of a range of pharmaceutically relevant molecules. Moreover, the low polarity of 1,4-dioxane was thought to be unsuitable to dissolve highly polar compounds such as pharmaceuticals.



Scheme 1. Ni-catalyzed C–H/C–X coupling of 1,3-azoles with haloarenes

This chapter describes the development of a new protocol based on Ni(OAc)₂/bipy

catalyst employing $\text{Mg}(\text{O}t\text{-Bu})_2$ as an alternative to $\text{LiO}t\text{-Bu}$ for the C–H arylation of 1,3-azoles with haloarenes (Scheme 2).^[7d] Mechanistic studies of this catalytic reaction are also discussed in detail. The synthetic utility of this newly developed methodology is demonstrated by the rapid synthesis of bioactive molecules such as febuxostat, tafamidis, and texaline.



Scheme 2. Development of a new protocol for nickel catalysis, mechanistic studies, and application to the synthesis of bioactive compounds

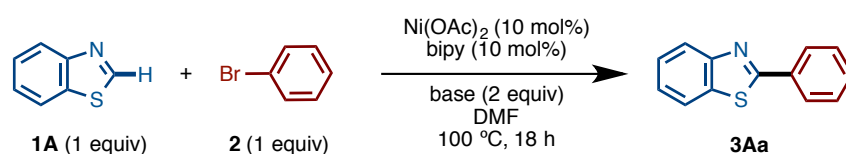
2. Results and Discussion

2-1. Discovery of the $\text{Mg}(\text{O}t\text{-Bu})_2$ Protocol

The author began the research project by exploring the use of new base additives for the Ni-catalyzed C–H arylation using benzothiazole (**1A**) and bromobenzene as model substrates (Table 1). In this screening, a highly polar solvent such as DMF was chosen in anticipation of the use of polar molecules in future synthetic applications. Reactions were carried out using various alkaline additives (2 equiv) under the action of $\text{Ni}(\text{OAc})_2/\text{bipy}$ catalyst in DMF at 100 °C for 18 hours. $\text{LiO}t\text{-Bu}$ was not an effective

additive in DMF (entry 1), and similarly to the previous screening using 1,4-dioxane as a solvent, sodium and potassium *tert*-butoxides were ineffective (entries 2 and 3). Interestingly, alkoxides of alkaline earth metals such as barium, calcium, and magnesium were rather effective (entries 4–8). Finally, an acceptable solution was discovered, in which the reaction was conducted with two equivalents of Mg(*Ot*-Bu)₂ in DMF, furnishing the corresponding product **3Aa** in 35% yield (entry 6). When the reaction time was elongated to 36 hours and 1.5 equivalent of Mg(*Ot*-Bu)₂ was used, the yield of **3Aa** was improved to 57%. It should be noted that Mg(*Ot*-Bu)₂ is less expensive and has milder basicity than Li*Ot*-Bu.

Table 1. Effect of base on the Ni-catalyzed C–H arylation in DMF



entry	base	yield (%) ^b
1	Li <i>Ot</i> -Bu	<1
2	Na <i>Ot</i> -Bu	<1
3	K <i>Ot</i> -Bu	0
4	Ca(OMe) ₂	6
5	Ba(<i>Ot</i> -Bu) ₂	20
6	Mg(<i>Ot</i> -Bu) ₂	35 (57) ^c
7	Mg(OEt) ₂	20
8	Mg(OMe) ₂	9
9	MgH ₂	0

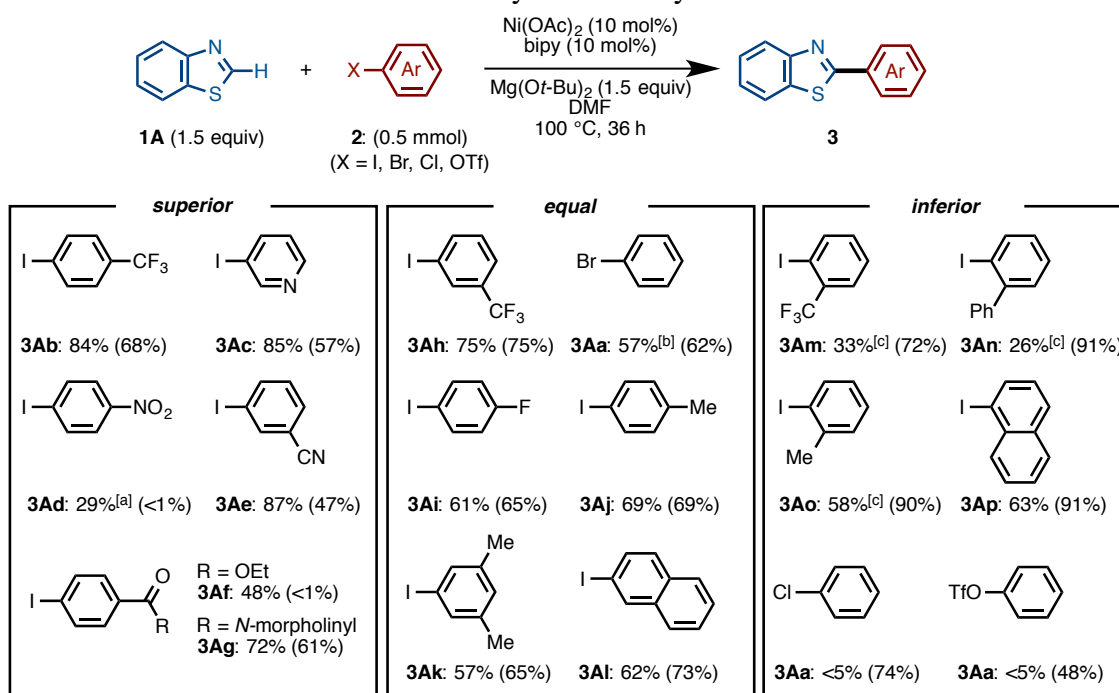
[a] Reaction conditions were as follows: **1A** (0.50 mmol), **2** (0.50 mmol), Ni(OAc)₂ (10 mol%), bipy (10 mol%), base (2.0 equiv), DMF (2.0 mL), 100 °C, 18 h. [b] GC yield [c] Using 1.5 equiv of **1A** and base, the reaction was conducted for 36 h.

2-2. Substrate Scope Using a Ni(OAc)₂/bipy/Mg(*Ot*-Bu)₂ System

With new conditions in hand, the reactivity of aryl electrophiles was tested under the action of Mg(*Ot*-Bu)₂ in DMF (Table 2). Using benzothiazole (**1A**) as a fixed coupling partner, various aryl electrophiles were classified as being “superior”, “equal”, or “inferior” by comparing the yields under Mg(*Ot*-Bu)₂-mediated conditions to those under Li*Ot*-Bu-mediated conditions. For example, in the case of bromobenzene, optimized conditions gave 57% of **3Aa**, which is nearly as good as the yield obtained

when Li*Ot*-Bu was used. Therefore, bromobenzene was classified as being “equal”. Haloarene substrates bearing electron-rich or electron-neutral substituents, such as fluoride, methyl, and 3,5-dimethyl groups, were also identified as being “equal”. In contrast, *ortho*-substituted haloarenes, chlorobenzene, and phenyl triflate were found to be “inferior” substrates. On the other hand, electron-deficient haloarenes, such as iodopyridine, iodobenzonitrile, and ester- or amide-substituted iodobenzenes, were found to be “superior” arylating agents. Notably, 4-nitroiodobenzene and ethyl 4-iodobenzoate were effective only under the Mg(*Ot*-Bu)₂ conditions. As a result, two useful sets of coupling conditions with the Ni(OAc)₂/bipy catalytic system have been established. Whereas the Li*Ot*-Bu/1,4-dioxane system generally works well for robust substrates, the Mg(*Ot*-Bu)₂/DMF system is, in many cases, superior for substrates with base-sensitive functional groups.

Table 2. Comparison between Li*Ot*-Bu/1,4-dioxane and Mg(*Ot*-Bu)₂/DMF systems in Ni-catalyzed C–H arylation



Numbers in the parenthesis show the reaction yield when reaction conducted using Li*Ot*-Bu in 1,4-dioxane. [a] The reaction was conducted at 85 °C. [b] The reaction was conducted at 120 °C.

Then, the reactivity of 1,3-azoles under the Mg(*Ot*-Bu)₂ protocol was examined, and this new protocol showed almost equal reactivity to the Li*Ot*-Bu protocol (Table 3). Benzothiazole (**1A**), thiazoles (**1B** and **1C**), and benzoxazole (**1D**) coupled with

iodobenzene to give the corresponding products in good to moderate yields.

Table 3. Substrate scope for 1,3-azoles using the Mg(*Ot*-Bu)₂ protocol

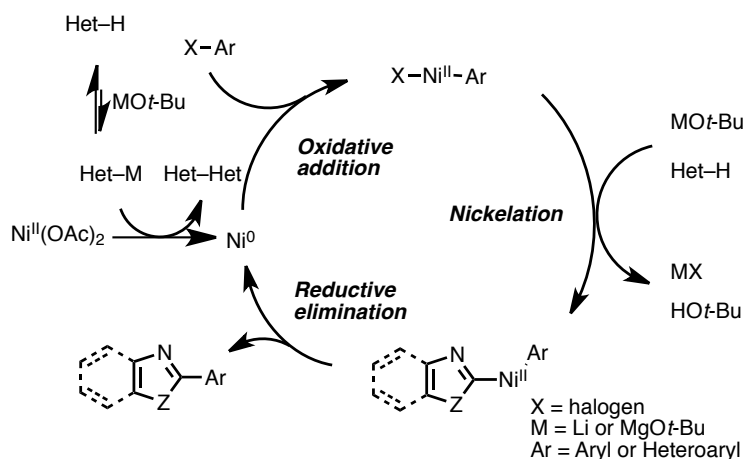
entry	azole	product	yield (%) ^{b, c}
1	1A	3Aa	73 (80)
2	1B	3Ba	31 (43)
3	1C	3Ca	68 (57)
4	1D	3Da	57 ^d (53)

[a] Reaction conditions were as follows: **1A** (0.50 mmol), **2** (0.50 mmol), Ni(OAc)₂ (10 mol%), bipy (10 mol%), Mg(*Ot*-Bu)₂ (1.5 equiv), DMF (2.0 mL), 100 °C, 36 h. [b] Isolated yield [c] The number in the parenthesis show the yield under the Li*Ot*-Bu protocol. [d] Zn powder (2.0 equiv) was added, and reaction was conducted at 140 °C.

2-3. Mechanistic Studies of the Ni-catalyzed C–H Arylation of Azoles

Mechanistic studies of transition-metal-catalyzed azole–haloarene coupling using palladium, rhodium, and copper catalysts had been performed by Ellman,^[2h] Daugulis,^[6a] and Zhuravlev.^[8] According to these reports, and previous investigation of the Itami group, a likely mechanism involves Ni(0)/Ni(II) redox catalysis (Scheme 3) that proceeds via: 1) oxidative addition of an aryl electrophile (Ar–X) to a Ni(0) species generated *in situ*; 2) nickelation of an azole (Het–H) with Ar–Ni^{II}–X to generate an Ar–Ni^{II}–Het species; and 3) reductive elimination of an heterobiaryl (Het–Ar) with regeneration of the Ni(0) catalyst. Ni(cod)₂ was also an effective catalyst, thus supporting the involvement of a Ni(0) species in the catalytic cycle. However, details were unclear regarding the elementary steps in the assumed mechanism, such as a) the way in which the Ni(0) species is produced from Ni(OAc)₂ under the reaction conditions; b) whether or not an Ar–Ni^{II}–X species is involved in the catalytic cycle; and c) the way in which azole nickelation occurs to give the Ar–Ni^{II}–Het species. With these questions in mind, a number of experiments were performed to shed some light on

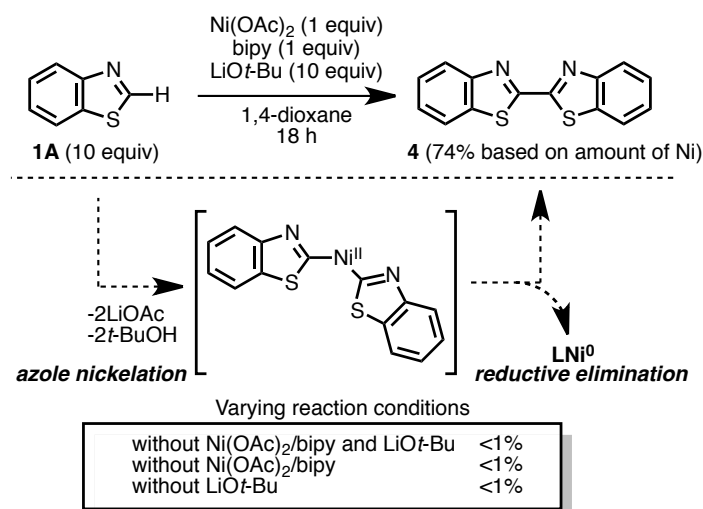
the mechanism of this reaction.



Scheme 3. A plausible catalytic cycle of Ni-catalyzed C–H arylation of 1,3-azoles with haloarenes

2-4. Generation of a Ni⁰ Species from Ni(OAc)₂

It was initially presumed that the active Ni(0) species can be generated from Ni(OAc)₂ by the action of sacrificial azole (in a catalytic amount) because less than 10% yield of an azole dimer was observed after every coupling reaction of azoles under the standard conditions. In other words, it might be possible that the nickelation of two azole molecules using one molecule of Ni(OAc)₂, followed by reductive elimination, could afford the necessary Ni(0) species along with an azole dimer (Scheme 3). Based upon this hypothesis, the experiments shown in Scheme 4 were performed. As anticipated, the dimerization of benzothiazole occurred in the presence of Ni(OAc)₂/bipy and LiOt-Bu to give the dimer **4** in 74% yield based on the amount of nickel. Intriguingly, when one of the two components (Ni(OAc)₂/bipy or LiOt-Bu) were omitted, the dimerization reaction did not occur. The possible role of LiOt-Bu will be discussed later in this chapter.

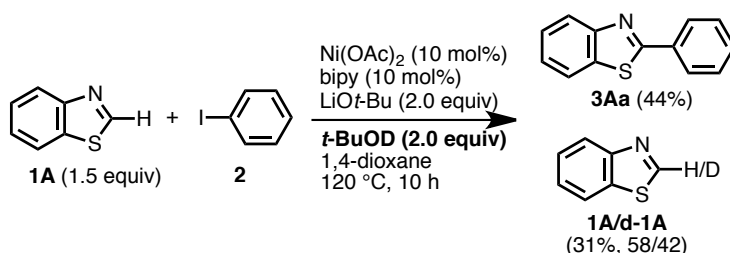


Scheme 4. Studies on the generation of an active Ni(0) species

2-5. Deprotonation of 1,3-Azoles with LiOt-Bu

Having identified that LiOt-Bu is critical for generating a Ni(0) species, the study was aimed to investigate another assumed role of LiOt-Bu as a deprotonating agent within the catalytic cycle (azole nickelation step). In early experiments, benzothiazole (**1A**) was deprotonated with *n*-butyllithium instead of LiOt-Bu and the nickel-catalyzed reaction with iodobenzene was then conducted. However, the expected coupling product was not obtained, and benzothiazole completely decomposed under the coupling conditions. In line with this observation, Itoh and co-workers reported that the C2-lithiated benzothiazole (**Li-1A**) is very unstable even at $-50\text{ }^\circ\text{C}$.^[9] To evaluate whether the deprotonation is taking place under our nickel-catalyzed conditions, the coupling in the presence of *t*-BuOD as a deuterium source was conducted (Scheme 5). When benzothiazole (**1A**: 1.5 equiv) was treated with iodobenzene (**2**: 1.0 equiv), Ni(OAc)₂ (10 mol%), bipy (10 mol%), LiOt-Bu (2.0 equiv), and *t*-BuOD (2.0 equiv), in 1,4-dioxane at $120\text{ }^\circ\text{C}$ for 10 h, coupling product was obtained in 42% and **1A** recovered was deuterated at the C2 position (**1A**/**d-1A** = 58:42). Although this result clearly indicates that the deprotonation occurs under the coupling conditions, a more important implication may be the following. With the instability of C2-lithiated benzothiazole (**Li-1A**) in mind, one of the important factors of the Ni-catalyzed coupling would be the existence of a pre-equilibrium between **1A** and **Li-1A**. This deprotonation-protonation shuttle should help to prevent decomposition of **Li-1A**. Similarly, this plausible effect of LiOt-Bu is operating in the generation of Ni(0) species

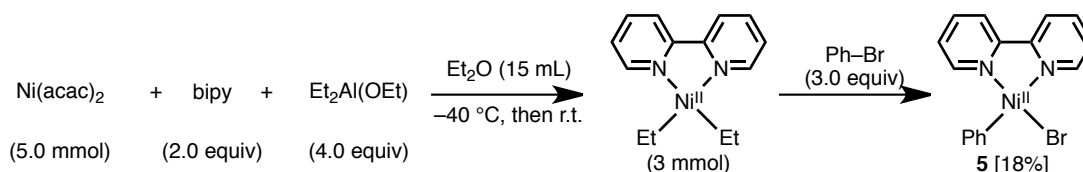
at initiation step (Scheme 4).



Scheme 5. Protonation-deprotonation shuttle

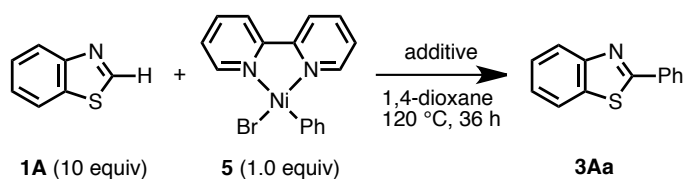
2-6. Nickelation of azoles with Ar–Ni^{II}–X and subsequent reductive elimination

In the mechanistic picture shown in Scheme 3, the nickelation of azoles with Ar–Ni^{II}–X is the step after the oxidative addition of Ar–X to Ni(0) species. To study the nickelation step in detail, Ar–Ni(bipy)–Br complex **5** was prepared by the procedure reported by Yamamoto (Scheme 6).^[10]



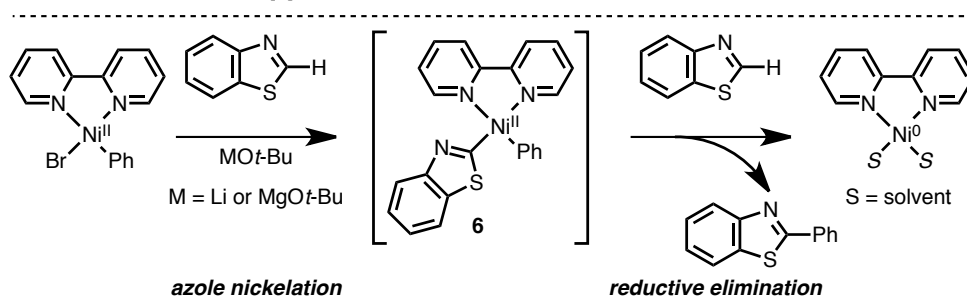
Scheme 6. Preparation of nickel complex **5**

Nickel complex **5** was treated with benzothiazole (**1A**) in 1,4-dioxane at 120 °C (Scheme 7). Without an added base, this reaction condition furnished no coupling product (entry 1). However, it was found that the addition of either LiOt-Bu or $\text{Mg}(\text{Ot-Bu})_2$ to the reaction between **1A** and **5** was essential; **3Aa** was produced in 72% and 84% yield, respectively. This result alludes to the possibility of sequence of 1) oxidative addition, 2) azole nickelation (supported by LiOt-Bu or $\text{Mg}(\text{Ot-Bu})_2$) to produce **6**, and 3) reductive elimination in catalysis which is consistent with the proposed Ni(0)/Ni(II) redox catalytic cycle.



entry	additive	yield (%)
1	none	0
2	<i>t</i> -BuOH (10 equiv)	0
3	Li <i>Ot</i> -Bu (10 equiv)	72
4 ^a	Mg(<i>Ot</i> -Bu) ₂ (10 equiv)	84

[a] Reaction was carried out in DMF.

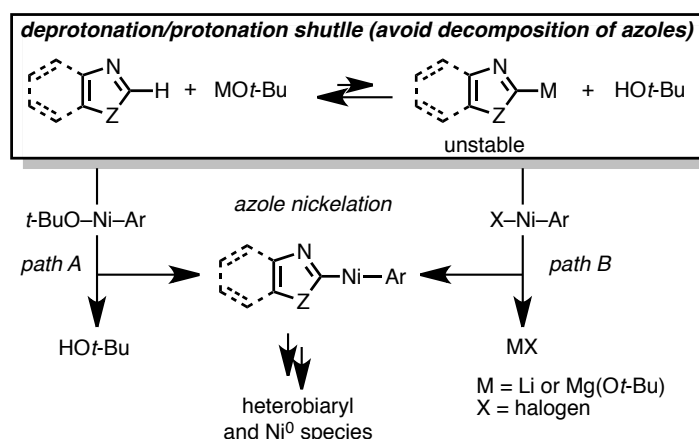


Scheme 7. Reaction of phenylnickel bromide complex and benzothiazole

2-7. Possible Pathways for Azole Nickelation and the Importance of the Protonation-Deprotonation Shuttle

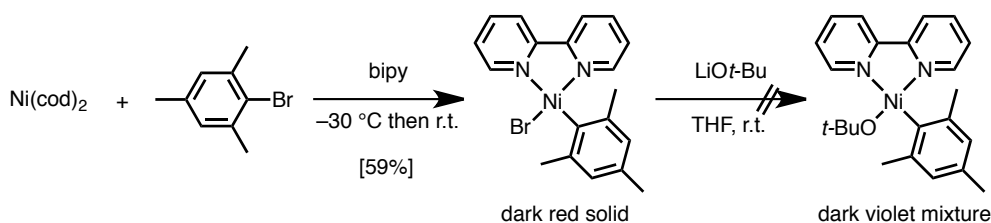
Although the mechanism of nickel-catalyzed arylation of azoles with haloarenes is not yet entirely clear, a number of experiments are in line with the proposed Ni(0)/Ni(II) catalytic cycle shown in Scheme 3. It is worth noting that Li*Ot*-Bu and Mg(*Ot*-Bu)₂ most likely play a critical role in the 1,3-azole nickelation step, which should be involved both in the product-generating catalytic cycle and the generation of catalytically active Ni(0) species from Ni(II) precursor, Ni(OAc)₂.

However, the way of nickelation of 1,3-azole with Ar-Ni(II)-X is particularly unclear. It is assumed that there exist possible mechanisms for this step; via 1) concerted metalation-deprotonation of 1,3-azole with Ar-Ni(II)-*Ot*-Bu species, which could be generated from substitution reaction of Ar-Ni-X with *tert*-butoxide (path A),^[11] and 2) *tert*-butoxide-mediated deprotonation of azoles followed by transmetalation of azolyl lithium (or magnesium) species with Ar-Ni-X (path B), namely, *in situ* Kumada-Tamao-Corriu type coupling (Scheme 8).



Scheme 8. Possible pathways of azole nickelation

In one of the attempts to support path A, preparation of a plausible Ar-Ni(II)-Ot-Bu species was carried out. However, this experiment resulted in only observation of a change in reaction color, and complex mixtures that did not contain the desired Ni(II) complex (Scheme 9).



Scheme 9. Attempts to isolate a plausible Ar-Ni(II)-Ot-Bu species.

Although the attempts to isolate Ar-Ni-Ot-Bu complex resulted in failure, it should be emphasized that even if path B were to occur, the deprotonation-protonation shuttle of 1,3-azoles (which avoids azole substrate decomposition) is essential for achieving the heterobiaryl coupling (path B).^[12] In this regard, the present Ni-catalyzed 1,3-azole arylation is not merely an *in situ* Kumada-Tamao-Corriu type coupling.

2-8. Applications of Ni-catalyzed C–H Arylation to the Synthesis of Biologically Active Compounds

To illustrate the utility of Ni-catalyzed azole arylation in the production of biologically active compounds, febuxostat, tafamidis and texaline were selected as aryl-substituted azole targets (Figure 1).

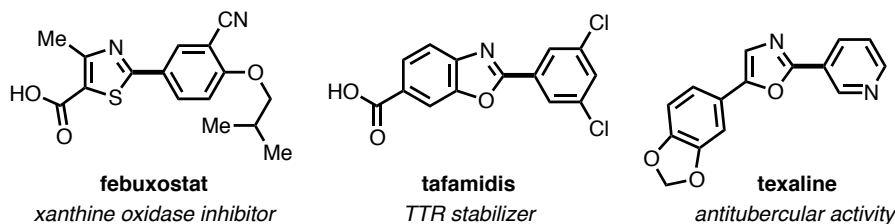
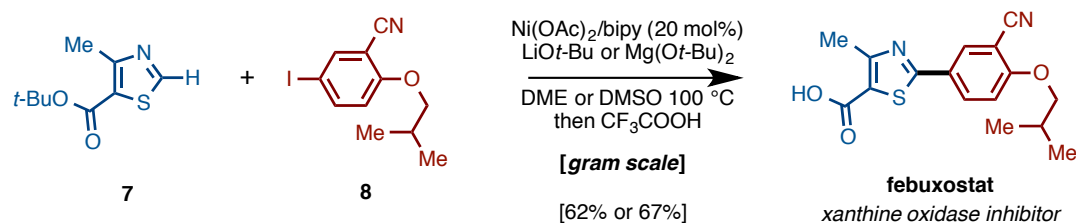


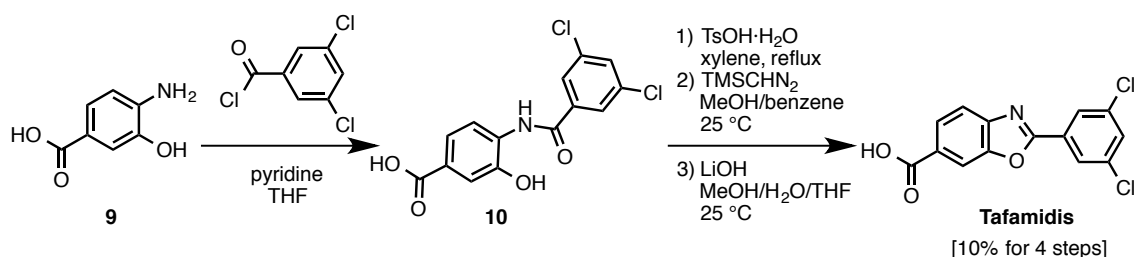
Figure 1. Targets for the illustration of synthetic utility of the Ni-catalyzed heterobiaryl coupling reaction.

Febuxostat is an inhibitor of xanthine oxidase that has been developed by Teijin Phama as a new drug for the treatment of gout and hyperuricemia. It has been 40 years since a drug of this kind has been developed, and febuxostat has gained a lot of popularity; it has already been accepted for commercial use in Europe, USA, Korea, and Japan. Therefore, the development of an efficient synthesis of febuxostat is currently ongoing in process chemistry. The current synthesis requires 6 steps (10% yield), which is a linear synthetic route.^[13a] Under the influence of Ni(OAc)₂/bipy catalyst and Li*O**t*-Bu, thiazole **7** and iodoarene **8** underwent cross-coupling in DME at 100 °C to furnish the corresponding coupling product (Scheme 10). The Mg(*O**t*-Bu)₂/DMSO system was equally effective for the coupling. Subsequent treatment with CF₃CO₂H afforded febuxostat in 62–67% overall yield. Following the present synthetic route, it is required only 3 steps (43–46% overall yield) to accomplish the synthesis of febuxostat. Furthermore, it should be mentioned that both of the coupling precursor **7** and **8** can be quickly diversified in one step from commercially available 4-methyl-5-thiazole carboxylic acid and 2-fluoro-5-iodobenzonitrile, respectively.



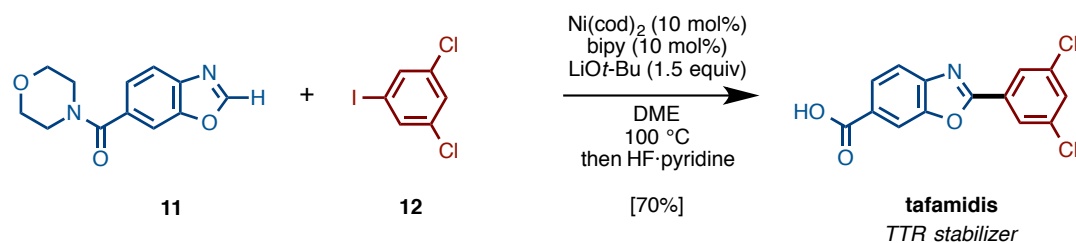
Scheme 10. Rapid synthesis of febuxostat using Ni-catalyzed direct C–H arylation

Tafamidis, which was first synthesized by Kelly and co-workers, is effective for the treatment of TTR amyloid polyneuropathy,^[14] and is currently commercially available in Europe from the beginning of 2012. Kelly's synthetic route is shown in Scheme 11, where the synthesis of tafamidis was achieved in 4 steps and 10% overall yield.



Scheme 11. Synthesis of tafamidis reported by Kelly

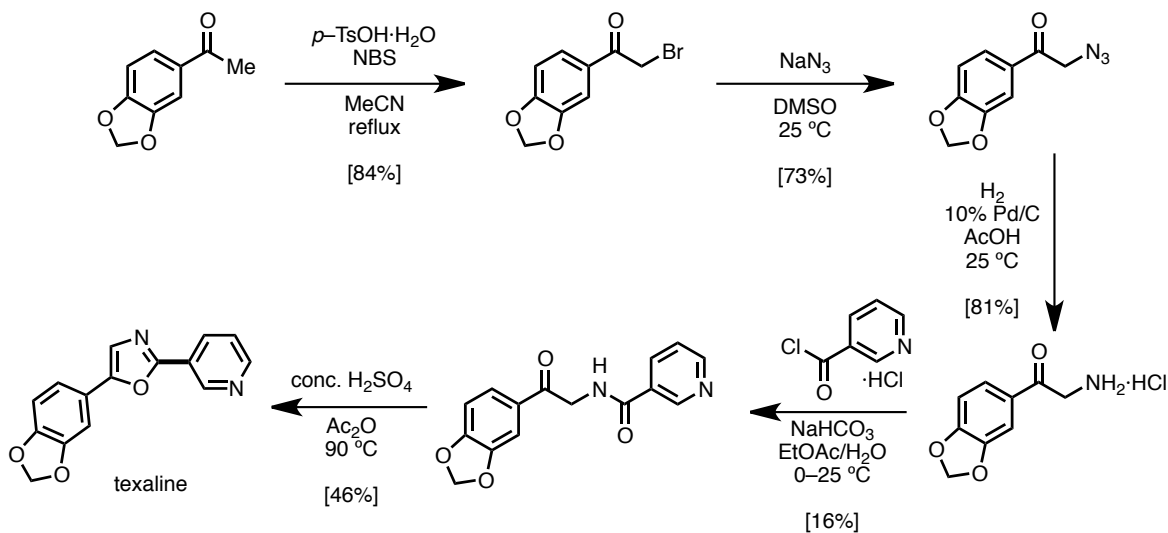
In contrast, the newly designed synthetic approach is more convergent than that of Kelly's group. A morpholinyl amide substituted benzoxazole **11** was coupled with 1,3-dichloro-5-iodobenzene (**12**) to serve the corresponding product. Subsequent hydrolysis of the amide using HF·pyridine provided tafamidis in 70% overall yield (Scheme 12).



Scheme 12. Rapid synthesis of tafamidis using Ni-catalyzed direct C–H arylation

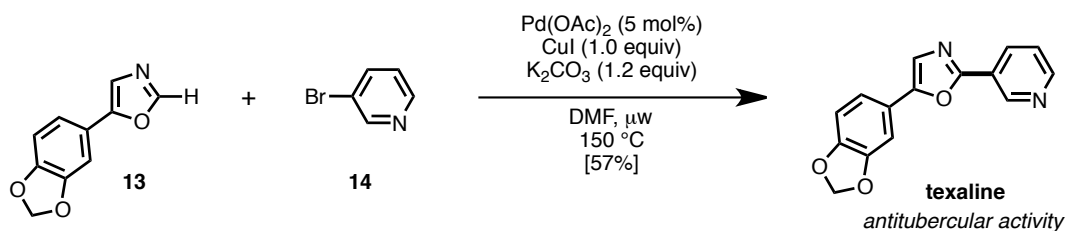
As the third example in this project, the synthesis of a natural product, texaline,

which displays antitubercular activity, was undertaken. The first synthesis of texaline was accomplished by the group of Copp, which required 5 steps (Scheme 13).^[15b]



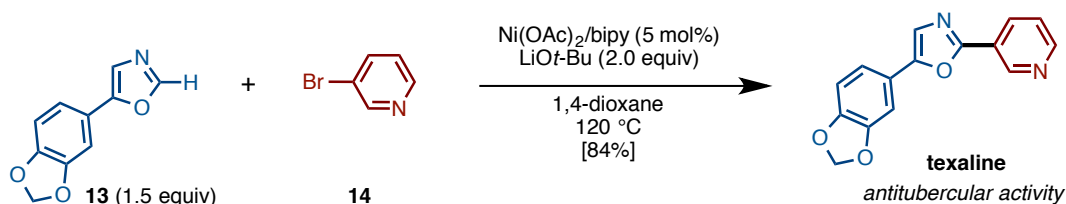
Scheme 13. First synthesis of texaline

Piguel and co-workers had already reported an elegant synthesis of texaline using a Pd-catalyzed direct arylation method under microwave conditions (Scheme 14).^[15c]



Scheme 14. Synthesis of texaline via Pd-catalyzed direct C–H arylation

It was found that texaline could be obtained in a superior 84% yield under the action of the Ni(OAc)₂/bipy/LiOt-Bu catalytic system in 1,4-dioxane at 120 °C (Scheme 15).



Scheme 15. Rapid synthesis of texaline using Ni-catalyzed direct C–H arylation

3. Conclusion

A new protocol for a Ni-catalyzed C–H arylation of azoles with haloarenes, using $\text{Mg}(\text{O}t\text{-Bu})_2$ as a milder and less expensive alternative to $\text{LiO}t\text{-Bu}$, has been developed. Compared to $\text{LiO}t\text{-Bu}$ protocol, the $\text{Mg}(\text{O}t\text{-Bu})_2$ protocol is more effective for electron deficient haloarenes.^[7d] It was succeeded to expand the substrate generality by using these two protocols. A number of mechanistic experiments supported that the C–H arylation takes place with Ni(0)/Ni(II) redox catalysis consisting of 1) oxidative addition of an aryl electrophile to Ni(0) species generated *in situ*, 2) nickelation of an azole with arylnickel(II) species, and 3) reductive elimination of a heterobiaryl product with regeneration of the Ni(0) catalyst. The efficient and rapid syntheses of febuxostat, tafamidis, and texaline speak well for the potential of the present nickel catalysis in a range of synthetic applications.

4. Experimental

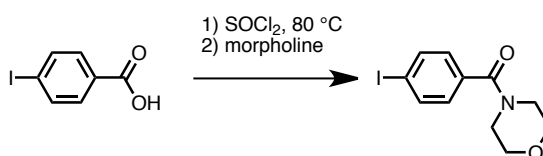
4-1. General

Unless otherwise noted, all materials including dry solvents were obtained from commercial suppliers and used as received. NiPh(bipy)Br (**5**),^[10] *tert*-butyl 4-methylthiazole-5-carboxylate (**6**),^[7a] 5-iodo-2-isobutoxybenzotrile (**8**)^[7a] and 5-benzo[1,3]dioxol-5-yl-oxazole (**13**)^[15c] were synthesized according to procedures reported in the literature. Unless otherwise noted, all reactions were performed with dry solvents under an atmosphere of argon in flame-dried glassware using standard vacuum-line techniques. Almost C–H bond arylation reactions were performed in 20-mL glass vessel tubes equipped with J. Young[®] O-ring tap and heated in an 8-well reaction block (heater + magnetic stirrer). All work-up and purification procedures were carried out with reagent-grade solvents in air.

Analytical thin-layer chromatography (TLC) was performed using E. Merck silica gel 60 F₂₅₄ precoated plates (0.25 mm). The developed chromatogram was analyzed by UV lamp (254 nm). Flash column chromatography was performed with E. Merck silica gel 60 (230–400 mesh). Preparative thin-layer chromatography (PTLC) was performed using Wakogel B5-F silica coated plates (0.75 mm) prepared in our laboratory. Gas chromatography (GC) analysis was conducted on a Shimadzu GC-2010 instrument equipped with a HP-5 column (30 m × 0.25 mm, Hewlett-Packard). GCMS analysis was conducted on a Shimadzu GCMS-QP2010 instrument equipped with a HP-5 column (30 m × 0.25 mm, Hewlett-Packard). High-resolution mass spectra (HRMS) was obtained from a JEOL JMS-700 (Electron Ionization High Resolution Mass Spectroscopy, EIHRMS) or a JMS-T100TD instrument (DART). Nuclear magnetic resonance (NMR) spectra was recorded on a JEOL JNM-ECA-600 (¹H 600 MHz, ¹³C 150 MHz) spectrometer and a JEOL A-400 (¹H 400 MHz, ¹³C 100 MHz) spectrometer. Chemical shifts for ¹H NMR are expressed in parts per million (ppm) relative to tetramethylsilane (δ 0.00 ppm) or residual peak of DMSO (δ 2.50 ppm). Chemical shifts for ¹³C NMR are expressed in ppm relative to CDCl₃ (δ 77.0 ppm) or DMSO (δ 39.5 ppm). Data are reported as follows: chemical shift, multiplicity (s = singlet, d = doublet, dd = doublet of doublets, t = triplet, q = quartet, m = multiplet, br = broad signal), coupling constant (Hz), and integration.

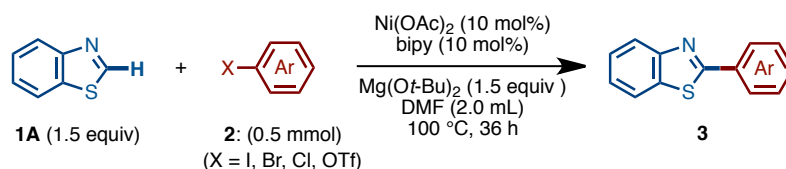
4-2. Preparation of Haloarene

4-(4-Iodobenzoyl)morpholine



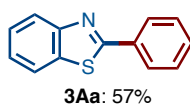
A mixture of 4-iodobenzoic acid (1.24 g, 5 mmol) and SOCl₂ (4.3 mL) was heated at 80 °C for 7 h. After cooling to room temperature, thionyl chloride was removed under reduced pressure to yield the corresponding acid chloride as a solid. The acid chloride was added morpholine (2.2 mL) at 0 °C, then stirred at room temperature for 5 h. After removing solvents under reduced pressure, the mixture was treated with saturated aqueous sodium bicarbonate (20 mL) and EtOAc (20 mL). The layers were separated, and the aqueous layer was extracted with ethyl acetate (2 × 20 mL). The combined organic layer was evacuated solvent under reduced pressure and the crude product was filtrated and washed with H₂O, Et₂O and hexane. A white precipitate appeared and was collected by filtration and dried under reduced pressure to afford haloarene **2g** (1.01 g, 64%) as a white solid. R_f = 0.27 (EtOAc/hexane = 2:1). ¹H NMR (600 MHz, CDCl₃) δ 7.77 (d, *J* = 6.2 Hz, 2H), 7.15 (d, *J* = 6.2 Hz, 2H), 3.99–3.19 (br, 8H). ¹³C NMR (150 MHz, CDCl₃) δ 169.47, 137.74, 134.65, 128.83, 96.12, 66.81. HRMS (DART) *m/z* calcd for C₁₁H₁₃INO₂ [MH]⁺: 317.9991, found 317.9992.

4-3. Typical Procedure for Ni-Catalyzed Arylation of Heteroarenes with Aryl Iodides/ Bromides using Mg(*Ot*-Bu)₂

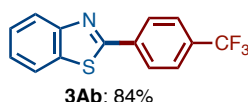


A 20-mL glass vessel equipped with J. Young[®] O-ring tap containing a magnetic stirring bar and Ni(OAc)₂·4H₂O (10.6 mg, 0.05 mmol) was dried with a heatgun under vacuum and filled with argon after cooling to room temperature. To this vessel were added 2,2'-bipyridyl (7.8 mg, 0.05 mmol), Mg(*Ot*-Bu)₂ (127.9 mg, 0.75 mmol), azole

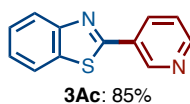
(**1**: 0.75 mmol, 1.5 equiv), and haloarene (**2**, 0.50 mmol), followed by dry DMF (2.0 mL) under a stream of argon. The vessel was sealed with an O-ring tap and then heated at 100 °C for 36 h in an 8-well reaction block with stirring. After cooling the reaction mixture to room temperature, the mixture was concentrated under vacuum. The crude product was dissolved in EtOAc, filtrated through Celite[®]. The filtrate was concentrated and the residue was subjected to preparative thin-layer chromatography (hexane/EtOAc) to afford 2-arylatediazole **3** as a coupling product.



3Aa^[7a] Purification by preparative thin-layer chromatography (hexane : EtOAc = 9 : 1) afford 2-phenylbenzothiazole **3Aa** (57% yield) as a light tan solid. $R_f = 0.45$ (hexane : EtOAc = 9 : 1). ¹H NMR (600 MHz, CDCl₃) δ 8.12–8.07 (m, 3H), 7.88 (d, $J = 8.2$ Hz, 1H), 7.53–7.42 (m, 4H), 7.38 (d, $J = 8.2, 1.1$ Hz, 1H). ¹³C NMR (150 MHz, CDCl₃) δ 168.04, 154.11, 135.03, 133.59, 130.95, 129.00, 127.53, 126.29, 125.16, 123.20, 121.59. HRMS (EI) m/z calcd for C₁₃H₉NS: 211.0456, found 211.0445.

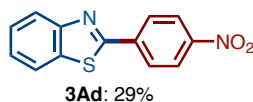


3Ab^[7a] Purification by preparative thin-layer chromatography (hexane : EtOAc = 9 : 1) afford 2-(4-(trifluoromethyl)phenyl)benzothiazole **3Ab** (84% yield) as a light tan solid. $R_f = 0.38$ (hexane : EtOAc = 9 : 1); ¹H NMR (600 MHz, CDCl₃) δ 8.22 (d, $J = 7.6$ Hz, 2H), 8.11 (d, $J = 8.2$ Hz, 1H), 7.94 (d, $J = 7.6$ Hz, 1H), 7.76 (d, $J = 8.3$ Hz, 2H), 7.54 (t, $J = 8.2$ Hz, 1H), 7.44 (t, $J = 8.3$ Hz, 1H). HRMS (EI) m/z calcd for C₁₄H₈NF₃S: 279.0330, found 279.0343.

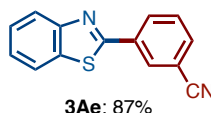


3Ac^[7a] Purification by preparative thin-layer chromatography (hexane : EtOAc = 4 : 1) afford 3-(2-benzothiazolyl)pyridine (**3Ac**: 85% yield) as a white solid. $R_f = 0.47$ (hexane : EtOAc = 4 : 1); ¹H NMR (600 MHz, CDCl₃) δ 9.30 (s, 1H), 8.73 (d, $J = 5.0$ Hz, 1H), 8.39 (d, $J = 8.3$ Hz, 1H), 8.11 (d, $J = 8.3$ Hz, 1H), 7.94 (d, $J = 7.5$ Hz, 1H), 7.53 (t, $J = 8.3$ Hz, 1H), 7.49–7.41 (m, 2H). HRMS (EI) m/z calcd for C₁₂H₈N₂S:

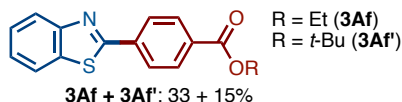
212.0408, found 212.0411.



3Ad Purification by preparative thin-layer chromatography (CHCl_3) afford 2-(4-nitrophenyl) benzothiazole (**3Ad**: 29% yield) as a white solid. $R_f = 0.44$ (CHCl_3); ^1H NMR (600 MHz, CDCl_3) δ 8.35 (d, $J = 8.2$ Hz, 2H), 8.27 (d, $J = 8.2$ Hz, 2H), 8.13 (d, $J = 8.2$ Hz, 1H), 7.96 (d, $J = 8.2$ Hz, 1H), 7.56 (dd, $J = 8.2, 6.9$ Hz, 1H), 7.47 (dd, $J = 8.2, 6.9$ Hz, 1H). ^{13}C NMR (150 MHz, CDCl_3) δ 164.79, 154.05, 148.95, 139.12, 135.44, 128.19, 126.89, 126.20, 124.28, 123.90, 121.82. HRMS (DART) m/z calcd for $\text{C}_{13}\text{H}_9\text{N}_2\text{O}_2\text{S}$ $[\text{MH}]^+$: 257.0385, found 257.0385.



3Ae Purification by preparative thin-layer chromatography (hexane : EtOAc = 5 : 1) afford 2-(3-cyanophenyl)benzothiazole (**3Ae**: 87% yield) as a white solid. $R_f = 0.27$ (hexane : EtOAc = 5 : 1); ^1H NMR (600 MHz, CDCl_3) δ 8.40 (d, $J = 1.4$ Hz, 1H), 8.29 (dd, $J = 7.6, 1.4$ Hz, 1H), 8.10 (d, $J = 8.3$ Hz, 1H), 7.93 (d, $J = 8.3$ Hz, 1H), 7.75 (dd, $J = 7.6, 1.4$ Hz, 1H), 7.62 (dd, $J = 7.6, 7.6$ Hz, 1H), 7.53 (dd, $J = 7.6, 7.6$ Hz, 1H), 7.44 (dd, $J = 7.6, 7.6$ Hz, 1H). ^{13}C NMR (150 MHz, CDCl_3) δ 165.00, 153.89, 135.04, 134.78, 133.81, 131.42, 130.84, 129.89, 126.76, 125.92, 123.64, 121.80, 118.02, 113.46. HRMS (DART) m/z calcd for $\text{C}_{14}\text{H}_9\text{N}_2\text{S}$ $[\text{MH}]^+$: 237.0487, found 237.0487.

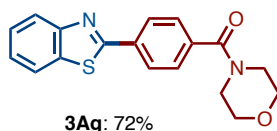


3Af^[16] Purification by preparative thin-layer chromatography (hexane : EtOAc = 10 : 1) afford ethyl 4-(benzothiazolyl)benzoate (**3Af**: 33% yield) and *t*-butyl 4-(2-benzothiazolyl)benzoate (**3Af'**: 15% yield) as white solids.

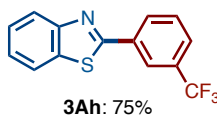
3Af: $R_f = 0.29$ (hexane : EtOAc = 10 : 1); ^1H NMR (600 MHz, CDCl_3) δ 8.17 (s, 4H), 8.11 (d, $J = 8.2$ Hz, 1H), 7.94 (d, $J = 8.2$ Hz, 1H), 7.53 (dd, $J = 7.6, 7.6$ Hz, 1H), 7.43

(dd, $J = 7.6, 6.9$ Hz, 1H), 4.42 (q, $J = 6.9$ Hz, 2H), 1.43 (t, $J = 6.9$ Hz, 3H). ^{13}C NMR (150 MHz, CDCl_3) δ 166.64, 165.92, 154.10, 137.33, 135.25, 132.37, 130.20, 127.36, 126.58, 125.67, 123.56, 121.71, 61.31, 14.31. HRMS (DART) m/z calcd for $\text{C}_{16}\text{H}_{14}\text{NO}_2\text{S}$ $[\text{MH}]^+$: 284.0745, found 284.0745.

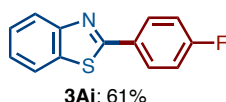
3Aaf: $R_f = 0.34$ (hexane : EtOAc = 10 : 1); ^1H NMR (600 MHz, CDCl_3) δ 8.21–8.05 (m, 5H), 7.93 (d, $J = 8.3$ Hz, 1H), 7.52 (dd, $J = 8.3, 7.6$ Hz, 1H), 7.42 (dd, $J = 8.3, 7.6$ Hz, 1H), 1.63 (s, 9H). ^{13}C NMR (150 MHz, CDCl_3) δ 166.80, 165.03, 154.11, 136.96, 135.23, 133.95, 130.06, 127.25, 126.54, 125.61, 123.52, 121.70, 81.55, 28.17. HRMS (DART) m/z calcd for $\text{C}_{18}\text{H}_{18}\text{NO}_2\text{S}$ $[\text{MH}]^+$: 312.1058, found 312.1058.



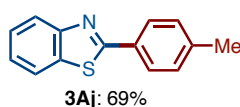
3Ag Purification by preparative thin-layer chromatography (hexane : EtOAc = 2 : 1) afford [4-(2-benzothiazolyl)phenyl]-4-morpholinylmethanone (**3Ag**: 72% yield) as a yellow solid. $R_f = 0.15$ (hexane : EtOAc = 2 : 1); ^1H NMR (600 MHz, CDCl_3) δ 8.15 (d, $J = 8.3$ Hz, 2H), 8.09 (d, $J = 8.3$ Hz, 1H), 7.92 (d, $J = 7.6$ Hz, 1H), 7.55 (d, $J = 8.3$ Hz, 2H), 7.52 (ddd, $J = 8.3, 7.6, 1.4$ Hz, 1H), 7.42 (ddd, $J = 7.6, 7.6, 1.4$ Hz, 1H), 3.95–3.39 (m, 8H). ^{13}C NMR (150 MHz, CDCl_3) δ 169.46, 166.64, 154.04, 137.45, 135.09, 134.92, 127.84, 127.67, 126.51, 125.53, 123.42, 121.67, 66.82. HRMS (DART) m/z calcd for $\text{C}_{18}\text{H}_{17}\text{N}_2\text{O}_2\text{S}$ $[\text{MH}]^+$: 325.1011, found 325.1011.



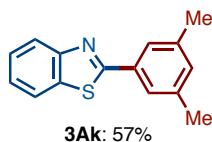
3Ah^[7a] Purification by preparative thin-layer chromatography (hexane : EtOAc = 9 : 1) afford 2-(3-trifluoromethylphenyl)benzothiazole (**3Ah**: 75% yield) as a white solid. $R_f = 0.34$ (hexane : EtOAc = 9 : 1); ^1H NMR (600 MHz, CDCl_3) δ 8.38 (s, 1H), 8.24 (d, $J = 8.3$ Hz, 1H), 8.11 (d, $J = 8.3$ Hz, 1H), 7.93 (d, $J = 7.6$ Hz, 1H), 7.75 (d, $J = 8.3$ Hz, 1H), 7.62 (t, $J = 8.3$ Hz, 1H), 7.52 (t, $J = 7.6$ Hz, 1H), 7.43 (d, $J = 7.6$ Hz, 1H). HRMS (EI) m/z calcd for $\text{C}_{14}\text{H}_8\text{NF}_3\text{S}$: 279.0330, found 279.0336.



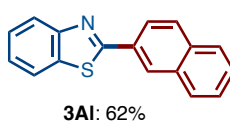
3Ai^[7a] Purification by preparative thin-layer chromatography (hexane : EtOAc = 9 : 1) afford 2-(4-fluorophenyl)benzothiazole (**3Ai**: 61% yield) as a tan solid. $R_f = 0.42$ (hexane : EtOAc = 9 : 1); $^1\text{H NMR}$ (400 MHz, CDCl_3) δ 8.11–8.05 (m, 3H), 7.90 (d, $J = 8.0$ Hz, 1H), 7.50 (t, $J = 7.2$ Hz, 1H), 7.39 (dd, $J = 8.0, 0.8$ Hz, 1H), 7.21–7.17 (m, 2H). HRMS (EI) m/z calcd for $\text{C}_{13}\text{H}_8\text{NF}$: 229.0361, found 229.0366.



3Aj^[7a] Purification by preparative thin-layer chromatography (hexane : EtOAc = 9 : 1) afford 2-(4-methylphenyl)benzothiazole (**3Aj**: 69% yield) as a white solid. $R_f = 0.45$ (hexane : EtOAc = 9 : 1); $^1\text{H NMR}$ (600 MHz, CDCl_3) δ 8.06 (d, $J = 8.3$ Hz, 1H), 7.99 (d, $J = 8.3$ Hz, 2H), 7.89 (d, $J = 7.6$ Hz, 1H), 7.48 (t, $J = 7.6$ Hz, 1H), 7.37 (t, $J = 7.6$ Hz, 1H), 7.30 (d, $J = 7.6$ Hz, 2H), 2.43 (s, 3H). HRMS (EI) m/z calcd for $\text{C}_{14}\text{H}_{11}\text{NS}$: 225.0612, found 225.0606.

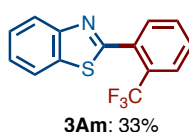


3Ak^[16] Purification by preparative thin-layer chromatography (hexane : EtOAc = 10 : 1) afford 2-(3,5-dimethylphenyl)benzothiazole (**3Ak**: 57% yield) as a white solid. $R_f = 0.42$ (hexane : EtOAc = 10 : 1); $^1\text{H NMR}$ (600 MHz, CDCl_3) δ 8.06 (d, $J = 8.3$ Hz, 1H), 7.88 (d, $J = 7.6$ Hz, 1H), 7.70 (s, 2H), 7.47 (d, $J = 8.3$ Hz, 1H), 7.36 (dd, $J = 8.3, 7.6$ Hz, 1H), 7.11 (s, 1H), 2.40 (s, 6H). $^{13}\text{C NMR}$ (150 MHz, CDCl_3) δ 168.53, 154.05, 138.68, 134.95, 133.38, 132.73, 126.20, 125.30, 125.00, 123.05, 121.54, 21.19. HRMS (DART) m/z calcd for $\text{C}_{15}\text{H}_{14}\text{NS}$ $[\text{MH}]^+$: 240.0847, found 240.0847.

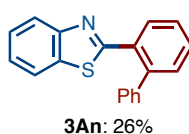


3Al^[17] Purification by preparative thin-layer chromatography (hexane : EtOAc = 10 : 1)

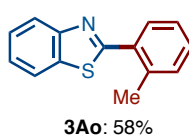
afford 2-(2-naphthyl)benzothiazole (**3A1**: 62% yield) as a white solid. $R_f = 0.37$ (hexane : EtOAc = 10 : 1); $^1\text{H NMR}$ (600 MHz, CDCl_3) δ 8.56 (s, 1H), 8.20 (dd, $J = 8.3$, 1.2 Hz, 1H), 8.11 (d, $J = 8.4$ Hz, 1H), 7.98–7.89 (m, 3H), 7.89–7.83 (m, 1H), 7.58–7.52 (m, 2H), 7.51 (td, $J = 7.6$, 1.3 Hz, 1H), 7.39 (td, $J = 7.6$, 1.3 Hz, 1H). $^{13}\text{C NMR}$ (150 MHz, CDCl_3) δ 168.08, 154.21, 135.10, 134.57, 133.15, 130.95, 128.80, 127.85, 127.56, 127.44, 126.87, 126.37, 125.23, 124.41, 123.21, 121.63. HRMS (DART) m/z calcd for $\text{C}_{17}\text{H}_{12}\text{NS}$ $[\text{MH}]^+$: 262.0690, found 262.0690.



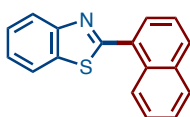
3Am^[18] Purification by preparative thin-layer chromatography (hexane : EtOAc = 5 : 1) afford 2-(3-cyanophenyl)benzothiazole (**3Ak**: 33% yield) as a yellow oil. $R_f = 0.34$ (hexane : EtOAc = 5 : 1); $^1\text{H NMR}$ (600 MHz, CDCl_3) δ 8.14 (d, $J = 8.3$ Hz, 1H), 7.95 (d, $J = 8.3$ Hz, 1H), 7.85 (d, $J = 8.3$ Hz, 1H), 7.72 (d, $J = 7.2$ Hz, 1H), 7.66 (dd, $J = 8.3$, 8.3 Hz, 1H), 7.63 (dd, $J = 8.3$, 8.3 Hz, 1H), 7.55 (dd, $J = 7.8$, 7.8 Hz, 1H), 7.46 (dd, $J = 8.3$, 7.2 Hz, 1H). $^{13}\text{C NMR}$ (150 MHz, CDCl_3) δ 164.60, 153.28, 136.17, 132.77, 132.21, 131.63, 130.06, 129.10 (q, $^2J_{\text{CF}} = 120.6$ Hz), 126.79 (q, $^3J_{\text{CF}} = 23.0$ Hz), 126.39, 125.57, 123.79, 123.55 (q, $^1J_{\text{CF}} = 1091.5$ Hz), 121.36. HRMS (DART) m/z calcd for $\text{C}_{14}\text{H}_9\text{NF}_3\text{S}$ $[\text{MH}]^+$: 280.0408, found 280.0408.



3An^[7a] Purification by preparative thin-layer chromatography (hexane : EtOAc = 9 : 1) afford 2-(2-biphenyl)benzothiazole (**3An**: 26% yield) as a colorless oil. $R_f = 0.48$ (hexane : EtOAc = 9 : 1); $^1\text{H NMR}$ (600 MHz, CDCl_3) δ 8.07 (d, $J = 7.6$ Hz, 1H), 8.05 (d, $J = 8.3$ Hz, 1H), 7.71 (d, $J = 7.6$ Hz, 1H), 7.55–7.49 (m, 2H), 7.46–7.43 (m, 2H), 7.36–7.30 (m, 6H). HRMS (EI) m/z calcd for $\text{C}_{19}\text{H}_{13}\text{NS}$: 287.0769, found 287.0761.

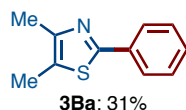


3Ao^[7a] Purification by preparative thin-layer chromatography (hexane : EtOAc = 9 : 1) afford 2-(2-methylphenyl)benzothiazole (**3Ao**: 58% yield) as a white solid. $R_f = 0.48$ (hexane : EtOAc = 9 : 1); $^1\text{H NMR}$ (600 MHz, CDCl_3) δ 8.12 (d, $J = 8.3$ Hz, 1H), 7.94 (d, $J = 7.6$ Hz, 1H), 7.77 (d, $J = 7.6$ Hz, 1H), 7.53 (t, $J = 8.3$ Hz, 1H), 7.42 (t, $J = 7.6$ Hz, 1H), 7.38 (d, $J = 8.3$ Hz, 1H), 7.35 (t, $J = 6.8$ Hz, 1H), 7.32 (t, $J = 6.8$ Hz, 1H), 2.68 (s, 3H). HRMS (EI) m/z calcd for $\text{C}_{14}\text{H}_{11}\text{NS}$: 225.0612, found 225.0605.



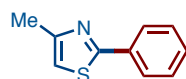
3Ap: 63%

3Ap^[7a] Purification by preparative thin-layer chromatography (hexane : EtOAc = 9 : 1) afford 2-(1-naphthyl)benzothiazole (**3Ap**: 63% yield) as a white solid. $R_f = 0.45$ (hexane : EtOAc = 9 : 1); $^1\text{H NMR}$ (600 MHz, CDCl_3) δ 8.96 (d, $J = 8.3$ Hz, 1H), 8.22 (d, $J = 7.5$ Hz, 1H), 8.00 (d, $J = 8.3$ Hz, 1H), 7.97 (d, $J = 7.5$ Hz, 1H), 7.93 (d, $J = 7.0$ Hz, 2H), 7.63 (t, $J = 7.0$ Hz, 1H), 7.60–7.55 (m, 3H), 7.46 (t, $J = 8.3$ Hz, 1H). HRMS (EI) m/z calcd for $\text{C}_{17}\text{H}_{11}\text{NS}$: 261.0612, found 261.0604.



3Ba: 31%

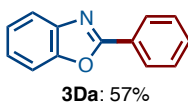
3Ba^[4a] Purification by preparative thin-layer chromatography (hexane : EtOAc = 10 : 1) afford 4,5-dimethyl-2-phenylthiazole (**3Ba**: 31% yield) as a colorless oil. $R_f = 0.40$ (hexane : EtOAc = 10 : 1); $^1\text{H NMR}$ (600 MHz, CDCl_3) δ 7.86 (dd, $J = 8.3, 1.4$ Hz, 2H), 7.40–7.35 (m, 3H), 2.38 (s, 6H). $^{13}\text{C NMR}$ (150 MHz, CDCl_3) δ 163.32, 149.26, 133.93, 129.31, 128.77, 126.49, 126.06, 14.81, 11.45. HRMS (DART) m/z calcd for $\text{C}_{11}\text{H}_{12}\text{NS}$ $[\text{MH}]^+$: 190.0690, found 190.0690.



3Ca: 68%

3Ca^[19] Purification by preparative thin-layer chromatography (hexane : EtOAc = 10 : 1) afford 4-methyl-2-phenylthiazole (**3Ca**: 68% yield) as a colorless oil. $R_f = 0.38$ (hexane : EtOAc = 10 : 1); $^1\text{H NMR}$ (600 MHz, CDCl_3) δ 7.93 (d, $J = 6.2, 1.4$ Hz, 2H),

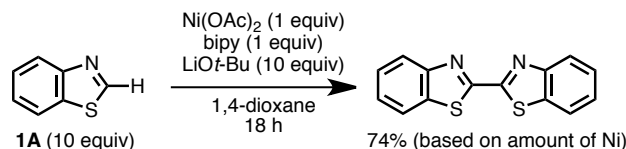
7.43–7.25 (m, 3H), 6.87 (s, 1H) 2.51 (s, 3H). ^{13}C NMR (150 MHz, CDCl_3) δ 167.55, 153.80, 133.75, 129.74, 128.83, 126.42, 113.39, 17.25. HRMS (DART) m/z calcd for $\text{C}_{10}\text{H}_{10}\text{NS}$ $[\text{MH}]^+$: 176.0533, found 176.0534.



3Da^[7a] Purification by preparative thin-layer chromatography (hexane : EtOAc = 9 : 1) afford 2-(phenyl)benzoxazole (**3Da**: 57% yield) as a white solid. R_f = 0.45 (hexane : EtOAc = 9 : 1); ^1H NMR (600 MHz, CDCl_3) δ 8.28–8.25 (m, 2H), 7.79–7.75 (m, 1H), 7.61–7.58 (m, 1H), 7.57–7.53 (m, 3H), 7.38–7.34 (m, 2H). HRMS (EI) m/z calcd for $\text{C}_{13}\text{H}_9\text{NO}$: 195.0684, found 195.0691.

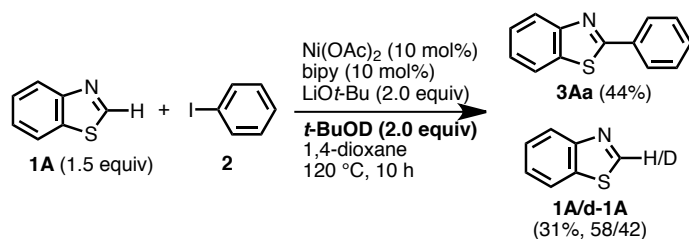
4-4. Procedure for Mechanistic Studies

4-4-1. Dimerization of Benzothiazole by the Action of $\text{Ni}(\text{OAc})_2/\text{bipy}$ and LiOt-Bu .



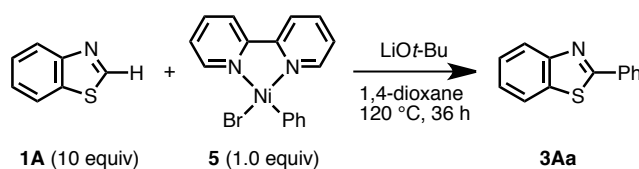
A 20-mL glass vessel equipped with J. Young[®] O-ring tap containing a magnetic stirring bar and $\text{Ni}(\text{OAc})_2 \cdot 4\text{H}_2\text{O}$ (10.6 mg, 0.05 mmol) was dried with a heatgun under vacuum and filled with argon after cooling to room temperature. To this vessel were added 2,2'-bipyridyl (7.8 mg, 0.05 mmol), LiOt-Bu (60.0 mg, 0.75 mmol) and benzothiazole (**1A**: 101.3 mg, 0.75 mmol), followed by dry 1,4-dioxane (2.0 mL) under a stream of argon. The vessel was sealed with an O-ring tap and then heated at 120 °C for 18 h in an 8-well reaction block with stirring. After cooling the reaction mixture to room temperature, the mixture was passed through a short silica gel pad (CHCl_3). The filtrate was concentrated and the residue was subjected to preparative thin-layer chromatography (CHCl_3) to afford **4** (9.8 mg, 74%) as a light tan solid. R_f = 0.35 (CHCl_3). ^1H NMR (600 MHz, CDCl_3) δ 8.17 (d, J = 8.2 Hz, 2H), 7.99 (d, J = 8.2 Hz, 2H), 7.56 (dd, J = 8.3, 6.8 Hz, 2H), 7.50 (dd, J = 8.3, 6.8 Hz, 2H). ^{13}C NMR (150 MHz, CDCl_3) δ 161.54, 153.56, 135.80, 126.85, 126.65, 124.09, 122.05. HRMS (DART) m/z calcd for $\text{C}_{14}\text{H}_9\text{N}_2\text{S}_2$ $[\text{MH}]^+$: 269.0207, found 269.0207.

4-4-2. Protonation/Deprotonation Shuffle



A 20-mL glass vessel equipped with J. Young[®] O-ring tap containing a magnetic stirring bar and $\text{Ni}(\text{OAc})_2 \cdot 4\text{H}_2\text{O}$ (10.6 mg, 0.05 mmol) was dried with a heatgun under vacuum and filled with argon after cooling to room temperature. To this vessel were added 2,2'-bipyridyl (7.8 mg, 0.05 mmol), LiOt-Bu (80.0 mg, 1.0 mmol), benzothiazole (**1A**: 101.3 mg, 0.75 mmol), $t\text{-BuOD}$ (74.1 mg, 1.0 mmol) and bromobenzene (77.9 mg, 0.50 mmol), followed by dry 1,4-dioxane (2.0 mL) under a stream of argon. The vessel was sealed with an O-ring tap and then heated at 120 °C for 10 h in an 8-well reaction block with stirring. After cooling the reaction mixture to room temperature, the mixture was passed through a short silica gel pad (EtOAc). The filtrate was concentrated and the residue was subjected to preparative thin-layer chromatography (hexane/EtOAc) to afford 2-phenylbenzothiazole (**3Aa**: 44%) as a light tan solid and benzothiazole and 2-deuteriobenzothiazole (**1A** and **d-1A**: 31%) as a colorless liquid. The rate of benzothiazole and 2-deuteriobenzothiazole were determined by ¹H NMR spectroscopy (**1A** : **d-1A** = 58 : 42).

4-4-3. Reaction of Phenylnickel Bromide Complex and Benzothiazole

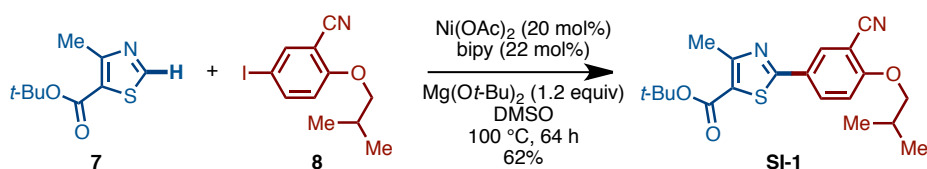


A 20-mL glass vessel equipped with J. Young[®] O-ring tap containing a magnetic stirring bar was dried with a heatgun under vacuum and filled with argon after cooling to room temperature. To this vessel were added $\text{NiPh}(\text{bipy})\text{Br}$ (**5**: 37.2 mg, 0.10 mmol), LiOt-Bu (80.1 mg, 1.0 mmol) and benzothiazole (**1A**: 135.2 mg, 1.0 mmol), followed by dry 1,4-dioxane (2.7 mL) under a stream of argon. The vessel was sealed with an

O-ring tap and then heated at 120°C for 36 h in an 8-well reaction block with stirring. After cooling the reaction mixture to room temperature, the mixture was passed through a short silica gel pad (EtOAc). The filtrate was concentrated and the residue was subjected to preparative thin-layer chromatography (hexane/EtOAc) to afford 2-phenylbenzothiazole (**3Aa**: 15.3 mg, 72%) as a light tan solid.

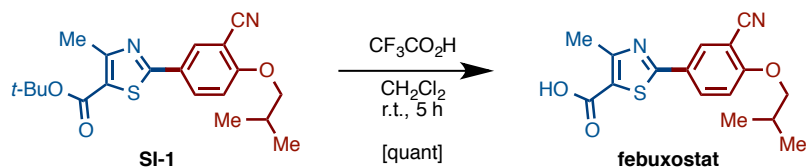
4-5-1. Synthesis of Febuxostat

tert-Butyl 2-(3-cyano-4-isobutoxyphenyl)-4-methylthiazole-5-carboxylate (**SI-1**)



To a 50-mL screw-top test tube containing a magnetic stirring bar was added Ni(OAc)₂ (176.8 mg, 1.0 mmol), 2,2'-bipyridyl (171.8 mg, 1.1 mmol), Mg(O*t*-Bu)₂ (1.02 g, 6.0 mmol), **7** (1.49 g, 7.5 mmol), **8** (1.27 g, 5.0 mmol) and distilled DMSO (5 mL). The vessel was sealed with an O-ring tap and then heated at 100 °C in an 8-well reaction block with stirring for 64 h. After cooling the reaction mixture to room temperature, toluene (30 mL) was added. The mixture was thermal filtrated and partitioned between water (100 mL×2) and toluene (150 mL). The organic layer washed with brine (50 mL), dried over MgSO₄, filtrated through a short silica gel pad (EtOAc). The filtrate was concentrated and the residue was subjected to purify by flash column chromatography (EtOAc/hexane = 1:19). The mixture was stirred for 30 min in hexane (30 mL), filtrated through a plug of cotton, and dried to afford **SI-1** (1.15 g, 62 %) as a white solid. R_f = 0.45 (EtOAc/hexane = 1:19). ¹H NMR (400 MHz, CDCl₃) δ 8.16 (d, *J* = 2.4 Hz, 1H), 8.08 (dd, *J* = 8.8, 2.4 Hz, 1H), 7.00 (d, *J* = 8.8 Hz, 1H), 3.89 (d, *J* = 6.8 Hz, 2H), 2.73 (s, 3H), 2.24–162. (m, 1H), 1.59 (s, 9H), 1.19 (d, *J* = 7.2 Hz, 6H). HRMS (EI) *m/z* calcd for C₂₀H₂₄N₂O₃S: 372.1508, found 372.1511.

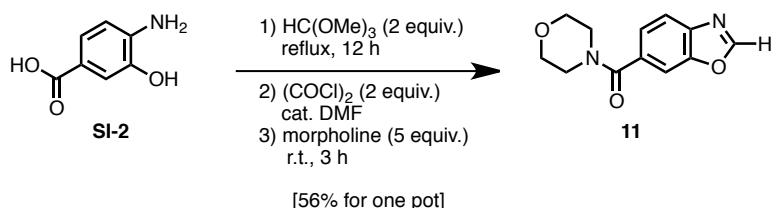
Febuxostat (TMX-67, Feburic®)



To a solution of **SI-1** (34.6 mg, 0.093 mmol) in CH_2Cl_2 (0.5 mL) was added trifluoroacetic acid (0.5 mL), and the reaction mixture was stirred at room temperature for 5 h. It was azeotroped with toluene (1 mL) three times under reduced pressure to afford febuxostat (29.4 mg, 0.093 mmol, quant.) as a white solid. ^1H NMR (400 MHz, CDCl_3) δ 8.17 (d, $J = 2.4$ Hz, 1H), 8.08 (dd, $J = 8.8, 2.4$ Hz, 1H), 7.01 (d, $J = 8.8$ Hz, 1H), 3.90 (d, $J = 6.8$ Hz, 2H), 2.79 (s, 3H), 2.25–2.15 (m, 1H), 1.09 (d, $J = 6.8$ Hz, 6H). HRMS (EI) m/z calcd for $\text{C}_{16}\text{H}_{16}\text{N}_2\text{O}_3\text{S}$: 316.0882, found 316.0879.

4-5-2. Synthesis of Tafamidis

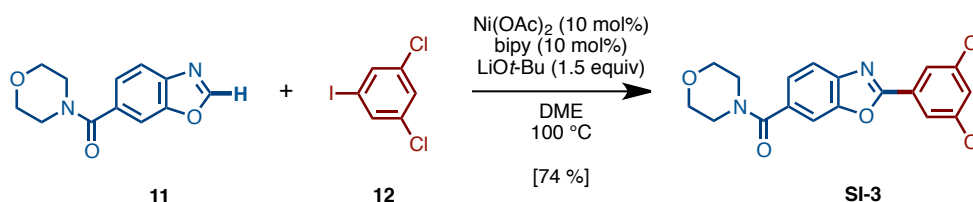
4-(6-Benzoxazoloyl)morpholine (**11**)



A mixture of 4-amino-3-hydroxybenzoic acid (**SI-2** : 1.53 g, 10 mmol) and trimethyl orthoformate (3 mL) was heated at 100 °C for 5 h. After cooling to room temperature, trimethyl orthoformate was removed under reduced pressure. To a solution of benzoxazole 6-carboxylic acid in CH_2Cl_2 (10 mL) were added DMF (0.1 mL) and oxalyl chloride (1.8 mL, 20 mmol) and the resultant mixture was stirred at room temperature for 12 h. After cooling to room temperature, DMF and oxalyl chloride were removed under reduced pressure to yield the corresponding acid chloride as a solid. Thus, generated acid chloride and morpholine (2.2 mL) were stirred at room temperature for 3 h. After removing solvents under reduced pressure, the mixture was treated with saturated aqueous sodium bicarbonate (20 mL) and ethyl acetate (20 mL). The layers were separated, and the aqueous layer was extracted with ethyl acetate (2 × 20 mL). The combined organic layer was washed with brine (20 mL), dried with anhydrous magnesium sulfate, and the solvent removed under reduced pressure. Purification of the resulting oil by flash column chromatography on silica (5% methanol

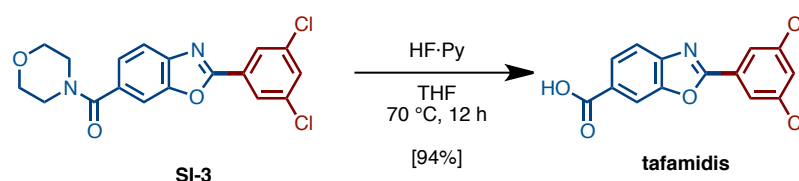
in CHCl_3 as eluent) afforded heteroarene **11** (1.30 g, 56%) as a white solid. $R_f = 0.47$ (MeOH/ $\text{CHCl}_3 = 1:20$). $^1\text{H NMR}$ (600 MHz, CDCl_3) δ 8.23 (s, 1H), 7.83 (d, $J = 8.3$ Hz, 1H), 7.71 (s, 1H) 7.44 (d, $J = 7.6$ Hz, 1H), 4.00–3.25 (br, 8H). $^{13}\text{C NMR}$ (150 MHz, CDCl_3) δ 169.52, 153.87, 149.67, 141.24, 132.90, 123.79, 120.76, 110.48, 66.81. HRMS (DART) m/z calcd for $\text{C}_{12}\text{H}_{13}\text{N}_2\text{O}_3$ $[\text{MH}]^+$: 233.0926, found 233.0926.

4-(3,5-Dichlorophenyl 6-Benzoxazolyl)morpholine (SI-3)



To a 20-mL glass vessel equipped with J. Young[®] O-ring tap containing a magnetic stirring bar were added Ni(cod)_2 (13.9 mg, 0.05 mmol), 2,2'-bipyridyl (7.8 mg, 0.05 mmol), LiOt-Bu (60 mg, 0.75 mmol), **11** (174.2 mg, 0.5 mmol), 3,5-dichloriodobenzene (**12**: 203.9 mg, 0.75 mmol), followed by dry 1,2-dimethoxyethane (2.0 mL). The vessel was sealed with an O-ring tap and then heated at 100 °C in an 8-well reaction block with stirring for 24 h. After cooling the reaction mixture to room temperature, the mixture was passed through a short silica gel pad (EtOAc). The filtrate was concentrated and the residue was subjected to preparative thin-layer chromatography (5% methanol in CHCl_3 as eluent) to afford **SI-2** (139.6 mg, 74 %) as a white foam. $R_f = 0.70$ (MeOH/ $\text{CHCl}_3 = 1:20$). $^1\text{H NMR}$ (600 MHz, CDCl_3) δ 8.16 (d, $J = 2.0$ Hz, 2H), 7.82 (d, $J = 7.6$ Hz, 1H), 7.70 (s, 1H), 7.55 (d, $J = 2.0$ Hz, 1H), 7.45 (d, $J = 7.6$ Hz, 1H), 4.00–3.25 (br, 8H). $^{13}\text{C NMR}$ (150 MHz, CDCl_3) δ 169.38, 161.78, 150.40, 142.90, 135.82, 132.95, 131.61, 129.26, 125.91, 124.23, 120.41, 110.26, 66.77. HRMS (DART) m/z calcd for $\text{C}_{18}\text{H}_{15}\text{Cl}_2\text{N}_2\text{O}_3$ $[\text{MH}]^+$: 377.0460 found 377.0465.

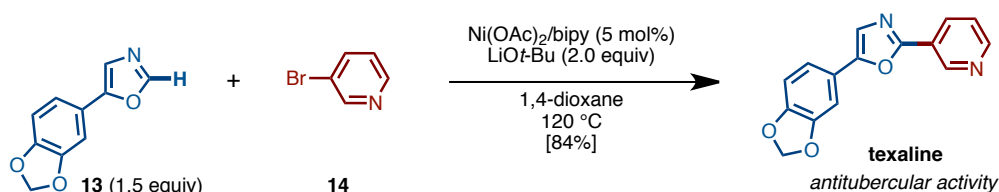
Tafamidis^[14]



HF·pyridine (0.5 mL) was added to a stirred solution of **SI-2** (32 mg, 0.09 mmol) in THF (0.5 mL) at 70 °C for 12 h. After cooling the reaction mixture to room temperature, the mixture was diluted with EtOAc and washed sequentially with sat. NaHCO₃, 2N HCl and brine. The organic layer was concentrated and the residue was subjected to preparative thin-layer chromatography (1% acetic acid, 5% methanol in CHCl₃ as eluent) to afford tafamidis (24.7 mg, 94%) as a white foam. ¹H NMR (600 MHz, DMSO-*d*₆) δ 8.23 (s, 1H), 8.08 (d, *J* = 1.4 Hz, 2H), 8.00 (d, *J* = 8.3 Hz, 1H), 7.88 (m, 2H). ¹³C NMR (150 MHz, DMSO-*d*₆) δ 166.6, 162.0, 150.0, 144.6, 135.1, 131.7, 129.1, 128.7, 126.5, 125.8, 120.0, 112.2. HRMS (DART) *m/z* calcd for C₁₄H₈Cl₂NO₃ [MH]⁺: 307.9881, found 307.9881.

4-5-3. Synthesis of Texaline

Texaline^[15b]



To a 20-mL glass vessel equipped with J. Young[®] O-ring tap containing a magnetic stirring bar were added Ni(OAc)₂ (8.8 mg, 0.05 mmol), 2,2'-bipyridyl (7.8 mg, 0.05 mmol), LiOt-Bu (160 mg, 2.00 mmol), **13** (286 mg, 1.5 mmol), **14** (158 mg, 1.0 mmol), and dry 1,4-dioxane (4.0 mL). The vessel was sealed with an O-ring tap and then heated at 120 °C in an 8-well reaction block with stirring for 36 h. After cooling the reaction mixture to room temperature, the mixture was passed through a short silica gel pad (CHCl₃). The filtrate was concentrated and the residue was subjected to preparative thin-layer chromatography (CHCl₃/MeOH = 20:1) to afford texaline (224 mg, 84%) as a yellow foam. R_f = 0.34 (CHCl₃/MeOH = 20:1). ¹H NMR (600 MHz, CDCl₃) δ 9.31 (s, 1H), 8.69 (d, *J* = 4.8 Hz, 1H), 8.34 (d, *J* = 8.4 Hz, 1H), 8.34 (d, *J* = 4.8 Hz, 1H), 7.34 (s, 1H), 7.24 (d, *J* = 7.8 Hz, 1H), 7.17 (s, 1H), 6.89 (d, *J* = 7.8 Hz, 1H), 6.03 (s, 2H). ¹³C NMR (150 MHz, CDCl₃) δ 151.13, 151.87, 150.73, 148.25, 148.17, 147.34, 133.23, 123.67, 123.58, 122.49, 121.68, 118.56, 108.88, 104.84, 101.45. HRMS (DART) *m/z* calcd for C₁₅H₁₁N₂O₃ [MH]⁺: 267.0770, found 267.0769.

Reference and Notes

1. (a) *Metal-Catalyzed Cross-coupling Reactions*, 2nd ed. (Eds.: de Meijere, A.; Diederich, F.), Wiley-VCH, Weinheim, **2004**. (b) *Topics in Current Chemistry, Vol. 219, Cross-Coupling Reactions: A Practical Guide* (Ed.: Miyaura, N.), Springer, Berlin, 2002.
2. For selected reviews on catalytic C–H bond arylation of arenes, see: (a) Campeau, L.-C.; Fagnou, K. *Chem. Commun.* **2006**, 1253. (b) Daugulis, O.; Zaitsev, V. G.; Shabashov, D.; Pham, Q.-N.; Lazareva, A. *Synlett* **2006**, 3382. (c) Alberico, D.; Scott, M. E.; Lautens, M.; *Chem. Rev.* **2007**, *107*, 174. (d) Seregin, I. V.; Gevorgyan, V. *Chem. Soc. Rev.* **2007**, *36*, 1173. (e) Satoh, T.; Miura, M. *Chem. Lett.* **2007**, *36*, 200. (f) Kakiuchi, F.; Kochi, T. *Synthesis* **2008**, 3013. (g) Li, B.-J.; Yang, S.-D.; Shi, Z.-J. *Synlett* **2008**, 949. (h) Lewis, J. C.; Bergman, R. G.; Ellman, J. A. *Acc. Chem. Res.* **2008**, *41*, 1013. (i) Miura, M.; Satoh, T. in *Modern Arylation Methods* (Ed. : Ackermann, L.), Wiley-VCH, Weinheim, **2009**, pp. 335–361. (j) Chen, X.; Engle, K. M.; Wang, D.-H.; Yu, J.-Q. *Angew. Chem., Int. Ed.* **2009**, *48*, 5094. (k) Ackermann, L.; Vicente, R.; Kapdi, A.R. *Angew. Chem., Int. Ed.* **2009**, *48*, 9792.
3. For selected report on catalytic C–H bond arylation of azoles, see: (a) Mori, A.; Sekiguchi, A.; Masui, K.; Shimada, T.; Horie, M.; Osakada, K.; Kawamoto, M.; Ikeda, T. *J. Am. Chem. Soc.* **2003**, *125*, 1700. (b) Bellina, F.; Cauteruccio, S.; Rossi, R. *Eur. J. Org. Chem.* **2006**, 1379. (c) Chiong, H. A.; Daugulis, O.; *Org. Lett.* **2007**, *9*, 1449. (d) Bellina, F.; Calandri, C.; Cauteruccio, S.; Rossi, R. *Tetrahedron* **2007**, *63*, 1970. (e) Turner, G. L.; Morris, J. A.; Greaney, M. F. *Angew. Chem., Int. Ed.* **2007**, *46*, 7996. (f) Campeau, L.-C.; Bertrand-Laperle, M.; Leclerc, J.-P.; Villemure, E.; Gorelsky, S.; Fagnou, K. *J. Am. Chem. Soc.* **2008**, *130*, 3276. (g) Ackermann, L.; Althammer, A.; Fenner, S. *Angew. Chem., Int. Ed.* **2008**, *48*, 201. (h) Shibahara, F.; Yamaguchi, E.; Murai, T. *Chem. Commun.* **2010**, 46, 2471. (i) Huang, J.; Chan, J.; Chen, Y.; Borths, C. J.; Baucom, K. D.; Larsen, R. D.; Faul, M. M. *J. Am. Chem. Soc.* **2010**, *132*, 3674.
4. For selected recent examples of Cu-catalyzed or mediated direct C–H arylations, see: (a) Do, H.-Q.; Daugulis, O. *J. Am. Chem. Soc.* **2007**, *129*, 12404. (b) Yoshizumi, T.; Tsurugi, H.; Satoh, T.; Miura, M. *Tetrahedron Lett.* **2008**, *49*,

- 1598; (c) Do, H.-Q.; Khan, R. M. K.; Daugulis, O. *J. Am. Chem. Soc.* **2008**, *130*, 15185. (d) Phipps, R. J.; Grimster, N. P.; Gaunt, M. J. *J. Am. Chem. Soc.* **2008**, *130*, 8172. (e) Phipps, R. J.; Gaunt, M. J. *Science* **2009**, *323*, 1593. (f) Ban, I.; Sudo, T.; Taniguchi, T.; Itami, K. *Org. Lett.* **2008**, *10*, 3607. (g) Kitahara, M.; Umeda, N.; Hirano, K.; Satoh, T.; Miura, M. *J. Am. Chem. Soc.* **2011**, *133*, 2160. (h) Nishino, M.; Hirano, K.; Satoh, T.; Miura, M. *Angew. Chem., Int. Ed.* **2012**, *51*, 6993.
5. For recent of Fe-catalyzed or mediated direct C–H arylations, see: (a) Norinder, J.; Matsumoto, A.; Yoshikai, N.; Nakamura, E. *J. Am. Chem. Soc.* **2008**, *130*, 5858. (b) Yoshikai, N.; Matsumoto, A.; Norinder, J.; Nakamura, E. *Angew. Chem., Int. Ed.* **2009**, *48*, 2925.
 6. For recent examples of Co-catalyzed or mediated direct C–H arylations, see: (a) Li, B.; Wu, Z.-H.; Gu, Y.-F.; Sun, C.-L.; Wang, B.-Q.; Shi, Z.-J. *Angew. Chem., Int. Ed.* **2011**, *50*, 1109. (b) Song, W.; Ackermann, L.; *Angew. Chem., Int. Ed.* **2012**, *51*, 8251. (c) Gao, K.; Lee, P.-S.; Long, C.; Yoshikai, N. *Org. Lett.* **2012**, *14*, 4234.
 7. For recent Ni-catalyzed direct C–H arylations, see: (a) Canivet, J.; Yamaguchi, J.; Ban, I.; Itami, K. *Org. Lett.* **2009**, *11*, 1733. (b) Hachiya, H.; Hirano, K.; Satoh, T.; Miura, M. *Org. Lett.* **2009**, *11*, 1737. (c) Kobayashi, O.; Uruguchi, D.; Yamanaka, T. *Org. Lett.* **2009**, *11*, 2679. (d) Yamamoto, T.; Muto, K.; Komiyama, M.; Canivet, J.; Yamaguchi, J.; Itami, K. *Chem. Eur. J.* **2011**, *17*, 10113. For C–H/C–M coupling, see: (e) Tobisu, M.; Hyodo, I.; Chatani, N. *J. Am. Chem. Soc.* **2009**, *131*, 12070. (f) Hachiya, H.; Hirano, K.; Satoh, T.; Miura, M. *ChemCatChem* **2010**, *2*, 1403. (g) Hachiya, H.; Hirano, K.; Satoh, T.; Miura, M. *Angew. Chem., Int. Ed.* **2010**, *49*, 2202. (h) Hyodo, I.; Tobisu, M.; Chatani, N. *Chem. Asian J.* **2012**, *7*, 1357–1365. (i) Hyodo, I.; Tobisu, M.; Chatani, N. *Chem. Commun.* **2012**, *48*, 308–310.
 8. Sanchez, R. S.; Zhuravlev, F. A. *J. Am. Chem. Soc.* **2007**, *129*, 5824.
 9. Chikashita, H.; Ishibaba, M.; Ori, K.; Itoh, K. *Bull. Chem. Soc. Jpn.* **1988**, *61*, 3637.
 10. Uchino, M.; Asagi, K.; Yamamoto, A.; Ikeda, S. *J. Organomet. Chem.* **1975**, *84*, 93.
 11. (a) Feth, M. P.; Klein, A.; Bertagnolli, H. *Eur. J. Inorg. Chem.* **2003**, 839. (b) Bryndza, H. E.; Tam, W. *Chem. Rev.* **1988**, *88*, 1163.
 12. For successful and unsuccessful examples of organolithium cross-coupling, see: (a)

- Murahashi, S.-I.; *J. Organomet. Chem.* **2002**, 653, 27. (b) Millard, A. A.; Rathke, M. W. *J. Am. Chem. Soc.* **1977**, 99, 4833. (c) Bumagin, N. A.; Ponomaryov, A. B.; Beletskaya, I. P. *J. Organomet. Chem.* **1985**, 291, 129. (d) Pelter, A.; Rowlands, M.; Clements, G. *Synthesis* **1987**, 51. (e) Negishi, E.-I.; Takahashi, T.; Baba, S.; Van Horn, D. E.; Okukado, N. *J. Am. Chem. Soc.* **1987**, 109, 2393. (f) Itami, K.; Mineno, M.; Muraoka, N.; Yoshida, J. *J. Am. Chem. Soc.* **2004**, 126, 11778. (g) Jhaveri, S. B.; Carter, K. R. *Chem. Eur. J.* **2008**, 14, 6845.
13. For the synthesis of febuxostat, see: (a) Watanabe, K.; Tanaka, T.; Kondo, S. *Jpn. Kokai Tokkyo Koho* **1994**, 329647; Treatment study and mechanism of febuxostat: (b) Becker, M. A.; Schumacher, H. R., Jr.; Wortmann, R. L.; MacDonald, P. A.; Eustace, D.; Palo, W. A.; Streit, J.; Joseph-Ridge, N. *New Engl. J. Med.* **2005**, 353, 2450. (c) Okamoto, K.; Eger, B. T.; Nishino, T.; Kondo, S.; Pai, E. F.; Nishino, T. *J. Biol. Chem.* **2003**, 278, 1848.
14. Razavi, H.; Palaninathan, S. K.; Powers, E. T.; Wiseman, R. L.; Purkey, H. E.; Mohamedmohaideen, N. N.; Deechongkit, S.; Chiang, K. P.; Dendle, M. T. A.; Sacchettini, J. C.; Kelly, J. W. *Angew. Chem., Int. Ed.* **2003**, 42, 2758.
15. For the isolation of texaline, see: (a) Domínguez, X. A.; de La Fuente, G.; Gonzalez, A. G.; Reina, M.; Timon, I. *Heterocycles* **1988**, 27, 35. Synthesis of texaline: (b) Giddens, A. C.; Boshoff, H. I. M.; Franzblau, S. G.; Barry, C. E.; Copp, B. R. *Tetrahedron Lett.* **2005**, 46, 7355. (c) Besselièvre, F.; Mahuteau-Betzer, F.; Grierson, D. S.; Piguel, S. *J. Org. Chem.* **2008**, 73, 3278.
16. Saha, D.; Adak, L.; Ranu B. C. *Tetrahedron Lett.* **2010**, 51, 5624.
17. Rudrawar, S.; Kondaskar, A.; Chakraborti, A. K. *Synthesis* **2005**, 2521.
18. Dmettey, Y.; Michaud, S.; Vierfond, J. M. *Heterocycles* **1994**, 38, 1001.
19. Asaumi, T.; Matsuo, T.; Fukuyama, T.; Ie, Y.; Kakiuchi, F.; Chatani, N. *J. Org. Chem.* **2004**, 69, 4433.

Decarbonylative Cross-Coupling of Esters and Organoborons by Nickel Catalysis

Abstract

Nickel-catalyzed decarbonylative cross-coupling of phenyl carboxylates and organoboron compounds has been developed. With a user-friendly and inexpensive nickel catalyst, a range of esters were coupled with boronic acids to construct valuable C–C bonds. Overall, a phenyl ester moiety works as the leaving group. This reaction is selective for phenyl ester, as alkyl esters are totally unreactive. Theoretical calculations revealed key mechanistic features including the phenyl ester selectivity of the coupling reaction. The developed decarbonylative reaction allows for a transformation of structurally complex drug molecules and a variety of orthogonal coupling reactions.

1. Introduction

The Suzuki–Miyaura coupling, a Pd- or Ni-catalyzed cross-coupling reaction of boron-based nucleophiles and organic electrophiles,^[1,2] is one of the most reliable reactions in synthetic organic chemistry, resulting in its indispensability in the synthesis of various functional organic materials ranging from pharmaceuticals, agrochemicals, organic electronic devices and liquid crystals. Conventionally, the Suzuki–Miyaura coupling uses organic halides as the electrophilic component (Figure 1).^[3] The development of a new mode of bond/group activation is expected to offer great opportunities, particularly when it leads to unconventional, streamlined organic syntheses. Recent advances in this field include the utilization of aniline derivatives, such as diazonium^[4] and ammonium salts,^[5] as C–N bond electrophiles. Phenol-based electrophiles such as anisoles and aryl pivalates have also been of use for coupling with organoborons.^[6] In addition, other compounds including C–S bond-containing electrophiles could be applied to the Suzuki–Miyaura coupling reaction.^[7-11]

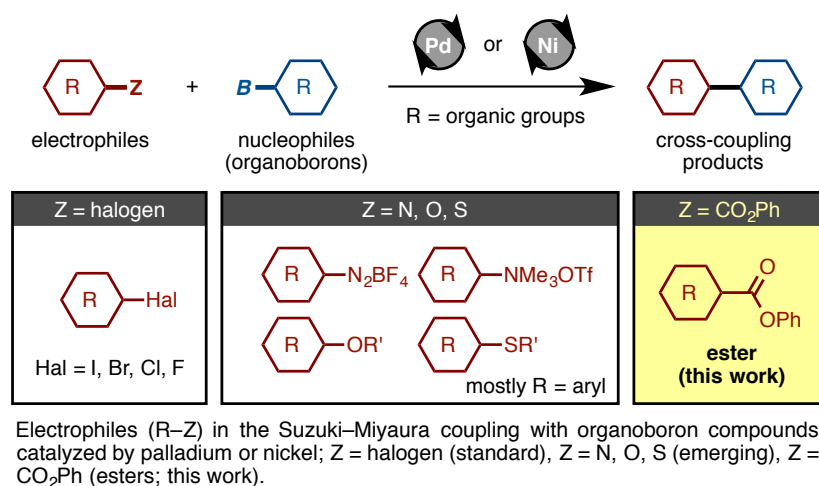


Figure 1. Electrophiles in the Suzuki–Miyaura coupling

The use of esters in the Suzuki–Miyaura coupling is important not only because it avoids the production of caustic halide-containing waste, but also because it allows the employment of a vast number of commercially and synthetically available ester-containing molecules (Figure 2). Moreover, ester groups are often associated with heteroaromatic synthesis, for example, Feist–Bénary furan synthesis and Hantzsch dihydropyridine synthesis, where these functionalities are important components of the

heterocyclic products. Thus, the successful implementation of this simple ester-based Suzuki–Miyaura coupling would allow these ester groups to be used directly as leaving groups. Given the recent rapid progress in C–H borylation chemistry,^[12] which has increased the accessibility of boron-based reagents, the target ester-based Suzuki–Miyaura coupling is expected to significantly advance organic synthesis. Furthermore, the use of earth-abundant first-row metal nickel as catalyst in the desired coupling makes this reaction commercially more appealing.

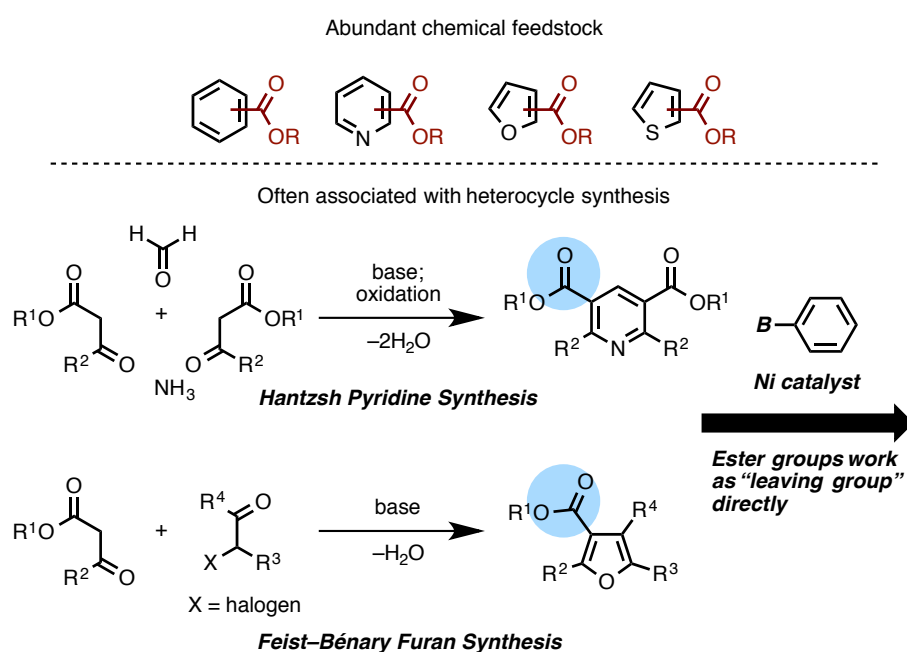


Figure 2. Advantages of using esters as electrophilic coupling partners in Suzuki–Miyaura coupling

Although recent efforts have realized the use of aryl compounds in metal-catalyzed cross-coupling in decarbonylative and decarboxylative fashion,^[13–17] ester groups have remained elusive electrophiles in the Suzuki–Miyaura coupling. Thus, a decarbonylative cross-coupling manifold employing Ni⁰/Ni^{II} redox catalysis was devised (Figure 3). According to prior experimental and theoretical investigations,^[18–25] oxidative addition of the C(acyl)–O bond of certain esters to Ni⁰ complexes could lead to the formation of an acyl–Ni(II) intermediate that could then undergo (i) transmetalation reaction with a boronic acid and (ii) decarbonylation to produce a diorganonickel (II) intermediate. Subsequent reductive elimination would release the

decarbonylative cross-coupling product and regenerates the Ni⁰ species. Armed with this knowledge and the beneficial impact of the phenyl substituent on the cleavage of C(acyl)–O bonds by nickel catalysts,^[21,22] this project focused on the use of phenyl arenecarboxylates (ArCO₂Ph).

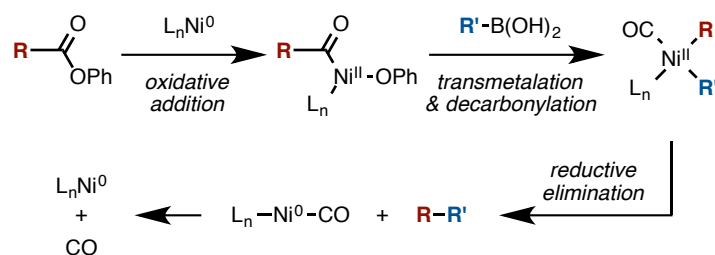


Figure 3. Mechanistic blueprint for the study of decarbonylative couplings

In this chapter, the development of Ni-catalyzed decarbonylative organoboron cross-coupling of esters is described. With inexpensive catalyst Ni(OAc)₂/P(*n*-Bu)₃ in the presence of Na₂CO₃, phenyl esters of aromatics as well as aliphatics can undergo decarbonylative cross-coupling with boronic acids. Ni(OAc)₂/(P*n*-Bu)₃ catalyst recognizes only phenyl esters, whereas alkyl esters remain intact under the developed conditions. The observed “phenyl ester” selectivity is discussed with the support of theoretical calculations. Furthermore, the developed decarbonylative cross-coupling realizes the transformation of structurally complex molecules and several classes of orthogonal cross-coupling reactions (Figure 4).

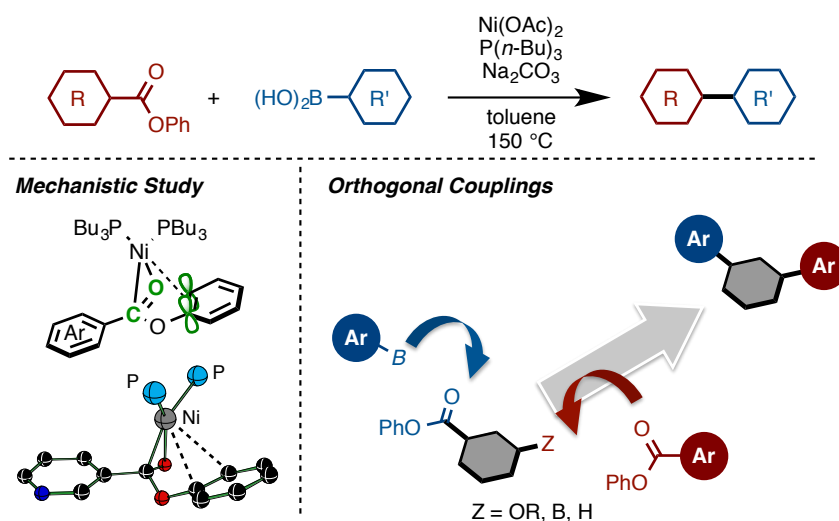
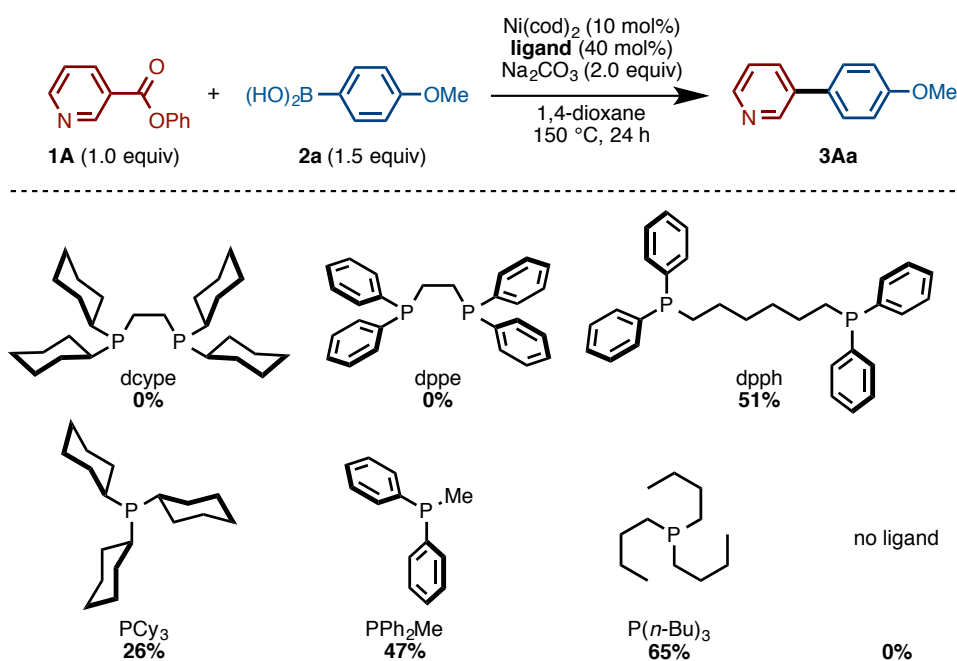


Figure 4. Decarbonylative organoboron coupling of esters by nickel catalysis

2. Results and Discussion

2-1. Discovery of Decarbonylative Organoboron Cross-Coupling of Esters and Investigation of Ligand Effect

This study was initiated to find suitable catalytic conditions for the decarbonylative cross-coupling of esters and arylboronic acids using phenyl 3-pyridinecarboxylate (**1A**) and *p*-anisylboronic acid (**2a**) as model substrates (Scheme 1). With the advantage of their low cost as well as prior knowledge in catalyst reactivity and selectivity,^[26-34] this study focused primarily on the use of nickel catalysts. Initially, the ligand effect was investigated by using Ni(cod)₂ (10 mol%) and Na₂CO₃ at 150 °C. The use of bidentate phosphines,^[22,25,31-34] such as dcype (1,2-bis(dicyclohexylphosphino)ethane) and dppe (1,2-bis(diphenylphosphino)ethane) as ligands did not produce the coupling product **3Aa**. Gratifyingly, further screening showed that the use of dpph (1,6-bis(diphenylphosphino)hexane) furnished **3Aa** in 51% yield. With the assumption that dpph, which has a long alkyl chain between two phosphorus atoms, is acting as a monodentate ligand rather than a bidentate ligand, the screening was turned to monodentate phosphine ligands. Rather expectedly, commercially available and inexpensive P(*n*-Bu)₃ showed the best performance in the decarbonylative cross-coupling (PCy₃, 26%; PPh₂Me, 47%; P(*n*-Bu)₃, 65%). It is worth mentioning that this cross-coupling reaction did not proceed without ligands.



Reaction conditions were as follows: **1A** (0.40 mmol), **2a** (0.60 mmol), Ni(cod)₂ (10 mol%), ligand (40 mol% for monodentate, 20 mol% for bidentate), Na₂CO₃ (2.0 equiv), 1,4-dioxane (1.6 mL), 150 °C, 24 h.

Scheme 1. Ligand effect in Ni-catalyzed decarbonylative cross-coupling of **1A** and **2a**

2-2. Investigation of Base and Solvent Effects

Having identified P(*n*-Bu)₃ as an optimal ligand, other parameters such as base, solvent, and temperature were examined (Table 2). This reaction worked best with weak bases such as Na₂CO₃, Li₂CO₃, and Et₃N (entries 1, 2, and 5). In the presence of slightly stronger bases such as K₂CO₃ or Cs₂CO₃, the coupling reaction competed with decomposition of the phenyl ester, resulting in low yields (entries 3 and 4). The reaction also proceeded without base (entry 6), even though halide-based Suzuki–Miyaura coupling typically requires exogenous base.^[1,2] Although the coupling could be conducted in various solvents such as ethers, hydrocarbons, and even alcohols, toluene was preferred as solvent giving **3Aa** in 95% yield (entries 7–10). Pleasingly, Ni(OAc)₂, which is air-stable and less expensive than Ni(cod)₂ or palladium catalyst in general, was found to function as an appropriate pre-catalyst, producing **3Aa** in 88% yield even with lower catalyst loading (5 mol%, entry 11). The effect of temperature was also investigated, demonstrating that this reaction is optimal at 150 °C (entries 12–14). Specifically, the generation of the product **3Aa** stopped at around 20% yield when the reaction was conducted below 120 °C. Thus, an operationally simple, economically/ecologically sound, user-friendly, nickel-based catalytic system for

organoboron-based, decarbonylative cross-coupling reactions using esters as electrophilic coupling partners was established.

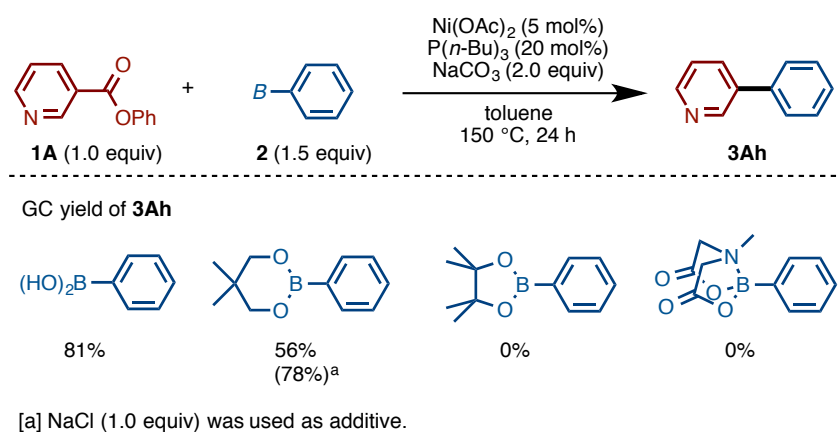
Table 2. Effect of various reaction parameters in the Ni-catalyzed decarbonylative cross-coupling of **1A** and **2a**

entry	base	solvent	T (°C)	yield of 3Aa (%) ^a
1	Na ₂ CO ₃	1,4-dioxane	150	65
2	Li ₂ CO ₃	1,4-dioxane	150	64
3	K ₂ CO ₃	1,4-dioxane	150	23
4	Cs ₂ CO ₃	1,4-dioxane	150	15
5	Et ₃ N	1,4-dioxane	150	68
6	none	1,4-dioxane	150	49
7	Na ₂ CO ₃	toluene	150	95
8	Na ₂ CO ₃	<i>m</i> -xylene	150	38
9	Na ₂ CO ₃	DME	150	56
10	Na ₂ CO ₃	<i>t</i> -AmylOH	150	53
11	Na ₂ CO ₃	toluene	150	88 ^b
12	Na ₂ CO ₃	toluene	140	75
13	Na ₂ CO ₃	toluene	130	60
14	Na ₂ CO ₃	toluene	120	18

Reaction conditions were as follows: **1A** (0.40 mmol), **2a** (0.60 mmol), Ni(cod)₂ (10 mol%), P(*n*-Bu)₃ (40 mol%), base (2.0 equiv), solvent (1.6 mL), 150 °C, 24 h. [a] GC yield using dodecane as an internal standard. [b] The reaction was conducted for 24 h using Ni(OAc)₂ (5 mol%) and P(*n*-Bu)₃ (20 mol%) as catalyst.

2-3. Investigation of Boron Groups

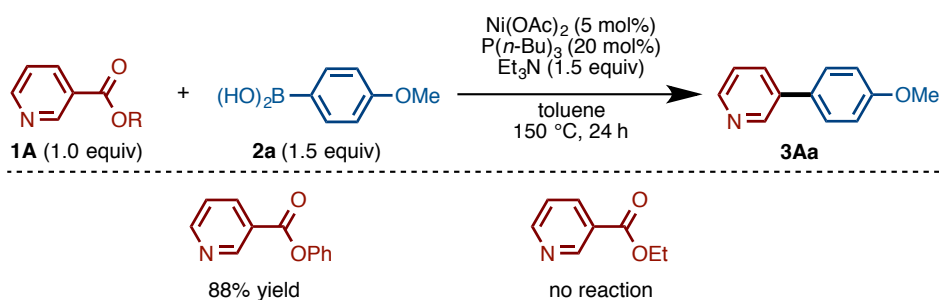
With the establishment of optimal conditions, applicable boron agents were examined (Scheme 2). Under the optimal conditions [Ni(OAc)₂ (5 mol%), P(*n*-Bu)₃ (20 mol%), and Na₂CO₃ in toluene at 150 °C], arylboronic acid and neopentyl arylboronic acid ester were found to be reactive. Unfortunately, pinacol boronic acid ester and MIDA (MIDA: *N*-methyliminodiacetic acid) boronate did not undergo this decarbonylative coupling. Additionally, it was found that the reaction of neopentyl boronic acid ester was accelerated by adding external NaCl salt to afford the coupling product **3Ah** in 78% yield. The effect of the NaCl additive is still unclear at this stage.



Scheme 2. The investigation of boron groups

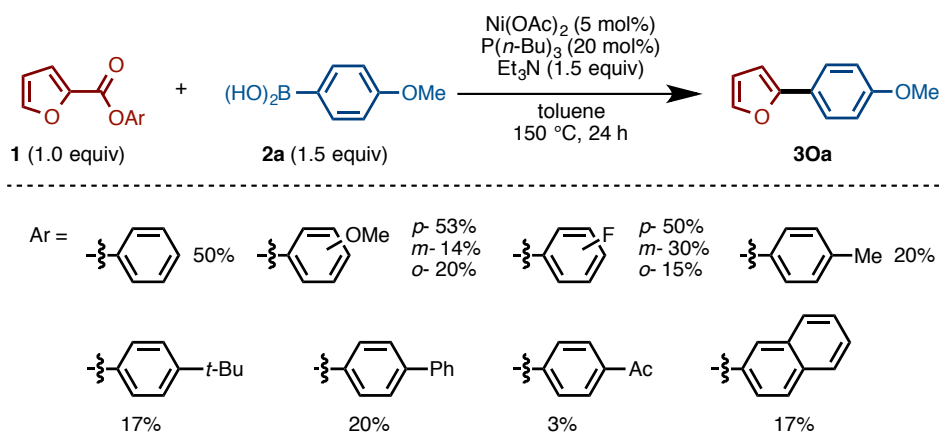
2-4. Investigation of Ester Substituents

Phenyl esters were effective substrates in this coupling, however, alkyl esters were found to be completely unreactive under otherwise identical conditions (Scheme 3).



Scheme 3. Comparison of the reactivity between phenyl and ethyl nicotinate

As for other aromatic esters, it was confirmed that the reaction proceeds albeit in lower yields (Scheme 4). Neither electron-donating nor withdrawing groups on the phenyl component improved the reaction progress, even when these functional groups were located at the sterically inconsequential *p*-position on the phenyl ring.



Scheme 4. The effect of substituents on the phenyl ester

2-5. Mechanistic Considerations

In order to confirm the proposed mechanistic blueprint depicted in Figure 3 and elucidate key mechanistic features of this decarbonylative Suzuki–Miyaura coupling, comprehensive theoretical calculations were conducted using phenyl nicotinate (**1A**) and *p*-anisylboronic acid (**2a**) as model substrates. The operative mechanism of the reaction in the presence of base (Na_2CO_3) and its potential energy surface are shown in Figure 4. At first, $\text{Ni}(\text{P}(n\text{-Bu})_3)_2$ (**A**) forms the π -complex with phenyl nicotinate (**B**) to undergo C(acyl)–O oxidative addition. Subsequently, the generated acyl–Ni(II) complex **C** then reacts with Na_2CO_3 with almost no energy barrier to form $\text{Ni}[\text{Na}_2\text{CO}_3\text{NaOPh}]$ cluster complex **D**,^[24,25,35-37] followed by transmetalation to give acyl–Ni(II)–aryl complex **E**. In this step, 20.5 kcal/mol of energy is required. The following decarbonylation occurs with an even higher energy barrier of 29.2 kcal/mol to give intermediate **F**, which furnishes the decarbonylative cross-coupling product and Ni(0) species **G** after reductive elimination. These computational studies suggest that transmetalation can take place prior to decarbonylation. Furthermore, compared with the transmetalation energy barrier of 20.5 kcal/mol, the decarbonylation energy barrier is 28.0 kcal/mol from nickel complex **D**. Thus, it can be said that the decarbonylation is the rate-determining step of the overall reaction in the presence of Na_2CO_3 . It is worth mentioning that the calculations have also identified a slight high-energy reaction pathway in the absence of Na_2CO_3 , in which the rate-determining step would be transmetalation from **C** with an energy barrier of 31.9 kcal/mol. Therefore, the computational studies shed light on the reason why this reaction can occur without base,

and why it is somewhat accelerated with the addition of Na_2CO_3 .

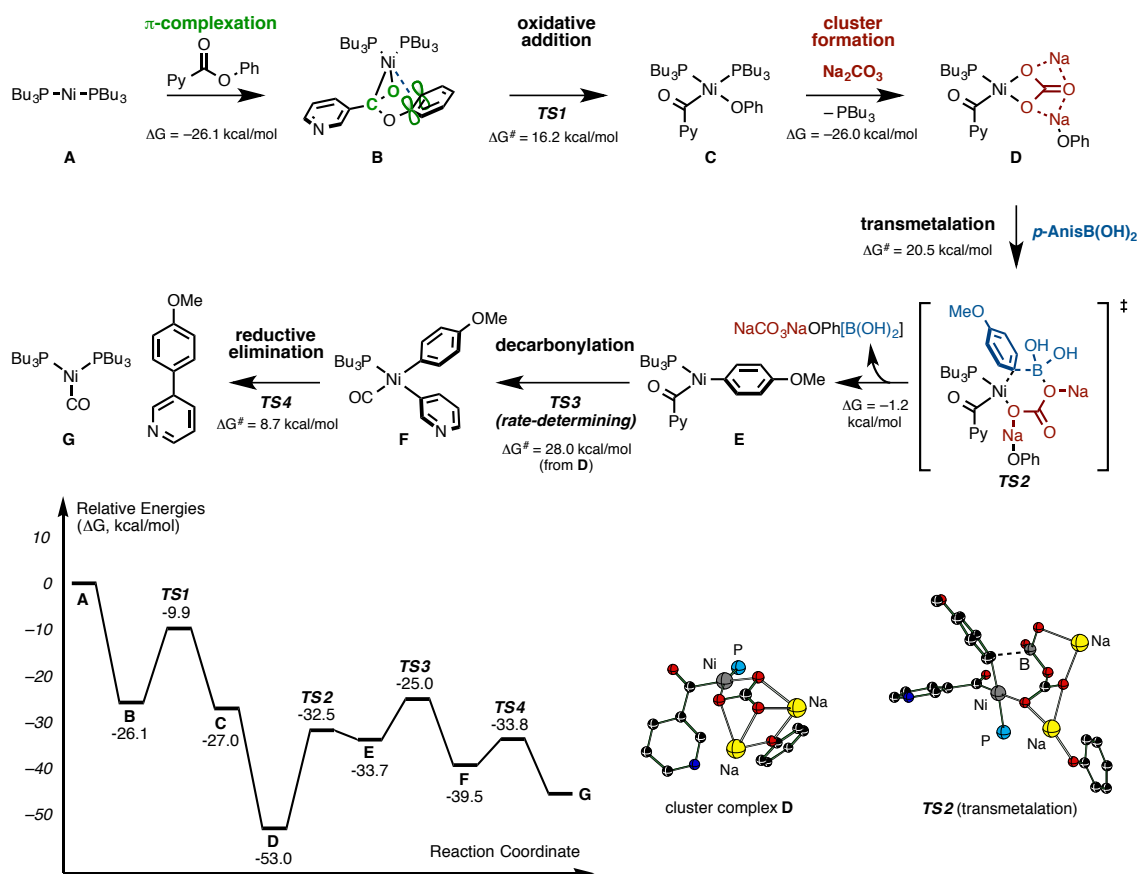


Figure 4. The possible reaction pathway identified by the calculations and the potential energy surface of the Ni-catalyzed coupling reaction. Relative energies of representative intermediates and transition states. The presented Gibbs free relative energies (ΔG) are obtained at the M06/{Lanl2dz_{Ni} + [6-31G(d,p)]} level of theory, in toluene solution (by using the PCM solvation method), and at the experimentally reported temperature (423.15 K) and pressure (1 atm).

Furthermore, these computational studies suggested the significant features of phenyl ester selectivity of the catalytic decarbonylative reaction (Figure 5). As previously mentioned, the oxidative addition is likely initiated by the formation of π -complex **B** between **A** and the phenyl ester reactant with the release of 26.1 kcal/mol of energy. It was expected that the existing donor-acceptor interaction between π -bonds of phenyl as well as the pyridyl ring and empty d-orbitals of nickel in the π -complex **B** play a key role in C(acyl)–O activation because ethyl ester was unreactive under these reaction

conditions. The theoretical calculations have also shown that the addition of Na_2CO_3 has no impact on the C–O oxidative addition step.

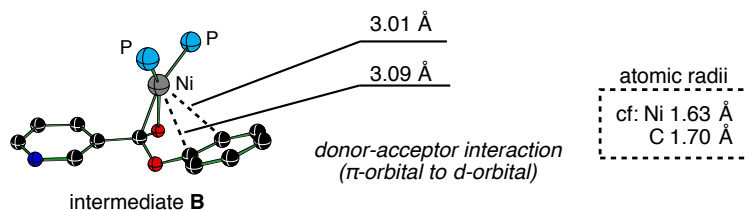
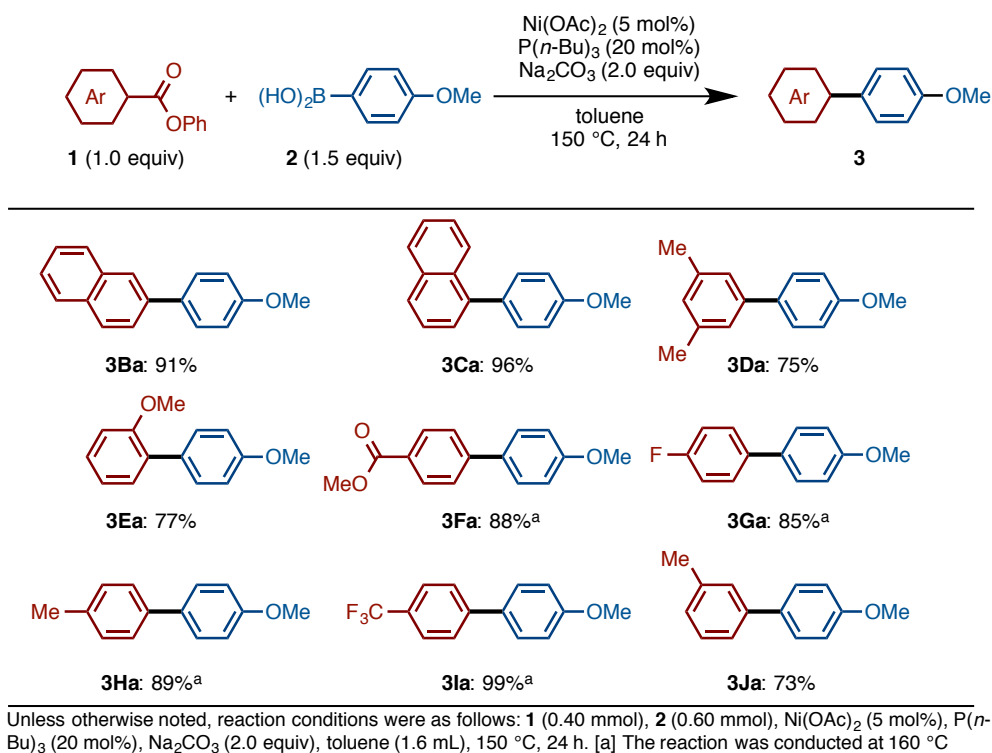


Figure 5. The importance of reactive intermediate **B**

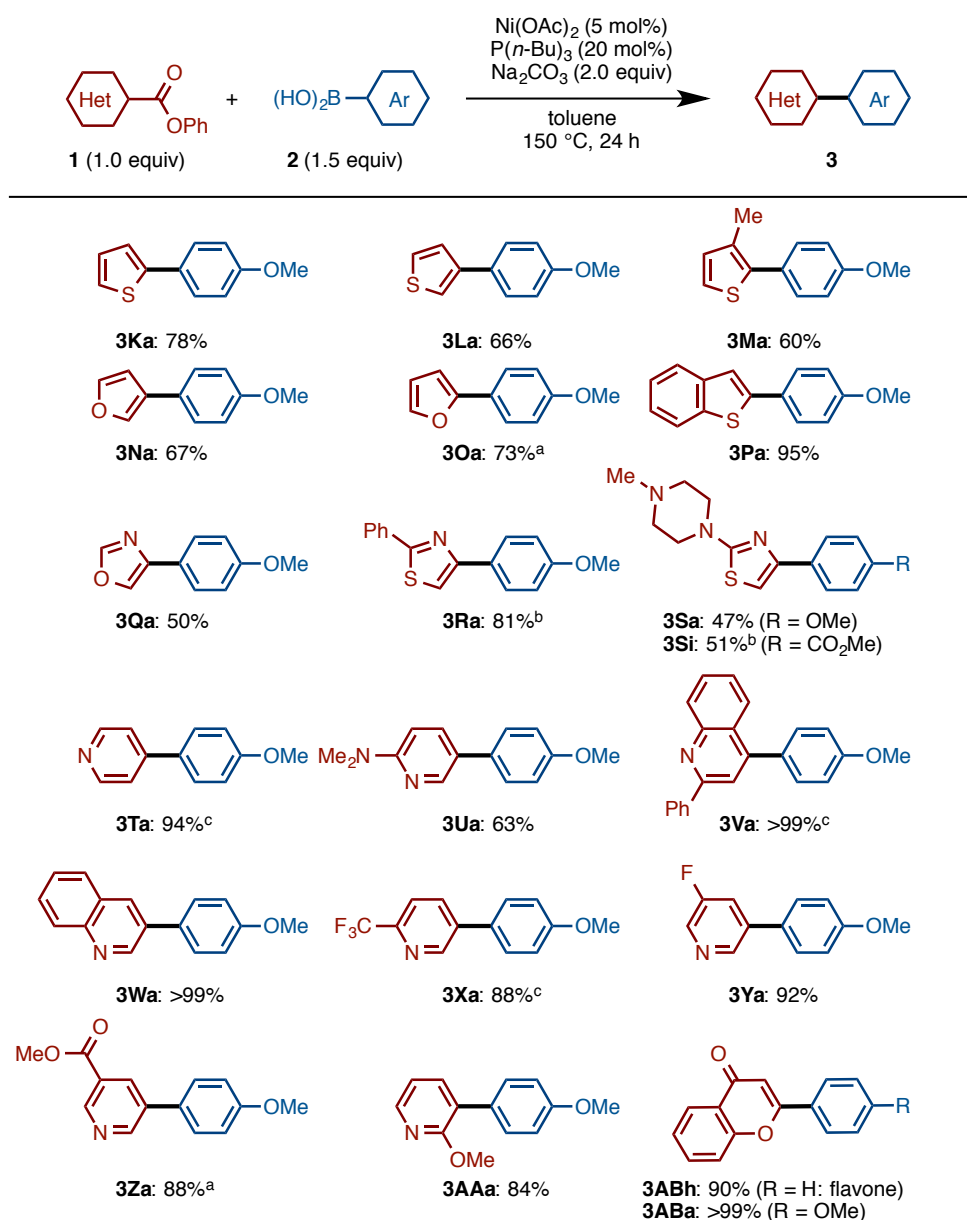
2-6. Scope of Decarbonylative Organoboron Cross-Coupling of Esters

Next, a wide range of compounds was subjected to the decarbonylative cross-coupling for the examination of the scope and limitation of this reaction (Scheme 5). As a result, the substrate scope was broad with regard to both coupling partners, for example, electronically and sterically diverse phenyl benzoates **1** were found to cross-couple with *p*-anisylboronic acid (**2a**) in high to excellent yields. It should be emphasized here that previous decarboxylative protocols by Gooßen required nitro, fluoro, and methoxy groups at the *ortho* position on the phenyl group to achieve reaction efficiency,^[15] but this decarbonylative coupling could couple a range of benzoic acid derivatives without such *ortho* substituents.



Scheme 5. Scope of phenyl benzoates

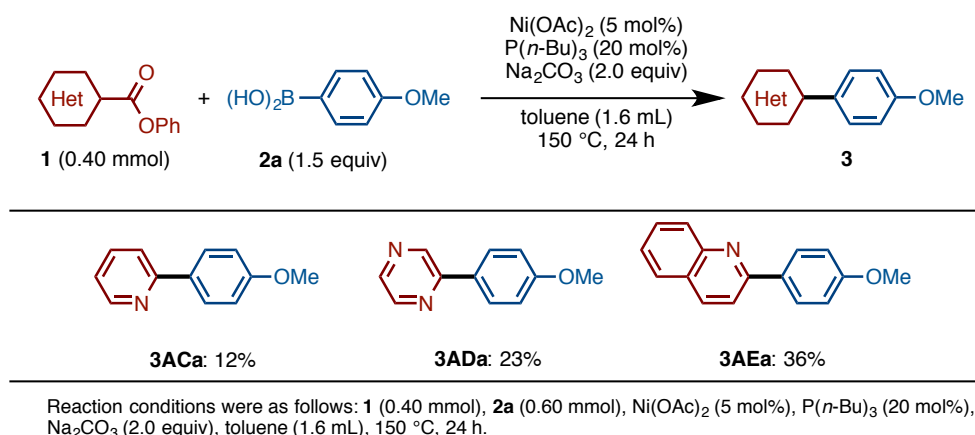
Esters of heterocycles such as thiophenes, furans, benzothiophenes, oxazoles, thiazoles, pyridines, and quinolines reacted smoothly to provide the corresponding heterobiaryls (Scheme 6). Easy access to heteroarene coupling participants is worth mentioning, for example, esters of oxazoles and thiazole **1Q–1S** could be prepared easily, while several steps are necessary for the synthesis of halogen analogues of these coupling partners. The present decarbonylative cross-coupling is also applicable to the synthesis of flavone and derivatives (**3ABh** and **3ABa**), which are compounds of significant interest to the scientific as well as general communities.



Unless otherwise noted, reaction conditions were as follows: **1** (0.40 mmol), **2** (0.60 mmol), Ni(OAc)₂ (5 mol%), P(*n*-Bu)₃ (20 mol%), Na₂CO₃ (2.0 equiv), toluene (1.6 mL), 150 °C, 24 h. [a] 1.2 equiv of Na₂CO₃ was used. [b] The reaction was conducted at 160 °C. [c] Et₃N was used instead of Na₂CO₃.

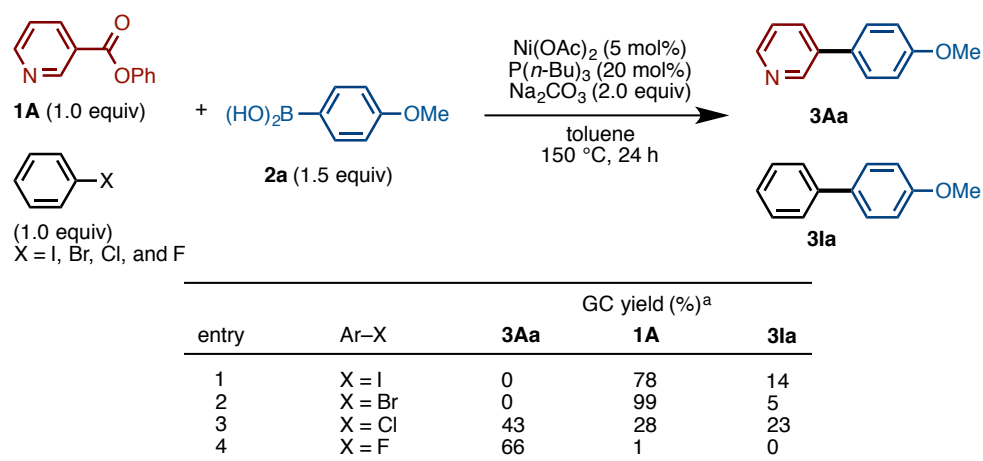
Scheme 6. Scope of heteroarene-carboxylates

Regarding the limitations of this coupling method, 2-azinecarboxylates showed poor reactivity (Scheme 7). For example, the reactions of 2-pyridyl, 2-pyrazyl, and 2-quinolonyl carboxylates furnished the corresponding coupling products in 12%, 23% and 36% yield, respectively.



Scheme 7. Limitations of the decarbonylative coupling: azines

Furthermore, with the exception of organofluorines, halide-containing substrates are problematic due to the competitive aryl–halogen bond activation and arylation by the Ni(OAc)₂/P(*n*-Bu)₃ catalyst (Scheme 8). Through competitive experiments, the reactivity order of Ar–I ≥ Ar–Br > Ar–Cl ≥ Ar–CO₂Ph ≫ Ar–F can be estimated. Although fluorine-bearing aromatic molecules are compatible with the decarbonylative reaction, iodine-, bromine-, and chlorine-bearing molecules are not suitable coupling partners.

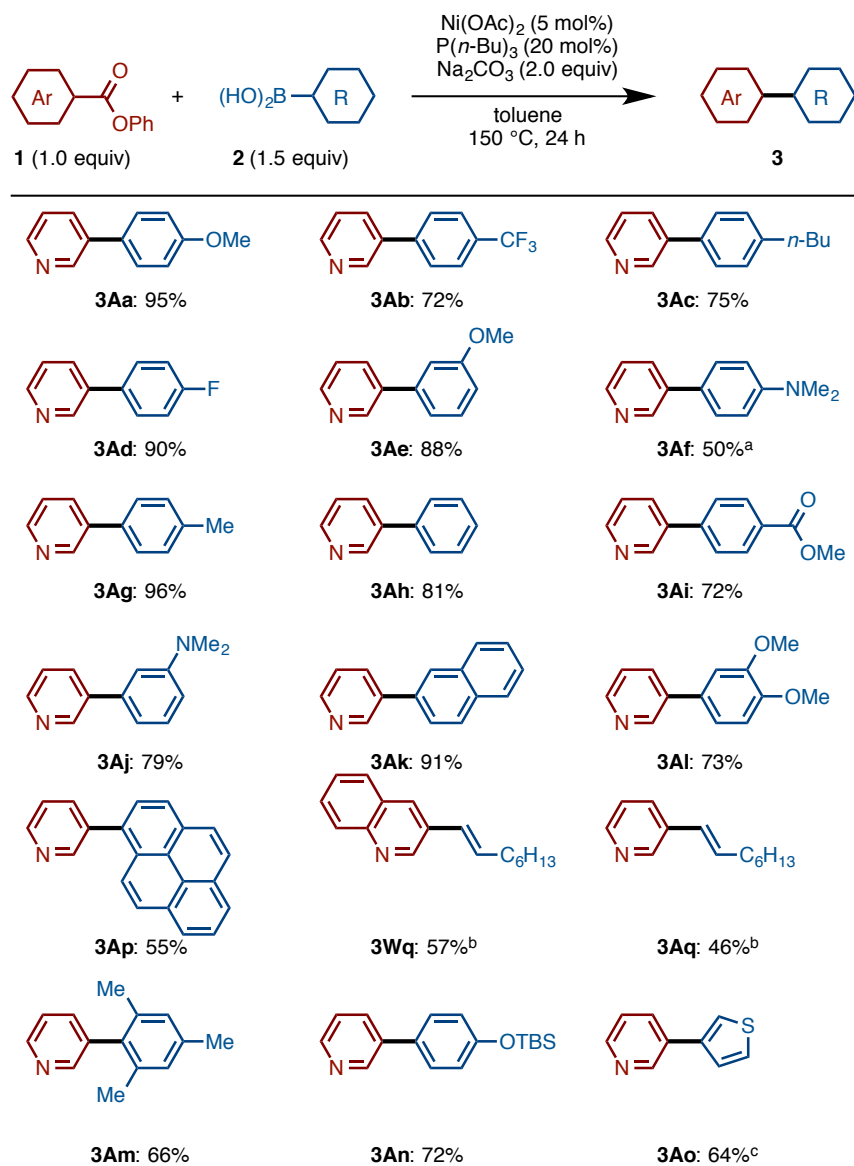


[a] GC yield using dodecane as an internal standard.

Scheme 8. Limitations of the decarbonylative coupling: halogens

The scope of this reaction with respect to arylboronic acids is also very broad (Scheme 9). In addition to various substituted phenyl groups including sterically

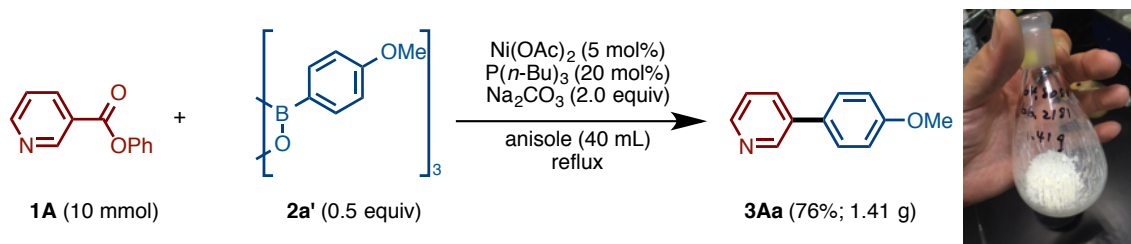
hindered *ortho*-disubstituted groups (**3Am**), heteroarene **3Ao** and polycyclic aromatic hydrocarbon **3Ap** could also be coupled. Moreover, alkenylboronic acids also participated well in this coupling reaction to afford the corresponding substituted alkenes in good yields (**3Wq** and **3Aq**), when NaCl was employed as an additive. The effect of NaCl or related salts remains unclear, but one possibility could be that it works as a dehydrating agent for the water that is generated from arylboronic acids. As mentioned above, the present coupling is selective for phenol-derived esters. Thus, methyl esters in either of the coupling partners are left intact (**3Fa**, **3Za** and **3Ai**). In almost all cases, the formation of carbonylated coupling product (diarylketone)¹³ was not observed, which indicates the high capability of nickel to facilitate the decarbonylation process.



Unless otherwise noted, reaction conditions were as follows: **1** (0.40 mmol), **2** (0.60 mmol), Ni(OAc)_2 (5 mol%), $\text{P}(n\text{-Bu})_3$ (20 mol%), Na_2CO_3 (2.0 equiv), toluene (1.6 mL), 150 °C, 24 h. [a] Et_3N was used instead of Na_2CO_3 . [b] NaCl (1.0 equiv) was added. [c] 1.2 equiv of Na_2CO_3 was used.

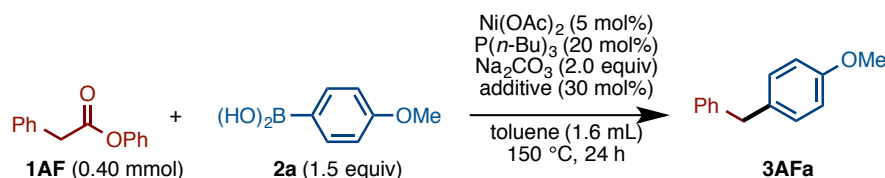
Scheme 9. Scope of boronic acids

It should also be highlighted that the present coupling has been conducted on a gram-scale in high yield with some modification of the reaction conditions, where arylboroxine and anisole were used (Scheme 10).



Scheme 10. Gram-scale coupling reaction of **1A** with **2a'**

This study primarily focused on the development of biaryl- and heterobiaryl-forming reactions with the goal of accessing privileged structures in a useful and unconventional way. Broadening the scope of present catalysis to an aliphatic system ($\text{sp}^3\text{-sp}^2$ cross-coupling) would have significant impact in synthetic chemistry. Though still preliminary, it was found that this type of coupling is feasible (Scheme 11). The decarbonylative coupling of **1AF** and **2a** under the optimal conditions afforded the target product **3AFa** in 27% yield. The addition of a catalytic amount of *N,N*-dimethylaminopyridine (DMAP) to the reaction led to improvement of the reaction yield (47% yield, entry 3), although its effect still remains unclear.

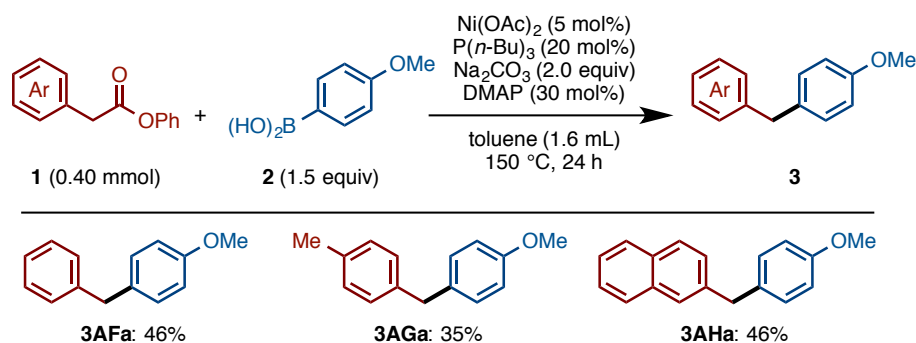


entry	additive	Isolated yield of 3
1	none	27%
2	none	43% ^a
3	DMAP (30 mol%)	46%
4	DMAP (1.0 equiv)	26%

Reaction conditions were as follows: **1AF** (0.40 mmol), **2a** (0.60 mmol), $\text{Ni}(\text{OAc})_2$ (5 mol%), $\text{P}(n\text{-Bu})_3$ (20 mol%), Na_2CO_3 (2.0 equiv), additive (30 mol%), toluene (1.6 mL), 150 °C, 24 h.[a] The reaction was 48 h.

Scheme 11. Investigation of $\text{sp}^3\text{-sp}^2$ coupling

The scope of the $\text{sp}^3\text{-sp}^2$ cross-coupling was examined (Scheme 12). The reactive substrate is still limited to phenyl arylacetates, but the present method successfully furnished diarylmethane **3AFa**, **3AGa**, and **3AHa**. Although there is room for further optimization of this particular coupling partner, this successful alkyl–aryl cross-coupling speaks well for the potential of the present nickel catalysis in the development of unconventional yet streamlined synthetic chemistry.

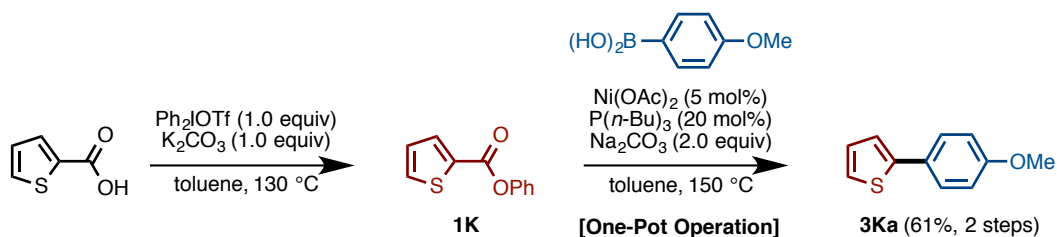


Unless otherwise noted, reaction conditions were as follows: **1** (0.40 mmol), **2a** (0.60 mmol), Ni(OAc)₂ (5 mol%), P(*n*-Bu)₃ (20 mol%), Na₂CO₃ (2.0 equiv), DMAP (30 mol%), toluene (1.6 mL), 150 °C, 24 h.

Scheme 12. Scope of aliphatic carboxylate coupling partners

2-7. One-pot Operation Starting from a Carboxylic Acid

While highly chemoselective coupling at the phenol-derived ester moiety is an advantage of the present protocol, there is still the need to transform a molecule of interest into a phenyl ester form prior to the cross-couplings. In order to simplify this pre-activation step, a one-pot protocol starting directly from carboxylic acids has also been established (Scheme 13). For example, 2-thiophenecarboxylic acid could be converted to the corresponding phenyl ester **1K** by treatment with diphenyliodonium triflate (Ph₂IOTf) and K₂CO₃ in toluene at 130 °C for 2 h.^[38] After removing iodobenzene (co-product of esterification) under reduced pressure, **2a**, Ni catalyst, and Na₂CO₃ were added to the same reaction flask, and the corresponding decarbonylative cross-coupling product **3Ka** was obtained in 61% yield (over the one-pot, two-step protocol) after stirring the mixture at 150 °C.

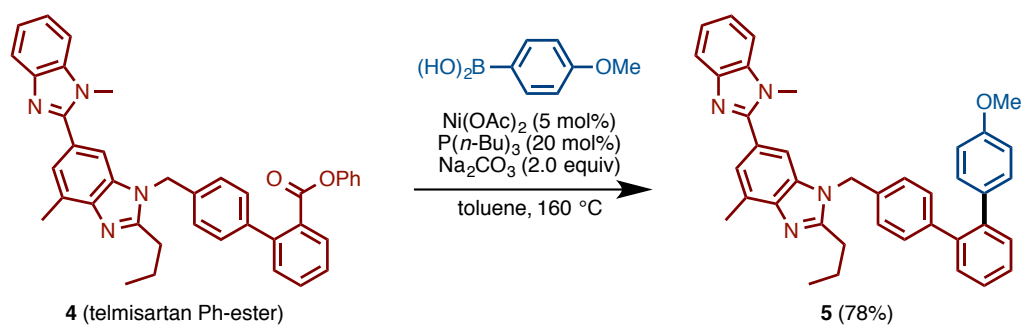


Scheme 13. One-pot transformation of thiophene-2-carboxylic acid to biaryl **3Ka**

2-8. Transformation of Complex Molecules by Ni-catalyzed Decarbonylative Coupling

This Ni-catalyzed decarbonylative cross-coupling was viable with complex-molecule precursors. For example, telmisartan, an angiotensin blocker that is

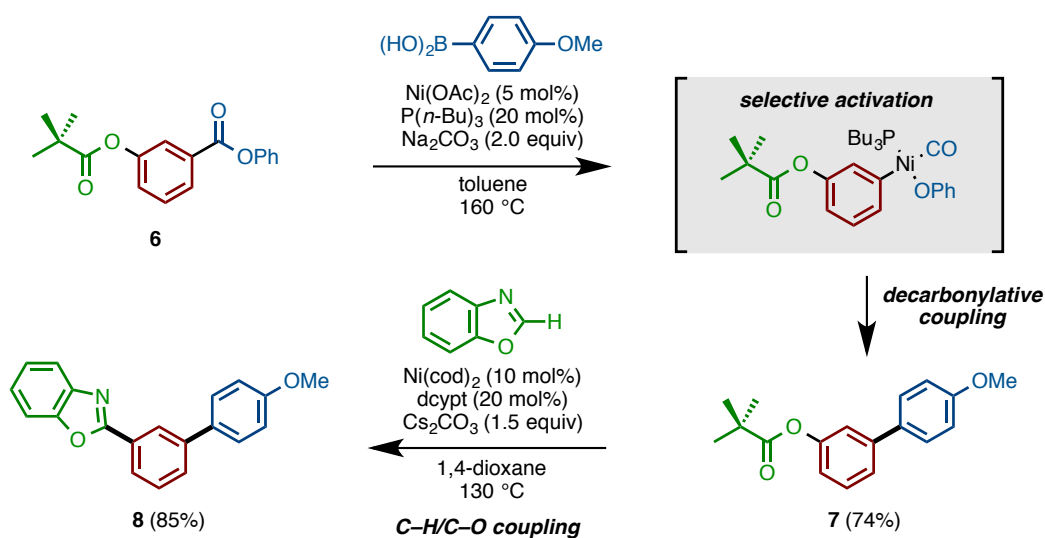
used for treatment of hypertension,^[39] could undergo decarbonylative cross-coupling with **2a** (after esterification) to provide aryl analogue **5** in 78% yield (Scheme 14). The successful coupling of heterocycle-rich compound **4** bodes well for the high versatility of present catalysis in many molecular transformations particularly in complex-molecule synthesis.



Scheme 14. Application to the synthesis of telmisartan derivatives

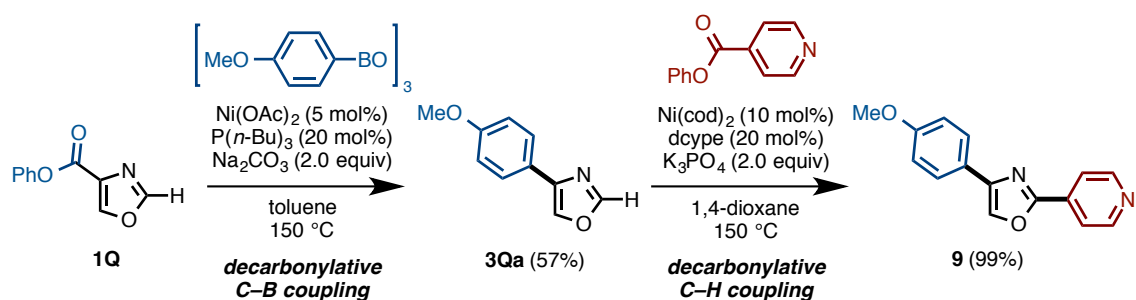
2-9. Orthogonal Coupling Based on the Present Decarbonylative Coupling

The molecular recognition ability and chemoselectivity of the $\text{Ni}(\text{OAc})_2/\text{P}(n\text{-Bu})_3$ catalyst is remarkably high (Scheme 15). 3-Hydroxybenzoic acid derivative **6**, in which the phenol terminus and the acid terminus are protected as a pivalate and phenyl ester respectively, provides an interesting example. This compound underwent selective activation of the latter phenyl ester moiety (highlighted in blue in Scheme 15) by the $\text{Ni}(\text{OAc})_2/\text{P}(n\text{-Bu})_3$ catalyst, leading to selective coupling with **2a** to produce **7** in 74% yield. There are a number of reports in which nickel complexes catalyze the Suzuki–Miyaura coupling of a range of aryl pivalates and related aryl C–O bonds with arylboronic acids.^[6,40–43] However, under the present conditions, the aryl pivalate moiety (highlighted in green) remained intact. This result underlines the capability of the $\text{Ni}(\text{OAc})_2/\text{P}(n\text{-Bu})_3$ catalyst to distinguish subtle difference in the steric environment of the two aryl ester moieties. Moreover, the remaining phenyl ester moiety of **7** could be activated by another catalyst developed in the Itami laboratory,^{31,34} $\text{Ni}(\text{cod})_2/\text{dcypt}$ (dcypt = 3,4-bis(dicyclohexylphosphino)thiophene) to achieve a C–H/C–O coupling reaction with benzoxazole to give teraryl **8** in 85% yield.



Scheme 15. Orthogonal coupling of **6**: decarbonylative cross-coupling catalyzed by $\text{Ni}(\text{OAc})_2/\text{P}(n\text{-Bu})_3$ (first step) and C-H/C-O coupling catalyzed by $\text{Ni}(\text{cod})_2/\text{dcypt}$ (second step).

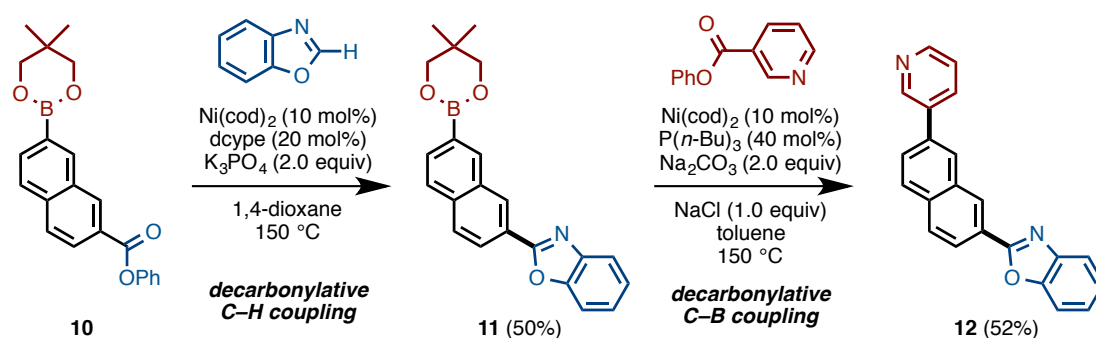
A sequence involving the present decarbonylative organoboron coupling and decarbonylative C-H coupling^[22] is also possible (Scheme 16). For example, under the influence of catalytic $\text{Ni}(\text{OAc})_2/\text{P}(n\text{-Bu})_3$, phenyl oxazole-4-carboxylate (**1Q**) reacted with (4-methoxyphenyl)boroxine in a decarbonylative organoboron coupling manner to afford aryloxazole **3Qa** in 57% yield. Subsequently, the oxazole C-H bond of **3Qa** can be further arylated by decarbonylative C-H coupling with phenyl isonicotinate in the presence of catalytic $\text{Ni}(\text{cod})_2/\text{dcypt}$ to give diaryloxazole **9** in 99% yield.



Scheme 16. Sequential coupling of **1Q**: decarbonylative C-B coupling catalyzed by $\text{Ni}(\text{OAc})_2/\text{P}(n\text{-Bu})_3$ (first step) and decarbonylative C-H coupling catalyzed by $\text{Ni}(\text{cod})_2/\text{dcypt}$ (second step)

Furthermore, another sequential coupling was demonstrated starting from bifunctional aromatic **10** having both boron and phenyl ester groups (Scheme 17). The

first decarbonylative C–H coupling proceeded well in the presence of the $\text{Ni}(\text{cod})_2/\text{dcype}$ catalyst, producing heterobiaryl **11** in 50% yield. It is worth noting that boronate moiety was compatible under these conditions. The remaining boron group was further converted to give teraryls **12** in 52% yield by the present decarbonylative organoboron coupling with phenyl nicotinate with $\text{Ni}/\text{P}(n\text{-Bu})_3$ catalyst.



Scheme 17. Orthogonal coupling of **10**: decarbonylative C–H coupling catalyzed by $\text{Ni}(\text{cod})_2/\text{dcype}$ (first step) and decarbonylative C–B coupling catalyzed by $\text{Ni}(\text{OAc})_2/\text{P}(n\text{-Bu})_3$ (second step)

3. Conclusion

In conclusion, a user-friendly Ni-based catalytic system ($\text{Ni}(\text{OAc})_2/\text{P}(n\text{-Bu})_3$) for the decarbonylative organoboron cross-coupling with esters as coupling partner, has been developed. This chapter described (1) the elucidation of key mechanistic features of this newly developed reaction by comprehensive theoretical calculation, (2) the broad scope with regard to both coupling partners (esters and boron), (3) successful aliphatic cross-coupling, (4) a gram-scale cross-coupling, (5) one-pot cross-coupling protocol starting directly from carboxylic acids, (6) application to complex-molecule settings, and (7) remarkably high molecular recognition ability of $\text{Ni}(\text{OAc})_2/\text{P}(n\text{-Bu})_3$ catalyst that enables unconventional orthogonal cross-couplings. Overall, the new Suzuki–Miyaura “ester coupling” described herein not only is useful as an alternative to the standard halide-based cross-coupling, but also allows strategic and unconventional utilization of ubiquitous ester functionalities in chemical synthesis. Further optimization of catalyst and reaction conditions to achieve broader scope to allow for lower temperature coupling is part of the future work of this research program.

4. Experimental

4-1. General

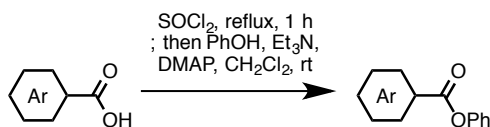
Unless otherwise noted, all materials including dry solvents were obtained from commercial suppliers and used as received. Ni(OAc)₂·4H₂O and P(*n*-Bu)₃ were obtained from Kanto Chemicals. Na₂CO₃ was obtained from Wako Chemicals. Toluene was purified by Glass Contour. Anisole and 1,4-dioxane were distilled with Na/ketyl before the use. Phenyl nicotinate (**1A**),^[22] phenyl 2-naphthoate (**1B**),^[22] phenyl thiophene-2-carboxylate (**1K**),^[22] phenyl thiophene-3-carboxylate (**1L**),^[22] phenyl furan-3-carboxylate (**1N**),^[22] phenyl furan-2-carboxylate (**1O**),^[22] phenyl 2-phenylthiazole-4-carboxylate (**1R**),^[22] phenyl isonicotinate (**1T**),^[22] phenyl 2-phenylquinoline-4-carboxylate (**1V**),^[22] phenyl picolinatephenyl (**1AC**),^[22] pyrazine-2-carboxylate (**1AD**),^[22] 4-oxo-4*H*-chromene-2-carboxylic acid (**1AB**),^[44] 5-(methoxycarbonyl)nicotinic acid (**1AA**),^[45] and 4-methylpiperazine-1-carbothioamide (**1S**)^[46] were synthesized according to procedures reported in the literature. Phenyl 3-methylbenzoate (**1J**),^[47] phenyl 4-fluorobenzoate (**1G**),^[47] methyl phenyl terephthalate (**1F**),^[49] phenyl 4-methylbenzoate (**1H**),^[49] phenyl 1-naphthoate (**1C**),^[50] phenyl 2-methoxybenzoate (**1E**),^[50] and phenyl quinoline-3-carboxylate (**1W**)^[50] were synthesized by known procedures using the corresponding carboxylic acids, phenol, EDC·HCl, and DMAP, and the spectra matched with those of reported compounds in the literature. Unless otherwise noted, all reactions were performed with dry solvents under an atmosphere of N₂ gas in dried glassware using standard vacuum-line techniques. All coupling reactions were performed in 20-mL glass vessel tubes equipped with J. Young[®] O-ring tap and heated in an 8-well reaction block (heater + magnetic stirrer) unless otherwise noted. All work-up and purification procedures were carried out with reagent-grade solvents in air.

Analytical thin-layer chromatography (TLC) was performed using E. Merck silica gel 60 F₂₅₄ precoated plates (0.25 mm). The developed chromatogram was analyzed by UV lamp (254 nm). Flash column chromatography was performed with E. Merck silica gel 60 (230–400 mesh) or Biotage Isolera[®] equipped with Biotage SNAP Cartridge KP-Sil columns using hexane/EtOAc as an eluent. Preparative thin-layer chromatography (PTLC) was performed using Wakogel B5-F silica coated plates (0.75 mm) prepared in our laboratory. Preparative high performance liquid chromatography (preparative

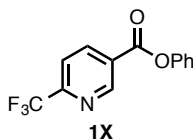
HPLC) was performed with a Biotage Isolera[®], one equipped with Biotage SNAP Cartridge KP-C18-HS columns using acetonitrile/water as an eluent. Preparative gel permeation chromatography (GPC) was performed with a JAI LC-9204 instrument equipped with JAIGEL-1H/JAIGEL-2H columns using chloroform as an eluent. Gas chromatography (GC) analysis was conducted on a Shimadzu GC-2010 instrument equipped with a HP-5 column (30 m × 0.25 mm, Hewlett-Packard) with dodecane as an internal standard. GCMS analysis was conducted on a Shimadzu GCMS-QP2010 instrument equipped with a HP-5 column (30 m × 0.25 mm, Hewlett-Packard). High-resolution mass spectra (HRMS) were obtained from a JEOL JMS-T100TD instrument (DART), Thermo Scientific Exactive Plus Orbitrap MS (ESI) and MSI.TOKYO Inc. MULTUM-FAB (FAB). Nuclear magnetic resonance (NMR) spectra were recorded on a JEOL JNM-ECA-400 (¹H 400 MHz, ¹³C 100 MHz) and JNM-ECA-600 (¹H 600 MHz, ¹³C 150 MHz) spectrometer. Chemical shifts for ¹H NMR are expressed in parts per million (ppm) relative to tetramethylsilane (δ 0.00 ppm). Chemical shifts for ¹³C NMR are expressed in ppm relative to CDCl₃ (δ 77.0 ppm). Data are reported as follows: chemical shift, multiplicity (s = singlet, d = doublet, dd = doublet of doublets, t = triplet, td = triplet of doublets, q = quartet, m = multiplet, br = broad signal), coupling constant (Hz), and integration.

4-2. Preparation of Arenecarboxylic Acid Phenyl Esters 1

Method A

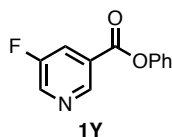


Thionyl chloride (0.5 M) was added to the carboxylic acid (1.0 equiv) and the mixture was refluxed for 1 h. The solution was concentrated *in vacuo*. To the residue were added CH₂Cl₂ (0.5 M), phenol (1.0 equiv), and then *N,N*-dimethyl-4-aminopyridine (DMAP: 1 mol%). After cooling the mixture to 0 °C, triethylamine (Et₃N: 1.2 equiv) was slowly added and then the reaction mixture was warmed to room temperature. After stirring the mixture for 1 h, NaHCO₃aq was added to the resulting mixture to quench the reaction. The mixture was extracted three times with CH₂Cl₂. The combined organic layer was dried over Na₂SO₄, and then filtrated. The filtrate was concentrated *in vacuo* and the residue was purified by recrystallization or flash column chromatography to afford the corresponding phenyl ester **1**.



Phenyl 6-(trifluoromethyl)nicotinate (**1X**)

Following the method A, purification by recrystallization (hexane) afforded **1X** as a white solid (741 mg, 88% yield; 3.15 mmol scale). ¹H NMR (CDCl₃, 400 MHz) δ 9.48 (s, 1H), 8.64 (d, *J* = 8.0 Hz, 1H), 7.86 (d, *J* = 8.0 Hz, 1H), 7.47 (t, *J* = 8.0 Hz, 2H), 7.33 (t, *J* = 8.0 Hz, 1H), 7.24 (d, *J* = 8.0 Hz, 2H); ¹³C NMR (CDCl₃, 100 MHz) δ 162.6, 151.7 (q, *J*_{C-F} = 35 Hz), 151.4, 150.2, 139.3, 129.7, 128.1, 126.5, 121.4, 121.0 (q, *J*_{C-F} = 279 Hz), 120.3 (q, *J*_{C-F} = 3.0 Hz); HRMS (DART) *m/z* calcd for C₁₃H₉F₃NO₂ [M+H]⁺: 268.0585, found: 268.0585.

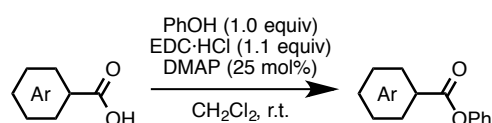


Phenyl 5-fluoronicotinate (**1Y**)

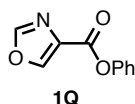
Following the method A, purification by flash column chromatography (hexane/EtOAc

= 5:1) afforded **1Y** as a white solid (470 mg, 77% yield; 2.65 mmol scale). ¹H NMR (CDCl₃, 400 MHz) δ 9.22 (s, 1H), 8.72 (d, *J* = 2.8 Hz, 1H), 8.16–8.11 (m, 1H), 7.45 (t, *J* = 8.0 Hz, 2H), 7.30 (t, *J* = 8.0 Hz, 1H), 7.23 (d, *J* = 8.0 Hz, 2H); ¹³C NMR (CDCl₃, 100 MHz) δ 161.5 (d, *J*_{C-F} = 238 Hz), 157.7, 150.3, 147.0 (d, *J*_{C-F} = 4.0 Hz), 142.6 (d, *J*_{C-F} = 24 Hz), 129.6, 126.9 (d, *J*_{C-F} = 3.0 Hz), 126.4, 124.0 (d, *J*_{C-F} = 20 Hz), 121.3; HRMS (DART) *m/z* calcd for C₁₂H₉FNO₂ [M+H]⁺: 218.0617, found: 218.0620.

2-2. Method B

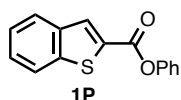


To a round-bottomed flask with the carboxylic acid (1.0 equiv) were added phenol (1.0 equiv), 1-(3-dimethylaminopropyl)-3-ethylcarbodiimide hydrochloride (EDC·HCl: 1.1 equiv), *N,N*-dimethyl-4-aminopyridine (DMAP: 0.25 equiv) and CH₂Cl₂ (0.5 M). After stirring the mixture for several hours with monitoring reaction progress with TLC, the reaction was quenched with saturated NaHCO₃aq and extracted three times with CH₂Cl₂. The combined organic layer was dried over Na₂SO₄, filtrated, and concentrated *in vacuo*. The residue was purified by recrystallization or flash column chromatography to afford the corresponding phenyl ester **1**.



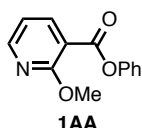
Phenyl oxazole-4-carboxylate (**1Q**)

Following the method B, purification by flash column chromatography (hexane/EtOAc = 5:1) afforded **1Q** as a white solid (800 mg, 96% yield; 4.4 mmol scale). ¹H NMR (CDCl₃, 400 MHz) δ 8.45 (s, 1H), 8.02 (s, 1H), 7.43 (t, *J* = 7.6 Hz, 2H), 7.28 (t, *J* = 7.6 Hz, 1H), 7.22 (d, *J* = 7.6 Hz, 2H); ¹³C NMR (CDCl₃, 100 MHz) δ 159.2, 151.6, 150.1, 145.1, 132.7, 129.5, 126.2, 121.5; HRMS (DART) *m/z* calcd for C₁₀H₈NO₃ [M+H]⁺: 190.0504, found: 190.0505.



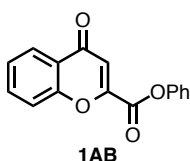
Phenyl benzo[*b*]thiophene-2-carboxylate (**1P**)

Following the method B, purification by recrystallization (hexane) afforded **1P** as a white solid (708 mg, 93% yield; 3.0 mmol scale). ¹H NMR (CDCl₃, 400 MHz) δ 8.25 (s, 1H), 7.93 (d, *J* = 8.0 Hz, 1H), 7.91 (d, *J* = 8.4 Hz, 1H), 7.50 (dd, *J* = 8.4, 7.2 Hz, 1H), 7.47–7.40 (m, 3H), 7.31–7.23 (m, 3H); ¹³C NMR (CDCl₃, 100 MHz) δ 161.2, 150.6, 142.6, 138.6, 132.7, 131.9, 129.5, 127.3, 126.1, 125.7, 125.1, 122.8, 121.6; HRMS (DART) *m/z* calcd for C₁₅H₁₁O₂S [M+H]⁺: 255.0480, found: 255.0477.



Phenyl 2-methoxynicotinate (**1AA**)

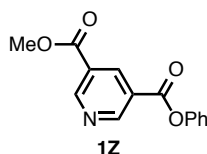
Following the method B, purification by flash column chromatography (hexane/EtOAc = 7:1) afforded **1AA** as colorless liquid (1.22 g, 91% yield; 6.0 mmol scale). ¹H NMR (CDCl₃, 400 MHz) δ 8.38 (d, *J* = 5.2 Hz, 1H), 8.35 (d, *J* = 7.6 Hz, 1H), 7.42 (t, *J* = 8.0 Hz, 2H), 7.27 (t, *J* = 8.0 Hz, 1H), 7.23 (d, *J* = 8.0 Hz, 2H), 7.01 (dd, *J* = 7.6, 5.2 Hz, 1H), 4.08 (s, 3H); ¹³C NMR (CDCl₃, 100 MHz) δ 163.4, 163.0, 151.6, 150.8, 141.8, 129.5, 126.0, 121.8, 116.5, 113.4, 54.3; HRMS (DART) *m/z* calcd for C₁₃H₁₂NO₃ [M+H]⁺: 230.0817, found: 230.0819.



Phenyl 4-oxo-4*H*-chromene-2-carboxylate (**1AB**)

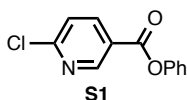
Following the method B, purification by flash column chromatography (hexane/EtOAc = 10:1) afforded **1AB** as a yellow solid (462 mg, 30% yield; 5.8 mmol scale). ¹H NMR (CDCl₃, 400 MHz) δ 8.23 (d, *J* = 8.4 Hz, 1H), 7.78 (t, *J* = 8.8 Hz, 1H), 7.65 (d, *J* = 8.8 Hz, 1H), 7.51–7.43 (m, 3H), 7.33 (t, *J* = 7.6 Hz, 1H), 7.31 (s, 1H), 7.25 (d, *J* = 7.6 Hz, 2H); ¹³C NMR (CDCl₃, 100 MHz) δ 178.2, 159.1, 156.0, 151.6, 150.0, 134.9, 129.7, 126.7, 126.1, 125.8, 124.4, 121.1, 118.8, 115.7; HRMS (DART) *m/z* calcd for C₁₆H₁₁O₄

[M+H]⁺: 267.0657, found: 267,0654.



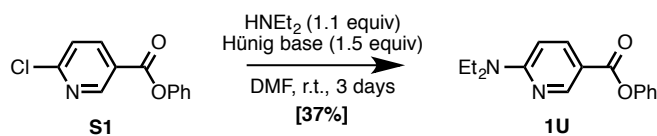
3-Methyl 5-phenyl pyridine-3,5-dicarboxylate (**1Z**)

Following the method B, purification by recrystallization from hexane afforded **1Z** as a white solid (570 mg, 44% yield; 5.0 mmol scale). ¹H NMR (CDCl₃, 400 MHz) δ 9.53 (d, *J* = 0.8 Hz, 1H), 9.44 (d, *J* = 2.0 Hz, 1H), 9.03 (dd, *J* = 2.0, 0.8 Hz, 1H), 7.46 (t, *J* = 8.0 Hz, 2H), 7.32 (t, *J* = 8.0 Hz, 1H), 7.24 (d, *J* = 8.0 Hz, 2H), 4.02 (s, 3H); ¹³C NMR (CDCl₃, 100 MHz) δ 164.8, 163.0, 154.7, 154.6, 150.3, 138.5, 129.6, 126.4, 126.1, 125.6, 121.4, 52.8; HRMS (DART) *m/z* calcd for C₁₄H₁₂NO₄ [M+H]⁺: 258.0766, found: 258.0770.



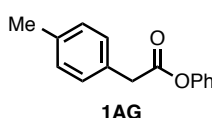
Phenyl 6-chloronicotinate (**S1**)

Following the method B, purification by recrystallization (hexane) afforded **S1** as a white solid (1.82 g, 79% yield; 10 mmol scale). ¹H NMR (CDCl₃, 400 MHz) δ 9.17 (d, *J* = 2.8 Hz, 1H), 8.39 (dd, *J* = 8.4, 2.8 Hz, 1H), 7.50 (d, *J* = 8.4 Hz, 1H), 7.46 (dd, *J* = 8.0, 7.6 Hz, 2H), 7.31 (t, *J* = 8.0 Hz, 1H), 7.22 (d, *J* = 7.6 Hz, 2H); ¹³C NMR (CDCl₃, 100 MHz) δ 163.0, 156.3, 151.6, 150.3, 140.0, 129.6, 126.4, 124.6, 124.4, 121.4; HRMS (DART) *m/z* calcd for C₁₂H₉ClNO₂ [M+H]⁺: 234.0322, found: 234.0318.



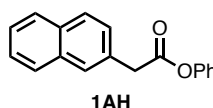
To a solution of phenyl 6-chloronicotinate (**S1**: 467 mg, 2.0 mmol) in DMF (4.0 mL) were added diethylamine (160.9 mg, 2.2 mmol, 1.1 equiv) and *N,N*-diisopropylethylamine (Hünig base: 510 mL, 3.0 mmol, 1.5 equiv). The mixture was stirred for 3 days at room temperature. The reaction was quenched with NH₄Cl aq and extracted four times with EtOAc. The combined organic layers were washed with brine, and then dried over Na₂SO₄. After filtration of the organic layer, the mixture was

concentrated *in vacuo*. Purification by flash column chromatography (hexane/EtOAc = 15:1 to 10:1) afforded **1U** as a white solid (198 mg, 37% yield). ¹H NMR (CDCl₃, 400 MHz) δ 8.96 (d, *J* = 2.0 Hz, 1H), 8.08 (dd, *J* = 9.2, 2.0 Hz, 1H), 7.40 (t, *J* = 8.0 Hz, 2H), 7.24 (t, *J* = 8.0 Hz, 1H), 7.19 (d, *J* = 8.0 Hz, 2H), 6.48 (d, *J* = 9.2 Hz, 1H), 3.59 (q, *J* = 7.2 Hz, 4H), 1.22 (t, *J* = 7.2 Hz, 6H); ¹³C NMR (CDCl₃, 100 MHz) δ 164.8, 159.5, 152.3, 151.0, 138.4, 129.3, 125.5, 121.8, 112.2, 104.4, 42.9, 12.8; HRMS (DART) *m/z* calcd for C₁₆H₁₉N₂O₂ [M+H]⁺: 271.1447, found: 271.1451.



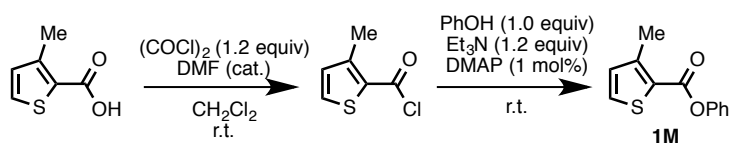
Phenyl 2-(*p*-tolyl)acetate (**1AG**)

Following the method B, purification by flash column chromatography (hexane/EtOAc = 20:1) afforded **1AG** as colorless oil (1.12 g, 99% yield; 5 mmol scale). ¹H NMR (CDCl₃, 400 MHz) δ 7.34 (t, *J* = 7.6 Hz, 2H), 7.27 (d, *J* = 8.0 Hz, 2H), 7.21 (t, *J* = 7.6 Hz, 1H), 7.16 (d, *J* = 8.0 Hz, 2H), 7.05 (d, *J* = 7.6 Hz, 2H), 3.81 (s, 2H), 2.35 (s, 3H); ¹³C NMR (CDCl₃, 100 MHz) δ 170.2, 150.8, 137.0, 130.4, 129.4, 129.3, 129.1, 125.8, 121.4, 41.0, 21.1; HRMS (ESI) *m/z* calcd for C₁₅H₁₄O₂Na [M+Na]⁺: 249.0886, found: 249.0876.



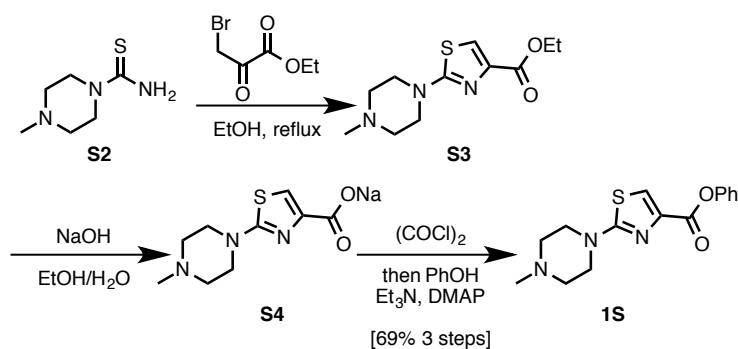
Phenyl 2-(naphthalen-2-yl)acetate (**1AH**)

Following the method B, purification by recrystallization (hexane) afforded **1AH** as a white solid (1.10 g, 76% yield; 5 mmol scale). ¹H NMR (CDCl₃, 400 MHz) δ 7.88–7.80 (m, 4H), 7.54–7.44 (m, 3H), 7.35 (dd, *J* = 8.0, 7.6 Hz, 2H), 7.21 (t, *J* = 7.6 Hz, 1H), 7.06 (d, *J* = 8.0 Hz, 2H), 4.02 (s, 2H); ¹³C NMR (CDCl₃, 100 MHz) δ 170.0, 150.7, 133.5, 132.6, 130.9, 129.4, 128.4, 128.1, 127.71, 127.67, 127.2, 126.3, 126.0, 125.9, 121.4, 41.6; HRMS (ESI) *m/z* calcd for C₁₈H₁₄O₂Na [M+Na]⁺: 285.0886, found: 285.0876.



Phenyl 3-methylthiophene-2-carboxylate (**1M**)

To a solution of 3-methylthiophene-2-carboxylic acid (713 mg, 5.0 mmol, 1.0 equiv) in CH_2Cl_2 (10 mL) were added oxalyl chloride (762 mg, 6.0 mmol, 1.2 equiv) and a portion of DMF. After stirring for 1.5 h at room temperature, phenol (470 mg, 5.0 mmol, 1.0 equiv) and *N,N*-dimethyl-4-aminopyridine (DMAP: 6.1 mg, 0.05 mmol, 1 mol%) were added to the mixture. Triethylamine (Et_3N : 470 mg, 6.0 mmol, 1.2 equiv) was slowly added to the mixture at 0 °C. After stirring the solution overnight, the reaction mixture was quenched with saturated NaHCO_3 aq and extracted three times with CH_2Cl_2 . The combined organic layer was dried over Na_2SO_4 , filtrated, and concentrated *in vacuo*. Purification by flash column chromatography (hexane/ EtOAc = 20:1) afforded **1M** as brown oil (990 mg, 91% yield). ^1H NMR (CDCl_3 , 400 MHz) δ 7.49 (d, J = 5.2 Hz, 1H), 7.42 (t, J = 8.0 Hz, 2H), 7.26 (t, J = 8.0 Hz, 1H), 7.21 (d, J = 8.0 Hz, 2H), 6.99 (d, J = 5.2 Hz, 1H), 2.61 (s, 3H); ^{13}C NMR (CDCl_3 , 100 MHz) δ 161.1, 150.5, 148.0, 131.9, 131.1, 129.4, 125.9, 125.6, 121.8, 16.1; HRMS (DART) m/z calcd for $\text{C}_{12}\text{H}_{11}\text{O}_2\text{S}$ $[\text{M}+\text{H}]^+$: 219.0480, found: 219.0483.



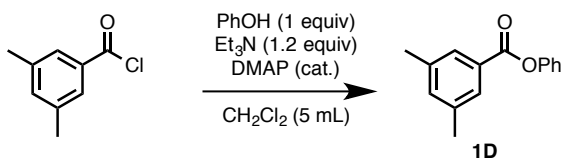
Phenyl 2-(4-methylpiperazin-1-yl)thiazole-4-carboxylate (**1S**)

A mixture of 4-methylpiperazine-1-carbothioamide (1.1 g, 6.7 mmol, 1.0 equiv) and ethyl 3-bromo-2-oxopropanoate (935 mL, 7.4 mmol, 1.1 equiv) in EtOH (10 mL) was refluxed overnight. After cooling to room temperature, the mixture was concentrated *in vacuo*. NaHCO_3 aq was added to the resulted solid and the mixture was extracted with Et_2O . The combined organic layer was dried over MgSO_4 , filtrated, and concentrated *in vacuo* to afford ethyl 2-(4-methylpiperazin-1-yl)thiazole-4-carboxylate (**S3**: 1.57 g, 91%

yield) as orange oil. **S3** was used without further purification.

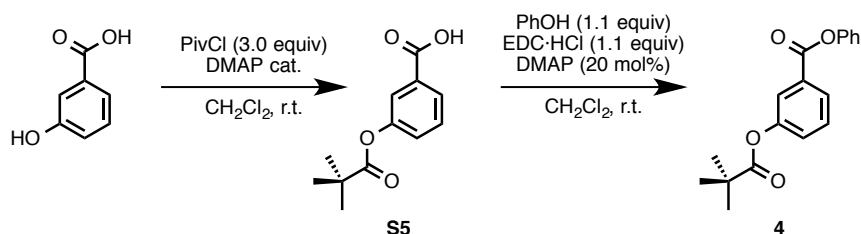
The obtained oil **S3** (1.57 g, 6.1 mmol) was treated with NaOH (270 mg, 6.7 mmol, 1.1 equiv) in EtOH/H₂O (10 mL/5 mL) at room temperature. After stirring overnight, the mixture was concentrated *in vacuo* to afford sodium 2-(4-methylpiperazin-1-yl)thiazole-4-carboxylate **S4** (1.53 g, quant.) as a yellow solid.

To a solution of the sodium carboxylate **S4** (1.53 g, 6.14 mmol) in CH₂Cl₂ (20 mL) were added oxalyl chloride (791 mL, 9.2 mmol, 1.5 equiv) and a portion of DMF. After stirring for 1.5 h, phenol (866 mg, 9.2 mmol, 1.5 equiv) and *N,N*-dimethyl-4-aminopyridine (DMAP: 10.0 mg, 0.05 mmol, 1 mol%) were added to the mixture. Then, triethylamine (Et₃N: 1.72 mL, 12 mmol, 2.0 equiv) was slowly added to the mixture at 0 °C. After stirring the solution overnight, the reaction mixture was quenched with saturated NaHCO₃aq and extracted three times with CH₂Cl₂. The combined organic layer was dried over Na₂SO₄, filtrated, and concentrated *in vacuo*. Purification by flash column chromatography (CHCl₃/MeOH = 20:1) and then preparative HPLC (H₂O/MeCN) afforded phenyl 2-(4-methylpiperazin-1-yl)thiazole-4-carboxylate **1S** as a brown solid (1.38 g, 74% yield). ¹H NMR (CDCl₃, 400 MHz) δ 7.67 (s, 1H), 7.40 (dd, *J* = 8.0, 7.6 Hz, 2H), 7.24 (t, *J* = 8.0 Hz, 1H), 7.19 (d, *J* = 7.6 Hz, 2H), 3.59 (t, *J* = 4.8 Hz, 4H), 2.53 (t, *J* = 4.8 Hz, 4H), 2.34 (s, 3H); ¹³C NMR (CDCl₃, 100 MHz) δ 170.9, 159.9, 150.7, 143.0, 129.4, 125.8, 121.7, 118.2, 54.1, 48.3, 46.1; HRMS (DART) *m/z* calcd for C₁₅H₁₈N₃O₂S [M+H]⁺: 304.1120, found: 304.1125.



To a solution of phenol (470 mg, 5.0 mmol, 1.0 equiv), DMAP (6.0 mg, 0.05 mmol, 1 mol%) and Et₃N (607 mg, 6.0 mmol, 1.2 equiv) in CH₂Cl₂ (5 mL) was slowly added 3,5-dimethylbenzoyl chloride (0.74 mL, 5.0 mmol, 1.0 equiv) at 0 °C. After stirring for 3 h, the reaction mixture was quenched with saturated NaHCO₃aq and extracted three times with CH₂Cl₂. The combined organic layer was dried over Na₂SO₄, filtrated, and concentrated *in vacuo*. Purification by flash column chromatography (hexane/EtOAc = 50:1) afforded **1D** as colorless liquid (1.13 g, quant). ¹H NMR (CDCl₃, 400 MHz) δ 7.83 (s, 2H), 7.43 (t, *J* = 8.4 Hz, 2H), 7.30–7.24 (m, 2H), 7.21 (d, *J* = 8.4 Hz, 2H), 2.41

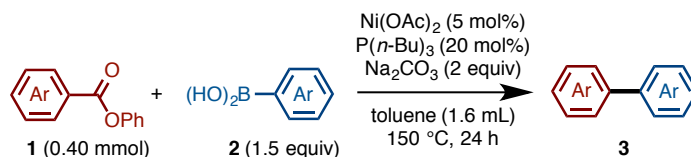
(s, 6H); ^{13}C NMR (CDCl_3 , 100 MHz) δ 165.5, 151.0, 138.3, 135.2, 129.5, 129.4, 127.9, 125.8, 121.7, 21.2; HRMS (DART) m/z calcd for $\text{C}_{15}\text{H}_{15}\text{O}_2$ $[\text{M}+\text{H}]^+$: 227.1072, found: 227.1075.



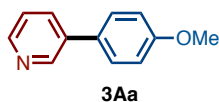
To a solution of 3-hydroxybenzoic acid (1.38 g, 10 mmol) and DMAP (12.0 mg, 0.1 mmol, 1 mol%) in pyridine (12 mL) was added pivaloyl chloride (3.62 g, 30 mmol, 3.0 equiv) at 0 °C. This solution was allowed to warm to room temperature and stirred for 1 h. To the mixture was carefully added water (30 mL) and stirred overnight at room temperature. This solution was extracted three times with CH_2Cl_2 . The combined organic layer was washed with 2.0M H_2SO_4 (20 mL) three times. The organic layer was dried over Na_2SO_4 and filtrated. The filtrate was concentrated *in vacuo* to afford 3-(pivaloyloxy)benzoic acid (**S5**: 2.15 g, 97% yield) as a white solid.

A mixture of **S5** (2.15 g, 9.7 mmol, 1.0 equiv), phenol (1.0 g, 10.7 mmol, 1.1 equiv), 1-(3-dimethylaminopropyl)-3-ethylcarbodiimide hydrochloride (EDC·HCl: 2.0 g, 10.7 mmol, 1.1 equiv), and *N,N*-dimethylaminopyridine (DMAP: 237 mg, 1.9 mmol, 0.2 equiv) in CH_2Cl_2 (20 mL) was stirred for 3 h at room temperature. After quenching the reaction with NaHCO_3aq , the mixture was extracted three times with CH_2Cl_2 . The combined organic layer was dried over Na_2SO_4 , filtrated, and then concentrated *in vacuo*. The residue was purified by flash column chromatography (hexane/EtOAc = 20:1) to afford phenyl 3-(pivaloyloxy)benzoate **4** as a white solid (2.56 g, 88% yield). ^1H NMR (CDCl_3 , 400 MHz) δ 8.07 (d, J = 8.0 Hz, 1H), 7.88 (s, 1H), 7.52 (t, J = 8.0 Hz, 1H), 7.43 (t, J = 8.0 Hz, 2H), 7.34 (d, J = 8.0 Hz, 1H), 7.27 (t, J = 8.0 Hz, 1H), 7.20 (d, J = 8.0 Hz, 2H), 1.36 (s, 9H); ^{13}C NMR (CDCl_3 , 100 MHz) δ 176.9, 164.3, 151.2, 150.8, 131.0, 129.54, 129.50, 127.4, 127.0, 126.0, 123.3, 121.6, 39.1, 27.1; HRMS (DART) m/z calcd for $\text{C}_{18}\text{H}_{19}\text{O}_4$ $[\text{M}+\text{H}]^+$: 299.1283, found: 299.1285.

4-3. Procedure for the Ni-Catalyzed Decarbonylative Cross-Coupling of 1 and 2

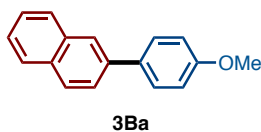


General Procedure: A 20-mL glass vessel equipped with J. Young[®] O-ring tap containing a magnetic stirring bar and $\text{Ni}(\text{OAc})_2 \cdot 4\text{H}_2\text{O}$ (5.0 mg, 0.020 mmol, 5 mol%) was dried with a heatgun under reduced pressure and filled with N_2 gas after cooling to room temperature. To this vessel was added phenyl arenecarboxylic acid phenyl ester **1** (0.40 mmol, 1.0 equiv), arylboronic acid **2** (0.60 mmol, 1.5 equiv), and Na_2CO_3 (84.8 mg, 0.8 mmol, 2.0 equiv). The vessel was vacuumed and refilled N_2 gas three times. To this was added $\text{P}(n\text{-Bu})_3$ (19.0 mL, 0.08 mmol, 20 mol%) and toluene (1.6 mL). The vessel was sealed with O-ring tap and then heated at $150\text{ }^\circ\text{C}$ for 24 h in an 8-well reaction block with stirring. After cooling the reaction mixture to room temperature, the mixture was passed through a short silica gel pad with EtOAc. The filtrate was concentrated and the residue was purified by flash column chromatography or PTLC to afford the corresponding cross-coupling product **3**.



3-(4-Methoxyphenyl)pyridine (**3Aa**)^[51]

Purification by flash column chromatography (hexane/ Et_2O = 2:1) afforded **3Aa** as a white solid (using 5 mol% catalyst, for 24 h; 69.7 mg, 95% yield; using 3 mol% catalyst, for 48 h; 73.4 mg, >99% yield). ^1H NMR (CDCl_3 , 400 MHz) δ 8.82 (d, J = 2.4 Hz, 1H), 8.55 (d, J = 4.8 Hz, 1H), 7.83 (dd, J = 8.0, 2.4 Hz, 1H), 7.53 (d, J = 9.2 Hz, 2H), 7.34 (dd, J = 8.0, 4.8 Hz, 1H), 7.02 (d, J = 9.2 Hz, 2H), 3.87 (s, 3H); ^{13}C NMR (CDCl_3 , 100 MHz) δ 159.7, 147.9, 147.8, 136.2, 133.8, 130.2, 128.1, 123.4, 114.5, 55.3; HRMS (ESI) m/z calcd for $\text{C}_{12}\text{H}_{12}\text{NO}$ [$\text{M}+\text{H}$]⁺: 186.0913, found: 186.0912.



2-(4-Methoxyphenyl)naphthalene (**3Ba**)^[41]

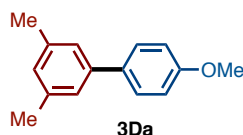
Purification by flash column chromatography (hexane/CHCl₃ = 5:1) afforded **3Ba** as a white solid (84.9 mg, 91% yield). ¹H NMR (CDCl₃, 400 MHz) δ 7.98 (s, 1H), 7.91–7.82 (m, 3H), 7.71 (dd, *J* = 8.4, 1.6 Hz, 1H), 7.65 (d, *J* = 8.8 Hz, 2H), 7.52–7.42 (m, 2H), 7.01 (d, *J* = 8.8 Hz, 2H), 3.86 (s, 3H); ¹³C NMR (CDCl₃, 100 MHz) δ 159.2, 138.1, 133.7, 133.6, 132.3, 128.4, 128.3, 128.0, 127.6, 126.2, 125.6, 125.4, 125.0, 114.3, 55.4; HRMS (DART) *m/z* calcd for C₁₇H₁₅O [M+H]⁺: 235.1123, found: 235.1120.



3Ca

1-(4-Methoxyphenyl)naphthalene (**3Ca**)^[52]

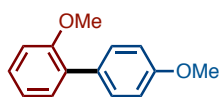
Purification by flash column chromatography (hexane/EtOAc = 100:1) afforded **3Ca** as a white solid (90.2 mg, 96% yield). ¹H NMR (CDCl₃, 400 MHz) δ 7.92 (d, *J* = 8.4 Hz, 1H), 7.86 (d, *J* = 8.0 Hz, 1H), 7.80 (d, *J* = 8.0 Hz, 1H), 7.85–7.35 (m, 6H), 6.99 (d, *J* = 8.8 Hz, 2H), 3.83 (s, 3H); ¹³C NMR (CDCl₃, 100 MHz) δ 158.9, 139.9, 133.8, 133.1, 131.8, 131.1, 128.2, 127.3, 126.9, 126.0, 125.9, 125.7, 125.4, 113.7, 55.3; HRMS (DART) *m/z* calcd for C₁₇H₁₅O [M+H]⁺: 235.1123, found: 235.1122.



3Da

4'-Methoxy-3,5-dimethyl-1,1'-biphenyl (**3Da**)^[53]

Purification by flash column chromatography (hexane/EtOAc = 100:1) afforded **3Da** as colorless liquid (63.8 mg, 75% yield). ¹H NMR (CDCl₃, 400 MHz) δ 7.49 (d, *J* = 9.2 Hz, 2H), 7.16 (s, 2H), 6.97–6.91 (m, 3H), 3.81 (s, 3H), 2.35 (s, 6H); ¹³C NMR (CDCl₃, 100 MHz) δ 159.0, 140.8, 138.1, 133.9, 128.3, 128.1, 124.6, 114.0, 55.2, 21.4; HRMS (DART) *m/z* calcd for C₁₅H₁₇O [M+H]⁺: 213.1279, found: 213.1277.

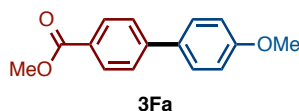


3Ea

2,4'-Dimethoxy-1,1'-biphenyl (**3Ea**)^[54]

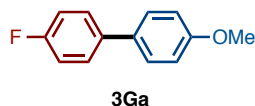
Purification by PTLC (hexane/EtOAc = 20:1) afforded **3Ea** as colorless oil (66.1 mg,

77% yield). ^1H NMR (CDCl_3 , 400 MHz) δ 7.46 (d, $J = 8.8$ Hz, 2H), 7.32–7.25 (m, 2H), 7.00 (dd, $J = 8.0, 7.2$ Hz, 1H), 6.97–6.91 (m, 3H), 3.82 (s, 3H), 3.79 (s, 3H); ^{13}C NMR (CDCl_3 , 100 MHz) δ 158.6, 156.4, 130.8, 130.63, 130.55, 130.2, 128.1, 120.8, 113.4, 111.1, 55.5, 55.2; HRMS (DART) m/z calcd for $\text{C}_{14}\text{H}_{15}\text{O}_2$ $[\text{M}+\text{H}]^+$: 215.1072, found: 215.1076.



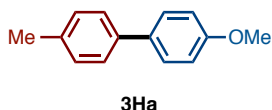
Methyl 4'-methoxy-[1,1'-biphenyl]-4-carboxylate (**3Fa**)^[55]

Purification by flash column chromatography (hexane/ $\text{CHCl}_3 = 4:1$ to $1:1$) afforded **3Fa** as a white solid (85.0 mg, 88% yield). ^1H NMR (CDCl_3 , 400 MHz) δ 8.07 (d, $J = 8.4$ Hz, 2H), 7.61 (d, $J = 8.4$ Hz, 2H), 7.56 (d, $J = 8.4$ Hz, 2H), 6.98 (d, $J = 8.4$ Hz, 2H), 3.92 (s, 3H), 3.85 (s, 3H); ^{13}C NMR (CDCl_3 , 100 MHz) δ 167.0, 159.8, 145.1, 132.3, 130.0, 128.3, 128.2, 126.4, 114.3, 55.3, 52.0; HRMS (DART) m/z calcd for $\text{C}_{15}\text{H}_{15}\text{O}_3$ $[\text{M}+\text{H}]^+$: 243.1021, found: 243.1019.



4-Fluoro-4'-methoxy-1,1'-biphenyl (**3Ga**)^[51]

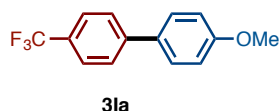
Purification by flash column chromatography (hexane/ $\text{CHCl}_3 = 10:1$ to $4:1$) afforded **3Ga** as a white solid (68.9 mg, 85% yield). ^1H NMR (CDCl_3 , 400 MHz) δ 7.51–7.43 (m, 4H), 7.12–7.06 (m, 2H), 6.97 (d, $J = 8.8$ Hz, 2H), 3.86 (s, 3H); ^{13}C NMR (CDCl_3 , 100 MHz) δ 162.1 (d, $J_{\text{C-F}} = 249$ Hz), 159.1, 136.9 (d, $J_{\text{C-F}} = 4.0$ Hz), 132.8, 128.2 (d, $J_{\text{C-F}} = 8.0$ Hz), 128.0, 115.5 (d, $J_{\text{C-F}} = 21$ Hz), 114.2, 55.3; HRMS (DART) m/z calcd for $\text{C}_{13}\text{H}_{12}\text{FO}$ $[\text{M}+\text{H}]^+$: 203.0872, found: 203.0870.



4-Methoxy-4'-methyl-1,1'-biphenyl (**3Ha**)^[56]

Purification by flash column chromatography (hexane/ $\text{CHCl}_3 = 10:1$ to $4:1$) afforded **3Ha** as a white solid (70.3 mg, 89% yield). ^1H NMR (CDCl_3 , 400 MHz) δ 7.50 (d, $J =$

8.8 Hz, 2H), 7.44 (d, $J = 8.0$ Hz, 2H), 7.22 (d, $J = 8.0$ Hz, 2H), 6.95 (d, $J = 8.8$ Hz, 2H), 3.84 (s, 3H), 2.38 (s, 3H); ^{13}C NMR (CDCl_3 , 100 MHz) δ 158.9, 137.9, 136.3, 133.7, 129.4, 127.9, 126.6, 114.1, 55.3, 21.0; HRMS (DART) m/z calcd for $\text{C}_{14}\text{H}_{15}\text{O}$ $[\text{M}+\text{H}]^+$: 199.1123, found: 199.1121.



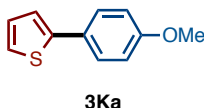
4-Methoxy-4'-(trifluoromethyl)-1,1'-biphenyl (**3Ia**)^[51]

The reaction was conducted at 160 °C. Purification by flash column chromatography (hexane/ $\text{CHCl}_3 = 4:1$) afforded **3Ia** as a white solid (99.5 mg, 99% yield). ^1H NMR (CDCl_3 , 400 MHz) δ 7.67–7.62 (m, 4H), 7.53 (d, $J = 8.8$ Hz, 2H), 6.99 (d, $J = 8.8$ Hz, 2H), 3.85 (s, 3H); ^{13}C NMR (CDCl_3 , 100 MHz) δ 159.8, 144.3, 132.1, 128.7 (q, $J_{\text{C-F}} = 33$ Hz), 128.3, 126.8, 125.7 (q, $J_{\text{C-F}} = 4$ Hz), 124.4 (q, $J_{\text{C-F}} = 276$ Hz), 114.4, 55.3; HRMS (DART) m/z calcd for $\text{C}_{14}\text{H}_{12}\text{F}_3\text{O}$ $[\text{M}+\text{H}]^+$: 253.0840, found: 253.0838.



4'-Methoxy-3-methyl-1,1'-biphenyl (**3Ja**)^[57]

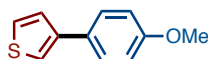
Purification by PTLC (hexane/ $\text{EtOAc} = 20:1$) afforded **3Ja** as a white solid (57.8 mg, 73% yield). ^1H NMR (CDCl_3 , 400 MHz) δ 7.51 (d, $J = 9.2$ Hz, 2H), 7.38–7.25 (m, 3H), 7.10 (d, $J = 7.6$ Hz, 1H), 6.94 (d, $J = 9.2$ Hz, 2H), 3.80 (s, 3H), 2.39 (s, 3H); ^{13}C NMR (CDCl_3 , 100 MHz) δ 159.0, 140.7, 138.2, 133.8, 128.6, 128.1, 127.5, 127.4, 123.8, 114.1, 55.2, 21.5; HRMS (DART) m/z calcd for $\text{C}_{14}\text{H}_{15}\text{O}$ $[\text{M}+\text{H}]^+$: 199.1123, found: 199.1120.



2-(4-Methoxyphenyl)thiophene (**3Ka**)^[53]

Purification by PTLC (hexane/ $\text{EtOAc} = 30:1$) afforded **3Ka** as a white solid (59.3 mg, 78% yield). ^1H NMR (CDCl_3 , 400 MHz) δ 7.53 (d, $J = 8.4$ Hz, 2H), 7.21–7.16 (m, 2H),

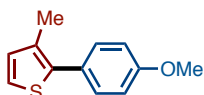
7.03 (d, $J = 4.4$ Hz, 1H), 6.89 (d, $J = 8.4$ Hz, 2H), 3.81 (s, 3H); ^{13}C NMR (CDCl_3 , 100 MHz) δ 159.1, 144.3, 127.9, 127.23, 127.16, 123.8, 122.0, 114.2, 55.3; HRMS (ESI) m/z calcd for $\text{C}_{11}\text{H}_{11}\text{OS}$ $[\text{M}+\text{H}]^+$: 191.0525, found: 191.0522.



3La

3-(4-Methoxyphenyl)thiophene (**3La**)^[58]

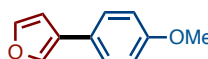
Purification by flash column chromatography (hexane/EtOAc = 100:1) afforded **3La** as a white solid (50.6 mg, 66% yield). ^1H NMR (CDCl_3 , 400 MHz) δ 7.52 (d, $J = 7.6$ Hz, 2H), 7.38–7.30 (m, 3H), 6.92 (d, $J = 7.6$ Hz, 2H), 3.84 (s, 3H); ^{13}C NMR (CDCl_3 , 100 MHz) δ 158.8, 142.0, 128.7, 127.5, 126.2, 126.0, 118.9, 114.1, 55.3; HRMS (DART) m/z calcd for $\text{C}_{11}\text{H}_{10}\text{OS}$ $[\text{M}+\text{H}]^+$: 191.0531, found: 191.0533.



3Ma

2-(4-Methoxyphenyl)-3-methylthiophene (**3Ma**)

Purification by flash column chromatography (hexane/EtOAc = 100:1) afforded **3Ma** as colorless liquid (49.4 mg, 60% yield). ^1H NMR (CDCl_3 , 400 MHz) δ 7.37 (d, $J = 7.6$ Hz, 2H), 7.13 (d, $J = 5.6$ Hz, 1H), 6.93 (d, $J = 7.6$ Hz, 2H), 6.88 (d, $J = 5.6$ Hz, 1H), 3.81 (s, 3H), 2.28 (s, 3H); ^{13}C NMR (CDCl_3 , 100 MHz) δ 158.8, 137.6, 132.5, 130.9, 130.2, 127.1, 122.6, 113.9, 55.2, 14.8; HRMS (ESI) m/z calcd for $\text{C}_{12}\text{H}_{13}\text{OS}$ $[\text{M}+\text{H}]^+$: 205.0682, found: 205.0680

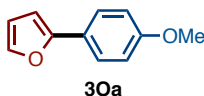


3Na

3-(4-Methoxyphenyl)furan (**3Na**)^[53]

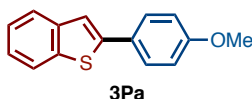
Purification by flash column chromatography (hexane/EtOAc = 100:1) afforded **3Na** as a white solid (46.9 mg, 67% yield). ^1H NMR (CDCl_3 , 400 MHz) δ 7.65 (d, $J = 1.6$ Hz, 1H), 7.44 (t, $J = 1.6$ Hz, 1H), 7.40 (d, $J = 8.8$ Hz, 2H), 6.91 (d, $J = 8.8$ Hz, 2H), 6.64 (d, $J = 1.6$ Hz, 1H), 3.81 (s, 3H); ^{13}C NMR (CDCl_3 , 100 MHz) δ 158.7, 143.5, 137.6, 127.0, 126.0, 125.0, 114.2, 108.8, 55.3; HRMS (ESI) m/z calcd for $\text{C}_{11}\text{H}_{11}\text{O}_2$ $[\text{M}+\text{H}]^+$:

175.0754, found: 175.0752.



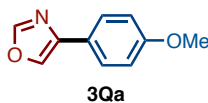
2-(4-Methoxyphenyl)furan (**30a**)^[59]

The reaction was conducted using 1.2 equiv of Na₂CO₃. Purification by flash column chromatography (hexane/EtOAc = 100:1) afforded **30a** as a white solid (51.0 mg, 73% yield). ¹H NMR (CDCl₃, 400 MHz) δ 7.60 (d, *J* = 8.8 Hz, 2H), 7.41 (d, *J* = 1.6 Hz, 1H), 6.91 (d, *J* = 8.8 Hz, 2H), 6.50 (d, *J* = 3.2 Hz, 1H), 6.43 (dd, *J* = 3.2, 1.6 Hz, 1H), 3.81 (s, 3H); ¹³C NMR (CDCl₃, 100 MHz) δ 159.0, 154.0, 141.3, 125.2, 124.0, 114.0, 111.5, 103.3, 55.3; HRMS (ESI) *m/z* calcd for C₁₁H₁₁O₂ [M+H]⁺: 175.0754, found: 175.0752.



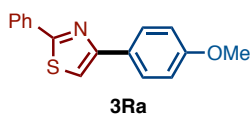
2-(4-Methoxyphenyl)benzo[*b*]thiophene (**3Pa**)^[60]

Purification by precipitation of the crude mixture in Et₂O and filtration of the suspension afforded **3Pa** as a white solid (91.7 mg, 95% yield). ¹H NMR (CDCl₃, 400 MHz) δ 7.80 (d, *J* = 8.0 Hz, 1H), 7.74 (d, *J* = 7.2 Hz, 1H), 7.64 (d, *J* = 8.8 Hz, 2H), 7.42 (s, 1H), 7.36–7.25 (m, 2H), 6.96 (d, *J* = 8.8 Hz, 2H), 3.85 (s, 3H); ¹³C NMR (CDCl₃, 100 MHz) δ 159.8, 144.1, 140.9, 139.1, 127.7, 127.0, 124.4, 123.9, 123.2, 122.2, 118.2, 114.3, 55.4; HRMS (ESI) *m/z* calcd for C₁₅H₁₃OS [M+H]⁺: 241.0682, found: 241.0678.



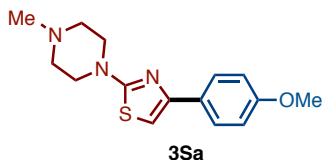
4-(4-Methoxyphenyl)oxazole (**3Qa**)^[61]

Purification by PTLC (hexane/EtOAc = 5:1) afforded **3Qa** as a white solid (35.5 mg, 50% yield). ¹H NMR (CDCl₃, 400 MHz) δ 7.91 (s, 1H), 7.86 (s, 1H), 7.68 (d, *J* = 8.4 Hz, 2H), 6.95 (d, *J* = 8.4 Hz, 2H), 3.85 (s, 3H); ¹³C NMR (CDCl₃, 100 MHz) δ 159.6, 151.2, 140.2, 132.6, 126.9, 123.4, 114.2, 55.3; HRMS (ESI) *m/z* calcd for C₁₀H₁₀NO₂ [M+H]⁺: 176.0706, found: 176.0704.



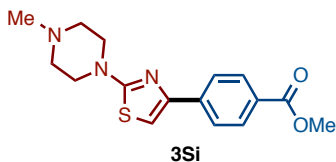
4-(4-Methoxyphenyl)-2-phenylthiazole (**3Ra**)^[62]

The reaction was conducted at 160 °C. Purification by PTLC (hexane/CHCl₃ = 1:1) afforded **3Ra** as a white solid (86.8 mg, 81% yield). ¹H NMR (CDCl₃, 400 MHz) δ 8.03 (dd, *J* = 8.4, 2.0 Hz, 2H), 7.92 (d, *J* = 8.4 Hz, 2H), 7.47–7.38 (m, 3H), 7.31 (s, 1H), 6.96 (d, *J* = 7.2 Hz, 2H), 3.84 (s, 3H); ¹³C NMR (CDCl₃, 100 MHz) δ 167.6, 159.6, 156.0, 133.8, 129.9, 128.9, 127.7, 127.5, 126.5, 114.0, 110.9, 55.3; HRMS (DART) *m/z* calcd for C₁₆H₁₄NOS [M+H]⁺: 268.0796, found: 268.0795.



4-(4-Methoxyphenyl)-2-(4-methylpiperazin-1-yl)thiazole (**3Sa**)

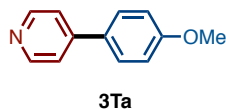
Purification by PTLC (CHCl₃/MeOH = 50:1) afforded **3Sa** as a yellow solid (54.5 mg, 47% yield). ¹H NMR (CDCl₃, 400 MHz) δ 7.76 (d, *J* = 8.4 Hz, 2H), 6.90 (d, *J* = 8.4 Hz, 2H), 6.62 (s, 1H), 3.82 (s, 3H), 3.56 (t, *J* = 5.2 Hz, 4H), 2.54 (t, *J* = 5.2 Hz, 4H), 2.35 (s, 3H); ¹³C NMR (CDCl₃, 100 MHz) δ 170.9, 159.2, 151.6, 128.1, 127.3, 113.8, 99.6, 55.2, 54.5, 48.2, 46.2; HRMS (DART) *m/z* calcd for C₁₅H₂₀N₃OS [M+H]⁺: 290.1327, found: 290.1329.



Methyl 4-(2-(4-methylpiperazin-1-yl)thiazol-4-yl)benzoate (**3Si**)

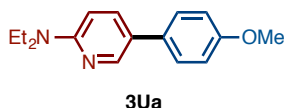
The reaction was conducted at 160 °C. Purification by PTLC (CHCl₃/MeOH = 50:1) afforded **3Si** as a brown solid (63.2 mg, 51% yield). ¹H NMR (CDCl₃, 400 MHz) δ 8.03 (d, *J* = 8.4 Hz, 2H), 7.90 (d, *J* = 8.4 Hz, 2H), 6.91 (s, 1H), 3.92 (s, 3H), 3.59 (t, *J* = 5.2 Hz, 4H), 2.55 (t, *J* = 5.2 Hz, 4H), 2.36 (s, 3H); ¹³C NMR (CDCl₃, 100 MHz) δ 171.0, 167.0, 150.8, 139.1, 129.9, 128.8, 125.8, 103.7, 54.2, 52.0, 48.3, 46.2; HRMS (DART)

m/z calcd for $C_{16}H_{20}N_3O_2S$ $[M+H]^+$: 318.1276, found: 318.1275.



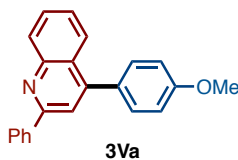
4-(4-Methoxyphenyl)pyridine (**3Ta**)^[63]

The reaction was conducted using 1.5 equiv of Et_3N instead of Na_2CO_3 . Purification by flash column chromatography (hexane/ Et_2O = 1:1) afforded **3Ta** as a white solid (69.7 mg, 94% yield). 1H NMR ($CDCl_3$, 600 MHz) δ 8.62 (d, J = 6.4 Hz, 2H), 7.59 (d, J = 8.4 Hz, 2H), 7.46 (d, J = 6.4 Hz, 2H), 7.00 (d, J = 8.4 Hz, 2H), 3.85 (s, 3H); ^{13}C NMR ($CDCl_3$, 150 MHz) δ 160.5, 150.1, 147.7, 130.3, 128.1, 121.0, 114.5, 55.3; HRMS (ESI) m/z calcd for $C_{12}H_{12}NO$ $[M+H]^+$: 186.0913, found: 186.0910.



N,N-Diethyl-5-(4-methoxyphenyl)pyridin-2-amine (**3Ua**)

Purification by PTLC (hexane/ $EtOAc$ = 10:1) and then GPC afforded **3Ua** as a white solid (64.3 mg, 63% yield). 1H NMR ($CDCl_3$, 400 MHz) δ 8.37 (d, J = 2.4 Hz, 1H), 7.60 (dd, J = 9.2, 2.4 Hz, 1H), 7.41 (d, J = 9.2 Hz, 2H), 6.95 (d, J = 9.2 Hz, 2H), 6.51 (d, J = 9.2 Hz, 1H), 3.82 (s, 3H), 3.52 (q, J = 7.2 Hz, 4H), 1.20 (t, J = 7.2 Hz, 6H); ^{13}C NMR ($CDCl_3$, 100 MHz) δ 158.4, 156.4, 145.9, 135.5, 131.4, 126.9, 123.6, 114.2, 105.3, 55.3, 42.5, 13.0; HRMS (DART) m/z calcd for $C_{16}H_{21}N_2O$ $[M+H]^+$: 257.1654, found: 257.1658.



4-(4-Methoxyphenyl)-2-phenylquinoline (**3Va**)^[64]

The reaction was conducted using 1.5 equiv of Et_3N instead of Na_2CO_3 . Purification by flash column chromatography (hexane/ $EtOAc$ = 30:1) afforded **3Va** as a white solid (125.6 mg, >99% yield). 1H NMR ($CDCl_3$, 600 MHz) δ 8.23 (d, J = 8.4 Hz, 1H), 8.18 (d, J = 7.2 Hz, 2H), 7.94 (d, J = 8.4 Hz, 1H), 7.79 (s, 1H), 7.71 (td, J = 8.4, 1.2 Hz, 1H),

7.54–7.42 (m, 6H), 7.07, (d, $J = 8.4$ Hz, 2H), 3.90 (s, 3H); ^{13}C NMR (CDCl_3 , 150 MHz) δ 159.8, 156.9, 148.9, 148.8, 139.7, 130.8, 130.6, 130.1, 129.4, 129.2, 128.8, 127.5, 126.2, 125.9, 125.6, 119.3, 114.0, 55.4; HRMS (DART) m/z calcd for $\text{C}_{22}\text{H}_{18}\text{NO}$ $[\text{M}+\text{H}]^+$: 312.1388, found: 312.1389.



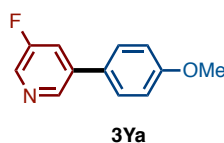
3-(4-Methoxyphenyl)quinoline (**3Wa**)^[54]

Purification by PTLC (hexane/EtOAc = 5:1) afforded **3Wa** as a white solid (98.7 mg, >99% yield). ^1H NMR (CDCl_3 , 400 MHz) δ 9.16 (d, $J = 2.4$ Hz, 1H), 8.21 (d, $J = 2.4$ Hz, 1H), 8.12 (d, $J = 8.4$ Hz, 1H), 7.83 (d, $J = 8.4$ Hz, 1H), 7.68 (dd, $J = 8.4, 7.8$ Hz, 1H), 7.63 (d, $J = 9.2$ Hz, 2H), 7.54 (dd, $J = 8.4, 7.8$ Hz, 1H), 7.03 (d, $J = 9.2$ Hz, 2H), 3.85 (s, 3H); ^{13}C NMR (CDCl_3 , 100 MHz) δ 159.7, 149.8, 146.9, 133.3, 132.3, 130.2, 129.1, 129.0, 128.4, 128.0, 127.8, 126.8, 114.6, 55.3; HRMS (ESI) m/z calcd for $\text{C}_{16}\text{H}_{14}\text{NO}$ $[\text{M}+\text{H}]^+$: 236.1070, found: 236.1073.



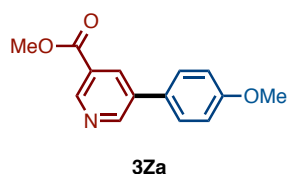
5-(4-Methoxyphenyl)-2-(trifluoromethyl)pyridine (**3Xa**)

The reaction was conducted using 1.5 equiv of Et_3N instead of Na_2CO_3 . Purification by flash column chromatography (hexane/EtOAc = 10:1) afforded **3Xa** as a white solid (89 mg, 88% yield). ^1H NMR (CDCl_3 , 400 MHz) δ 8.90 (s, 1H), 7.98 (d, $J = 8.4$ Hz, 1H), 7.71 (d, $J = 8.4$ Hz, 1H), 7.54 (d, $J = 9.0$ Hz, 2H), 7.03 (d, $J = 9.0$ Hz, 2H), 3.87 (s, 3H); ^{13}C NMR (CDCl_3 , 100 MHz) δ 160.4, 148.0, 146.0 (q, $J_{\text{C-F}} = 35$ Hz), 139.0, 134.7, 128.6, 128.4, 121.7 (q, $J_{\text{C-F}} = 275$ Hz), 120.3, 114.8, 55.3; HRMS (DART) m/z calcd for $\text{C}_{13}\text{H}_{11}\text{F}_3\text{NO}$ $[\text{M}+\text{H}]^+$: 254.0793, found: 254.0790.



3-Fluoro-5-(4-methoxyphenyl)pyridine (**3Ya**)

Purification by PTLC (hexane/EtOAc = 4:1) afforded **3Ya** as a white solid (75.2 mg, 92% yield). ¹H NMR (CDCl₃, 400 MHz) δ 8.62 (s, 1H), 8.39 (s, 1H), 7.54–7.47 (m, 3H), 6.99 (d, *J* = 8.8 Hz, 2H), 3.84 (s, 3H); ¹³C NMR (CDCl₃, 100 MHz) δ 160.0, 159.6 (d, *J*_{C-F} = 260 Hz), 143.6 (d, *J*_{C-F} = 4 Hz), 137.7 (d, *J*_{C-F} = 4 Hz), 135.7 (d, *J*_{C-F} = 24 Hz), 128.5, 128.2, 120.2 (d, *J*_{C-F} = 19 Hz), 114.5, 55.2; HRMS (ESI) *m/z* calcd for C₁₂H₁₁FNO [M+H]⁺: 204.0819, found: 204.0820.



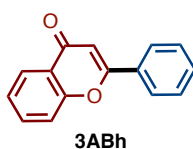
Methyl 5-(4-methoxyphenyl)nicotinate (**3Za**)

The reaction was conducted using 1.2 equiv of Na₂CO₃. Purification by flash column chromatography (hexane/EtOAc = 4:1) afforded **3Za** as a white solid (85.8 mg, 88% yield). ¹H NMR (CDCl₃, 400 MHz) δ 9.14 (s, 1H), 8.96 (d, *J* = 2.0 Hz, 1H), 8.43 (d, *J* = 2.0 Hz, 1H), 7.56 (d, *J* = 8.0 Hz, 2H), 7.02 (d, *J* = 8.0 Hz, 2H), 3.98 (s, 3H), 3.86 (s, 3H); ¹³C NMR (CDCl₃, 100 MHz) δ 165.8, 160.0, 151.3, 148.6, 135.9, 134.5, 128.8, 128.2, 125.8, 114.6, 55.3, 52.4; HRMS (DART) *m/z* calcd for C₁₄H₁₄NO₃ [M+H]⁺: 244.0974, found: 244.0971.



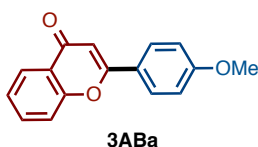
2-Methoxy-3-(4-methoxyphenyl)pyridine (**3AAa**)^[65]

Purification by PTLC (hexane/EtOAc = 10:1) afforded **3AAa** as a white solid (72.4 mg, 84% yield). ¹H NMR (CDCl₃, 400 MHz) δ 8.12 (dd, *J* = 4.8, 1.2 Hz, 1H), 7.57 (dd, *J* = 8.0, 1.2 Hz, 1H), 7.50 (d, *J* = 8.0 Hz, 2H), 6.99–6.92 (m, 3H), 3.97 (s, 3H), 3.83 (s, 3H); ¹³C NMR (CDCl₃, 100 MHz) δ 160.8, 159.0, 145.1, 138.1, 130.2, 129.0, 124.3, 117.1, 113.6, 55.2, 53.5; HRMS (ESI) *m/z* calcd for C₁₃H₁₄NO₂ [M+H]⁺: 216.1019, found: 216.1020.



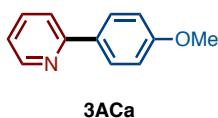
2-Phenyl-4*H*-chromen-4-one (**3ABh**)^[66]

Purification by flash column chromatography (hexane/EtOAc = 6:1) afforded **3ABh** as a white solid (80.0 mg, 90% yield). ¹H NMR (CDCl₃, 400 MHz) δ 8.22 (d, *J* = 8.0 Hz, 1H), 7.91 (d, *J* = 7.6 Hz, 2H), 7.68 (dd, *J* = 8.0, 7.6 Hz, 1H), 7.60–7.46 (m, 4H), 7.40 (dd, *J* = 8.0, 7.6 Hz, 1H), 6.81 (s, 1H); ¹³C NMR (CDCl₃, 100 MHz) δ 178.3, 163.2, 156.1, 133.7, 131.6, 131.5, 128.9, 126.2, 125.6, 125.1, 123.8, 118.0, 107.5; HRMS (ESI) *m/z* calcd for C₁₅H₁₁O [M+H]⁺: 223.0754, found: 223.0756.



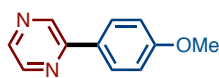
2-(4-Methoxyphenyl)-4*H*-chromen-4-one (**3ABa**)^[66]

Purification by PTLC (hexane/Et₂O = 1:1, hexane/EtOAc = 3:1, and then CHCl₃) afforded **3ABa** as a white solid (100.8 mg, >99% yield). ¹H NMR (CDCl₃, 400 MHz) δ 8.21 (d, *J* = 7.6 Hz, 1H), 7.86 (d, *J* = 8.0 Hz, 2H), 7.66 (dd, *J* = 7.6, 7.2 Hz, 1H), 7.52 (d, *J* = 7.6 Hz, 1H), 7.39 (dd, *J* = 7.6, 7.2 Hz, 1H), 6.99 (d, *J* = 8.0 Hz, 2H), 6.72 (s, 1H), 3.86 (s, 3H); ¹³C NMR (CDCl₃, 100 MHz) δ 178.2, 163.3, 162.3, 156.1, 133.5, 127.9, 125.5, 125.0, 123.9, 117.9, 114.4, 106.1, 55.4; HRMS (DART) *m/z* calcd for C₁₆H₁₃O₃ [M+H]⁺: 253.0865, found: 253.0861.



2-(4-Methoxyphenyl)pyridine (**3ACa**)^[67]

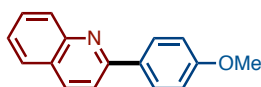
Purification by flash column chromatography (hexane/Et₂O = 5:1 to 7:3) afforded **3ACa** as a white solid (9.0 mg, 12% yield). ¹H NMR (CDCl₃, 400 MHz) δ 8.66 (d, *J* = 4.4 Hz, 1H), 7.95 (d, *J* = 8.4 Hz, 2H), 7.75–7.64 (m, 2H), 7.17 (dd, *J* = 7.2, 4.4 Hz, 1H), 7.00 (d, *J* = 8.4 Hz, 2H), 3.87 (s, 3H); ¹³C NMR (CDCl₃, 100 MHz) δ 160.5, 157.1, 149.5, 136.6, 132.0, 128.1, 121.4, 119.8, 114.1, 55.3; HRMS (ESI) *m/z* calcd for C₁₂H₁₂NO [M+H]⁺: 186.0913, found: 186.0909.



3ADa

2-(4-Methoxyphenyl)pyrazine (**3ADa**)^[68]

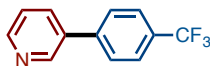
Purification by flash column chromatography (hexane/Et₂O = 1:1) afforded **3ADa** as a white solid (17.0 mg, 23% yield). ¹H NMR (CDCl₃, 400 MHz) δ 8.98 (s, 1H), 8.58 (d, *J* = 2.4 Hz, 1H), 8.44 (d, *J* = 2.4 Hz, 1H), 7.98 (d, *J* = 7.2 Hz, 2H), 7.03 (d, *J* = 7.2 Hz, 2H), 3.88 (s, 3H); ¹³C NMR (CDCl₃, 100 MHz) δ 161.1, 152.5, 144.0, 142.1, 141.6, 128.8, 128.3, 114.4, 55.4; HRMS (ESI) *m/z* calcd for C₁₁H₁₁N₂O [M+H]⁺: 187.0866, found: 187.0864.



3AEa

2-(4-Methoxyphenyl)quinoline (**3AEa**)^[69]

Purification by flash column chromatography (hexane/EtOAc = 20:1) afforded **3AEa** as a white solid (34.3 mg, 36% yield). ¹H NMR (CDCl₃, 400 MHz) δ 8.20–8.11 (m, 4H), 7.83 (d, *J* = 8.8 Hz, 1H), 7.80 (d, *J* = 8.8 Hz, 1H), 7.71 (td, *J* = 7.2, 1.2 Hz, 1H), 7.50 (td, *J* = 7.2, 1.2 Hz, 1H), 7.05 (d, *J* = 9.2 Hz, 2H), 3.89 (s, 3H); ¹³C NMR (CDCl₃, 100 MHz) δ 160.8, 156.9, 148.3, 136.6, 132.2, 129.6, 129.5, 128.9, 127.4, 126.9, 125.9, 118.5, 114.2, 55.4; HRMS (ESI) *m/z* calcd for C₁₆H₁₄NO [M+H]⁺: 236.1070, found: 236.1078.

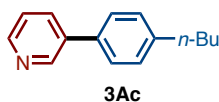


3Ab

3-(4-(Trifluoromethyl)phenyl)pyridine (**3Ab**)^[70]

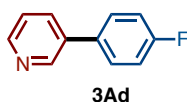
Purification by flash column chromatography (hexane/Et₂O = 2:1) afforded **3Ab** as a white solid (64.5 mg, 72% yield). ¹H NMR (CDCl₃, 400 MHz) δ 8.87 (s, 1H), 8.66 (d, *J* = 4.0 Hz, 1H), 7.89 (d, *J* = 8.0 Hz, 1H), 7.74 (d, *J* = 8.8 Hz, 2H), 7.68 (d, *J* = 8.8 Hz, 2H), 7.41 (dd, *J* = 8.0, 4.0 Hz, 1H); ¹³C NMR (CDCl₃, 100 MHz) δ 149.3, 148.3, 141.3, 135.2, 134.4, 130.2 (q, *J*_{C-F} = 32 Hz), 127.4, 126.0 (q, *J*_{C-F} = 4.0 Hz), 124.0 (q, *J*_{C-F} = 277 Hz), 123.6; HRMS (ESI) *m/z* calcd for C₁₂H₉F₃N [M+H]⁺: 224.0682, found:

224.0684.



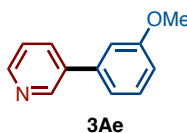
3-(4-Butylphenyl)pyridine (**3Ac**)^[71]

Purification by PTLC (hexane/EtOAc = 4:1) afforded **3Ac** as colorless liquid (63.0 mg, 75% yield). ¹H NMR (CDCl₃, 400 MHz) δ 8.84 (d, *J* = 2.4 Hz, 1H), 8.56 (dd, *J* = 4.8, 2.4 Hz, 1H), 7.87 (dd, *J* = 8.0, 4.8 Hz, 1H), 7.50 (d, *J* = 8.0 Hz, 2H), 7.35 (dd, *J* = 8.0, 4.8 Hz, 1H), 7.29 (d, *J* = 8.0 Hz, 2H), 2.67 (t, *J* = 8.0 Hz, 2H), 1.70–1.59 (m, 2H), 1.46–1.32 (m, 2H), 0.95 (t, *J* = 7.8 Hz, 3H); ¹³C NMR (CDCl₃, 100 MHz) δ 148.24, 148.19, 143.0, 136.6, 135.1, 134.1, 129.2, 127.0, 123.5, 35.3, 33.6, 22.4, 13.9; HRMS (ESI) *m/z* calcd for C₁₅H₁₈N [M+H]⁺: 212.1434, found: 212.1433.



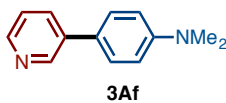
3-(4-Fluorophenyl)pyridine (**3Ad**)^[70]

Purification by flash column chromatography (hexane/EtOAc = 6:1) afforded **3Ad** as a white solid (62.1 mg, 90% yield). ¹H NMR (CDCl₃, 400 MHz) δ 8.81 (s, 1H), 8.59 (d, *J* = 4.8 Hz, 1H), 7.82 (d, *J* = 8.0 Hz, 1H), 7.59–7.50 (m, 2H), 7.36 (dd, *J* = 8.0, 4.8 Hz, 1H), 7.20–7.11 (m, 2H); ¹³C NMR (CDCl₃, 100 MHz) δ 162.8 (d, *J*_{C-F} = 249 Hz), 148.4, 148.1, 135.6, 134.1, 133.8, 128.7 (d, *J*_{C-F} = 8.0 Hz), 123.9, 116.0 (d, *J*_{C-F} = 21 Hz); HRMS (ESI) *m/z* calcd for C₁₁H₉FN [M+H]⁺: 174.0714, found: 174.0711.



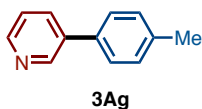
3-(3-Methoxyphenyl)pyridine (**3Ae**)^[72]

Purification by PTLC (hexane/Et₂O = 1:1) afforded **3Ae** as colorless liquid (65.2 mg, 88% yield). ¹H NMR (CDCl₃, 400 MHz) δ 8.85 (s, 1H), 8.59 (d, *J* = 4.8 Hz, 1H), 7.86 (dd, *J* = 8.0, 2.4 Hz, 1H), 7.42–7.32 (m, 2H), 7.16 (dd, *J* = 8.0, 4.8 Hz, 1H), 7.10 (s, 1H), 6.94 (dd, *J* = 8.0, 2.4 Hz, 1H), 3.86 (s, 3H); ¹³C NMR (CDCl₃, 100 MHz) δ 160.0, 148.6, 148.3, 139.2, 136.4, 134.3, 130.1, 123.4, 119.5, 113.3, 112.9, 55.3; HRMS (ESI) *m/z* calcd for C₁₂H₁₂ON [M+H]⁺: 186.0913, found: 186.0910.



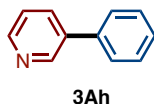
***N,N*-Dimethyl-4-(pyridin-3-yl)aniline (3Af)** ^[73]

The reaction was conducted using 1.5 equiv of Et₃N instead of Na₂CO₃. Purification by flash column chromatography (hexane/EtOAc = 4:1) afforded **3Af** as a white solid (39.3 mg, 50% yield). ¹H NMR (CDCl₃, 400 MHz) δ 8.82 (s, 1H), 8.48 (d, *J* = 4.8 Hz, 1H), 7.83 (d, *J* = 8.0 Hz, 1H), 7.49 (d, *J* = 8.8 Hz, 2H), 7.30 (dd, *J* = 8.0, 4.8 Hz, 1H), 6.82 (d, *J* = 8.8 Hz, 2H), 3.01 (s, 6H); ¹³C NMR (CDCl₃, 100 MHz) δ 150.4, 147.7, 147.1, 136.6, 133.2, 127.7, 125.4, 123.4, 112.8, 40.4; HRMS (ESI) *m/z* calcd for C₁₃H₁₅N₂ [M+H]⁺: 199.1230, found: 199.1228.



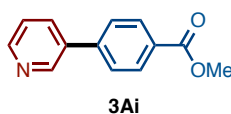
3-(4-Methyl)pyridine (3Ag) ^[70]

Purification by flash column chromatography (hexane/EtOAc = 6:1) afforded **3Ag** as a white solid (64.7 mg, 96% yield). ¹H NMR (CDCl₃, 400 MHz) δ 8.84 (d, *J* = 2.0 Hz, 1H), 8.56 (dd, *J* = 4.8, 2.0 Hz, 1H), 7.85 (dd, *J* = 8.0, 2.0 Hz, 1H), 7.47 (d, *J* = 8.4 Hz, 2H), 7.34 (dd, *J* = 8.0, 4.8 Hz, 1H), 7.28 (d, *J* = 8.4 Hz, 2H), 2.41 (s, 3H); ¹³C NMR (CDCl₃, 100 MHz) δ 148.1 (one carbon overlap), 138.0, 136.5, 134.9, 134.1, 129.7, 126.9, 123.5, 21.1; HRMS (ESI) *m/z* calcd for C₁₂H₁₂N [M+H]⁺: 170.0964, found: 170.0961.



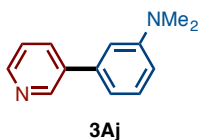
3-Phenylpyridine (3Ah) ^[70]

Purification by flash column chromatography (hexane/EtOAc = 4:1) afforded **3Ah** as colorless oil (50.1 mg, 81% yield). ¹H NMR (CDCl₃, 400 MHz) δ 8.86 (d, *J* = 2.4 Hz, 1H), 8.59 (d, *J* = 5.2 Hz, 1H), 7.87 (dd, *J* = 8.0, 2.4 Hz, 1H), 7.58 (d, *J* = 8.0 Hz, 2H), 7.48 (dd, *J* = 8.0, 2.4 Hz, 2H), 7.41 (dd, *J* = 8.0, 5.2 Hz, 1H), 7.37 (d, *J* = 8.0 Hz, 1H); ¹³C NMR (CDCl₃, 100 MHz) δ 148.4, 148.3, 137.8, 136.6, 134.3, 129.0, 128.1, 127.1, 123.5; HRMS (ESI) *m/z* calcd for C₁₁H₁₀N [M+H]⁺: 156.0808, found: 156.0805.



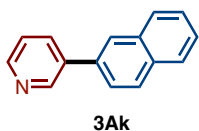
Methyl 4-(pyridin-3-yl)benzoate (**3Ai**)^[74]

Purification by flash column chromatography (hexane/EtOAc = 5:1) afforded **3Ai** as a white solid (61.1 mg, 72% yield). ¹H NMR (CDCl₃, 400 MHz) δ 8.89 (d, *J* = 2.4 Hz, 1H), 8.65 (dd, *J* = 4.8, 2.4 Hz, 1H), 8.15 (d, *J* = 8.8 Hz, 2H), 7.92 (dd, *J* = 8.0, 2.4 Hz, 1H), 7.66 (d, *J* = 8.8 Hz, 2H), 7.40 (dd, *J* = 8.0, 4.8 Hz, 1H), 3.96 (s, 3H); ¹³C NMR (CDCl₃, 100 MHz) δ 166.6, 149.2, 148.3, 142.1, 135.4, 134.4, 130.3, 129.6, 127.0, 123.6, 52.2; HRMS (ESI) *m/z* calcd for C₁₃H₁₁NO₂ [M+H]⁺: 214.0863, found: 214.0863.



N,N-Dimethyl-3-(pyridin-3-yl)aniline (**3Aj**)

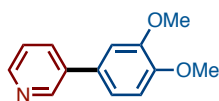
Purification by PTLC (hexane/EtOAc = 3:1) afforded **3Aj** as yellow oil (62.6 mg, 79% yield). ¹H NMR (CDCl₃, 400 MHz) δ 8.85 (d, *J* = 1.6 Hz, 1H), 8.57 (dd, *J* = 4.8, 1.6 Hz, 1H), 7.87 (dd, *J* = 8.0, 1.6 Hz, 1H), 7.36–7.31 (m, 2H), 6.91 (d, *J* = 7.6 Hz, 1H), 6.88 (d, *J* = 2.8 Hz, 1H), 6.77 (dd, *J* = 8.4, 2.8 Hz, 1H), 3.00 (s, 6H); ¹³C NMR (CDCl₃, 100 MHz) δ 150.9, 148.4, 148.2, 138.7, 137.5, 134.4, 129.7, 123.3, 115.4, 112.1, 111.1, 40.5; HRMS (ESI) *m/z* calcd for C₁₃H₁₅N₂ [M+H]⁺: 199.1230, found: 199.1227.



3-(Naphthalen-2-yl)pyridine (**3Ak**)^[75]

Purification by flash column chromatography (hexane/EtOAc = 5:1 to 4:1) afforded **3Ak** as a white solid (74.9 mg, 91% yield). ¹H NMR (CDCl₃, 400 MHz) δ 8.99 (d, *J* = 2.4 Hz, 1H), 8.63 (d, *J* = 4.8 Hz, 1H), 8.05 (d, *J* = 2.0 Hz, 1H), 8.00 (dd, *J* = 8.0, 2.4 Hz, 1H), 7.96 (d, *J* = 8.8 Hz, 1H), 7.94–7.87 (m, 2H), 7.72 (dd, *J* = 8.8, 2.0 Hz, 1H), 7.58–7.49 (m, 2H), 7.40 (dd, *J* = 8.0, 4.8 Hz, 1H); ¹³C NMR (CDCl₃, 100 MHz) δ 148.6, 148.5, 136.6, 135.2, 134.6, 133.6, 132.9, 128.9, 128.2, 127.7, 126.6, 126.4, 126.2, 125.0,

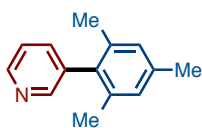
123.6; HRMS (ESI) m/z calcd for $C_{15}H_{12}N$ $[M+H]^+$: 206.0964, found: 206.0964.



3AI

3-(3,4-Dimethoxyphenyl)pyridine (**3AI**)^[76]

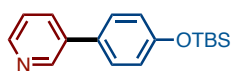
Purification by flash column chromatography (hexane/EtOAc = 1:1) afforded **3AI** as a white solid (62.6 mg, 73% yield). ¹H NMR (CDCl₃, 400 MHz) δ 8.82 (d, J = 2.0 Hz, 1H), 8.56 (dd, J = 4.8, 2.0 Hz, 1H), 7.84 (dd, J = 8.0, 2.0 Hz, 1H), 7.34 (dd, J = 8.0, 4.8 Hz, 1H), 7.14 (dd, J = 8.4, 2.0 Hz, 1H), 7.08 (d, J = 2.0 Hz, 1H), 6.97 (d, J = 8.4 Hz, 1H), 3.97 (s, 3H), 3.93 (s, 3H); ¹³C NMR (CDCl₃, 100 MHz) δ 149.3, 149.1, 148.0, 147.9, 136.4, 133.9, 130.6, 123.4, 119.5, 111.6, 110.1, 55.9 (one peak overlap); HRMS (ESI) m/z calcd for $C_{13}H_{14}NO_2$ $[M+H]^+$: 216.1019, found: 216.1020.



3Am

3-Mesitylpyridine (**3Am**)^[71]

Purification by PTLC (hexane/EtOAc = 4:1) afforded **3Am** as a white solid (52.0 mg, 66% yield). ¹H NMR (CDCl₃, 400 MHz) δ 8.59 (dd, J = 4.8, 1.6 Hz, 1H), 8.43 (d, J = 1.6 Hz, 1H), 7.50 (dd, J = 8.0, 1.6 Hz, 1H), 7.36 (dd, J = 8.0, 4.8 Hz, 1H), 6.97 (s, 2H), 2.34 (s, 3H), 2.00 (s, 6H); ¹³C NMR (CDCl₃, 100 MHz) δ 150.3, 148.0, 137.5, 136.9, 136.6, 136.2, 135.0, 128.3, 123.3, 21.0, 20.8; HRMS (ESI) m/z calcd for $C_{14}H_{16}N$ $[M+H]^+$: 198.1277, found: 198.1273.

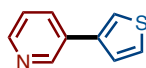


3An

3-(4-((*tert*-Butyldimethylsilyloxy)phenyl)pyridine (**3An**)

Purification by flash column chromatography (hexane/EtOAc = 5:1) afforded **3An** as colorless oil (82.4 mg, 72% yield). ¹H NMR (CDCl₃, 400 MHz) δ 8.81 (d, J = 2.4 Hz, 1H), 8.54 (d, J = 4.8 Hz, 1H), 7.82 (dd, J = 8.0, 2.4 Hz, 1H), 7.46 (d, J = 6.8 Hz, 2H),

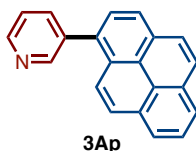
7.32 (dd, $J = 8.0, 4.8$ Hz, 1H), 6.94 (d, $J = 6.8$ Hz, 2H), 1.01 (s, 9H), 0.24 (s, 6H); ^{13}C NMR (CDCl_3 , 100 MHz) δ 156.0, 148.0, 147.8, 136.3, 133.8, 130.8, 128.1, 123.4, 120.7, 25.6, 18.2, -4.4; HRMS (DART) m/z calcd for $\text{C}_{17}\text{H}_{24}\text{NOSi}$ $[\text{M}+\text{H}]^+$: 286.1627, found: 286.1621.



3Ao

3-(Thiophen-3-yl)pyridine (3Ao)^[77]

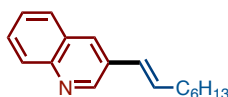
The reaction was conducted using 1.2 equiv of Na_2CO_3 . Purification by PTLC (hexane/ $\text{Et}_2\text{O} = 1:1$) and then GPC afforded **3Ao** as a white solid (41.3 mg, 64% yield). ^1H NMR (CDCl_3 , 400 MHz) δ 8.88 (s, 1H), 8.53 (d, $J = 4.4$ Hz, 1H), 7.85 (d, $J = 8.0$ Hz, 1H), 7.52 (dd, $J = 2.8, 1.2$ Hz, 1H), 7.44 (dd, $J = 5.2, 2.8$ Hz, 1H), 7.39 (dd, $J = 5.2, 1.2$ Hz, 1H), 7.31 (dd, $J = 8.0, 4.4$ Hz, 1H); ^{13}C NMR (CDCl_3 , 100 MHz) δ 148.2, 147.6, 138.7, 133.4, 131.4, 126.9, 125.8, 123.6, 121.3; HRMS (ESI) m/z calcd for $\text{C}_9\text{H}_8\text{NS}$ $[\text{M}+\text{H}]^+$: 162.0372, found: 162.0369.



3Ap

3-(Pyren-1-yl)pyridine (3Ap)

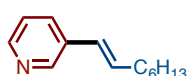
Purification by PTLC (hexane/ $\text{Et}_2\text{O} = 1:1$) afforded **3Ap** as a yellow solid (61.7 mg, 55% yield). ^1H NMR (CDCl_3 , 400 MHz) δ 8.88 (s, 1H), 8.72 (d, $J = 4.8$ Hz, 1H), 8.24–8.10 (m, 3H), 8.10–7.95 (m, 5H), 7.94–7.79 (m, 2H), 7.46 (dd, $J = 8.8, 4.8$ Hz, 1H); ^{13}C NMR (CDCl_3 , 100 MHz) δ 151.0, 148.4, 137.6, 136.7, 133.4, 131.3, 131.0, 130.7, 128.5, 128.0, 127.8, 127.4, 127.2, 126.1, 125.4, 125.0, 124.8, 124.64, 124.61, 124.2, 123.2; HRMS (DART) m/z calcd for $\text{C}_{21}\text{H}_{14}\text{N}$ $[\text{M}+\text{H}]^+$: 280.1126, found: 280.1122.



3Wq

(*E*)-3-(Oct-1-en-1-yl)quinoline (3Wq)

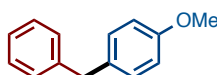
The reaction was conducted using NaCl (1.0 equiv) as additive. Purification by PTLC (hexane/EtOAc = 8:1) and then GPC afforded **3Wq** as colorless oil (57.8 mg, 57% yield). ¹H NMR (CDCl₃, 600 MHz) δ 8.97 (s, 1H), 8.06 (d, *J* = 8.8 Hz, 1H), 7.98 (s, 1H), 7.76 (d, *J* = 8.8 Hz, 1H), 7.64 (t, *J* = 8.8 Hz, 1H), 7.51 (t, *J* = 8.8 Hz, 1H), 6.54–6.43 (m, 2H), 2.28 (q, *J* = 8.0 Hz, 2H), 1.56–1.46 (m, 2H), 1.42–1.27 (m, 6H), 0.91 (q, *J* = 6.8 Hz, 3H); ¹³C NMR (CDCl₃, 150 MHz) δ 149.4, 147.1, 134.1, 131.5, 130.8, 129.2, 128.7, 128.2, 127.6, 126.8, 126.5, 33.3, 31.7, 29.2, 28.9, 22.6, 14.1; HRMS (ESI) *m/z* calcd for C₁₇H₂₂N [M+H]⁺: 240.1747, found: 240.1752.



3Aq

(*E*)-3-(Oct-1-en-1-yl)pyridine (3Aq) ^[78]

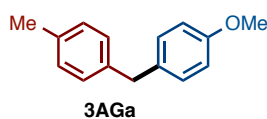
The reaction was conducted by using 1.0 equiv of NaCl as additive. Purification by PTLC (hexane/EtOAc = 5:1) afforded **3Aq** as colorless oil (35.0 mg, 46% yield). ¹H NMR (CDCl₃, 400 MHz) δ 8.56 (s, 1H), 8.42 (d, *J* = 4.4 Hz, 1H), 7.65 (d, *J* = 8.0 Hz, 1H), 7.21 (dd, *J* = 8.0, 4.4 Hz, 1H), 6.40–6.25 (m, 2H), 2.23 (q, *J* = 8.0 Hz, 2H), 1.52–1.43 (m, 2H), 1.40–1.32 (m, 6H), 0.88 (t, *J* = 6.8 Hz, 3H); ¹³C NMR (CDCl₃, 100 MHz) δ 147.94, 147.86, 133.7, 133.5, 132.3, 126.2, 123.3, 33.1, 31.7, 29.1, 28.9, 22.6, 14.1; HRMS (ESI) *m/z* calcd for C₁₃H₂₀N [M+H]⁺: 190.1590, found: 190.1586.



3AFa

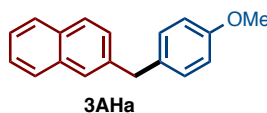
1-Benzyl-4-methoxybenzene (3AFa) ^[79]

The reaction was conducted using *N,N*-dimethyl-4-aminopyridine (DMAP: 14.7 mg, 0.12 mmol, 30 mol%) as additive. Purification by PTLC (hexane/EtOAc = 20:1) afforded **3AFa** as colorless oil (36.5 mg, 46% yield). ¹H NMR (CDCl₃, 400 MHz) δ 7.27 (dd, *J* = 7.6, 7.2 Hz, 2H), 7.21–7.15 (m, 3H), 7.10 (d, *J* = 8.4 Hz, 2H), 6.82 (d, *J* = 8.4 Hz, 2H), 3.92 (s, 2H), 3.78 (s, 3H); ¹³C NMR (CDCl₃, 100 MHz) δ 157.9, 141.6, 133.2, 129.8, 128.8, 128.4, 126.0, 113.9, 55.2, 41.0; HRMS (DART) *m/z* calcd for C₁₄H₁₅O [M+H]⁺: 199.1123, found: 199.1122.



1-Methoxy-4-(4-methylbenzyl)benzene (**3AGa**)^[79]

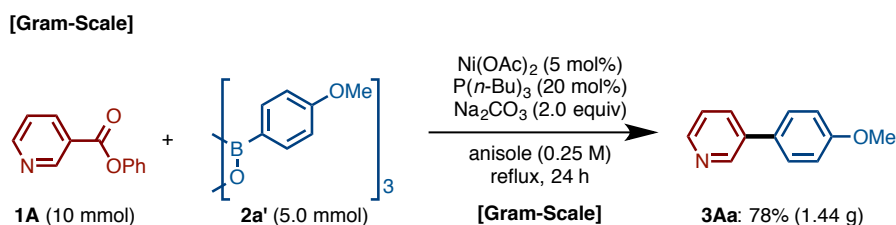
The reaction was conducted using *N,N*-dimethyl-4-aminopyridine (DMAP: 14.7 mg, 0.12 mmol, 30 mol%) as additive. Purification by PTLC (hexane/EtOAc = 20:1) afforded **3AGa** as colorless oil (30.0 mg, 35% yield). ¹H NMR (CDCl₃, 400 MHz) δ 7.12–7.03 (m, 6H), 6.81 (d, *J* = 8.4 Hz, 2H), 3.88 (s, 2H), 3.77 (s, 3H), 2.31 (s, 3H); ¹³C NMR (CDCl₃, 100 MHz) δ 157.9, 138.5, 135.4, 133.5, 129.8, 129.1, 128.7, 113.8, 55.2, 40.6, 21.0; HRMS (FAB) *m/z* calcd for C₁₅H₁₆O [M]: 212.1201, found: 212.1203



2-(4-Methoxybenzyl)naphthalene (**3AHa**)^[79]

The reaction was conducted using *N,N*-dimethyl-4-aminopyridine (DMAP: 14.7 mg, 0.12 mmol, 30 mol%) as additive. Purification by PTLC (hexane/EtOAc = 20:1) afforded **3AHa** as a white solid (45.8 mg, 46% yield). ¹H NMR (CDCl₃, 400 MHz) δ 7.81–7.77 (m, 3H), 7.60 (s, 1H), 7.47–7.35 (m, 2H), 7.29 (dd, *J* = 8.4, 1.6 Hz, 1H), 7.12 (dd, *J* = 8.8, 1.6 Hz, 2H), 6.82 (dd, *J* = 8.8, 1.6 Hz, 2H), 4.07 (s, 2H), 3.77 (s, 3H); ¹³C NMR (CDCl₃, 100 MHz) δ 158.0, 139.0, 133.6, 133.0, 132.0, 129.9, 128.0, 127.6, 127.54, 127.50, 126.9, 125.9, 125.3, 113.9, 55.2, 41.2; HRMS (FAB) *m/z* calcd for C₁₈H₁₆O [M]⁺: 248.1201, found: 248.1207.

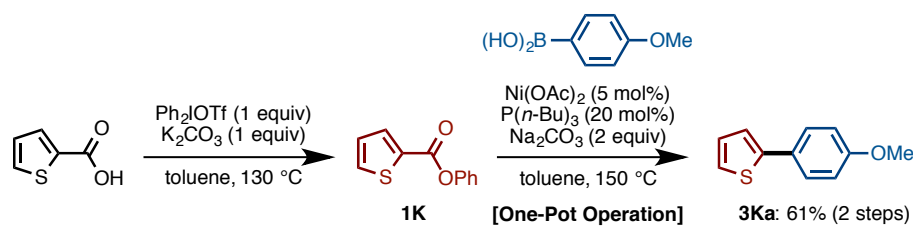
Gram-scale Reaction



A 100-mL Schlenk tube equipped with a condenser and balloon containing a magnetic stirring bar and Ni(OAc)₂·4H₂O (124 mg, 0.5 mmol, 5 mol%) was dried with a heatgun

in vacuo and filled with N₂ gas after cooling to room temperature. To this was added phenyl nicotinate (**1A**: 1.99 g, 10 mmol, 1.0 equiv), tri(*p*-methoxyphenyl)boroxine (**2a'**: 2.00 g, 5.0 mmol, 0.5 equiv), and Na₂CO₃ (2.12 g, 20 mmol, 2.0 equiv). The tube was vacuumed and refilled N₂ gas three times. To this was added P(*n*-Bu)₃ (0.49 mL, 2.0 mmol, 20 mol%) and anisole (40 mL). The Schlenk cock was closed and then this mixture was refluxed for 24 h in an oil bath (oil bath temperature was 160 °C) with stirring. After cooling the reaction mixture to room temperature, the mixture was passed through a short silica gel pad with EtOAc. The filtrate was concentrated *in vacuo* and the residue was purified by flash column chromatography (hexane/Et₂O = 3:2 to 2:3) to afford 3-(4-methoxyphenyl)pyridine (**3Aa**: 1.44 g, 78% yield) as a white solid.

4-4. One-pot Transformation of Thiophene-2-carboxylic Acid to Biaryl 3Ka

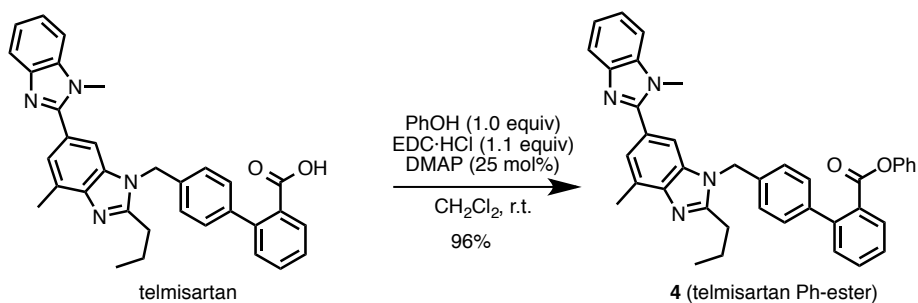


A 20-mL glass vessel equipped with J. Young[®] O-ring tap containing a magnetic stirring bar was dried with heatgun under reduced pressure and filled with N₂ gas after cooling to room temperature. To this was added thiophene-2-carboxylic acid (51.3 mg, 0.40 mmol), diphenyliodonium triflate (172.0 mg, 0.40 mmol, 1.0 equiv), K₂CO₃ (55.2 mg, 0.40 mmol, 1.0 equiv), and then toluene (2.0 mL). The vessel was sealed with O-ring tap and then heated at 130 °C for 2 h in an 8-well reaction block with stirring. After cooling the reaction mixture to room temperature, this mixture was concentrated *in vacuo* to remove toluene and iodobenzene.

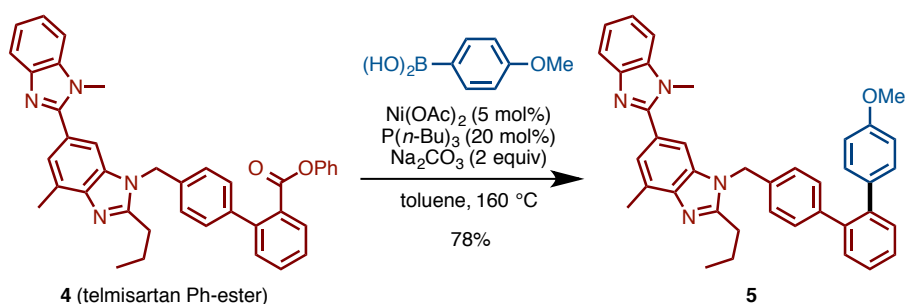
To the same tube containing obtained crude product **1K** were added Ni(OAc)₂ (3.5 mg, 0.02 mmol, 5 mol%), *p*-methoxyphenylboronic acid **3** (0.60 mmol, 91.9 mg, 1.5 equiv), and Na₂CO₃ (84.8 mg, 0.8 mmol, 2.0 equiv). The vessel was vacuumed and refilled N₂ gas three times. To this was added P(*n*-Bu)₃ (19.0 mL, 0.08 mmol, 20 mol%) and toluene (1.6 mL). The vessel was sealed with O-ring tap and then heated at 150 °C for 24 h in an 8-well reaction block with stirring. After cooling the reaction mixture to room temperature, the mixture was passed through a short silica gel pad with EtOAc.

The filtrate was concentrated and the residue was purified by flash column chromatography (hexane/EtOAc = 100:1) to afford 2-(4-methoxyphenyl)thiophene (**3Ka**: 46.2 mg, 61% yield over 2 steps) as a white solid.

4-5. Application to the Synthesis of Telmisartan Derivatives



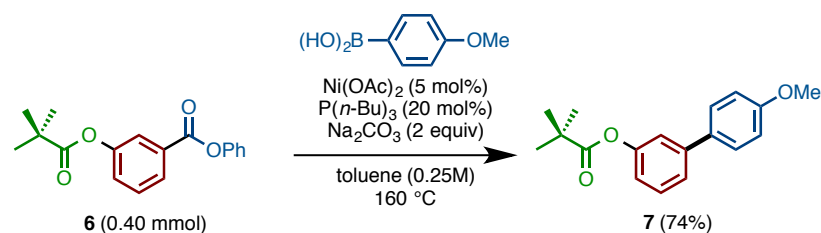
To a test tube equipped with screw cap containing a magnetic stirring bar were added telmisartan (772 mg, 1.5 mmol, 1.0 equiv), phenol (155 mg, 1.65 mmol, 1.1 equiv), 1-(3-dimethylaminopropyl)-3-ethylcarbodiimide hydrochloride (EDC·HCl: 316 mg, 1.65 mmol, 1.1 equiv), *N,N*-dimethyl-4-aminopyridine (DMAP: 18.3 mg, 0.15 mmol, 0.1 equiv) and CH₂Cl₂ (3.0 mL). After stirring for 6 h, the reaction mixture was quenched with saturated NaHCO₃aq and extracted three times with CH₂Cl₂. The combined organic layer was dried over Na₂SO₄, filtrated, and concentrated *in vacuo*. The residue was purified by flash column chromatography (hexane/EtOAc = 2:1 to EtOAc) to afford telmisartan Ph-ester (**4**: 850 mg, 96% yield) as a white solid. ¹H NMR (CDCl₃, 400 MHz) δ 8.03 (dd, *J* = 8.0, 1.6 Hz, 1H), 7.83–7.80 (m, 1H), 7.60 (td, *J* = 8.0, 1.6 Hz, 1H), 7.52–7.44 (m, 3H), 7.40–7.35 (m, 3H), 7.32–7.28 (m, 3H), 7.21 (t, *J* = 8.0 Hz, 2H), 7.12 (d, *J* = 8.0 Hz, 2H), 7.04 (t, *J* = 8.0 Hz, 1H), 6.85 (d, *J* = 8.0 Hz, 2H), 5.45 (s, 2H), 3.71 (s, 3H), 2.91 (t, *J* = 8.0 Hz, 2H), 2.79 (s, 3H), 1.91–1.81 (m, 2H), 1.03 (t, *J* = 8.0 Hz, 3H); ¹³C NMR (CDCl₃, 100 MHz) δ 166.6, 156.4, 154.7, 150.6, 143.2, 142.9, 142.3, 141.1, 136.7, 135.0, 131.9, 130.9, 130.4, 129.9, 129.5, 129.25, 129.20, 127.6, 125.9, 125.7, 124.0, 123.9, 122.4, 122.3, 121.1, 119.6, 109.5, 108.8, 46.9, 31.7, 29.8, 21.8, 16.9, 14.1; HRMS (DART) *m/z*. calcd for C₃₉H₃₅N₄O₂ [M+H]⁺: 591.2760, found: 591.2770.



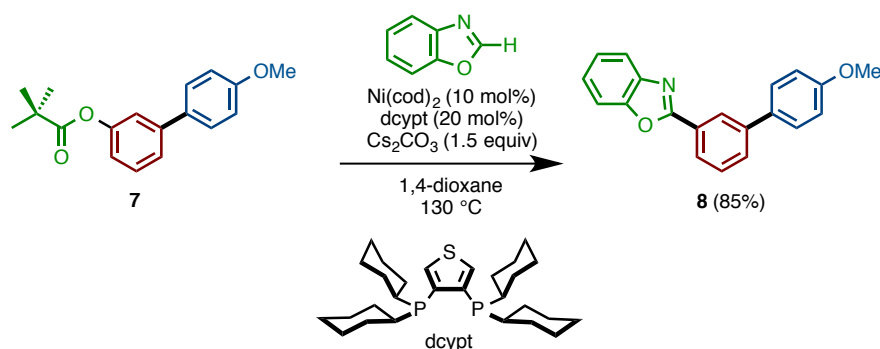
A 20-mL glass vessel equipped with J. Young[®] O-ring tap containing a magnetic stirring bar and $\text{Ni}(\text{OAc})_2 \cdot 4\text{H}_2\text{O}$ (3.5 mg, 0.0125 mmol, 5 mol%) was dried with a heatgun under reduced pressure and filled with N_2 gas after cooling to room temperature. To this vessel was added telmisartan Ph-ester **4** (145 mg, 0.25 mmol, 1.0 equiv), *p*-methoxyphenylboronic acid (**2a**: 58.0 mg, 0.375 mmol, 1.5 equiv), and Na_2CO_3 (53 mg, 0.50 mmol, 2.0 equiv). The vessel was vacuumed and refilled N_2 gas three times. To this were added $\text{P}(n\text{-Bu})_3$ (12.5 mL, 0.05 mmol, 20 mol%) and toluene (1.0 mL). The vessel was sealed with O-ring tap and then heated at 160 °C for 24 h in an 8-well reaction block with stirring. After cooling the reaction mixture to room temperature, the mixture was passed through Celite[®] with EtOAc. The filtrate was concentrated and the residue was purified by flash column chromatography (hexane/EtOAc = 1:2 to EtOAc), followed by reverse-phase HPLC (Isolera[®]; $\text{H}_2\text{O}/\text{MeCN}$) to afford a coupling product **5** as a white solid (111 mg, 78% yield). ¹H NMR (CDCl_3 , 400 MHz) δ 7.84–7.81 (m, 1H), 7.51 (s, 1H), 7.44 (s, 1H), 7.40–7.28 (m, 7H), 7.10 (d, $J = 8.0$ Hz, 2H), 7.01 (d, $J = 8.8$ Hz, 2H), 6.94 (d, $J = 8.0$ Hz, 2H), 6.71 (d, $J = 8.8$ Hz, 2H), 5.36 (s, 2H), 3.80 (s, 3H), 3.72 (s, 3H), 2.87 (t, $J = 7.6$ Hz, 2H), 2.78 (s, 3H), 1.85–1.76 (m, 2H), 1.03 (t, $J = 7.6$ Hz, 3H); ¹³C NMR (CDCl_3 , 100 MHz) δ 158.3, 156.4, 154.7, 143.1, 142.9, 141.5, 140.1, 139.5, 136.7, 135.2, 133.9, 133.6, 130.8, 130.6, 130.4, 127.6, 125.8, 123.9, 123.7, 122.4, 122.3, 119.5, 113.3, 109.5, 108.7, 55.1, 47.0, 31.8, 29.8, 21.7, 16.8, 14.0; HRMS (DART) m/z calcd for $\text{C}_{39}\text{H}_{37}\text{N}_4\text{O}$ $[\text{M}+\text{H}]^+$: 577.2967, found: 577.2969.

4-6. Orthogonal Coupling of 6, 1Q, and 10

Orthogonal Coupling of 6



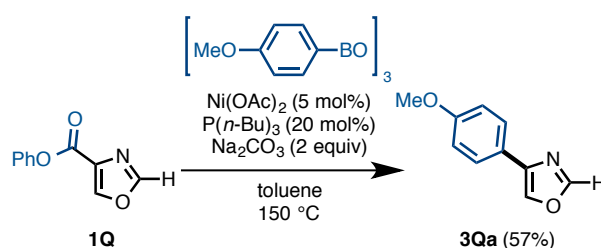
A 20-mL glass vessel equipped with J. Young[®] O-ring tap containing a magnetic stirring bar and $\text{Ni}(\text{OAc})_2 \cdot 4\text{H}_2\text{O}$ (5.0 mg, 0.020 mmol, 5 mol%) was dried with a heatgun under reduced pressure and filled with N_2 gas after cooling to room temperature. To this vessel was added phenyl 3-(pivaloyloxy)benzoate (**6**: 119.2 mg, 0.40 mmol, 1.0 equiv), *p*-methoxyphenylboronic acid (**2a**: 91.8 mg, 0.60 mmol, 1.5 equiv), and Na_2CO_3 (85.0 mg, 0.8 mmol, 2.0 equiv). The vessel was vacuumed and refilled N_2 gas three times. To this were added $\text{P}(\textit{n}\text{-Bu})_3$ (20 mL, 0.08 mmol, 20 mol%) and toluene (1.6 mL). The vessel was sealed with O-ring tap and then heated at 150 °C for 24 h in an 8-well reaction block with stirring. After cooling the reaction mixture to room temperature, the mixture was passed through a short silica gel pad with EtOAc. The filtrate was concentrated *in vacuo* and the residue was purified by flash column chromatography (hexane/EtOAc = 100:1), and then GPC to afford 4'-methoxy-[1,1'-biphenyl]-3-yl pivalate **7** (84.2 mg, 74% yield) as colorless oil. ¹H NMR (CDCl_3 , 400 MHz) δ 7.51 (d, J = 8.8 Hz, 2H), 7.41–7.37 (m, 2H), 7.22 (s, 1H), 7.01–6.98 (m, 1H), 6.96 (d, J = 8.8 Hz, 2H), 3.83 (s, 3H), 1.39 (s, 9H); ¹³C NMR (CDCl_3 , 100 MHz) δ 177.1, 159.3, 151.4, 142.4, 132.7, 129.5, 128.2, 123.9, 119.7, 119.6, 114.1, 55.3, 39.1, 27.1; HRMS (DART) m/z calcd for $\text{C}_{18}\text{H}_{21}\text{O}_3$ $[\text{M}+\text{H}]^+$: 285.1491, found: 285.1494.



A 20-mL glass vessel equipped with J. Young[®] O-ring tap containing a magnetic

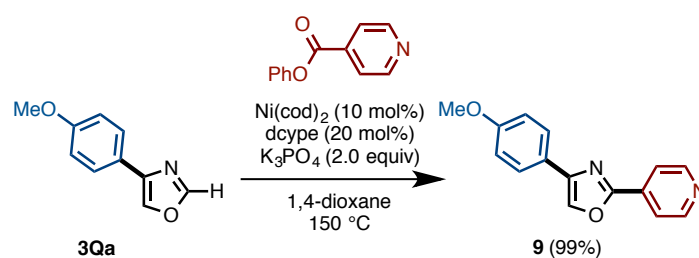
stirring bar and Cs₂CO₃ (146.6 mg, 0.45 mmol, 1.5 equiv) was dried with a heatgun under reduced pressure and filled with N₂ gas after cooling to room temperature. To this vessel was added 4'-methoxy-[1,1'-biphenyl]-3-yl pivalate (**7**: 85.3 mg, 0.30 mmol, 1.0 equiv) and 2,3-bis(dicyclohexylphosphine)thiophene (dcypt: 28.3 mg, 0.06 mmol, 20 mol%), and then introduced into an argon-atmosphere glovebox. To the reaction vessel was added Ni(cod)₂ (8.3 mg, 0.03 mmol, 10 mol%), and then taken out of the glovebox. To this tube were added benzoxazole (47.6 mg, 0.40 mmol, 1.3 equiv) and 1,4-dioxane (1.5 mL) under a stream of N₂. The vessel was sealed with O-ring tap and then heated at 130 °C for 12 h in an 8-well reaction block with stirring. After cooling the reaction mixture to room temperature, the mixture was passed through a short silica gel pad with EtOAc. The filtrate was concentrated *in vacuo* and the residue was purified by flash column chromatography (hexane/EtOAc = 100:1) to afford 2-(4'-methoxy-[1,1'-biphenyl]-3-yl)benzo[d]oxazole (**8**: 76.8 mg, 85% yield) as a white solid. ¹H NMR (CDCl₃, 400 MHz) δ 8.46 (s, 1H), 8.18 (d, *J* = 8.0 Hz, 1H), 7.83–7.77 (m, 1H), 7.72 (d, *J* = 8.0 Hz, 1H), 7.65–7.53 (m, 4H), 7.40–7.33 (m, 2H), 7.01 (d, *J* = 8.8 Hz, 2H), 3.87 (s, 3H); ¹³C NMR (CDCl₃, 100 MHz) δ 163.0, 159.5, 150.7, 142.1, 141.5, 132.5, 129.7, 129.3, 128.2, 127.5, 125.7, 125.1, 124.6, 120.0, 114.3, 110.6, 55.3 (one peak overlap); HRMS (DART) *m/z* calcd for C₂₀H₁₆NO₂ [M+H]⁺: 302.1181, found: 302.1178.

Orthogonal Coupling of **1Q**



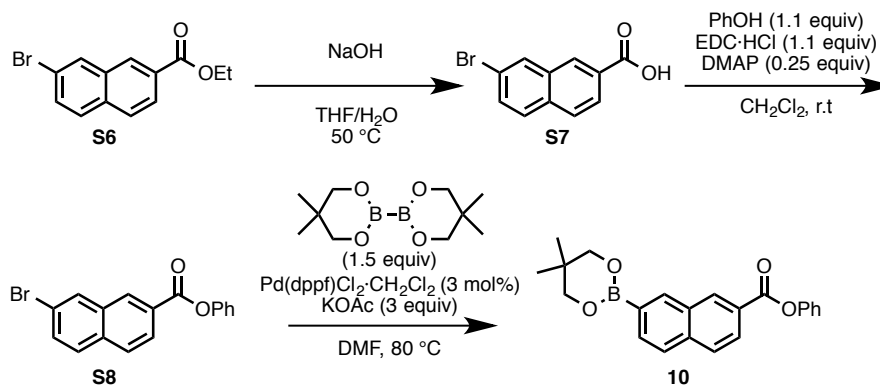
A 20-mL glass vessel equipped with J. Young[®] O-ring tap containing a magnetic stirring bar and Ni(OAc)₂·4H₂O (5.0 mg, 0.020 mmol, 5 mol%) was dried with a heatgun for 1 min under reduced pressure and filled with N₂ gas after cooling to room temperature. To this vessel was added phenyl oxazole-4-carboxylate (**1Q**: 75.7 mg, 0.40 mmol, 1.0 equiv), *p*-methoxyphenylboroxine (**2a'**: 80.3 mg, 0.20 mmol, 0.50 equiv), and Na₂CO₃ (85.0 mg, 0.8 mmol, 2.0 equiv). The vessel was vacuumed and refilled with

N₂ gas three times. To this were added P(*n*-Bu)₃ (20 mL, 0.08 mmol, 20 mol%) and toluene (1.6 mL). The vessel was sealed with O-ring tap and then heated at 150 °C for 24 h in an 8-well reaction block with stirring. After cooling the reaction mixture to room temperature, the mixture was passed through a short silica gel pad with EtOAc. The filtrate was concentrated *in vacuo* and the residue was purified by flash column chromatography by using Isolera[®] (hexane/EtOAc = 95:5 to 4:1), and then GPC to afford 4-(4-methoxyphenyl)oxazole (**3Qa**: 40.7 mg, 57% yield) as a white solid.



A 20-mL glass vessel equipped with J. Young[®] O-ring tap containing a magnetic stirring bar and K₃PO₄ (169.8 mg, 0.80 mmol, 2.0 equiv) was dried with a heatgun for 3 minutes *in vacuo* and filled with N₂ gas after cooling to room temperature. To this vessel was added 4-(4-methoxyphenyl)oxazole (**3Qa**: 70.7 mg, 0.40 mmol, 1.0 equiv) and phenyl 4-nicotinate (119.5 mg, 0.60 mmol, 1.5 equiv), and then introduced into an argon-atmosphere glovebox. To the reaction vessel was added Ni(cod)₂ (11.0 mg, 0.04 mmol, 10 mol%) and 1,2-bis(dicyclohexylphosphino)ethane (dcype: 33.8 mg, 0.08 mmol, 20 mol%), and then taken out of the glovebox. To this tube was added 1,4-dioxane (1.6 mL) under a stream of N₂. The vessel was sealed with O-ring tap and then heated at 150 °C for 24 h in an 8-well reaction block with stirring. After cooling the reaction mixture to room temperature, the mixture was passed through a Celite[®] pad with EtOAc as an eluent. The filtrate was concentrated *in vacuo* and the residue was purified by PTLC (hexane/EtOAc = 1:1) to afford 4-(4-methoxyphenyl)-2-(pyridin-4-yl)oxazole (**9**: 100.5 mg, 99% yield) as a white solid. ¹H NMR (CDCl₃, 400 MHz) δ 8.76 (dd, *J* = 4.4, 1.2 Hz, 2H), 7.96–7.92 (m, 3H), 7.75 (dd, *J* = 7.2, 2.4 Hz, 2H), 6.98 (dd, *J* = 7.2, 2.4 Hz, 2H), 3.86 (s, 3H); ¹³C NMR (CDCl₃, 100 MHz) δ 159.8, 159.4, 150.5, 142.5, 134.3, 133.5, 127.0, 123.1, 120.0, 114.2, 55.3; HRMS (DART) *m/z* calcd for C₁₅H₁₃N₂O₂ [M+H]⁺: 253.0977, found: 253.0972.

Orthogonal Coupling of 10

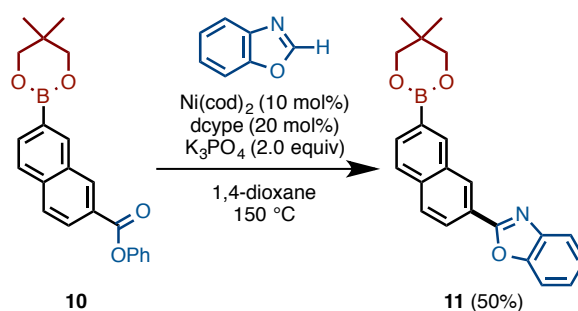


The solution of **S6** (1.95 g, 7.0 mmol, 1.0 equiv) in THF (28 mL) was treated with 1M NaOH_{aq} (14 mL, 2.0 equiv) at 50 °C. After stirring overnight, the mixture was diluted with Et₂O and washed two times with Et₂O. 1 M HCl_{aq} was added to the combined water phase to adjust the pH to 2, and then resulted solution was extracted three times with Et₂O. The combined organic phase was concentrated *in vacuo* to afford 7-bromo-2-naphthoic acid (**S7**: 1.76 g) as a white solid. This was used without further purification.

To a round-bottomed flask with the carboxylic acid **S7** (1.76 g, 7.0 mmol, 1.0 equiv) were added phenol (725 mg, 7.7 mmol, 1.1 equiv), 1-(3-dimethylaminopropyl)-3-ethylcarbodiimide hydrochloride (EDC·HCl: 1.48 g, 7.7 mmol, 1.1 equiv), *N,N*-dimethyl-4-aminopyridine (DMAP: 213.8 mg, 1.75 mmol, 0.25 equiv) and CH₂Cl₂ (28 mL). After stirring the mixture for several hours with monitoring reaction progress on TLC, the reaction was quenched with saturated NaHCO₃_{aq} and extracted three times with CH₂Cl₂. The combined organic layer was dried over Na₂SO₄, passed a short silica gel pad, and concentrated *in vacuo*. The residue was purified by recrystallization (hexane/CH₂Cl₂) to afford phenyl 7-bromo-2-naphthoate (**S8**: 2.15 g, 94% yield) as a white solid.

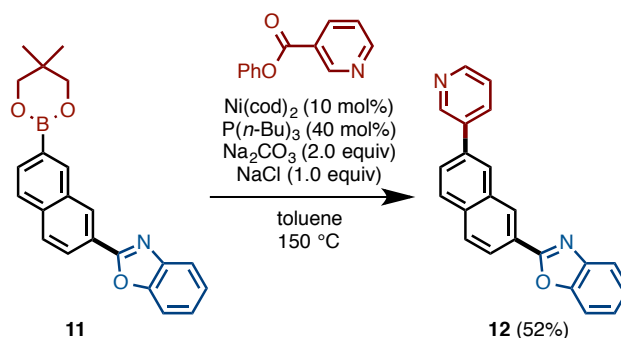
To a dried 50-mL Schlenk tube were added dehydrated KOAc (883 mg, 9.0 mmol, 3.0 equiv), phenyl 7-bromo-2-naphthoate (**S8**: 982 mg, 3.0 mmol, 1.0 equiv), Pd(dppf)Cl₂·CH₂Cl₂ (73.5 mg, 0.090 mmol, 3 mol%), and bis(neopentyl glycolato)diboron (1.01 g, 4.5 mmol, 1.5 equiv). The tube was vacuumed and filled with N₂ gas three times. DMF (12 mL) was added under a stream of N₂ gas and the

mixture was heated at 80 °C for 12 h in an oil bath. After cooling the mixture to room temperature, the mixture was diluted with EtOAc and passed a silica-gel pad with EtOAc as an eluent. The mixture was washed with brine, dried over Na₂SO₄, filtered, and then concentrated *in vacuo*. The resulted crude product was purified by silica-gel column chromatography by using Isolera[®] (hexane/EtOAc = 10:1 to 1:1) to afford phenyl 7-(5,5-dimethyl-1,3,2-dioxaborinan-2-yl)-2-naphthoate (**10**: 940 mg, 87% yield) as a white solid. ¹H NMR (CDCl₃, 400 MHz) δ 8.77 (s, 1H), 8.41 (s, 1H), 8.19 (d, *J* = 8.4 Hz, 1H), 8.01–7.91 (m, 3H), 7.45 (d, *J* = 8.4 Hz, 2H), 7.32–7.22 (m, 3H), 3.84 (s, 4H), 1.07 (s, 6H); ¹³C NMR (CDCl₃, 100 MHz) δ 165.4, 151.1, 135.2, 134.7, 133.8, 131.7, 130.9, 129.5, 129.1, 128.3, 127.3, 125.9, 125.2, 121.8, 72.5, 32.0, 21.9; HRMS (DART) *m/z* calcd for C₂₂H₂₂BO₄ [M+H]⁺: 361.1611, found: 361.1611.



A 20-mL glass vessel equipped with J. Young[®] O-ring tap containing a magnetic stirring bar and K₃PO₄ (169.8 mg, 0.80 mmol, 2.0 equiv) was dried with a heatgun for 3 min *in vacuo* and filled with N₂ gas after cooling to room temperature. To this vessel was added phenyl 7-(5,5-dimethyl-1,3,2-dioxaborinan-2-yl)-2-naphthoate (**10**: 144.1 mg, 0.40 mmol, 1.0 equiv), and then introduced into an argon-atmosphere glovebox. To the reaction vessel was added Ni(cod)₂ (11.0 mg, 0.04 mmol, 10 mol%) and 1,2-bis(dicyclohexylphosphino)ethane (dcype: 33.8 mg, 0.08 mmol, 20 mol%), and then taken out of the glovebox. To this tube were added benzoxazole (60 μL, 71.4 mg, 0.60 mmol, 1.5 equiv) and 1,4-dioxane (1.6 mL) under a stream of N₂. The vessel was sealed with O-ring tap and then heated at 150 °C for 12 h in an 8-well reaction block with stirring. After cooling the reaction mixture to room temperature, the mixture was passed through a silica-gel pad with EtOAc as an eluent. The filtrate was concentrated *in vacuo* and the residue was purified by silica-gel column chromatography by using Isolera[®] (hexane/EtOAc = 100:1 to EtOAc) to afford a pale yellow solid (82 mg). This solid was

further purified by silica-gel column chromatography by using Isolera[®] (hexane/CHCl₃ = 4:1 to CHCl₃) to afford 2-(7-(5,5-dimethyl-1,3,2-dioxaborinan-2-yl)naphthalen-2-yl)benzo[d]oxazole (**11**: 71.3 mg, 50% yield) as a white solid. ¹H NMR (CDCl₃, 400 MHz) δ 8.77 (s, 1H), 8.40 (s, 1H), 8.31 (dd, *J* = 9.0, 1.2 Hz, 1H), 8.01 (d, *J* = 9.0 Hz, 1H), 7.98–7.92 (m, 2H), 7.83–7.80 (m, 1H), 7.65–7.62 (m, 1H), 7.40–7.35 (m, 2H), 3.85 (s, 4H), 1.08 (s, 6H); ¹³C NMR (CDCl₃, 100 MHz) δ 163.2, 150.8, 142.2, 134.8, 134.3, 134.1, 131.0, 129.5, 127.9, 127.7, 125.1, 124.9, 124.6, 123.7, 120.0, 110.6, 72.4, 31.9, 21.9; HRMS (DART) *m/z* calcd for C₂₂H₂₁BNO₃ [M+H]⁺: 358.1615, found: 358.1618.



A 20-mL glass vessel equipped with J. Young[®] O-ring tap containing a magnetic stirring bar was dried with a heatgun *in vacuo* and filled with N₂ gas after cooling to room temperature. To this vessel was added a phenyl 3-nicotinate (**1A**: 59.8 mg, 0.30 mmol, 1.5 equiv), 2-(7-(5,5-dimethyl-1,3,2-dioxaborinan-2-yl)naphthalen-2-yl)benzo[d]oxazole (**11**: 71.4 mg, 0.20 mmol, 1.0 equiv), Na₂CO₃ (42.4 mg, 0.4 mmol, 2.0 equiv), and NaCl (11.9 mg, 0.20 mmol, 1.0 equiv). The vessel was introduced into an argon-atmosphere glovebox. To the reaction vessel was added Ni(cod)₂ (5.5 mg, 0.020 mmol, 10 mol%), and then taken out of the glovebox. To this were added P(*n*-Bu)₃ (10 mL, 0.08 mmol, 40 mol%) and toluene (0.8 mL) under a stream of N₂. The vessel was sealed with O-ring tap and then heated at 150 °C for 48 h in an oil bath with stirring. After cooling the reaction mixture to room temperature, the mixture was passed through a short silica gel pad with EtOAc. The filtrate was concentrated *in vacuo* and the residue was purified by silica-gel column chromatography by using Isolera[®] (hexane/EtOAc = 4:1 to EtOAc) to afford

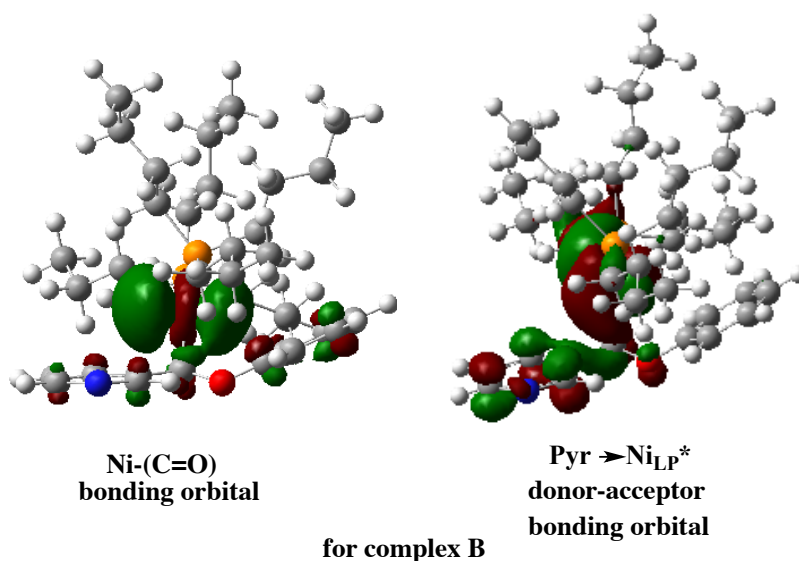
2-(7-(pyridin-3-yl)naphthalen-2-yl)benzo[*d*]oxazole (**12**: 33.8 mg, 52% yield) as a white solid. ¹H NMR (CDCl₃, 600 MHz) δ 9.00 (s, 1H), 8.79 (s, 1H), 8.66 (d, *J* = 4.2 Hz, 1H), 8.36 (d, *J* = 9.0 Hz, 1H), 8.10–8.07 (m, 2H), 8.05–7.98 (m, 2H), 7.84–7.75 (m, 2H), 7.64–7.60 (m, 1H), 7.45–7.41 (m, 1H), 7.40–7.34 (m, 2H); ¹³C NMR (CDCl₃, 150 MHz) δ 162.9, 150.8, 148.9, 148.5, 142.2, 137.0, 136.1, 134.9, 134.6, 132.4, 129.9, 129.1, 127.8, 126.1, 125.3, 124.9, 124.7, 123.7, 120.1, 110.6; HRMS (DART) *m/z* calcd for C₂₂H₁₅N₂O [M+H]⁺: 323.1184, found: 323.1181.

4-7. Computational Details

Calculations were performed by Gaussian 09 quantum chemical package.^[80] The geometries of all reported structures were optimized without symmetry constraints in toluene at the M06L level of density functional theory^[81] in conjunction with the LanL2dz basis set and corresponding Hay–Wadt ECP for Ni.^[82,83] Standard 6-31G(d) basis sets were used for all other atoms. Below, this approach will be called as M06L/{LanL2dz + [6-31G(d)]} or M06L/BS1. Solvent effects were estimated by using the PCM solvation method.^[84–86] Previously, we have shown that this approach reasonable describes geometries and energetics of the Ni-complexes and Ni-catalyzed coupling reactions²⁷. In order to incorporate disperse interactions into calculations we also performed geometry optimization and energy calculations of selected important intermediates and transition states at the M06/BS1 level of theory.^[87]

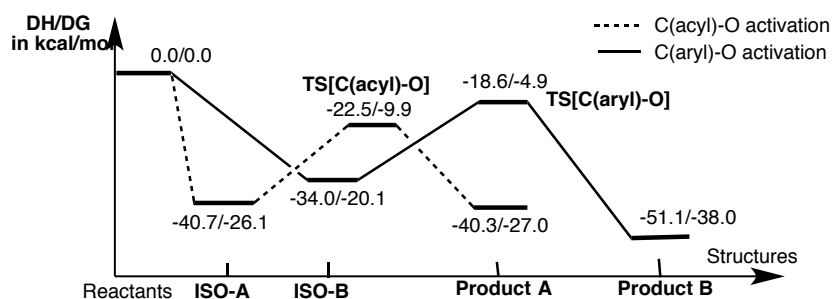
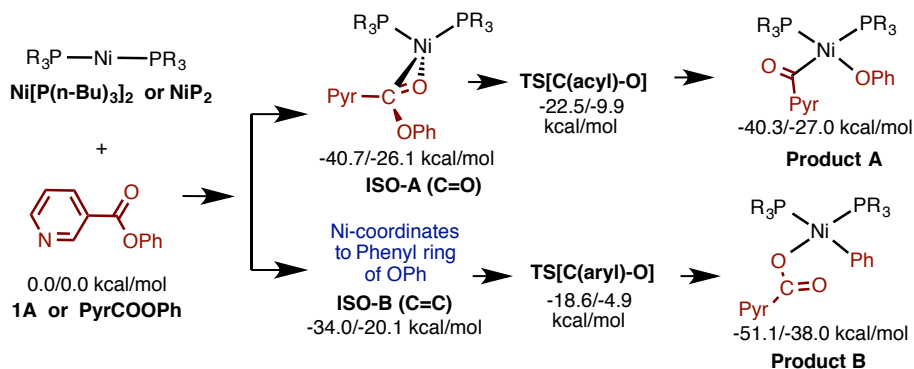
The nature of each stationary point was characterized by performing normal mode analysis at the appropriate (i.e. same as a geometry optimization) levels of theory. Relative free energies and enthalpies of all reported structures were calculated under standard conditions (1 atm and 298.15 K). In the presented figures and tables, we give both relative Gibbs free energies and enthalpies (in kcal/mol) as ΔG/ΔH. Cartesian coordinates and total energies of all reported structures are also presented below. In this paper, the M06/BS1 calculated free energies (i.e. ΔG values) at 298.15 K are mainly discussed unless otherwise specified.

4-8. NBO Analysis of the Intermediate Complex B



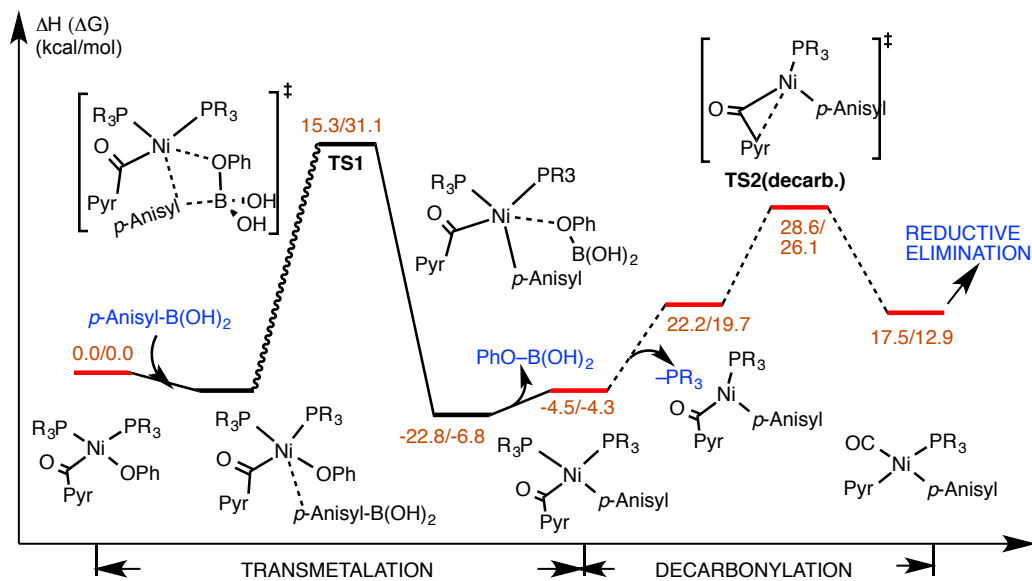
4-9. Computational data

Oxidative Addition of Phenyl 3-Pyridinecarboxylate to Ni[P(*n*-Bu)₃]₂ Catalyst



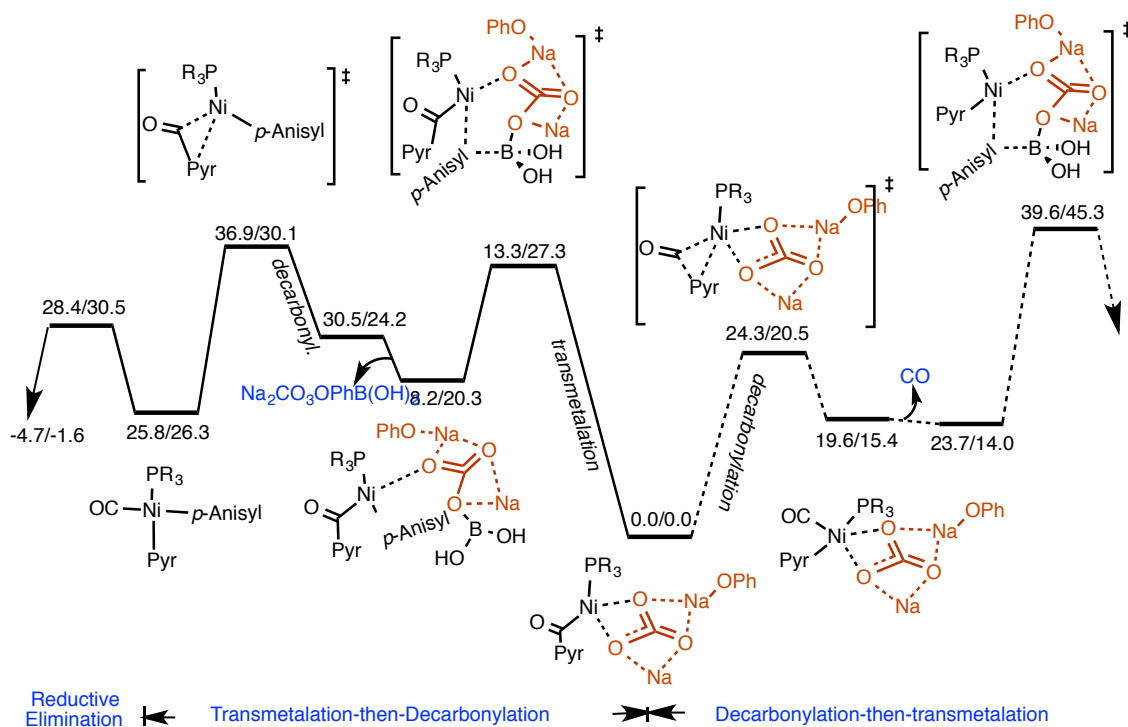
Transmetalation-then-Decarbonylation Pathway in the No-Base Condition

(M06L/BS1 level of theory)



Transmetalation-then-Decarbonylation Pathway in the Presence of Na₂CO₃

(M06L/BS1 level of theory)



Calculated Total and Relative Energies (in kcal/mol) (M06L/BS1 level of theory)

Structure	Energies				Relative Energies			
	-E _{tot}	-(E + ZPC)	-H	-G	ΔE	Δ(E+ZPC)	ΔH	ΔG
Ni[P(n-Bu) ₃] ₂ → Ni[P(n-Bu) ₃] + [P(n-Bu) ₃]								
Ni[P(n-Bu) ₃] ₂	1799.047953	1798.302214	1798.262328	1798.375858	-42.1	-41.5	-41.1	-28
Ni[P(n-Bu) ₃] ₂	984.149528	983.776269	983.755037	983.826269				
[P(n-Bu) ₃]	814.831310	814.459779	814.441825	814.504941				
Ni[P(n-Bu) ₃] ₂ + [P(n-Bu) ₃]	1798.980838	1798.236048	1798.196862	1798.33121	0.0	0.0	0.0	0.0
Oxidative addition of phenyl 3-pyridinecarboxylate (1A) to Ni[P(n-Bu) ₃] ₂ catalyst								
Ni[P(n-Bu) ₃] ₂ + (PyrCOOPh)	2466.886649	2466.956609	2465.904096	2466.070012	0	0	0	0
Ni[P(n-Bu) ₃] ₂ (PyrCOOPh)								
ISO-A(C=O)	2466.955448	2466.022313	2465.969010	2466.111613	-43.2/0	-41.2/0	-40.7/0	-26.1/0
ISO-B(C=C)	2466.943787	2466.012035	2465.958304	2466.102092	-35.9	-34.8	-34	-20.1
TS[C(acyl)-O]	2466.924214	2465.994081	2465.940003	2466.085737	-23.6/19.6	-23.5/17.7	-22.5/18.2	-9.9/16.2
TS[C(aryl)-O]	2466.918790	2465.987373	2465.933787	2466.077801	-20.2	-19.3	-18.6	-4.9
Ni[P(n-Bu) ₃] ₂ (PyrCO)(OPh), from TS[C(acyl)-O]	2466.954329	2466.022239	2465.968331	2466.112966	-42.5	-41.2	-40.3	-27
Ni[P(n-Bu) ₃] ₂ (PyrCO)(Ph), from TS[C(aryl)-O]	2466.973059	2466.039236	2465.985560	2466.130675	-54.2	-51.9	-51.1	-38.1
Ni[P(n-Bu) ₃] ₂ + Na ₂ CO ₃ → Ni[P(n-Bu) ₃] ₂ [Na ₂ CO ₃]								
NiP ₂ [Na ₂ CO ₃]								
iso2	2387.576020	2386.809538	2386.761115	2386.894495	-21.0	-19.0	-18.2	-6.4
iso1	2387.580192	2386.814613	2386.766031	2386.899542	-23.6	-22.2	-21.3	-9.6
Na ₂ CO ₃	588.494676	588.4770470	588.469801	588.508414				
Ni[P(n-Bu) ₃] ₂	1799.047953	1798.302214	1798.262328	1798.375858				
Ni[P(n-Bu) ₃] ₂ + Na ₂ CO ₃	2387.542629	2386.779261	2386.732129	2386.884272	0.0	0.0	0.0	0.0
Ni[P(n-Bu) ₃] ₂ [Na ₂ CO ₃] → Ni[P(n-Bu) ₃] ₂ [Na ₂ CO ₃] + [P(n-Bu) ₃]								
NiP ₂ [Na ₂ CO ₃], iso1	2387.580192	2386.814613	2386.766031	2386.899542	0.0	0.0	0.0	0.0
NiP[Na ₂ CO ₃], iso1	1572.707774	1572.316435	1572.287108	1572.380429				
[P(n-Bu) ₃]	814.831310	814.459779	814.441825	814.504940				
NiP[Na ₂ CO ₃] + [P(n-Bu) ₃]	2387.539084	2386.776214	2386.728933	2386.885369	25.8	24.1	23.2	8.9

Calculated total and Relative Energies (in kcal/mol) of Decarbonylative Transmetalation in the Absence of Na₂CO₃ Base (M06L/BS1 level of theory)

Structure	Energies				Relative Energies			
	-E _{tot}	-(E + ZPC)	-H	-G	ΔE	Δ(E+ZPC)	ΔH	ΔG
I. Decarbonylation-then-transmetalation from the oxidative addition product Ni[P(n-Bu) ₃] ₂ (PyrCO)(OPh), after one of the ligands [i.e. P(n-Bu) ₃] dissociation.								
I.A.1. P(n-Bu) ₃ - dissociation								
Ni[P(n-Bu) ₃] ₂ (PyrCO)(OPh)	2466.954329	2466.022239	2465.968331	2466.112966	[0.0]	[0.0]	[0.0]	[0.0]
[P(n-Bu) ₃]	814.831310	814.459779	814.441825	814.504941				
Ni[P(n-Bu) ₃](PyrCO)(OPh)+[P(n-Bu) ₃]	2466.905400	2466.976871	2466.924291	2466.090237	[30.7]	[28.5]	[27.6]	[14.3]
I.A.2. Decarbonylation								
Ni[P(n-Bu) ₃](PyrCO)(OPh)	1652.074090	1651.517092	1651.482466	1651.585296	0.0	0.0	0.0	0.0
TS [(OC-C(Pyr))]	1652.062105	1651.506432	1651.472146	1651.573609	7.5	6.7	6.5	7.3
Ni[P(n-Bu) ₃](CO)(OPh)(Pyr)	1652.071579	1651.515716	1651.480567	1651.584590	1.6	0.9	1.2	0.4
I.B. Transmetalation from the Ni[P(n-Bu) ₃](CO)(OPh)(Pyr) complex								
Ni[P(n-Bu) ₃](CO)(OPh)(Pyr)	1652.071579	1651.515716	1651.480567	1651.584590				
MeOPh ₂ B(OH) ₂	522.743995	522.585484	522.574127	522.622372				
Ni[P(n-Bu) ₃](CO)(OPh)(Pyr)	2174.825574	2174.101200	2174.054694	2174.206962	0.0	0.0	0.0	0.0
+MeOPh ₂ B(OH) ₂	2174.846852	2174.129090	2174.082738	2174.211641	-13.4	-17.5	-17.6	-2.9
Ni[P(n-Bu) ₃](CO)(Pyr)(OPh)	1691.334516	1690.750869	1690.71358	1690.822796				
[MeOPh ₂ B(OH) ₂], B-C, pre-reaction complex	2174.845932	2174.129063	2174.082710	2174.208173				
TS(B-C act.)	2174.804872	2174.091779	2174.046422	2174.169626				
	2174.805385	2174.091461	2174.045258	2174.170968	12.7	6.1	5.9	22.6
Ni[P(n-Bu) ₃](Pyr)(CO)(PhOMe)((HO) ₂ B-OPh)								
CO-N trans, iso1	2174.832348	2174.116384	2174.069275	2174.200053	-4.3	-9.5	-9.2	4.3
CO-N trans, iso2	2174.831376	2174.115632	2174.068231	2174.201346				
Ni[P(n-Bu) ₃](Pyr)(CO)(PhOMe)								
N-CO trans	1691.334065	1690.750683	1690.71358	1690.822796				
P-CO trans	1691.334516	1690.750869	1690.71376	1690.823534				
[(HO) ₂ B-OPh], iso2	483.482975	483.352792	483.343067	483.387441				
Ni[P(n-Bu) ₃](Pyr)(CO)(PhOMe), N-CO trans + [(HO) ₂ B-OPh]	2174.817040	2174.103475	2174.056647	2174.210237	5.4	-1.4	-1.2	-2.1
I.C. Reductive Elimination								
Ni[P(n-Bu) ₃]	1799.047953	1798.302214	1798.262328	1798.375858				
N-CO trans	1691.334065	1690.750683	1690.713580	1690.822796	0.0	0.0	0.0	0.0

	Iso-3b	3055.499666	3054.549503	3054.487244	3054.650785				
C. Ligand Exchange: Ni[P(n-Bu) ₃](PyrCO)(Na ₂ CO ₃ Oph) → Ni[P(n-Bu) ₃](PyrCO)(NaCO ₃) + NaOph									
Ni[P(n-Bu) ₃](PyrCO)(Na ₂ CO ₃ Oph)	Iso-3a	3055.505151	3054.555050	3054.492800	3054.656882	0.0	0.0	0.0	0.0
	Iso-3b	3055.499666	3054.549503	3054.487244	3054.650785				
Ni[P(n-Bu) ₃](PyrCO)(NaCO ₃)	Down Iso-3a	2586.260084	2585.404600	2585.350746	2585.497264				
	UP iso-3b	2586.262707	2585.407175	2585.353485	2585.498639				
Na_Oph		469.175242	469.082344	469.074299	469.114741				
Ni[P(n-Bu) ₃](PyrCO)(NaCO ₃), iso3b_UP + NaOph		3055.437949	3054.489519	3054.427784	3054.613380	42.2	41.1	40.8	27.3
D. Reaction: Ni[P(n-Bu) ₃](PyrCO)(Na ₂ CO ₃ Oph) → Ni[P(n-Bu) ₃](PyrCO)(NaCO ₃ Oph) + [P(n-Bu) ₃]									
Ni[P(n-Bu) ₃](PyrCO)(Na ₂ CO ₃ Oph), Iso-3a		3055.505151	3054.555050	3054.492800	3054.656882	0.0	0.0	0.0	0.0
Ni[P(n-Bu) ₃](PyrCO)(Na ₂ CO ₃ Oph)	Iso1	2240.650977	2240.074859	2240.032693	2240.151469				
	Iso2	2240.653829	2240.076958	2240.035154	2240.150825				
[P(n-Bu) ₃]		814.831310	814.459779	814.441825	814.504941				
Ni[P(n-Bu) ₃](PyrCO)(Na ₂ CO ₃ Oph), iso2 + [P(n-Bu) ₃]		3055.485139	3054.536737	3054.476979	3054.655766	12.6	11.5	9.9	0.7

Calculated Total and Relative Energies (in kcal/mol) of Product, Intermediate, and Transition State the Reaction in the Presence of Na₂CO₃ (M06L/BS1 level of theory)

Structure		-E _{tot}	-(E + ZPC)	-H	-G	ΔE	Relative Energies Δ(E+ZPC)	ΔH	ΔG
arbylation-then-transmetalation from the Ni[P(n-Bu) ₃](PyrCO)(Na ₂ CO ₃ Oph) cluster complex									
ecarbonylation: Ni[P(n-Bu) ₃](PyrCO)(Na ₂ CO ₃ Oph) → Ni[P(n-Bu) ₃](CO)(Pyr)(Na ₂ CO ₃ Oph)									
i-Bu) ₃](PyrCO)(Na ₂ CO ₃ Oph)	Iso-2	2240.653829	2240.076958	2240.035154	2240.150825	0.0	0.0	0.0	0.0
	TS	2240.612500	2240.039326	2239.996498	2240.118211	25.9	23.6	24.3	20.5
i-Bu) ₃](CO)(Pyr)(Na ₂ CO ₃ Oph), Trans-O		2240.621459	2240.047162	2240.003860	2240.126299	20.3	18.7	19.6	15.4
CO-dissociation: Ni[P(n-Bu) ₃](Pyr)(CO)(Na ₂ CO ₃ Oph) → Ni[P(n-Bu) ₃](Pyr)(Na ₂ CO ₃ Oph) + CO									
i-Bu) ₃](PyrCO)(Na ₂ CO ₃ Oph)	Trans-O	2240.621459	2240.047162	2240.003860	2240.126299	0.0	0.0	0.0	0.0
	Trans-N	2240.614635	2240.040420	2239.997244	2240.119472				
		113.296662	113.291641	113.288337	113.3107850				
i-Bu) ₃](Pyr)(Na ₂ CO ₃ Oph),		2127.308317	2126.742004	2126.701406	2126.817765				
Ni[P(n-Bu) ₃](Pyr)(Na ₂ CO ₃ Oph) + CO		2240.604979	2240.033645	2239.989743	2240.128550	10.3	8.5	8.9	-1.4
I.B. Transmetalation from the Ni[P(n-Bu) ₃](Pyr)(Na ₂ CO ₃ Oph) complex									
Ni[P(n-Bu) ₃](Pyr)(Na ₂ CO ₃ Oph),		2127.308317	2126.742004	2126.701406	2126.817765				
MeOph_B(OH) ₂		522.743995	522.585484	522.574127	522.622372				
Ni[P(n-Bu) ₃](Pyr)(Na ₂ CO ₃ Oph) + MeOph_B(OH) ₂		2650.052312	2649.327488	2649.275533	2649.440137	0.0	0.0	0.0	0.0
COMPLEX _x		2650.054169	2649.328488	2649.276691	2649.413974	-1.2	-0.6	-0.7	16.4
TS1, B-O formation									
B-O complex		2650.053240	2649.327730	2649.275783	2649.414957	-0.6	-0.2	-0.2	15.8
TS2, B-C active.		2650.025711	2649.302276	2649.250183	2649.390267	16.7	15.8	15.9	31.3
B-C complex: Ni[P(n-Bu) ₃](Pyr)(MeOph)(Na ₂ CO ₃ Oph)B(OH) ₂	iso1	2650.040433	2649.315553	2649.263193	2649.403507	7.5	7.5	7.7	23
	iso2	2650.031954	2649.307755	2649.255311	2649.396236				
Ni[P(n-Bu) ₃](Pyr)(MeOph), O-P trans, Iso-1		1577.980792	1577.406174	1577.371479	1577.476373				
Na ₂ CO ₃ (Oph)B(OH) ₂		1072.020568	1071.872413	1071.854530	1071.919027				
Ni[P(n-Bu) ₃](Pyr)(MeOph) + Na ₂ CO ₃ (Oph)B(OH) ₂		2650.001360	2649.278587	2649.226009	2649.395400	32.0	30.7	31.1	28.1
I.C. Reductive elimination									
Ni[P(n-Bu) ₃](Pyr)(MeOph)(Na ₂ CO ₃ Oph)B(OH) ₂	iso1	2650.040433	2649.315553	2649.263193	2649.403507	0.0	0.0	0.0	0.0
	iso2	2650.031954	2649.307755	2649.255311	2649.396236				
TS, iso2		2650.027094	2649.303384	2649.251479	2649.390739	8.4	7.6	7.4	8.0
COMPLEX _{prod} ,	iso-1	2650.065887	2649.340579	2649.288578	2649.427124				
	iso-2	2650.083236	2649.357099	2649.305590	2649.442512	-26.9	-26.1	-26.6	-24.5
Ni[P(n-Bu) ₃](Na ₂ CO ₃ Oph)B(OH) ₂		2056.249575	2055.728396	2055.689485	2055.802417				
MeOph_Pyr		593.806680	593.603521	593.591395	593.641012				
Ni[P(n-Bu) ₃](Na ₂ CO ₃ Oph)B(OH) ₂ + MeOph_Pyr		2650.056255	2649.331917	2649.280880	2649.443429	-9.9	-10.3	-11.1	-25.1
II. Transmetalation-then-decarbonylation from the Ni[P(n-Bu) ₃](PyrCO)(Na ₂ CO ₃ Oph) cluster complex									
II.A. Transmetalation from Ni[P(n-Bu) ₃](PyrCO)(Na ₂ CO ₃ Oph)									
Ni[P(n-Bu) ₃](PyrCO)(Na ₂ CO ₃ Oph), Iso-1		2240.653829	2240.076958	2240.035154	2240.150825				
MeOph_B(OH) ₂		522.743995	522.585484	522.574127	522.622372				
Ni[P(n-Bu) ₃](PyrCO)(Na ₂ CO ₃ Oph) + MeOph_B(OH) ₂		2763.397824	2762.662442	2762.609281	2762.773197	0.0	0.0	0.0	0.0
TS(B-C active.)	Iso2_down	2763.364975	2762.630124	2762.576682	2762.718606	20.6	20.3	20.5	34.3
	Iso2_up	2763.375548	2762.641315	2762.588054	2762.729615	14.0	13.3	13.3	27.3
Ni[P(n-Bu) ₃](PyrCO)(PhOMe)(Na ₂ CO ₃ Oph)B(OH) ₂	Iso2_down	2763.384351	2762.648868	2762.594958	2762.738319				
	Iso2_up	2763.385586	2762.650096	2762.596291	2762.740707	7.7	7.8	8.2	20.3
II.B. Ni[P(n-Bu) ₃](PyrCO)(PhOMe)(Na ₂ CO ₃ Oph)B(OH) ₂ → Ni[P(n-Bu) ₃](PyrCO)(PhOMe) + (Na ₂ CO ₃ Oph)B(OH) ₂									
Ni[P(n-Bu) ₃](PyrCO)(PhOMe)(Na ₂ CO ₃ Oph)B(OH) ₂ , Iso2_up		2763.385586	2762.650096	2762.596291	2762.739707	0.0	0.0	0.0	0.0
Ni[P(n-Bu) ₃](PyrCO)(PhOMe)		1691.327612	1690.742389	1690.706162	1690.811668				
Na ₂ CO ₃ OphB(OH) ₂		1072.020568	1071.872413	1071.854530	1071.919027				
Ni[P(n-Bu) ₃](PyrCO)(PhOMe) + [Na ₂ CO ₃ Oph)B(OH) ₂]		2763.348180	2762.614802	2762.560692	2762.733495	23.5	22.1	22.3	3.8
II.C. Decarbonylation: Ni[P(n-Bu) ₃](PyrCO)(PhOMe) → Ni[P(n-Bu) ₃](Pyr)(CO)(PhOMe)									
See Supplementary Table 9, section II.B									
II.D. Reduction Elimination from the decarbonylated product Ni[P(n-Bu) ₃](Pyr)(CO)(PhOMe)									
See Supplementary Table 9, section I.C									

Calculated Total and Relative Energies (in kcal/mol) of Product, Intermediate, and Transition State the Reaction in the Absence of Na₂CO₃ (M06L/BS1 level of theory)

Structure	Energies				ΔE	Relative Energies		
	-E _{tot}	-(E +ZPC)	-H	-G		Δ(E+ZPC)	ΔH	ΔG
Ni[P(n-Bu) ₃] ₂ → Ni[P(n-Bu) ₃] + [P(n-Bu) ₃]								
[P(n-Bu) ₃]	814.490909	814.122914	814.103415	814.170490				
Na ₂ CO ₃	588.394747	588.377485	588.369946	588.409119				
MeOPh-B(OH) ₂	522.478119	522.320396	522.308972	522.357204				
Na ₂ CO ₃ (OPh)[B(OH) ₂]	1071.684273	1071.535321	1071.517884	1071.581034				
NaOPh	468.986985	468.894407	468.886389	468.926895				
PyrCOOPh	667.449129	667.265396	667.252733	667.305218				
Transmetalation from the Ni[P(n-Bu)₃]₂(OPh)(PyrCO) oxidative addition complex (i.e. in the absence of Na₂CO₃)								
Ni[P(n-Bu) ₃] ₂ (PyrCO)(OPh)	2465.849470	2464.923877	2464.870386	2465.012720				
Ni[P(n-Bu) ₃] ₂ (PyrCO)(OPh) + MeOPh-B(OH) ₂	2988.327589	2987.244273	2987.179358	2987.369924	0.0	0.0	0.0	0.0
TS(TRME, no base)	2988.310009	2987.223803	2987.159129	2987.323873	11.1	12.8	12.7	28.9
Prod., iso1	2988.378488	2987.292071	2987.227559	2987.392273	-31.9	-30.0	-30.2	-14.0
Reaction Ni[P(n-Bu)₃]₂(PyrCO)(OPh) + Na₂CO₃ → Ni[P(n-Bu)₃]₂(PyrCO)(Na₂CO₃OPh)								
Ni[P(n-Bu) ₃] ₂ (PyrCO)(OPh) + Na ₂ CO ₃	3054.244217	3053.301362	3053.240332	3053.421839	0.0	0.0	0.0	0.0
Ni[P(n-Bu) ₃] ₂ (PyrCO)(Na ₂ CO ₃ OPh)	3054.299150	3053.355753	3053.293809	3053.455389	-34.5	-34.1	-33.6	-21.1
Reaction Ni[P(n-Bu)₃]₂(PyrCO)(Na₂CO₃OPh) → Ni[P(n-Bu)₃]₂(PyrCO)(Na₂CO₃OPh) + [P(n-Bu)₃]								
Ni[P(n-Bu) ₃] ₂ (PyrCO)(Na ₂ CO ₃ OPh)	3054.29915	3053.355753	3053.293809	3053.455389	0.0	0.0	0.0	0.0
<hr/>								
Ni[P(n-Bu) ₃] ₂ (PyrCO)(Na ₂ CO ₃ OPh)	2239.79129	2239.217874	2239.176036	2239.292649				
Ni[P(n-Bu) ₃] ₂ (PyrCO)(Na ₂ CO ₃ OPh) + [P(n-Bu) ₃]	3054.282199	3053.340788	3053.279451	3053.463139	10.6	9.4	9.0	-4.9
Transmetalation from the Ni[P(n-Bu)₃]₂(Pyr)(Na₂CO₃OPh) complex								
Ni[P(n-Bu) ₃] ₂ (PyrCO)(Na ₂ CO ₃ OPh) + MeOPh-B(OH) ₂	2762.269409	2761.538270	2761.485008	2761.649853	0.0	0.0	0.0	0.0
B-O complex	2762.273253	2761.541162	2761.488113	2761.627769	-2.4	-1.8	-2.0	13.9
TS(TRME, Na ₂ CO ₃ OPh)	2762.260184	2761.529096	2761.476239	2761.617153	5.8	5.8	5.5	20.5
Product	2762.270430	2761.537494	2761.484054	2761.626846	-0.7	0.5	0.6	14.4
Ni[P(n-Bu) ₃] ₂ (PyrCO)(MeOPh) + Na ₂ CO ₃ (OPh)[B(OH) ₂]	2762.232157	2761.502610	2761.448586	2761.619122	23.4	22.4	22.9	19.3
Decarbonylation: Ni[P(n-Bu)₃]₂(PyrCO)(PhOMe) → Ni[P(n-Bu)₃]₂(Pyr)(CO)(PhOMe)								
Ni[P(n-Bu) ₃] ₂ (PyrCO)(MeOPh)	1690.547884	1689.967289	1689.930702	1690.038088	0.0	0.0	0.0	0.0
TS (decarbonylation)	1690.534837	1689.955043	1689.919302	1690.024305	8.2	7.7	7.2	8.7
Ni[P(n-Bu) ₃] ₂ (Pyr)(CO)(MeOPh)	1690.553265	1689.974446	1689.937195	1690.047382	-3.4	-4.5	-4.1	-5.8
Reductive Elimination								
Ni[P(n-Bu) ₃] ₂ (Pyr)(CO)(MeOPh)	1690.553265	1689.974446	1689.937195	1690.047382	0.0	0.0	0.0	0.0
TS	1690.546591	1689.968420	1689.932022	1690.038307	4.2	3.8	3.3	5.7

References and Notes

1. *Cross-Coupling Reactions: A Practical Guide*; Miyaura, N., Ed.; Topics in Current Chemistry, Vol. 219; Springer: Berlin, **2002**.
2. Miyaura, N.; Suzuki, A. *Chem. Rev.* **1995**, *95*, 2457.
3. Lee, J. C. H. & Hall, D. G.; *State-of-the-art in metal-catalyzed Cross-Coupling Reactions of organoboron compounds with organic electrophiles*, in *Metal-catalyzed cross-coupling reactions and more*: de Meijere, A.; Bräse, S.; Oestreich, M. Eds: pp. 65–132; Wiley-VCH: Weinheim, **2014**.
4. Roglans, A.; Pla-Quintana, A.; Moreno-Mañas, M. *Chem. Rev.* **2006**, *106*, 4622.
5. Blakey, S. B.; MacMillan, D. W. C. *J. Am. Chem. Soc.* **2003**, *125*, 6046.
6. Rosen, B. M.; Quasdorf, K. W.; Wilson, D. A.; Zhang, N.; Resmerita, A.-M.; Garg, N. K.; Percec, V. *Chem. Rev.* **2011**, *111*, 1346.
7. Modha, S. G.; Mehta, V. P.; Van der Eycken, E. V. *Chem. Soc. Rev.* **2013**, *42*, 5042.
8. Yu, D.-G.; Yu, M.; Guan, B.-T.; Li, B.-J.; Zheng, Y.; Wu, Z.-H.; Shi, Z.-J. *Org. Lett.* **2009**, *11*, 3374.
9. Chen, X.; Engle, K. M.; Wang, D.-H.; Yu, J.-Q. *Angew. Chem., Int. Ed.* **2009**, *48*, 5094.
10. Sun, C.-L.; Li, B.-J.; Shi, Z.-J. *Chem. Commun.* **2010**, *46*, 677.
11. Yamaguchi, J.; Itami, K.; *Biaryl synthesis through metal-catalyzed C–H arylation*, in *Metal-catalyzed cross-coupling reactions and more*: de Meijere, A.; Bräse, S.; Oestreich, M. Eds: pp. 1315–1387; Wiley-VCH: Weinheim, **2014**.
12. Mkhaliid, I. A. I.; Barnard, J. H.; Marder, T. B.; Murphy, J. M.; Hartwig, J. F. *Chem. Rev.* **2010**, *110*, 890.
13. Gooßen, L. J.; Rodríguez, N.; Gooßen, K. *Angew. Chem., Int. Ed.* **2008**, *47*, 3100.
14. Dzik, W. I.; Lange, P. P.; Gooßen, L. J. *Chem. Sci.* **2012**, *3*, 2671.
15. Gooßen, L. J.; Deng, G.; Levy, L. M. *Science* **2006**, *313*, 662.
16. Gooßen, L. J.; Paetzold, J. *Adv. Synth. Catal.* **2004**, *346*, 1665.
17. Wang, J.; Liu, B.; Zhao, H.; Wang, J. *Organometallics* **2012**, *31*, 8598.
18. Trost, B. M.; Chen, F. *Tetrahedron Lett.* **1971**, *12*, 2603.
19. O'Brien, E. M.; Bercot, E. A.; Rovis, T. *J. Am. Chem. Soc.* **2003**, *125*, 10498.
20. Havlik, S. E.; Simmons, J. M.; Winton, V. J.; Johnson, J. B. *J. Org. Chem.* **2011**, *76*, 3588.

21. Yamamoto, T.; Ishizu, J.; Kohara, T.; Komiya, S.; Yamamoto, A. *J. Am. Chem. Soc.* **1980**, *102*, 3758.
22. Amaike, K.; Muto, K.; Yamaguchi, J.; Itami, K. *J. Am. Chem. Soc.* **2012**, *134*, 13573.
23. Hong, X.; Liang, Y.; Houk, K. N. *J. Am. Chem. Soc.* **2014**, *136*, 2017.
24. Lu, Q.; Yu, H.; Fu, Y. *J. Am. Chem. Soc.* **2014**, *136*, 8252.
25. Xu, H.; Muto, K.; Yamaguchi, J.; Zhao, C.; Itami, K.; Musaev, D. G. *J. Am. Chem. Soc.* **2014**, *136*, 14834.
26. Tasker, S. Z.; Standley, E. A.; Jamison, T. F. *Nature* **2014**, *509*, 299.
27. Yamaguchi, J.; Muto, K.; Itami, K. *Eur. J. Org. Chem.* **2012**, *2013*, 19.
28. Nakao, Y.; Oda, S. A.; Hiyama, T. *J. Am. Chem. Soc.* **2004**, *126*, 13904.
29. Watson, M. P.; Jacobsen, E. N. *J. Am. Chem. Soc.* **2008**, *130*, 12594.
30. Murakami, M.; Ashida, S.; Matsuda, T. *J. Am. Chem. Soc.* **2005**, *127*, 6932.
31. Muto, K.; Yamaguchi, J.; Itami, K. *J. Am. Chem. Soc.* **2012**, *134*, 169.
32. Meng, L.; Kamada, Y.; Muto, K.; Yamaguchi, J.; Itami, K. *Angew. Chem., Int. Ed.* **2013**, *52*, 10048.
33. Muto, K.; Yamaguchi, J.; Lei, A.; Itami, K. *J. Am. Chem. Soc.* **2013**, *135*, 16384.
34. Takise, R.; Muto, K.; Yamaguchi, J.; Itami, K. *Angew. Chem., Int. Ed.* **2014**, *53*, 6791.
35. Liu, L.; Zhang, S.; Chen, H.; Lv, Y.; Zhu, J.; Zhao, Y. *Chem. Asian J.* **2013**, *8*, 2592.
36. Ananikov, V. P. *ACS Catal.* **2015**, *5*, 1964.
37. Figg, T. M.; Wasa, M.; Yu, J.-Q.; Musaev, D. G. *J. Am. Chem. Soc.* **2013**, *135*, 14206.
38. Petersen, T. B.; Khan, R.; Olofsson, B. *Org. Lett.* **2011**, *13*, 3462.
39. Battershill, A. J.; Scott, L. J. *Drugs* **2006**, *66*, 51.
40. Quasdorf, K. W.; Tian, X.; Garg, N. K. *J. Am. Chem. Soc.* **2008**, *130*, 14422.
41. Guan, B.-T.; Wang, Y.; Li, B.-J.; Yu, D.-G.; Shi, Z.-J. *J. Am. Chem. Soc.* **2008**, *130*, 14468.
42. Tobisu, M.; Shimasaki, T.; Chatani, N. *Angew. Chem., Int. Ed.* **2008**, *47*, 4866.
43. Antoft-Finch, A.; Blackburn, T.; Snieckus, V. *J. Am. Chem. Soc.* **2009**, *131*, 17750.
44. Ladouceur, G. H., Connell, R. D., Baryza, J., Campbell, A.-M., Lease, T. G. & Cook, J. H. U. S. Patent 1998024627.

45. Eickmeier, C., Fuchs, K., Peters, S., Dorner-Ciossek, C., Heine, N., Handschuh, S., Klinder, K. & Kostka, M. Eur. Patent 2006002769.
46. Palmer, J. T.; Bryant, C.; Wang, D.-X.; Davis, D. E.; Setti, E. L.; Rydzewski, R. M.; Venkatraman, S.; Tian, Z.-Q.; Burrill, L. C.; Mendonca, R. V.; Springman, E.; McCarter, J.; Chung, T.; Cheung, H.; Janc, J. W.; McGrath, M.; Somoza, J. R.; Enriquez, P.; Yu, Z. W.; Strickley, R. M.; Liu, L.; Venuti, M. C.; Percival, M. D.; Falgueyret, J.-P.; Prasit, P.; Oballa, R.; Riendeau, D.; Young, R. N.; Wesolowski, G.; Rodan, S. B.; Johnson, C.; Kimmel, D. B.; Rodan, G. *J. Med. Chem.* **2005**, *48*, 7520.
47. Roy, H. N.; Al Mamun, A. H. *Synth. Commun.* **2006**, *36*, 2975.
48. Bottalico, D.; Fiandanese, V.; Marchese, G.; Punzi, A. *Synlett* **2007**, *2007*, 0974.
49. Qin, C.; Wu, H.; Chen, J.; Liu, M.; Cheng, J.; Su, W.; Ding, J. *Org. Lett.* **2008**, *10*, 1537.
50. Ueda, T.; Konishi, H.; Manabe, K. *Org. Lett.* **2012**, *14*, 3100.
51. Ackermann, L.; Althammer, A. *Org. Lett.* **2006**, *8*, 3457.
52. Shen, H.-C.; Pal, S.; Lian, J.-J.; Liu, R.-S. *J. Am. Chem. Soc.* **2003**, *125*, 15762.
53. Tang, Y.-Q.; Lv, H.; Lu, J.-M.; Shao, L.-X. *J. Organomet. Chem.* **2011**, *696*, 2576.
54. Denmark, S. E.; Smith, R. C.; Chang, W.-T. T.; Muhuhi, J. M. *J. Am. Chem. Soc.* **2009**, *131*, 3104.
55. Kwong, F. Y.; Chan, K. S.; Yeung, C. H.; Chan, A. S. C. *Chem. Commun.* **2004**, 2336.
56. Hoshiya, N.; Shimoda, M.; Yoshikawa, H.; Yamashita, Y.; Shuto, S.; Arisawa, M. *J. Am. Chem. Soc.* **2010**, *132*, 7270.
57. Leowanawat, P.; Zhang, N.; Resmerita, A.-M.; Rosen, B. M.; Percec, V. *J. Org. Chem.* **2011**, *76*, 9946.
58. Molander, G. A.; Trice, S. L. J.; Dreher, S. D. *J. Am. Chem. Soc.* **2010**, *132*, 17701.
59. Molander, G. A.; Canturk, B.; Kennedy, L. E. *J. Org. Chem.* **2009**, *74*, 973.
60. Tamba, S.; Okubo, Y.; Tanaka, S.; Monguchi, D.; Mori, A. *J. Org. Chem.* **2010**, *75*, 6998.
61. Whitney, S. E.; Winters, M.; Rickborn, B. *J. Org. Chem.* **1990**, *55*, 929.
62. Kirchberg, S.; Tani, S.; Ueda, K.; Yamaguchi, J.; Studer, A.; Itami, K. *Angew. Chem., Int. Ed.* **2011**, *50*, 2387.
63. Kobayashi, O.; Uraguchi, D.; Yamakawa, T. *Org. Lett.* **2009**, *11*, 2679.

64. Cao, K.; Zhang, F.-M.; Tu, Y.-Q.; Zhuo, X.-T.; Fan, C.-A. *Chem. Eur. J.* **2009**, *15*, 6332.
65. Nguyen, T. T.; Marquise, N.; Chevallier, F.; Mongin, F. *Chem. Eur. J.* **2011**, *17*, 10405.
66. Zhao, J.; Zhao, Y.; Fu, H. *Angew. Chem., Int. Ed.* **2011**, *50*, 3769.
67. Parmentier, M.; Gros, P.; Fort, Y. *Tetrahedron* **2005**, *61*, 3261.
68. Saito, R.; Tokita, M.; Uda, K.; Ishikawa, C.; Satoh, M. *Tetrahedron* **2009**, *65*, 3019.
69. Tobisu, M.; Hyodo, I.; Chatani, N. *J. Am. Chem. Soc.* **2009**, *131*, 12070.
70. Chiba, S.; Xu, Y.-J.; Wang, Y.-F. *J. Am. Chem. Soc.* **2009**, *131*, 12886.
71. Barder, T. E.; Walker, S. D.; Martinelli, J. R.; Buchwald, S. L. *J. Am. Chem. Soc.* **2005**, *127*, 4685.
72. Molander, G. A.; Iannazzo, L. *J. Org. Chem.* **2011**, *76*, 9182.
73. Vella, S. J.; Tiburcio, J.; Gault, J. W.; Loeb, S. J. *Org. Lett.* **2006**, *8*, 3421.
74. Chen, G.-J.; Huang, J.; Gao, L.-X.; Han, F.-S. *Chem. Eur. J.* **2011**, *17*, 4038.
75. Gooßen, L. J.; Rodríguez, N.; Lange, P. P.; Linder, C. *Angew. Chem. Int. Ed.* **2010**, *49*, 1111.
76. Hiraoka, S.; Sakata, Y.; Shionoya, M. *J. Am. Chem. Soc.* **2008**, *130*, 10058.
77. Billingsley, K.; Buchwald, S. L. *J. Am. Chem. Soc.* **2007**, *129*, 3358.
78. Nakao, Y.; Imanaka, H.; Sahoo, A. K.; Yada, A.; Hiyama, T. *J. Am. Chem. Soc.* **2005**, *127*, 6952.
79. Inés, B.; Moreno, I.; SanMartin, R.; Domínguez, E. *J. Org. Chem.* **2008**, *73*, 8448.
80. *Gaussian 09, Revision D.01*, Frisch, M. J.; Trucks, G. W.; Schlegel, H. B.; Scuseria, G. E.; Robb, M. A.; Cheeseman, J. R.; Scalmani, G.; Barone, V.; Mennucci, B.; Petersson, G. A.; Nakatsuji, H.; Caricato, M.; Li, X.; Hratchian, H. P.; Izmaylov, A. F.; Bloino, J.; Zheng, G.; Sonnenberg, J. L.; Hada, M.; Ehara, M.; Toyota, K.; Fukuda, R.; Hasegawa, J.; Ishida, M.; Nakajima, T.; Honda, Y.; Kitao, O.; Nakai, H.; Vreven, T.; Montgomery, Jr. J. A.; Peralta, J. E.; Ogliaro, F.; Bearpark, M.; Heyd, J. J.; Brothers, E.; Kudin, K. N.; Staroverov, V. N.; Keith, T.; Kobayashi, R.; Normand, J.; Raghavachari, K.; Rendell, A.; Burant, J. C.; Iyengar, S. S.; Tomasi, J.; Cossi, M.; Rega, N.; Millam, J. M.; Klene, M.; Knox, J. E.; Cross, J. B.; Bakken, V.; Adamo, C.; Jaramillo, J.; Gomperts, R.; Stratmann, R. E.; Yazyev, O.; Austin, A. J.; Cammi, R.; Pomelli, C.; Ochterski, J. W.; Martin, R. L.; Morokuma, K.; Zakrzewski, V. G.; Voth, G. A.; Salvador, P.; Dannenberg, J. J.; Dapprich, S.;

Daniels, A. D.; Farkas, O.; Foresman, J. B.; Ortiz, J. V.; Cioslowski, J.; Fox, D. J. Gaussian, Inc., Wallingford CT, **2013**.

81. Zhao, Y.; Truhlar, D. G. A. *J. Chem. Phys.* **2006**, *125*, 194101.
82. Wadt, W. R.; Hay, P. J. *J. Chem. Phys.* **1985**, *82*, 284.
83. Hay, P. J.; Wadt, W. R. *J. Chem. Phys.* 1985, *82*, 299.
84. Mennucci, B.; Tomasi, J. *J. Chem. Phys.* **1997**, *106*, 3032.
85. Mennucci, B.; Tomasi, J. *J. Chem. Phys.* **1997**, *106*, 5151.
86. Scalmani, G.; Frisch, M. J. *J. Chem. Phys.* **2010**, *132*, 114110.
87. For M06 method see: (a) Zhao, Y.; Truhlar, D. G. *Theor. Chem. Acc.* **2008**, *120*, 215. (b) Zhao, Y.; Truhlar, D. G. *Acc. Chem. Res.* **2008**, *41*, 157. (c) Zhao, Y.; Truhlar, D. G. *J. Chem. Theory Comput.* **2008**, *5*, 324.

Nickel-Catalyzed C–H Coupling Reaction of Azoles with Phenol and Enol Derivatives

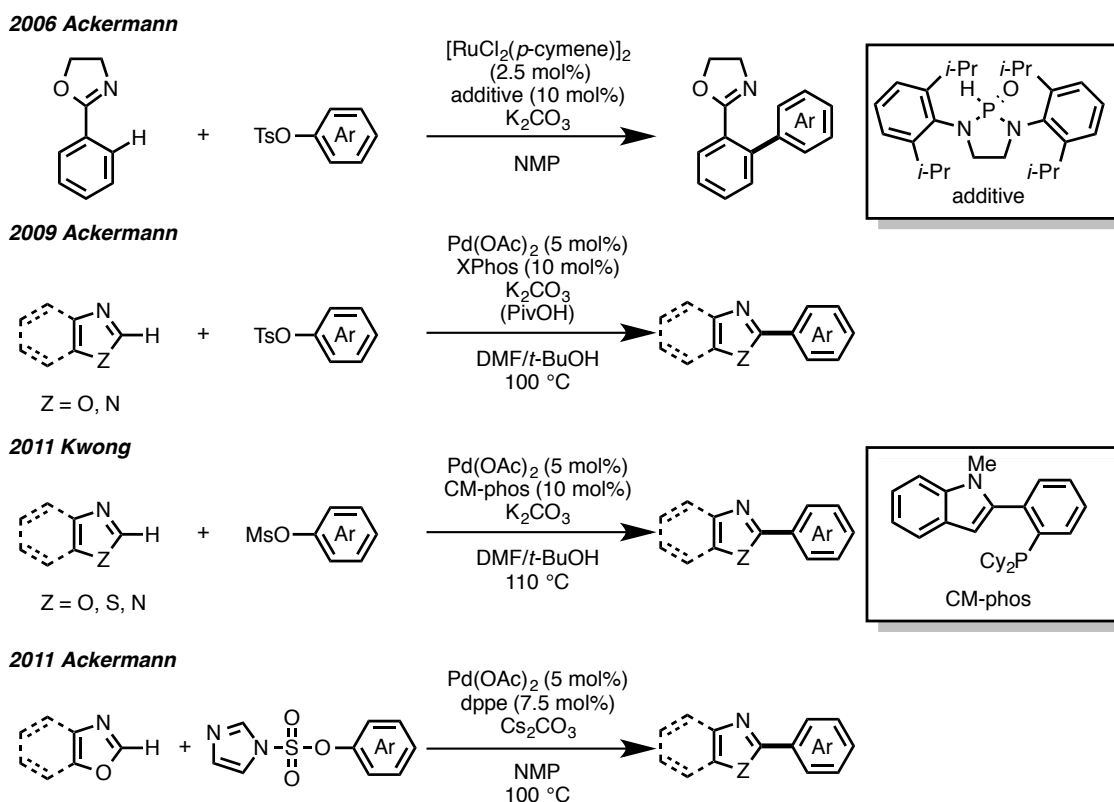
Abstract

The development of the first Ni-catalyzed C–H bond arylation and alkenylation of azoles with phenol and enol derivatives (C–H/C–O coupling) is described. A new Ni(cod)₂/dcype catalytic system promotes the coupling of various phenol derivatives, such as carbamates, carbonates, sulfamates, triflates, tosylates, and mesylates. With this C–H/C–O coupling, a series of 2-aryl- and alkenylazoles can be synthesized. Moreover, the synthetic utility of the present coupling reaction is successfully demonstrated through the rapid synthesis of biologically active alkaloids and functionalization of naturally occurring molecules, such as estrone and quinine.

1. Introduction

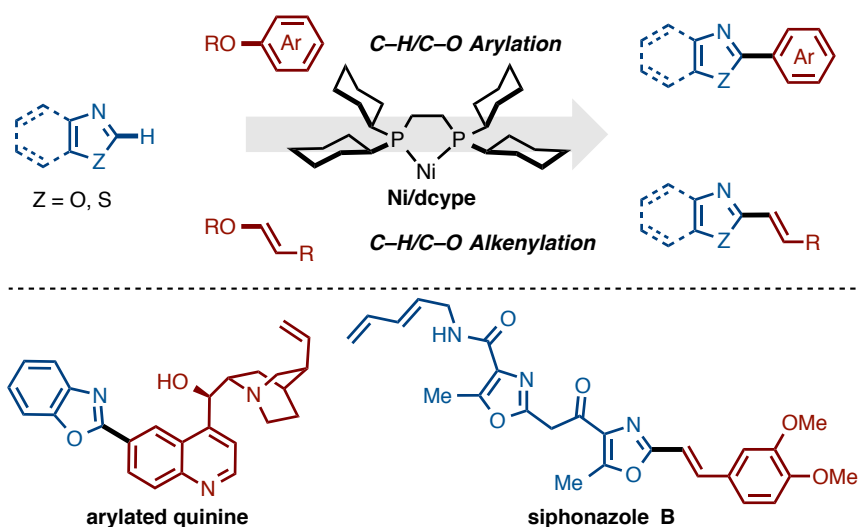
The discovery of a new protocol for Ni-catalyzed C–H/C–X coupling reaction using $\text{Mg}(\text{O}t\text{-Bu})_2$ as an alternative to $\text{LiO}t\text{-Bu}$ was described in Chapter 1.^[1] By using the $\text{LiO}t\text{-Bu}$ or $\text{Mg}(\text{O}t\text{-Bu})_2$ protocol, the Ni-catalyzed C–H/C–X coupling reaction was successfully applied to the rapid synthesis of bioactive molecules. Although there is one example using phenyl triflate as an aryl electrophile,^[1a] the coupling reaction generally requires the use of haloarenes. Recently, phenol derivatives, such as aryl carboxylates (Ar-OCOR) or aryl ethers (Ar-OR), have been attracting attention as new sources of aryl electrophile.^[2] The advantage of using phenol derivatives as aryl electrophiles is apparent, as they are often readily available and less expensive. While many examples of Ni-catalyzed cross-coupling of phenol derivatives with metalloarenes have been reported (C–M/C–O coupling), the employment of phenol derivatives with (hetero)arenes (C–H/C–O coupling) has remained a challenging theme.

Some examples of metal-catalyzed coupling reaction between (hetero)arenes and phenol derivatives with sulfur-containing leaving group such as aryl tosylates, mesylates, or imidazolylsulfamates have been reported (Scheme 1).^[3] In 2006, Ackermann reported the first aromatic C–H arylation with aryl tosylates using a ruthenium catalyst.^[3a] Thereafter, a direct arylation of heteroarenes with aryl tosylates using a palladium catalyst was also developed by Ackermann.^[3d] Recently, two examples of C–H arylation using aryl mesylates were also demonstrated. In 2011, Kwong reported the direct arylation of azoles with aryl mesylates using a palladium catalyst system.^[3f] Furthermore, Ackermann succeeded to develop a Pd-catalyzed C–H arylation of 1,3-azoles with aryl imidazolylsulfamates.^[3h] Although these are pioneering works on C–H arylation using phenol derivatives, the generation of sulfur-containing waste could not be avoided.



Scheme 1. Aromatic C–H arylation using aryl tosylates, mesylates and imidazolylsulfamates

In Chapter 3, the first example of C–H arylation of 1,3-azoles with phenol derivatives (C–H/C–O coupling) by Ni/dcype catalysis is described (Scheme 2).^[4] Notably, a dramatic ligand effect has been observed, as no reaction occurs when other ligands are used. In the presence of catalytic Ni/dcype, a range of phenol derivatives such as aryl pivalates, carbamates, carbonates, sulfamates, and sulfonates can react with 1,3-azoles to provide coupling products. The newly developed Ni/dcype catalyst was found to be practical for a C–H/C–O alkenylation of oxazoles with enol derivatives.^[5] Enols, which are prepared from the corresponding aldehydes and ketones, can couple with oxazoles. The synthetic utility of these C–H/C–O couplings was demonstrated by a late-stage arylation of complex natural products and a short-step synthesis of siphonazole B.

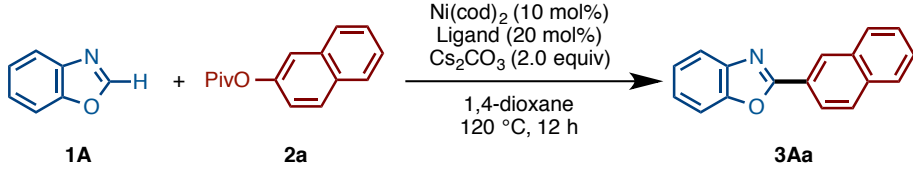


Scheme 2. Ni-catalyzed C–H/C–O coupling reaction of 1,3-azoles and phenol derivatives

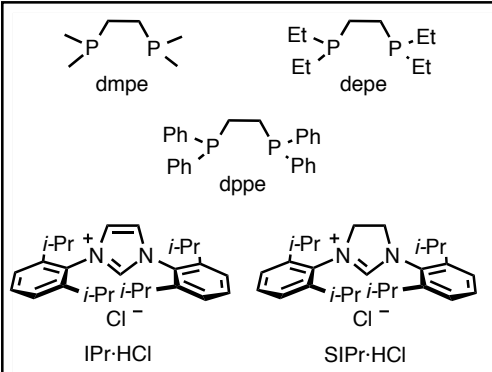
2. Results and Discussion

2-1. Development of Ni-catalyzed C–H/C–O Coupling Reaction

Using 10 mol% of Ni(cod)₂ as a catalyst precursor, several ligands were examined in the presence of Cs₂CO₃ in 1,4-dioxane at 120 °C (Table 1). As a result, only dcype was effective (entry 1) for the Ni-catalyzed C–H arylation of benzoxazole (**1A**) with naphthalen-2-yl pivalate (**2a**). It was found that tricyclohexylphosphine (PCy₃), a standard ligand to activate aryl C–O bonds for C–M/C–O coupling,^[6,7] was ineffective for the present C–H/C–O coupling (entry 2). Similarly, *N*-heterocyclic carbene ligands, 1,3-bis-(2,6-diisopropylphenyl)imidazolium chloride (IPr·HCl) and 1,3-bis-(2,6-di-isopropylphenyl)imidazolium chloride (SIPr·HCl) were also ineffective (entries 3 and 4).^[8] Structurally similar methyl-, ethyl-, and phenyl-substituted diphosphine ligands (dmpe, depe and dppe) as well as 2,2'-bipyridyl (bipy), a standard ligand for Ni-catalyzed C–H/C–X coupling,^[11] were also ineffective (entries 5–8). Furthermore, the coupling between **1A** and **2a** using Pd(OAc)₂ instead of Ni(cod)₂ as a catalyst afforded no coupling product (entry 9).

Table 1. Influence of the ligand in the coupling of **1A** and **2a**

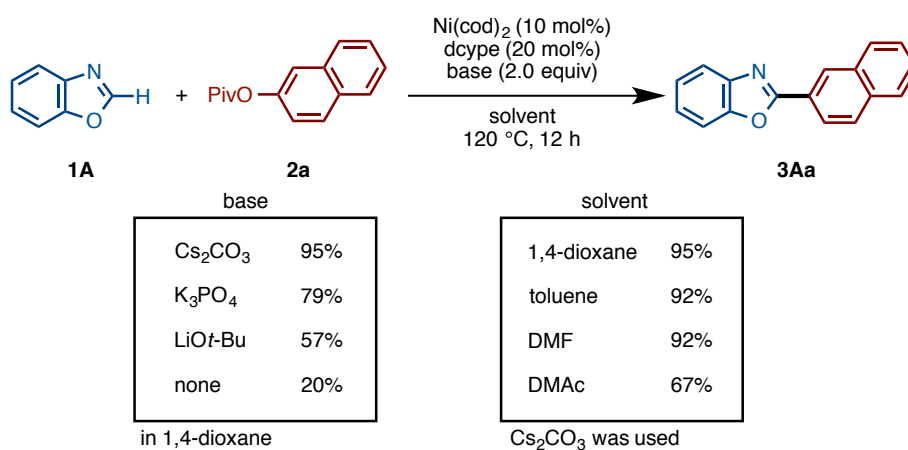
entry	Ligand	GC yield ^a
1	dcype	95
2	PCy ₃	0
3	IPr-HCl	0
4	SIPr-HCl	0
5	dmpe	0
6	depe	2
7	dppe	0
8	bipy	0
9 ^b	dcype	0



dmpe: $\text{P}(\text{CH}_2\text{CH}_2)_2\text{P}(\text{CH}_2\text{CH}_2)_2$
depe: $\text{Et}_2\text{P}(\text{CH}_2\text{CH}_2)_2\text{P}(\text{Et})_2$
dppe: $\text{Ph}_2\text{P}(\text{CH}_2\text{CH}_2)_2\text{P}(\text{Ph})_2$
IPr-HCl: $[\text{IPr}]^+\text{Cl}^-$
SIPr-HCl: $[\text{SIPr}]^+\text{Cl}^-$

Reaction conditions were as follows: **1A** (0.40 mmol), **2a** (0.60 mmol), Ni(cod)₂ (10 mol%), Ligand (20 mol%), Cs₂CO₃ (2.0 equiv), 1,4-dioxane (1.6 mL), 120 °C, 12 h. [a] Decane was used as an internal standard. [b] Pd(OAc)₂ was used instead of Ni(cod)₂.

As shown in Scheme 3, it was found that operative bases and solvents are not limited to Cs₂CO₃ and 1,4-dioxane. Regarding the base, K₃PO₄ and LiOt-Bu were also effective but the reaction yields were lower than that with Cs₂CO₃. Notably, this reaction also proceeds without base albeit in lower yield (20%). This result illustrated that the C–H bond at the C2 position of 1,3-azole can be cleaved by this nickel catalyst without any action of the base. In addition to 1,4-dioxane, toluene and polar solvent such as DMF and DMAc were also viable solvents.



Reaction conditions were as follows: **1A** (0.40 mmol), **2a** (0.60 mmol), Ni(cod)₂ (10 mol%), dcype (20 mol%), base (2.0 equiv), solvent (1.6 mL), 120 °C, 12 h. The yield was determined on GC using decane as an internal standard

Scheme 3. Influence of bases and solvents in the coupling of **1A** and **2a**

Next, a variety of nickel precursors were tested (Table 2). Compared to Ni(cod)₂, Ni(PPh₃)₄ showed almost equal catalytic activity (entry 1). With regard to using nickel(I) or nickel(II) precursor, it was found that the use of both Ni(PPh₃)₃Cl and Ni(PPh₃)₂Cl₂ as the nickel source provided **3Aa** in good yields (71% and 89%, respectively; entries 3 and 4). However, neither Ni(acac)₂ nor NiBr₂ were effective for the cross-coupling reaction of **1A** and **2a** (entries 5 and 6). Although Ni(cod)₂ gave the best result, it is notable that an air-stable nickel(II) precursor, Ni(PPh₃)₂Cl₂ also functions in the present coupling reaction.

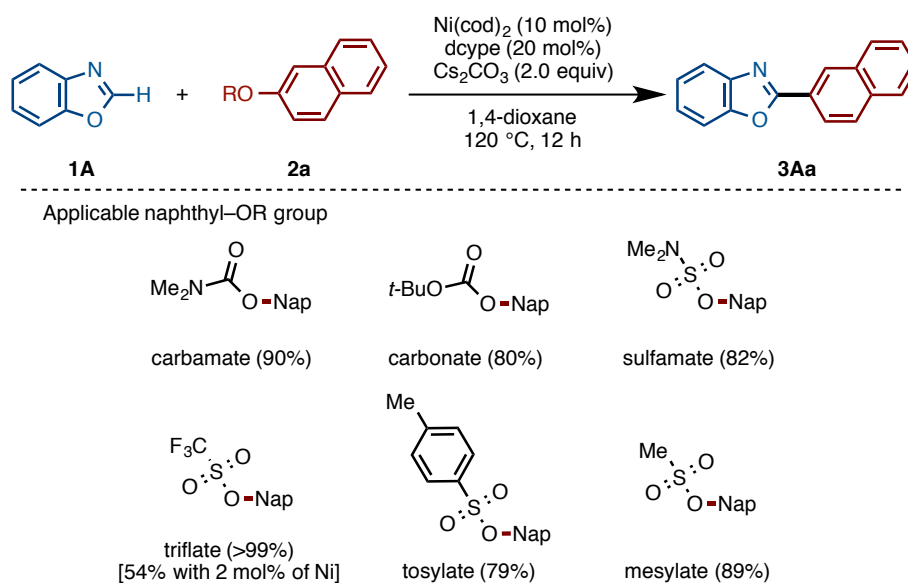
Table 2. Influence of the nickel precursors in the coupling of **1A** and **2a**

entry	Ni precursor	yield ^a
1	Ni(cod) ₂	95
2	Ni(PPh ₃) ₄	92
3	Ni(PPh ₃) ₂ Cl ₂	71
4	Ni(PPh ₃) ₃ Cl	89
5	Ni(acac) ₂	18
6	NiBr ₂	16

Reaction conditions were as follows: **1A** (0.40 mmol), **2a** (0.60 mmol), Nickel (10 mol%), dcype (20 mol%), Cs₂CO₃ (2.0 equiv), 1,4-dioxane (1.6 mL), 120 °C, 12 h. [a] GC yield

2-2. Survey of Applicable Naphthalene-ORs

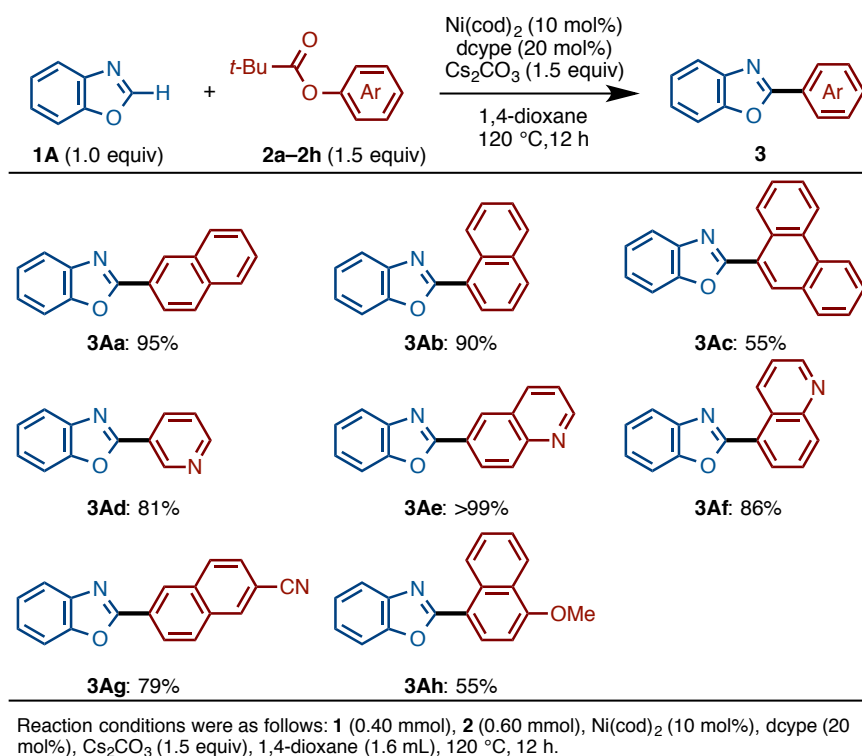
Gratifyingly, the present Ni(cod)₂/dcype catalyst was found to be active for the coupling of other phenol derivatives such as carbamates, carbonates, sulfamates, triflates, tosylates, and mesylates (79–99% yield; Scheme 4). It was also confirmed that the reaction also takes place with catalyst loadings as low as 2 mol% (54% yield with triflate).



Scheme 4. Scope of Ar-OR electrophiles

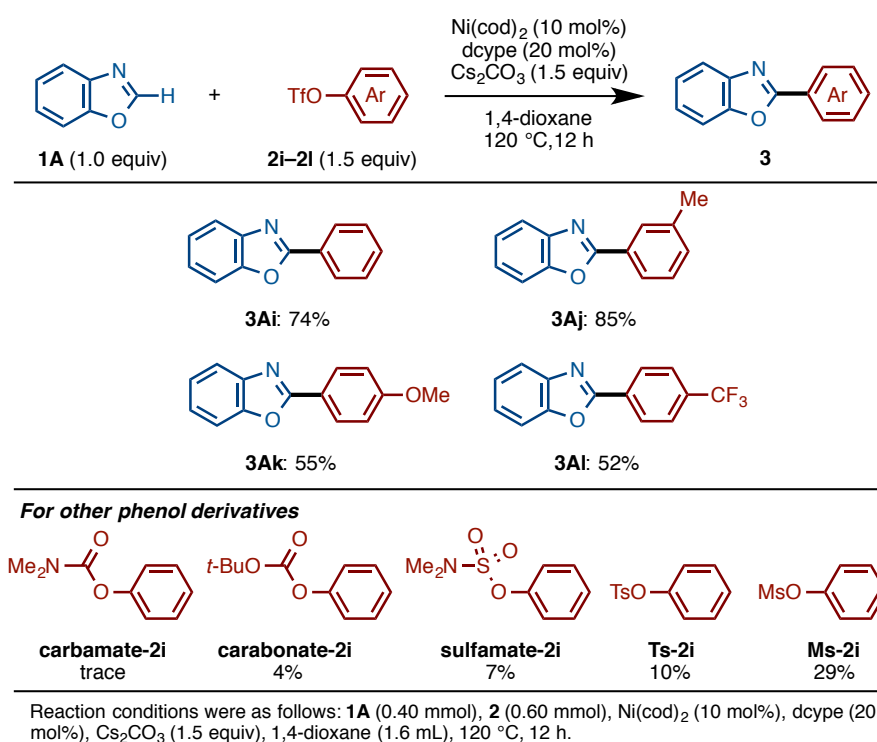
2-3. Substrate Scope

On the basis of these findings, applicable C–O substrates were examined by using benzoxazole (**1A**) under the influence of Ni(cod)₂/dcype/Cs₂CO₃ (Scheme 5). **1A** was successfully coupled with 1-naphthyl, 2-naphthyl, and 9-phenanthrenyl pivalates, giving the corresponding coupling products **3Aa–3Ac** in moderate to excellent yields. The present Ni-catalyzed reaction using aryl pivalates was also found to be effective for nitrogen-containing heteroarenes of 3-pyridyl and quinolinyl pivalates. Aryl-methoxy^[6,7a] and aryl-cyano^[9] bonds, which could be activated with nickel catalysts, were well tolerated under the present conditions.



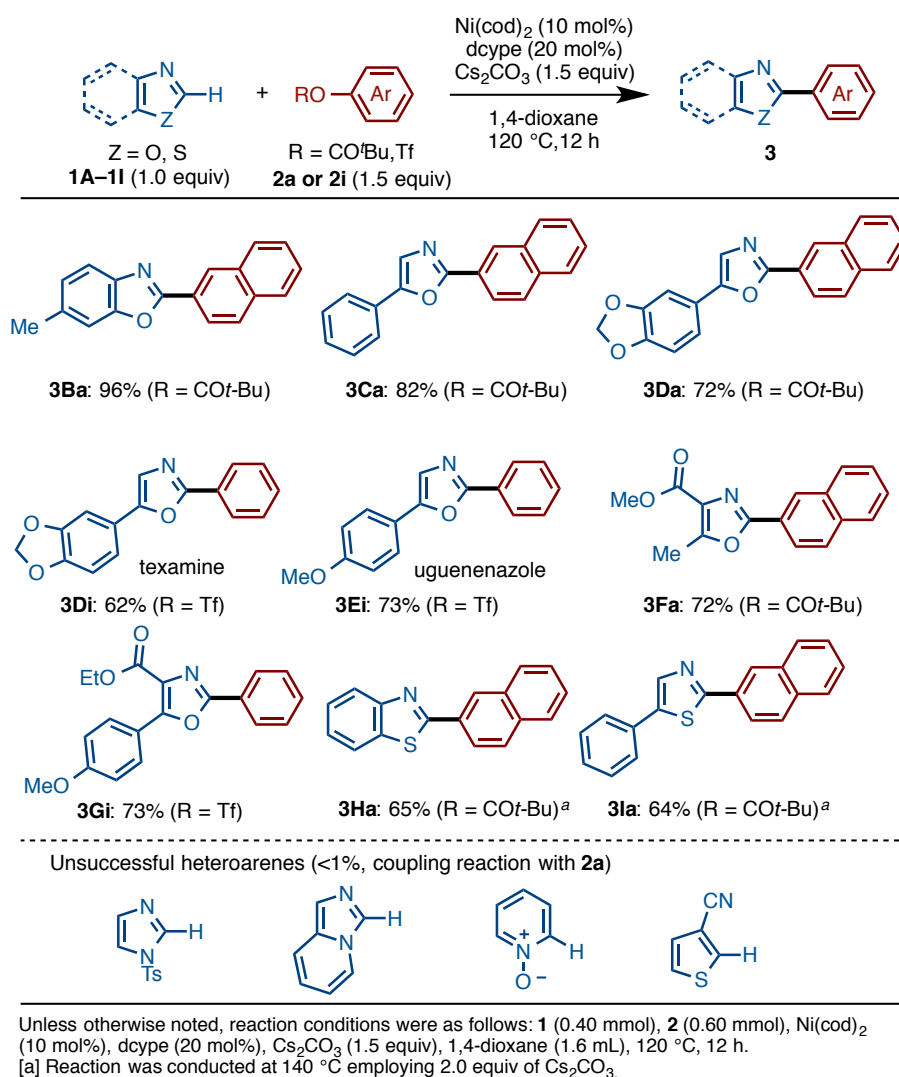
Scheme 5. Substrate scope for aryl pivalates in the Ni-catalyzed C–H/C–O coupling of benzoxazole (**1A**)

Unfortunately, it was found that the yield of the reaction using phenyl pivalates was much lower than other aryl pivalates **2a–2h** (11% yield). In order to solve this drawback, the scope of usable phenyl–OR substrates was reinvestigated (Scheme 6). As a result, it was revealed that phenyl triflate reacts smoothly under the present nickel catalysis, producing 2-phenylbenzoxazole (**3Ai**) in 74% yield. Under these conditions, both electron-rich and electron-deficient phenyl triflates were successfully coupled with **1A**. With regard to other phenyl–OR substrates, the coupling reaction of **1A** with phenyl carbamate, carbonate, tosylate, and mesylate also provided coupling products, albeit with lower yields compared to that with phenyl triflate.



Scheme 6. Substrate scope for aryl triflates in the Ni-catalyzed C–H/C–O coupling of benzoxazole (**1A**)

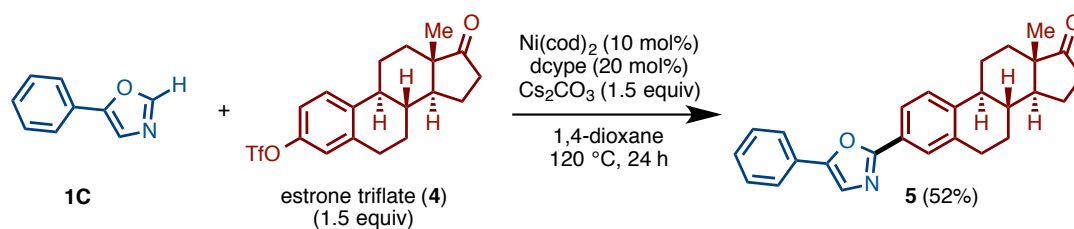
By using both aryl pivalates and triflates, the scope of heteroarenes was investigated in the present Ni-catalyzed arylation (Scheme 7). In addition to benzoxazoles, oxazoles, thiazoles, and benzothiazoles were found to couple smoothly with phenol derivatives to furnish the corresponding coupling products. However, it was found that this nickel catalytic system could not be applied to the reaction of imidazoles, imidazopyridines, pyridine *N*-oxides, and thiophenes. It is of note that the present reaction allowed for the concise synthesis of oxazole-containing alkaloids texamine (**3Di**)^[10] and uguenenazole (**3Ei**).^[11]



Scheme 7. Ni/dcype-catalyzed coupling reaction of various heteroarenes with phenol derivatives

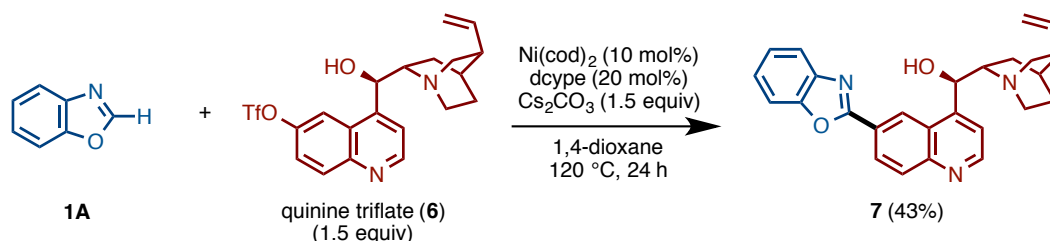
2-4. Application of Ni-Catalyzed C–H/C–O Coupling to Complex Natural Products

It was envisioned that the C–H/C–O biaryl coupling should find use in the rapid identification of new biologically active compounds by functionalization of C–O bond-containing naturally occurring structures.^[12] Thus, to demonstrate the feasibility of this approach, the Ni-catalyzed C–H/C–O coupling to functionalize estrone and quinine was attempted. The coupling of estrone triflate (**4**) and **1C** proceeded smoothly under the standard conditions to afford heteroarylated estrone **5** in 52% yield (Scheme 8).



Scheme 8. Ni-catalyzed arylation of estrone triflate (4)

The C–H/C–O coupling of quinine triflate (6)^[13] with 1A also occurred, giving the quinine–benzoxazole hybrid molecule 7, albeit with somewhat lower efficiency (Scheme 9). Notably, the hydroxyl, amine, and olefin functionalities were tolerated under the coupling conditions. This successful application to the functionalization of the quinine structure, which is known to be sensitive under acidic, basic, and redox conditions, speaks well for the potential of the present nickel catalysis for further development and applications.



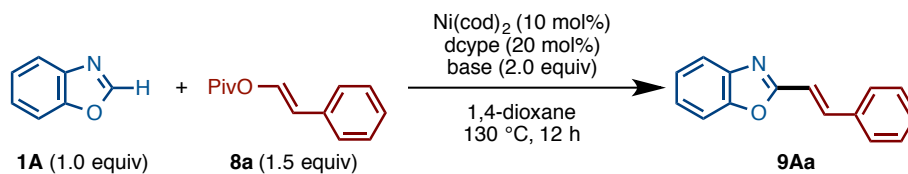
Scheme 9. Ni-catalyzed direct arylation of quinine triflate 6

2-5. Discovery of Nickel-Catalyzed C–H Alkenylation by Using Enols

With the success of the development of Ni-catalyzed C–H/C–O arylation using phenols, it was hypothesized that C–H/C–O alkenylation should be feasible by using enols as the electrophilic coupling component. To this end, the development of C–H alkenylation of azoles using enol derivatives was examined (Table 3). Gratifyingly, under the conditions with $\text{Ni}(\text{cod})_2$ (10 mol%), dcype (20 mol%), and Cs_2CO_3 (2.0 equiv) in 1,4-dioxane at 130 °C, desired coupling product 9Aa was obtained from benzoxazole (1A) with styryl pivalate 8a, albeit in low yield (15%: entry 1). Encouraged by this result, the reaction conditions were optimized. It was found that this C–H alkenylation prefers weaker bases than Cs_2CO_3 . Accordingly K_2CO_3 and K_3PO_4 gave better yields (entries 2, 5, and 6). Finally, lower temperature (120 °C) led to

further improvement of the reaction, as 46% yield of **9Aa** was obtained (entry 6).

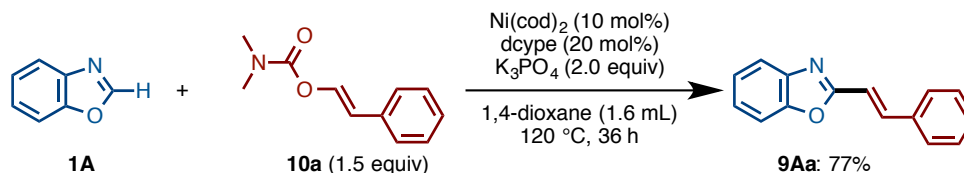
Table 3. Discovery of Ni-catalyzed C–H alkenylation by using enols



entry	base	yield (%) ^a
1	Cs_2CO_3	15
2	K_2CO_3	36
3	Na_2CO_3	0
4	Li_2CO_3	0
5	K_3PO_4	38
6 ^b	K_3PO_4	46

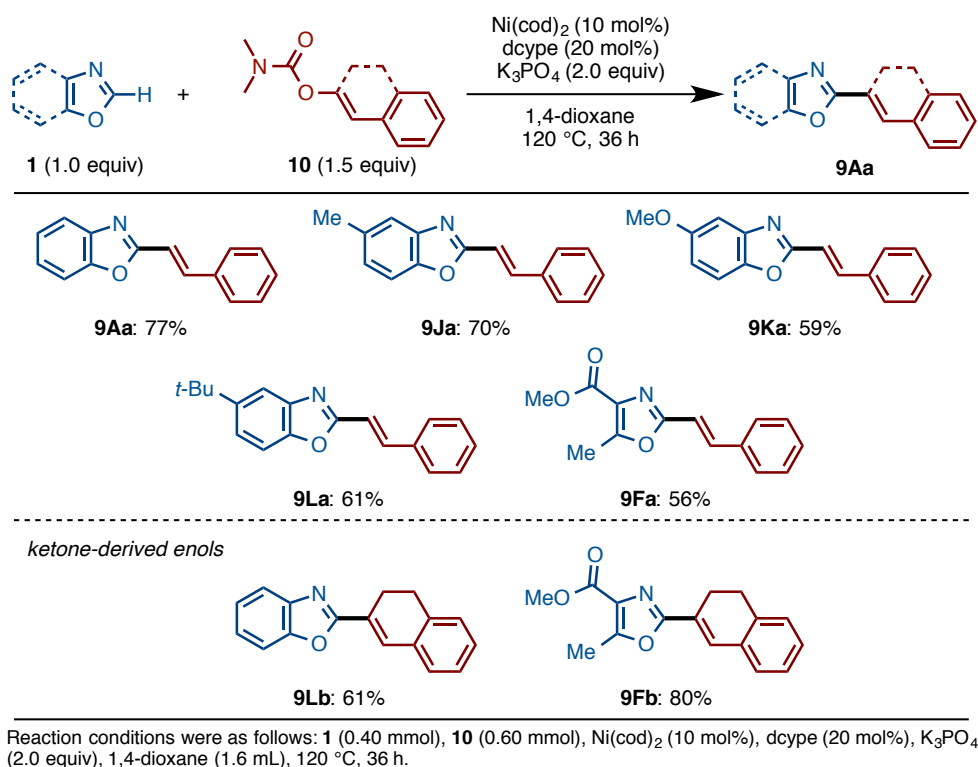
Reaction conditions were as follows: **1A** (0.40 mmol), **8a** (0.60 mmol), $\text{Ni}(\text{cod})_2$ (10 mol%), dcype (20 mol%), base (2.0 equiv), 1,4-dioxane (1.6 mL), 130 °C, 12 h. [a] GC yield [b] Under 120 °C

Furthermore, during the survey of applicable enols, it was found that carbamates were superior to pivalates as the alkenylating component in the present reaction (Scheme 10). Under the similar reaction conditions, styryl carbamate **10a** furnished **9Aa** in 77% yield.



Scheme 10. C–H alkenylation of benzoxazole (**1A**) with carbamate **10a** by nickel catalysis

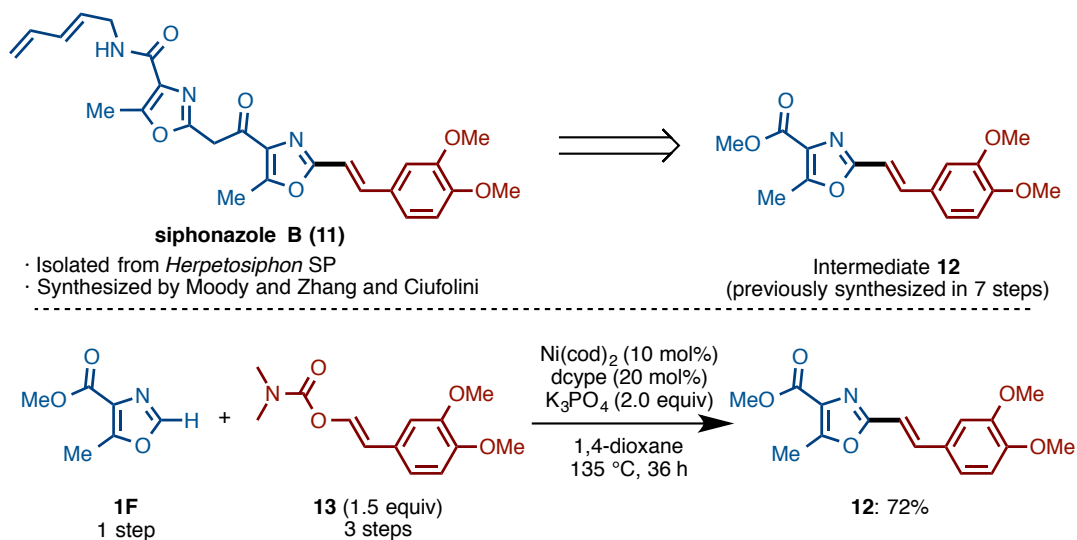
With the optimal conditions in hand, the substrate generality of this reaction was next examined (Scheme 11). C5-methyl (**1J**), methoxy (**1K**), and *t*-butyl (**1L**) substituted benzoxazole could couple with **10a** in moderate to good yield. As well as benzoxazoles, ester substituted oxazole **1E** could react well to produce **9Ea** in moderate yield. In addition to enols prepared from aldehydes, enols prepared from ketones **10b** also underwent the C–H alkenylation to furnish **9Lb** and **9Fb** in 61% and 80% yield, respectively. Unfortunately, however, thiazoles and benzothiazoles could not couple with enols in the Ni-catalyzed C–H alkenylation at all.



Scheme 11. Substrate scope of Ni-catalyzed C–H alkenylation of azoles with alkenyl carbamates

2-6. Application to the Synthesis of Siphonazole B

Finally, to showcase the utility of the new azole alkenylation method, this reaction was applied to the synthesis of siphonazole B (**11**), a natural product isolated from a metabolite from *Herpetosiphon* sp.^[14] Although siphonazole B (**11**) has already been synthesized by Moody and co-workers^[15] and Zhang and Ciufolini,^[16] their synthesis took a lot of steps because of parallel repetition of linear synthetic sequences. To tackle this problem, the convergent synthesis of siphonazole B through Ni-catalyzed C–H alkenylation reaction was designed (Scheme 12). Although **12** is an intermediate in the previous synthesis, this needs to be synthesized in seven steps. Thus, this was retrosynthetically broken up the intermediate into oxazole **1F** and alkenyl enol **13**. Pleasingly, C–H/C–O alkenylation of **1F** and **13** delivered **12** in good yield over 4 linear steps, thus, accomplishing the formal synthesis of siphonazole B.



Scheme 12. Synthesis of siphonazole B (**11**) by Ni-catalyzed C–H/C–O alkenylation

3. Conclusion

In summary, it was revealed that Ni/dcybe catalyst can promote efficient C–H coupling reactions, a C–H/C–O coupling of 1,3-azoles with phenol and enol derivatives.^[4,5] Under Ni(cod)₂/dcybe catalysis, C–H/C–O coupling was achieved using various pivalates, triflates, tosylates, mesylates, carbamates, carbonates, and sulfamates. In addition, a C–H alkenylation was also achieved by employing enol derivatives with the same nickel catalyst. The present findings not only push the limit of *sp*²-*sp*² cross-coupling into the C–H/C–O manifold but should also open an avenue for a range of new catalytic C–O bond transformations of phenol derivatives with Ni(cod)₂/dcybe.^[17]

4. Experimental

4-1. General

Unless otherwise noted, all reactants or reagents including dry solvents were obtained from commercial suppliers and used as received. Ni(cod)₂ and Cs₂CO₃ were obtained from Wako Chemicals. 1,2-Bis(dicyclohexylphosphino)ethane was obtained from Sigma-Aldrich. 1,4-Dioxane was freshly distilled by calcium hydride before coupling reaction. Unless otherwise noted, all reactions were performed with dry solvents under an atmosphere of argon in flame-dried glassware using standard vacuum-line techniques. All C–H bond arylation reactions were performed in 20-mL glass vessel tubes equipped with J. Young[®] O-ring tap and heated in an 8-well reaction block (heater + magnetic stirrer). All work-up and purification procedures were carried out with reagent-grade solvents in air.

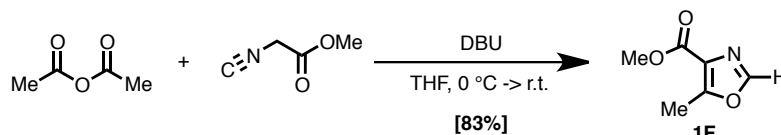
Analytical thin-layer chromatography (TLC) was performed using E. Merck silica gel 60 F₂₅₄ precoated plates (0.25 mm). The developed chromatogram was analyzed by UV lamp (254 nm). Flash column chromatography was performed with E. Merck silica gel 60 (230–400 mesh). Preparative thin-layer chromatography (PTLC) was performed using Wakogel B5-F silica coated plates (0.75 mm) prepared in our laboratory. Preparative high performance liquid chromatography (preparative HPLC) was performed with a Biotage Isolera One equipped with Biotage[®] SNAP Cartridge KP-C18-HS columns using acetonitrile/water as an eluent. Gas chromatography (GC) analysis was conducted on a Shimadzu GC-2010 instrument equipped with a HP-5 column (30 m × 0.25 mm, Hewlett-Packard) with decane as an internal standard. GCMS analysis was conducted on a Shimadzu GCMS-QP2010 instrument equipped with a HP-5 column (30 m × 0.25 mm, Hewlett-Packard). High-resolution mass spectra (HRMS) was obtained from a JEOL JMS-T100TD instrument (DART). Nuclear magnetic resonance (NMR) spectra was recorded on a JEOL JNM-ECA-400 (¹H 400 MHz, ¹³C 100 MHz) spectrometer. Chemical shifts for ¹H NMR are expressed in parts per million (ppm) relative to tetramethylsilane (δ 0.00 ppm). Chemical shifts for ¹³C NMR are expressed in ppm relative to CDCl₃ (δ 77.0 ppm). Data are reported as follows: chemical shift, multiplicity (s = singlet, d = doublet, dd = doublet of doublets, t = triplet, q = quartet, m = multiplet, br = broad signal), coupling constant (Hz), and integration.

4-2. Procedure for Synthesis of Azoles

Note:

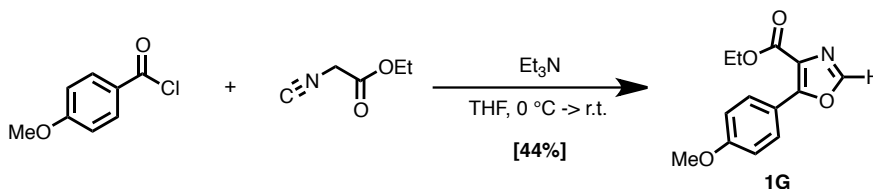
Azoles **1B**,^[18] **1C**,^[10c] **1D**,^[10c] **1E**,^[10c] **1I**,^[18b] **1J**,^[19] **1K**^[19], and **1L**^[20] were synthesized according to procedures reported in the literature.

Methyl-5-methyloxazole carboxylate (**1F**)^[21]



To a solution of methyl 2-isocyanoacetate (1.98 g, 20 mmol) in 24 mL of THF was in a dry 50 mL round bottom flask was added DBU (1,8-diazabicyclo[5.4.0]undec-7-ene, 3.39 g, 22 mmol, 1.1 equiv). Cooling the reaction mixture to 0 °C, the solution of acetic anhydride (2.25 g, 22 mmol, 1.1 equiv) in 6 mL of THF was added slowly. Warming up to room temperature, the reaction mixture was stirred. The progress of the reaction was monitored by TLC. On completion of reaction, the reaction mixture was concentrated in vacuo. To this vessel was added 30 mL of EtOAc and 20 mL of water. The aqueous layer was extracted with EtOAc (20 mL x 3) and the combined organic layer was treated with Na₂SO₄ and then filtered. Following evaporation of the solvent under reduced pressure, the crude residue was purified by flash column chromatography (hexane/EtOAc = 3:1) to afford **1F** as a white solid (2.35 g, 83% yield). R_f 0.43 (hexane/EtOAc = 1:1); ¹H NMR (400 MHz, CDCl₃): δ 7.76 (s, 1H), 3.92 (s 3H), 2.65 (s, 3H).

Ethyl-5-(4-methoxyphenyl)oxazole-4-carboxylate (**1G**)^[22]



To a solution of ethyl 2-isocyanoacetate (903 mg, 8.0 mmol) and triethylamine (3.34 mL, 24 mmol, 3.0 equiv) in 15 mL of THF in a 50 mL round bottomed flask was added a solution of *p*-methoxybenzoyl chloride (1.61 g, 9.5 mmol) in 4 mL of THF slowly at 0 °C. After stirring for 40 minutes under 0 °C, the reaction mixture was warmed to

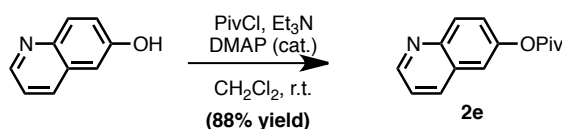
room temperature. After stirring 12 h, the reaction mixture was concentrated in vacuo, then to this vessel was added 30 mL of EtOAc and 20 mL of water. The aqueous layer was extracted with EtOAc (20 mL x 2) and the combined organic layer was treated with Na₂SO₄ and then filtered. Following evaporation of the solvent under reduced pressure, the crude residue was purified by flash column chromatography (hexane/EtOAc = 5:1) to afford **1G** as a yellow solid (865 mg, 44% yield). R_f 0.07 (hexane/EtOAc = 5:1); ¹H NMR (400 MHz, CDCl₃): δ 8.07 (d, *J* = 9.2 Hz, 2H), 7.86 (s, 1H), 6.99 (d, *J* = 9.2 Hz, 2H), 4.42 (q, *J* = 7.1 Hz, 2H), 3.87 (s, 3H), 1.42 (t, *J* = 7.1 Hz, 3H).

4-3. Procedure for Synthesis of Phenol Derivatives

Note:

Aryl pivalates **2a**,^[7b] **2b**,^[7b] **2c**,^[7b] **2d**,^[7b] *N,N*-dimethyl-2-naphthalenylcarbamate (**carbamate-2a**),^[23a] *N,N*-dimethyl-2-naphthalenylsulfamate (**sulfamate-2a**),^[8c] *tert*-butyl-2-naphthalenylcarbonate (**carbonate-2a**),^[7d] 2-naphthalenyltosylate (**Ts-2a**),^[23b] and 2-naphthalenylmesylate (**Ms-2a**)^[23c] were synthesized according to procedures reported in the literature.

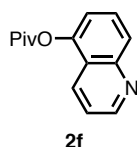
Procedure for Synthesis of Aryl Pivalates



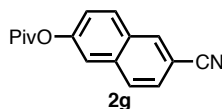
Representative procedure (6-quinolinylpivalate (**2e**) was used as an example)

To a solution of 2-quinolinol (1.60 g, 11 mmol) and a piece of 4,4-dimethylaminopyridine (DMAP) in CH₂Cl₂ (20 mL) was added triethylamine (1.84 mL, 13.2 mmol, 1.2 equiv) at room temperature. Then pivaloyl chloride (1.62 mL, 13.2 mmol, 1.2 equiv) was added dropwise over 3 min at 0 °C. After stirring for 15 min., the reaction mixture was quenched with sat. NaHCO₃ aq. (10 mL), then the layers were separated. The aqueous layer was extracted with CH₂Cl₂ (25 mL x 3) and the combined organic layer was treated with Na₂SO₄ and then filtrated. Following evaporation of the solvent under reduced pressure, the crude residue was purified by flash column chromatography (hexane/EtOAc = 5:1) to afford **2e** as a yellow solid (2.21 g, 88% yield). R_f 0.49 (hexane/EtOAc = 1:1); ¹H NMR (400 MHz, CDCl₃): δ 8.90 (dd, *J* = 1.2,

4.0 Hz, 1H), 8.11 (dd, $J = 2.8, 9.2$ Hz, 2H), 7.53 (d, $J = 2.4$ Hz, 1H), 7.43 (dd, $J = 2.4, 8.8$ Hz, 1H), 7.41–7.35 (m, 1H), 1.41 (s, 9H); ^{13}C NMR (100 MHz, CDCl_3): δ 177.0, 150.1, 148.9, 146.2, 135.7, 130.9, 128.5, 124.7, 121.5, 118.2, 39.1, 27.1; HRMS (DART) m/z calcd for $\text{C}_{14}\text{H}_{15}\text{NO}_2$ $[\text{MH}]^+$: 230.1181 found 230.1181.

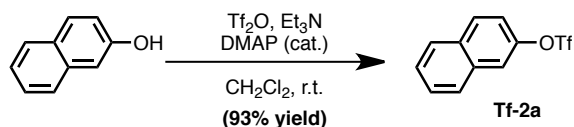


Quinolin-5-yl pivalate (2f) Purification by flash column chromatography (hexane/EtOAc = 3:1) afforded **2f** as a white solid (95 % yield). R_f 0.50 (hexane/EtOAc = 1:1); ^1H NMR (400 MHz, CDCl_3): δ 8.94 (dd, $J = 1.2, 4.0$ Hz, 1H), 8.18 (dq, $J = 1.2, 8.7$ Hz, 1H), 8.01 (d, $J = 8.7$ Hz, 1H), 7.71 (t, $J = 8.0$ Hz, 1H), 7.42 (q, $J = 4.0$ Hz, 1H), 7.29 (dd, $J = 1.2, 8.0$ Hz, 1H), 1.49 (s, 9H); ^{13}C NMR (100 MHz, CDCl_3): δ 176.8, 150.8, 148.9, 146.3, 129.7, 128.8, 127.3, 122.4, 121.3, 118.5, 39.5, 27.3; HRMS (DART) m/z calcd for $\text{C}_{14}\text{H}_{15}\text{NO}_2$ $[\text{MH}]^+$: 230.1181 found 230.1181.



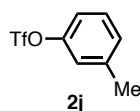
6-Cyanonaphthalen-2-yl pivalate (2g) Purification by flash column chromatography (hexane/ CHCl_3 = 5:1) afforded **2g** as a white solid (85 % yield). R_f 0.08 (hexane/ CHCl_3 = 5:1); ^1H NMR (400 MHz, CDCl_3): δ 8.23 (s, 1H), 7.94–7.83 (m, 2H), 7.66–7.58 (m, 2H), 7.33 (dd, $J = 2.4, 8.8$ Hz, 1H), 1.41 (s, 9H); ^{13}C NMR (100 MHz, CDCl_3): δ 176.9, 151.2, 135.3, 133.9, 130.1, 129.9, 128.8, 127.1, 123.2, 119.1, 118.8, 109.1, 39.2, 27.1; HRMS (DART) m/z calcd for $\text{C}_{16}\text{H}_{16}\text{NO}_2$ $[\text{MH}]^+$: 254.1181 found 254.1181.

4-4. Procedure for Synthesis of Aryl Triflates

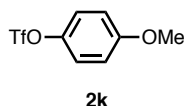


Representative procedure (naphthalen-2-yl triflate (**Tf-2a**)^[24] was used as an example).

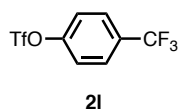
To a solution of 2-naphthalene (1.59 g, 11 mmol) and a piece of 4,4-dimethylaminopyridine (DMAP) in CH₂Cl₂ (20 mL) was added triethylamine (1.84 mL, 13.2 mmol, 1.2 equiv) at room temperature. Then trifluoromethanesulfonic anhydride (1.99 mL, 13.2 mmol, 1.2 equiv) was added dropwise over 3 min at 0 °C. After stirring for 2 h, the reaction mixture was quenched with water (10 mL), then the layers were separated. The aqueous layer was extracted with CH₂Cl₂ (25 mL × 3) and the combined organic layer was treated with Na₂SO₄ and then filtrated. Following evaporation of the solvent under reduced pressure, the crude residue was purified by flash column chromatography (hexane/EtOAc = 10:1) to afford **S1-2a** as a colorless oil (2.82 g, 93% yield). ¹H NMR (400 MHz, CDCl₃): δ 7.94 (d, *J* = 9.0 Hz, 1H), 7.91-7.86 (m, 2H), 7.77 (d, *J* = 2.5 Hz, 1H), 7.60-7.57 (m, 2H), 7.38 (dd, 2.5, 9.0 Hz, 1H).



***m*-Tolyl trifluoromethanesulfonate (2j)**^[25] Purification by flash column chromatography (hexane : EtOAc/8:1) afforded **2d** as a yellow oil (86 % yield). *R*_f 0.54 (hexane/EtOAc = 5:1); ¹H NMR (400 MHz, CDCl₃): δ 7.32 (t, *J* = 7.6 Hz) , 1H, 7.18 (d, *J* = 7.6 Hz, 1H), 7.12-7.05 (m, 2H), 2.40 (s, 3H).



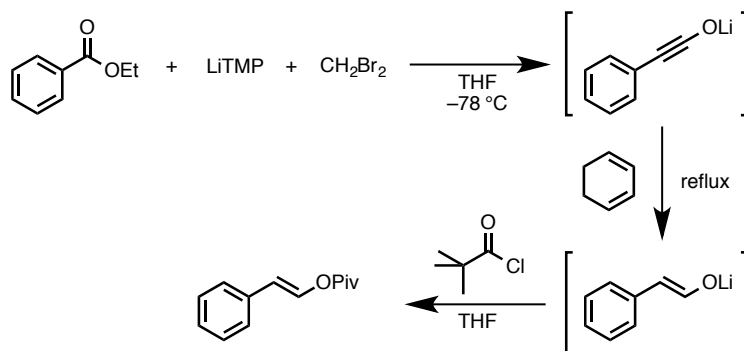
4-Methoxyphenyl trifluoromethanesulfonate (2k)^[26] Purification by flash column chromatography (hexane/EtOAc = 9:1) afforded **2e** as a colorless oil (70 % yield). *R*_f 0.57 (hexane/EtOAc = 5:1); ¹H NMR (400 MHz, CDCl₃): δ 7.20 (d, *J* = 9.2 Hz, 2H), 6.92 (d, *J* = 9.2 Hz, 2H), 3.82 (s, 3H).



4-(Trifluoromethyl)phenyl trifluoromethanesulfonate (2l)^[27] Purification by flash column chromatography (hexane/EtOAc = 3:1) afforded **2d** as a colorless oil (64 %

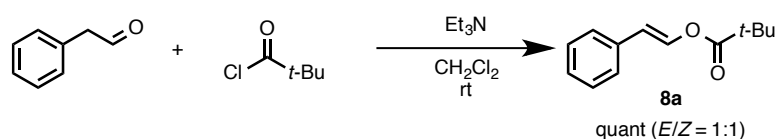
yield). R_f 0.57 (hexane/EtOAc = 5:1); $^1\text{H NMR}$ (400 MHz, CDCl_3): δ 7.76 (d, $J = 8.8$ Hz, 2H), 7.43 (d, $J = 8.8$ Hz, 2H).

***E*-Selective^[28] synthesis of (*E*)-styryl pivalate (**8a**)^[29]**



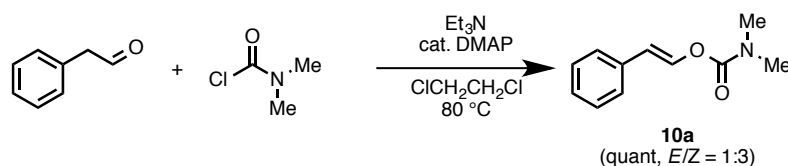
To a solution of 2,2,6,6-tetramethylpiperidine (678 mg, 4.8 mmol, 2.2 equiv) in THF (6.0 mL) was added *n*-butyllithium in hexane (1.6 M, 4.8 mmol, 2.2 equiv) at $0\text{ }^\circ\text{C}$. This mixture was transferred into the THF solution (6 mL) of CH_2Br_2 (383 mg, 2.2 mmol, 1.1 equiv) via cannula slowly at $-90\text{ }^\circ\text{C}$ (Et_2O with dry ice). After stirring for 5 min, a solution of ethyl benzoate (300 mg, 2.0 mmol) in THF (4.0 mL) was added dropwise, and further 5 min later, a solution of *n*-butyllithium in hexane (10.0 mmol, 5.0 equiv) was added dropwise. The mixture was warmed to room temperature and stirred for 30 min. Then 1,3-cyclohexadiene (1.60 g, 20.0 mmol, 10 equiv) was added and the reaction mixture was refluxed for 60 min. To the reaction mixture was added pivaloyl chloride (3.62 g, 30 mmol, 15 equiv) at $0\text{ }^\circ\text{C}$. After stirring over 5 min at room temperature, saturated NaHCO_3aq was added. The mixture was extracted three times with ether. The combined organic phase was washed with brine, and dried over MgSO_4 . The filtrate was concentrated under reduced pressure. The residue was purified by flash column chromatography on silica gel to afford the desired styryl pivalate as a colorless oil (**8a**: 52 mg, 13% yield, $E/Z = >20/1$). $^1\text{H NMR}$ (CDCl_3 , 400 MHz) δ 7.84 (d, $J = 13.0$ Hz, 1H), 7.34–7.26 (m, 4H), 7.25–7.21 (m, 1H), 6.41 (d, $J = 13.0$ Hz, 1H), 1.29 (s, 9H); $^{13}\text{C NMR}$ (CDCl_3 , 100 MHz) δ 175.6, 136.7, 134.3, 128.7, 127.3, 126.2, 115.0, 38.8, 27.0; HRMS calcd for $\text{C}_{13}\text{H}_{17}\text{O}_2$ $[\text{M}+\text{H}]^+$: 205.1229, found: 205.1230.

Synthesis of styryl pivalate (8a**, $E/Z = 1:1$)**



To a dichloroethane solution (30 mL) of phenyl acetaldehyde (1.81 g, 15 mmol) were added Et₃N (3.6 mL, 25 mmol, 1.7 equiv) and pivaloyl chloride (2.4 g, 20 mmol, 1.3 equiv). This mixture was stirred overnight at room temperature. The reaction was quenched by saturated NH₄Cl aq., and then the mixture was extracted three times with CH₂Cl₂. The combined organic layer was dried over Na₂SO₄, concentrated under reduced pressure. The residue was purified by flash column chromatography on silica gel (hexane/EtOAc = 20:1) to afford styryl pivalate **8a** (3.04 g, quant, *E/Z* = 1:1) as a yellow oil. ¹H NMR (CDCl₃, 400 MHz) δ 7.84 (d, *J* = 13.0 Hz, 1H, (*E*)), 7.59 (dd, *J* = 8.8, 1.2 Hz, 2H, (*Z*)) 7.34–7.26 (m, 9H, (*E* and *Z*)), 6.41 (d, *J* = 13.0 Hz, 1H), 5.71 (d, *J* = 7.2 Hz, 1H, (*Z*)), 1.34 (s, 9H, (*Z*)), 1.29 (s, 9H, (*E*)).

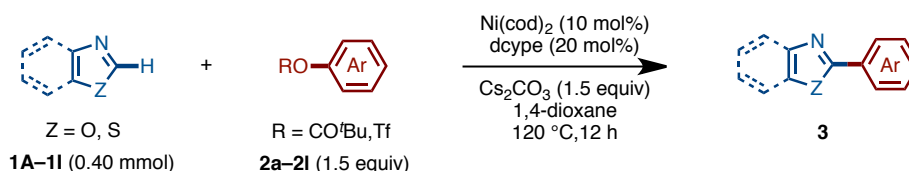
(*E*)-Styryl dimethylcarbamate (10a *E/Z* = 1:3)



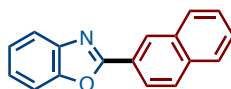
To a dichloroethane solution (30 mL) of phenyl acetaldehyde (1.81 g, 15 mmol) were added Et₃N (3.6 mL, 25 mmol, 1.7 equiv), *N,N*-dimethyl amino pyridine (DMAP: 457 mg, 3.7 mmol, 25 mol%) and *N,N*-dimethylcarbamoyl chloride (2.14 g, 20 mmol, 1.3 equiv). This mixture was stirred overnight at 80 °C. The reaction was quenched by saturated NH₄Cl aq., and then the mixture was extracted three times with CH₂Cl₂. The combined organic layer was dried over Na₂SO₄, concentrated under reduced pressure. The residue was purified by flash column chromatography on silica gel (hexane/EtOAc = 5:1) to afford styryl dimethylcarbamate **10a** (2.86 g, quant, *E/Z* = 1:3) as a yellow oil. ¹H NMR (CDCl₃, 400 MHz) δ 7.78 (d, *J* = 13.1 Hz, 1H (*E*)), 7.53 (d, *J* = 7.8 Hz, 6H (*Z*)), 7.34–7.15 (m, 17H, (*E* and *Z*)), 6.30 (d, *J* = 13.1 Hz, 1H, (*E*)), 5.61 (d, *J* = 7.8 Hz, 3H, (*Z*)), 3.07 (s, 9H, (*Z*)), 2.99 (s, 12H, (*E* and *Z*)), 2.97 (s, 3H); ¹³C NMR (CDCl₃, 100 MHz) δ 153.6, 153.4, 137.9, 135.5, 134.7, 134.5, 128.63, 128.56, 128.3, 126.8, 126.7, 125.9, 112.8, 109.6, 36.7, 36.6, 36.2, 35.9; HRMS calcd for C₁₁H₁₄NO₂ [M+H]⁺:

192.1025, found: 192.1024.

4-6. General Procedure for the Nickel-Catalyzed C–H/C–O Coupling of Azoles with Phenol Derivatives



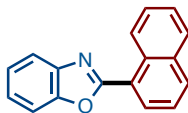
A 20-mL glass vessel equipped with J. Young[®] O-ring tap containing a magnetic stirring bar and Cs_2CO_3 (195.5 mg, 0.60 mmol, 1.5 equiv) was dried with a heatgun under reduced pressure and filled with argon after cooling to room temperature. To this vessel was added phenol derivatives **2** (0.60 mmol, 1.5 equiv) then introduced inside an argon atmosphere glovebox. In the glovebox, to the vessel was added $\text{Ni}(\text{cod})_2$ (11.2 mg, 0.04 mmol, 10 mol%) and 1,2-bis(dicyclohexylphosphino)ethane (dcype) (33.8 mg, 0.08 mmol, 20 mol%). The vessel was taken out of the glovebox, then to it was added azole **1** (0.40 mmol) and then 1,4-dioxane (1.6 mL) under a stream of argon. The vessel was sealed with O-ring tap and then heated at 120 °C for 12 h in an 8-well reaction block with stirring. After cooling the reaction mixture to room temperature, the mixture was passed through a short silica gel pad with EtOAc. The filtrate was concentrated and the residue was subjected to preparative thin-layer chromatography to afford 2-arylated azoles **3** as a coupling product.



3Aa: 95%

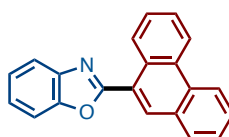
2-(Naphthalen-2-yl)benzoxazole (3Aa)^[3g] Purification by preparative thin-layer chromatography (hexane/EtOAc = 10:1) afford **3Aa** (93.2 mg, 95%) as a white solid. R_f = 0.48 (hexane/EtOAc = 5:1); ^1H NMR (400 MHz, CDCl_3): δ 8.79 (s, 1H), 8.33 (dd, J = 1.4, 8.7 Hz, 1H), 8.03–7.96 (m, 2H), 7.93–7.87 (m, 1H), 7.82 (dd, J = 3.7, 6.0 Hz, 1H), 7.63 (dd, J = 2.7, 6.4 Hz, 1H), 7.60–7.52 (m, 2H), 7.41–7.31 (m, 2H); ^{13}C NMR (100 MHz, CDCl_3): δ 163.2, 150.9, 142.2, 134.7, 133.0, 128.9, 128.8, 128.1, 127.9, 127.8, 126.9, 125.2, 124.6, 124.4, 124.0, 120.0, 110.6. HRMS (DART) m/z calcd for $\text{C}_{17}\text{H}_{12}\text{NO}$

[MH]⁺: 246.0919 found 246.0919.



3Ab: 90%

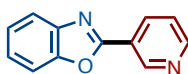
2-(Naphthalen-1-yl)benzoxazole (3Ab)^[30 a] Purification by preparative thin-layer chromatography (hexane/EtOAc = 10:1) afforded **3Ab** (88.2 mg, 90%) as a white solid. $R_f = 0.61$ (hexane/EtOAc = 5:1); ¹H NMR (400 MHz, CDCl₃): δ 9.47 (d, $J = 8.4$ Hz, 1H), 8.38 (d, $J = 7.2$ Hz, 1H), 7.97 (d, $J = 8.0$ Hz, 1H), 7.91–7.82 (m, 2H), 7.68 (t, $J = 8.0$ Hz, 1H), 7.62–7.57 (m, 1H), 7.54 (t, $J = 8.4$ Hz, 2H), 7.40–7.31 (m, 2H); ¹³C NMR (100 MHz, CDCl₃): δ 162.7, 150.1, 142.3, 133.9, 132.2, 130.6, 129.2, 128.6, 127.8, 126.4, 126.2, 125.2, 124.8, 124.4, 123.5, 120.2, 110.4; HRMS (DART) m/z calcd for C₁₇H₁₂NO [MH]⁺: 246.0919 found 246.0918.



3Ac: 55%

2-(Phenanthren-9-yl)benzoxazole (3Ac)^[30b]

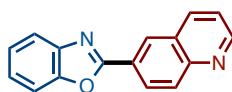
Purification by preparative thin-layer chromatography (hexane/EtOAc = 10:1) afforded **3Ac** (65.2 mg, 55%) as a white solid. $R_f = 0.61$ (hexane/EtOAc = 5:1); ¹H NMR (400 MHz, CDCl₃): δ 9.54 (dd, $J = 2.0, 8.0$ Hz, 1H), 8.80 (dd, $J = 2.0, 8.0$ Hz, 1H), 8.78–8.72 (m, 2H), 8.04 (d, $J = 8.0$ Hz, 1H), 7.95–7.88 (m, 1H), 7.84–7.74 (m, 3H), 7.73–7.63 (m, 2H), 7.46–7.39 (m, 2H); ¹³C NMR (100 MHz, CDCl₃): δ 162.6, 150.1, 142.2, 131.6, 131.5, 130.7, 130.4, 129.7, 128.61, 128.58, 127.55, 127.0, 125.3, 124.5, 122.9, 122.6, 122.4, 120.3, 110.4; HRMS (DART) m/z calcd for C₂₁H₁₄NO [MH]⁺: 296.1075 found 296.1075.



3Ad: 81%

2-(Pyridin-3-yl)benzoxazole (3Ad)^[30c]

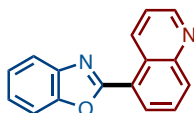
Purification by preparative thin-layer chromatography (hexane/EtOAc = 3:1) afforded **3Ad** (63.2 mg, 81%) as a tan solid. $R_f = 0.23$ (hexane/EtOAc = 2:1); ^1H NMR (400 MHz, CDCl_3): δ 9.48 (s, 1H), 8.76 (dd, $J = 2.0, 3.6$ Hz, 1H), 8.51 (d, $J = 8.0$ Hz, 1H), 7.84–7.76 (m, 1H), 7.65–7.58 (m, 1H), 7.50–7.43 (m, 1H), 7.43–7.35 (m, 2H); ^{13}C NMR (100 MHz, CDCl_3): δ 160.5, 151.9, 150.6, 148.6, 141.6, 134.5, 125.6, 124.8, 123.5, 123.4, 120.1, 110.6; HRMS (DART) m/z calcd for $\text{C}_{12}\text{H}_9\text{N}_2\text{O}[\text{MH}]^+$: 197.0715 found 197.0715.



3Ae: 99%

2-(Quinolin-6-yl)benzoxazole (**3Ae**)^[3f]

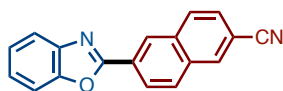
Purification by preparative thin-layer chromatography (hexane/EtOAc = 5:1) afforded **3Ae** (98.0 mg, 99%) as a white solid. $R_f = 0.17$ (hexane/EtOAc = 4:1); ^1H NMR (400 MHz, CDCl_3): δ 9.04–8.97 (m, 1H), 8.76 (s, 1H), 8.56 (dt, $J = 2.0, 7.2$ Hz, 1H), 8.29 (d, $J = 8.0$ Hz, 1H), 8.24 (d, $J = 8.0$ Hz, 1H), 7.86–7.79 (m, 1H), 7.68–7.59 (m, 1H), 7.53–7.46 (m, 1H), 7.44–7.36 (m, 2H); ^{13}C NMR (100 MHz, CDCl_3): δ 162.4, 152.0, 150.9, 149.5, 142.1, 136.8, 130.4, 128.0, 127.9, 127.7, 125.5, 125.2, 124.8, 122.1, 120.2, 110.7; HRMS (DART) m/z calcd for $\text{C}_{16}\text{H}_{11}\text{N}_2\text{O}[\text{MH}]^+$: 247.0871 found 247.0871.



3Af: 86% (R = CO^tBu)

2-(Quinolin-5-yl)benzoxazole (**3Af**)

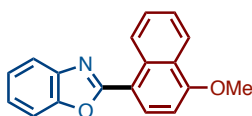
Purification by preparative thin-layer chromatography (hexane/EtOAc = 3:1) afforded **3Af** (84.4 mg, 86%) as a white solid. $R_f = 0.23$ (hexane/EtOAc = 2:); ^1H NMR (400 MHz, CDCl_3): δ 9.93 (d, $J = 8.0$ Hz, 1H), 9.00 (dd, $J = 1.6, 4.0$ Hz, 1H), 8.49 (dd, $J = 1.6, 7.2$ Hz, 1H), 8.29 (d, $J = 8.0$ Hz, 1H), 7.90–7.78 (m, 2H), 7.67–7.56 (m, 2H), 7.45–7.36 (m, 2H); ^{13}C NMR (100 MHz, CDCl_3): δ 161.6, 150.8, 150.0, 148.4, 142.1, 135.0, 133.6, 129.3, 128.5, 126.3, 125.6, 124.7, 123.7, 122.5, 120.3, 110.6; HRMS (DART) m/z calcd for $\text{C}_{16}\text{H}_{11}\text{N}_2\text{O}[\text{MH}]^+$: 247.0871 found 247.0872.



3Ag: 79%

2-(6-Cyanonaphthalen-2-yl)benzoxazole (**3Ag**)

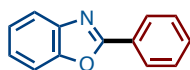
Purification by preparative thin-layer chromatography (hexane/CHCl₃ = 1:1) afforded **3Ag** (85.6 mg, 79%) as a white solid. $R_f = 0.27$ (hexane/CHCl₃ = 1:1); ¹H NMR (400 MHz, CDCl₃): δ 8.73 (s, 1H), 8.38 (dd, $J = 1.6, 8.8$ Hz, 1H), 8.22 (s, 1H), 8.00 (t, $J = 8.8, 10.4$ Hz, 2H), 7.84–7.76 (m, 1H), 7.64 (dd, $J = 0.8, 8.8$ Hz, 1H), 7.63–7.57 (m, 1H), 7.45–7.35 (m, 2H); ¹³C NMR (100 MHz, CDCl₃): δ 161.9, 150.8, 142.0, 134.2, 133.8, 133.3, 130.0, 129.2, 127.6, 127.34, 127.28, 125.8, 125.6, 124.9, 120.3, 118.7, 111.0, 110.7; HRMS (DART) m/z calcd for C₁₈H₁₁N₂O [MH]⁺: 271.0871 found 271.0872.



3Ah: 55%

2-(4-Methoxynaphthalen-1-yl)benzo[*d*]oxazole (**3Ah**)

Purification by preparative thin-layer chromatography (hexane/CHCl₃ = 1:1) afforded **3Ah** (60.4 mg, 55%) as a white solid. $R_f = 0.27$ (hexane/CHCl₃ = 1:1); ¹H NMR (400 MHz, CDCl₃): δ 8.73 (s, 1H), 8.38 (dd, 1H, $J = 1.4, 8.7$ Hz), 8.22 (s, 1H), 8.00 (t, 2H, $J = 9.2, 10.5$ Hz), 7.84–7.76 (m, 1H), 7.64 (dd, 1H, $J = 0.9, 8.7$ Hz), 7.63–7.57 (m, 1H), 7.45–7.35 (m, 2H); ¹³C NMR (100 MHz, CDCl₃): δ 161.9, 150.8, 142.0, 134.2, 133.8, 133.3, 130.0, 129.2, 127.6, 127.34, 127.28, 125.8, 125.6, 124.9, 120.3, 118.7, 111.0, 110.7.

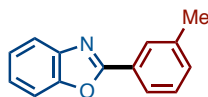


3Ai: 11% (R = CO^tBu)
75% (R = Tf)

2-Phenylbenzoxazole **3Ai**^[30d]

Purification by preparative thin-layer chromatography (hexane/EtOAc = 10:1) afforded **3Ai** (8.6 mg, 11%, R = CO^tBu; 58.6 mg, 75%, R = Tf) as a white solid. $R_f = 0.40$ (hexane/EtOAc = 5:1); ¹H NMR (400 MHz, CDCl₃): δ 8.27 (dd, $J = 2.0, 8.0$ Hz, 2H), 7.78 (dd, $J = 3.2, 6.4$ Hz, 1H), 7.59 (dd, $J = 3.2, 6.4$ Hz, 1H), 7.56–7.49 (m, 3H) 7.38–

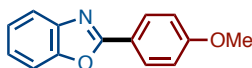
7.34 (m, 2H); ^{13}C NMR (100 MHz, CDCl_3): δ 163.0, 150.7, 142.1, 131.4, 128.8, 127.6, 127.1, 125.0, 124.5, 120.0, 110.5; HRMS (DART) m/z calcd for $\text{C}_{13}\text{H}_{10}\text{NO}$ $[\text{MH}]^+$: 196.0762 found 196.0762.



3Aj: 85%

2-(3-Methylphenyl)benzoxazole (**3Aj**)^[30e]

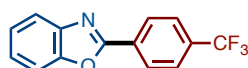
Purification by preparative thin-layer chromatography (hexane/EtOAc = 10:1) afforded **3Aj** (71.4 mg, 85%) as a white solid. Spectral data match those previously reported. R_f = 0.56 (hexane/EtOAc = 5:1); ^1H NMR (400 MHz, CDCl_3): δ 8.07 (s, 1H), 8.02 (d, J = 7.6 Hz, 1H), 7.79–7.71 (m, 1H), 7.58–7.49 (m, 1H), 7.41–7.27 (m, 4H), 2.41 (s, 3H); ^{13}C NMR (100 MHz, CDCl_3): δ 163.1, 150.6, 142.1, 138.6, 132.2, 128.7, 128.1, 126.9, 124.9, 124.6, 124.4, 119.8, 110.4, 21.2; HRMS (DART) m/z calcd for $\text{C}_{14}\text{H}_{12}\text{NO}$ $[\text{MH}]^+$: 210.0919 found 210.0919.



3Ak: 55%

2-(4-Methoxyphenyl)benzoxazole (**3Ak**)^[30d]

Purification by preparative thin-layer chromatography (hexane/EtOAc = 10:1) afforded **3Ak** (49.6 mg, 55%) as a white solid. R_f = 0.32 (hexane/EtOAc = 5:1); ^1H NMR (400 MHz, CDCl_3): δ 8.18 (dd, J = 1.6, 9.2 Hz, 2H), 7.72 (dd, J = 2.4, 6.8 Hz, 1H), 7.53 (dd, J = 2.4, 6.8 Hz, 1H), 7.37–7.27 (m, 2H), 7.00 (dd, J = 1.6, 9.2 Hz, 2H), 3.85 (s, 3H); ^{13}C NMR (100 MHz, CDCl_3): δ 163.1, 162.2, 150.6, 142.2, 129.3, 124.5, 124.3, 119.6, 119.5, 114.3, 110.3, 55.4; HRMS (DART) m/z calcd for $\text{C}_{14}\text{H}_{12}\text{NO}_2$ $[\text{MH}]^+$: 226.0868 found 226.0868.

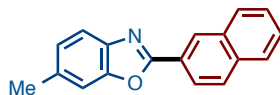


3Al: 52%

2-(4-Trifluoromethylphenyl)benzoxazole (**3Al**)^[30d]

Purification by preparative thin-layer chromatography (hexane/EtOAc = 10:1) afforded

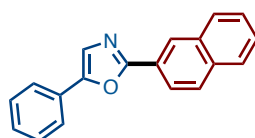
3A1 (54.4 mg, 52%) as a white solid. $R_f = 0.61$ (hexane/EtOAc = 5:1); $^1\text{H NMR}$ (400 MHz, CDCl_3): δ 8.34 (d, $J = 7.6$ Hz, 2H), 7.82–7.73 (m, 3H), 7.62–7.55 (m, 1H), 7.41–7.34 (m, 2H); $^{13}\text{C NMR}$ (100 MHz, CDCl_3): δ 161.4, 150.8, 141.9, 132.9 ($J_{\text{C-F}} = 33.5$ Hz), 130.4, 127.8, 125.9 ($J_{\text{C-F}} = 3.8$ Hz), 125.8, 124.9, 123.7 ($J_{\text{C-F}} = 274.0$ Hz), 120.4, 110.8; HRMS (DART) m/z calcd for $\text{C}_{14}\text{H}_9\text{F}_3\text{NO}$ $[\text{MH}]^+$: 264.0636 found 264.0635.



3Ba: 96% (R = COt-Bu)

6-Methyl-2-(naphthalen-2-yl)benzoxazole (**3Ba**)^[30f]

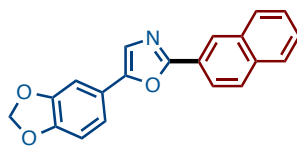
Purification by preparative thin-layer chromatography (hexane/EtOAc = 10:1) afforded **3Ba** (99.7 mg, 96%) as a white solid. $R_f = 0.44$ (hexane/EtOAc = 5:1); $^1\text{H NMR}$ (400 MHz, CDCl_3): δ 8.67 (s, 1H), 8.24 (dd, $J = 1.6, 8.8$ Hz, 1H), 7.95–7.86 (m, 2H), 7.85–7.77 (m, 1H), 7.63 (d, $J = 8.2$ Hz, 1H), 7.54–7.46 (m, 2H), 7.33 (s, 1H), 7.12 (d, $J = 8.2$ Hz, 1H), 2.46 (s, 3H); $^{13}\text{C NMR}$ (100 MHz, CDCl_3): δ 162.6, 151.0, 139.9, 135.5, 134.5, 132.9, 128.8, 128.6, 127.8, 127.7, 127.5, 126.7, 125.7, 124.5, 123.8, 119.2, 110.7, 21.7; HRMS (DART) m/z calcd for $\text{C}_{18}\text{H}_{14}\text{NO}$ $[\text{MH}]^+$: 260.1075 found 260.1075.



3Ca: 82% (R = COt-Bu)

2-(Naphthalen-1-yl)-5-phenyloxazole (**3Ca**)^[10c]

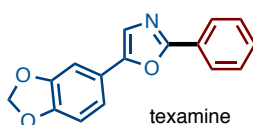
Purification by preparative thin-layer chromatography (hexane/EtOAc = 5:1) afforded **3Ca** (88.6 mg, 82%) as a white solid. $R_f = 0.36$ (hexane/EtOAc = 5:1); $^1\text{H NMR}$ (400 MHz, CDCl_3): δ 8.55 (s, 1H), 8.16 (dd, $J = 1.6, 8.0$ Hz, 1H), 7.95–7.86 (m, 2H), 7.86–7.77 (m, 1H), 7.72 (d, $J = 8.0$ Hz, 2H), 7.53–7.47 (m, 2H), 7.47–7.38 (m, 3H), 7.32 (t, $J = 8.0$ Hz, 1H); $^{13}\text{C NMR}$ (100 MHz, CDCl_3): δ 162.2, 151.3, 134.1, 133.0, 128.9, 128.62, 128.58, 128.4, 127.9, 127.8, 127.1, 126.7, 126.0, 124.6, 124.2, 123.6, 123.2; HRMS (DART) m/z calcd for $\text{C}_{19}\text{H}_{14}\text{NO}$ $[\text{MH}]^+$: 272.1075 found 272.1075.



3Da: 72% (R = CO_t-Bu)

5-(Benzo[*d*][1,3]dioxol-5-yl)-2-(naphthalen-2-yl)oxazole (**3Da**)

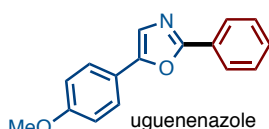
Purification by preparative thin-layer chromatography (hexane/EtOAc = 3:1) afforded **3Da** (90.2 mg, 72%) as a white solid. R_f = 0.55 (hexane/EtOAc = 2:1); ¹H NMR (400 MHz, CDCl₃): δ 8.49 (s, 1H), 8.11 (dd, J = 1.6, 8.4 Hz, 1H), 7.93–7.78 (m, 3H), 7.52–7.45 (m, 2H), 7.30 (s, 1H), 7.22 (dd, J = 1.6, 8.4 Hz, 1H), 7.14 (s, 1H), 6.84 (d, J = 8.4 Hz, 1H), 5.94 (s, 2H); ¹³C NMR (100 MHz, CDCl₃): δ 160.6, 151.2, 148.1, 147.8, 133.9, 133.0, 128.6, 128.5, 127.8, 127.0, 126.6, 125.8, 124.6, 123.1, 122.4, 122.1, 118.3, 108.7, 104.7, 101.3; HRMS (DART) m/z calcd for C₂₀H₁₄NO₃ [MH]⁺: 316.0974 found 316.0973.



3Di: 62% (R = Tf)

Texamine (**3Di**)^[10c]

Purification by preparative thin-layer chromatography (hexane/EtOAc = 4:1) afforded texamine (**3Di**; 65.8 mg, 62%) as a white solid. R_f = 0.46 (hexane/EtOAc = 3:1); ¹H NMR (400 MHz, CDCl₃): δ 8.06 (dd, J = 1.6, 8.4 Hz, 2H), 7.50–7.39 (m, 3H), 7.28 (s, 1H), 7.20 (dd, J = 1.6, 8.4 Hz, 1H), 7.14 (s, 1H), 6.84 (d, J = 8.4 Hz, 1H), 5.97 (s, 2H); ¹³C NMR (100 MHz, CDCl₃): δ 160.5, 151.0, 148.1, 147.8, 130.1, 128.7, 127.4, 126.1, 122.3, 122.1, 118.2, 108.7, 104.7, 101.3; HRMS (DART) m/z calcd for C₁₆H₁₂NO₃ [MH]⁺: 266.0817 found 266.0817.

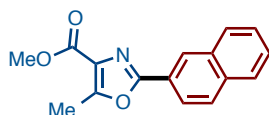


3Ei: 73% (R = Tf)

Uguenenazole (**3Ei**)^[11b]

Purification by preparative thin-layer chromatography (hexane/EtOAc = 4:1) afforded uguenenazole (**3Ei**; 73.8 mg, 73%) as a white solid. R_f = 0.46 (hexane/EtOAc = 3:1); ¹H NMR (400 MHz, CDCl₃): δ 8.08 (dd, J = 1.6, 8.0 Hz, 2H), 7.62 (dd, J = 2.4, 9.2 Hz,

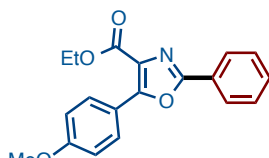
2H), 7.50–7.39 (m, 3H), 7.31 (s, 1H), 6.95 (dd, $J = 2.4, 9.2$ Hz, 2H), 3.83 (s, 3H); ^{13}C NMR (100 MHz, CDCl_3): δ 160.5, 159.7, 151.2, 130.0, 128.7, 127.5, 126.1, 125.7, 121.9, 120.8, 114.3, 55.3; HRMS (DART) m/z calcd for $\text{C}_{16}\text{H}_{14}\text{NO}_2$ $[\text{MH}]^+$: 252.1025 found 252.1025.



3Fa: 72% (R = COt-Bu)

Methyl 5-methyl-2-(naphthalen-2-yl)oxazole-4-carboxylate (**3Fa**)

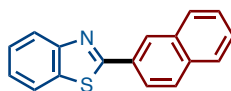
Purification by preparative thin-layer chromatography (hexane/EtOAc = 3:1) afforded **3Fa** (76.7 mg, 72%) as a white solid. $R_f = 0.29$ (hexane/EtOAc = 3:1); ^1H NMR (400 MHz, CDCl_3): δ 8.54 (s, 1H), 8.11 (dd, $J = 1.6, 8.8$ Hz, 1H), 7.93–7.78 (m, 3H), 7.53–7.47 (m, 2H), 3.95 (s, 3H), 2.71 (s, 3H); ^{13}C NMR (100 MHz, CDCl_3): δ 162.7, 159.7, 156.4, 134.1, 132.8, 128.6, 128.53, 128.48, 127.7, 127.3, 126.7, 126.5, 123.7, 123.1, 51.9, 12.1; HRMS (DART) m/z calcd for $\text{C}_{16}\text{H}_{14}\text{NO}_3$ $[\text{MH}]^+$: 268.0974 found 268.0974.



3Gi: 73% (R = Tf)

Ethyl 5-(4-methoxyphenyl)-2-phenyloxazole-4-carboxylate (**3Gi**)

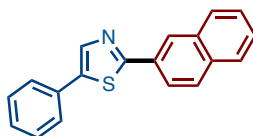
Purification by preparative thin-layer chromatography (CHCl_3) afforded **3Gi** (94.3 mg, 73%) as a white solid. $R_f = 0.47$ (hexane/EtOAc = 2:1); ^1H NMR (400 MHz, CDCl_3): δ 8.17–8.06 (m, 4H), 7.49–7.43 (m, 3H), 7.00 (dd, $J = 2.4, 9.2$ Hz, 2H), 4.45 (q, $J = 7.2$ Hz, 2H), 3.86 (s, 3H), 1.43 (t, $J = 7.2$ Hz, 3H); ^{13}C NMR (100 MHz, CDCl_3): δ 162.4, 161.0, 159.0, 155.3, 130.7, 130.1, 128.6, 126.9, 126.6, 126.4, 119.5, 113.7, 61.2, 55.3, 14.2; HRMS (DART) m/z calcd for $\text{C}_{19}\text{H}_{18}\text{NO}_4$ $[\text{MH}]^+$: 324.1236 found 324.1236.



3Ha: 65% (R = CO t -Bu)

2-(Naphthalen-2-yl)benzo[*d*]thiazole (**3Ha**)^[1b]

Purification by preparative thin-layer chromatography (hexane/EtOAc = 5:1) afforded **3Ha** (71.6 mg, 65%) as a white solid. R_f = 0.48 (hexane/EtOAc = 5:1); ^1H NMR (400 MHz, CDCl_3): δ 8.57 (s, 1H), 8.21 (dd, J = 2.0, 8.4 Hz, 1H), 8.12 (d, J = 8.4 Hz, 1H), 8.01–7.92 (m, 3H), 7.91–7.84 (m, 1H), 7.60–7.49 (m, 3H), 7.41 (t, J = 8.4 Hz, 1H); ^{13}C NMR (100 MHz, CDCl_3): δ 168.0, 154.2, 135.0, 134.5, 133.1, 130.1, 128.7, 127.8, 127.5, 127.4, 126.8, 126.3, 125.1, 124.3, 123.1, 121.6; HRMS (DART) m/z calcd for $\text{C}_{17}\text{H}_{12}\text{NS}$ $[\text{MH}]^+$: 262.0690 found 262.0690.

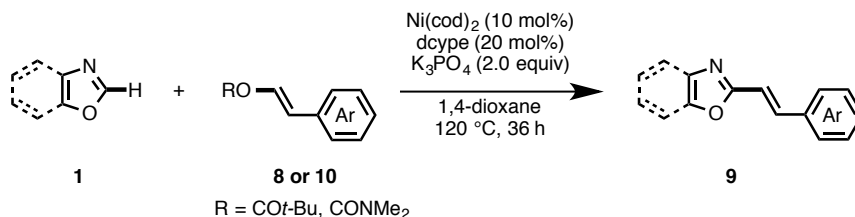


3Ia: 64% (R = CO t -Bu)

2-(Naphthalen-2-yl)-5-phenylthiazole (**3Ia**)

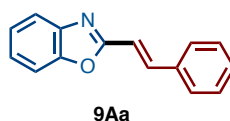
Purification by preparative thin-layer chromatography (hexane/ CH_2Cl_2 = 1:1) afforded **3Ia** (73.7 mg, 64%) as a slightly yellow solid. R_f = 0.44 (hexane/ CH_2Cl_2 = 1:1); ^1H NMR (400 MHz, CDCl_3): δ 8.42 (s, 1H), 8.09–8.00 (m, 2H), 7.93–7.78 (m, 3H), 7.60 (d, J = 8.0 Hz, 2H), 7.52–7.48 (m, 2H), 7.40 (t, J = 8.0 Hz, 2H), 7.32 (t, J = 8.0 Hz, 1H); ^{13}C NMR (100 MHz, CDCl_3): δ 167.1, 139.4, 139.3, 134.1, 133.2, 131.4, 131.0, 129.1, 128.7, 128.6, 128.3, 127.8, 127.0, 126.8, 126.6, 125.7, 123.7; HRMS (DART) m/z calcd for $\text{C}_{19}\text{H}_{14}\text{NS}$ $[\text{MH}]^+$: 288.0847 found 288.0846.

4-7. Ni-Catalyzed C–H/C–O Alkenylation of Azoles with Enol Derivatives



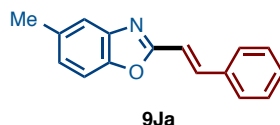
General Procedure: A 20-mL glass vessel equipped with J. Young[®] O-ring tap

containing a magnetic stirring bar and K_3PO_4 (169.7 mg, 0.80 mmol, 2.0 equiv) was dried with a heatgun under reduced pressure and filled with N_2 gas after cooling to room temperature. To this vessel was added an alkenyl pivalate **8** (or carbamate **10**) (0.60 mmol, 1.5 equiv calculated based on the amount of (*E*)-**8**, (*E*)-**10**), and then introduced into an argon-atmosphere glovebox. To the reaction vessel were added $Ni(cod)_2$ (11.2 mg, 0.04 mmol, 10 mol%) and 1,2-bis(dicyclohexylphosphino)ethane (dcype) (33.8 mg, 0.08 mmol, 20 mol%). The vessel was taken out of the glovebox, then to it were added an azole **1** (0.40 mmol) and 1,4-dioxane (1.6 mL) under a stream of N_2 . The vessel was sealed with O-ring tap and then heated at 120 °C for 36 h in an 8-well reaction block with stirring. After cooling the reaction mixture to room temperature, the mixture was passed through a short silica gel pad with EtOAc. The filtrate was concentrated and the residue was subjected to preparative thin-layer chromatography (PTLC) to afford a 2-alkenylated azole **9**.



(*E*)-2-(2-Phenylethenyl)-benzoxazole (9Aa)^[31]

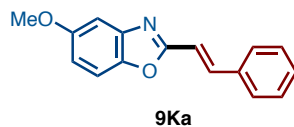
Purification by preparative thin-layer chromatography afforded **9Aa** as a white solid (68.2 mg, 77% yield). 1H NMR ($CDCl_3$, 400 MHz) δ 7.81 (d, $J = 16.5$ Hz, 1H), 7.75–7.69 (m, 1H), 7.61 (d, $J = 7.8$ Hz, 2H), 7.56–7.50 (m, 1H), 7.46–7.38 (m, 3H), 7.36–7.31 (m, 2H), 7.09 (d, $J = 16.5$ Hz, 1H); ^{13}C NMR ($CDCl_3$, 100 MHz) δ 162.8, 150.4, 142.2, 139.5, 135.1, 129.8, 129.0, 127.6, 125.2, 124.5, 119.9, 114.0, 110.3; HRMS calcd for $C_{15}H_{12}NO$ $[M+H]^+$: 222.0919, found: 222.0917.



(*E*)-5-Methyl-2-styrylbenzoxazole (9Ja)

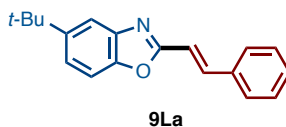
Purification by preparative thin-layer chromatography afforded **9Ja** as a white solid (66.0 mg, 70% yield). 1H NMR ($CDCl_3$, 400 MHz) δ 7.77 (d, $J = 16.8$ Hz, 1H), 7.60 (d, $J = 6.8$ Hz, 2H), 7.50 (s, 1H), 7.46–7.35 (m, 4H), 7.15 (dd, $J = 8.4, 1.6$ Hz, 1H), 7.07 (d, $J = 16.8$ Hz, 1H), 2.48 (s, 3H); ^{13}C NMR ($CDCl_3$, 100 MHz) δ 162.8, 148.6, 142.3,

139.0, 135.1, 134.3, 129.6, 128.9, 127.4, 126.3, 119.7, 114.0, 109.6, 21.4; HRMS calcd for C₁₆H₁₄NO [M+H]⁺: 236.1075, found: 236.1075.



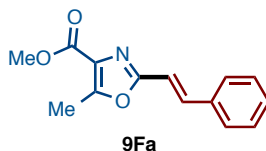
(E)-5-Methoxy-2-(2-phenylethenyl)benzoxazole (9Ka)

Purification by preparative thin-layer chromatography afforded **9Ka** as a yellow solid (59.4 mg, 59% yield). ¹H NMR (CDCl₃, 400 MHz) δ 7.76 (d, *J* = 16.5 Hz), 7.59 (d, *J* = 8.4 Hz, 2H), 7.43–7.39 (m, 4H), 7.19 (d, *J* = 2.5 Hz, 1H), 7.05 (d, *J* = 16.5 Hz, 1H), 6.93 (dd, *J* = 8.4, 2.5 Hz, 1H), 3.86 (s, 3H); ¹³C NMR (CDCl₃, 100 MHz) δ 163.6, 157.3, 145.0, 143.0, 139.1, 135.2, 129.7, 128.9, 127.5, 114.0, 113.8, 110.4, 102.7, 55.9; HRMS calcd for C₁₆H₁₄NO₂ [M+H]⁺: 252.1025, found: 252.1024.



(E)-5-(tert-Butyl)-2-(2-phenylethenyl)benzoxazole (9La)

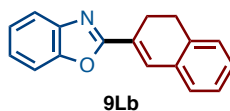
Purification by preparative thin-layer chromatography afforded **9La** as a white solid (67.5 mg, 61% yield). ¹H NMR (CDCl₃, 400 MHz) δ 7.77 (d, *J* = 16.4 Hz, 1H), 7.73 (d, *J* = 1.6 Hz, 1H), 7.60 (d, *J* = 6.8 Hz, 2H), 7.46–7.39 (m, 5H), 7.07 (d, *J* = 16.4 Hz, 1H), 1.39 (s, 9H); ¹³C NMR (CDCl₃, 100 MHz) δ 162.9, 148.4, 148.0, 142.1, 138.9, 135.2, 129.6, 128.9, 127.4, 122.9, 116.3, 114.1, 109.4, 34.8, 31.7; HRMS calcd for C₁₉H₂₀NO [M+H]⁺: 278.1545, found: 278.1541.



(E)-Methyl 5-methyl-2-styryloxazole-4-carboxylate (9Fa)

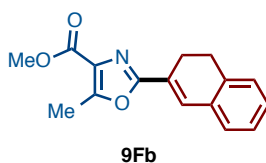
Purification by preparative thin-layer chromatography afforded **9Fa** as a white solid (54.6 mg, 56% yield). ¹H NMR (CDCl₃, 400 MHz) δ 7.53 (d, *J* = 16.8 Hz, 1H), 7.51 (d, *J* = 6.8 Hz, 2H), 7.41–7.34 (m, 3H), 6.89 (d, *J* = 16.8 Hz, 1H), 3.93 (s, 3H), 2.68 (s, 3H); ¹³C NMR (CDCl₃, 100 MHz) δ 162.7, 159.3, 156.0, 137.0, 135.1, 129.4, 128.9,

128.4, 127.2, 113.0, 51.9, 12.0; HRMS calcd for C₁₄H₁₄NO₃ [M+H]⁺: 244.0974, found: 244.0970.



2-(3,4-Dihydronaphthalen-2-yl)benzoxazole (**9Lb**)

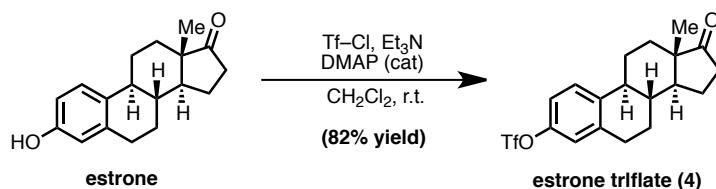
Purification by preparative thin-layer chromatography afforded **9Lb** as a white solid (60.4 mg, 61% yield). ¹H NMR (CDCl₃, 400 MHz) δ 7.76–7.69 (m, 1H), 7.74 (s, 1H), 7.55–7.47 (m, 1H), 7.36–7.27 (m, 2H), 7.26–7.15 (m, 4H), 3.05–2.90 (m, 4H); ¹³C NMR (CDCl₃, 100 MHz) δ 163.5, 150.4, 142.1, 136.3, 132.8, 132.2, 128.9, 127.9, 127.7, 126.8, 125.5, 125.1, 124.3, 119.8, 110.2, 27.4, 22.9; HRMS calcd for C₁₇H₁₄NO [M+H]⁺: 248.1075, found: 248.1076.



Methyl 2-(3,4-dihydronaphthalen-2-yl)-5-methyloxazole-4-carboxylate (**9Fb**)

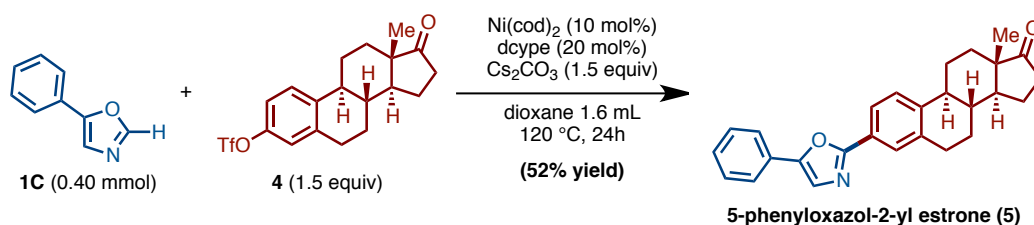
Purification by preparative thin-layer chromatography afforded **9Fb** as a white solid (86.1 mg, 80% yield). ¹H NMR (CDCl₃, 400 MHz) δ 7.38 (s, 1H), 7.23–7.13 (m, 4H), 3.93 (s, 3H), 2.93–2.91 (m, 2H), 2.89–2.82 (m, 2H), 2.68 (s, 3H); ¹³C NMR (CDCl₃, 100 MHz) δ 162.7, 160.0, 156.1, 135.8, 129.6, 128.5, 127.5, 126.6, 51.8, 27.2, 22.7, 12.0; HRMS calcd for C₁₆H₁₆NO₃ [M+H]⁺: 270.1130, found: 270.1133.

4-7. Nickel-Catalyzed Arylation of Complex Steroid and Alkaloid Scaffolds



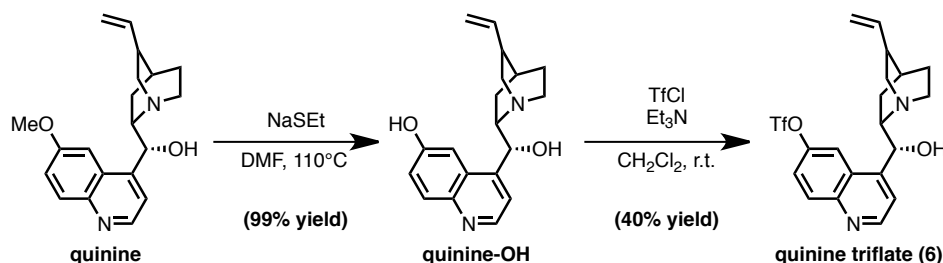
To a solution of estrone (1.62 g, 6.0 mmol) in CH₂Cl₂ (10 mL) was added triethylamine (1.0 mL, 7.2 mmol, 1.2 equiv) at room temperature. Then trifluoromethanesulfonyl chloride (760 μL, 7.2 mmol, 1.2 equiv) was added dropwise over 3 min at 0°C. After

stirring for 6 h, the reaction mixture was quenched with sat. NaHCO₃ aq. (10 mL), then the layers were separated. The aqueous layer was extracted with CH₂Cl₂ (20 mL × 3) and the combined organic layer was treated with Na₂SO₄ and then filtrated. Following evaporation of the solvent *in vacuo*, the crude residue was purified by flash column chromatography (hexane/EtOAc = 5:1) to afford estrone triflate **4** as a white solid (1.98 g, 82% yield).^[27] R_f 0.36 (hexane/EtOAc = 5:1); ¹H NMR (400 MHz, CDCl₃): δ 7.34 (d, *J* = 9.2 Hz, 1H), 7.03 (d, *J* = 9.2 Hz, 1H), 6.99 (s, 1H), 2.95 (t, 2H, *J* = 4.0, 4.4 Hz), 2.52 (qd, *J* = 2.8, 9.2 Hz, 1H), 2.50–2.36 (m, 1H), 2.36–2.25 (m, 1H), 2.24–2.01 (m, 3H), 1.98 (dd, *J* = 2.8, 9.6 Hz, 1H), 1.69–1.44 (m, 6H), 0.92 (s, 3H).



A 20-mL glass vessel equipped with J. Young[®] O-ring tap containing a magnetic stirring bar and Cs₂CO₃ (195.5 mg, 0.60 mmol, 1.5 equiv) was dried with a heatgun under reduced pressure and filled with argon after cooling to room temperature. To this vessel was added 5-phenyloxazole (**1C**: 58.0 mg, 0.40 mmol) and estrone triflate (**4**: 241.5 mg, 0.60 mmol, 1.5 equiv) then introduced inside an argon atmosphere glovebox. In the glovebox, to the vessel was added Ni(cod)₂ (11.2 mg, 0.04 mmol, 10 mol%) and 1.2-bis(dicyclohexylphosphino)ethane (dcype) (33.8 mg, 0.08 mmol, 20 mol%). The vessel was taken out of the glovebox, then to it was added 1,4-dioxane (1.6 mL) under a stream of argon. The vessel was sealed with O-ring tap and then heated at 120 °C for 24 h in an 8-well reaction block with stirring. After cooling the reaction mixture to room temperature, the mixture was passed through a short silica gel pad with EtOAc. The filtrate was concentrated and the residue was subjected to preparative thin-layer chromatography (hexane/CHCl₃ = 5:1) to afford 5-phenyloxazol-2-yl estrone (**5**: 83.3 mg, 52%) as a white solid. R_f = 0.50 (hexane/EtOAc = 3:1); ¹H NMR (400 MHz, CDCl₃): δ 7.87–7.79 (m, 2H), 7.70 (d, *J* = 7.6 Hz, 2H), 7.46–7.39 (m, 3H), 7.38–7.29 (m, 2H), 3.01–2.92 (m, 2H), 2.50 (q, *J* = 9.2 Hz, 1H), 2.44–2.38 (m, 1H), 2.33–2.25 (m, 1H), 2.18–1.94 (m, 4H), 1.68–1.39 (m, 6H), 0.91 (s, 3H); ¹³C NMR (100 MHz, CDCl₃): δ 220.5, 161.2, 150.8, 142.3, 137.0, 128.8, 128.2, 127.9, 126.6, 125.7, 124.8, 124.0,

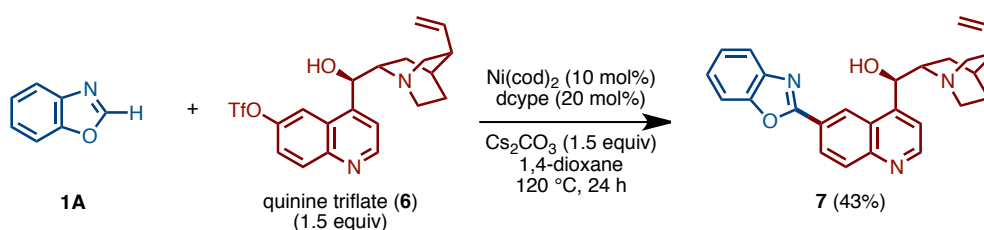
123.5, 123.2, 50.3, 47.8, 44.4, 37.7, 35.7, 31.4, 29.2, 26.2, 25.5, 21.4, 13.7; HRMS (DART) m/z calcd for $C_{27}H_{28}NO_2$ $[MH]^+$: 398.2120 found 398.2119.



A 100-mL two necked round flask containing a magnetic stirring bar was dried with a heatgun under reduced pressure and filled with argon after cooling to room temperature. To this vessel was added quinine (1.33 g, 4.1 mmol), sodium ethane sulfide (1.38 g, 16.4 mmol, 4.0 equiv), and then DMF 30 mL. This vessel was heated 120 °C in an oil bath overnight. After cooling reaction vessel to room temperature, reaction mixture was quenched with sat. NH₄Cl (30 mL), then the layers were separated. The aqueous layer was extracted with EtOAc (25 mL × 5), then the combined organic layer was washed with brine (25 ml × 3). The organic layer was treated with Na₂SO₄ and then filtrated. Following evaporation of the solvent under reduced pressure, the crude mixture was triturated with 10% CH₂Cl₂ in hexane to afford 1.27 g of quinine-OH as a white solid (99% yield).^[32] ¹H NMR (400 MHz, CD₃OD): δ 8.60 (d, J = 4.4 Hz, 1H), 7.91 (d, J = 9.2 Hz, 1H), 7.63 (d, J = 4.4 Hz, 1H), 7.34 (dd, J = 2.4, 9.2 Hz, 1H), 7.29 (d, J = 2.4 Hz, 1H), 5.81–5.69 (m, 1H), 5.57 (d, J = 2.4 Hz, 1H), 5.03–4.90 (m, 2H), 3.78 (br, 1H), 3.24–3.12 (m, 2H), 2.86–2.72 (m, 2H), 2.43 (br, 1H), 1.97–1.86 (m, 2H), 1.84 (br, 1H), 1.65 (br, 1H), 1.51–1.41 (m, 1H).

Without further purification, to a dry 30 mL two necked round flask containing a magnetic stirring bar was added quinine-OH (465.6 mg, 1.5 mmol). To this vessel was added triethylamine (238 mL, 1.1 equiv), CH₂Cl₂ (3.0 mL) then trifluoromethanesulfonyl chloride (166 mL, 1.05 equiv) at 0 °C. After stirring 8 h under room temperature, the reaction mixture was quenched with sat. NaHCO₃ (5 mL). The aqueous layer was extracted with CH₂Cl₂ (15 mL × 5) and the combined organic layer was treated with Na₂SO₄ and then filtrated. Following evaporation of the solvent under reduced pressure, the crude residue was purified by flash column chromatography (CHCl₃/MeOH = 9:1) then reversed phase HPLC (H₂O/MeCN gradient) afforded 265.9 mg of quinine triflate **6** as a white solid (40% yield).^[32] R_f = 0.26 (CHCl₃/MeOH = 10:1); ¹H NMR (400 MHz,

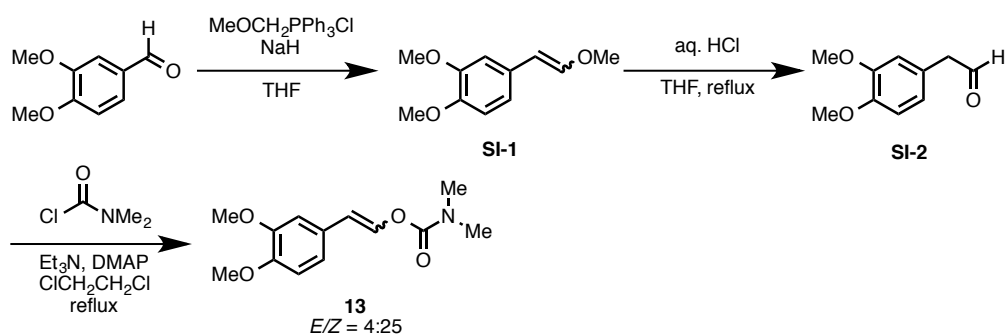
CD₃OD): δ 8.91 (d, J = 4.4 Hz, 1H), 8.36 (d, J = 2.4 Hz, 1H), 8.20 (d, J = 9.6 Hz, 1H), 7.77–7.71 (m, 2H), 5.82–5.71 (m, 1H), 5.45 (d, J = 4.4 Hz, 1H), 5.01–4.85 (m, 2H), 3.58–3.46 (br, 1H), 3.20–3.12 (br, 1H), 3.05 (dd, J = 10.8, 14.0 Hz, 1H), 2.71–2.60 (m, 2H), 2.39–2.29 (br, 1H), 1.89–1.78 (m, 3H), 1.68–1.52 (m, 2H); ¹³C NMR (100 MHz, CD₃OD): δ 153.9, 149.9, 149.3, 144.0, 134.5, 128.8, 125.5, 123.0, 121.6 (q, J_{C-F} = 322.0 Hz), 119.2, 116.3, 74.6, 63.2, 58.6, 45.0, 42.1, 30.4, 29.5, 24.5.



A 20-mL glass vessel equipped with J. Young[®] O-ring tap containing a magnetic stirring bar and Cs₂CO₃ (122.2 mg, 0.375 mmol, 1.5 equiv) was dried with a heatgun under reduced pressure and filled with argon after cooling to room temperature. To this vessel was added quinine triflate (**6**: 165.9 mg, 0.375 mmol, 1.5 equiv) then introduced inside an argon atmosphere glovebox. In the glovebox, to the vessel was added Ni(cod)₂ (7.0 mg, 0.025 mmol, 10 mol%) and 1,2-bis(dicyclohexylphosphino)ethane (dcype) (20.8 mg, 0.05 mmol, 20 mol%). The vessel was taken out of the glovebox, then to it was added benzoxazole (**1A**: 29.8 mg, 0.25 mmol) and 1,4-dioxane (1.0 mL) under a stream of argon. The vessel was sealed with O-ring tap and then heated at 120 °C for 24 h in an 8-well reaction block with stirring. After cooling the reaction mixture to room temperature, the mixture was passed through a short silica gel pad with EtOAc. The filtrate was concentrated and the residue was subjected to preparative thin-layer chromatography (CHCl₃:MeOH = 10/1), then reversed phase HPLC (H₂O/MeCN gradient) afforded benzoxazol-2-yl quinine (**7**: 43.9 mg, 43%) as a white solid. R_f = 0.17 (CHCl₃/MeOH = 10:1); ¹H NMR (400 MHz, CDCl₃): δ 8.55 (s, 1H), 8.28 (d, J = 4.4 Hz, 1H), 8.08 (d, J = 8.8 Hz, 1H), 7.93 (d, J = 8.8 Hz, 1H), 7.72–7.65 (m, 1H), 7.64–7.57 (m, 1H), 7.44 (d, J = 4.4 Hz, 1H), 7.42–7.35 (m, 2H), 5.82 (d, J = 2.8 Hz, 1H), 5.72–5.61 (m, 1H), 4.96–4.82 (m, 2H), 3.73–3.58 (m, 1H), 3.13 (dd, J = 10.4, 14.0 Hz, 1H), 3.04–2.94 (m, 1H), 2.82–2.68 (m, 1H), 2.60 (dd, J = 3.2, 14.0 Hz, 1H), 2.30 (br, 1H), 2.00–1.85 (m, 2H), 1.82 (d, J = 3.2 Hz, 1H), 1.62–1.49 (m, 1H), 1.48–1.38 (m, 1H); ¹³C NMR (100 MHz, CDCl₃): δ 161.9, 151.3, 150.7, 150.6, 148.7, 141.4, 141.3,

130.7, 126.4, 125.5, 124.9, 124.8, 123.9, 122.8, 119.8, 118.8, 114.4, 110.9, 70.5, 60.7, 56.4, 42.9, 39.6, 27.9, 27.1, 20.4; HRMS (DART) m/z calcd for $C_{26}H_{26}N_3O_2$ $[MH]^+$: 412.2025 found 412.2025.

(E)-3,4-Dimethoxystyryl dimethylcarbamate (13)



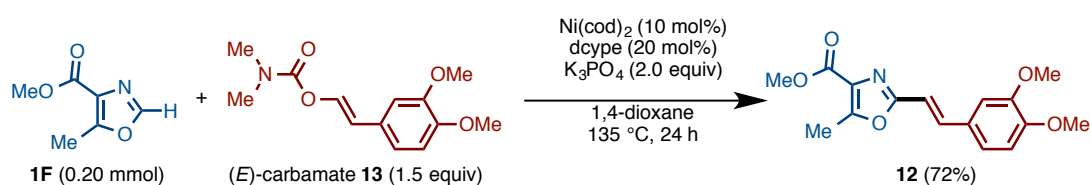
To a THF solution (90 mL) of (methoxymethyl)triphenylphosphonium chloride (15.4 g, 45 mmol, 1.5 equiv) was added NaH 60% dispersion in mineral oil (1.80 g, 45 mmol, 1.5 equiv). After stirring this solution for 30 min, 3,4-dimethoxybenzaldehyde (4.98 g, 30 mmol) was added to this mixture and it was refluxed. By monitoring the progress of the reaction by TLC, the reaction was quenched by adding H_2O . This was extracted five times with Et_2O , the combined organic phase was dried over $MgSO_4$, and filtrated. After concentration of filtrate, Et_2O was added to the resulted crude product. Triphenylphosphine oxide was removed by filtration, and then the resulted solution was concentrated. The residue was purified by flash column chromatography on silica gel (hexane/ $EtOAc$ = 5:1) to afford enol ether **SI-1** (4.89 g, 84% yield).

To a solution of **SI-1** (4.89 g, 25 mmol) in THF (160 mL) was added 1 M HCl (80 mL), and it was refluxed 3 hours. The reaction mixture was quenched with saturated $NaHCO_3$ aq. After the removal of THF under the reduced pressure, the reaction mixture was extracted three times with Et_2O . The combined organic layer was washed with brine, and then dried over $MgSO_4$. After the filtration, the solution was concentrated under the reduced pressure to afford aldehyde **SI-2** as a yellow oil (4.58 g). This oil was used without further purification.

To a dichloroethane solution (50 mL) of **SI-2** (4.58 g, 25 mmol) were added Et_3N (4.6 mL, 32.5 mmol, 1.3 equiv), N,N -dimethyl amino pyridine (DMAP: catalytic amount) and N,N -dimethyl carbamoyl chloride (3.0 mL, 32.5 mmol, 1.3 equiv). This mixture was refluxed overnight. The reaction was quenched by saturated NH_4Cl aq., and

then the mixture was extracted three times with CH₂Cl₂. The combined organic layer was dried over Na₂SO₄, concentrated under reduced pressure. The residue was subjected for flash column chromatography on silica gel to afford enol carbamate **13** (4.47 g, 71% yield in 2 steps, *E/Z* =4:25) as a white solid. The (*E*)-isomer was isolated by flash column chromatography on silica gel. ¹H NMR (CDCl₃, 400 MHz) δ 7.69 (d, *J* = 13.0 Hz, 1H), 6.90–6.78 (m, 3H), 6.27 (d, *J* = 13.0 Hz, 1H), 3.91 (s, 3H), 3.87 (s, 3H), 3.02 (s, 3H), 2.99 (s, 3H); ¹³C NMR (CDCl₃, 100 MHz) δ 153.8, 149.1, 148.3, 136.7, 127.6, 119.1, 112.8, 111.3, 108.3, 55.9, 55.8, 36.6, 36.0; HRMS calcd for C₁₃H₁₈NO₄ [M+H]⁺: 252.1236, found: 252.1233.

Ni-Catalyzed C–H/C–O Alkenylation of **1F** with **13**^[16a]



A 20-mL tube equipped with J. Young[®] O-ring tap containing magnetic stirring bar and K₃PO₄ (84.9 mg, 0.40 mmol, 2.0 equiv) was dried with heatgun under the reduced pressure. After cooling to room temperature and being filled with N₂ gas, to it were added carbamate **13** (75.4 mg, 0.30 mmol, 1.5 equiv) and **1F** (28.2 mg, 0.20 mmol). This tube was introduced into an argon atmosphere in glovebox. In the glovebox, Ni(cod)₂ (5.5 mg, 0.02 mmol, 10 mol%) and dcype (16.6 mg, 0.04 mmol, 20 mol%) were added, and the vessel was taken out from glovebox. 1,4-Dioxane (0.8 mL) was added under the stream of N₂ gas, and this tube was sealed with J. Young O-ring tap. After heating this reaction mixture in oil bath at 135 °C for 24 hours, the reaction mixture was cooled to room temperature. The reaction mixture was passed through a silica-gel pad with EtOAc, and concentrated. The residue was subjected to PTLC (hexane/EtOAc = 1:1) to afford methyl (*E*)-2-(3,4-dimethoxystyryl)-5-methyloxazole-4-carboxylate (**12**) as a yellow solid (42.8 mg, 72% yield). ¹H NMR (CDCl₃, 400 MHz) δ 7.47 (d, *J* = 16.7 Hz, 1H), 7.08 (dd, *J* = 8.2, 1.3 Hz, 1H), 7.04 (s, 1H), 6.88 (d, *J* = 8.2 Hz, 1H), 6.76 (d, *J* = 16.7 Hz, 1H), 4.00–3.85 (m, 9H), 2.67 (s, 3H); ¹³C NMR (CDCl₃, 100 MHz) δ 162.8, 159.6, 155.8, 150.4, 149.2, 136.8, 128.3, 128.2, 121.2, 111.1, 111.0, 109.0, 55.9, 55.8, 51.9, 12.0; HRMS calcd for C₁₆H₁₈NO₅ [M+H]⁺: 304.1185, found: 304.1187.

Reference and Notes

- 1 (a) Canivet, J.; Yamaguchi, J.; Ban, I.; Itami, K. *Org. Lett.* **2009**, *11*, 1733. (b) Yamamoto, T.; Muto, K.; Komiyama, M.; Canivet, J.; Yamaguchi, J.; Itami, K. *Chem. Eur. J.* **2011**, *17*, 10113.
- 2 For reviews of cross-coupling involving C–O bond activation, see: (a) Li, B.-J.; Yu, D.-G.; Sun, C.-L.; Shi, Z.-J. *Chem. Eur. J.* **2011**, *17*, 1728. (b) Rosen, B. M.; Quasdorf, K. W.; Wilson, D. A.; Zhang, N.; Resmerita, A.-M.; Garg, N. K.; Percec, V. *Chem. Rev.* **2011**, *111*, 1346. (c) Yu, D.-G.; Li, B.-J.; Shi, Z.-J. *Acc. Chem. Res.* **2010**, *43*, 1486.
- 3 Metal-catalyzed C–H/C–O biaryl coupling of aryl tosylates, mesylates, and imidazolylcarbamates are known: Ru-catalyzed reaction using aryl tosylates: (a) Ackermann, L.; Althammer, A.; Born, R. *Angew. Chem., Int. Ed.* **2006**, *45*, 2619. (b) Ackermann, L.; Vicente, R.; Althammer, A. *Org. Lett.* **2008**, *10*, 2299. (c) Ackermann, L.; Mulzer, M. *Org. Lett.* **2008**, *10*, 5043. Pd-catalyzed reaction using aryl tosylates: (d) Ackermann, L.; Althammer, A.; Fenner, S. *Angew. Chem., Int. Ed.* **2009**, *48*, 201. (e) Ackermann, L.; Fenner, S. *Chem. Commun.* **2011**, *47*, 430. Using aryl mesylates: (f) So, C. M.; Lau, C. P.; Kwong, F. Y. *Chem. Eur. J.* **2011**, *17*, 761. (g) Ferguson, D. M.; Rudolph, S. R.; Kalyani, D. *ACS Catal.* **2014**, *4*, 2395. Using aryl imidazolylsulfamates: (h) Ackermann, L.; Barfüsser, S.; Pospesch, J. *Org. Lett.* **2010**, *12*, 724.
- 4 Muto, K.; Yamaguchi, J.; Itami, K. *J. Am. Chem. Soc.* **2012**, *134*, 169.
- 5 Meng, L.; Kamada, Y.; Muto, K.; Yamaguchi, J.; Itami, K. *Angew. Chem., Int. Ed.* **2013**, *52*, 10048.
- 6 For Ni-catalyzed C–Mg/C–O and C–Zn/C–O biaryl coupling, see: (a) Wenkert, E.; Michelotti, E. L.; Swindell, C. S. *J. Am. Chem. Soc.* **1979**, *101*, 2246. (b) Wenkert, E.; Michelotti, E. L.; Swindell, C. S.; Tingoli, M. *J. Org. Chem.* **1984**, *49*, 4894. (c) Hayashi, T.; Katsuro, Y.; Okamoto, Y.; Kumada, M. *Tetrahedron Lett.* **1981**, *22*, 4449. (d) Dankwardt, J. W. *Angew. Chem., Int. Ed.* **2004**, *43*, 2428. (e) Macklin, T. K.; Snieckus, V. *Org. Lett.* **2005**, *7*, 2519. (f) Li, B.-J.; Li, Y.-Z.; Lu, X.-Y.; Liu, J.; Guan, B.-T.; Shi, Z.-J. *Angew. Chem., Int. Ed.* **2008**, *47*, 10124. (g) Yu, D.-G.; Li,

- B.-J.; Zheng, S.-F.; Guan, B.-T.; Wang, B.-Q.; Shi, Z.-J. *Angew. Chem., Int. Ed.* **2010**, *49*, 4566. (h) Wang, C.; Ozaki, T.; Takita, R.; Uchiyama, M. *Chem. Eur. J.* **2012**, *18*, 3482.
- 7 For Ni/PCy₃-catalyzed C–B/C–O biaryl coupling using phenol derivatives (ethers, esters, carbamates, carbonates, sulfamates, phosphates, and metal salts), see: (a) Tobisu, M.; Shimasaki, T.; Chatani, N. *Angew. Chem., Int. Ed.* **2008**, *47*, 4866. (b) Quasdorf, K. W.; Tian, X.; Garg, N. K. *J. Am. Chem. Soc.* **2008**, *130*, 14422. (c) Guan, B.-T.; Wang, Y.; Li, B.-J.; Yu, D.-G.; Shi, Z.-J. *J. Am. Chem. Soc.* **2008**, *130*, 14468. (d) Quasdorf, K. W.; Riener, M.; Petrova, K. V.; Garg, N. K. *J. Am. Chem. Soc.* **2009**, *131*, 17748. (e) Antoft-Finch, A.; Blackburn, T.; Snieckus, V. *J. Am. Chem. Soc.* **2009**, *131*, 17750. (f) Xi, L.; Li, B.-J.; Wu, Z.-H.; Lu, X.-Y.; Guan, B.-T.; Wang, B.-Q.; Zhao, K.-Q.; Shi, Z.-J. *Org. Lett.* **2010**, *12*, 884. (g) Quasdorf, K. W.; Antoft-Finch, A.; Liu, P.; Silberstein, A. L.; Komaromi, A.; Blackburn, T.; Ramgren, S. D.; Houk, K. N.; Snieckus, V.; Garg, N. K. *J. Am. Chem. Soc.* **2011**, *133*, 6352. (h) Chen, H.; Huang, Z.; Hu, X.; Tang, G.; Xu, P.; Zhao, Y.; Cheng, C.-H. *J. Org. Chem.* **2011**, *76*, 2338. (i) Yu, D.-G.; Shi, Z.-J. *Angew. Chem., Int. Ed.* **2011**, *50*, 7097. For reactions using a ferrocenyl bisphosphine ligand, see: (j) Kuwano, R.; Shimizu, R. *Chem. Lett.* **2011**, *40*, 913.
- 8 Ni/N-heterocyclic carbene catalyzed aromatic C–O bond transformation: For C–O amination, see: (a) Tobisu, M.; Shimasaki, T.; Chatani, N. *Chem. Lett.* **2009**, *38*, 710. (b) Shimasaki, T.; Tobisu, M.; Chatani, N. *Angew. Chem., Int. Ed.* **2010**, *49*, 2929. (c) Ramgren, S. D.; Silberstein, A. L.; Yang, Y.; Garg, N. K. *Angew. Chem., Int. Ed.* **2011**, *50*, 2171. (d) Mesganaw, T.; Silberstein, A. L.; Ramgren, S. D.; Fine Nathel, N. F.; Hong, X.; Liu, P.; Garg, N. K. *Chem. Sci.* **2011**, *2*, 1766. For C–O reduction with H₂, see: (e) Sergeev, A. G.; Hartwig, J. F. *Science* **2011**, *332*, 439.
- 9 (a) Abla, M.; Yamamoto, T. *J. Organomet. Chem.* **1997**, *532*, 267. (b) Garcia, J. J.; Brunkan, N. M.; Jones, W. D. *J. Am. Chem. Soc.* **2002**, *124*, 9547. (c) Nakao, Y.; Oda, S.; Hiyama, T. *J. Am. Chem. Soc.* **2004**, *126*, 13904. (d) Nakao, Y.; Yada, A.; Ebata, S.; Hiyama, T. *J. Am. Chem. Soc.* **2007**, *129*, 2428.

- 10 For isolation, see: (a) Dominguez, X. A.; de la Fuente, G.; Gonzalez, A. G.; Reina, M.; Timon, I. *Heterocycles* **1988**, *27*, 35. For synthesis, see: (b) Ciddens, A. C.; Boshoff, H. I. M.; Franzblau, S. G.; Barry, C. E.; Copp, B. R. *Tetrahedron Lett.* **2005**, *46*, 7355. (c) Besselievre, F.; Mahuteau-Betzer, F.; Grierson, D. S.; Piguel, S. *J. Org. Chem.* **2008**, *73*, 3278.
- 11 For isolation, see: (a) Cheplogoi, P.; Mulholland, D.; Coombes, P.; Randrianarivelojosia, M. *Phytochemistry* **2008**, *69*, 1384. For synthesis, see: (b) Besselievre, F.; Lebrequier, S.; Mahuteau-Betzer, F.; Piguel, S. *Synthesis* **2009**, 3511.
- 12 For selected recent examples, see: (a) Seiple, I. B.; Su, S.; Rodriguez, R. A.; Gianatassio, R.; Fujiwara, Y.; Sobel, A. L.; Baran, P. S. *J. Am. Chem. Soc.* **2010**, *132*, 13194. (b) Tang, P.; Furuya, T.; Ritter, T. *J. Am. Chem. Soc.* **2010**, *132*, 12150. (c) Fujiwara, Y.; Domingo, V.; Seiple, I. B.; Gianatassio, R.; Bel, M. D.; Baran, P. S. *J. Am. Chem. Soc.* **2011**, *133*, 3292.
- 13 The reaction employing quinine pivalate did not provide the coupling product.
- 14 Nett, M.; Erol, Ö.; Kehraus, S.; Köck, M.; Krick, A.; Eguereva, E.; Neu, E.; König, G. M. *Angew. Chem., Int. Ed.* **2006**, *45*, 3863.
- 15 Linder, J. R.; Moody, C. J. *Chem. Commun.* **2007**, 1508.
- 16 (a) Linder, J.; Blake, A. J.; Moody, C. J. *Org. Biomol. Chem.* **2008**, *6*, 3908. (b) Zhang, J.; Ciufolini, M. A. *Org. Lett.* **2009**, *11*, 2389.
- 17 After this work, Ni-catalyzed intramolecular C–H/C–O coupling as well as Co-catalyzed C–H/C–O coupling were reported by Kalyani and Ackermann, respectively. See: (a) Wang, J.; Ferguson, D. M.; Kalyani, D. *Tetrahedron* **2013**, *69*, 5780. (b) Song, W.; Ackermann, L. *Angew. Chem., Int. Ed.* **2012**, *51*, 8251. (c) Moselage, M.; Sauermann, N.; Richter, S. C.; Ackermann, L. *Angew. Chem., Int. Ed.* **2015**, *54*, 6352.
- 18 Preparation of **1**, For **1B**: (a) Cho, S. H.; Kim, J. Y.; Lee, S. Y.; Chang, S. *Angew. Chem., Int. Ed.* **2009**, *48*, 9127. For **1I**: (b) Parisien, M.; Valette, D.; Fagnou, K. J. *Org. Chem.* **2005**, *70*, 7578.
- 19 Lee, J. J.; Kim, J.; Jun, Y. M.; Lee, B. M.; Kim, B. H. *Tetrahedron* **2009**, *65*, 8821.

- 20 Li, Y.; Xie, Y.; Zhang, R.; Jin, K.; Wang, X.; Duan, C. *J. Org. Chem.* **2011**, *76*, 5444.
- 21 Suzuki, M.; Iwasaki, T.; Miyoshi, M.; Okumura, K.; Matsumoto, K. *J. Org. Chem.* **1973**, *38*, 3571.
- 22 Reader, J. C.; Ellard, J. M.; Boffey, H.; Taylor, S.; Carr, A. D.; Cherry, M.; Wilson, M.; Owoare, R. B. PCT. Int. Appl. WO2008/139161
- 23 For preparation of **2**: For **carbamate-2a**: (a) Li, B.-J.; Xu, L.; Wu, Z.-H.; Guan, B.-T.; Sun, C.-L.; Wang, B.-Q.; Shi, Z. *J. Am. Chem. Soc.* **2009**, *131*, 14656. For **Ts-2a**: (b) Ogata, T.; Hartwig, J. F. *J. Am. Chem. Soc.* **2008**, *130*, 13848. For **Ms-2a**: (c) Wilson, D. A.; Wilson, C. J.; Moldoveanu, C.; Resmerita, A.-M.; Corcoran, P.; Hoang, L. M.; Rosen, B. M.; Percec, V. *J. Am. Chem. Soc.* **2010**, *132*, 1800.
- 24 For **Tf-2a**: Neuville, L.; Bigot, A.; Dau, M. E. T. H.; Zhu, J. *J. Org. Chem.* **1999**, *64*, 7638.
- 25 For **2j**: Lee, D.-Y.; Hartwig, J. F. *Org. Lett.* **2005**, *7*, 1169.
- 26 For **2k**: Echavarren, A. M.; Stille, J. K. *J. Am. Chem. Soc.* **1987**, *109*, 5478.
- 27 For **2l**: Gill, D.; Hester, A. J.; Lloyd-Jones, G. C. *Org. Biomol. Chem.* **2004**, *2*, 2547.
- 28 Kowalski, C. J.; Haque, M. S. *J. Am. Chem. Soc.* **1986**, *108*, 1325.
- 29 Tan, S. T.; Fan, W. Y. *Eur. J. Inorg. Chem.* **2010**, 4631.
- 30 Compounds data of **3**: For **3Ab**: (a) Do, H.-Q.; Daugulis, O. *J. Am. Chem. Soc.* **2007**, *129*, 12404. For **3Ac**: (b) Hachiya, H.; Hirano, K.; Satoh, T.; Miura, M. *Org. Lett.* **2009**, *11*, 1737. For **3Ad**: (c) Evindar, G.; Batey, R. A. *J. Org. Chem.* **2006**, *71*, 1802. For **3Ai**, **3Ak** and **3Al**: (d) Kawashita, Y.; Nakamichi, N.; Kawabata, H.; Hayashi, M. *Org. Lett.* **2003**, *5*, 3713. For **3Aj**: (e) Johnson, S. M.; Connelly, S.; Wilson, I. A.; Kelly, J. W. *J. Med. Chem.* **2008**, *51*, 260. For **3Ba**: (f) Barbero, N.; Carril, M.; SanMartin, R.; Domínguez, E. *Tetrahedron* **2007**, *63*, 10425. For **3Ar**: (g) Derridj, F.; Djebbar, S.; Benali-Baitich, O.; Doucet, H. *J. Organomet. Chem.* **2008**, *693*, 135.
- 31 Chen, Y.-X.; Qian, L.-F.; Zhang, W.; Han, B. *Angew. Chem., Int. Ed.* **2008**, *47*, 9330.
- 32 Furuya, T.; Storm, A. E.; Ritter, T. *J. Am. Chem. Soc.* **2009**, *131*, 1662.

Mechanistic Studies of Nickel-Catalyzed C–H Arylation of Azoles with Phenol Derivatives

Abstract

Mechanistic studies of the Ni-catalyzed C–H arylation of 1,3-azoles with phenol derivatives (C–H/C–O coupling) are discussed. Combined experimental and computational studies not only support a catalytic cycle consisting of C–O oxidative addition, C–H nickelation, and reductive elimination, but also provide significant insight into dramatic ligand and base effects in the C–H/C–O coupling. This chapter contains the first synthesis, isolation and characterization of an arylnickel(II) pivalate, which is an intermediate in the catalytic cycle after the oxidative addition of a C–O bond. Kinetic studies and kinetic isotope effect investigations revealed that the C–H nickelation is the turnover-limiting step in the catalytic cycle. Furthermore, theoretical calculations unveiled a key role of base especially on the C–H nickelation step where Cs_2CO_3 forms a Cs–Ni cluster to facilitate C–H cleavage.

1. Introduction

Invention, understanding, and utilization of a new mode of inert bond activation by transition-metal catalysts offer great opportunities in organic synthesis. In particular, when coupled with strategic synthetic approaches, the activation of ubiquitous and inert bonds such as C–H and C–O bonds can lead to an unconventional, streamlined method for assembling molecules.^[1] In parallel to experimental screening for optimizing reaction conditions, mechanistic studies such as kinetic analysis, isolation and reaction of a possible intermediates, and computational analysis are crucial for the rational design of catalysts, conditions, and new transformations.^[2]

As mentioned in Chapter 3, C–H/C–O coupling of 1,3-azoles and phenol derivatives, promoted by catalytic amount of Ni(cod)₂/dcype (dcype: 1,2-bis(dicyclohexylphosphino)ethane) and Cs₂CO₃, was developed. In this reaction, the use of dcype was essential, as reputed ligands for C–M/C–O coupling such as PCy₃ and *N*-heterocyclic carbene (NHC) were totally ineffective.^[3] This reaction was developed based on a mechanistic blueprint of a Ni(0)/Ni(II) redox catalytic cycle (Figure 1) consisting of (i) C–O bond oxidative addition of a phenol derivative (Ar–OR) to Ni(0) **A** to form Ar–Ni(II)–OR complex **B**, (ii) C–H nickelation of an azole (Az–H) to produce Ar–Ni(II)–Az complex **C**, and (iii) reductive elimination to release the coupling product (Ar–Az) with regeneration of Ni(0) species **A**. However, there was no evidence for this pathway at the time when the reaction was developed. Moreover, it was difficult to provide any rationale explanation for the dramatic ligand effects in the C–H/C–O coupling.

In this chapter, mechanistic studies of the Ni/dcype-catalyzed C–H/C–O coupling of 1,3-azoles and phenol derivatives are discussed. These studies were conducted by combined experimental and computational analyses, including the isolation of a possible catalytic intermediate, kinetic studies, and density functional theory (DFT) studies. To this end, the synthesis of an Ar–Ni(II)–OR complex, which is a proposed intermediate in the Ni(0)/Ni(II) redox catalytic cycle, was attempted. Moreover, stoichiometric reaction of a 1,3-azole with this Ni(II) complex, and kinetic investigations by using *in situ* FTIR elucidated the effect of dcype. Besides these experimental studies, DFT studies were conducted to reveal the effect of Cs₂CO₃ especially on the C–H nickelation step.

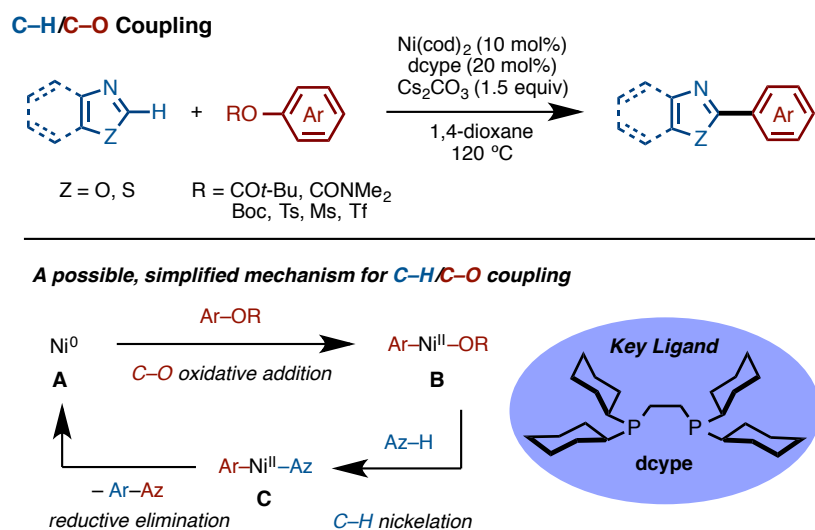


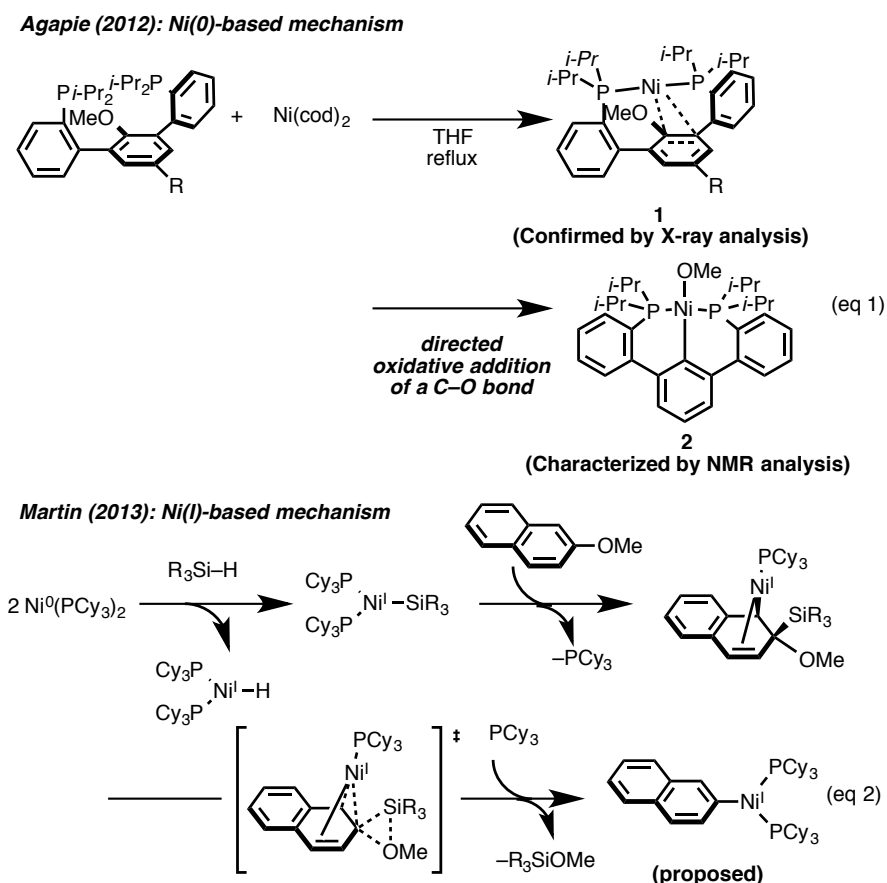
Figure 1. Heterobiaryl-forming C–H/C–O coupling catalyzed by Ni/dcype

2. Results and Discussions

2-1. C–O Oxidative Addition: Experimental Mechanistic Study

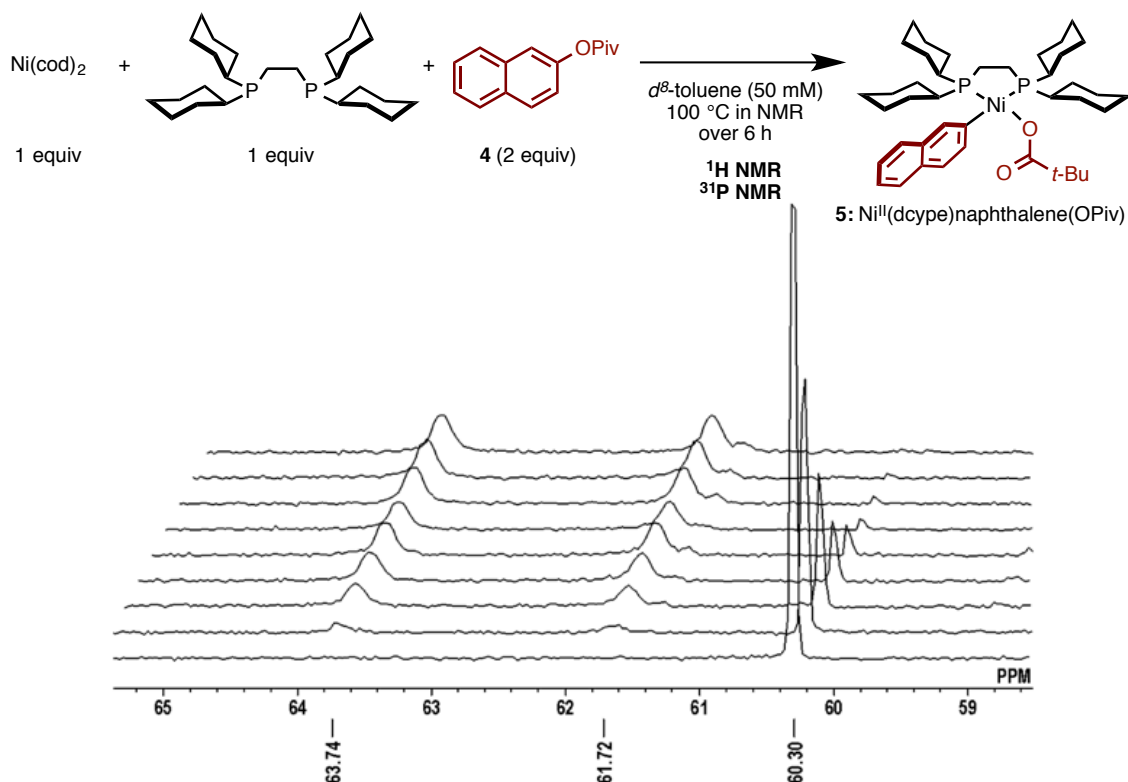
In the proposed catalytic cycle, Ar–Ni(II)–OR would be generated from an oxidative addition of an aromatic C–O bond to a Ni(0) species. Although this type of intermediate has been also proposed in the Ni-catalyzed C–M/C–O coupling reaction of arylboronic acids and phenol derivatives, the support for the C–O bond oxidative addition has remained inadequate (Scheme 1).^[4,5] Agapie and co-workers reported the ¹H NMR characterization of Ar–Ni(II)–OMe species **2**, which was generated from nickel complex **1** (formed by mixing a pincer-type ligand with Ni(cod)₂; eq 1).^[6] Their DFT calculations also supported a mechanistic hypothesis wherein Ni-catalyzed C–M/C–O coupling proceeds via oxidative addition of an aromatic C–O bond to Ni(0) producing an Ar–Ni(II)–OR species. In contrast, Martin reported an interesting oxidative addition mechanism that proceeds through a Ni(I) species in their combined experimental and computational mechanistic studies on C–OMe bond reduction using catalytic Ni/PCy₃ and hydrosilanes as reducing agents (eq 2).^[7] Meanwhile, C–O oxidative addition has also been studied by using other transition metals such as ruthenium and rhodium.^[8] In the case of ruthenium, Kakiuchi and co-workers successfully prepared ruthenium complex by oxidative addition of aryl ethers (bearing an *ortho*-directing group) to RuH₂(CO)(PPh₃)₃, and obtained an X-ray crystal structure of a species resembling in **1**.^[8a] For rhodium, the group of Ozerov also observed the oxidative addition of an

aromatic C–O bond to a rhodium pincer complex and characterized by X-ray analysis, a rhodium complex that has undergone C–O oxidative addition.^[8b] Herein, the first synthesis of an Ar–Ni(II)–OR species with dcype ligand is described and the reactivity of this species is investigated.



Scheme 1. Previous studies on the oxidative addition of aromatic C–O bonds

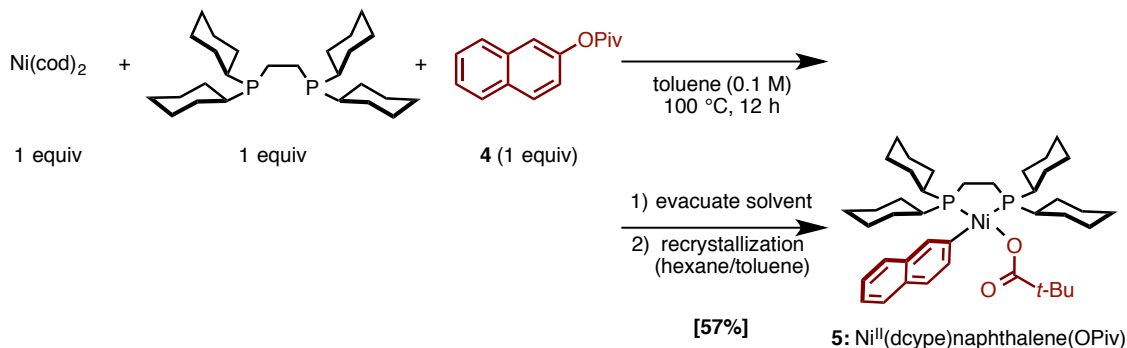
The author began by monitoring the stoichiometric reaction of naphthalen-2-yl pivalate (**4**) with Ni(cod)₂/dcype using ³¹P NMR spectroscopy to identify the C–O oxidative addition intermediate. The reaction did not proceed at room temperature. When the reaction temperature was elevated to 100 °C, two new downfield peaks (δ = 63.7 and 61.7 ppm) appeared along with the signal for the Ni(cod)₂/dcype complex (δ = 60.3 ppm) (Scheme 2). As two phosphorus atoms are in different chemical environments in complex **5**, it was postulated that the aromatic C–O bond underwent oxidative addition. Additionally, the fact that the NMR spectra are displayed with clarity suggested that the reaction does not generate a paramagnetic Ni(I) species.



Scheme 2. ^{31}P NMR monitoring of the oxidative addition of **4** to $\text{Ni}(\text{cod})_2/\text{dcype}$.

Encouraged by this result, isolation of the presumed nickel complex was attempted (Scheme 3). After the stoichiometric reaction, the solvent was completely removed to afford a crude orange solid. The resulting solid was recrystallized from toluene/hexane to give orange crystals in 57% isolated yield. The structure of this mononuclear Ni(II) complex **5** (C–O oxidative addition complex) was unambiguously confirmed by X-ray crystallographic analysis.^[9] The X-ray crystal structure showed that the nickel atom is in a square-planar geometry surrounded by two phosphorus, a carbon, and an oxygen atom (Figure 2). The dcype ligand is indeed coordinated to the nickel atom in a *cis*-configuration. Most importantly, nickel complex **5** not only matches our proposed intermediate **B**, but also represents the first isolation and characterization of an Ar–Ni(II)–OR species via the oxidative addition of an aromatic C–O bond to a Ni(0) species. It should also be noted that virtually no decomposition of nickel complex **5** has been detected after extended (>3 months) exposure to air, indicating the effect of dcype in the stability of nickel complexes. Though stable in solid state, complex **5** gradually

decomposes in solution when exposed to an atmosphere of air.



Scheme 3. Procedure for the synthesis of Ni(II) complex **5**

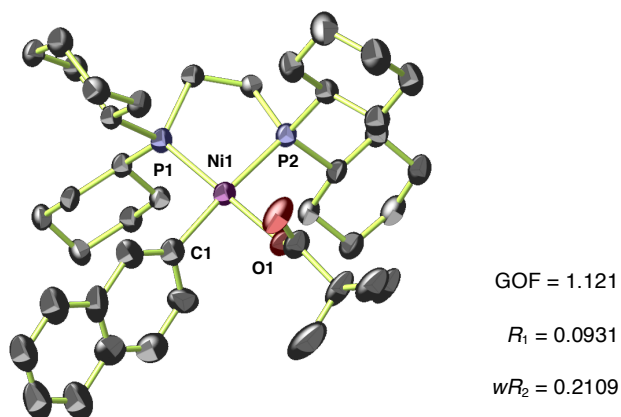
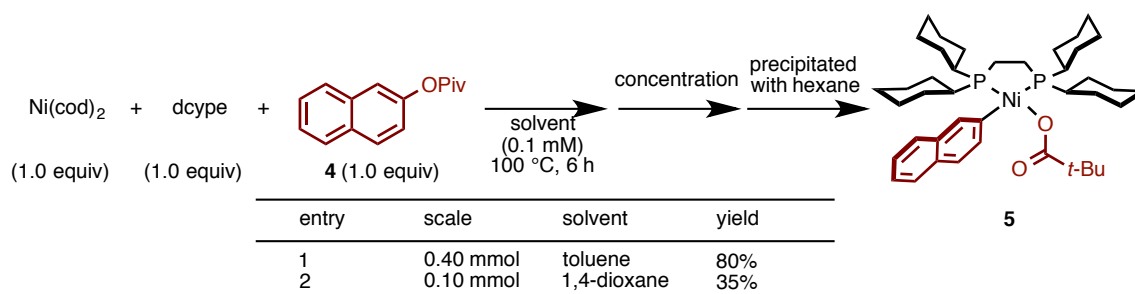


Figure 2. ORTEP drawing of one of two independent molecules of **5**. Hydrogen atoms are omitted for clarity; thermal ellipsoids are drawn at 50% probability. Selected bond lengths (Å) and angles (deg): Ni1–C1 = 1.940(6), Ni1–O1 = 1.919(4), Ni–P1 = 2.1401(16), Ni1–P2 = 2.2192(17), P1–Ni1–P2 = 88.56(8), P1–Ni1–C1 = 91.85(18), C1–Ni1–O1 = 88.8(2), O1–Ni1–P2 = 89.89(13), P1–Ni1–O1 = 175.10(14), P2–Ni1–C1 = 168.9(2).

To improve the reaction yield of **5**, the isolation method was modified from recrystallization to precipitation without a decrease in purity (80% yield; Scheme 4, entry 1). 1,4-Dioxane, which is the best solvent for the Ni-catalyzed C–H/C–O coupling reaction, also turned out to be a usable solvent for the synthesis of **5**, albeit in lower yield (35% yield, entry 2).



Scheme 4. Optimization of the synthetic procedure for Ni(II) complex **5**

When studying applicable solvents for the oxidative addition of **4** to $\text{Ni}(\text{cod})_2/\text{dcype}$, an interesting phenomenon was observed. When the reaction rate was examined using a variety of solvents, it was unexpectedly found that the reaction in *t*-AmylOH was faster than the reaction in other solvents, such as toluene and 1,4-dioxane (Figure 3).

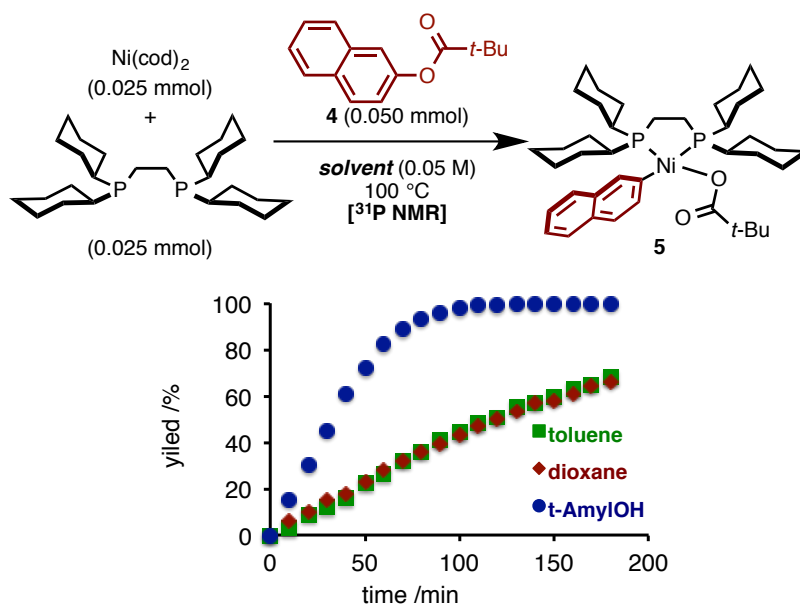


Figure 3. Comparison of reaction rate between the reaction in *t*-AmylOH, toluene, and 1,4-dioxane

Judging from this result, it was hypothesized that the proton of *t*-AmylOH can activate a C–O electrophile toward the oxidative addition. In order to confirm this hypothesis, solvent kinetic isotope effect (solvent KIE) was evaluated by using *t*-BuOH and *t*-BuOD as solvents (Figure 4). Surprisingly, a significant inverse kinetic isotope effect was obtained ($k_{\text{H}}/k_{\text{D}} = 0.29$).

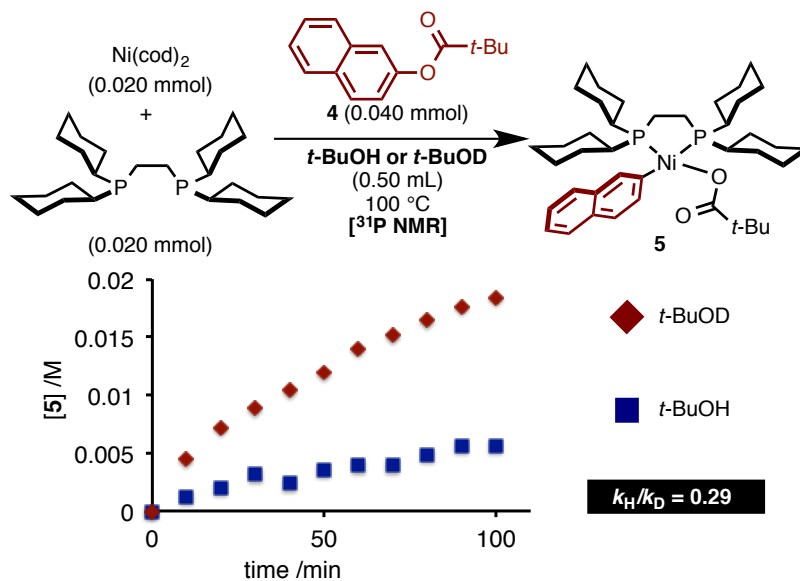


Figure 4. Investigation of solvent KIE

The obtained solvent KIE value suggested that a proton of a tertiary solvent can coordinate to a C–O electrophile (Figure 5). At this stage, it is unclear how many solvent molecules can coordinate to the C–O electrophile. However, it can be anticipated that this alcohol-mediated C–O bond activation mode will provide numerous opportunities to design new transformations of inert C–O bonds such as Ar–OMe bonds.

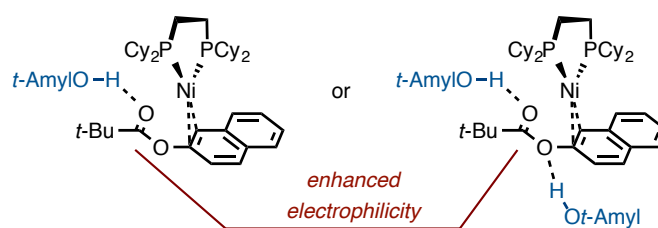
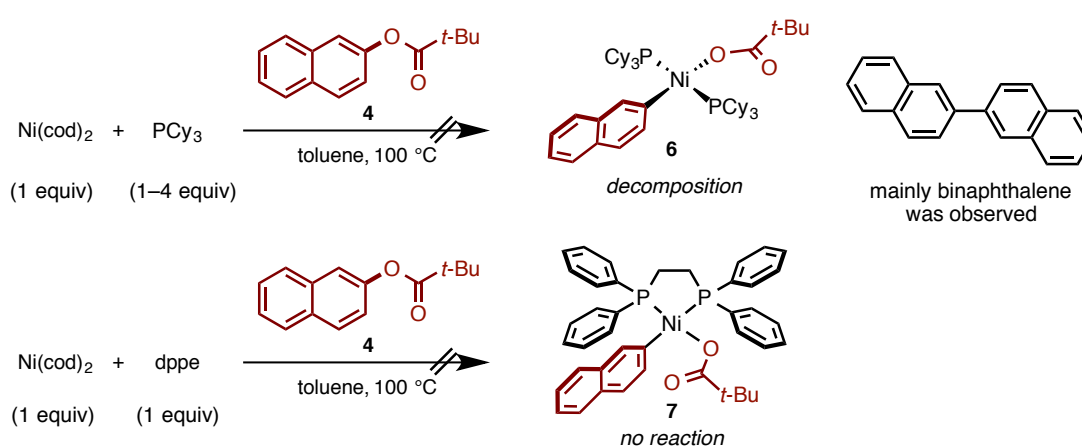


Figure 5. Postulated effect of the tertiary alcohol

2-2. Attempts for the Synthesis of Other Ar–Ni–OPiv Complexes as a Comparison with Ni(dcype)naphthalene(OPiv)

Synthesis and isolation of other Ar–Ni(II)–OPiv species were attempted in order to compare the reactivity between dcype and other ligands (Scheme 5). As reference ligands in this study, PCy₃ and dppe (1,2-diphenylphosphinoethane), which do not

promote catalytic C–H/C–O coupling,^[3] were chosen. When PCy₃ (known as a useful ligand for Ni-catalyzed C–M/C–O coupling reaction) was employed, the corresponding oxidative addition complex **6** was not isolated. Instead, the reaction afforded 2,2'-binaphthyl, which is likely generated by disproportionation of **6** similarly to the production of biaryl from Ar–Ni–X (X = halogen).^[10] In the case of the reaction using dppe, oxidative addition complex **7** was not observed and **4** remained almost unchanged.



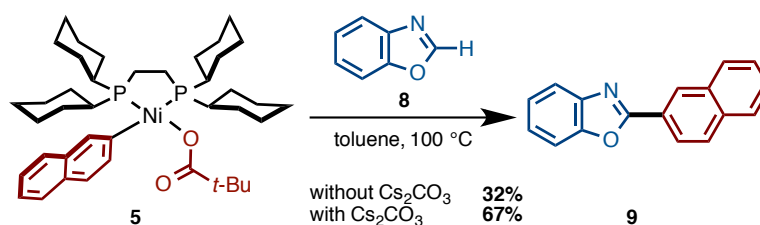
Scheme 5. Attempts for the isolation of Ar–Ni^{II}–OPiv species **6** and **7**

According to these results, the dcype ligand might be playing two roles in the oxidative addition of aryl C–O bonds as well as in the catalytic reaction. The first is that the electron-donating cyclohexyl moieties on the phosphorus atoms help increase the electron density of the Ni(0) center to facilitate the C–O oxidative addition. The other is that the bidentate structure of dcype could stabilize the generated Ar–Ni(II)–OR species after the oxidative addition.

2-3. Stoichiometric Reaction of Benzoxazole (**8**) with Ni(II) Complex A

With plausible oxidative addition intermediate **5** in hand, a stoichiometric reaction of **5** and benzoxazole (**8**) was next examined to support a plausible intermediate in the catalytic cycle of the C–H/C–O coupling reaction (Scheme 6). The reaction of **8** with **5** in toluene at 100 °C furnished the desired product **9** in 32% yield. The reaction yield was improved by the addition of Cs₂CO₃ (1.0 equiv), resulting in the generation of **9** in 67% yield. These results suggest that nickel complex **5** is likely involved in the catalytic

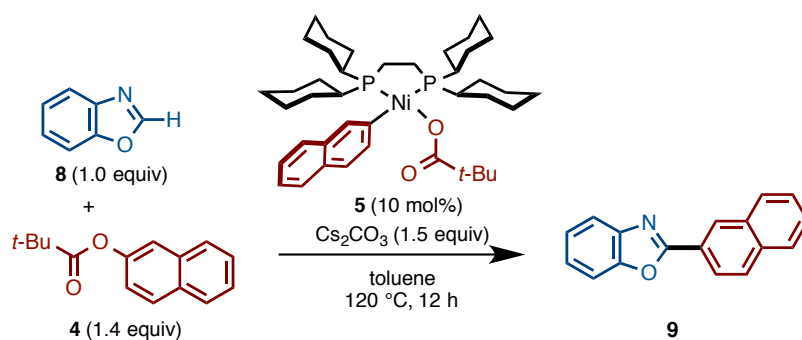
cycle. Although it is difficult to observe the assumed diarylnickel(II) intermediate (C: Ar–Ni(II)–Az), it is postulated that product **9** is formed via C–H nickelation, followed by reductive elimination (Figure 1). The product generation in the absence of the base indicates that the C–H nickelation pathway from **5** would take place through a concerted metalation-deprotonation (CMD) mechanism.^[11] It is envisaged that the rate acceleration by Cs₂CO₃ in the C–H nickelation step might arise from the generation of a more active nickel catalytic intermediate, Ar–Ni(II)–OCO₂Cs, via ligand exchange from pivaloyl (OPiv) to carbonate (OCO₂Cs). However, further investigation is needed to prove this particular step (*vide infra*).



Scheme 6. Stoichiometric reaction between **8** and **5**

2-3. Application of Nickel complex A to Catalytic C–H/C–O Coupling

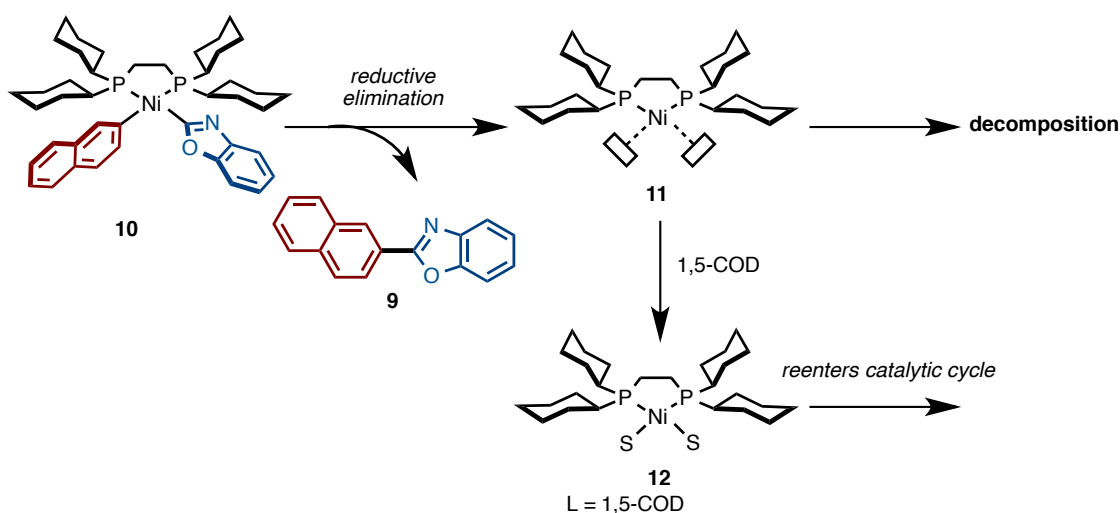
As part of these studies investigating the reactivity of oxidative addition complex **5**, a C–H/C–O coupling using nickel complex **5** as a catalyst was examined (Scheme 7). Although the C–H/C–O coupling of **8** and **4** proceeded in toluene when using **5** as a catalyst, the coupling reaction did not proceed well and afforded the corresponding coupling product **9** in only 8% yield. This result indicates that the product was likely formed much like the stoichiometric reaction shown in Scheme 6, but the regenerated Ni(0) species decomposed under the reaction conditions. With the assumption that some additional ligands exist in the catalytic reaction to prevent the decomposition or aggregation of Ni(0), catalytic amount of 1,5-COD, which is present in the optimal catalytic conditions as shown in Figure 1, was added into the reaction using **5**. Indeed, the product yield was much improved by adding 10 mol% of 1,5-COD (70% yield).



entry	variation	yield
1	none	8%
2	added 1,5-cod (10 mol%)	70%

Scheme 7. C–H/C–O coupling using nickel complex **5** as catalyst

These results illustrate that coordinatively unsaturated Ni(0) species **11**, which is regenerated after the reductive elimination, might be unstable, and it can be inactivated (aggregated) prior to the oxidative addition of naphthalen-2-yl pivalate (**4**) to Ni (Scheme 8). In order to prevent this catalyst decomposition, it is likely that 1,5-COD plays a key role in the catalytic cycle as Ni(0)-stabilizing ligand.



Scheme 8. Effect of 1,5-COD after the reductive elimination step

2-4. Kinetic Studies for the Ni-Catalyzed C–H/C–O Coupling Reaction

Based on the catalytic cycle shown in Figure 1, kinetic studies by *in situ* FTIR (react IR) were conducted to gain further insight into the reaction mechanism. Revealing the rate-determining step of the C–H/C–O coupling would help design an optimal ligand

and control the reaction conditions.

Initially, the Ni-catalyzed C–H/C–O coupling reaction between benzoxazole (**8**) and naphthalen-2-yl pivalate (**4**; 1.5 equiv) under the standard conditions was monitored by *in situ* FTIR for 8 h (Figure 6). The product was detected as a peak at 824 cm⁻¹. While a gradual acceleration of the reaction rate was observed, the yield was low (11% yield) after 2 h (Table 2, entry 1). When non-dried Cs₂CO₃ was used, the yield slightly increased (35% yield).

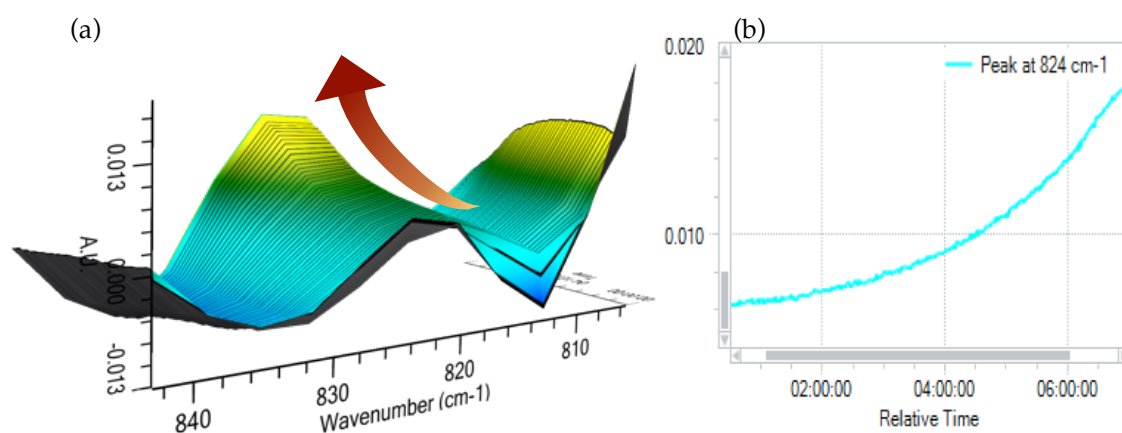
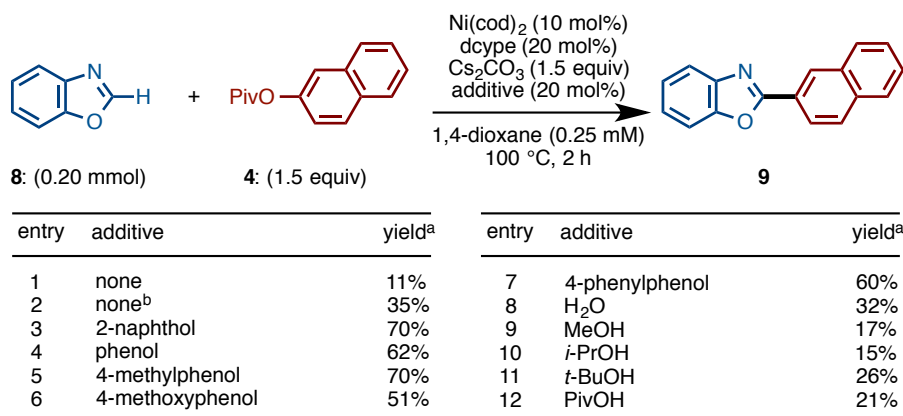


Figure 6. (a) Product peak at 824 cm⁻¹ observed by *in situ* FTIR;
(b) Area of peak at 824 cm⁻¹

After investigation of the reaction profiles, it was concluded that 2-naphthol might be produced as a byproduct from **4** under the reaction conditions and play a role in accelerating the reaction rate. Therefore, 20 mol% of 2-naphthol was added to the standard conditions, after which the reaction afforded the desired coupling product **9** in 70% yield after 2 h (Table 1, entry 3). Similarly, several phenol derivatives were also effective and afforded **9** in 51–70% yield (entries 3–7). Finally, the use of 20 mol% of 2-naphthol as an additive was taken as the optimal conditions for *in situ* FTIR experiments although its accelerating effect is still unclear.

Table 1. Additive effects on the Ni-catalyzed C–H/C–O coupling of **8** and **4**

[a] GC yield [b] Non-dried Cs₂CO₃ was used.

With these optimized reaction conditions in hand, kinetic studies with *in situ* FTIR were conducted to gain further insight into the mechanism of the C–H/C–O coupling. The results obtained by observing the initial rate of reaction, are summarized in Figure 7. The kinetic profile for **4** demonstrated that the reaction rate of C–H/C–O coupling of **8** with **4** is zero-order in [**4**]. In contrast to [**4**], first-order kinetic profiles were observed for both [**8**] and [Ni(cod)₂/dcype]. The kinetic profiles for each substrate suggest that the turnover-limiting step of this Ni-catalyzed reaction is the C–H nickelation step. Furthermore, it was found that the active catalyst is a monometallic nickel species because a first-order dependence on the amount of catalyst was observed.

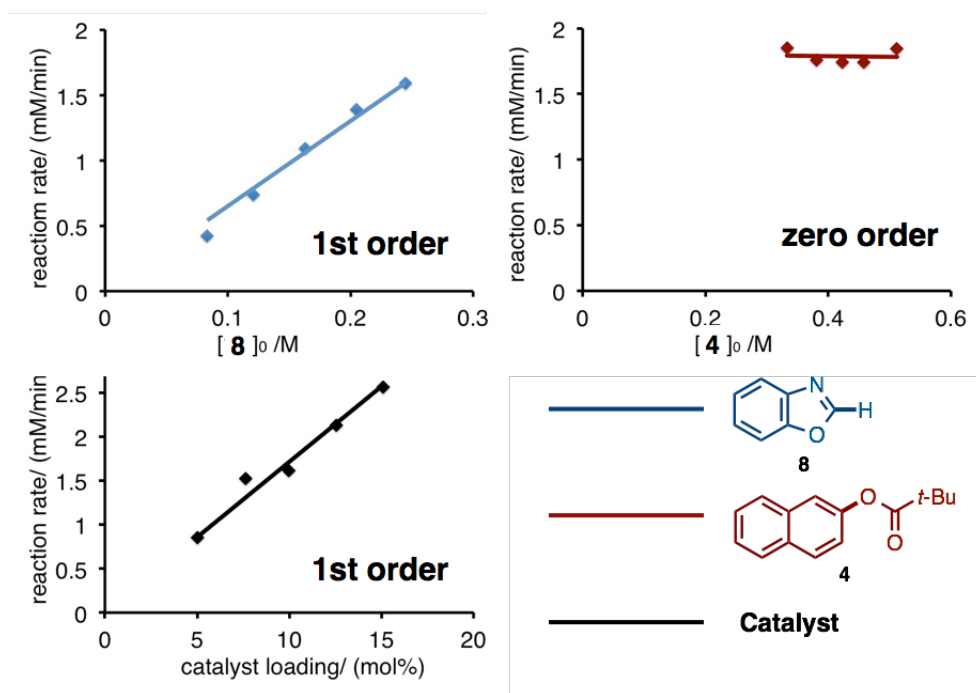


Figure 7. Kinetic profiles for the Ni-catalyzed C–H/C–O coupling

Kinetic isotope effect (KIE) experiments were also carried out using the reaction of **4** with **8** and its C2-deuterated derivative (**D-8**) under optimized conditions (Figure 8).^[12] Since an initial KIE was observed ($k_H/k_D = 2.4$), it is likely that the C–H nickelation (C–H cleavage) of 1,3-azole is the rate-determining step in the catalytic reaction.

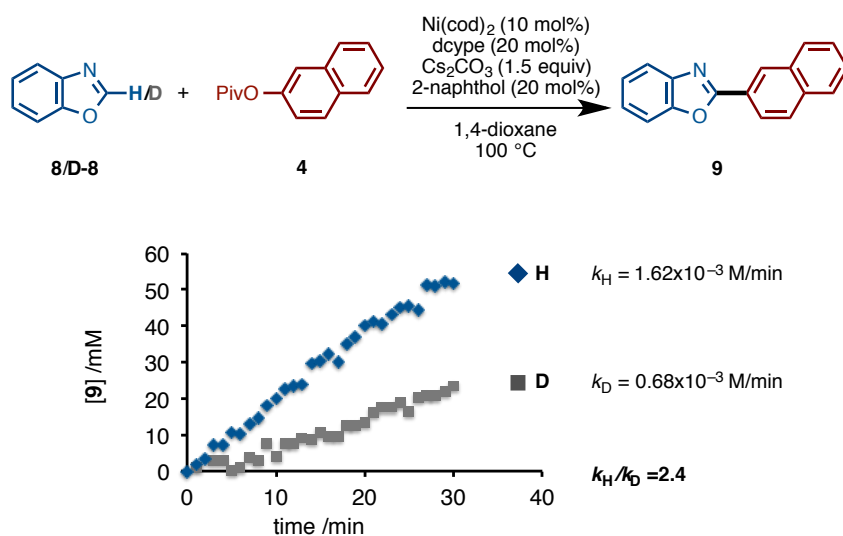
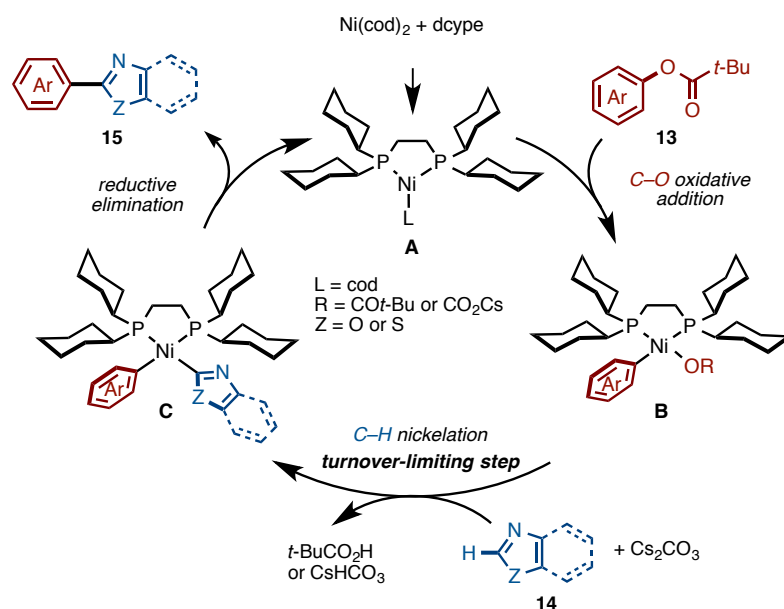


Figure 8. Investigation of KIE for the Ni-catalyzed coupling **8** and **4**

2-5. Possible Mechanism

Taking all these experimental data into consideration, the mechanism of the C–H/C–O coupling reaction is proposed in Scheme 9. The key Ni(0) species, L–Ni(0)-dcype (A) (L = cod), is firstly generated from Ni(cod)₂ and dcype. The dissociation of L would generate a coordinatively unsaturated Ni(0)-dcype complex, which undergoes the C–O oxidative addition of **13** to produce arylnickel(II) pivalate **B** (R = CO*t*-Bu). The turnover-limiting, Cs₂CO₃-accelerated C–H nickelation of **B** with azoles affords a diarylnickel(II) intermediate **C**. Finally, the coupling product **15** is produced by the reductive elimination of **C** and Ni(0)-dcype, which should be trapped by L for stabilization.



Scheme 9. Possible mechanism of C–H/C–O coupling

2-6. Computational Studies

As mentioned above, through experimental mechanistic studies, the catalytic cycle and the dcype ligand effect were successfully unveiled. Additionally, Houk and Fu independently reported computational studies on both Ni/dcype-catalyzed C–H/C–O coupling and decarbonylative C–H coupling reactions.^[13] In spite of these advances, several aspects of this C–H/C–O coupling reaction, especially those related to the nature of the C–H substrate and the role of base in the C–H/C–O coupling, remained unanswered. Thus, the next study was intended to elucidate in particular the effect of

base in the C–O oxidative addition and/or the C–H nickelation steps through combined experimental and theoretical studies.

2-7. Oxidative Addition: Computational Mechanistic Studies

The oxidative addition of a C–O bond to the Ni/dcype species was further studied by DFT calculations. At first, this study examined the oxidative addition of the C–O bond in the absence of base. The present catalytic reaction should be initiated by an active catalyst formation before the oxidative addition. The calculations showed that active catalyst formation would be exergonic by 12.5 kcal/mol (Scheme 10).^[14]



Scheme 10. The formation of the active catalyst before the oxidative addition

In the oxidative addition step, there are two possible pathways; one is a C(aryl)–O oxidative addition, and the other is a C(acyl)–O oxidative addition. However, the present C–H/C–O coupling can only proceed via C(aryl)–O oxidative addition. Factors affecting the selectivity of the C(aryl)–O and C(acyl)–O bond activation have been the subject of several recent investigations by others.^[5g,13] These calculations mostly agreed with previous studies but also provided slightly different results. Firstly, it was found that the C(acyl)–O bond cleavage proceeding via a three-centered transition state requires a 26.7 kcal/mol energy barrier and is endergonic by 11.4 kcal/mol (calculated relative to the reactants [Ni(cod)(dcype) + NaphOPiv]). Secondly, the C(aryl)–O oxidative addition occurring via the five-centered transition state **TS1** (Figure 9) requires a slightly higher (29.1 kcal/mol) energy barrier and leads to product **5**. However, the C(aryl)–O oxidative addition is found to be exergonic by 3.5 kcal/mol. Based on these findings, it was predicted that the C–O oxidative addition product resulting from the reaction of Ni(cod)(dcype) with **4** would be Ni(Naph)(OPiv)(dcype) **5**, which is a complex associated with the C(aryl)–O oxidative addition. This prediction is consistent with the experimental result showing that the reaction of Ni(cod)(dcype) with NaphOPiv leads to isolable and stable Ni(Naph)(OPiv)(dcype) product **5**.^[3] It

should be mentioned that the calculated geometry parameters of oxidative addition product **5** are well consistent with their experimental values.

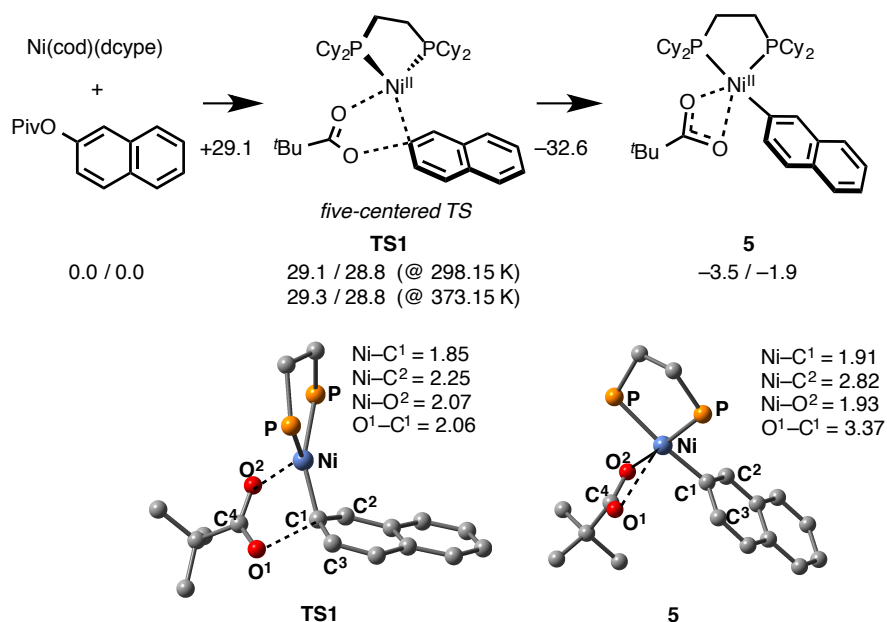


Figure 9. Important geometry parameters (in Å) and relative energies [in kcal/mol, relative to reactants Ni(cod)(dcype) plus NaphOPiv] of the lowest C(aryl)-O oxidative addition five-centered transition state and the corresponding oxidative addition product **5** (cyclohexyl groups and hydrogen atoms are omitted for clarity).

The actual catalytic C-H/C-O coupling was conducted in the presence of base, thus, it was also thought that the base can coordinate the resulting oxidative addition nickel complex **5**. This time, the limited computational data indicated that the C(aryl)-O oxidative addition of **4** to Ni(cod)(dcype) is a facile process in the presence of both Cs₂CO₃ and K₂CO₃. However, these computational studies have also indicated that it is difficult to conclude that the base effect is unrelated to the oxidative addition. Thus, experimental study was next examined as comprehensive approaches.

With the above aspects in mind, the influence of the base was examined by monitoring the oxidative addition of **4** to Ni(cod)₂/dcype in the presence and absence of Cs₂CO₃ and K₂CO₃ using ³¹P NMR. As depicted in Figure 10, the use of neither Cs₂CO₃ nor K₂CO₃ showed significant effect on the oxidative addition. Furthermore, it is worth noting that during the course of these reactions, only ³¹P NMR peaks derived from **5** and reactant Ni(cod)(dcype) were observed. These results indicate that C-O oxidative

additions are not affected by the base.

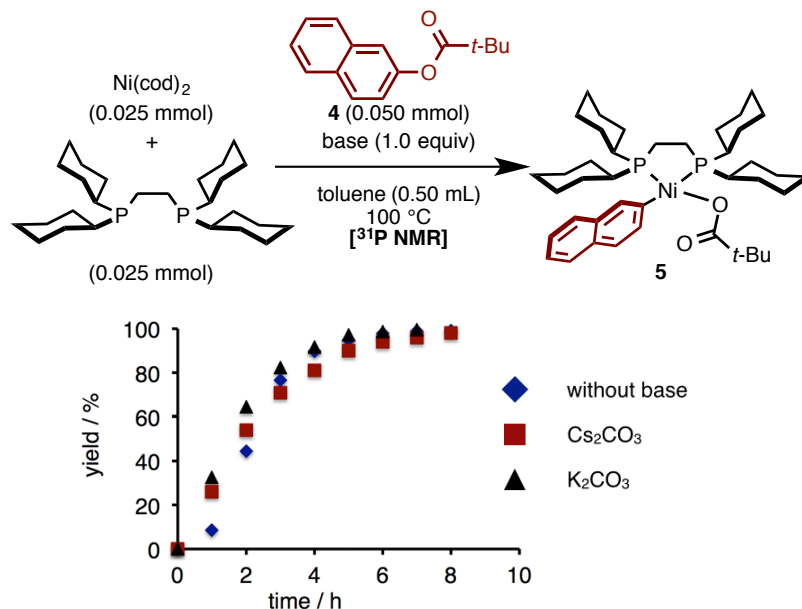


Figure 10. Monitoring the C–O oxidative addition of **4** to Ni(cod)(dcype) in the presence (black; K₂CO₃ and red; Cs₂CO₃) and absence (blue) of base.

2-8. C–H Nickelation: Computational Mechanistic Studies

As described in Section 2-3, the stoichiometric reaction of nickel complex **5** and benzoxazole (**8**) gave the coupling product **9**. The addition of Cs₂CO₃ resulted in the improvement of the reaction yield from 32% to 67% yield. Moreover, this time, the kinetic studies on this stoichiometric reaction in the presence and absence of base showed that the rate of the reaction with Cs₂CO₃ is three-fold faster than the reaction without base (Figure 11). This experimental finding indicates the involvement of base in the mechanism of the C–H nickelation step. Thus, in order to elucidate the mechanism of the C–H nickelation step as well as the role of the base in this particular step, studies were aimed to computationally investigate two discrete reactions of **4** with benzoxazole (**8**) in the presence and absence of Cs₂CO₃.

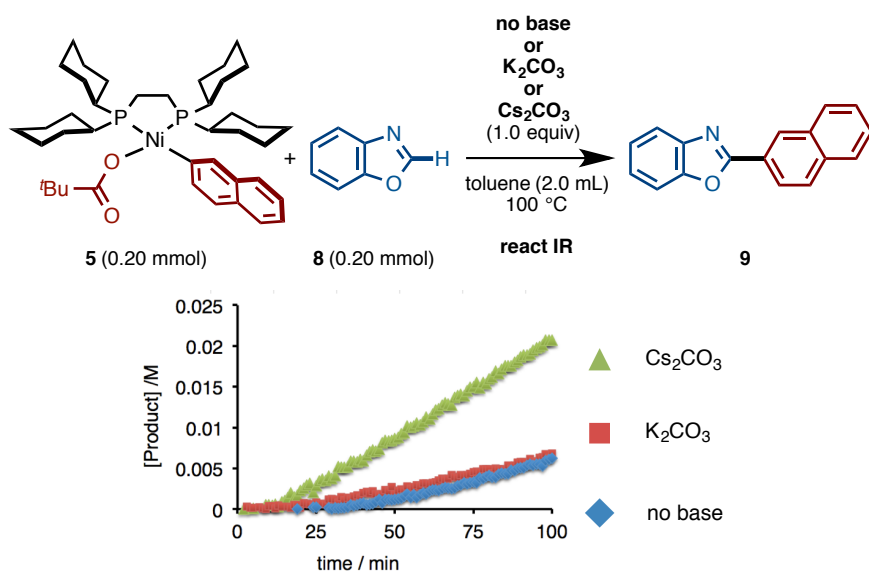


Figure 11. The kinetics of the stoichiometric reaction of **5** with benzoxazole (**8**) in the presence and absence of bases

2-9. C–H Nickelation Step in the Absence of Base: A Computational Study

The C–H nickelation step is expectedly triggered by coordination of benzoxazole (**8**) to nickel complex **5** after the oxidative addition. This coordination results in the formation of intermediate **16**, which lies 15.2 kcal/mol higher in free energy than the dissociation limit of **5** with azole (Figure 12). The following azole C–H nickelation step takes place to produce azole-Ni(II) species **17** through a typical concerted metalation/deprotonation (CMD) transition state **TS2**.^[11] The energy barrier required in this pathway is 31.0 kcal/mol. In order to find an energetically more favored pathway, the other possible pathway was studied. An “arm-off” mechanism, which is a process undergoing the formation of a coordinatively unsaturated nickel complex by the dissociation of one of two phosphorus atoms from the nickel center, was previously discussed in the literature^[13b,15]. However, it was found that the arm-off mechanism requires a higher activation barrier of 37.7 kcal/mol, therefore, this type of mechanism will be ruled out from further discussion.

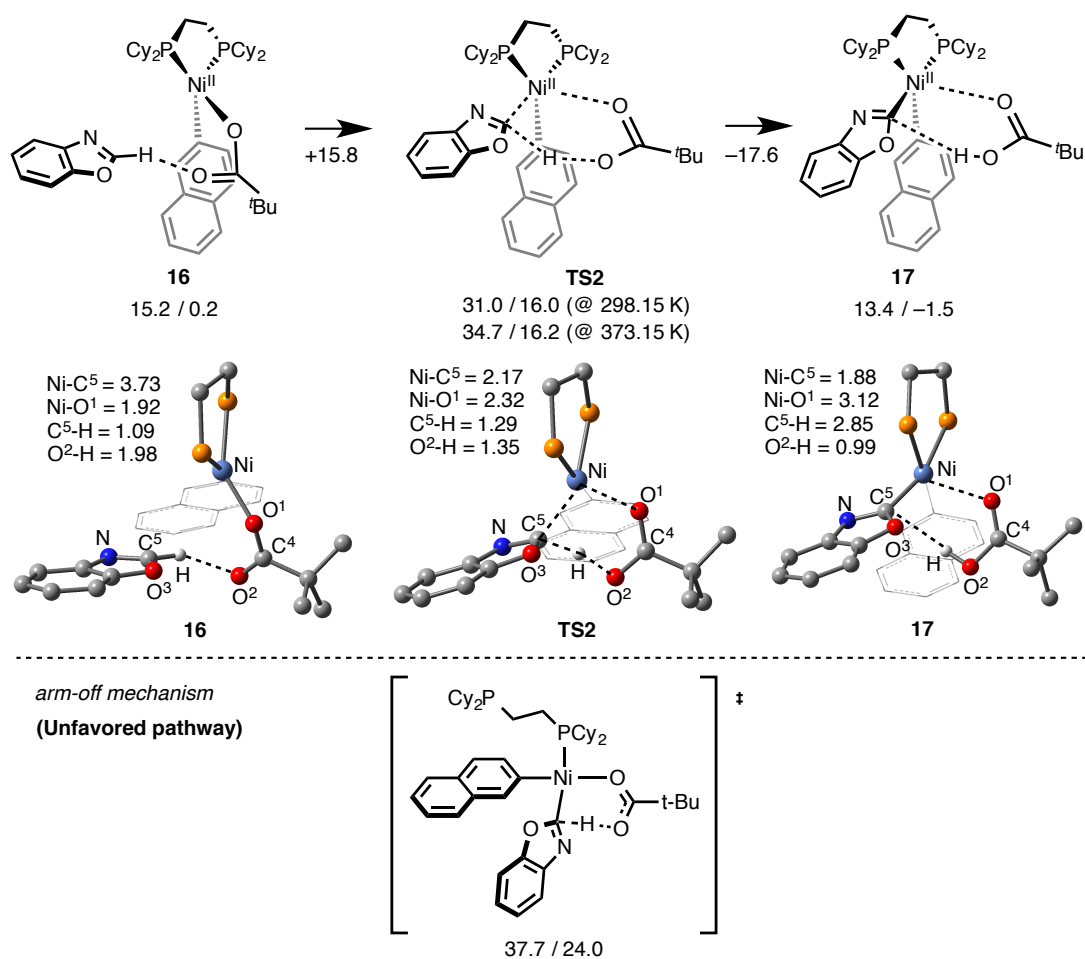


Figure 12. The mechanism of C–H nickelation in the absence of Cs₂CO₃ and relative energies of the transformation [in kcal/mol, relative to intermediate Ni(dcype)(Naph)(OPiv). left numbers show ΔG , and right numbers show ΔH]

The following reductive elimination was initiated by the dissociation of PivOH from **17**. The first step of the dissociation is exergonic by 4.5 kcal/mol, and the second reductive elimination requires only 9.1 kcal/mol of activation energy at transition state **TS3** (Figure 13).

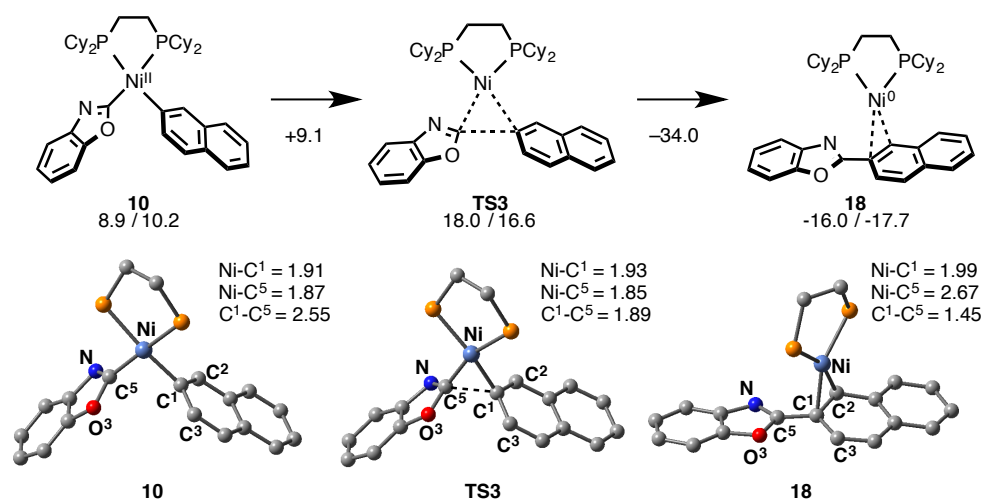


Figure 13. Mechanism of the reductive elimination and relative energies [in kcal/mol, relative to intermediate $\text{Ni}(\text{dcype})(\text{Naph})(\text{OPiv})$. left numbers show ΔG , and right numbers show ΔH]

Summarizing these computational data, Figure 14 illustrates the overall potential energy surface of the coupling reaction in the absence of base. As the reductive elimination requires a much smaller energy barrier, the former step of C–H nickelation is thought to be irreversible. Thus, the reaction of **5** with benzoxazole (**8**) in the absence of Cs_2CO_3 requires 31.0 kcal/mol of energy at transition state **TS2** of the C–H nickelation step. This conclusion is well in agreement with the experimentally reported high reaction temperature of 100–120 °C and the rate-determining C–H nickelation step.

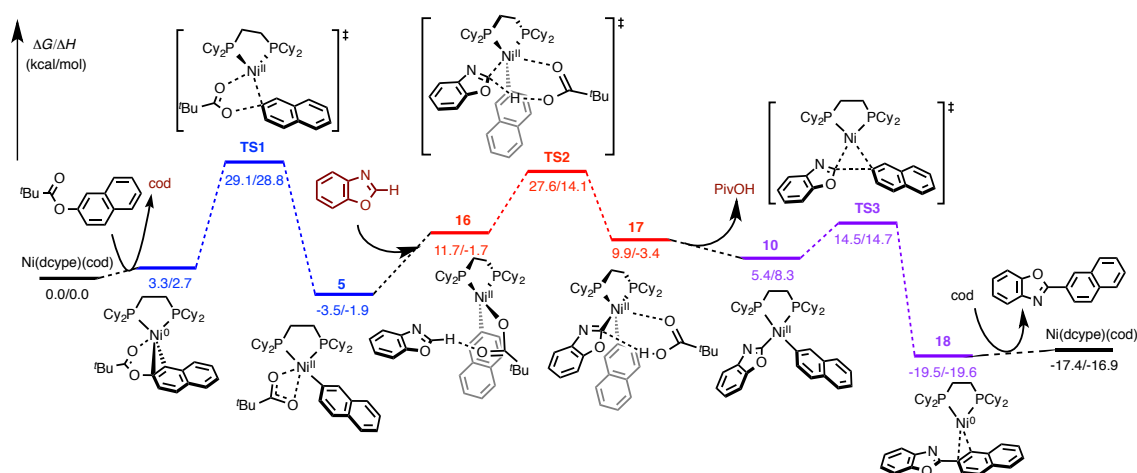


Figure 14. The overall potential energy surface

2-10. C–H Nickelation Step in the Presence of Base

Through computational studies, the C–H/C–O coupling of benzoxazole (**8**) and naphthalen-2-yl pivalate (**4**) was found to proceed via a CMD pathway in the C–H nickelation step with a 31.0 kcal/mol energy barrier. The following studies were aimed to investigate the reaction in the presence of Cs_2CO_3 . As mentioned already, it was experimentally revealed that this reaction, especially the C–H nickelation step, can be accelerated by the addition of Cs_2CO_3 .

The addition of Cs_2CO_3 into the reaction of nickel complex **5** with **8** was found to be exergonic by 9.7 kcal/mol and led to the formation of intermediate **1-Cs** (Figure 15). **1-Cs** is likely to be kinetically unstable and results in the generation of thermodynamically more favored intermediate **2-Cs** with a release of 30.3 kcal/mol of energy.

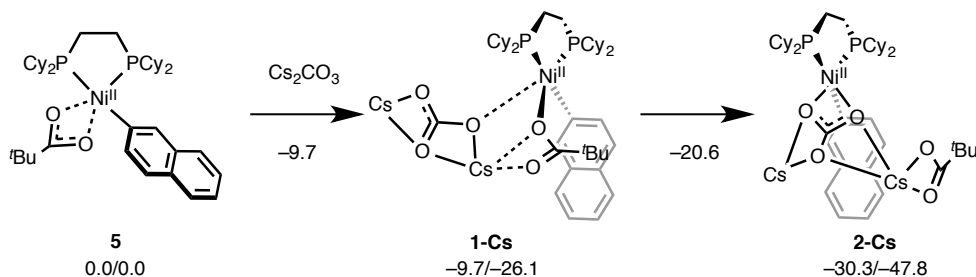


Figure 15. Computational studies of the reaction of intermediate **5** with Cs_2CO_3 , along with relative energies [in kcal/mol, relative to intermediate **5**. left number show ΔG , and right numbers show ΔH]

From resulting complex **2-Cs**, two different processes would be feasible. One can be named a “PivOCs dissociation pathway”, and another can be named an “isomerization pathway” (Figure 16). The PivOCs dissociation pathway starts with the elimination of the Cs–OPiv moiety from **2-Cs** to generate **3-Cs**. The formation of **3-Cs** is uphill from **2-Cs** by 10.2 kcal/mol. Next, the C–H nickelation event would proceed via two further kinds of possible pathways, in which the dcype ligand can coordinate to the nickel center bidentately and monodentately. However, both pathways require rather high activation barriers (35.3 and 37.9 kcal/mol, respectively). The obtained energy barriers are higher than that of the reaction in the absence of Cs_2CO_3 (31.0 kcal/mol). In contrast to this process, the calculations showed another possible pathway of isomerization from

2-Cs that can take place rather easily. In the isomerization pathway, **2-Cs** isomerizes to thermodynamically stable Cs-Ni cluster complex **3-Cs-Clus**. This transformation of **2-Cs** to **3-Cs-Clus** is an exothermic process (5.8 kcal/mol). With this observation, further studies were directed to investigate the reaction from **3-Cs-Clus**.

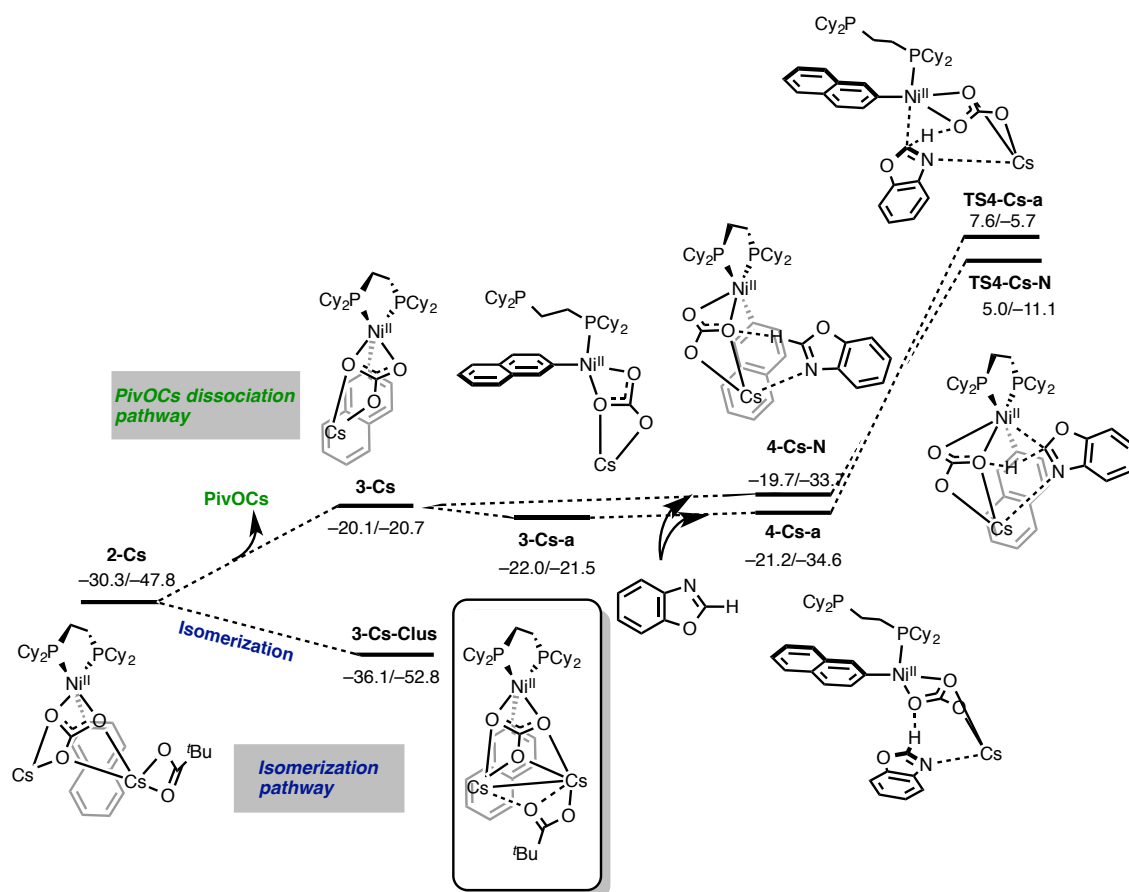


Figure 16. Two possible pathways from **2-Cs** and relative energies [in kcal/mol, relative to intermediate Ni(dcype)(Naph)(OPiv) **5**. left numbers show ΔG , and right numbers show ΔH]

After the generation of **3-Cs-Clus**, the next process goes through substrate coordination to **3-Cs-Clus** (Figure 17). Benzoxazole (**8**) was found to coordinate to the cesium cation on **3-Cs-Clus** with the requirement of 4.3 kcal/mol of energy. In this coordination process, interaction between a cesium and a nitrogen atom is 3.0 kcal/mol more favored than that between a cesium and an oxygen atom. The resulting benzoxazole coordinating complex, **4-Cs-Clus-N**, undergoes C–H nickelation step through transition state **Ts5-Cs-Clus-N**. At this transition state, the C–H activation

energy barrier is 27.0 kcal/mol, which is 4.0 kcal/mol less than the rate-determining barrier of 31.0 kcal/mol for the reaction in the absence of Cs_2CO_3 . Furthermore, at 373.15 K, the C–H activation energy barrier is 31.1 kcal/mol where it is 1.8 kcal/mol higher than the 29.3 kcal/mol energy barrier for the oxidative addition of a C–O bond to $\text{Ni}(\text{cod})(\text{dcype})$. This result represents demonstrates that the C–H nickelation step also remains the rate-determining step of the reaction in the presence of Cs_2CO_3 .

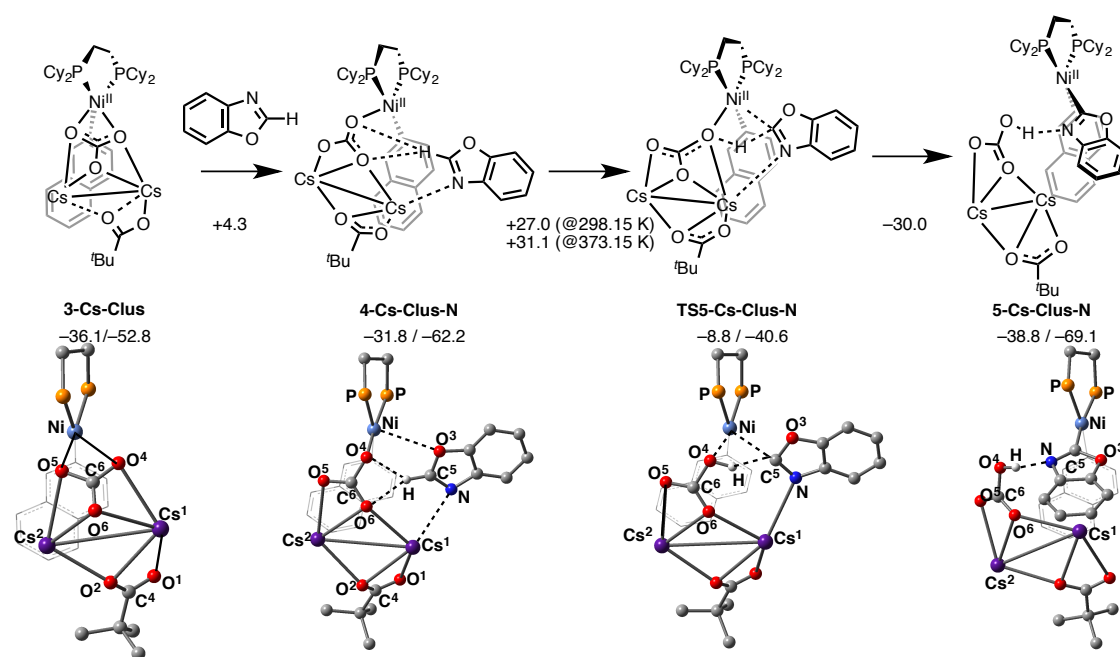


Figure 17. Mechanism of the C–H nickelation in the presence of Cs_2CO_3 and relative energies [in kcal/mol, relative to intermediate $\text{Ni}(\text{dcype})(\text{Naph})(\text{OPiv})$ **5**. left numbers show ΔG , and right numbers show ΔH]

Further detailed studies were concentrated on the effect of the cluster formation for the C–H activation step (Figure 18). It is predicted that the formation of **4-Cs-Clus-N** would be affected by the acidity of the C–H bond of azole. The existence of the Cs–N interaction in **4-Cs-Clus-N** likely plays a key role to reduce the rate-limiting C–H activation energy barrier. This computational finding is consistent with experimental results in which the addition of Cs_2CO_3 to the reaction of **5** with benzoxazole (**8**) increase the reaction yield from 32% to 67% and also makes the reaction three times faster. Moreover, comparison of C–H activation transition states **TS2** and **TS5-Cs-Clus-N** shows that the addition of Cs_2CO_3 to **5** changes the nature of the C–H

activation transition state from the six-membered CMD transition state to the four-membered σ -bond metathesis transition state where one oxygen bearing nickel acts as a proton acceptor.

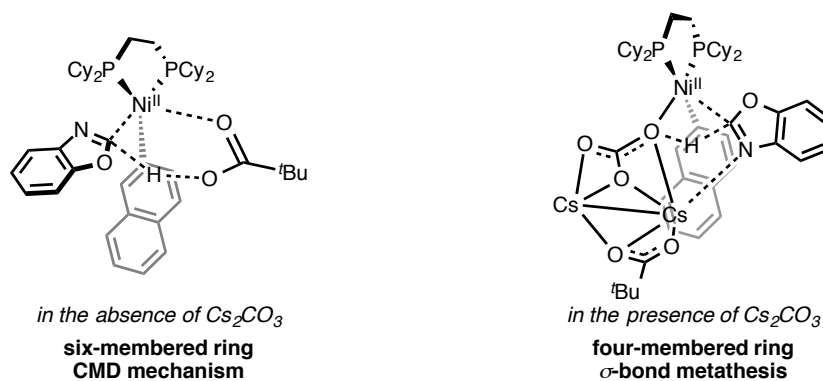
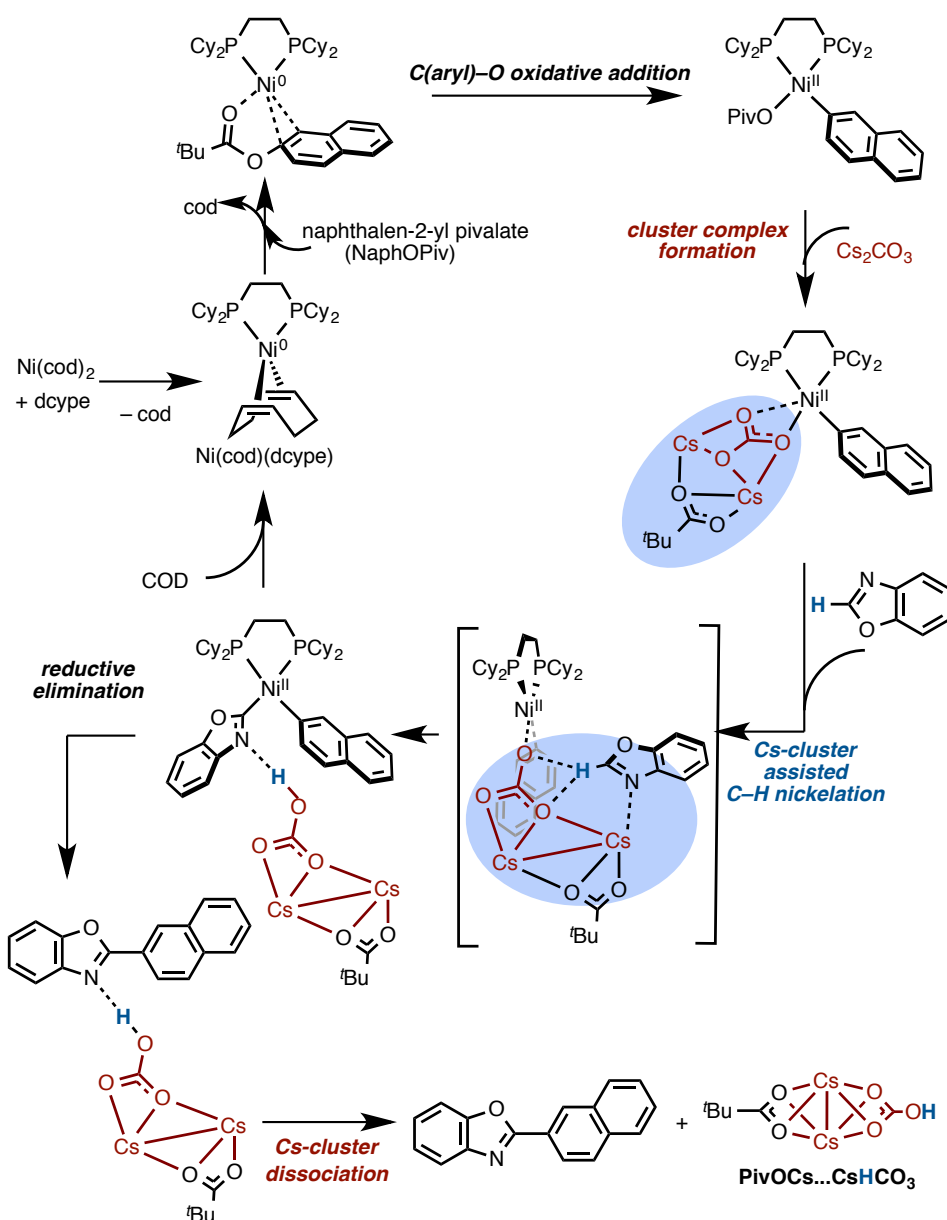


Figure 18. Comparison of the C–H activation transition states of CMD mechanism (in the absence of base) and σ -bond metathesis mechanism (in the presence of base)

With these combined experimental and theoretical studies, the plausible catalytic cycle shown in Scheme 9 is modified as depicted in Scheme 11. This reaction involves: (1) active catalyst generation and Ni(dcype)(NaphOPiv) intermediate formation, (2) C(aryl)–O oxidative addition via the five-centered transition state leading to the Ni(dcype)(Naph)(OPiv) intermediate, (3) Cs₂CO₃ coordination and Ni(dcype)(Naph)[PivOCs·CsCO₃] cluster complex formation, (4) C–H activation/nickelation by the Cs-clustered nickel complex via the σ -bond metathesis transition state, and (5) C–C reductive elimination and catalyst regeneration.



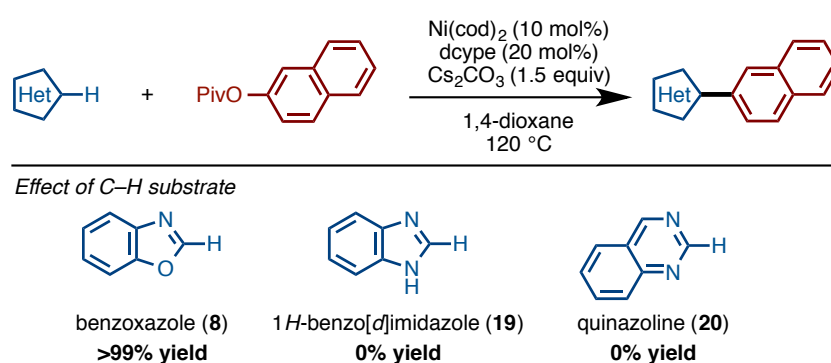
Scheme 11. Modified catalytic cycle of the $\text{Ni}(\text{cod})(\text{dcype})$ -catalyzed and $\text{PivOCs}\cdot\text{CsCO}_3$ -mediated C-H/C-O coupling of benzoxazole and NaphOPiv

2-11. Effect of C-H Substrates

It was predicted above that the existence of the interaction between a cesium atom of **3-Cs-Clus** and a nitrogen atom of benzoxazole facilitates the C-H activation by increasing its acidity. Additionally, the pK_a value was previously indicated to be one of the important factors of C-H bond activation by transition metal systems.^[16] However, there still remains a question to be answered and investigated: that is, whether the presence of this Cs-N interaction and related pK_a values is the only factor controlling

the C–H activation by **3-Cs-Clus** or not. In order to elucidate other factors affecting the C–H activation, the catalytic reactions of benzimidazole (**19**) and quinazoline (**20**) in the presence of Cs_2CO_3 were evaluated both computationally and experimentally.

Although benzoxazole (**8**) can cross-couple with **4** quantitatively under the standard catalytic conditions, it was revealed that neither **19** nor **20** reacts with **4** under otherwise identical conditions (Scheme 12). Careful comparison of these substrates shows that the π -electron density in the azole system decreases in the order **8** > **19** > **20**. This electronic feature of the examined azoles may have a large effect on Cs–N interaction in **4-Cs-Clus-N**, and in the following C–H activation transition state **TS5-Cs-Clus-N**.



Scheme 12. Effect of C–H substrates in the nickel catalysis

Consistent with these experimental findings, accompanying calculations show a large increase in the C–H activation barrier when replacing **8** by **19** or **20** from 26.6 kcal/mol in **8** to 40.2 and 48.6 kcal/mol in **19** and **20**, respectively (Figure 19, ΔG^\ddagger). These values indicate that **19** and **20** cannot undergo the C–H coupling even in the presence of Cs_2CO_3 .

In order to shed light on the plausible reasons of the observed and calculated trends in the reactivity of **8**, **19** and **20** by **3-Cs-Clus** (**8** >> **19** > **20**), distortion/interaction analysis was next performed.^[13a,17,18] As seen in Figure 19, the negative value of the total interaction energy E_{int} is 16.5 and 40.5 kcal/mol smaller for **19** and **20**, respectively, compared to **8**. Since E_{int} is combination of the Cs–N interaction energy and Ni–C2 (heteroarenes) interaction energy, it is expected that the increasing electron density of heteroarene (**8** > **19** > **20**) defines the Ni–C2 interaction.

π -electron density in these heteroarenes. Thus, more π -electron-rich azoles have a smaller C–H activation barrier (Figure 20).

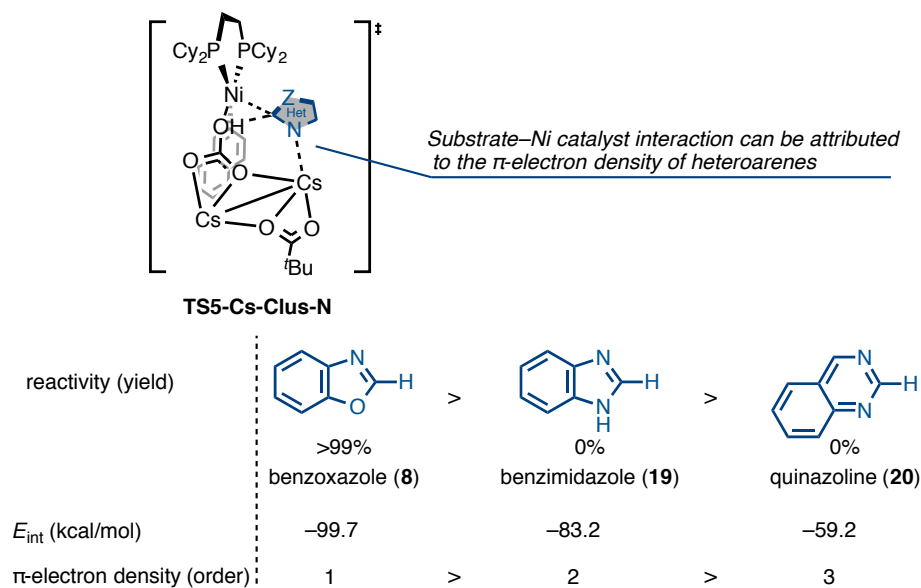


Figure 20. Relationship of Het–Ni catalyst interaction and π -electron density of heteroarenes

4. Conclusion

Combined experimental and computational studies shed light on the Ni-catalyzed C–H/C–O coupling of azoles and phenol derivatives. The isolation of a key intermediate **5** resulting from C–O oxidative addition, as well as the stoichiometric reaction of **5**, supports the plausible Ni(0)/Ni(II) redox catalytic cycle. The rate-determining step of the catalytic reaction was also found to be the C–H nickelation step. Through these experimental studies, some insights into the dcype ligand effect were obtained. The cyclohexyl substituents on the phosphines facilitate the oxidative addition of an aromatic C–O bond owing to its high σ -donating property. The bidentate structure also plays a key role to stabilize the generated intermediate **5** after the oxidative addition. Further computational studies demonstrated the key role of the Cs_2CO_3 base on the C–H nickelation step. Although the C–H nickelation step can proceed in the absence of base via a CMD mechanism with 31.0 kcal/mol of activation energy for the transition state **TS2**, this step can be accelerated by the addition of Cs_2CO_3 leading to the formation of

Cs-Ni cluster **3-Cs-Clus**. The generated Cs-Ni cluster **3-Cs-Clus** undergoes the following C–H nickelation step through a σ -bond metathesis mechanism, where the energy barrier is 27.0 kcal/mol. These obtained mechanistic data are expected to lead to the new design and development of further advanced catalysis for C–H/C–O coupling.

4. Experimental

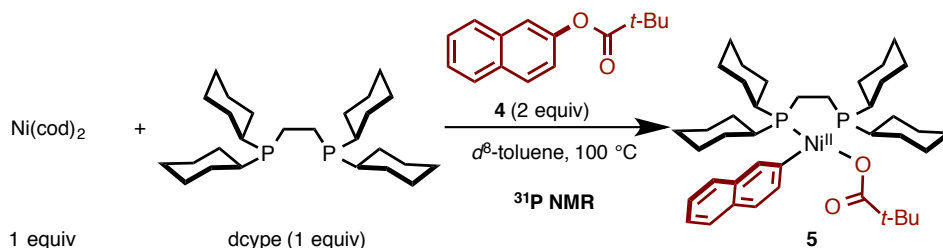
4-1. General

Unless otherwise noted, all materials including dry solvents were obtained from commercial suppliers and used as received. Ni(cod)₂ and Cs₂CO₃ were obtained from Wako Chemicals. 1,2-Bis(dicyclohexylphosphino)ethane (dcype) was obtained from Sigma-Aldrich. 1,4-Dioxane was freshly distilled over Na metal with benzophenone. 2-Deuterated benzoxazole (**D-8**) was synthesized according to procedures reported in the literature.^[19] Unless otherwise noted, all reactions were performed with dry solvents under an atmosphere of N₂ gas in flame-dried glassware using standard vacuum-line techniques. Unless otherwise noted, all C–H/C–O coupling reactions were performed in 20-mL glass vessel tubes equipped with J. Young® O-ring tap and heated in an 8-well reaction block (heater + magnetic stirrer). Monitoring experiments by nuclear magnetic resonance (NMR) was performed with an NMR tube equipped with a screwed cap. All work-up and purification procedures were carried out with reagent-grade solvents in air.

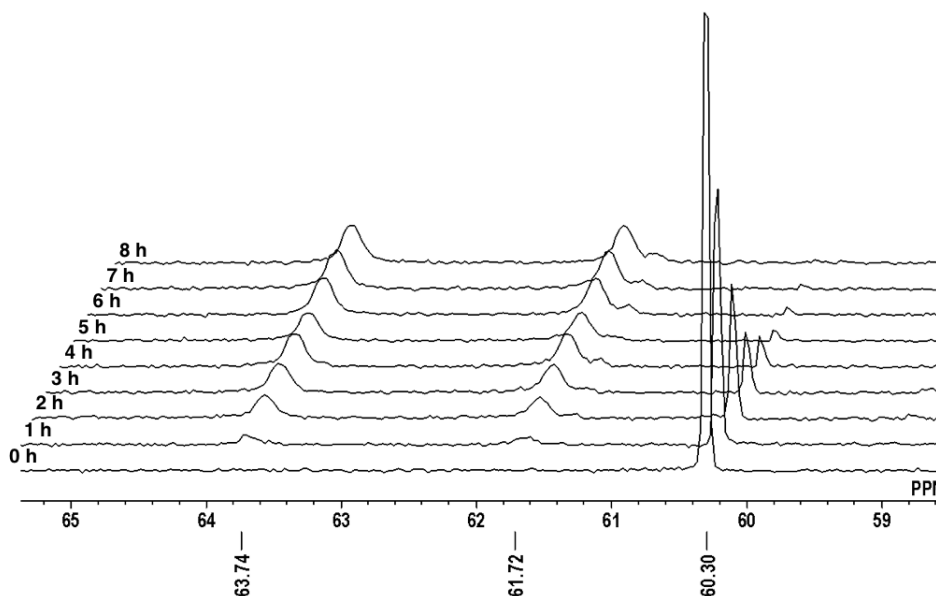
Analytical thin-layer chromatography (TLC) was performed using E. Merck silica gel 60 F₂₅₄ precoated plates (0.25 mm). The developed chromatogram was analyzed by UV lamp (254 nm). Flash column chromatography was performed with E. Merck silica gel 60 (230–400 mesh). Preparative thin-layer chromatography (PTLC) was performed using Wakogel B5-F silica coated plates (0.75 mm) prepared in our laboratory. Gas chromatography (GC) analysis was conducted on a Shimadzu GC-2010 instrument equipped with a HP-5 column (30 m × 0.25 mm, Hewlett-Packard) with decane as an internal standard. High-resolution mass spectra (HRMS) were obtained from a Thermo Scientific Exactive Plus Orbitrap MS (ESI). Nuclear magnetic resonance (NMR) spectra were recorded on a JEOL JMA-ECA-600 (¹H 600 MHz, ¹³C 150 MHz, ³¹P 243 MHz). Chemical shifts for ¹H NMR are expressed in parts per million (ppm) relative to *d*⁸-toluene (δ 2.18 ppm), when *d*⁸-toluene was used. Chemical shifts for ¹³C NMR are expressed in ppm relative to *d*⁸-toluene (δ 20.8 ppm). Data are reported as follows: chemical shift, multiplicity (s = singlet, d = doublet, dd = doublet of doublets, t = triplet, q = quartet, m = multiplet, br = broad signal), coupling constant (Hz), and integration. For kinetic experiments using *in situ* IR, the reaction spectra were recorded using an IC 15 from Mettler-Toledo AutoChem. Data processing was carried out using Microsoft® Excel® for Mac ver 14.2.5.

4-2. Monitoring Oxidative Addition Reaction by NMR

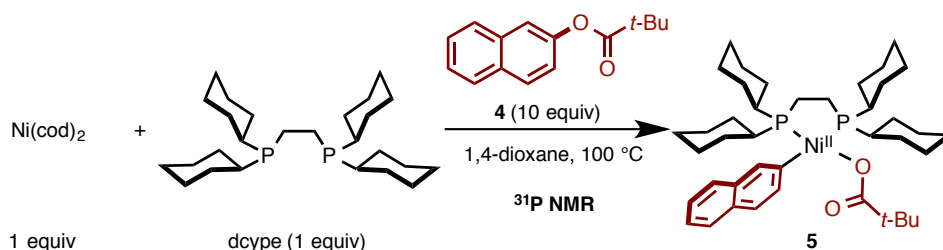
Oxidative Addition of **4** with Ni(cod)₂/dcype



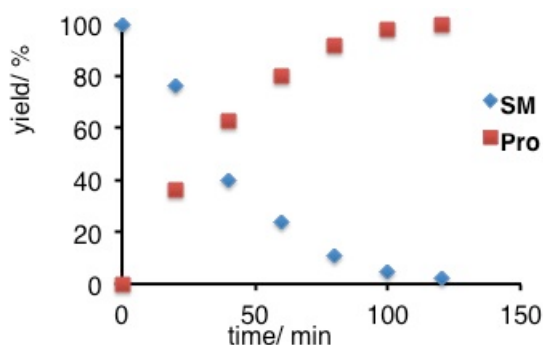
An NMR tube equipped with a screwed cap was dried with a heat-gun under reduced pressure and filled with N₂ after cooling to room temperature. **4** (11.4 mg, 0.050 mmol, 2.0 equiv) was added to this tube, which was introduced inside an argon atmosphere glovebox. To the vessel were added Ni(cod)₂ (6.9 mg, 0.025 mmol, 1.0 equiv), 1,2-bis(dicyclohexylphosphino)ethane (dcype: 10.6 mg, 0.025 mmol, 1.0 equiv), and *d*⁸-toluene (0.50 mL). This tube was capped, and then it was taken out of the glovebox. This tube was set into the NMR spectrometer, and the reaction was monitored by ³¹P NMR spectroscopy (0 h – 8 h) at 100 °C. During the course of the reaction, two new downfield peaks ($\delta = 63.7$ and 61.7 ppm) appeared alongside the signal of the Ni(cod)₂/dcype complex ($\delta = 60.3$ ppm) on ³¹P NMR.



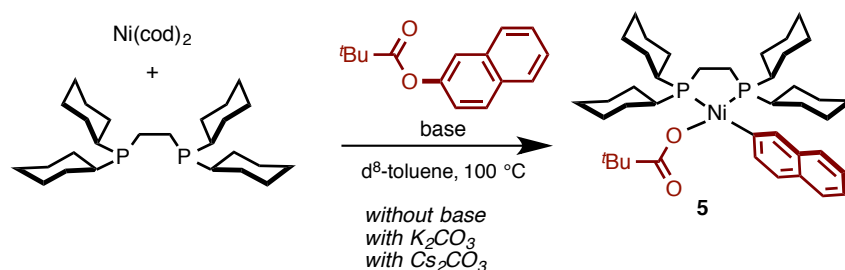
Oxidative Addition of Excess Amount of **4** with Ni(cod)₂/dcype



An NMR tube equipped with a screw cap was dried with a heat-gun under reduced pressure and filled with N₂ after cooling to room temperature. **4** (28.7 mg, 0.125 mmol, 10.0 equiv) was added to this tube, which was introduced inside an argon atmosphere glovebox. To the vessel were added Ni(cod)₂ (3.4 mg, 0.0125 mmol, 1.0 equiv), 1,2-bis(dicyclohexylphosphino)ethane (dcype: 5.3 mg, 0.0125 mmol, 1.0 equiv), and 1,4-dioxane (0.50 mL). This tube was capped, and then it was taken out of the glovebox. This tube was set into the NMR spectrometer, and the reaction was monitored by ³¹P NMR spectroscopy (0 h – 3 h) at 100 °C. The plots of time vs the reaction yield show that the oxidative addition is much faster than the catalytic reaction.

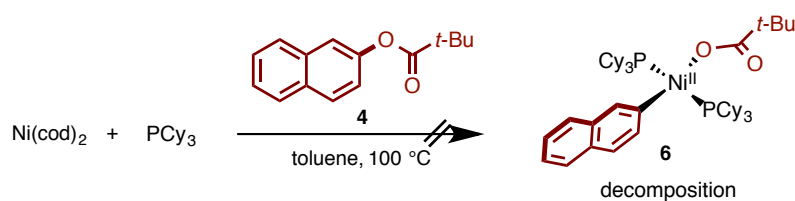


Oxidative Addition of **4** with Ni(cod)₂/dcype in the Presence of Bases

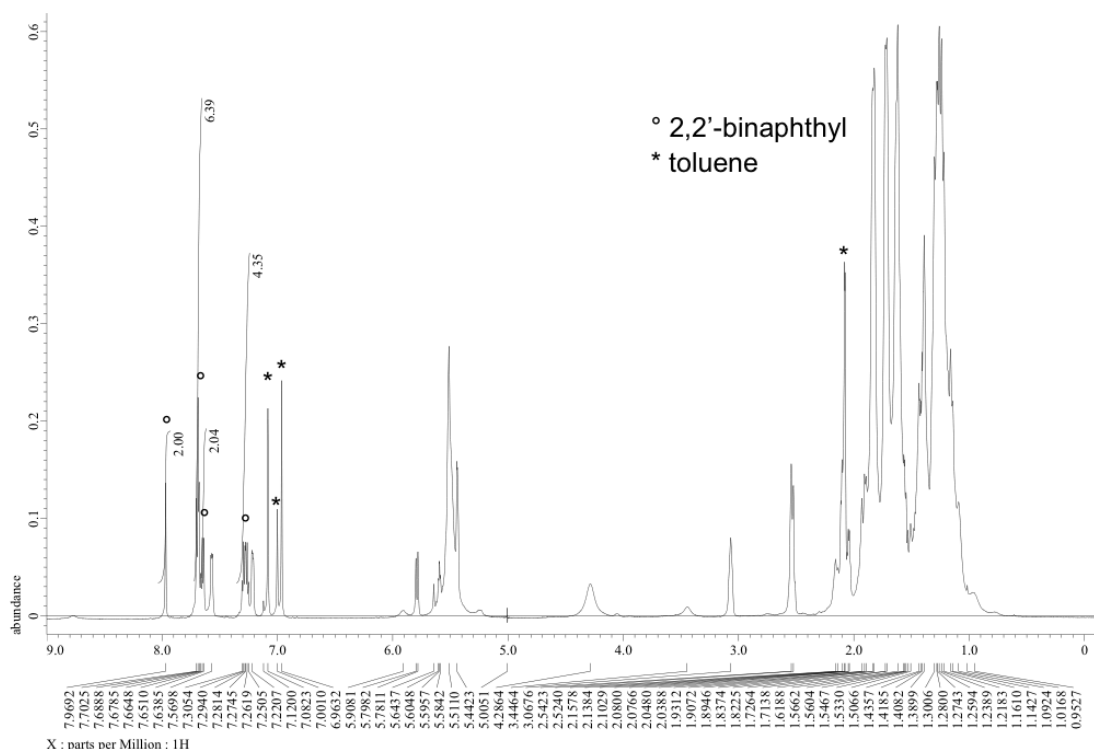


An NMR tube equipped with a screw cap containing base (0.025 mmol, 1.0 equiv) was dried with a heat-gun under reduced pressure and filled with N₂ after cooling to room temperature. Naphthalen-2-yl pivalate (**4**: 11.4 mg, 0.050 mmol, 2.0 equiv) was added to this tube, which was introduced inside an argon atmosphere glovebox. To the vessel were added Ni(cod)₂ (6.9 mg, 0.025 mmol, 1.0 equiv), 1,2-bis(dicyclohexylphosphino)ethane (dcype: 10.6 mg, 0.025 mmol, 1.0 equiv), and *d*⁸-toluene (0.50 mL). This tube was capped, and then it was taken out of the glovebox. This tube was set into the NMR spectrometer, and the reaction was monitored by ³¹P NMR spectroscopy (0 h–8 h) at 100 °C. During the course of the reaction, two new downfield peaks (δ = 63.7 and 61.7 ppm) gradually appeared alongside the signal of the Ni(cod)₂/dcype complex (δ = 60.3 ppm) on ³¹P NMR.

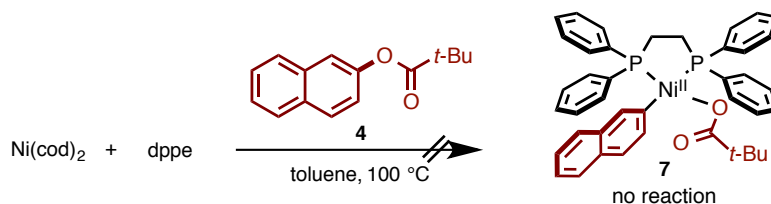
Oxidative Addition of **4** with Ni(cod)₂/PCy₃



An NMR tube equipped with a screw cap was dried with a heat-gun under reduced pressure and filled with N₂ after cooling to room temperature. **4** (11.4 mg, 0.050 mmol, 2.0 equiv) was added to this tube, which was introduced inside an argon atmosphere glovebox. To the vessel were added Ni(cod)₂ (6.9 mg, 0.025 mmol, 1.0 equiv), tricyclohexylphosphine (PCy₃: 14.0 mg, 0.050 mmol, 2.0 equiv), and *d*⁸-toluene (0.50 mL). This tube was capped and then taken out of the glovebox. This tube was set into the NMR spectrometer, and the reaction was monitored by ¹H NMR and ³¹P NMR spectroscopy at 100 °C. The main product was 2,2'-binaphthyl, as observed by ¹H NMR and GCMS, and the complex **6** was not obtained. Compound data of 2,2'-binaphthyl: ¹H NMR (600 MHz, *d*⁸-toluene): δ 7.98 (s, 2H), 7.76–7.75 (m, 6H), 7.65 (d, *J* = 5.5 Hz, 2H), 7.34–7.24 (m, 4H).

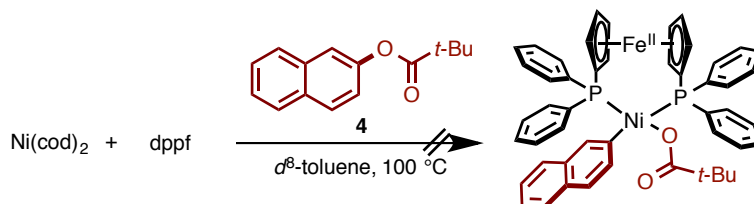


Oxidative Addition of **4** with $\text{Ni}(\text{cod})_2/\text{dppe}$



An NMR tube equipped with a screw cap was dried with a heat-gun under reduced pressure and filled with N_2 after cooling to room temperature. **4** (11.4 mg, 0.050 mmol, 2.0 equiv) was added to this tube, which was introduced inside an argon-atmosphere glovebox. To the vessel were added $\text{Ni}(\text{cod})_2$ (6.9 mg, 0.025 mmol, 1.0 equiv), 1,2-bis(diphenylphosphino)ethane (dppe: 10.0 mg, 0.025 mmol, 1.0 equiv), and d^8 -toluene (0.50 mL). This tube was capped and then taken out of the glovebox. This tube was set into the NMR spectrometer, and the reaction was monitored by ^{31}P NMR spectroscopy (0 h–8 h) at 100 °C. This experiment resulted in the observation of no ^{31}P NMR peak shift (δ 44.8 ppm).

Oxidative Addition of **4** with Ni(cod)₂/dppf

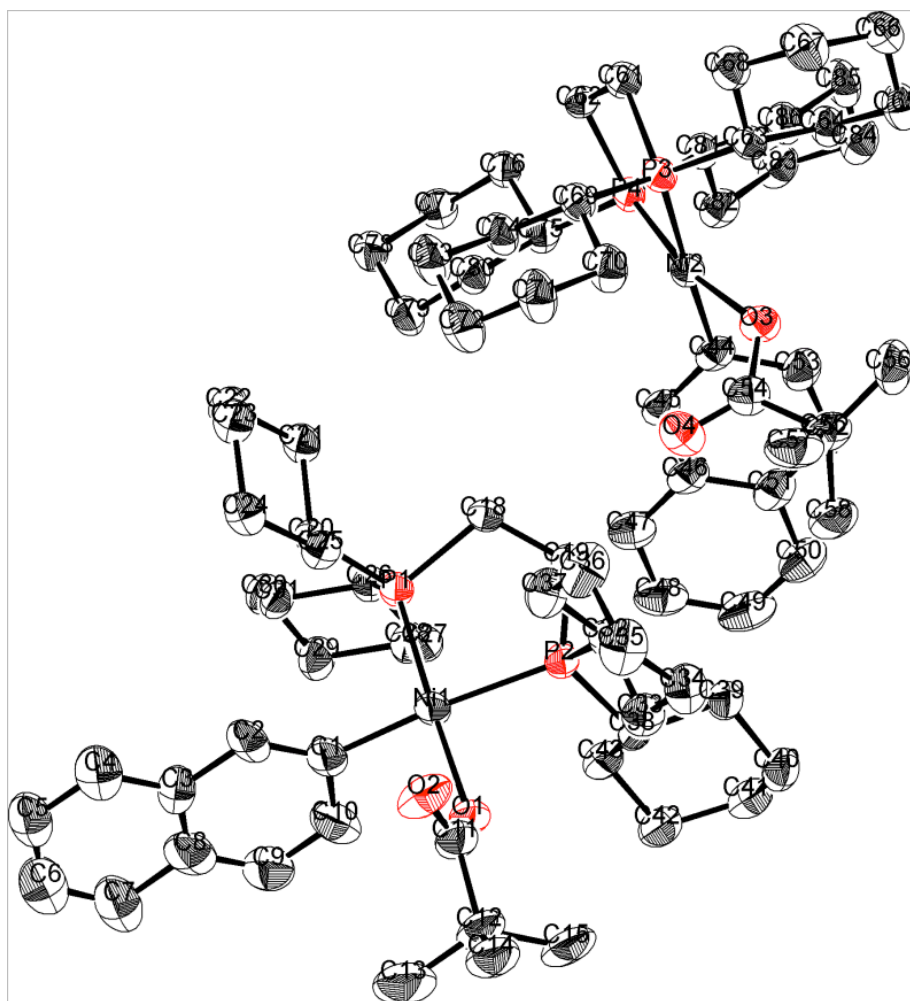


An NMR tube equipped with a screw cap was dried with a heat-gun under reduced pressure and filled with N₂ after cooling to room temperature. **4** (11.4 mg, 0.050 mmol, 2.0 equiv) was added to this tube, which was introduced inside an argon-atmosphere glovebox. To the vessel were added Ni(cod)₂ (6.9 mg, 0.025 mmol, 1.0 equiv), 1,2-bis(diphenylphosphino)ferrocene (dppf: 13.9 mg, 0.025 mmol, 1.0 equiv), and d⁸-toluene (0.50 mL). This tube was capped and then taken out of the glovebox. This tube was set into the NMR spectrometer, and the reaction was monitored by ¹H and ³¹P NMR spectroscopy (0 h – 8 h) at 100 °C. During the course of the reaction, none of new downfield peaks appeared alongside the signal of the Ni(cod)(dppf) complex (d = 33.7 ppm) on ³¹P NMR, however, some of new peaks (30.4, 25.8, 23.5, 16.5, 12.5) appeared alongside the signal of the Ni(cod)(dppf) complex. According to the ¹H NMR, the peak of *tert*-butyl on pivaloyl group did not shifted (δ = 1.27 ppm). These results indicated the no oxidative addition had occurred.

4-3. X-ray Crystal Structure Analysis of **5**

A suitable crystal of **5** was mounted with mineral oil on a glass fiber and transferred to the goniometer of a Rigaku Saturn CCD diffractometer. Graphite-monochromated Mo K α radiation ($\lambda = 0.71070 \text{ \AA}$) was used. The structures were solved by direct methods with (SIR-97)^[20] and refined by full-matrix least-squares techniques against F^2 (SHELXL-97).^[21] The intensities were corrected for Lorentz and polarization effects. The non-hydrogen atoms were refined anisotropically. Hydrogen atoms were placed using AFIX instructions. Details of the crystal data and a summary of the intensity data collection parameters for **5** are listed below.

formula	C42.5H67.5NiO2P2
fw	731.12
<i>T</i> (K)	103(2)
<i>l</i> (Å)	0.71070
cryst syst	Monoclinic
space group	<i>C2/c</i>
<i>a</i> , (Å)	35.830(12)
<i>b</i> , (Å)	25.083(6)
<i>c</i> , (Å)	27.462(8)
<i>a</i> , (deg)	90°
<i>b</i> , (deg)	136.700(5)°
<i>g</i> , (deg)	90°
<i>V</i> , (Å ³)	16926(9)
<i>Z</i>	16
<i>D</i> _{calc} , (g / cm ³)	1.148
<i>m</i> (mm ⁻¹)	0.566
F(000)	6344
cryst size (mm)	0.20 × 0.20 × 0.20
2 <i>q</i> range, (deg)	3.03–25.00
reflns collected	56141
indep reflns/ <i>R</i> _{int}	14770/0.0732
params	924
GOF on <i>F</i> ²	1.117
<i>R</i> ₁ , w <i>R</i> ₂ [<i>I</i> > 2 <i>s</i> (<i>I</i>)]	0.0926, 0.2029
<i>R</i> ₁ , w <i>R</i> ₂ (all data)	0.1166, 0.2198

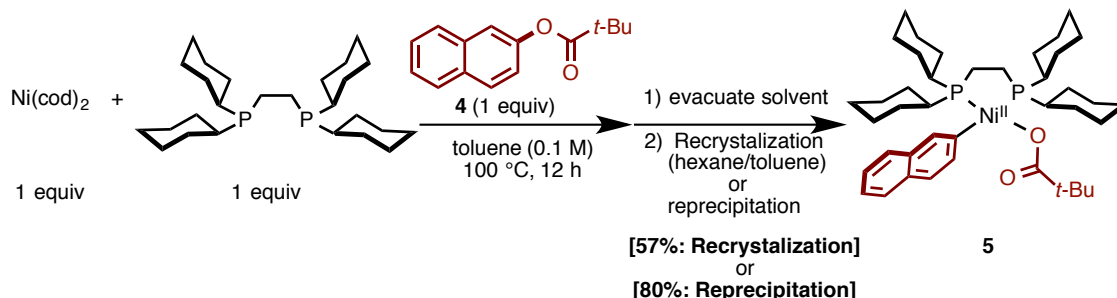


ORTEP drawing of **5** with 50% thermal ellipsoid. All hydrogen atoms are omitted for clarity. Obtained X-ray crystal structure displayed two independent molecules in an asymmetric unit.

Selected bond lengths (Å) and angles (deg)

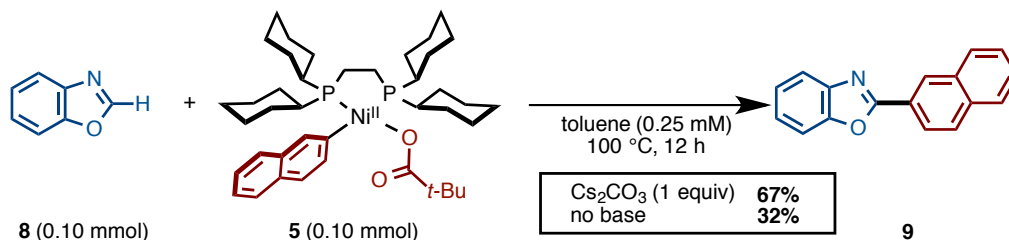
Ni1–P1 = 2.1401(16)	Ni2–P4 = 2.1381(16)
Ni1–P2 = 2.2192(17)	Ni2–P3 = 2.2100(17)
Ni1–O1 = 1.919(4)	Ni2–O3 = 1.908(4)
Ni1–C1 = 1.940(6)	Ni2–C44 = 1.933(6)
O1–Ni1–C1 = 88.8(2)	O3–Ni2–C44 = 89.6(2)
O1–Ni1–P1 = 175.10(14)	O3–Ni2–P4 = 167.69(13)
C1–Ni1–P1 = 91.85(18)	C44–Ni2–P4 = 91.28(16)
O1–Ni1–O1 = 89.89(13)	O3–Ni2–P3 = 89.33(13)
C1–Ni1–P1 = 168.9(2)	C44–Ni2–P3 = 178.35(18)
P1–Ni1–P2 = 88.56(6)	P4–Ni2–P3 = 89.45(6)

4-4. Isolation of Nickel Complex 5



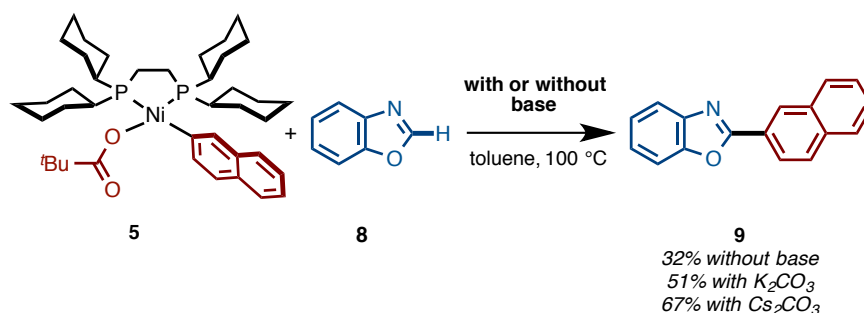
A 20-mL glass vessel equipped with J. Young[®] O-ring tap containing a magnetic stirring bar was dried with a heat-gun under reduced pressure and filled with N_2 after cooling to room temperature. **4** (45.7 mg, 0.20 mmol) was added to this vessel, which was then introduced inside an argon-atmosphere glovebox. To the vessel were added $\text{Ni}(\text{cod})_2$ (55.3 mg, 0.20 mmol, 1.0 equiv), 1,2-bis(dicyclohexylphosphino)ethane (dcype: 86.1 mg, 0.20 mmol, 1.0 equiv), and toluene (2.0 mL). After sealing this vessel with O-ring tap, it was taken out of the glovebox, then stirred at 100 °C in an oil bath for 12 h. After cooling the reaction mixture to room temperature, this vessel was transferred into the glovebox, and then solvent and 1,5-cyclooctadiene were completely removed to afford the crude solid. The residue was azeotroped with hexane to obtain a yellow solid. The obtained solid was purified by 1) recrystallization from the mixed solvent of toluene (0.5 mL)/hexane (2.0 mL) at 0 °C to afford an orange crystal (**5**: 80.6 mg, 57% yield) or 2) reprecipitation using hexane to afford a yellow solid (**5**: 227 mg (0.40 mmol scale), 80% yield): ^1H NMR (600 MHz, d^8 -toluene) δ 8.21 (s, 1H), 8.16 (d, $J = 5.5$ Hz, 1H), 7.71 (d, $J = 8.0$ Hz, 1H), 7.64 (d, $J = 8.0$ Hz, 1H), 7.57 (d, $J = 8.0$ Hz, 1H), 7.25 (t, $J = 8.8$ Hz, 1H), 7.15 (t, $J = 8.8$ Hz, 1H), 2.70–2.50 (m, 2H), 2.40–2.25 (m, 2H), 2.05–0.69 (m, 53H). ^{31}P NMR (243 MHz, d^8 -toluene) δ 63.8 (d, $J_{\text{pp}} = 13.3$ Hz, 1P), 61.6 (d, $J_{\text{pp}} = 13.3$ Hz, 1P). HRMS (ESI) m/z calcd for $\text{C}_{41}\text{H}_{64}\text{NiO}_2\text{P}_2 + \text{Cl}$ [$\text{M} + \text{Cl}$] $^-$: 745.3393, found 745.3412.

4-5. Stoichiometric Reaction of **8** with **5**



A test tube equipped with a screw cap containing a magnetic stirring bar and Cs_2CO_3 (32.5 mg, 0.10 mmol, 1.0 equiv) was dried with a heatgun under reduced pressure and filled with N_2 after cooling to room temperature. **5** (70.1 mg, 0.10 mmol, 1.0 equiv) was added to this vessel, then evacuated and purged with N_2 for three times. To this were added **8** (11.9 mg, 0.10 mmol) and 1,4-dioxane (0.4 mL) under a stream of N_2 . The vessel was sealed with the screw cap and then heated at 100 °C for 12 h in an 8-well reaction block with stirring. After cooling the reaction mixture to room temperature, the mixture was passed through a short silica gel pad with EtOAc. The filtrate was concentrated and the residue was purified by preparative thin-layer chromatography (hexane/EtOAc = 10:1) to afford **9** (15.2 mg, 67%) as a white solid. ^1H NMR (600 MHz, CDCl_3) δ 8.79 (s, 1H), 8.33 (dd, $J = 8.7, 1.4$ Hz, 1H), 8.03–7.96 (m, 2H), 7.93–7.87 (m, 1H), 7.82 (dd, $J = 6.4, 3.7$ Hz, 1H), 7.63 (dd, $J = 6.4, 2.7$ Hz, 1H), 7.60–7.52 (m, 2H), 7.41–7.31 (m, 2H).

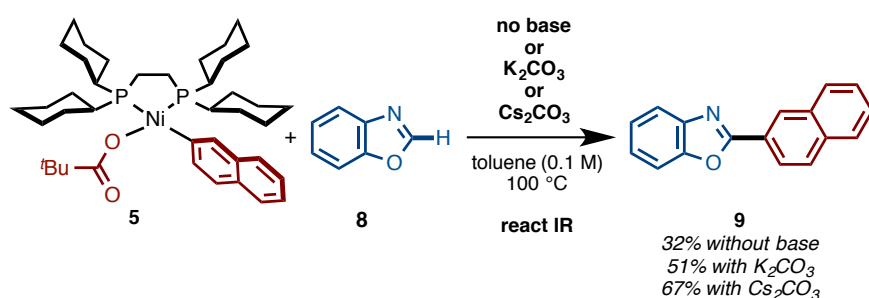
Stoichiometric Reaction of **5** with **8** in the Presence and Absence of Bases



A test tube equipped with a screw cap containing a magnetic stirring bar and base (0.10 mmol, 1.0 equiv) was dried with a heatgun under reduced pressure and filled with N_2 after cooling to room temperature. **5** (70.1 mg, 0.10 mmol, 1.0 equiv) was added to this vessel, then evacuated and purged with N_2 for three times. To this were added benzoxazole (11.9 mg, 0.10 mmol) and toluene (0.4 mL) under a stream of N_2 . The vessel was sealed with the screw cap and then heated at 100 °C for 12 h in an 8-well

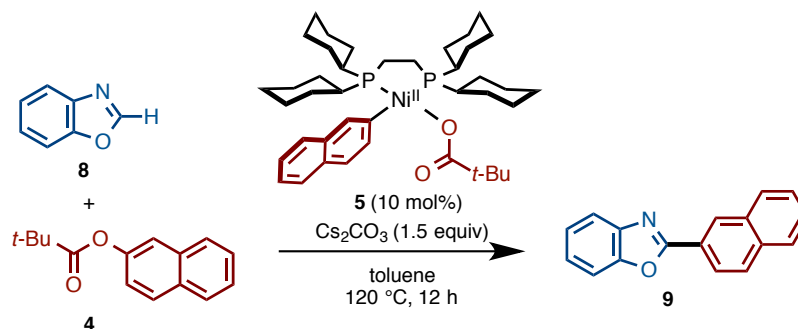
reaction block with stirring. After cooling the reaction mixture to room temperature, the mixture was passed through a short silica gel pad with EtOAc. The filtrate was concentrated and the residue was purified by preparative thin-layer chromatography (hexane/EtOAc = 10:1) to afford 2-(naphthalen-2-yl) benzoxazole (**9**) as a white solid (without base; 7.8 mg, 32% yield, with K_2CO_3 ; 12.4 mg, 51% yield, with Cs_2CO_3 ; 15.2 mg, 67% yield)

Kinetic Study on the Stoichiometric Reaction of **5** with **8** in the Presence or Absence of Bases



To a three-necked reaction vessel containing magnetic stirring bar and base (0.20 mmol, 1.0 equiv) was dried with a heatgun under reduced pressure and filled with N_2 after cooling to room temperature. **5** (141.9 mg, 0.20 mmol, 1.0 equiv) was added to this vessel, then vacuumed and purged with N_2 for three times. The IR probe was inserted into the middle neck through an adapter; another neck was capped by a rubber septum for injections, and the other one was jointed three-way cock in order to flow N_2 gas. To this were added toluene (2.0 mL) under a stream of N_2 . The mixture was allowed to stir at 100 °C in an oil bath. After 5 min, to the reaction mixture was added benzoxazole (23.8 mg, 0.20 mmol, 1.0 equiv) to start the C–H nickelation reaction. *In situ* IR spectra were minutely recorded over the course of the reaction. After 12 hours, the reaction mixture was cooled to room temperature and then EtOAc was added to quench the reaction. The reaction yield was confirmed by GC equipment.

4-6. Procedure for 5-Catalyzed Coupling Reaction of 8 with 4

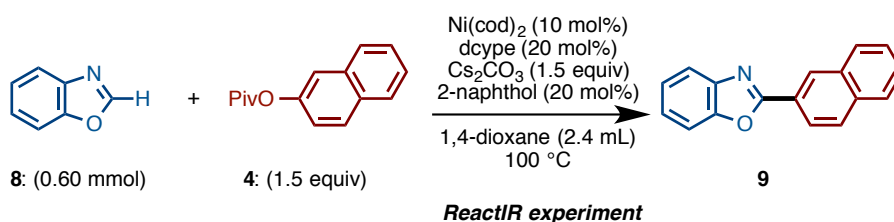


entry	variation	yield
1	none	8%
2	added dcype (10 mol%)	16%
3	added 1,5-COD (10 mol%)	70%
4	1,4-dioxane instead of toluene	quant

Representative Procedure (Entry 4)

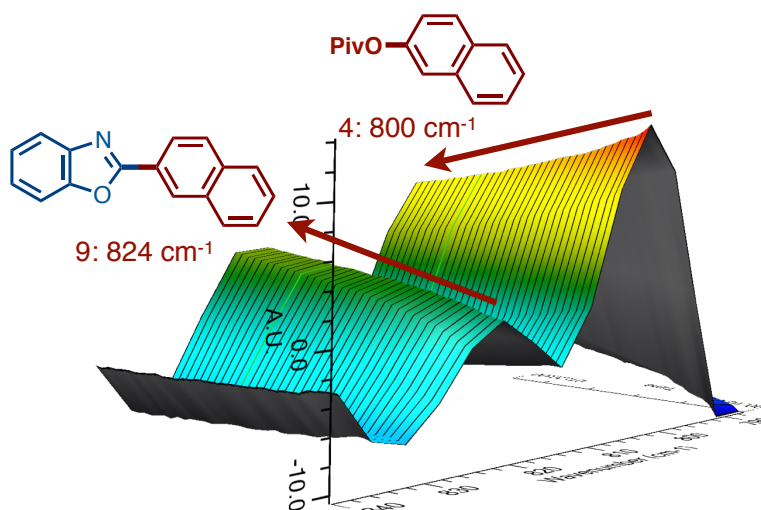
A 20-mL glass vessel equipped with J. Young[®] O-ring tap containing a magnetic stirring bar and Cs_2CO_3 (195.5 mg, 0.60 mmol, 1.5 equiv) was dried with a heatgun under reduced pressure and filled with N_2 after cooling to room temperature. To this vessel were added **4** (127.8 mg, 0.56 mmol, 1.4 equiv) and **5** (28.4 mg, 0.040 mmol, 10 mol%). The vessel was evacuated and purged with N_2 for three times. Then **8** (47.7 mg, 0.40 mmol) and 1,4-dioxane (1.6 mL) were added under a stream of N_2 . The vessel was sealed with the O-ring tap and then heated at 120 °C for 12 h in an 8-well reaction block with stirring. After cooling the reaction mixture to room temperature, the mixture was passed through a short silica gel pad with EtOAc. The filtrate was concentrated and the residue was purified by silica-gel flash column chromatography (hexane/EtOAc = 30:1) to afford **9** (98.0 mg, 99%).

4-7. Procedure for react IR Experiments for Kinetic Studies

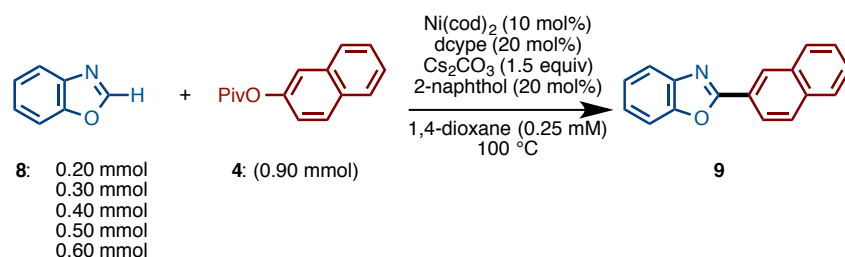


A three-necked reaction vessel containing a magnetic stirring bar and Cs₂CO₃ (292.5 mg, 0.90 mmol, 1.5 equiv) was dried with a heatgun. To this vessel were added **4** (205.3 mg, 0.90 mmol, 1.5 equiv) and 2-naphthol (17.3 mg, 0.12 mmol, 20 mol%). The IR probe was inserted into the middle neck through an adapter, another neck was capped by a rubber septum for the purpose of reagent injection, and the third one was attached to a three-way cock in order to flow N₂ gas. This vessel was evacuated and purged with N₂ three times. To this vessel was added 1,4-dioxane (1.4 mL) via a syringe. The mixture was allowed to stir at 100 °C in an oil bath. Then the data collection was started, followed by addition of benzoxazole (**8**). After 5 min, the solution of Ni(cod)₂ (16.5 mg, 0.06 mmol, 10 mol%) and dcype (50.7 mg, 0.12 mmol, 20 mol%) in 1,4-dioxane (1.0 mL) was added via syringe to start the coupling reaction. *In situ* IR spectra were recorded over the course of the reaction. After 1–3 h, the reaction mixture was cooled to room temperature and then EtOAc was added to quench the reaction. The reaction yield was confirmed by GC analysis.

The observed coupling product peak (824 cm⁻¹) is presented below.

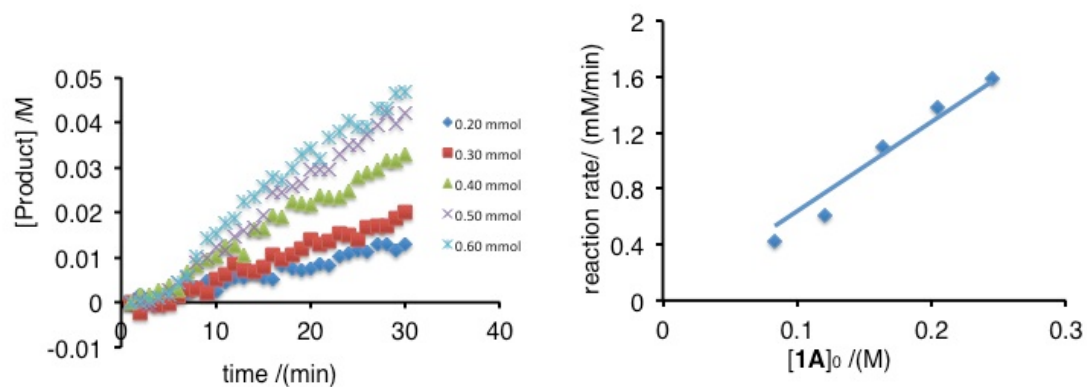


Dependence of the Reaction Rate on Concentration of Benzoxazole (**8**)



Kinetic profiles of different initial concentrations of **8** (from 0.0833 M to 0.250 M).

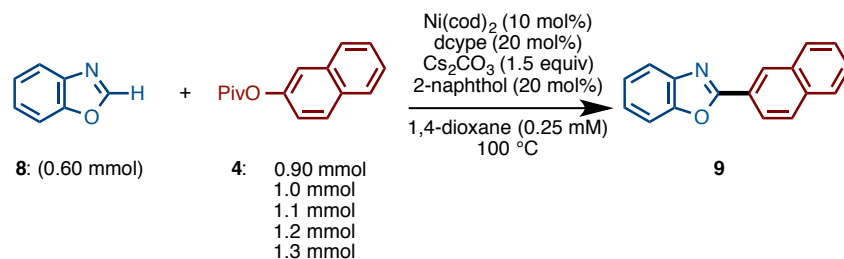
Reaction conditions: $[\mathbf{4}] = 0.375 \text{ M}$, $[\text{Ni}(\text{cod})_2] = 0.025 \text{ M}$, $[\text{dcype}] = 0.050 \text{ M}$, amount of $\text{Cs}_2\text{CO}_3 = 0.90 \text{ mmol}$, $[\text{2-naphthol}] = 0.050 \text{ M}$, 2.4 mL of 1,4-dioxane, 100 °C.



$[\mathbf{8}]_0 \text{ (M)}$	$k_{\text{obs}} \text{ (mM/min)}$
0.083249384	0.422396322
0.121026416	0.609195258
0.163350683	1.093873536
0.204625588	1.38735374
0.245200918	1.592728029

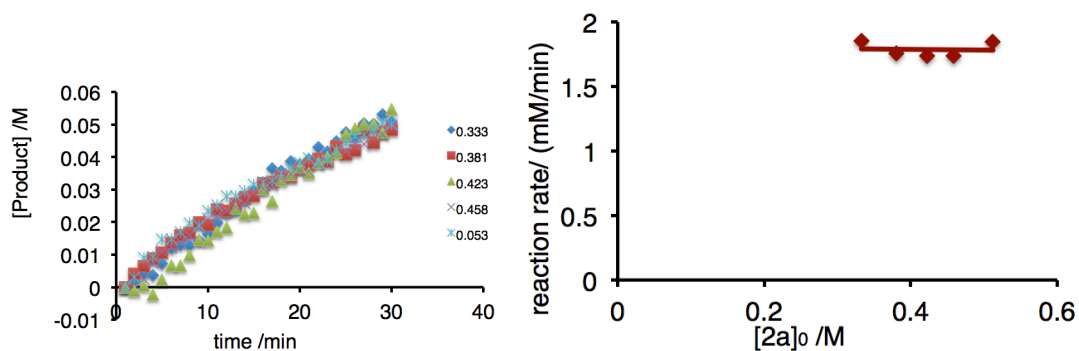
Dependence of the Reaction Rate on Concentration of Naphthalene-2-yl Pivalate

([4])



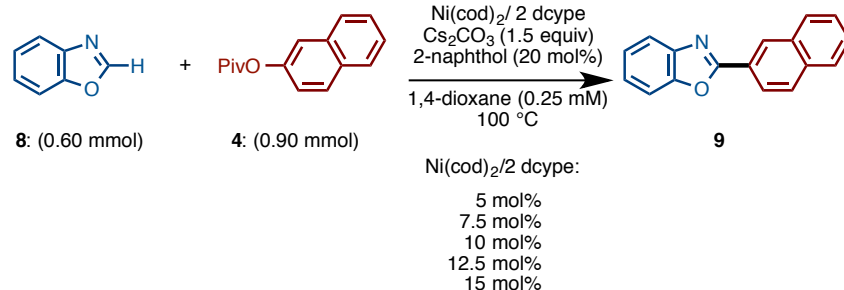
Kinetic profiles of different initial concentrations of **4** (from 0.375 M to 0.500 M).

Reaction conditions: [**8**] = 0.250 M, [Ni(cod)₂] = 0.025 M, [dcype] = 0.050 M, amount of Cs₂CO₃ = 0.90 mmol, [2-naphthol] = 0.050 M, 2.4 mL of 1,4-dioxane, 100 °C.

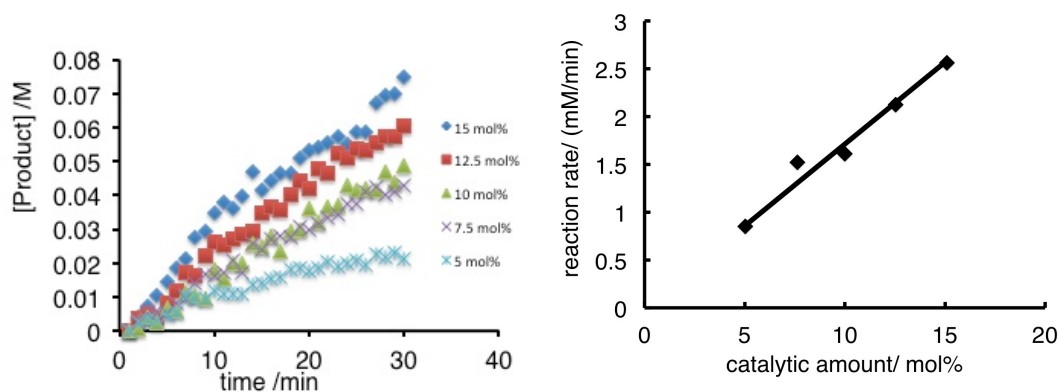


[4] ₀ (M)	<i>k</i> _{obs} / (mM/min)
0.332771109	1.850996024
0.380779228	1.759398981
0.422763515	1.740269529
0.457993808	1.739817114
0.5122083	1.845282981

Dependence of the Reaction Rate on Concentration of Ni(cod)₂/dcype ([catalyst])

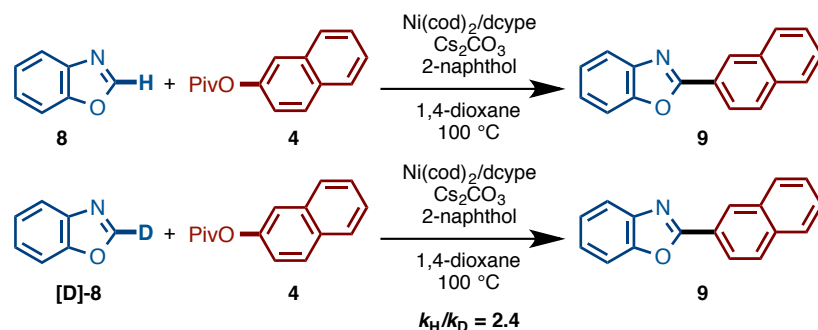


Kinetic profiles of different initial concentrations of [catalyst] (from 0.0125 M to 0.0375 M), Reaction conditions: **[8]** = 0.250 M, **[4]** = 0.375 M, amount of Cs₂CO₃ = 0.90 mmol, [2-naphthol] = 0.050 M, 2.4 mL of 1,4-dioxane, 100 °C.



catalytic amount/ (mol%)	k_{obs} / (mM/min)
5.029205749	0.853656913
7.634697884	1.523367959
9.997818658	1.610566149
12.54271795	2.12654159
15.08761725	2.56555144

4-8. Kinetic Isotope Effect



A three-necked reaction vessel containing a magnetic stirring bar and Cs_2CO_3 (292.5 mg, 0.90 mmol, 1.5 equiv) was dried with a heatgun. To this vessel were added **4** (205.3 mg, 0.90 mmol, 1.5 equiv) and 2-naphthol (17.3 mg, 0.12 mmol, 20 mol%). The IR probe was inserted through an adapter into the middle neck; another neck was capped by a rubber septum for the purpose of reagent injection, and the third one was jointed three-way cock in order to flow N_2 gas. This vessel was evacuated and purged with N_2 three times. To this vessel was added 1,4-dioxane (1.4 mL) via a syringes. The mixture was allowed to stir at $100\text{ }^\circ\text{C}$ in an oil bath. Then the data collection was started, followed by addition of benzoxazole (**8**) (71.5 mg, 0.60 mmol, 1 equiv) or 2-deuterated-benzoxazole (**d-8**) (72.1 mg, 0.60 mmol, 1 equiv). After 5 min, the solution of $\text{Ni}(\text{cod})_2$ (16.5 mg, 0.06 mmol, 10 mol%) and dcype (50.7 mg, 0.12 mmol, 20 mol%) in 1,4-dioxane (1.0 mL) was added via syringe to start the coupling reaction. *In situ* IR spectra were recorded over the course of the reaction. After 1–3 hours, the reaction mixture was cooled to room temperature and then EtOAc was added to quench the reaction. The reaction yield was confirmed by GC analysis.

4-9. Computational Methods

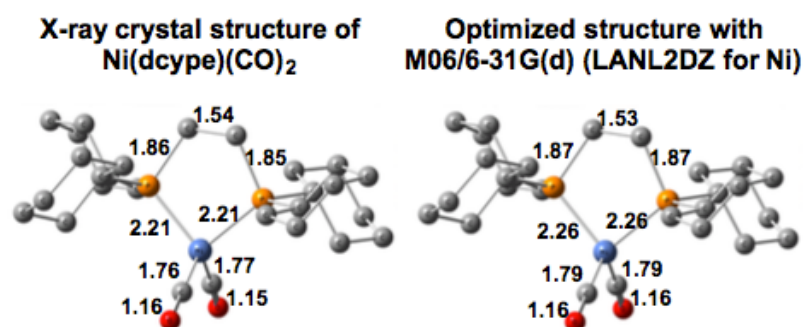
Calculations were performed by Gaussian 09 quantum chemical package.^[22] The geometries of all reported reactants, intermediates, transition states, and products were optimized without symmetry constraints in 1,4-dioxane solvent ($\epsilon = 2.21$) at the M06L level of density functional theory^[23] in conjunction with the Lanl2dz basis set and corresponding Hay–Wadt effective core potential (ECP) for Ni and Cs.^[24] Standard 6-31G(d) basis sets were used for all other atoms. Below, this approach will be called as

M06L/{Lan12dz + [6-31G(d)]} or M06L/BS1. Solvent effects were estimated by using the PCM solvation method.^[25] In order to incorporate disperse interactions into calculations, geometry optimization and energy calculations of selected important intermediates and transition states at the M06/BS1 level of theory were also performed.^[26] These calculations have shown that the M06L/BS1 and M06/BS1 optimized geometries are very close, while relative energies can vary by a few kcal/mol. The nature of each stationary point was characterized by performing normal-mode analysis. Relative free energies and enthalpies of all reported structures were calculated under standard conditions (1 atm and 298.15 K). Since the associated experiments were performed at 100 °C, the important energy barriers [i.e., C(aryl)–O oxidative addition and benzoxazole C–H bond activation] were also recalculated at 373.15 K. Briefly, it is found that increasing the temperature from 298.15 to 373.15 K only slightly increases energy barriers and does not affect the reported conclusions and reactivity trends. Therefore, below, in sake of consistency, we discuss the M06/BS1 calculated free energies (i.e., ΔG values) at 298.15 K unless otherwise specified. In the presented figures and tables, both relative Gibbs free energies and enthalpies (in kcal/mol) are given as $\Delta G/\Delta H$.

In order to evaluate the used M06L/BS1 and M06/BS1 approaches, the geometry of the Ni(dcype)(CO)₂ complex, which was previously isolated experimentally and characterized by X-ray technique, were investigated. Comparison of the calculated geometry parameters of this molecule with their X-ray values shows an excellent agreement between the calculated and experimental geometries of Ni(dcype)(CO)₂.

4-10. Computational Data

Comparison of Experimental and Calculated Geometry Parameters (Distances in Å) of Ni(dcype)(CO)₂



Comparison of Experimental and Computational Geometry Parameters of Ni(Naph)(OPiv)(dcype) (5) (Distances are given in Å, angles are in deg.)

Distances/angles	Exp.	5
Ni-C1	1.940(6)	1.90708
Ni-O1	1.919(4)	1.92619
Ni-P1	2.1401(16)	2.15955
Ni-P2	2.2192(17)	2.23531
P1-Ni-P2	88.56(8)	89.835
P1-Ni-C1	91.85(18)	91.323
C1-Ni-O1	88.8(2)	88.408
O1-Ni-P2	89.89(13)	90.442
P1-Ni-O1	175.10(14)	179.721
P2-Ni-C1	168.9(2)	171.065

Reference and Notes

- 1 Selected reviews on inert bond activation: (a) Godula, K.; Sames, D. *Science* **2006**, *312*, 67. (b) Alberico, D.; Scott, M. E.; Lautens, M. *Chem. Rev.* **2007**, *107*, 174. (c) Davies, H. W. L.; Manning, J. R. *Nature* **2008**, *451*, 417. (d) Ackermann, L.; Vicente, R.; Kapdi, A. R. *Angew. Chem., Int. Ed.* **2009**, *48*, 9792. (e) Chen, X.; Engle, K. M.; Wang, D.-H.; Yu, J.-Q. *Angew. Chem., Int. Ed.* **2009**, *48*, 5094. (f) Gutekunst, W. R.; Baran, P. S. *Chem. Soc. Rev.* **2011**, *40*, 1976. (g) Yamaguchi, J.; Yamaguchi, A.; Itami, K. *Angew. Chem., Int. Ed.* **2012**, *51*, 8960. (h) Amii, H.; Uneyama, K. *Chem. Rev.* **2009**, *109*, 2119. (i) Tobisu, M.; Chatani, N. *Chem. Soc. Rev.* **2008**, *37*, 300.
- 2 Selected examples: (a) Garcia-Cuadrado, D.; de Mendoza, P.; Braga, A. A. C.; Maseras, F.; Echavarren, A. M. *J. Am. Chem. Soc.* **2007**, *129*, 6880. (b) Lewis, J. C.; Berman, A. M.; Bergman, R. G.; Ellman, J. A. *J. Am. Chem. Soc.* **2008**, *130*, 2493. (c) Musaev, D. G.; Kaledin, A.; Shi, B.-F.; Yu, J.-Q. *J. Am. Chem. Soc.* **2012**, *134*, 1690. (d) Jiao, L.; Herdtweck, E.; Bach, T. *J. Am. Chem. Soc.* **2012**, *134*, 14563. (e) Tan, Y.; Barrios-Landeros, B.; Hartwig, J. F. *J. Am. Chem. Soc.* **2012**, *134*, 3683.
- 3 (a) Muto, K.; Yamaguchi, J.; Itami, K. *J. Am. Chem. Soc.* **2012**, *134*, 169. (b) Amaike, K.; Muto, K.; Yamaguchi, J.; Itami, K. *J. Am. Chem. Soc.* **2012**, *134*, 13573. (c) Meng, L.; Kamada, Y.; Muto, K.; Yamaguchi, J.; Itami, K. *Angew. Chem., Int. Ed.* **2013**, *52*, 10048.
- 4 Recent reviews, see: (a) Li, B.-J.; Yu, D.-G.; Sun, C.-L.; Shi, Z.-J. *Chem. Eur. J.* **2011**, *17*, 1728. (b) Rosen, B. M.; Quasdorf, K. W.; Wilson, D. A.; Zhang, N.; Resmerita, A.-M.; Garg, N. K.; Percec, V. *Chem. Rev.* **2011**, *111*, 1346. (c) Yu, D.-G.; Li, B.-J.; Shi, Z.-J. *Acc. Chem. Res.* **2010**, *43*, 1486. (d) Yamaguchi, J.; Muto, K.; Itami, K. *Eur. J. Org. Chem.* **2013**, 19. (e) Mesganaw, T.; Garg, N. K. *Org. Process Res. Dev.* **2013**, *17*, 29.
- 5 Ni/PCy₃-catalyzed C–B/C–O biaryl coupling using phenol derivatives (ethers, esters, carbamates, carbonates, sulfamates, phosphates, and metal salts): (a) Tobisu, M.; Shimasaki, T.; Chatani, N. *Angew. Chem., Int. Ed.* **2008**, *47*, 4866. (b) Quasdorf, K. W.; Tian, X.; Garg, N. K. *J. Am. Chem. Soc.* **2008**, *130*, 14422. (c) Guan, B.-T.; Wang, Y.; Li, B.-J.; Yu, D.-G.; Shi, Z.-J. *J. Am. Chem. Soc.* **2008**, *130*, 14468. (d) Quasdorf, K. W.; Riener, M.; Petrova, K. V.; Garg, N. K. *J. Am. Chem. Soc.* **2009**,

- 131, 17748. (e) Antoft-Finch, A.; Blackburn, T.; Snieckus, V. *J. Am. Chem. Soc.* **2009**, *131*, 17750. (f) Xi, L.; Li, B.-J.; Wu, Z.-H.; Lu, X.-Y.; Guan, B.-T.; Wang, B.-Q.; Zhao, K.-Q.; Shi, Z.-J. *Org. Lett.* **2010**, *12*, 884. (g) Quasdorf, K. W.; Antoft-Finch, A.; Liu, P.; Silberstein, A. L.; Komaromi, A.; Blackburn, T.; Ramgren, S. D.; Houk, K. N.; Snieckus, V.; Garg, N. K. *J. Am. Chem. Soc.* **2011**, *133*, 6352. (h) Chen, H.; Huang, Z.; Hu, X.; Tang, G.; Xu, P.; Zhao, Y.; Cheng, C.-H. *J. Org. Chem.* **2011**, *76*, 2338. (i) Yu, D.-G.; Shi, Z.-J. *Angew. Chem., Int. Ed.* **2011**, *50*, 7097. (j) Ramgren, S. D.; Hie, L.; Ye, Y.; Garg, N. K. *Org. Lett.* **2013**, *15*, 3950.
- 6 Kelly, P.; Lin, S.; Edouard, G.; Day, M. W.; Agapie, T. *J. Am. Chem. Soc.* **2012**, *134*, 5480.
- 7 Cornella, J.; Gómez-Bengoa, E.; Martin, R. *J. Am. Chem. Soc.* **2013**, *135*, 1997.
- 8 (a) Ueno, S.; Mizushima, E.; Chatani, N.; Kakiuchi, F. *J. Am. Chem. Soc.* **2006**, *128*, 16516. (b) Zhu, Y.; Smith, D. A.; Herbert, D. E.; Gatard, S.; Ozerov, O. V. *Chem. Commun.* **2012**, *48*, 218.
- 9 An asymmetric unit contains two independent molecules having only slightly different bond lengths and angles between them. One of them is omitted for clarity.
- 10 Yamamoto, T.; Wakabayashi, S.; Osakada, K. *J. Organomet. Chem.* **1992**, *428*, 223.
- 11 For reviews, see: (a) Lapointe, D.; Fagnou, K. *Chem. Lett.* **2010**, *39*, 1118. (b) Ackermann, L. *Chem. Rev.* **2011**, *11*, 1315.
- 12 Simmons, E. M.; Hartwig, J. F. *Angew. Chem., Int. Ed.* **2012**, *51*, 3066.
- 13 (a) Hong, X.; Liang, Y.; Houk, K. N. *J. Am. Chem. Soc.* **2014**, *136*, 2017. (b) Lu, Q.; Yu, H.; Fu, Y. *J. Am. Chem. Soc.* **2014**, *136*, 8252. (c) Li, Z.; Zhang, S.-L.; Fu, Y.; Guo, Q.-X.; Liu, L. *J. Am. Chem. Soc.* **2009**, *131*, 8815. (d) Liu, L.; Zhang, S.; Chen, H.; Lv, Y.; Zhu, J.; Zhao, Y. *Chem. Asian J.* **2013**, *8*, 2592.
- 14 (a) Garcia, J. J.; Brunkan, N. M.; Jones, W. D. *J. Am. Chem. Soc.* **2002**, *124*, 9547. (b) Yoshikai, N.; Matsuda, H.; Nakamura, E. *J. Am. Chem. Soc.* **2008**, *130*, 15258.
- 15 (a) Birkholz, M.-N.; Freixa, Z.; van Leeuwen, P. W. N. M. *Chem. Soc. Rev.* **2009**, *38*, 1099. (b) Clegg, W.; Eastham, G. R.; Elsegood, M. R. J.; Heaton, B. T.; Iggo, J. A.; Tooze, R. P.; Whyman, R.; Zacchini, S. *Organometallics* **2002**, *21*, 1832.
- 16 Shen, K.; Fu, Y.; Li, J.-N.; Liu, L.; Guo, Q.-X. *Tetrahedron* **2007**, *63*, 1568.
- 17 Mahler, J.; Persson, I. *Inorg. Chem.* **2012**, *51*, 425.

- 18 Gorelsky, S. I.; Lapointe, D.; Fagnou, K. *J. Org. Chem.* **2011**, *77*, 658.
- 19 Bayh, O.; Awad, H.; Mongin, F.; Hoarau, C.; Bischoff, L.; Trécourt, F.; Quéguiner, G.; Marsais, F.; Blanco, F.; Abarca, B.; Ballesteros, R. *J. Org. Chem.* **2005**, *70*, 5190.
- 20 Altomare, A.; Burla, M. C.; Camalli, M.; Cascarano, G. L.; Giacovazzo, C.; Guagliardi, A.; Moliterni, A. G. G.; Polidori, G.; Spagna, R. *J. Appl. Crystallogr.* **1999**, *32*, 115.
- 21 Sheldrick, G. M. University of Göttingen: Göttingen, Germany, **1997**.
- 22 Frisch, M. J.; Trucks, G. W.; Schlegel, H. B.; Scuseria, G. E.; Robb, M. A.; Cheeseman, J. R.; Scalmani, G.; Barone, V.; Mennucci, B.; Petersson, G. A.; Nakatsuji, H.; Caricato, M.; Li, X.; Hratchian, H. P.; Izmaylov, A. F.; Bloino, J.; Zheng, G.; Sonnenberg, J. L.; Hada, M.; Ehara, M.; Toyota, K.; Fukuda, R.; Hasegawa, J.; Ishida, M.; Nakajima, T.; Honda, Y.; Kitao, O.; Nakai, H.; Vreven, T.; Montgomery, J. A., Jr.; Peralta, J. E.; Ogliaro, F.; Bearpark, M.; Heyd, J. J.; Brothers, E.; Kudin, K. N.; Staroverov, V. N.; Keith, T.; Kobayashi, R.; Normand, J.; Raghavachari, K.; Rendell, A.; Burant, J. C.; Iyengar, S. S.; Tomasi, J.; Cossi, M.; Rega, N.; Millam, J. M.; Klene, M.; Knox, J. E.; Cross, J. B.; Bakken, V.; Adamo, C.; Jaramillo, J.; Gomperts, R.; Stratmann, R. E.; Yazyev, O.; Austin, A. J.; Cammi, R.; Pomelli, C.; Ochterski, J. W.; Martin, R. L.; Morokuma, K.; Zakrzewski, V. G.; Voth, G. A.; Salvador, P.; Dannenberg, J. J.; Dapprich, S.; Daniels, A. D.; Farkas, O.; Foresman, J. B.; Ortiz, J. V.; Cioslowski, J.; Fox, D. J. Gaussian 09, Revision D.01; Gaussian, Inc.: Wallingford CT, 2013.
- 23 Zhao, Y.; Truhlar, D. G. *J. Chem. Phys.* **2006**, *125*, 194101.
- 24 (a) Wadt, W. R.; Hay, P. J. *J. Chem. Phys.* **1985**, *82*, 284. (b) Hay, P. J.; Wadt, W. R. *J. Chem. Phys.* **1985**, *82*, 299.
- 25 (a) Mennucci, B.; Tomasi, J. *J. Chem. Phys.* **1997**, *106*, 3032. (b) Mennucci, B.; Tomasi, J. *J. Chem. Phys.* **1997**, *106*, 5151. (c) Scalmani, G.; Frisch, M. J. *J. Chem. Phys.* **2010**, *132*, 114110.
- 26 For M06 method see: (a) Zhao, Y.; Truhlar, D. G. *Theor. Chem. Acc.* **2008**, *120*, 215. (b) Zhao, Y.; Truhlar, D. G. *Acc. Chem. Res.* **2008**, *41*, 157. (c) Zhao, Y.; Truhlar, D. G. *J. Chem. Theory Comput.* **2009**, *5*, 324.

C–H Arylation and Alkenylation of Imidazoles with Nickel Catalyst

Abstract

In this chapter, the first Ni-catalyzed C–H coupling of imidazoles including benzimidazoles is described. Under the influence of Ni(OTf)₂/dcype/K₃PO₄ (dcype: 1,2-bis(dicyclohexylphosphino)ethane) in *t*-AmylOH, imidazoles can undergo C–H arylation with phenol derivatives. By changing the ligand to dcpyt (3,4-bis(dicyclohexylphosphino)thiophene), enol derivatives can be employed as C–H alkenylation participants. The key to success in this C–H coupling of imidazoles is the use of tertiary alcohol as solvent. This protocol allows the use of air-stable Ni(II) as a metal source. Using this inexpensive nickel catalytic system, various C2-arylated and alkenylated imidazoles can be synthesized.

1. Introduction

Imidazoles including benzimidazoles are recognized as important chemical motifs since they are frequently found in a range of natural products, pharmaceuticals, and organic materials. Because of the high potential of imidazole-containing compounds, functionalization and derivatization thereof are of significant importance in synthetic organic chemistry. Furthermore, C2-arylated and alkenylated imidazoles are one of the most privileged organic motifs in pharmaceuticals as well as drug candidates.^[1] Numerous synthetic methods to construct C2-aryl and alkenyl imidazoles have been reported thus far. Although cyclization or annulation reactions have found wide use, these methods often suffer from inefficiencies in terms of low reaction yields and multiple reaction sequences.^[2] Transition metal-catalyzed cross-coupling reactions of arylmetal compounds and aryl halides have also been employed, albeit requiring the pre-functionalization of metalated or halogenated imidazoles prior to the coupling reaction.^[3]

Recently, transition metal-catalyzed C–H functionalization has attracted attention as a method that enables the rapid and straightforward synthesis of various functional heteroarenes. Within this class of reactions, C–H arylation^[4] and alkenylation of imidazoles using transition metal catalysts have been reported, mainly involving palladium^[5] and rhodium.^[6] In 2009, Daugulis and co-workers discovered a Cu-catalyzed C–H arylation of imidazoles, which allowed the use of an inexpensive transition metal catalyst.^[7]

As mentioned in previous chapters, several nickel catalysts^[8] were developed and enabled the C–H arylation of 1,3-azoles with haloarenes (C–H/C–X coupling),^[9] phenol derivatives (C–H/C–O coupling),^[10] and arenecarboxylates (decarbonylative C–H coupling).^[11] Oxazoles, benzoxazoles, thiazoles, and benzothiazoles can undergo these Ni-catalyzed C–H couplings. The advantage of a nickel catalytic system is not only its low cost, but also its ability to activate and couple phenol derivatives (C–O electrophiles).^[12, 13] However, imidazoles and benzimidazoles still remained as challenging substrates for Ni-catalyzed C–H coupling (Figure 1).^[14]

Previous Metal-Catalyzed C–H Coupling of Imidazoles



Previous Ni-Catalyzed C–H Coupling of Oxazoles and Thiazoles

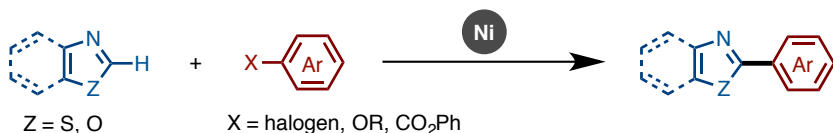
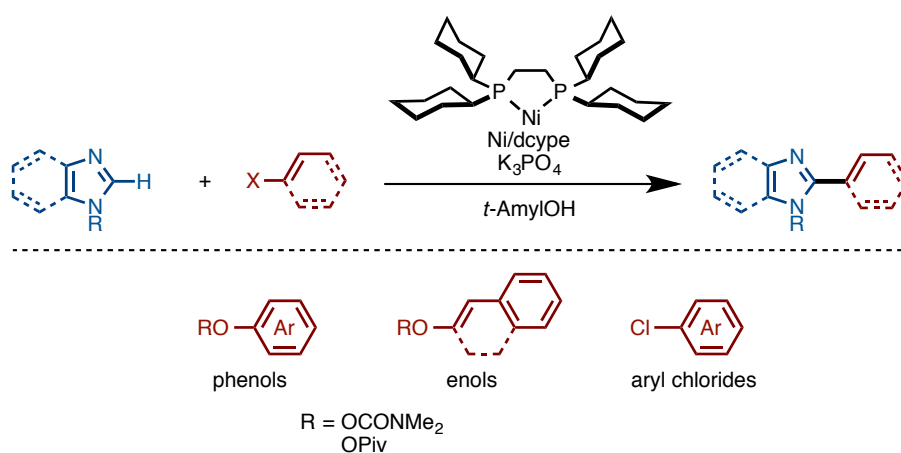


Figure 1. Transition metal-catalyzed C–H arylation of imidazoles and Ni-catalyzed C–H arylation of 1,3-azoles

In this chapter, the development of a new protocol for Ni/dcype-catalyzed C–H arylation and alkenylation of imidazoles is described. This new protocol using Ni/dcype as catalyst and K₃PO₄ as base in *t*-AmylOH enabled not only C–H/C–O arylation of imidazoles using phenol derivatives, but also C–H/C–O alkenylation with enol derivatives. The coupling conditions allowed even the use of aryl chlorides as coupling partners. Furthermore, this protocol has broader substrate generality than the previous protocol, allowing thiazoles as well as oxazoles to undergo C–H/C–O coupling. The key to success proved to be the use of *t*-AmylOH as solvent. The effect of *t*-AmylOH solvent is discussed through mechanistic investigations including kinetic studies.



Scheme 1. Ni-catalyzed C–H coupling of imidazoles

2. Results and Discussion

2-1. C–H Arylation of Imidazoles with Phenol Derivatives

This study was initiated by the re-optimization of the Ni/dcype-catalyzed system in the C–H coupling of 1,3-azoles and phenol derivatives. The reaction conditions using Ni(cod)₂/dcype as catalyst and Cs₂CO₃ as base in 1,4-dioxane can promote the C–H/C–O coupling of azoles and phenols. However, it was experimentally and computationally proven that imidazoles are not reactive under Ni/dcype catalysis. Thus, it was necessary to design a new reaction mode in the C–H activation step. While the Ni/dcype catalysis displayed a dramatic ligand effect, other parameters such as base and solvent were rather tunable. Additionally, mechanistic investigations described in Chapter 4 revealed that the choice of solvent impacts the oxidative addition of the C–O bond. The use of *t*-AmylOH can accelerate this particular step via proton coordination to the heteroatom of the C–O electrophile (i.e. hydrogen bonding). Furthermore, it was found that the reactivity of the azole in the C–H nickelation step depends on the acidity of the C–H bond. It was envisaged that *t*-AmylOH hydrogen bond can increase the acidity of the C–H bond of imidazole, and thus, it was presumed that the development of C–H coupling reaction of imidazoles is viable (Figure 2).

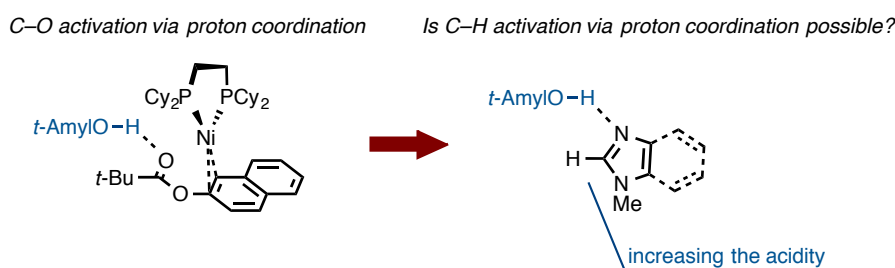
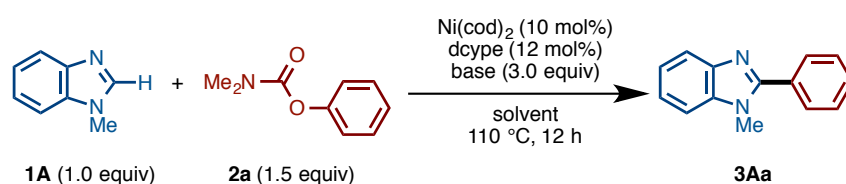


Figure 2. Mechanistic blueprint to activate imidazoles

With this blueprint in mind, this study embarked on the investigation of appropriate bases and solvents by using *N*-methylbenzimidazole (**1A**) and phenyl carbamate **2a** as model substrates (Table 1). The previous reaction conditions that employ Cs₂CO₃ as base in 1,4-dioxane afforded no coupling products (entry 1). Delightfully, the change of 1,4-dioxane to *t*-AmylOH promoted the desired C–H arylation of **1A**, generating **3Aa** in 44% yield (entry 2). The reaction yield was further improved when using K₃PO₄ as base, providing the desired product in 83% yield (entry 3). Additionally, the desired product

was obtained in lower yields in the presence of Cs₂CO₃ or LiOt-Bu compared to K₃PO₄ (entries 4 and 5). *In situ*-generated potassium tertiary alkoxide can be thought as potentially active species, however, the use of KOt-Bu completely shut down the catalytic activity (entry 6). Setting K₃PO₄ as the optimal base, the solvent effect on the C–H arylation of imidazoles was further investigated. As expected, the use of tertiary alcohol as solvent was crucial, while other aprotic and secondary alcohol solvents were completely ineffective for this reaction (entries 7–9).

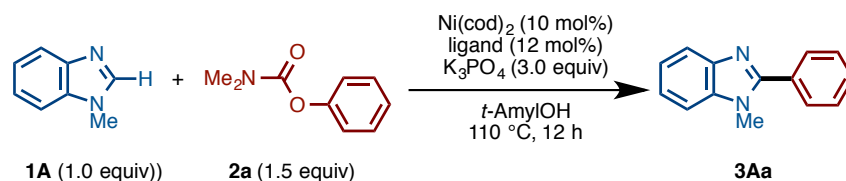
Table 1. Investigation of base and solvent in the Ni-catalyzed coupling of **1A** and **2a**



entry ^a	base	solvent	3Aa (%) ^b
1	Cs ₂ CO ₃	1,4-dioxane	0
2	Cs ₂ CO ₃	<i>t</i> -AmylOH	44
3	K ₃ PO ₄	<i>t</i> -AmylOH	83
4	LiOt-Bu	<i>t</i> -AmylOH	59
5	KOt-Bu	<i>t</i> -AmylOH	0
6	K ₃ PO ₄	<i>t</i> -BuOH	70
7	K ₃ PO ₄	1,4-dioxane	0
8	K ₃ PO ₄	DMF	0
9	K ₃ PO ₄	<i>i</i> -PrOH	0

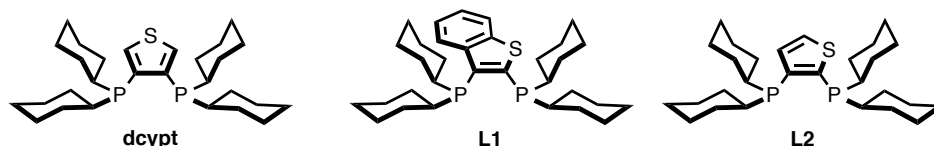
[a] Reaction conditions were as follows: **1A** (0.40 mmol), **2a** (1.5 equiv), Ni(cod)₂ (10 mol%), dcype (12 mol%), base (3.0 equiv), solvent (1.6 mL), 110 °C, 12 h. [b] GC yield determined by using dodecane as an internal standard

Regarding the ligand effect, PCy₃ and an *N*-heterocyclic carbene ligand were inactive for the present reaction (Table 2, entries 1 and 2). A thiophene-based diphosphine ligand, dcyp^t (3,4-bis(dicyclohexylphosphino)thiophene),^[15] as well as other dcype derivatives such as **L1** and **L2** furnished **3Aa** in moderate yields (entries 3–5). Gratifyingly, an air-stable Ni(OTf)₂ maintained the catalytic activity (entry 6). Finally, reaction conditions using catalytic Ni(OTf)₂/dcype and K₃PO₄ in *t*-AmylOH were identified as optimized conditions for the C–H coupling.

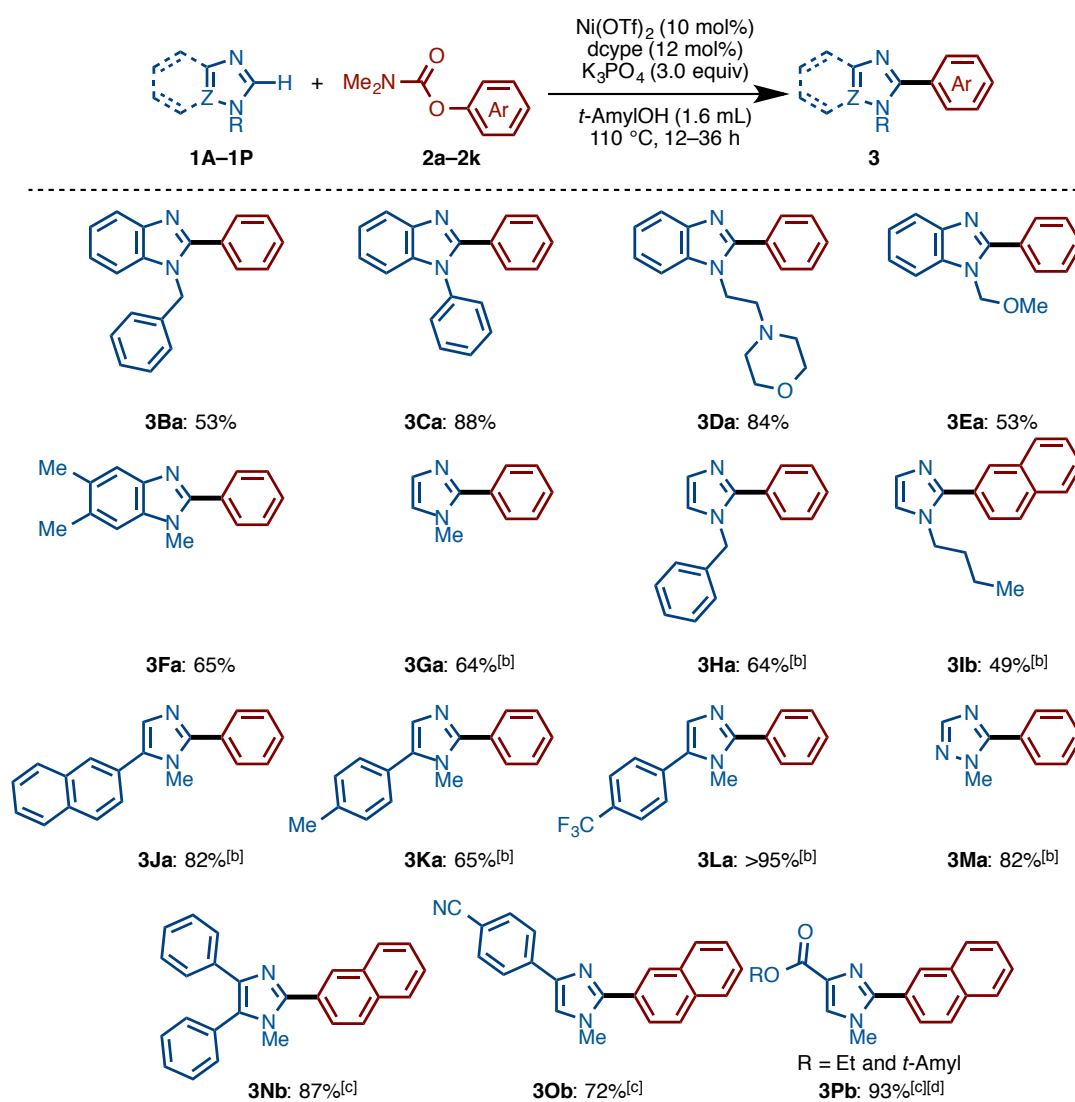
Table 2. Investigation of the ligand effect in the Ni-catalyzed imidazole coupling

entry ^a	ligand	3Aa (%) ^b
1	PCy ₃	0
2	IPr·HCl	0
3	dcypt	55
4	L1	53
5	L2	64
6	dcype	82 ^c

[a] Reaction conditions were as follows: **1A** (0.40 mmol), **2a** (1.5 equiv), Ni(cod)₂ (10 mol%), dcypt (12 mol%), K₃PO₄ (3.0 equiv), solvent (1.6 mL), 110 °C, 12 h.
[b] determined by using dodecane as an internal standard
[c] Ni(OTf)₂ was used instead of Ni(cod)₂.



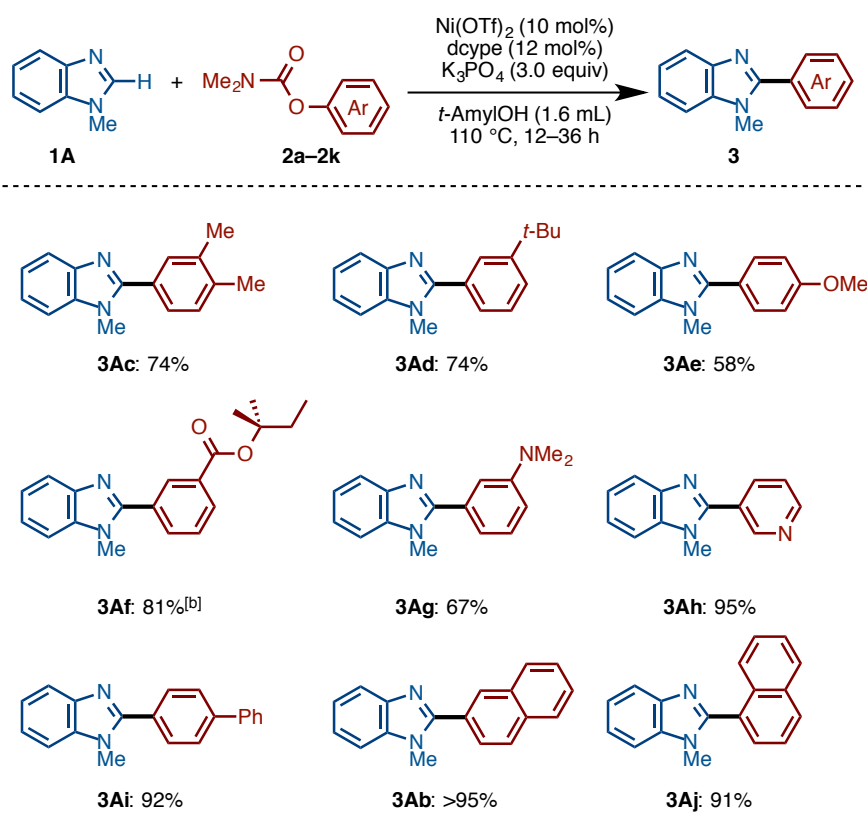
The substrate scope for the C-H/C-O coupling of imidazoles was then examined (Scheme 2). Several *N*-substituted benzimidazoles such as *N*-benzyl (**1B**), phenyl (**1C**), morpholinoethyl (**1D**), and methoxymethyl benzimidazoles (**1E**) underwent C-H/C-O coupling to afford the corresponding products in moderate to excellent yields. In addition to benzimidazoles, imidazoles were also successfully coupled with phenol derivatives, although the use of Ni(cod)₂ as the catalyst precursor as well as longer reaction times were required. This reaction likely preferred having electron-withdrawing groups over electron-donating groups on the phenyl ring at the C5 position of the imidazole. For example, the reaction of CF₃-substituted 5-arylimidazole furnished triaryl **3La** in superior yield (>95%) than that of Me-substituted triaryl **3Ka** (65%). Although the reason remains unclear at this stage, the dcypt ligand gave better results in the case of C4-substituted imidazoles (**1N**, **1O**, and **1P**). Notably, triazole **1M** also underwent C-H/C-O coupling with 5-phenyl-*N*-methyl-1,2,4-triazole (**3Ma**) in 82% yield. It should be emphasized that this coupling reaction proceeds with high regioselectivity at the C2 position of azoles, as both C4 and C5 positions on the imidazoles were intact under the developed nickel catalyst system.



[a] Unless otherwise noted, reaction conditions were as follows: **1** (0.40 mmol), **2** (1.5 equiv), Ni(OTf)₂ (10 mol%), dcype (12 mol%), K₃PO₄ (3.0 equiv), *t*-AmylOH (1.6 mL), 110 °C, 12–36 h. [b] Ni(cod)₂ (10 mol%) was used. [c] Ni(cod)₂ (10 mol%) and dcyp^t (12 mol%) was used. [d] Starting from ethyl 4-imidazolecarboxylate **1P**. (R = Et: 33%; *t*-Amyl: 60%).

Scheme 2. Substrate scope of the C–H/C–O arylation

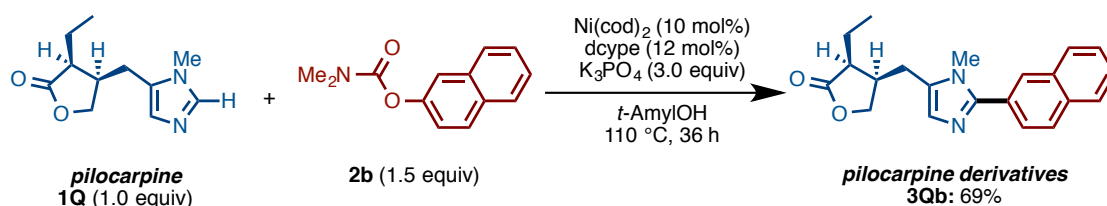
Regarding aryl electrophiles, a broad functional group tolerance was observed (Scheme 3). A catalyst-deactivating amino group did not inhibit the reaction when generating **3Ag**. Although transesterification took place when ethoxycarbonyl-substituted phenol electrophile **2f** was used, the corresponding product **3Af** was generated in good yield. Furthermore, heteroarene coupling partners such as 3-pyridyl **2h** could couple to generate pyridin-3-yl imidazoles **3Ah** in excellent yield.



^[a] Unless otherwise noted, reaction conditions were as follows: **1A** (0.40 mmol), **2** (1.5 equiv), Ni(OTf)₂ (10 mol%), dcype (12 mol%), K₃PO₄ (3.0 equiv), *t*-AmylOH (1.6 mL), 110 °C, 12–36 h. ^[b] Starting from methyl 3-((dimethylcarbamoyl)oxy)benzoate (**2f**).

Scheme 3. Substrate scope of C–H/C–O arylation

Delightfully, pilocarpine (**1Q**), which is a drug for the treatment of dry mouth,^[16] could be directly functionalized in 69% yield without lactone opening or epimerization at the α -position of the carbonyl group (Scheme 4).

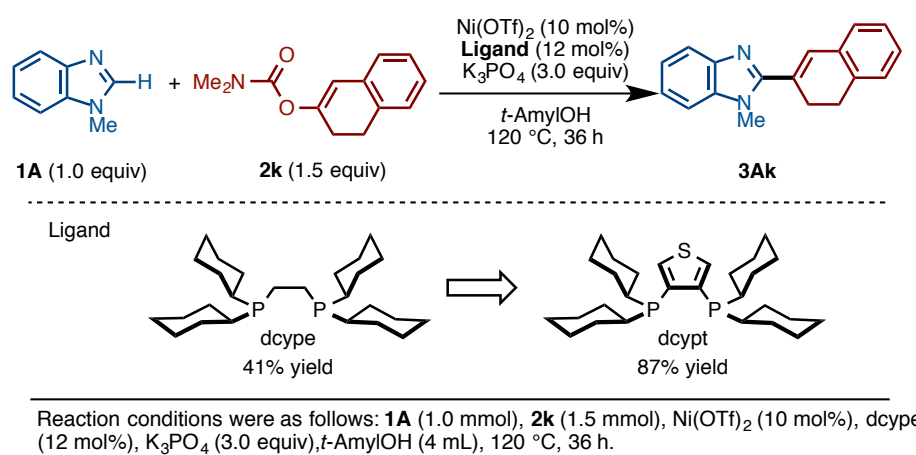


Scheme 4. C–H coupling of pilocarpine

2-2. C–H Alkenylation of Imidazoles with Enol Derivatives

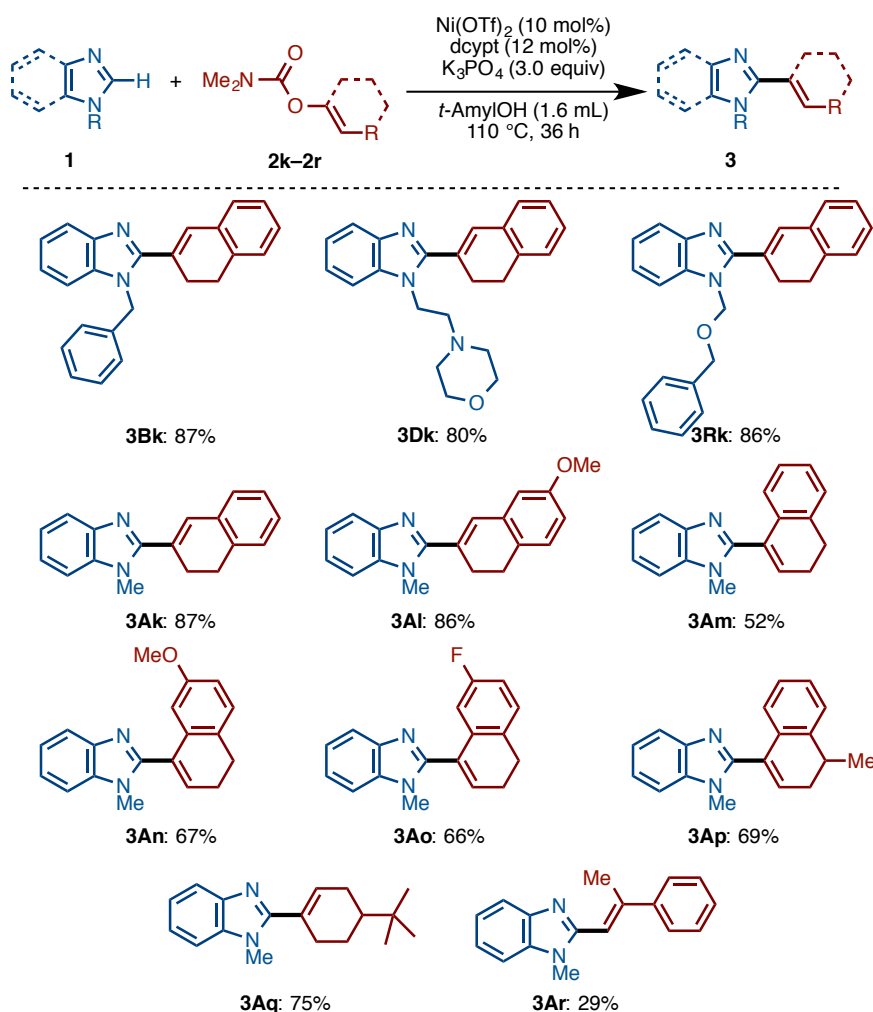
With the previous success of Ni-catalyzed C–H alkenylation of oxazoles with enol derivatives (C–H/C–O alkenylation),^[10b, 17] it was assumed that alkenylation of imidazoles under the optimized conditions would be feasible. The use of C–O alkenyl

electrophiles for coupling reactions is advantageous because they could be easily prepared from the corresponding ketones and aldehydes. Motivated by the fact that the alkenyl group is a versatile platform in organic synthesis, the present study next embarked on the development of C–H/C–O alkenylation of imidazoles (Scheme 5). Although the coupling reaction of **1A** with **2k** under Ni/dcype catalysis is feasible, it provided alkenylated product **3Ak** in only 41% yield. While changes in base and solvent did not lead to the improvement of the reaction yield, Ni/dcyp_t catalyst was drastically effective for the C–H/C–O alkenylation, providing the coupling product **3Ak** in 87% yield.



Scheme 5. Discovery of C–H alkenylation of imidazoles using dcyp_t

With the establishment of the reaction conditions for C–H/C–O alkenylation, it was found that the alkenylation reaction also had broad substrate generality (Scheme 6). As with the case of biaryl couplings, several *N*-alkylated benzimidazoles (such as **1B**, **1D**, **1R**) were successfully coupled with enol carbamates. Enol carbamates synthesized from both α - and β -tetralones were reactive using the Ni/dcyp_t catalyst to afford the coupling products **3Ak–3Ap**. Cyclohexenyl benzimidazole **3Aq** could be accessed from cyclohexanone-derived enols. Aldehyde-derived enol **2r** could be coupled, but was unfortunately found to be less operative owing to its fast decomposition under these reaction conditions. Although the cleavage of C–OMe^[13a,e] and C–F bonds^[18] are known reaction processes in nickel catalysis, these groups were completely tolerated in the present Ni-catalyzed coupling reaction.



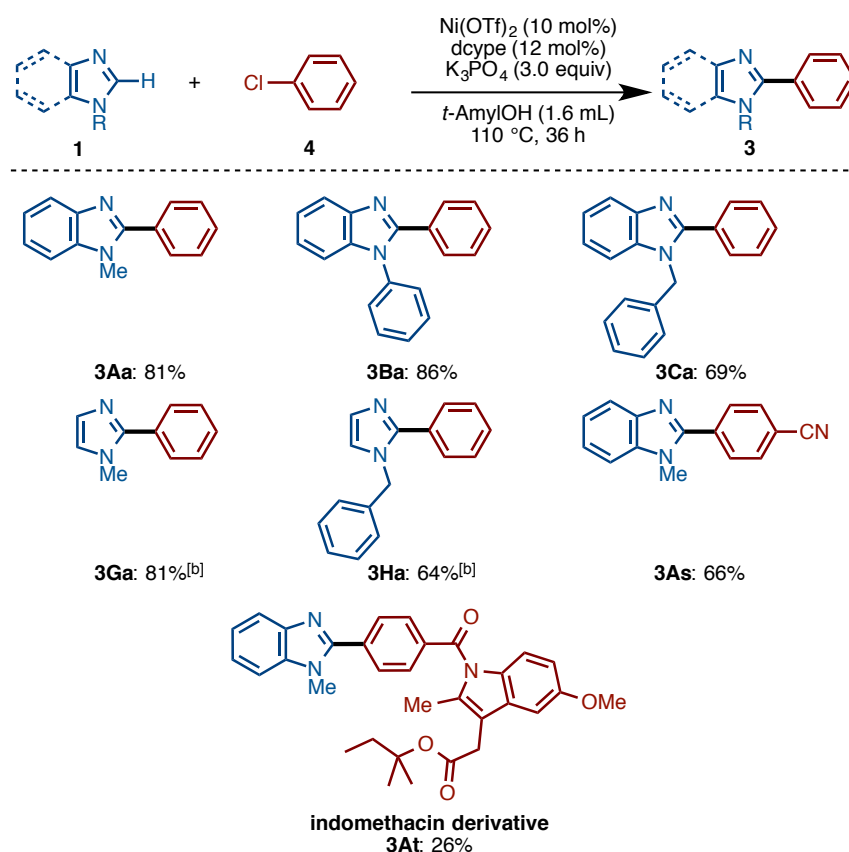
[a] Unless otherwise noted, reaction conditions were as follows: **1** (1.0 mmol), **2** (1.5 equiv), Ni(OTf)₂ (10 mol%), dcypt (12 mol%), K₃PO₄ (3.0 equiv), *t*-AmylOH (4.0 mL), 120 °C, 36 h.

Scheme 6. Scope of C–H/C–O alkenylation

2-3. C–H Arylation of Imidazoles with Chloroarenes

Strikingly, the developed Ni/dcypt catalytic system allowed the use of aryl chlorides as electrophiles, generating phenylated imidazoles in excellent yield without any modification of reaction conditions. Curiously, the reactions of aryl iodides and bromides resulted in poor or zero yields of product. The reactivity of imidazoles for the coupling reaction with aryl chlorides was identical to the reaction with phenol derivatives (Scheme 7). *N*-Methyl, phenyl, and benzyl benzimidazoles underwent C–H coupling with chlorobenzene (**4a**) to deliver phenylated imidazoles in good yield. *N*-Methyl (**1G**) and benzyl (**1H**) imidazoles also reacted well. Nitrile-substituted aryl chloride **4s** furnished the corresponding product **3As** in good yield. Although the

reaction yield was low (26%), indomethacin derivative **4t** could be applied to the reaction to give **3At**, but with significant amounts of homodimerization by-product.



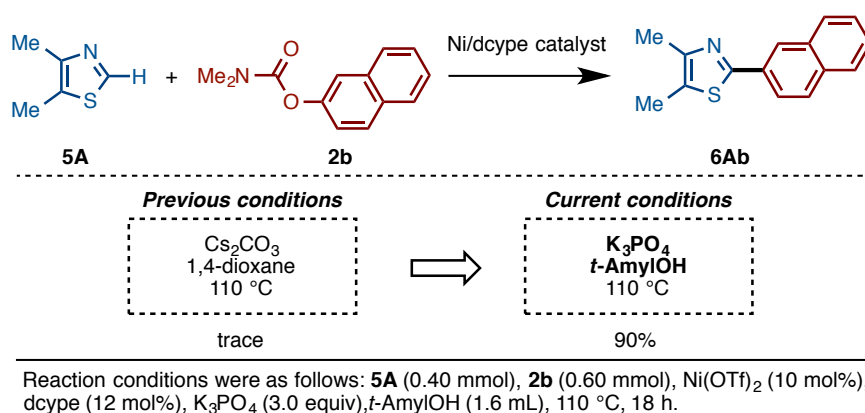
[a] Unless otherwise noted, reaction conditions were as follows: **1** (0.40 mmol), **4** (1.5 equiv), $\text{Ni}(\text{OTf})_2$ (10 mol%), dcype (12 mol%), K_3PO_4 (3.0 equiv), $t\text{-AmylOH}$ (1.6 mL), $110\text{ }^\circ\text{C}$, 36 h. [b] $\text{Ni}(\text{cod})_2$ (10 mol%) was used.

Scheme 7. Substrate scope of aryl chlorides in the C–H coupling of (benz)imidazoles

2-4. C–H/ C–O Coupling of Other 1,3-Azoles

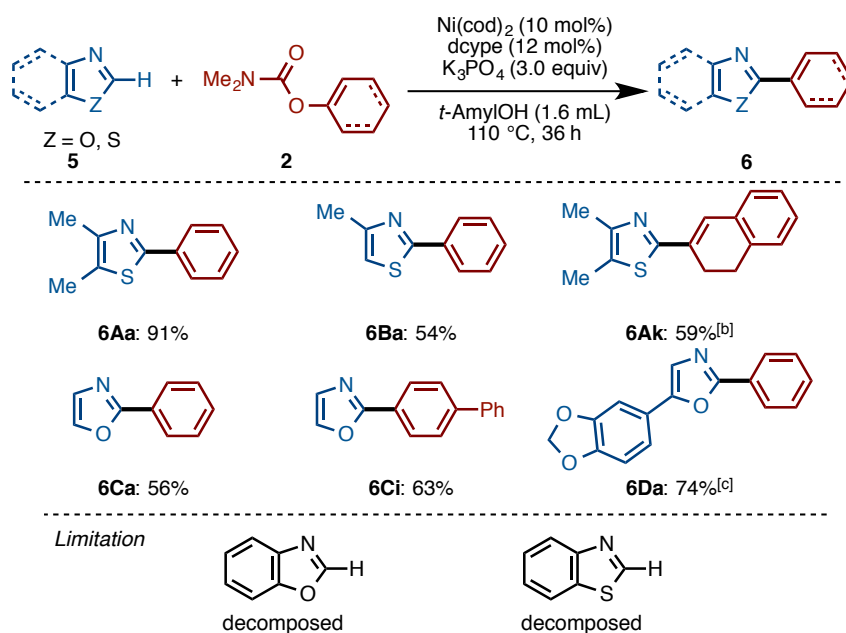
The present catalytic protocols were found to be practical not only for imidazoles, but also for thiazoles and oxazoles. The previous reaction protocol (Cs_2CO_3 in 1,4-dioxane) was active for oxazoles and thiazoles,^[10] and in particular, for benzo-fused 1,3-azoles. However, when relatively electron-rich azoles were employed under previous reaction protocol, the reaction efficiency was not satisfying. For example, the reaction of 4,5-dimethylthiazole (**5A**) with naphthyl carbamate **2b** under the previous conditions furnished no coupling product. Thus, the new protocol with K_3PO_4 in $t\text{-AmylOH}$ was applied to the reaction of previously unreactive azole **5A**. Fortunately, it was found that this new protocol is also operative for thiazoles, furnishing **6Ab** in excellent yield

(Scheme 8).



Scheme 8. Comparison of previous and present conditions for the reaction of **5A**

Shown in Scheme 9 are the results of the Ni-catalyzed reaction of other 1,3-azoles. In addition to thiazoles, oxazoles were also found to be appropriate substrates, generating the corresponding coupling product in good yield. Although previous alkenylation reactions with C–O electrophiles were limited to the reaction of oxazoles, the present Ni-catalyzed reaction in *t*-AmylOH was also applicable to thiazoles. However, more acidic C–H substrates such as benzoxazole and benzothiazole resulted in decomposition when exposed to the present *t*-AmylOH protocol despite being reactive under the previous C–H/C–O coupling condition.



[a] Unless otherwise noted, reaction conditions were as follows: **5** (0.40 mmol), **2** (1.5 equiv), Ni(OTf)₂ (10 mol%), dcype (12 mol%), K₃PO₄ (3.0 equiv), *t*-AmylOH (1.6 mL), 110 °C, 36 h. [b] Ni(OTf)₂ (10 mol%) and dcype (12 mol%) was used. [c] Ni(OTf)₂ (10 mol%) and dcype (12 mol%) was used.

Scheme 9. Substrate scope of oxazoles and thiazoles

2-5. Mechanistic Studies

A plausible catalytic cycle consisting of a Ni(0)/Ni(II) redox cycle is shown in Figure 3. First, oxidative addition of the aryl electrophile's C–O or C–Cl bond to Ni(0) **A** can take place to generate intermediate **B**. Then, base-promoted C–H nickelation of (benz)imidazole, followed by reductive elimination would furnish the cross-coupled product with regeneration of active Ni(0) species **A**. Previously, intermediate **B** was successfully isolated and characterized by using naphthalen-2-yl pivalates as a C–O electrophile,^[10c] which can support the hypothesized catalytic cycle. In this work, the use of *t*-AmylOH allowed imidazoles to participate in this catalytic cycle. However, the role of *t*-AmylOH to enhance the reactivity of imidazoles is unclear, and therefore this study next aimed at elucidating the solvent effect.

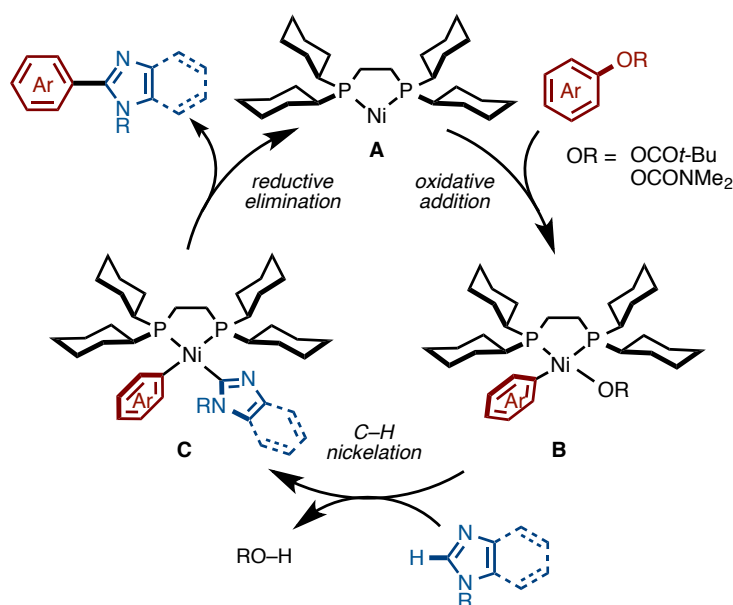


Figure 3. A plausible catalytic cycle for the Ni-catalyzed C–H/C–O coupling reaction

First, kinetic studies were performed with the “reaction progress kinetic analysis” (RPKA) method, which is advocated by Blackmond.^[19] The reaction progress of *N*-methylbenzimidazole (**1A**) with naphthalen-2-yl pivalate (**2b'**) under the standard conditions was monitored with gas chromatography. Before performing RPKA, it should be mentioned that “excess” is defined as shown in equation (1).

$$\text{excess} = [\mathbf{2b}']_0 - [\mathbf{1A}]_0 \quad (1)$$

RPKA consists two kinds of experiments, “same excess” and “different excess” experiments. Following the RPKA method, the “same excess” experiment was initially conducted. Figure 4 displays the two obtained reaction profiles [(a): $[\mathbf{1A}]_0 = 0.250$ M, $[\mathbf{2b}']_0 = 0.375$ M, excess = 0.125 M; green, and (b): $[\mathbf{1A}]_0 = 0.125$ M, $[\mathbf{2b}']_0 = 0.25$ M, excess = 0.125 M; red] and a concentration-adjusted profile (b') (light red). The reaction profile of run (a) and concentration-adjusted profile (b') were almost matching at the initial stage of the reaction, indicating that the reaction rate of C–H coupling of **1A** and **2b'** does not depend on the concentration of both substrates. In other words, the reaction rate of the Ni-catalyzed C–H coupling is likely zero order in both $[\mathbf{1A}]$ and $[\mathbf{2b}']$.

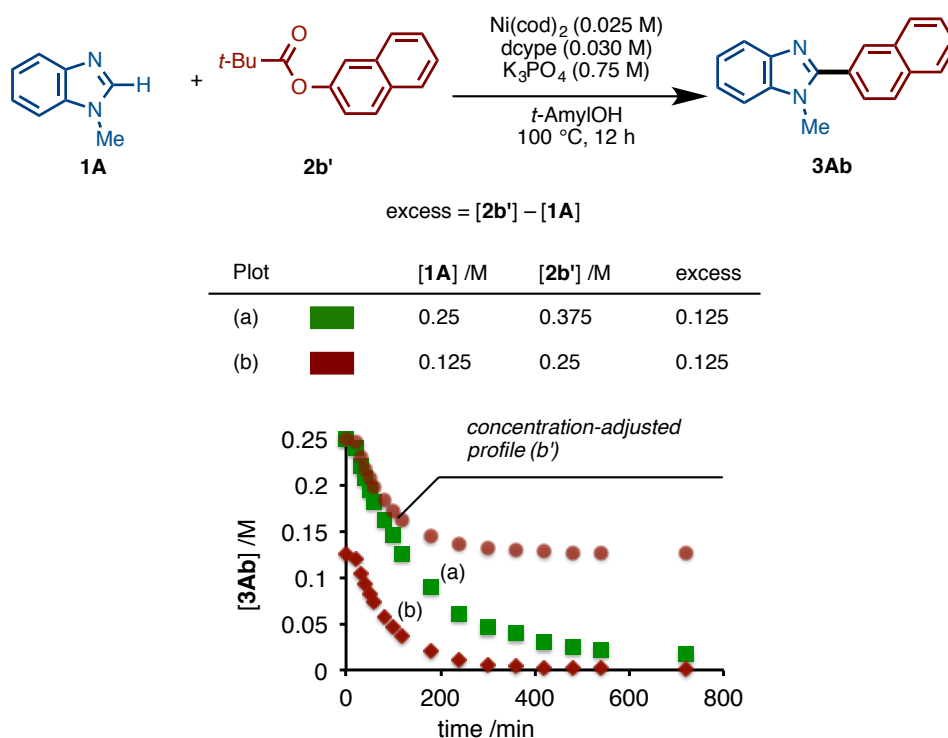


Figure 4. Same excess experiments for the Ni-catalyzed C–H/C–O coupling reaction

In order to confirm that the reaction rate of the present C–H coupling is zero order in [1A] and [2b'], different excess experiments were further conducted (Figure 5). The result of the reactions of different [1A]₀ are illustrated in Figure 5A. The reaction profiles at the initial reaction rate of run (a) and (b) were identical. Similarly, regarding the reactions of different [2b']₀, the profile at the initial reaction rate of run (a) and (c) also overlapped (Figure 5B). Thus, the “same excess” and “different excess” experiments support that this Ni-catalyzed C–H arylation of **1A** with **2b'** is zero order in both [1A] and [2b'].

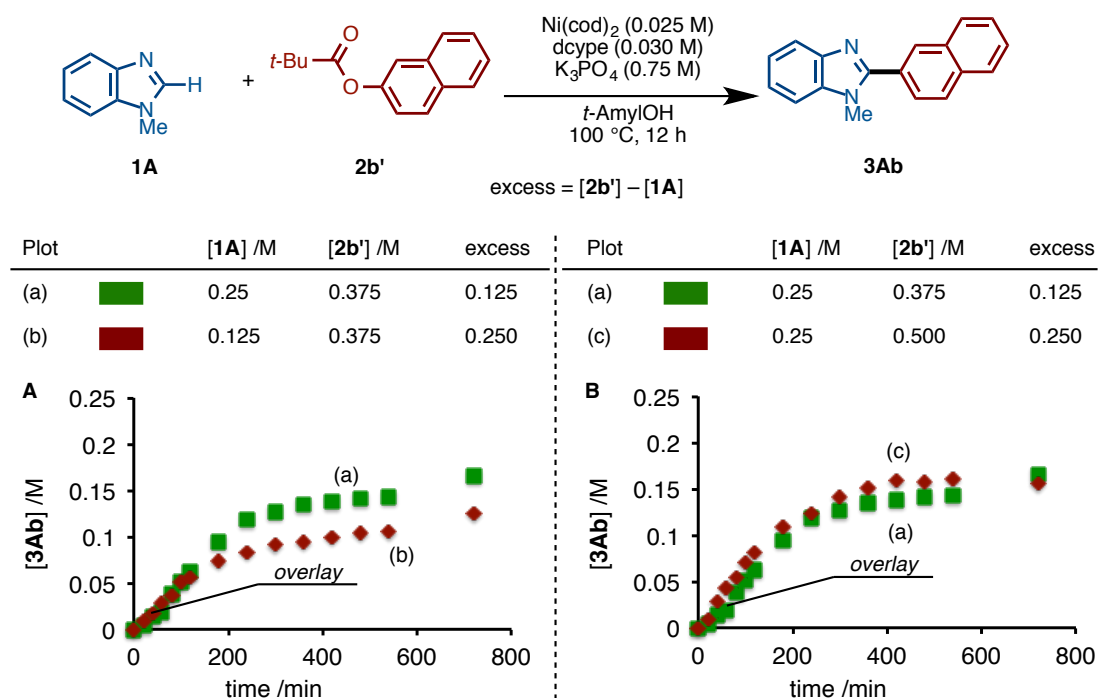
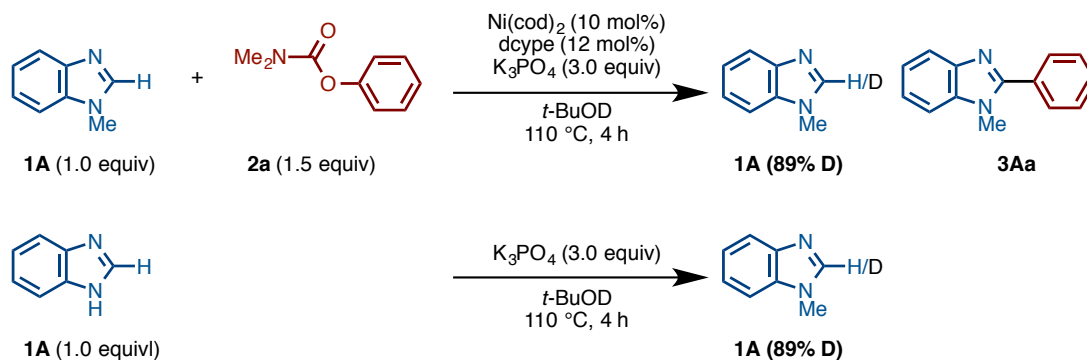


Figure 5. Different excess experiments for the Ni-catalyzed C–H/C–O coupling reaction

With this RPKA result, reductive elimination can be thought as the rate-determining step of the reaction. However, previous DFT studies described in Chapter 4 showed that the reductive elimination, albeit in the case of benzoxazole, is the energetically facile step, making it less reasonable to conclude that the reductive elimination is the rate-determining step of the present coupling reaction. On the other hand, this RPKA experiment implies another possible reason why the present reaction showed zero order kinetic character in both substrates. It may be possible that the nickelation of imidazole consists of base-mediated deprotonation followed by transmetalation of a potassium imidazolide species. If the latter transmetalation is the rate-determining step of the reaction, the observation of zero-order kinetic behavior on [1A] is rational because imidazoles themselves are not directly involved in the catalytic cycle.^[20]

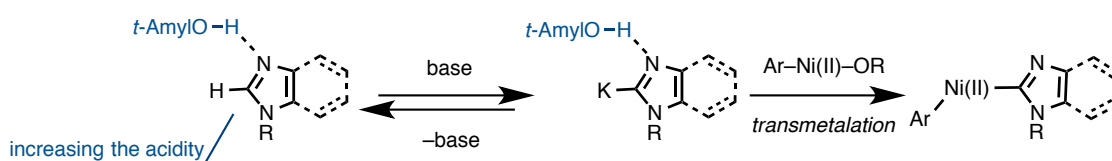
In order to confirm whether or not the deprotonation takes place prior to the transmetalation of imidazoles, a deuterium labeling experiment was conducted as shown in Scheme 10. *N*-Methylbenzimidazole (1A) was treated with *t*-BuOD under the catalytic coupling conditions for 4 h. ¹H NMR spectrum of an obtained crude material showed that deuterium was incorporated into the remaining *N*-methylbenzimidazole

(**1A** and **d-1A**) with H/D ratio of 11/89. This deuterium incorporation was also observed even without Ni/dcype catalyst. This result clearly shows that the deprotonation occurs only with K_3PO_4 in a tertiary alcohol solvent.



Scheme 10. Deuterium labeling experiments with and without a nickel catalyst.

Taking these mechanistic studies and the reported pK_a value of imidazoles ($pK_a = >32$ in DMSO)^[21] into consideration, it can be thought that *t*-AmylOH can coordinate to the sp^2 -nitrogen atom on imidazole, increasing the acidity of the C–H bond. Furthermore, the base can deprotonate the hydrogen atom at the C2 position of imidazole (Scheme 11). Although further investigations are still required, current data suggest that the transmetalation of an *in situ*-generated potassium imidazolide species is possibly the rate-determining step of the catalytic reaction.



Scheme 11. A possible deprotonation–nickelation pathway

A modified catalytic cycle including the plausible role of *t*-AmylOH is displayed in Figure 6. Particularly, imidazole nickelation would proceed through base-mediated deprotonation followed by transmetalation to afford diarylnickel(II) intermediate **C**. Although further studies including theoretical calculations are necessary, it was suggested that a tertiary alcohol solvent can increase the acidity of the C–H bond of imidazole, thus inducing deprotonation at the nickelation step.

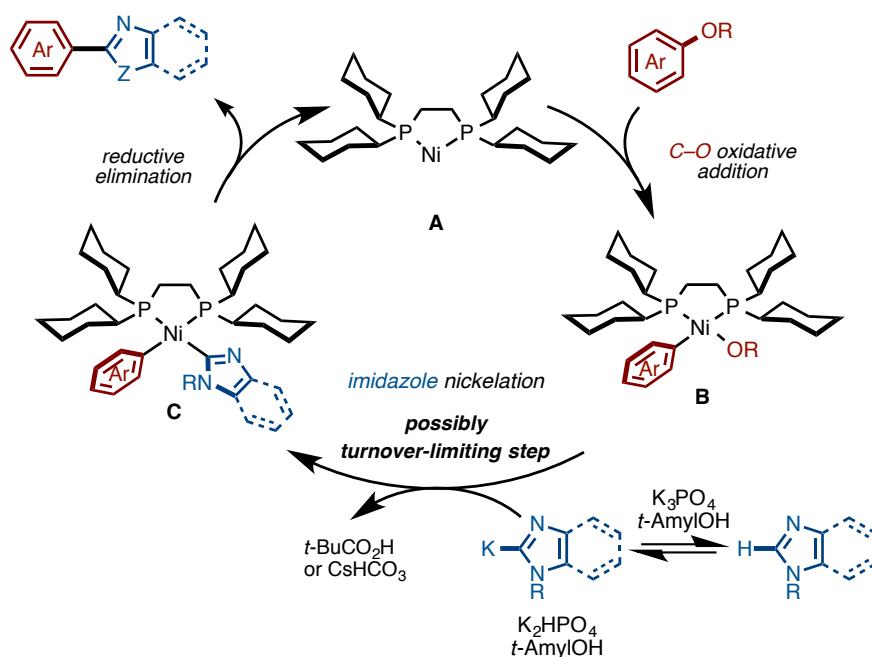


Figure 6. A modified reaction mechanism for the Ni-catalyzed C–H/C–O coupling reaction

3. Conclusions

In summary, a Ni-catalyzed C–H arylation/alkenylation of imidazoles was developed. Ni/dcypc and Ni/dcypc enabled a direct C–C bond-forming reaction of imidazoles including C–H/C–O arylation, C–H/C–O alkenylation, and C–H/C–Cl arylation. In the present Ni-catalyzed system, the key to success was the choice of a tertiary alcohol as solvent, as neither aprotic nor secondary alcohol solvents were completely effective. Kinetic studies and experiments using deuterated solvent indicated that the mechanism of C–H nickelation step most likely consists of base-mediated deprotonation followed by transmetalation of the generated potassium imidazolide species. With this mild and inexpensive catalyst system, it is envisaged that the present method can provide significant opportunities to synthesize and derivatize valuable functionalized imidazoles.

4. Experimental

4-1. General

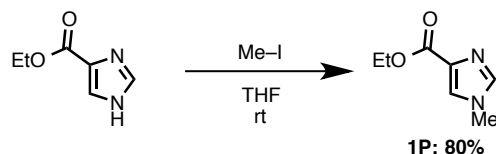
Unless otherwise noted, all materials including dry solvents were obtained from commercial suppliers and used as received. Ni(cod)₂ and K₃PO₄ were obtained from Wako Chemicals. 1,2-Bis(dicyclohexylphosphino)ethane (dcype) was obtained from Kanto Chemical. Dry *t*-AmylOH was purchased from Sigma-Aldrich and used as received. 1-Benzyl-1*H*-benzo[*d*]imidazole (**1B**)^[22], 1-phenyl-1*H*-benzo[*d*]imidazole (**1C**)^[23], 4-(2-(1*H*-benzo[*d*]imidazol-1-yl)ethyl)morpholine (**1D**)^[24], 1-(methoxymethyl)-1*H*-benzo[*d*]imidazole (**1E**)^[25], 1,5,6-trimethyl-1*H*-benzo[*d*]imidazole (**1F**)^[26], 1-benzyl-1*H*-imidazole (**1H**)^[27], 1-methyl-4,5-diphenyl-1*H*-imidazole (**1N**)^[28], 4-(1-methyl-1*H*-imidazol-4-yl)benzotrile (**1O**)^[29], 1-((benzyloxy)methyl)-1*H*-benzo[*d*]imidazole (**1Q**)^[30], phenyl dimethylcarbamate (**2a**)^[31], naphthalen-2-yl dimethylcarbamate (**2b**)^[31], naphthalen-1-yl dimethylcarbamate (**2k**)^[30], 4-methoxyphenyl dimethylcarbamate (**2e**)^[32], methyl 3-((dimethylcarbamoyl)oxy)benzoate (**2f**)^[32], [1,1'-biphenyl]-4-yl dimethylcarbamate (**2j**)^[31], 3,4-dihydronaphthalen-2-yl dimethylcarbamate (**2k**)^[33], 3,4-Dihydronaphthalen-1-yl dimethylcarbamate (**2m**)^[34], 5-(benzo[*d*][1,3]dioxol-5-yl)-2-phenyloxazole (**5D**)^[35], and 3,4-bis(dicyclohexylphosphanyl)thiophene (dcypt)^[15a] were synthesized according to procedures reported in the literature. Unless otherwise noted, all reactions were performed with dry solvents under an atmosphere of argon in flame-dried glassware using standard vacuum-line techniques. All C–H coupling reactions were performed in 20-mL glass vessel tubes equipped with J. Young[®] O-ring tap and heated in an 8-well reaction block (heater + magnetic stirrer) unless otherwise noted. All work-up and purification procedures were carried out with reagent-grade solvents in air.

Analytical thin-layer chromatography (TLC) was performed using E. Merck silica gel 60 F₂₅₄ precoated plates (0.25 mm). The developed chromatogram was analyzed by UV lamp (254 nm). Flash column chromatography was performed with E. Merck silica gel 60 (230–400 mesh) or Biotage Isolera[®] equipped with Biotage SNAP Cartridge KP-Sil columns using hexane/EtOAc as an eluent. Preparative thin-layer chromatography (PTLC) was performed using Wakogel B5-F silica coated plates (0.75 mm) prepared in our laboratory. High-resolution mass spectra (HRMS) were obtained from a JMS-T100TD instrument (DART) and Thermo Fisher Scientific Exactive (ESI).

Nuclear magnetic resonance (NMR) spectra were recorded on a JEOL JNM-ECA-600 (^1H 600 MHz, ^{13}C 150 MHz) spectrometer and a JEOL JNM-ECA-400 (^1H 400 MHz, ^{13}C 100 MHz) spectrometer. Chemical shifts for ^1H NMR are expressed in parts per million (ppm) relative to tetramethylsilane (δ 0.00 ppm). Chemical shifts for ^{13}C NMR are expressed in ppm relative to CDCl_3 (δ 77.0 ppm). Data are reported as follows: chemical shift, multiplicity (s = singlet, d = doublet, dd = doublet of doublets, t = triplet, q = quartet, m = multiplet, br = broad signal), coupling constant (Hz), and integration.

4-2. Preparation of Starting Materials

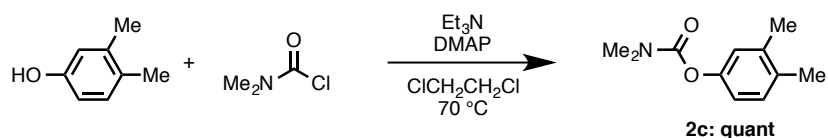
Ethyl 1-methyl-1*H*-imidazole-4-carboxylate (**1P**)



To a solution of ethyl 1*H*-imidazole-4-carboxylate (700 mg, 5.0 mmol, 1.0 equiv) in THF (15 mL) was added (NaH 60%, dispersion in paraffin liquid: 300 mg, 7.5 mmol, 1.5 equiv) at 0 °C. After stirring for 30 min, methyl iodide (781 mg, 5.5 mmol, 1.1 equiv) was added at 0 °C and the solution was stirred overnight at room temperature. The mixture was quenched by the addition of water, then extracted several times with EtOAc, dried over Na₂SO₄, and filtrated. The solution was concentrated *in vacuo*. The crude mixture was purified by Isolera[®] (hexane/EtOAc = 1:1 to EtOAc) to afford **1P** as a yellow solid (615 mg, 80% yield). ¹H NMR (400 MHz, CDCl₃): δ 7.58 (s, 1H), 7.45 (s, 1H), 4.36 (q, *J* = 7.2 Hz, 2H), 3.74 (s, 3H), 1.39 (t, *J* = 7.2 Hz, 3H); ¹³C NMR (100 MHz, CDCl₃): δ 162.5, 138.3, 133.8, 125.9, 60.1, 33.5, 14.1; HRMS (ESI) *m/z* calcd for C₇H₁₀N₂O₂Na [MNa]⁺: 177.0634, found 177.0633.

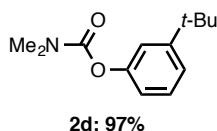
Synthesis of Aryl Carbamate: Representative Procedure

3,4-Dimethylphenyl dimethylcarbamate

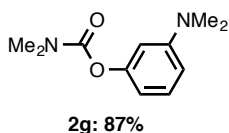


To a CICH₂CH₂Cl solution (4 mL) of 3,4-dimethylphenol (611 mg, 5.0 mmol, 1.0 equiv) and *N,N*-dimethylaminopyridine (DMAP: 6.1 mg, 0.050 mmol, 1 mol%) were added Et₃N (843 μL, 6.0 mmol, 1.2 equiv), and *N,N*-dimethylcarbamoyl chloride (505 μL, 5.5 mmol, 1.1 equiv). This mixture was stirred overnight at 80 °C. The reaction mixture was quenched by the addition of saturated NaHCO₃aq, and then the mixture was extracted four times with CH₂Cl₂. The combined organic layer was dried over Na₂SO₄, and concentrated *in vacuo*. The residue was purified by flash column chromatography (hexane/EtOAc = 10:1) to afford **2c** as a white solid (980 mg, quant). ¹H NMR (400 MHz, CDCl₃): δ 7.09 (d, *J* = 8.0 Hz, 1H), 6.89 (s, 1H), 6.83 (d, *J* = 8.0 Hz, 1H), 3.08 (s, 3H), 2.99 (s, 3H), 2.23 (s, 3H), 2.22 (s, 3H); ¹³C NMR (100 MHz,

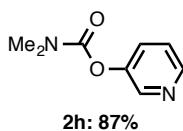
CDCl₃): δ 155.3, 149.4, 137.5, 133.4, 130.1, 122.7, 118.8, 36.6, 36.4, 19.8, 19.1; HRMS (ESI) m/z calcd for C₁₁H₁₅NO₂Na [MNa]⁺: 216.0995, found 216.0991.



3-(tert-Butyl)phenyl dimethylcarbamate (2d): Purification by flash column chromatography (hexane/EtOAc = 10:1) afforded **2d** as a white solid (751 mg, 97% yield). ¹H NMR (400 MHz, CDCl₃): δ 7.29 (dd, J = 8.4, 7.6 Hz, 1H), 7.21 (d, J = 7.6 Hz, 1H), 7.10 (s, 1H), 6.93 (d, J = 8.4 Hz, 1H), 3.10 (s, 3H), 3.01 (s, 3H), 1.32 (s, 9H); ¹³C NMR (100 MHz, CDCl₃): δ 155.0, 152.7, 151.3, 128.6, 122.2, 118.74, 118.71, 36.6, 36.4, 34.7, 31.2; HRMS (DART) m/z calcd for C₁₃H₂₀NO₂ [MH]⁺: 222.1494, found 222.1490.



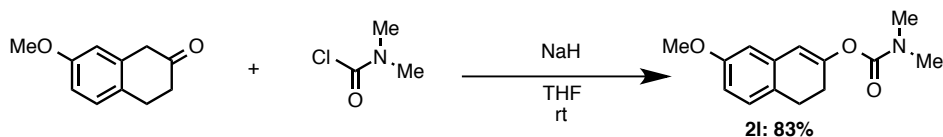
3-(Dimethylamino)phenyl dimethylcarbamate (2g): Purification by flash column chromatography (hexane/EtOAc = 4:1) afforded **2g** as a brown liquid (900 mg, 87% yield). ¹H NMR (400 MHz, CDCl₃): δ 7.18 (t, J = 8.0 Hz, 1H), 6.55 (d, J = 8.0 Hz, 1H), 6.45 (d, J = 8.0 Hz, 1H), 6.44 (s, 1H), 3.09 (s, 3H), 3.00 (s, 3H), 2.93 (s, 6H); ¹³C NMR (100 MHz, CDCl₃): δ 155.1, 152.5, 151.6, 129.4, 109.6, 109.5, 105.9, 40.5, 36.6, 36.4; HRMS (ESI) m/z calcd for C₁₁H₁₆N₂O₂Na [MNa]⁺: 231.1104, found 231.1100.



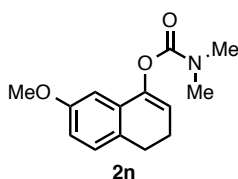
Pyridin-3-yl dimethylcarbamate (2h): Purification by flash column chromatography (hexane/EtOAc = 1:1 to EtOAc) afforded **2h** as a yellow liquid (721 mg, 87% yield). ¹H NMR (400 MHz, CDCl₃): δ 8.46–8.42 (m, 2H), 7.52 (dd, J = 8.4, 4.0 Hz, 1H), 7.30 (dd, J = 8.4, 4.0 Hz, 1H), 3.12 (s, 3H), 3.03 (s, 3H); ¹³C NMR (100 MHz, CDCl₃): δ 154.0, 148.1, 146.2, 143.5, 129.3, 123.6, 36.7, 36.4; HRMS (ESI) m/z calcd for C₈H₁₀N₂O₂Na [MNa]⁺: 189.0634, found 189.0630.

Representative Procedure:

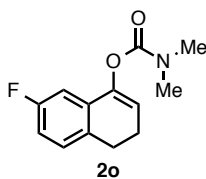
7-Methoxy-3,4-dihydronaphthalen-2-yl dimethylcarbamate (**2l**):



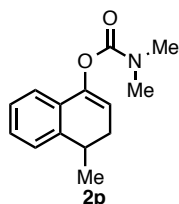
General Procedure: NaH (55% dispersion in paraffin liquid: 1.15 g, 27 mmol, 1.8 equiv) was placed in a 300-mL flask under a stream of argon, and THF (24 mL) was added into the flask. To this suspension, 7-methoxy-3,4-dihydronaphthalen-2(1H)-one (2.82 g, 16 mmol, 1.0 equiv) in THF (8 mL) was added dropwise. The resulting mixture was stirred at room temperature for 5 min. *N,N*-Dimethyl carbamoyl chloride (2.21 mL, 24 mmol, 1.5 equiv) in THF (4 mL) was added, and then the mixture was stirred for an additional 30 min. The reaction was quenched by the addition of water. The mixture was extracted three times with *tert*-butyl methyl ether, and the combined organic layer was washed with water and brine, dried over Na₂SO₄, and then filtered. The filtrate was concentrated *in vacuo*. The crude residue was purified by flash column chromatography (hexane/EtOAc = 3:1) to afford **2l** as a pale yellow oil (3.26 g, 83% yield). ¹H NMR (400 MHz, CDCl₃): δ 7.01 (d, *J* = 7.6 Hz, 1H), 6.63 (dd, *J* = 7.6, 2.4 Hz, 1H), 6.57 (d, *J* = 2.4 Hz, 1H), 6.17 (s, 1H), 3.77 (s, 3H), 3.01 (s, 3H), 2.97 (s, 3H), 2.92 (t, *J* = 8.0 Hz, 2H), 2.51 (t, *J* = 8.0 Hz, 2H); ¹³C NMR (100 MHz, CDCl₃): δ 158.3, 154.2, 152.1, 134.7, 127.7, 125.3, 113.9, 111.9, 111.2, 55.2, 36.44, 36.35, 27.7, 27.0; HRMS (DART) *m/z* calcd for C₁₄H₁₈NO₃ [MH]⁺: 248.1287, found 248.1287.



7-Methoxy-3,4-dihydronaphthalen-1-yl dimethylcarbamate (2n): 15 mmol scale. Purification by flash column chromatography (hexane/EtOAc = 3:1) afforded **2n** as a pale yellow oil (1.45 g, 39% yield). ¹H NMR (400 MHz, CDCl₃): δ 7.05 (d, *J* = 8.0 Hz, 1H), 6.72–6.68 (m, 2H), 5.73 (t, *J* = 4.4 Hz, 1H), 3.78 (s, 3H), 3.13 (s, 3H), 2.99 (s, 3H), 2.79 (t, *J* = 8.0 Hz, 2H), 2.41 (dt, *J* = 8.0, 4.4, 2H); ¹³C NMR (100 MHz, CDCl₃): δ 158.1, 154.5, 145.6, 132.2, 128.5, 128.0, 115.6, 111.6, 107.6, 55.1, 36.6, 36.2, 26.5, 22.3; HRMS (DART) *m/z* calcd for C₁₄H₁₈NO₃ [MH]⁺: 248.1287, found 248.1282.

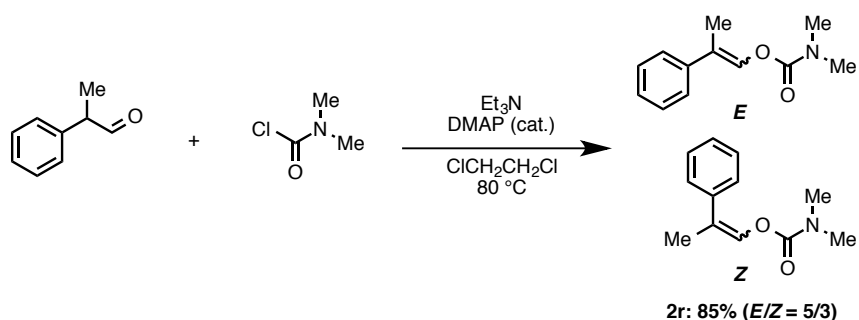


7-Fluoro-3,4-dihydronaphthalen-1-yl dimethylcarbamate (2o): 6.1 mmol scale. Purification by flash column chromatography (hexane/Et₂O = 1:1) afforded **2o** as a yellow oil (1.02 g, 71% yield). ¹H NMR (400 MHz, CDCl₃): δ 7.10–7.04 (m, 1H), 6.88–6.80 (m, 2H), 5.77 (t, *J* = 4.4 Hz, 1H), 3.12 (s, 3H), 2.99 (s, 3H), 2.81 (t, *J* = 7.6 Hz, 2H), 2.43 (dt, *J* = 7.6, 4.4 Hz, 2H); ¹³C NMR (100 MHz, CDCl₃): δ 161.7 (d, *J* = 241.2 Hz), 154.4, 145.1 (d, *J* = 1.9 Hz), 133.0 (d, *J* = 8.6 Hz), 131.7 (d, *J* = 2.9 Hz), 128.5 (d, *J* = 7.6 Hz), 116.3, 113.8 (d, *J* = 20.9 Hz), 107.9 (d, *J* = 23.9 Hz), 36.6, 36.3, 26.6, 22.1; HRMS (DART) *m/z* calcd for C₁₃H₁₆FNO₂ [MH]⁺: 236.1087, found 236.1087.



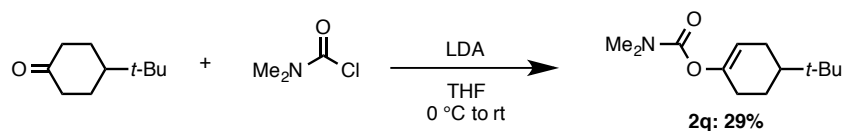
4-Methyl-3,4-dihydronaphthalen-1-yl dimethylcarbamate (2p): 15.5 mmol scale. Purification by flash column chromatography (hexane/EtOAc = 4:1) afforded **2p** as a white solid (2.34 g, 65% yield). ¹H NMR (400 MHz, CDCl₃): δ 7.26–7.10 (m, 4H), 5.64 (t, *J* = 4.4 Hz, 1H), 3.13 (s, 3H), 3.07–2.93 (m, 4H), 2.60 (ddd, *J* = 16.8, 6.4, 4.4 Hz, 1H), 2.23 (ddd, *J* = 16.8, 6.4, 4.4 Hz, 1H), 1.31 (d, *J* = 6.4 Hz, 3H); ¹³C NMR (100 MHz, CDCl₃): δ 154.9, 145.4, 141.4, 130.4, 127.9, 126.2, 126.1, 120.7, 113.6, 36.7, 36.4, 31.9, 29.9, 20.1; HRMS (DART) *m/z* calcd for C₁₄H₁₉NO₂ [MH]⁺: 232.1338, found 232.1339.

(*E*)-2-Phenylprop-1-en-1-yl dimethylcarbamate (2r)



To a $\text{ClCH}_2\text{CH}_2\text{Cl}$ solution (40 mL) of 2-phenylpropionaldehyde (2.7 mL, 20.2 mmol, 1.0 equiv) were added Et_3N (4.8 mL, 34.4 mmol, 1.7 equiv), *N,N*-dimethylaminopyridine (DMAP: 610.8 mg, 5 mmol, 25 mol%) and *N,N*-dimethylcarbamoyl chloride (2.5 mL, 27.2 mmol, 1.3 equiv). This mixture was stirred overnight at 80 °C. The reaction mixture was quenched by the addition of saturated NH_4Cl aq, and then the mixture was extracted three times with CH_2Cl_2 . The combined organic layer was washed with water and brine, dried over Na_2SO_4 , concentrated *in vacuo*. The residue was purified by flash column chromatography (hexane/EtOAc = 5/1) to afford **2r** as a colorless oil (3.48 g, 85% yield, *E/Z* ratio = 5:3). ^1H NMR (400 MHz, CDCl_3): δ 7.49–7.21 (m, 11H, (*E* and *Z*)), 7.16 (d, $J = 1.4$ Hz, 1H, (*Z*)), 3.01 (s, 3H, (*E*)), 2.96 (s, 3H, (*E*)), 2.91 (s, 3H, (*Z*)), 2.84 (s, 3H, (*Z*)), 2.07 (d, $J = 1.4$ Hz, 3H, (*E*)), 1.99 (d, $J = 1.4$ Hz, 3H, (*Z*)); ^{13}C NMR (100 MHz, CDCl_3): δ 153.5, 139.2, 137.8, 133.8, 131.8, 128.2, 127.7, 127.6, 126.6, 125.4, 118.7, 116.8, 36.3, 36.3, 35.7, 35.7, 18.5, 13.3; HRMS (DART) m/z calcd for $\text{C}_{14}\text{H}_{19}\text{NO}_2$ [MH] $^+$: 232.1338, found 232.1339.

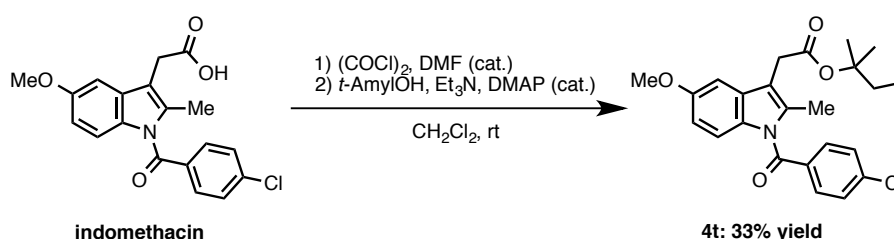
4-(*tert*-Butyl)cyclohex-1-en-1-yl dimethylcarbamate (**2q**)



To a solution of 4-(*tert*-butyl)cyclohexanone (462.8 mg, 3.0 mmol, 1.0 equiv) in THF (4.5 mL) was slowly added lithium diisopropylamide [LDA: prepared from diisopropylamine (333.9 mg, 3.3 mmol, 1.1 equiv) and 1.6 M of *n*-BuLi in hexane (2.06 mL, 3.3 mmol, 1.1 equiv) in 4.5 mL of THF] at 0 °C. After stirring the solution for 1 h, *N,N*-dimethylcarbamoyl chloride (413.6 mL, 4.5 mmol, 1.5 equiv) was added at 0 °C and was allowed to warm up to room temperature. The solution was stirred overnight, and then NaHCO_3 aq was added to quench the reaction. The mixture was extracted three

times with EtOAc, washed with brine, dried over Na_2SO_4 , and then filtered. The mixture was concentrated *in vacuo*. The crude mixture was purified by flash column chromatography (hexane/EtOAc = 50:1 to 10:1) to afford **2q** as a colorless liquid (193 mg, 29% yield). ^1H NMR (400 MHz, CDCl_3): δ 5.35 (t, J = 2.8 Hz, 1H), 2.95 (s, 3H), 2.93 (s, 3H), 2.38–2.21 (m, 1H), 2.17–2.05 (m, 2H), 1.96–1.80 (m, 2H), 1.42–1.30 (m, 2H), 0.89 (s, 9H); ^{13}C NMR (100 MHz, CDCl_3): δ 155.0, 148.7, 113.5, 43.4, 36.4, 36.2, 32.1, 28.2, 27.3, 25.0, 24.0; HRMS (DART) m/z calcd for $\text{C}_{13}\text{H}_{25}\text{NO}_2$ $[\text{MH}]^+$: 226.1807, found 226.1810.

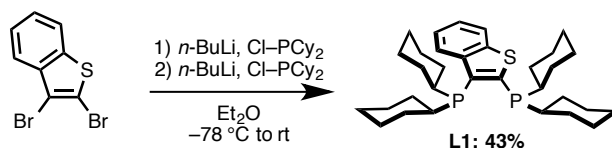
***tert*-Pentyl 2-(1-(4-chlorobenzoyl)-5-methoxy-2-methyl-1*H*-indol-3-yl)acetate (**4t**)**



To a solution of indomethacin (3.58 g, 10 mmol, 1.0 equiv) in CH_2Cl_2 (10 mL) were added oxalyl chloride (1.29 mL, 15 mmol, 1.5 equiv) and a few drops of DMF at room temperature, and then this solution was stirred for 1 h. To the mixture were added *t*-AmylOH (3.24 mL, 30 mmol, 3.0 equiv), Et_3N (3.06 mL, 22 mmol, 2.2 equiv), and *N,N*-dimethylamino pyridine (DMAP: 12.2 mg, 0.10 mmol, 1.0 equiv) at 0 °C. This solution was allowed to warm up to room temperature and stirred for 3 h. The reaction was quenched by the addition of NaHCO_3 aq and extracted three times with CH_2Cl_2 , dried over Na_2SO_4 , and then filtered. The resulting solution was concentrated *in vacuo*. The crude mixture was purified by flash column chromatography (hexane/EtOAc = 10:1 to 4:1) to afford **4t** as a yellow solid (1.41 g, 33% yield). ^1H NMR (400 MHz, CDCl_3): δ 7.65 (d, J = 8.8 Hz, 2H), 7.46 (d, J = 8.8 Hz, 2H), 6.96 (d, J = 2.0 Hz, 1H), 6.88 (d, J = 9.2 Hz, 1H), 6.66 (dd, J = 9.2, 2.0 Hz, 1H), 3.83 (s, 3H), 3.58 (s, 2H), 2.37 (s, 3H), 1.75 (q, J = 8.0 Hz, 2H), 1.41 (s, 6H), 0.81 (t, J = 8.0 Hz, 3H); ^{13}C NMR (100 MHz, CDCl_3): δ 170.0, 168.2, 155.9, 139.1, 135.6, 134.0, 131.1, 130.8, 130.7, 129.0, 114.9, 113.3, 111.6, 101.2, 83.5, 55.6, 33.3, 31.6, 25.5, 13.3, 8.1; HRMS (DART) m/z calcd for $\text{C}_{24}\text{H}_{27}\text{ClNO}_4$ $[\text{MH}]^+$: 428.1629, found 428.1627.

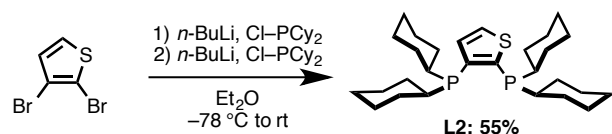
Synthesis of Thiophene-Based Diphosphine Ligand L1 and L2

Benzo[*b*]thiophene-2,3-diylbis(dicyclohexylphosphane) (L1)



To a 50-mL round-bottom glass flask containing a magnetic stirring bar were added 2,3-dibromobenzo[*b*]thiophene (1.46 g, 5.0 mmol, 1.0 equiv) and dry Et₂O (5 mL). After cooling at -78 °C, a solution of *n*-BuLi in hexane (1.6 M, 3.2 mL, 1.0 equiv) was added at -78 °C over 10 min. After stirring the mixture at -78 °C for 1 h, a solution of chlorodicyclohexylphosphine (1.22 g, 5.25 mmol, 1.05 equiv) in Et₂O (1.5 mL) was added at -78 °C over 15 min. The resulting mixture was further stirred at -78 °C for 30 min. Then a solution of *n*-BuLi in hexane (1.6 M, 3.2 mL, 1.0 equiv) was added at -78 °C over 10 min. After stirring the mixture at -78 °C for 1 h, a solution of chlorodicyclohexylphosphine (1.22 g, 5.25 mmol, 1.05 equiv) in Et₂O (1.5 mL) was added at -78 °C over 10 min. The resulting mixture was further stirred at -78 °C for 30 min. After warming to room temperature, the reaction was quenched with water, extracted with hexane, washed with brine, dried over Na₂SO₄, and concentrated under reduced pressure. The reaction mixture was purified by reprecipitation with toluene (0.50 mL) and methanol (25 mL) to afford benzo[*b*]thiophene-2,3-diylbis(dicyclohexylphosphane) (L1) as a white solid (1.13 g, 43% yield). ¹H NMR (400 MHz, CDCl₃) δ 8.07 (br s, 1H), 7.86 (dd, *J* = 8.4, 4.0 Hz, 1H), 7.42–7.31 (m, 2H), 2.49 (br s, 2H), 2.00 (br s, 6H), 1.90–1.50 (m, H), 1.49–0.95 (m, H); ³¹P NMR (162 MHz, CDCl₃) δ -13.2 (d, *J* = 160 Hz, 1P), -16.2 (d, *J* = 160 Hz, 1P); HRMS (ESI) *m/z* calcd for C₃₂H₄₉P₂S [MH]⁺: 527.3030 found 527.3034.

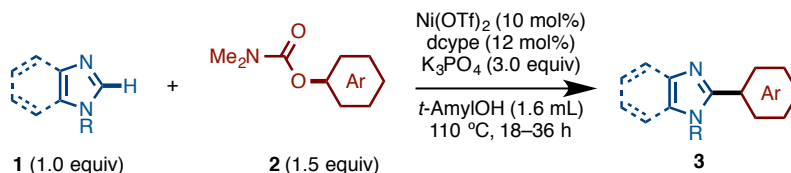
2,3-Bis(dicyclohexylphosphino)thiophene (L2)



To a 50-mL round-bottom glass flask containing a magnetic stirring bar were added 2,3-dibromothiophene (967 mg, 4.0 mmol, 1.0 equiv) and dry Et₂O (4 mL). After cooling at -78 °C, a solution of *n*-BuLi in hexane (1.6 M, 2.5 mL, 1.0 equiv) was added

at $-78\text{ }^{\circ}\text{C}$ over 10 min. After stirring the mixture at $-78\text{ }^{\circ}\text{C}$ for 1 h, a solution of chlorodicyclohexylphosphine (977 mg, 4.2 mmol, 1.05 equiv) in Et_2O (1.25 mL) was added at $-78\text{ }^{\circ}\text{C}$ over 15 min. The resulting mixture was further stirred at $-78\text{ }^{\circ}\text{C}$ for 30 min. Then a solution of *n*-BuLi in hexane (1.6 M, 2.5 mL, 1.0 equiv) was added at $-78\text{ }^{\circ}\text{C}$ over 10 min. After stirring the mixture at $-78\text{ }^{\circ}\text{C}$ for 1 h, a solution of chlorodicyclohexylphosphine (977 mg, 4.2 mmol, 1.05 equiv) in Et_2O (1.25 mL) was added at $-78\text{ }^{\circ}\text{C}$ over 10 min. The resulting mixture was further stirred at $-78\text{ }^{\circ}\text{C}$ for 30 min. After warming to room temperature, the reaction was quenched with water, extracted with hexane, washed with brine, dried over Na_2SO_4 , and concentrated under reduced pressure. The reaction mixture was purified by reprecipitation with toluene (0.40 mL) and methanol (20 mL) to afford 2,3-bis(dicyclohexylphosphino)thiophene (**L2**) as a white solid (1.05 g, 55% yield). ^1H NMR (400 MHz, CDCl_3) δ 7.56 (d, $J = 5.2$ Hz, 1H), 1.93–1.80 (m, 8H), 1.78–1.47 (m, 16H), 1.32–1.00 (m, 20H); ^{31}P NMR (162 MHz, CDCl_3) δ -19.0 (d, $J = 129$ Hz, 1P), -20.8 (d, $J = 129$ Hz, 1P); HRMS (ESI) m/z calcd for $\text{C}_{28}\text{H}_{47}\text{P}_2\text{S}$ $[\text{MH}]^+$: 477.2874 found 477.2867.

4-3. Nickel-Catalyzed C–H Arylation of Imidazoles

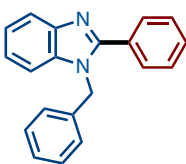


General Procedure: A 20-mL glass vessel equipped with a J. Young® O-ring tap containing a magnetic stirring bar and K₃PO₄ (255.0 mg, 1.20 mmol, 3.0 equiv) was dried with a heatgun for 3 min *in vacuo* and filled with N₂ after cooling to room temperature. To this vessel were added Ni(OTf)₂ (14.2 mg, 0.040 mmol, 10 mol%), imidazole **1** (0.40 mmol, 1.0 equiv) and aryl carbamate **2** (0.60 mmol, 1.5 equiv), and then introduced into an argon-atmosphere glovebox. To the reaction vessel was added 1,2-bis(dicyclohexylphosphino)ethane (dcype: 20.6 mg, 0.050 mmol, 12 mol%). The vessel was taken out of the glovebox, then dry *t*-AmylOH (1.6 mL) was added under a stream of N₂. The vessel was sealed with an O-ring tap and then heated at 110 °C for 18–36 h in an 8-well reaction block with stirring. After cooling the reaction mixture to room temperature, the mixture was passed through a short silica gel pad with EtOAc as the eluent. The filtrate was concentrated and the residue was subjected to PTLC to afford a C–H coupling product (2-arylated imidazole **3**).



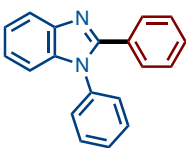
3Aa: 83% (C–H/C–O coupling)
81% (C–H/C–Cl coupling)

1-Methyl-2-phenyl-1H-benzo[*d*]imidazole (3Aa)^{l 36 l}: Purification by PTLC (hexane/EtOAc = 4:1) afforded **3Aa** as a white solid (69.0 mg, 83% yield from C–H/C–O coupling; 67.3 mg, 81% yield from C–H/C–Cl coupling). ¹H NMR (400 MHz, CDCl₃): δ 7.85–7.81 (m, 1H), 7.79–7.75 (m, 2H), 7.55–7.49 (m, 3H), 7.41–7.37 (m, 1H), 7.35–7.28 (m, 2H), 3.86 (s, 3H); ¹³C NMR (100 MHz, CDCl₃): δ 153.6, 142.9, 136.5, 130.1, 129.6, 129.3, 128.5, 122.6, 122.3, 119.7, 109.5, 31.5; HRMS (DART) *m/z* calcd for C₁₄H₁₃N₂ [MH]⁺: 209.1079, found 209.1076.



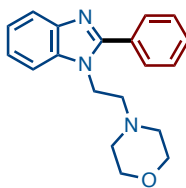
**3Ba: 53% (C–H/C–O coupling)
69% (C–H/C–Cl coupling)**

1-Benzyl-2-phenyl-1H-benzo[*d*]imidazole (3Ba)^[37]: Purification by Isolera[®] (hexane/EtOAc = 10/1 to EtOAc) afforded **3Ba** as a white solid (60.5 mg, 53% yield from C–H/C–O coupling: 78.1 mg, 69% yield from C–H/C–Cl coupling, 69% yield). ¹H NMR (400 MHz, CDCl₃): δ 7.87 (d, *J* = 8.0 Hz, 1H), 7.68 (d, *J* = 8.0 Hz, 2H), 7.48–7.38 (m, 3H), 7.35–7.24 (m, 4H), 7.22 (dd, *J* = 7.2, 5.4 Hz, 2H), 7.09 (d, *J* = 5.4 Hz, 2H), 5.44 (s, 2H); ¹³C NMR (100 MHz, CDCl₃): δ 154.1, 143.2, 136.3, 136.0, 130.1, 129.8, 129.2, 129.0, 128.7, 127.7, 125.9, 123.0, 122.6, 119.9, 110.5, 48.3; HRMS (DART) *m/z* calcd for C₂₀H₁₇N₂ [MH]⁺: 285.1392, found 285.1390



**3Ca: 88% (C–H/C–O coupling)
86% (C–H/C–Cl coupling)**

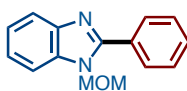
1,2-Diphenyl-1H-benzo[*d*]imidazole (3Ca)^[38]: Purification by Isolera[®] (hexane/EtOAc = 10/1 to EtOAc) afforded **3Ca** as a white solid (95.0 mg, 88% yield from C–H/C–O coupling: 93.2 mg, 86% yield from C–H/C–Cl coupling). ¹H NMR (400 MHz, CDCl₃): δ 7.89 (d, *J* = 7.2 Hz, 1H), 7.56 (d, *J* = 8.4 Hz, 2H), 7.53–7.41 (m, 3H), 7.38–7.22 (m, 8H); ¹³C NMR (100 MHz, CDCl₃): δ 152.3, 143.0, 137.2, 136.9, 129.9, 129.8, 129.39, 129.36, 128.5, 128.2, 127.3, 123.3, 122.9, 119.8, 110.4; HRMS (DART) *m/z* calcd for C₁₉H₁₅N₂ [MH]⁺: 271.1235, found 271.1230.



3Da: 84%

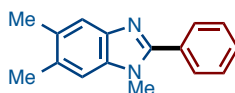
4-(2-(2-Phenyl-1H-benzo[*d*]imidazol-1-yl)ethyl)morpholine (3Da): Purification by

PTLC (EtOAc) afforded **3Da** as a yellow oil (103.3 mg, 84% yield). ^1H NMR (400 MHz, CDCl_3): δ 7.83 (dd, $J = 7.6, 2.4$ Hz, 1H), 7.79–7.74 (m, 2H), 7.55–7.45 (m, 3H), 7.43–7.38 (m, 1H), 7.34–7.26 (m, 2H), 4.35 (t, $J = 6.8$ Hz, 2H), 3.54 (t, $J = 4.4$ Hz, 4H), 2.70 (t, $J = 6.8$ Hz, 2H), 2.30 (t, $J = 4.4$ Hz, 4H); ^{13}C NMR (100 MHz, CDCl_3): δ 154.0, 143.0, 135.4, 130.5, 129.7, 129.4, 128.6, 122.7, 122.4, 119.9, 109.9, 66.6, 57.4, 53.7, 42.2; HRMS (DART) m/z calcd for $\text{C}_{19}\text{H}_{22}\text{N}_3\text{O} [\text{MH}]^+$: 308.1763, found 308.1767



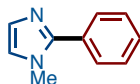
3Ea: 53%

1-(Methoxymethyl)-2-phenyl-1H-benzo[d]imidazole (3Ea): Purification by PTLC (hexane/EtOAc = 4/1) afforded **3Ea** as a yellow solid (50.1 mg, 53% yield). ^1H NMR (400 MHz, CDCl_3): δ 7.95–7.88 (m, 2H), 7.86–7.81 (m, 1H), 7.55–7.47 (m, 4H), 7.35–7.29 (m, 2H), 5.45 (s, 2H), 3.39 (s, 3H); ^{13}C NMR (100 MHz, CDCl_3): δ 154.4, 142.8, 136.0, 130.0, 129.7, 129.5, 128.6, 123.2, 122.9, 119.9, 110.0, 75.0, 56.5; HRMS (DART) m/z calcd for $\text{C}_{15}\text{H}_{15}\text{N}_2\text{O} [\text{MH}]^+$: 239.1184, found 239.1183



3Fa: 65%

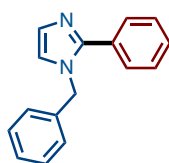
1,5,6-Trimethyl-2-phenyl-1H-benzo[d]imidazole (3Fa): Purification by Isolera[®] (hexane/EtOAc = 10/1 to 1:1) afforded **3Fa** as a white solid (69.1 mg, 65% yield). ^1H NMR (400 MHz, CDCl_3): δ 7.72 (d, $J = 7.6$ Hz, 2H), 7.57 (s, 1H), 7.51–7.41 (m, 3H), 7.12 (s, 1H), 3.76 (s, 3H), 2.40 (s, 3H), 2.39 (s, 3H); ^{13}C NMR (100 MHz, CDCl_3): δ 152.8, 141.5, 135.1, 131.8, 131.1, 130.4, 129.3, 129.2, 128.5, 119.7, 109.8, 31.5, 20.5, 20.2; HRMS (DART) m/z calcd for $\text{C}_{16}\text{H}_{17}\text{N}_2 [\text{MH}]^+$: 237.1392, found 237.1396.



**3Ga: 64% (C–H/C–O coupling)
81% (C–H/C–Cl coupling)**

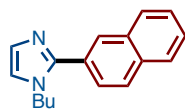
1-Methyl-2-phenyl-1H-imidazole (3Ga)^[7b]: The reaction was performed by using $\text{Ni}(\text{cod})_2$ (11.0 mg, 0.040 mmol, 10 mol%) instead of $\text{Ni}(\text{OTf})_2$ for 36 h. Purification by

PTLC (EtOAc) afforded **3Ga** as a colorless oil (40.5 mg, 64% yield from C–H/C–O coupling: 51.8 mg, 81% yield from C–H/C–Cl coupling). ^1H NMR (400 MHz, CDCl_3): δ 7.63 (d, $J = 8.0$ Hz, 2H), 7.49–7.38 (m, 3H), 7.13 (d, $J = 1.6$ Hz, 1H), 6.97 (d, $J = 1.6$ Hz, 1H), 3.76 (s, 3H); ^{13}C NMR (100 MHz, CDCl_3): δ 147.7, 130.5, 128.51, 128.47, 128.4, 128.3, 122.2, 34.4; HRMS (DART) m/z calcd for $\text{C}_{10}\text{H}_{11}\text{N}_2$ $[\text{MH}]^+$: 159.0922, found 159.0920.



3Ha: 64% (C–H/C–O coupling)
64% (C–H/C–Cl coupling)

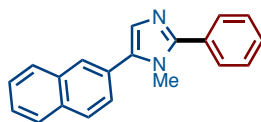
1-Benzyl-2-phenyl-1H-imidazole (3Ha): The reaction was performed by using $\text{Ni}(\text{cod})_2$ (11.0 mg, 0.040 mmol, 10 mol%) instead of $\text{Ni}(\text{OTf})_2$ for 36 h. Purification by PTLC (EtOAc) afforded **3Ha** as a yellow solid (59.8 mg, 64% yield from C–H/C–O coupling: 60.4 mg, 64% yield from C–H/C–Cl coupling). ^1H NMR (400 MHz, CDCl_3): δ 7.59–7.51 (m, 2H), 7.42–7.25 (m, 6H), 7.18 (s, 1H), 7.07 (d, $J = 7.2$ Hz, 2H), 6.95 (s, 1H), 5.20 (s, 2H); ^{13}C NMR (100 MHz, CDCl_3): δ 148.1, 136.9, 130.4, 128.9, 128.8, 128.68, 128.66, 128.4, 127.8, 126.4, 121.2, 50.2; HRMS (DART) m/z calcd for $\text{C}_{16}\text{H}_{15}\text{N}_2$ $[\text{MH}]^+$: 235.1235, found 235.1230.



3Ib: 49%^[b]

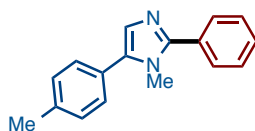
1-Butyl-2-(naphthalen-2-yl)-1H-imidazole (3Ib): The reaction was performed by using $\text{Ni}(\text{cod})_2$ (11.0 mg, 0.040 mmol, 10 mol%) instead of $\text{Ni}(\text{OTf})_2$ for 36 h. Purification by Isolera[®] (hexane/EtOAc = 10/1 to EtOAc) afforded **3Ib** as a yellow solid (48.7 mg, 49% yield). ^1H NMR (400 MHz, CDCl_3): δ 8.04 (s, 1H), 7.95–7.81 (m, 3H), 7.71 (d, $J = 7.6$ Hz, 1H), 7.55–7.46 (m, 2H), 7.19 (s, 1H), 7.05 (s, 1H), 4.06 (t, $J = 7.6$ Hz, 2H), 1.79–1.70 (m, 2H), 1.33–1.21 (m, 2H), 0.86 (q, $J = 7.6$ Hz, 3H); ^{13}C NMR (100 MHz, CDCl_3): δ 147.6, 133.0, 128.6, 128.3, 128.22, 128.17, 128.1, 127.7, 126.5, 126.4, 126.3, 120.5, 46.6, 33.1, 19.2, 13.5 (one peak is overlapping); HRMS (DART)

m/z calcd for $C_{17}H_{19}N_2$ $[MH]^+$: 251.1548, found 251.1542.



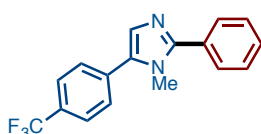
3Ja: 82%^[b]

1-Methyl-5-(naphthalen-2-yl)-2-phenyl-1H-imidazole (3Ja): The reaction was performed by using $Ni(cod)_2$ (11.0 mg, 0.040 mmol, 10 mol%) instead of $Ni(OTf)_2$ for 36 h. Purification by flash column chromatography (hexane/EtOAc = 4/1 to EtOAc) afforded **3Ja** as a white solid (93.3 mg, 82% yield). 1H NMR (400 MHz, $CDCl_3$): δ 7.95–7.84 (m, 4H), 7.73 (d, $J = 8.0$ Hz, 2H), 7.57 (d, $J = 8.0$ Hz, 1H), 7.56–7.46 (m, 4H), 7.42 (t, $J = 8.0$ Hz, 1H), 7.32 (s, 1H), 3.73 (s, 3H); ^{13}C NMR (100 MHz, $CDCl_3$): δ 149.6, 135.4, 133.3, 132.6, 130.9, 128.8, 128.7, 128.5, 128.4, 128.0, 127.7, 127.6, 127.4, 126.6, 126.44, 126.36, 33.9 (one peak is overlapping elsewhere); HRMS (DART) m/z calcd for $C_{20}H_{17}N_2$ $[MH]^+$: 285.1392, found 285.1397.



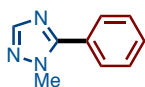
3Ka: 65%^[b]

1-Methyl-2-phenyl-5-(p-tolyl)-1H-imidazole (3Ka): The reaction was performed by using $Ni(cod)_2$ (11.0 mg, 0.040 mmol, 10 mol%) instead of $Ni(OTf)_2$ for 36 h. Purification by flash column chromatography (hexane/EtOAc = 4/1 to 1:1) afforded **3Ka** as a white solid (65.0 mg, 65% yield). 1H NMR (400 MHz, $CDCl_3$): δ 8.15 (s, 1H), 7.91–7.78 (m, 5H), 7.51–7.45 (m, 2H), 7.32–7.24 (m, 3H), 3.75 (s, 3H); ^{13}C NMR (100 MHz, $CDCl_3$): δ 153.5, 142.9, 136.5, 133.4, 132.7, 129.1, 128.3, 128.2, 127.6, 127.3, 127.0, 126.5, 126.1, 122.6, 122.3, 119.6, 109.5, 31.5; HRMS (DART) m/z calcd for $C_{17}H_{17}N_2$ $[MH]^+$: 249.1392, found 249.1395.



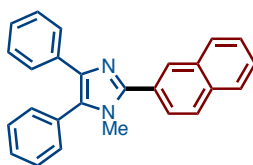
3La: >95%^[b]

1-Methyl-2-phenyl-5-(4-(trifluoromethyl)phenyl)-1*H*-imidazole (3La)^[5d]: The reaction was performed by using Ni(cod)₂ (11.0 mg, 0.040 mmol, 10 mol%) instead of Ni(OTf)₂ for 36 h. Purification by PTLC (hexane/EtOAc = 1/1) afforded **3La** as a white solid (122.4 mg, >95% yield). ¹H NMR (400 MHz, CDCl₃): δ 7.74–7.67 (m, 4H), 7.58 (d, *J* = 8.0 Hz, 2H), 7.52–7.41 (m, 3H), 7.28 (s, 1H), 3.70 (s, 3H); ¹³C NMR (100 MHz, CDCl₃): δ 150.4, 134.0, 133.8, 130.5, 129.7 (q, *J* = 32.5 Hz), 129.0, 128.8, 128.6, 128.5, 125.7 (q, *J* = 4.0 Hz), 124.0 (q, *J* = 273 Hz), 33.9 (one peak is overlapping elsewhere); HRMS (DART) *m/z* calcd for C₁₇H₁₄F₃N₂ [MH]⁺: 303.1109, found 303.1108.



3Ma: 82%^[b]

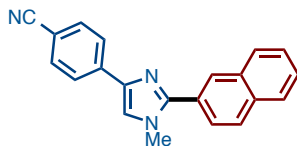
1-Methyl-5-phenyl-1*H*-1,2,4-triazole (3Ma)^[7b]: The reaction was performed by using Ni(cod)₂ (11.0 mg, 0.040 mmol, 10 mol%) instead of Ni(OTf)₂ for 36 h. Purification by PTLC (EtOAc) afforded **3Ma** as a white solid (52.2 mg, 82% yield). ¹H NMR (400 MHz, CDCl₃): δ 7.94 (s, 1H), 7.70–7.66 (m, 2H), 7.54–7.48 (m, 3H), 3.99 (s, 3H); ¹³C NMR (100 MHz, CDCl₃): δ 154.5, 150.6, 130.0, 128.8, 128.5, 127.8, 36.9; HRMS (DART) *m/z* calcd for C₉H₁₀N₃ [MH]⁺: 160.0875, found 160.0875.



3Nb: 87%^[c]

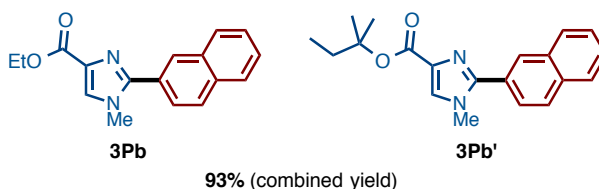
1-Methyl-2-(naphthalen-2-yl)-4,5-diphenyl-1*H*-imidazole (3Nb): The reaction was performed by using Ni(cod)₂ (11.0 mg, 0.040 mmol, 10 mol%) and dcypt (22.9 mg, 0.050 mmol, 12 mol%) instead of Ni(OTf)₂ and dcype for 36 h. Purification by Isolera[®] (hexane/EtOAc = 10/1 to EtOAc) afforded **3Nb** as a white solid (125.1 mg, 87% yield). ¹H NMR (400 MHz, CDCl₃): δ 8.21 (s, 1H), 7.98–7.85 (m, 4H), 7.58 (d, *J* = 8.4 Hz, 2H), 7.56–7.41 (m, 7H), 7.23 (t, *J* = 8.0 Hz, 2H), 7.15 (t, *J* = 7.6 Hz, 1H), 3.58 (s, 3H); ¹³C NMR (100 MHz, CDCl₃): δ 147.9, 138.0, 134.7, 133.2, 133.1, 131.2, 130.9, 130.7, 129.0, 128.6, 128.4, 128.33, 128.26, 128.1, 127.8, 127.0, 126.6, 126.52, 126.49, 126.3,

33.3 (one peak is overlapping); HRMS (DART) m/z calcd for $C_{26}H_{21}N_2$ $[MH]^+$: 361.1705, found 361.1708.



3Ob: 72%^[c]

4-(1-Methyl-2-(naphthalen-2-yl)-1H-imidazol-4-yl)benzonitrile (3Ob): The reaction was performed by using $Ni(cod)_2$ (11.0 mg, 0.040 mmol, 10 mol%) instead of $Ni(OTf)_2$ for 36 h. Purification by Isolera[®] (hexane/EtOAc = 10/1 to EtOAc) afforded **3Ob** as a yellow solid (89.2 mg, 72% yield). 1H NMR (400 MHz, $CDCl_3$): δ 8.12 (s, 1H), 7.98–7.86 (m, 5H), 7.80 (dd, $J = 8.4, 1.6$ Hz, 1H), 7.64 (d, $J = 8.4$ Hz, 2H), 7.58–7.50 (m, 2H), 7.39 (s, 1H), 3.83 (s, 3H); ^{13}C NMR (100 MHz, $CDCl_3$): δ 148.9, 139.4, 138.6, 133.3, 133.0, 132.4, 128.4, 128.3, 128.2, 127.8, 127.3, 126.9, 126.7, 126.0, 125.1, 120.1, 119.3, 110.0, 34.9; HRMS (DART) m/z calcd for $C_{21}H_{16}N_3$ $[MH]^+$: 310.1344, found 310.1349.

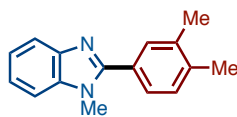


3Pb **3Pb'**
93% (combined yield)

Ethyl 1-methyl-2-(naphthalen-2-yl)-1H-imidazole-4-carboxylate (3Pb): The reaction was performed by $Ni(cod)_2$ (11.0 mg, 0.040 mmol, 10 mol%) instead of $Ni(OTf)_2$ for 36 h. Purification by Isolera[®] (hexane/EtOAc = 10/1 to EtOAc) afforded **3Pb** as a white solid (37.5 mg, 33% yield). 1H NMR (400 MHz, $CDCl_3$): δ 8.11 (s, 1H), 7.93–7.83 (m, 3H), 7.76 (d, $J = 8.8$ Hz, 1H), 7.69 (s, 1H), 7.55–7.48 (m, 2H), 4.41 (q, $J = 7.2$ Hz, 2H), 3.80 (s, 3H), 1.39 (t, $J = 7.2$ Hz, 3H); ^{13}C NMR (100 MHz, $CDCl_3$): δ 163.0, 148.8, 133.2, 132.9, 132.7, 128.6, 128.3, 128.2, 127.7, 126.9, 126.8, 126.6, 126.0, 60.4, 35.0, 14.4 (one peak is overlapping); HRMS (DART) m/z calcd for $C_{17}H_{17}N_2O_2$ $[MH]^+$: 281.1290, found 281.1289.

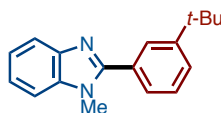
tert-Pentyl 1-methyl-2-(naphthalen-2-yl)-1H-imidazole-4-carboxylate (3Pb'): Purification by Isolera[®] (hexane/EtOAc = 10/1 to EtOAc) afforded **3Pb'** as a white solid (77.6 mg, 60% yield). 1H NMR (400 MHz, $CDCl_3$): δ 8.13 (s, 1H), 7.93–7.85 (m, 3H),

7.79 (d, $J = 8.0$ Hz, 1H), 7.58 (s, 1H), 7.54–7.50 (m, 2H), 3.82 (s, 3H), 1.94 (q, $J = 7.2$ Hz, 2H), 1.57 (s, 6H), 0.97 (t, $J = 7.2$ Hz, 3H); ^{13}C NMR (100 MHz, CDCl_3): δ 162.1, 148.6, 134.2, 133.3, 132.9, 128.5, 128.3, 128.2, 127.7, 127.6, 127.2, 126.9, 126.6, 126.2, 83.2, 35.0, 33.6, 25.8, 8.4; HRMS (DART) m/z calcd for $\text{C}_{20}\text{H}_{23}\text{N}_2\text{O}_2$ $[\text{MH}]^+$: 323.1760, found 323.1757.



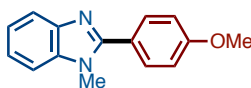
3Ac: 74%

2-(3,4-Dimethylphenyl)-1-methyl-1H-benzo[d]imidazole (3Ac): Purification by PTLC (hexane/EtOAc = 4/1) afforded **3Ac** as a white solid (69.6 mg, 74% yield). ^1H NMR (400 MHz, CDCl_3): δ 7.84–7.79 (m, 1H), 7.57 (s, 1H), 7.42 (d, $J = 7.6$ Hz, 1H), 7.35–7.22 (m, 4H), 3.79 (s, 3H), 2.324 (s, 3H), 2.317 (s, 3H); ^{13}C NMR (100 MHz, CDCl_3): δ 153.9, 142.8, 138.4, 137.0, 136.5, 130.5, 129.6, 127.5, 126.5, 122.4, 122.1, 119.5, 109.4, 31.5, 19.6 (one peak is overlapping); HRMS (DART) m/z calcd for $\text{C}_{16}\text{H}_{17}\text{N}_2$ $[\text{MH}]^+$: 237.1392, found 237.1387.



3Ad: 74%

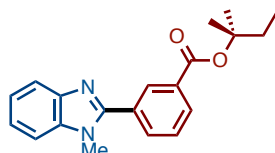
2-(3-(tert-Butyl)phenyl)-1-methyl-1H-benzo[d]imidazole (3Ad): Purification by PTLC (hexane/EtOAc = 4/1) afforded **3Ad** as a white solid (78.0 mg, 74% yield). ^1H NMR (400 MHz, CDCl_3): δ 7.87–7.83 (m, 1H), 7.82 (m, 1H), 7.57 (m, 2H), 7.46 (dd, $J = 8.0, 7.6$ Hz, 1H), 7.42–7.36 (m, 1H), 7.35–7.27 (m, 2H), 3.86 (s, 3H), 1.39 (s, 9H); ^{13}C NMR (100 MHz, CDCl_3): δ 154.4, 151.7, 143.0, 136.6, 129.9, 128.3, 126.8, 126.6, 126.5, 122.6, 122.3, 119.8, 109.5, 34.9, 31.6, 31.3; HRMS (DART) m/z calcd for $\text{C}_{18}\text{H}_{21}\text{N}_2$ $[\text{MH}]^+$: 265.1705, found 265.1700



3Ae: 58%

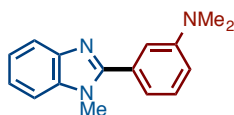
2-(4-Methoxyphenyl)-1-methyl-1H-benzo[d]imidazole (3Ae): Purification by PTLC (hexane/EtOAc = 1/1) afforded **3Ae** as a white solid (57.2 mg, 58% yield). ^1H NMR

(400 MHz, CDCl₃): δ 7.80 (dd, J = 8.0, 3.2 Hz, 1H), 7.67 (d, J = 8.0 Hz, 2H), 7.35–7.25 (m, 3H), 7.00 (d, J = 8.0 Hz, 2H), 3.84 (s, 3H), 3.78 (s, 3H); ¹³C NMR (100 MHz, CDCl₃): δ 160.6, 153.6, 142.8, 136.4, 130.7, 122.4, 122.3, 122.1, 119.4, 114.0, 109.4, 55.2, 31.5; HRMS (DART) m/z calcd for C₁₅H₁₅N₂O [MH]⁺: 239.1184, found 239.1181.



3Af: 81%

tert-Pentyl 3-(1-methyl-1H-benzo[d]imidazol-2-yl)benzoate (3Af): Purification by PTLC (hexane/EtOAc = 10/1) and then GPC afforded **3Af** as a colorless liquid (69.1 mg, 81% yield). ¹H NMR (400 MHz, CDCl₃): δ 8.37 (s, 1H), 8.13 (d, J = 6.8 Hz, 1H), 7.95 (d, J = 6.8 Hz, 1H), 7.84 (d, J = 4.0 Hz, 1H), 7.59 (t, J = 6.8 Hz, 1H), 7.42–7.30 (m, 3H), 3.85 (s, 3H), 1.94 (q, J = 7.2 Hz, 2H), 1.58 (s, 6H), 0.98 (t, J = 7.2 Hz, 3H); ¹³C NMR (100 MHz, CDCl₃): δ 164.8, 152.7, 142.8, 136.4, 133.3, 132.4, 130.4, 130.3, 129.9, 128.6, 122.8, 122.4, 119.7, 109.6, 83.9, 33.5, 31.5, 25.5, 8.2; HRMS (DART) m/z calcd for C₂₀H₂₃N₂O₂ [MH]⁺: 323.1760, found 323.1756.



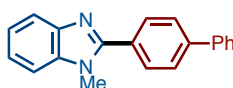
3Ag: 67%

***N,N*-Dimethyl-3-(1-methyl-1H-benzo[d]imidazol-2-yl)aniline (3Ag):** Purification by Isolera[®] (hexane/EtOAc = 10/1 to 1:2) afforded **3Ag** as a yellow oil (67.0 mg, 67% yield). ¹H NMR (400 MHz, CDCl₃): δ 7.86–7.80 (m, 1H), 7.41–7.27 (m, 4H), 7.11 (s, 1H), 7.00 (d, J = 8.4 Hz, 1H), 6.85 (d, J = 8.4 Hz, 1H), 3.84 (s, 3H), 3.01 (s, 6H); ¹³C NMR (100 MHz, CDCl₃): δ 154.7, 150.7, 142.9, 136.5, 130.8, 129.0, 122.5, 122.2, 119.7, 117.2, 113.6, 113.4, 109.5, 40.5, 31.6; HRMS (DART) m/z calcd for C₁₆H₁₈N₃ [MH]⁺: 252.1501, found 252.1501.



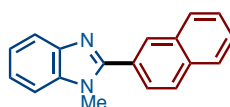
3Ah: 95%

1-Methyl-2-(pyridin-3-yl)-1H-benzo[d]imidazole (3Ah): Purification by Isolera[®] (hexane/EtOAc = 1/1 to EtOAc) afforded **3Ah** as a white solid (79.6 mg, 95% yield). ¹H NMR (400 MHz, CDCl₃): δ 9.02 (s, 1H), 8.75 (dd, *J* = 4.0, 1.6 Hz, 1H), 8.14 (dd, *J* = 8.0, 1.6 Hz, 1H), 7.85–7.80 (m, 1H), 7.52–7.30 (m, 4H), 3.89 (s, 3H); ¹³C NMR (100 MHz, CDCl₃): δ 150.6, 149.8, 143.0, 136.8, 136.5, 126.5, 123.5, 123.3, 122.7, 120.0, 109.7, 31.6; HRMS (DART) *m/z* calcd for C₁₃H₁₂N₃ [MH]⁺: 210.1031, found 210.1025.



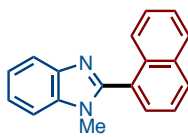
3Ai: 92%

2-([1,1'-Biphenyl]-4-yl)-1-methyl-1H-benzo[d]imidazole (3Ai)¹³⁹: Purification by Isolera[®] (hexane/EtOAc = 5/1 to EtOAc) afforded **3Ai** as a white solid (105.2 mg, 92% yield). ¹H NMR (400 MHz, CDCl₃): δ 7.98–7.80 (m, 3H), 7.72 (d, *J* = 8.4 Hz, 2H), 7.63 (d, *J* = 8.0 Hz, 2H), 7.46 (t, *J* = 8.0 Hz, 2H), 7.40–7.27 (m, 4H), 3.85 (s, 3H); ¹³C NMR (100 MHz, CDCl₃): δ 153.4, 142.9, 142.3, 140.0, 136.6, 129.7, 128.9, 128.8, 127.8, 127.2, 127.1, 122.7, 122.4, 119.7, 109.6, 31.7; HRMS (DART) *m/z* calcd for C₂₀H₁₇N₂ [MH]⁺: 285.1392, found 285.1393.



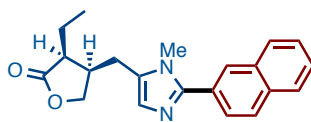
3Ab: >95%

1-Methyl-2-(naphthalen-2-yl)-1H-benzo[d]imidazole (3Ab): Purification by Isolera[®] (hexane/EtOAc = 10/1 to EtOAc) afforded **3Ab** as a white solid (103.0 mg, >95% yield). ¹H NMR (400 MHz, CDCl₃): δ 8.15 (s, 1H), 7.91–7.78 (m, 5H), 7.51–7.45 (m, 2H), 7.32–7.24 (m, 3H), 3.75 (s, 3H); ¹³C NMR (100 MHz, CDCl₃): δ 153.5, 142.9, 136.5, 133.4, 132.7, 129.1, 128.3, 128.2, 127.6, 127.3, 127.0, 126.5, 126.1, 122.6, 122.3, 119.6, 109.5, 31.5; HRMS (DART) *m/z* calcd for C₁₈H₁₅N₂ [MH]⁺: 259.1235, found 259.1235.



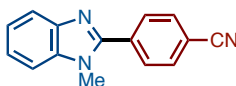
3Aj: 91%

1-Methyl-2-(naphthalen-1-yl)-1H-benzo[*d*]imidazole (3Aj): Purification by PTLC (hexane/EtOAc = 20/1 to EtOAc) afforded **3Aj** as a white solid (98.6 mg, 91% yield). ^1H NMR (400 MHz, CDCl_3): δ 8.01 (d, $J = 8.4$ Hz, 1H), 7.93 (d, $J = 8.4$ Hz, 1H), 7.92–7.87 (m, 1H), 7.73 (d, $J = 8.0$ Hz, 1H), 7.67 (d, $J = 8.0$ Hz, 1H), 7.59 (t, $J = 8.4$ Hz, 1H), 7.56–7.41 (m, 3H), 7.40–7.32 (m, 2H), 3.60 (s, 3H); ^{13}C NMR (100 MHz, CDCl_3): δ 152.9, 143.2, 135.9, 133.5, 132.1, 130.2, 128.8, 128.4, 127.8, 127.2, 126.3, 125.4, 125.0, 122.7, 122.3, 120.0, 109.5, 31.0; HRMS (DART) m/z calcd for $\text{C}_{18}\text{H}_{15}\text{N}_2$ $[\text{MH}]^+$: 259.1235, found 259.1230.



**pilocarpine derivative
3Qb: 69%**

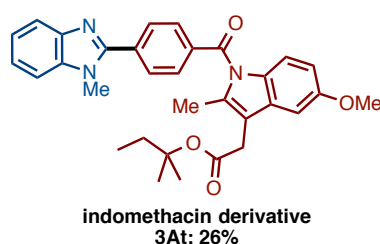
(3*S*,4*R*)-3-Ethyl-4-((1-methyl-2-(naphthalen-2-yl)-1H-imidazol-5-yl)methyl)dihydrofuran-2(3*H*)-one (3Qb): Purification by Isolera[®] (hexane/EtOAc = 10/1 to EtOAc) afforded **3Qb** as a colorless oil (92.2 mg, 69% yield). ^1H NMR (400 MHz, CDCl_3): δ 8.03 (s, 1H), 7.93–7.83 (m, 3H), 7.71 (dd, $J = 8.4, 2.0$ Hz, 1H), 7.54–7.48 (m, 2H), 6.94 (s, 1H), 4.47 (dd, $J = 9.2, 7.2$ Hz, 1H), 3.98 (dd, $J = 9.2, 7.2$ Hz, 1H), 3.66 (s, 3H), 2.92 (dd, $J = 15.6, 5.2$ Hz, 1H), 2.81–2.63 (m, 2H), 2.33 (q, $J = 6.4$ Hz, 1H), 1.85–1.73 (m, 2H), 1.08 (t, $J = 8.0$ Hz, 3H); ^{13}C NMR (100 MHz, CDCl_3): δ 178.1, 148.8, 133.3, 133.2, 129.8, 128.34, 128.28, 128.1, 127.8, 126.81, 126.76, 126.7, 126.6, 126.3, 71.1, 46.7, 39.2, 32.0, 28.5, 22.6, 11.1; HRMS (DART) m/z calcd for $\text{C}_{21}\text{H}_{23}\text{N}_2\text{O}_2$ $[\text{MH}]^+$: 335.1760, found 335.1762.



3As: 66%

4-(1-Methyl-1H-benzo[*d*]imidazol-2-yl)benzotrile (3As): The reaction was

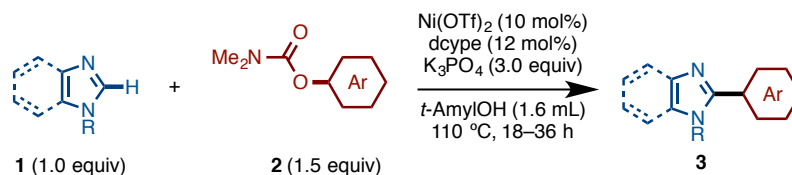
performed by using Ni(cod)₂ (11.0 mg, 0.040 mmol, 10 mol%) instead of Ni(OTf)₂ for 36 h with 4-chlorobenzonitrile. Purification by Isolera[®] (hexane/EtOAc = 10:1 to EtOAc) afforded **3As** as a white solid (62.0 mg, 66% yield). ¹H NMR (400 MHz, CDCl₃): δ 7.92 (d, *J* = 8.4 Hz, 2H), 7.86–7.78 (m, 3H), 7.45–7.31 (m, 3H), 3.90 (s, 3H); ¹³C NMR (100 MHz, CDCl₃): δ 151.4, 142.9, 136.7, 134.6, 132.4, 129.9, 123.6, 123.0, 120.2, 118.2, 113.3, 109.8, 31.8; HRMS (DART) *m/z* calcd for C₁₅H₁₂N₃ [MH]⁺: 234.1031, found 234.1038.



tert-Pentyl

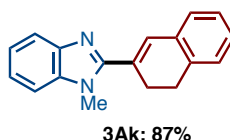
2-(5-methoxy-2-methyl-1-(4-(1-methyl-1*H*-benzo[*d*]imidazol-2-yl)benzoyl)-1*H*-indol-3-yl)acetate (3At**):** Purification by Isolera[®] (hexane/EtOAc = 1:0 to 0:1) afforded **3At** as a white solid (55.0 mg, 26% yield). ¹H NMR (400 MHz, CDCl₃): δ 7.92 (d, *J* = 8.4 Hz, 2H), 7.87–7.82 (m, 3H), 7.45–7.30 (m, 3H), 7.00–6.96 (m, 2H), 6.67 (dd, *J* = 8.8, 2.0 Hz, 1H), 3.91 (s, 3H), 3.83 (s, 3H), 3.59 (s, 2H), 2.40 (s, 3H), 1.76 (q, *J* = 8.0 Hz, 2H), 1.42 (s, 6H), 0.82 (t, *J* = 8.0 Hz, 3H); ¹³C NMR (100 MHz, CDCl₃): δ 170.0, 168.6, 156.0, 152.2, 142.9, 136.7, 135.6, 134.2, 130.8, 129.9, 129.7, 123.4, 122.8, 120.1, 115.1, 113.6, 111.7, 109.7, 101.4, 83.5, 55.6, 33.3, 31.8, 31.6, 25.5, 13.4, 8.1; HRMS (ESI) *m/z* calcd for C₃₂H₃₃N₃O₄Na [MNa]⁺: 546.2363, found 546.2360.

4-4. Nickel-Catalyzed C–H Alkenylation of Imidazoles with Enol Derivatives

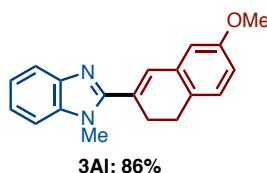


General Procedure: A 50-mL glass Schlenk tube containing a magnetic stirring bar and K₃PO₄ (670.3 mg, 3.0 mmol, 3.0 equiv) was dried with a heatgun for 3 min *in vacuo* and filled with argon after cooling to room temperature. Ni(OTf)₂ (35.7 mg, 0.10 mmol,

10 mol%), imidazole **1** (1.0 mmol, 1.0 equiv), alkenyl carbamate **2** (1.5 mmol, 1.5 equiv), and 3,4-bis(dicyclohexylphosphino)thiophene (dcypt: 57.2 mg, 0.12 mmol, 12 mol%) were placed in a 20-mL glass Schlenk tube under a argon atmosphere. Then, to it was added dry degassed *t*-AmylOH (2.0 mL) under a stream of argon. The *t*-AmylOH solution was transferred into the 50-mL Schlenk tube under a stream of argon via cannula. The 20 mL Schlenk was washed with *t*-AmylOH (2.0 mL), and then 2 mL of solution was transferred into 50 mL Schlenk via cannula. The reaction mixture was stirred at 120 °C for 36 h. After cooling the reaction mixture to room temperature, the mixture was diluted with ethyl acetate, and the organic layer was washed with water and brine, dried over Na₂SO₄, and filtered. The filtrate was concentrated and the residue was purified by silica-gel column chromatography to afford a C–H coupling product (2-alkenylated imidazole **3**).

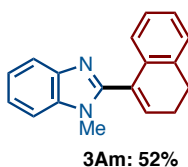


2-(3,4-Dihydronaphthalen-2-yl)-1-methyl-1H-benzo[d]imidazole (3Ak): Purification by silica-gel column chromatography (hexane/EtOAc = 3/1) afforded **3Ak** as a white solid (225.7 mg, 87% yield). ¹H NMR (400 MHz, CDCl₃): δ 7.82 (d, *J* = 7.2 Hz, 1H), 7.40–7.20 (m, 7H), 6.99 (s, 1H), 3.96 (s, 3H), 3.08–2.97 (m, 4H); ¹³C NMR (100 MHz, CDCl₃): δ 153.8, 142.7, 136.6, 135.6, 133.1, 131.1, 129.1, 128.3, 127.6, 127.3, 126.7, 122.8, 122.3, 119.6, 109.4, 32.1, 27.8, 26.3; HRMS (DART) *m/z* calcd for C₁₈H₁₇N₂ [MH]⁺: 261.1392, found 261.1392.



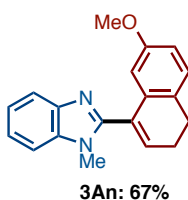
2-(7-Methoxy-3,4-dihydronaphthalen-2-yl)-1-methyl-1H-benzo[d]imidazole (3Al): Purification by silica-gel column chromatography (hexane/EtOAc = 2/1) afforded **3Al** as a white solid (249.2 mg, 86% yield). ¹H NMR (400 MHz, CDCl₃): δ 7.79 (dd, *J* = 6.8, 2.4 Hz, 1H), 7.40–7.27 (m, 3H), 7.13 (d, *J* = 8.0 Hz, 1H), 6.93 (s, 1H), 6.81–6.75 (m, 2H), 3.94 (s, 3H), 3.83 (s, 3H), 3.00–2.90 (m, 4H); ¹³C NMR (100 MHz, CDCl₃): δ

159.4, 153.8, 142.6, 136.6, 134.0, 131.1, 129.7, 128.4, 127.7, 122.9, 122.3, 119.6, 113.4, 112.9, 109.4, 55.3, 32.1, 26.9, 26.8; HRMS (DART) m/z calcd for $C_{19}H_{19}N_2O$ $[MH]^+$: 291.1497, found 291.1496.



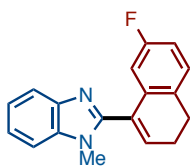
2-(3,4-Dihydronaphthalen-1-yl)-1-methyl-1H-benzo[d]imidazole (3Am):

Purification by silica-gel column chromatography (hexane/EtOAc = 2/1) afforded **3Am** as a pink solid (134.7 mg, 52% yield). 1H NMR (400 MHz, $CDCl_3$): δ 7.82 (d, J = 6.4 Hz, 1H), 7.40–7.27 (m, 3H), 7.24–7.16 (m, 2H), 7.10 (t, J = 7.2 Hz, 1H), 6.78 (d, J = 7.2 Hz, 1H), 6.53 (t, J = 4.8 Hz, 1H), 3.60 (s, 3H), 2.94 (t, J = 8.4 Hz, 2H), 2.60–2.50 (m, 2H); ^{13}C NMR (100 MHz, $CDCl_3$): δ 153.0, 143.0, 135.8, 135.4, 134.6, 132.8, 129.7, 127.8, 127.7, 126.8, 124.7, 122.6, 122.1, 119.9, 109.4, 31.0, 27.5, 23.4; HRMS (DART) m/z calcd for $C_{18}H_{17}N_2$ $[MH]^+$: 261.1392, found 261.1391.



2-(7-Methoxy-3,4-dihydronaphthalen-1-yl)-1-methyl-1H-benzo[d]imidazole (3An):

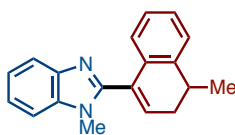
Purification by silica-gel column chromatography (hexane/EtOAc = 2/1) afforded **3An** as a yellow oil (193.4 mg, 67% yield). 1H NMR (400 MHz, $CDCl_3$): δ 7.81 (d, J = 6.4 Hz, 1H), 7.40–7.27 (m, 3H), 7.13 (d, J = 8.4 Hz, 1H), 6.74 (dd, J = 8.0, 2.8 Hz, 1H), 6.55 (t, J = 4.4 Hz, 1H), 6.38 (d, J = 2.8 Hz, 1H), 3.56 (s, 3H), 2.61 (s, 3H), 2.86 (t, J = 7.6 Hz, 2H), 2.56–2.48 (m, 2H); ^{13}C NMR (100 MHz, $CDCl_3$): δ 158.4, 152.7, 142.8, 135.7, 135.2, 133.7, 129.5, 128.4, 127.4, 122.5, 122.0, 119.7, 112.2, 111.0, 109.3, 55.2, 30.9, 26.5, 23.7; HRMS (DART) m/z calcd for $C_{19}H_{19}N_2O$ $[MH]^+$: 291.1497, found 291.1493.



3Ao: 66%

2-(7-Fluoro-3,4-dihydronaphthalen-1-yl)-1-methyl-1H-benzo[d]imidazole (3Ao):

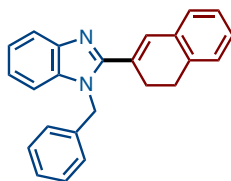
Purification by silica-gel column chromatography (hexane/EtOAc = 2/1) afforded **3Ao** as a white solid (184.9 mg, 66% yield). ¹H NMR (400 MHz, CDCl₃): δ 7.82 (d, *J* = 6.8 Hz, 1H), 7.42–7.29 (m, 3H), 7.17 (dd, *J* = 8.4, 5.6 Hz, 1H), 6.88 (td, *J* = 8.4, 2.8 Hz, 1H), 6.60–6.53 (m, 2H), 3.63 (s, 3H), 2.90 (t, *J* = 8.0 Hz, 2H), 2.59–2.51 (m, 2H); ¹³C NMR (100 MHz, CDCl₃): δ 161.8 (d, *J* = 241.8 Hz), 152.2, 142.8, 135.7, 134.5 (d, *J* = 7.6 Hz), 130.80, 130.78, 129.1, 128.9 (d, *J* = 7.6 Hz), 122.8, 122.2, 119.9, 114.1 (d, *J* = 21.0 Hz), 111.8 (d, *J* = 22.9 Hz), 109.5, 31.0, 26.7, 23.5; HRMS (DART) *m/z* calcd for C₁₈H₁₆FN₂ [MH]⁺: 279.1298, found 279.1293.



3Ap: 69%

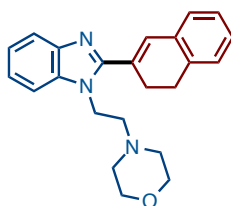
1-Methyl-2-(4-methyl-3,4-dihydronaphthalen-1-yl)-1H-benzo[d]imidazole (3Ap):

Purification by silica-gel column chromatography (hexane/EtOAc = 2/1) afforded **3Ap** as a yellow oil (187.9 mg, 69% yield). ¹H NMR (400 MHz, CDCl₃): δ 7.85–7.79 (m, 1H), 7.40–7.20 (m, 5H), 7.11 (td, *J* = 7.8, 1.6 Hz, 1H), 6.79 (d, *J* = 7.8 Hz, 1H), 6.46 (t, *J* = 7.8 Hz, 1H), 3.60 (s, 3H), 3.08 (q, *J* = 6.8 Hz, 1H), 2.71 (ddd, *J* = 16.8, 6.8, 4.0 Hz, 1H), 2.37 (ddd, *J* = 16.8, 6.8, 4.0 Hz, 1H), 1.36 (d, *J* = 6.8 Hz, 3H); ¹³C NMR (100 MHz, CDCl₃): δ 153.0, 142.9, 140.2, 135.8, 133.1, 131.9, 129.2, 128.0, 126.6, 126.4, 124.8, 122.5, 122.0, 119.8, 109.3, 31.6, 31.2, 30.9, 20.0; HRMS (DART) *m/z* calcd for C₁₉H₁₉N₂ [MH]⁺: 275.1548, found 275.1545



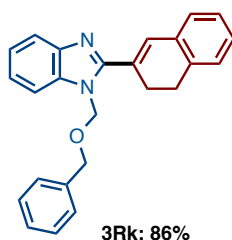
3Bk: 87%

1-Benzyl-2-(3,4-dihydronaphthalen-2-yl)-1H-benzo[d]imidazole (3Bk): Purification by silica-gel column chromatography (hexane/EtOAc = 3/1) afforded **3Bk** as a white solid (293.1 mg, 87% yield). ^1H NMR (400 MHz, CDCl_3): δ 7.84 (d, $J = 7.6$ Hz, 1H), 7.40–7.22 (m, 7H), 7.20–7.10 (m, 4H), 6.89 (d, $J = 7.6$ Hz, 1H), 6.76 (s, 1H), 5.54 (s, 2H), 3.00–2.93 (m, 4H); ^{13}C NMR (100 MHz, CDCl_3): δ 154.3, 143.0, 136.7, 136.5, 135.6, 133.1, 130.8, 129.1, 128.8, 128.4, 127.8, 127.6, 127.3, 126.6, 125.9, 123.2, 122.6, 119.8, 110.1, 48.7, 27.8, 26.4; HRMS (DART) m/z calcd for $\text{C}_{24}\text{H}_{21}\text{N}_2$ $[\text{MH}]^+$: 337.1705, found 337.1705.



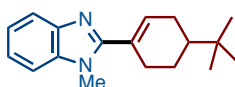
3Dk: 80%

4-(2-(2-(3,4-Dihydronaphthalen-2-yl)-1H-benzo[d]imidazol-1-yl)ethyl)morpholine (3Dk): Purification by silica-gel column chromatography ($\text{CH}_2\text{Cl}_2/\text{MeOH} = 24/1$) afforded **3Dk** as a pale yellow oil (288.6 mg, 80% yield). ^1H NMR (400 MHz, CDCl_3): δ 7.82–7.76 (m, 1H), 7.42–7.40 (m, 1H), 7.33–7.28 (m, 2H), 7.27–7.21 (m, 3H), 7.19–7.16 (m, 1H), 7.07 (s, 1H), 4.46 (t, $J = 7.6$ Hz, 2H), 3.68 (t, $J = 4.8$ Hz, 4H), 3.08–2.94 (m, 4H), 2.85 (t, $J = 7.6$ Hz, 2H), 2.51 (t, $J = 4.8$ Hz, 4H); ^{13}C NMR (100 MHz, CDCl_3): δ 153.9, 142.9, 135.8, 135.5, 133.1, 130.7, 129.2, 128.4, 127.7, 127.1, 126.7, 122.8, 122.4, 119.8, 109.7, 66.8, 57.5, 54.0, 42.9, 27.8, 26.7; HRMS (DART) m/z calcd for $\text{C}_{23}\text{H}_{26}\text{N}_3\text{O}$ $[\text{MH}]^+$: 360.2076, found 360.2077.



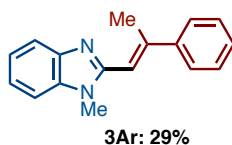
1-((Benzyloxy)methyl)-2-(3,4-dihydronaphthalen-2-yl)-1H-benzo[*d*]imidazole

(3Rk): Purification by silica-gel column chromatography (hexane/EtOAc = 4/1) afforded **3Rk** as a yellow oil (314.4 mg, 86% yield). ¹H NMR (400 MHz, CDCl₃): δ 7.87–7.83 (m, 1H), 7.45–7.30 (m, 9H), 7.25–7.18 (m, 3H), 7.15 (d, *J* = 7.6 Hz, 1H), 5.68 (s, 2H), 4.70 (s, 2H), 3.03–2.99 (m, 4H); ¹³C NMR (100 MHz, CDCl₃): δ 154.4, 142.4, 136.5, 136.1, 135.6, 133.1, 131.9, 131.8, 128.4, 128.3, 128.1, 127.9, 127.5, 127.4, 126.5, 123.3, 122.8, 119.6, 109.6, 72.9, 70.3, 27.6, 26.1; HRMS (DART) *m/z* calcd for C₂₅H₂₃N₂O [MH]⁺: 367.1810, found 367.1817.



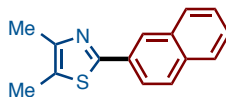
2-(4-(*tert*-Butyl)cyclohex-1-en-1-yl)-1-methyl-1H-benzo[*d*]imidazole **(3Aq):**

Purification by Isolera[®] (hexane/EtOAc = 10/1 to EtOAc) and then GPC afforded **3Aq** as a white solid (80.4 mg, 75% yield). ¹H NMR (400 MHz, CDCl₃): δ 7.73 (d, *J* = 8.8 Hz, 1H), 7.30–7.19 (m, 3H), 6.18 (dd, *J* = 2.8, 2.4 Hz, 1H), 3.76 (s, 3H), 2.77 (dd, *J* = 15.2, 3.6 Hz, 1H), 2.56–2.28 (m, 2H), 2.10–1.97 (m, 2H), 1.50–1.28 (m, 2H), 0.93 (s, 9H); ¹³C NMR (100 MHz, CDCl₃): δ 155.0, 142.5, 136.1, 133.4, 128.6, 122.2, 121.9, 119.4, 109.2, 43.5, 32.2, 31.4, 29.3, 27.4, 27.1, 23.9; HRMS (DART) *m/z* calcd for C₁₈H₂₅N₂ [MH]⁺: 269.2018, found 269.2018.



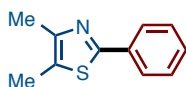
(*E*)-1-methyl-2-(2-phenylprop-1-en-1-yl)-1H-benzo[*d*]imidazole **(3Ar):** Purification by silica-gel column chromatography (hexane/ether = 3/1) afforded **3Ar** as a pale yellow solid (72.8 mg, 29% yield). ¹H NMR (400 MHz, CDCl₃): δ 7.83–7.78 (m, 1H), 7.58 (d, *J* = 8.0 Hz, 2H), 7.45–7.27 (m, 6H), 6.71 (s, 1H), 3.81 (s, 3H), 2.73 (s, 3H); ¹³C

NMR (100 MHz, CDCl₃): δ 151.0, 147.4, 143.1, 143.0, 135.0, 128.4, 128.2, 126.1, 122.4, 122.0, 119.5, 112.7, 108.9, 29.8, 18.5; HRMS (DART) m/z calcd for C₁₇H₁₇N₂ [MH]⁺: 249.1392, found 249.1391.



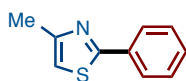
6Ab: 90%

4,5-Dimethyl-2-(naphthalen-2-yl)thiazole (6Ab): Purification by PTLC (hexane/EtOAc = 20/1) afforded **6Ab** as a pale yellow solid (86.0 mg, 90% yield). ¹H NMR (400 MHz, CDCl₃): δ 8.33 (s, 1H), 7.97 (dd, J = 8.8, 2.0 Hz, 1H), 7.91–7.78 (m, 3H), 7.51–7.43 (m, 2H), 2.41 (s, 3H), 2.39 (s, 3H); ¹³C NMR (100 MHz, CDCl₃): δ 163.3, 149.4, 133.7, 133.3, 131.2, 128.50, 128.46, 127.7, 126.7, 126.5, 125.1, 123.8, 14.8, 11.5; HRMS (DART) m/z calcd for C₁₅H₁₄NS [MH]⁺: 240.0847, found 240.0846.



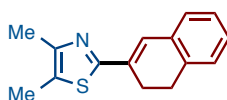
6Aa: 91%

4,5-Dimethyl-2-phenylthiazole (6Aa)^[9b]: Purification by PTLC (hexane/EtOAc = 10/1) afforded **6Aa** as a colorless liquid (69.1 mg, 91% yield). ¹H NMR (400 MHz, CDCl₃): δ 7.86 (dd, J = 8.0, 2.4 Hz, 2H), 7.42–7.33 (m, 3H), 2.38 (s, 6H); ¹³C NMR (100 MHz, CDCl₃): δ 163.3, 149.3, 133.9, 129.3, 128.8, 126.5, 126.1, 14.8, 11.4; HRMS (DART) m/z calcd for C₁₁H₁₂NS [MH]⁺: 190.0690, found 190.0686.



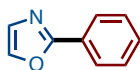
6Ba: 54%

4-Methyl-2-phenylthiazole (6Ba)^[9b]: Purification by Isolera[®] (hexane/EtOAc = 100/0 to 10/1) afforded **6Ba** as a yellow liquid (37.8 mg, 54% yield). ¹H NMR (400 MHz, CDCl₃): δ 7.92 (d, J = 7.6 Hz, 2H), 7.45–7.35 (m, 3H), 6.85 (s, 1H), 2.50 (s, 3H); ¹³C NMR (100 MHz, CDCl₃): δ 167.5, 153.8, 133.8, 129.7, 128.8, 126.4, 113.4, 17.2; HRMS (DART) m/z calcd for C₁₀H₁₀NS [MH]⁺: 176.0534, found 176.0535.



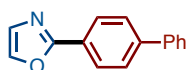
6Ak: 59%^[b]

2-(3,4-Dihydronaphthalen-2-yl)-4,5-dimethylthiazole (6Ak): Purification by silica-gel column chromatography (hexane/ether = 6/1) afforded **6Ak** as a yellow solid (141.8 mg, 59% yield). ¹H NMR (400 MHz, CDCl₃): δ 7.19–7.14 (m, 5H), 2.97–2.83 (m, 4H), 2.38 (s, 3H), 2.36 (s, 3H); ¹³C NMR (100 MHz, CDCl₃): δ 164.3, 148.9, 135.7, 133.7, 132.7, 127.7, 127.4, 127.1, 126.6, 126.2, 125.9, 27.8, 25.0, 14.8, 11.5; HRMS (DART) *m/z* calcd for C₁₅H₁₆NS [MH]⁺: 242.1003, found 242.1002.



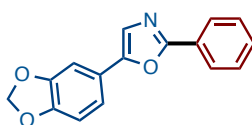
6Ca: 56%

2-Phenyloxazole (6Ca)^[9b]: Purification by PTLC (hexane/EtOAc = 20/1) afforded **6Ca** as a colorless liquid (32.6 mg, 56% yield). ¹H NMR (400 MHz, CDCl₃): δ 8.05 (d, *J* = 7.6 Hz, 2H), 7.69 (d, *J* = 2.0 Hz, 1H), 7.50–7.40 (m, 3H), 7.23 (d, *J* = 2.0 Hz, 1H); ¹³C NMR (100 MHz, CDCl₃): δ 161.9, 138.5, 130.3, 128.7, 128.3, 127.4, 126.3; HRMS (DART) *m/z* calcd for C₉H₈NO [MH]⁺: 146.0606, found 146.0603.



6Ci: 63%

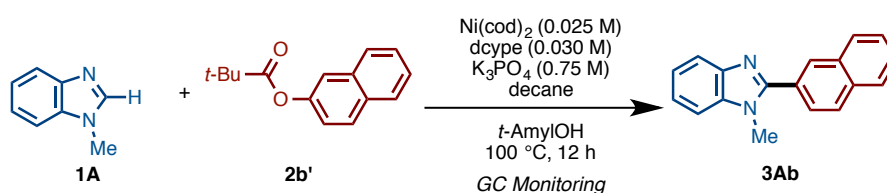
2-([1,1'-Biphenyl]-4-yl)oxazole (6Ci): Purification by PTLC (hexane/EtOAc = 10/1) afforded **6Ci** as white solid (55.8 mg, 63% yield). ¹H NMR (400 MHz, CDCl₃): δ 8.11 (d, *J* = 8.4 Hz, 2H), 7.69 (s, 1H), 7.66 (d, *J* = 8.4 Hz, 2H), 7.61 (d, *J* = 8.4 Hz, 2H), 7.44 (t, *J* = 8.4 Hz, 2H), 7.36 (t, *J* = 8.4 Hz, 1H), 7.24 (s, 1H); ¹³C NMR (100 MHz, CDCl₃): δ 161.8, 142.9, 140.1, 138.5, 128.8, 128.4, 127.8, 127.4, 127.0, 126.7, 126.3; HRMS (DART) *m/z* calcd for C₁₅H₁₂NO [MH]⁺: 222.0919, found 222.0920.



6Da: 74%^[c]

4,5-Dimethyl-2-phenylthiazole (6Da)^[10a]: Purification by flash column chromatography (hexane/EtOAc = 10:1 to 4:1) afforded **6Da** as a white solid (78.9 mg, 74% yield). ¹H NMR (400 MHz, CDCl₃): δ 8.05 (d, *J* = 8.4 Hz, 2H), 7.49–7.39 (m, 3H), 7.28 (s, 1H), 7.20 (d, *J* = 8.4 Hz, 1H), 7.14 (s, 1H), 6.85 (d, *J* = 8.4 Hz, 1H), 5.97 (s, 2H); ¹³C NMR (100 MHz, CDCl₃): δ 160.5, 151.0, 148.1, 147.8, 130.1, 128.7, 127.4, 126.1, 122.3, 122.1, 118.2, 108.7, 104.7, 101.3; HRMS (DART) *m/z* calcd for C₁₆H₁₂NO₃ [MH]⁺: 266.0817, found 266.0813.

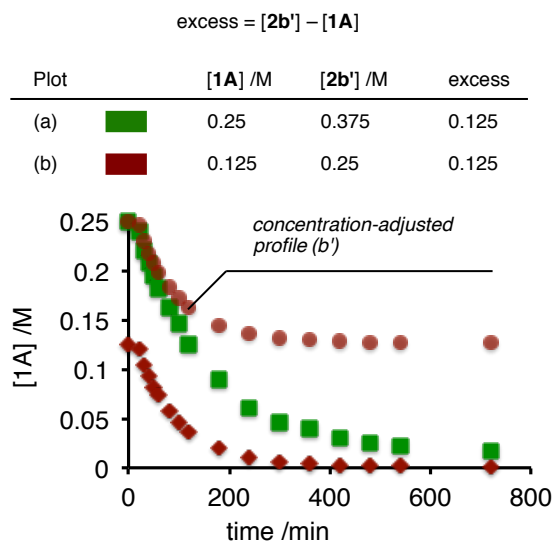
4-5. Reaction Progress Kinetic Analysis



A general procedure for RPKA

A 20-mL glass vessel equipped with a J. Young[®] O-ring tap containing a magnetic stirring bar and K₃PO₄ (509.4 mg, 2.4 mmol, 3.0 equiv) was dried with a heatgun for 3 min *in vacuo* and filled with N₂ after cooling to room temperature. To this vessel was added *N*-methylbenzimidazole (**1A**) and naphthalen-2-yl pivalate (**2a'**), which was then introduced into an argon-atmosphere glovebox. To the reaction vessel were added Ni(cod)₂ (22.0 mg, 0.080 mmol, 10 mol%) and 1,2-bis(dicyclohexylphosphino)ethane (dcype: 40.7 mg, 0.096 mmol, 12 mol%). The vessel was taken out of the glovebox, then dodecane (80 μL as an internal standard) and dry *t*-AmylOH (3.2 mL) were added under a stream of N₂. The vessel was sealed with O-ring tap and then heated at 110 °C for 18–36 h in an 8-well reaction block with stirring. The reaction progress was monitored by GC (taking every 50 μL of sample after 20, 40, 60, 80, 100, 120, 180, 240, 300, 360, 420, 480, 540, and 720 min). GC yield was determined by using dodecane as an internal standard.

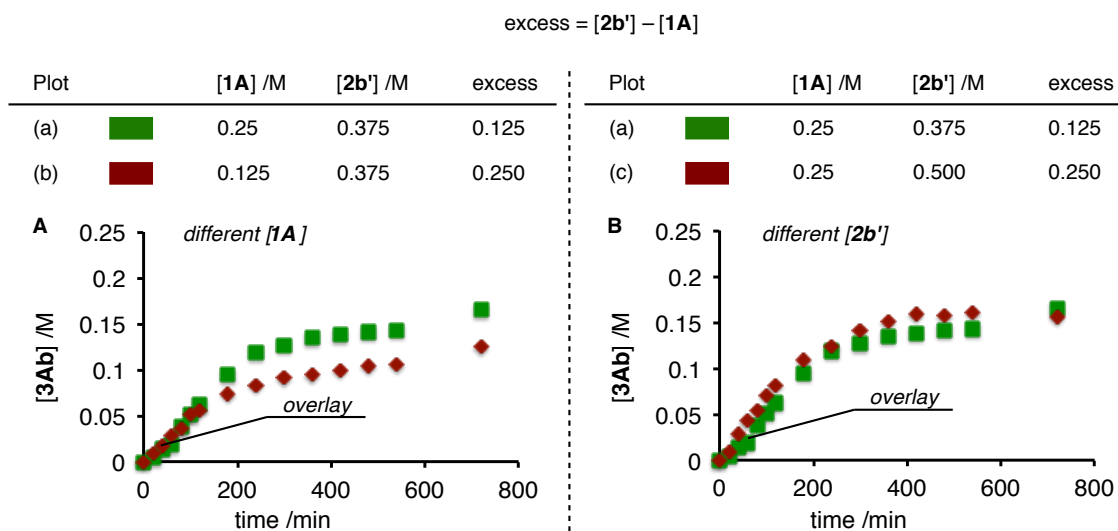
For “same excess” Experiment



For the reaction of (a): **1A** (105.7 mg, 0.80 mmol), **2a'** (274.0 mg, 1.20 mmol)

For the reaction of (b): **1A** (52.9 mg, 0.40 mmol), **2a'** (182.6 mg, 0.80 mmol)

For “different excess” Experiment

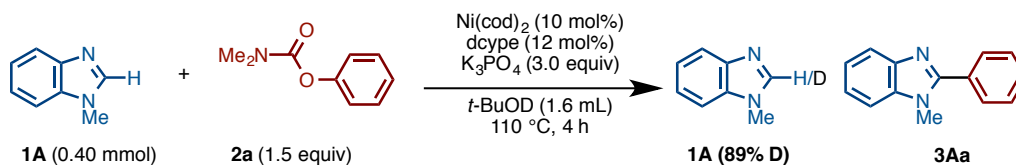


For the reaction of (a): **1A** (105.7 mg, 0.80 mmol), **2a'** (274.0 mg, 1.20 mmol)

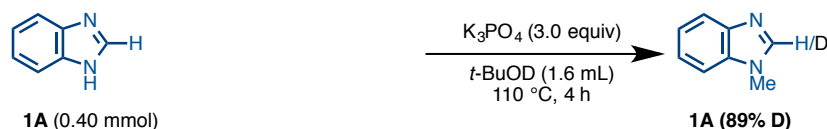
For the reaction of (b): **1A** (52.9 mg, 0.40 mmol), **2a'** (274.0 mg, 1.20 mmol)

For the reaction of (c): **1A** (105.7 mg, 0.40 mmol), **2a'** (365.3 mg, 1.60 mmol)

Deuterium Experiment



A 20-mL glass vessel equipped with a J. Young[®] O-ring tap containing a magnetic stirring bar and K₃PO₄ (255.0 mg, 1.20 mmol, 3.0 equiv) was dried with a heatgun for 3 min *in vacuo* and filled with N₂ after cooling to room temperature. To this vessel were added Ni(OTf)₂ (14.2 mg, 0.040 mmol, 10 mol%), *N*-methylbenzimidazole (**1A**) (52.9 mg, 0.40 mmol, 1.0 equiv) and phenyl carbamate **2a** (99.1 mg, 0.60 mmol, 1.5 equiv), then introduced into an argon-atmosphere glovebox. To the reaction vessel was added 1,2-bis(dicyclohexylphosphino)ethane (dcype: 20.6 mg, 0.050 mmol, 12 mol%). The vessel was taken out of the glovebox, then dry *t*-BuOD (1.6 mL) was added under a stream of N₂. The vessel was sealed with an O-ring tap and then heated at 110 °C for 4 h in an 8-well reaction block with stirring. After cooling the reaction mixture to room temperature, the mixture was passed through a Celite[®] pad with EtOAc as the eluent. The filtrate was concentrated and the residue was analyzed by ¹H NMR to determine the H/D ratio of remaining **1A**.



A 20-mL glass vessel equipped with J. Young[®] O-ring tap containing a magnetic stirring bar and K₃PO₄ (255.0 mg, 1.20 mmol, 3.0 equiv) was dried with a heatgun for 3 min *in vacuo* and filled with N₂ after cooling to room temperature. To this vessel was added *N*-methylbenzimidazole (**1A**) (52.9 mg, 0.40 mmol, 1.0 equiv). The vessel was evacuated and refilled nitrogen gas three times, and then *t*-BuOD (1.6 mL) was added under a stream of N₂. The vessel was sealed with O-ring tap and then heated at 110 °C for 4 h in an 8-well reaction block with stirring. After cooling the reaction mixture to room temperature, the mixture was passed through a Celite[®] pad with EtOAc. The filtrate was concentrated and the residue was analyzed by ¹H NMR to determine H/D ratio of remaining **1A**.

Reference and Notes

- 1 Luca, L. D. *Curr. Med. Chem.* **2006**, *13*, 1.
- 2 Grimmett M. R. *Imidazole and Benzimidazole Synthesis*, Academic Press, London, **1997**.
- 3 (a) Kosugi, M.; Koshiha, M.; Atoh, A.; Sano, H.; Migita, T. *Bull. Chem. Soc. Jpn.* **1986**, *59*, 677. (b) Bhanu Prasad, A. S.; Stevenson, T. M.; Citineni, J. R.; Nyzam, V.; Knochel, P. *Tetrahedron* **1997**, *53*, 7237.
- 4 For reviews, see: (a) Ackermann, L.; Vicente, R. N.; Kapdi, A. R. *Angew. Chem., Int. Ed.* **2009**, *48*, 9792. (b) Chen, X.; Engle, K. M.; Wang, D.-H.; Yu, J.-Q. *Angew. Chem., Int. Ed.* **2009**, *48*, 5094. (c) Alberico, D.; Scott, M. E.; Lautens, M. *Chem. Rev.* **2007**, *107*, 174. (d) Wencel-Delord, J.; Glorius, F. *Nat. Chem.* **2013**, *5*, 369. (e) Yamaguchi, J.; Yamaguchi, A. D.; Itami, K. *Angew. Chem., Int. Ed.* **2012**, *51*, 8960. (f) Segawa, Y.; Maekawa, T.; Itami, K. *Angew. Chem., Int. Ed.* **2014**, *54*, 66.
- 5 Pd-catalyzed C–H coupling of imidazoles, see: (a) Joo, J. M.; Touré, B. B.; Sames, D. *J. Org. Chem.* **2010**, *75*, 4911. (b) Campeau, L.-C.; Stuart, D. R.; Leclerc, J.-P.; Bertrand-Laperle, M.; Villemure, E.; Sun, H.-Y.; Lasserre, S.; Guimond, N.; Lecavallier, M.; Fagnou, K. *J. Am. Chem. Soc.* **2009**, *131*, 3291. (c) Zhao, D.; Wang, W.; Lian, S.; Yang, F.; Lan, J.; You, J. *Chem. Eur. J.* **2009**, *15*, 1337. (d) Shibahara, F.; Yamaguchi, E.; Murai, T. *J. Org. Chem.* **2011**, *76*, 2680.
- 6 Rh-catalyzed C–H coupling of imidazoles, see: (a) Lewis, J. C.; Wiedemann, S. H.; Bergman, R. G.; Ellman, J. A. *Org. Lett.* **2003**, *6*, 35. (b) Lewis, J. C.; Wu, J. Y.; Bergman, R. G.; Ellman, J. A. *Angew. Chem., Int. Ed.* **2006**, *45*, 1589. (c) Lewis, J. C.; Berman, A. M.; Bergman, R. G.; Ellman, J. A. *J. Am. Chem. Soc.* **2008**, *130*, 2493. (d) Lewis, J. C.; Bergman, R. G.; Ellman, J. A. *Acc. Chem. Res.* **2008**, *41*, 1013.
- 7 Cu-catalyzed C–H coupling of imidazoles, see: (a) Do, H.-Q.; Daugulis, O. *J. Am. Chem. Soc.* **2007**, *129*, 12404. (b) Do, H.-Q.; Khan, R. M. K.; Daugulis, O. *J. Am. Chem. Soc.* **2008**, *130*, 15185. (c) Zhao, D.; Wang, W.; Yang, F.; Lan, J.; Yang, L.; Gao, G.; You, J. *Angew. Chem., Int. Ed.* **2009**, *48*, 3296. (d) Daugulis, O.; Do, H.-Q.; Shabashov, D. *Acc. Chem. Res.* **2009**, *42*, 1074.

- 8 For reviews on nickel catalysis, see: (a) Tasker, S. Z.; Standley, E. A.; Jamison, T. F. *Nature* **2014**, *509*, 299. (b) Yamaguchi, J.; Muto, K.; Itami, K. *Eur. J. Org. Chem.* **2013**, 19.
- 9 (a) Canivet, J.; Yamaguchi, J.; Ban, I.; Itami, K. *Org. Lett.* **2009**, *11*, 1733. (b) Yamamoto, T.; Muto, K.; Komiyama, M.; Canivet, J.; Yamaguchi, J.; Itami, K. *Chem. Eur. J.* **2011**, *17*, 10113.
- 10 (a) Muto, K.; Yamaguchi, J.; Itami, K. *J. Am. Chem. Soc.* **2012**, *134*, 169. (b) Meng, L.; Kamada, Y.; Muto, K.; Yamaguchi, J.; Itami, K. *Angew. Chem., Int. Ed.* **2013**, *52*, 10048. (c) Muto, K.; Yamaguchi, J.; Lei, A.; Itami, K. *J. Am. Chem. Soc.* **2013**, *135*, 16384. (d) Xu, H.; Muto, K.; Yamaguchi, J.; Zhao, C.; Itami, K.; Musaev, D. G. *J. Am. Chem. Soc.* **2014**, *136*, 14834.
- 11 Amaike, K.; Muto, K.; Yamaguchi, J.; Itami, K. *J. Am. Chem. Soc.* **2012**, *134*, 13573.
- 12 Reviews on C–O activation: (a) Li, B.-J.; Yu, D.-G.; Sun, C.-L.; Shi, Z.-J. *Chem. Eur. J.* **2011**, *17*, 1728. (b) Rosen, B. M.; Quasdorf, K. W.; Wilson, D. A.; Zhang, N.; Resmerita, A.-M.; Garg, N. K.; Percec, V. *Chem. Rev.* **2011**, *111*, 1346. (c) Yu, D.-G.; Li, B.-J.; Shi, Z.-J. *Acc. Chem. Res.* **2010**, *43*, 1486. (d) Mesganaw, T.; Garg, N. K. *Org. Process Res. Dev.* **2013**, *17*, 29. (e) Kozhushkov, S. I.; Potukuchi, H. K.; Ackermann, L. *Catal. Sci. Technol.* **2013**, *3*, 562. (f) Tobisu, M.; Chatani, N. *Acc. Chem. Res.* **2015**, *48*, 1717.
- 13 For representative examples of C–O activation, see, (a) Tobisu, M.; Shimasaki, T.; Chatani, N. *Angew. Chem., Int. Ed.* **2008**, *47*, 4866. (b) Guan, B.-T.; Wang, Y.; Li, B.-J.; Yu, D.-G.; Shi, Z.-J. *J. Am. Chem. Soc.* **2008**, *130*, 14468. (c) Quasdorf, K. W.; Tian, X.; Garg, N. K. *J. Am. Chem. Soc.* **2008**, *130*, 14422. (d) Quasdorf, K. W.; Antoft-Finch, A.; Liu, P.; Silberstein, A. L.; Komaromi, A.; Blackburn, T.; Ramgren, S. D.; Houk, K. N.; Snieckus, V.; Garg, N. K. *J. Am. Chem. Soc.* **2011**, *133*, 6352. (e) Zarate, C.; Martin, R. *J. Am. Chem. Soc.* **2014**, *136*, 2236. (f) Zarate, C.; Manzano, R.; Martin, R. *J. Am. Chem. Soc.* **2015**, *137*, 6754.
- 14 For Ni-catalyzed C–H coupling reported by Miura, see: (a) Hachiya, H.; Hirano, K.; Satoh, T.; Miura, M. *Org. Lett.* **2009**, *11*, 1737. (b) Hachiya, H.; Hirano, K.; Satoh, T.; Miura, M. *Angew. Chem., Int. Ed.* **2010**, *49*, 2202. (c) Hachiya, H.; Hirano, K.;

- Satoh, T.; Miura, M. *ChemCatChem* **2010**, *2*, 1403. For Ni-catalyzed C–H coupling reported by Chatani, see: (d) Castro, L. C. M.; Chatani, N. *Chem. Lett.* **2015**, *44*, 410. (e) Tobisu, M.; Hyodo, I.; Chatani, N. *J. Am. Chem. Soc.* **2009**, *131*, 12070. (f) Aihara, Y.; Chatani, N. *J. Am. Chem. Soc.* **2013**, *135*, 5308. (g) Aihara, Y.; Chatani, N. *J. Am. Chem. Soc.* **2014**, *136*, 898. (h) Aihara, Y.; Tobisu, M.; Fukumoto, Y.; Chatani, N. *J. Am. Chem. Soc.* **2014**, *136*, 15509. (i) Yokota, A.; Aihara, Y.; Chatani, N. *J. Org. Chem.* **2014**, *79*, 11922.
- 15 (a) Takise, R.; Muto, K.; Yamaguchi, J.; Itami, K. *Angew. Chem., Int. Ed.* **2014**, *53*, 6791. (b) Koch, E.; Takise, R.; Studer, A.; Yamaguchi, J.; Itami, K. *Chem. Commun.* **2014**, *51*, 855. (c) Muto, K.; Yamaguchi, J.; Musaev, D. G.; Itami, K. *Nat. Commun.* **2015**, *6*, 7508.
- 16 Fox, P. C. *Arch. Intern. Med.* **1991**, *151*, 1149.
- 17 (a) Nakao, Y.; Kanyiva, K. S.; Oda, S.; Hiyama, T. *J. Am. Chem. Soc.* **2006**, *128*, 8146. (b) Kanyiva, K. S.; Löbermann, F.; Nakao, Y.; Hiyama, T. *Tetrahedron Lett.* **2009**, *50*, 3463. (c) Nakao, Y.; Kanyiva, K. S.; Hiyama, T. *J. Am. Chem. Soc.* **2008**, *130*, 2448. (d) Tsai, C.-C.; Shih, W.-C.; Fang, C.-H.; Li, C.-Y.; Ong, T.-G.; Yap, G. P. A. *J. Am. Chem. Soc.* **2010**, *132*, 11887.
- 18 For representative examples of C–F activation by Ni catalysts, see: (a) Yoshikai, N.; Matsuda, H.; Nakamura, E. *J. Am. Chem. Soc.* **2009**, *131*, 9590. (b) Tobisu, M.; Xu, T.; Shimasaki, T.; Chatani, N. *J. Am. Chem. Soc.* **2011**, *133*, 19505.
- 19 (a) Blackmond, D. G. *Angew. Chem., Int. Ed.* **2005**, *44*, 4302. (b) Mathew, J. S.; Klussmann, M.; Iwamura, H.; Valera, F.; Futran, A.; Emanuelsson, E. A. C.; Blackmond, D. G. *J. Org. Chem.* **2006**, *71*, 4711.
- 20 Similar conclusion is discussed in the case of Pd-catalyzed Sonogashira coupling where transmetalation of copper-acetylide to palladium is a rate-determining step, see: He, C.; Ke, J.; Xu, H.; Lei, A. *Angew. Chem., Int. Ed.* **2012**, *52*, 1527.
- 21 Shen, K.; Fu, Y.; Li, J.-N.; Liu, L.; Guo, Q.-X. *Tetrahedron* **2007**, *63*, 1568.
- 22 Kose, O.; Saito, S. *Org. Biomol. Chem.* **2010**, *8*, 896.
- 23 Zou, L.-H.; Reball, J.; Mottweiler, J.; Bolm, C. *Chem. Commun.* **2012**, *48*, 11307.
- 24 Özdemir, İ.; Şahin, N.; Gök, Y.; Demir, S.; Çetinkaya, B. *J. Mol. Catal. A: Chem.* **2005**, *234*, 181.

- 25 Rivera, A.; Maldonado, M.; Ríos-Motta, J.; Navarro, M. A.; González-Salas, D. *Tetrahedron Lett.* **2009**, *51*, 102.
- 26 Collins, E. A.; Garcia-Losada, P.; Hamdouchi, C.; Hipskind, P. A.; Lu, J.; Takakuwa, T. Patent WO 2006-US12072
- 27 Tang, W.; Yuan, W.-G.; Zhao, B.; Zhang, H.-L.; Xiong, F.; Jing, L.-H.; Qin, D.-B. *J. Organomet. Chem.* **2013**, *743*, 147.
- 28 LaRonde, F. J.; Brook, M. A. *Inorganica Chimica Acta* **1999**, *296*, 208.
- 29 Lin, L. S.; Chioda, M. D.; Liu, P.; Nargund, R. P. Patent WO 2009-US46241
- 30 Glunz, P. W.; Wurtz, N.; Cheng, X. Patent WO 2005-US44113
- 31 Yang, X.; Sun, Y.; Chen, Z.; Rao, Y. *Adv. Synth. Catal.* **2014**, *356*, 1625.
- 32 Zhao, X.; Yeung, C. S.; Dong, V. M. *J. Am. Chem. Soc.* **2010**, *132*, 5832.
- 33 Olofson, R. A.; Cuomo, J. *Tetrahedron Lett.* **1980**, *21*, 819.
- 34 Gong, T.-J.; Su, W.; Liu, Z.-J.; Cheng, W.-M.; Xiao, B.; Fu, Y. *Org. Lett.* **2014**, *16*, 330.
- 35 Giddens, A. C.; Boshoff, H. I. M.; Franzblau, S. G.; Barry, C. E., III; Copp, B. R. *Tetrahedron Lett.* **2005**, *46*, 7355.
- 36 Huang, J.; Chan, J.; Chen, Y.; Borths, C. J.; Baucom, K. D.; Larsen, R. D.; Faul, M. M. *J. Am. Chem. Soc.* **2010**, *132*, 3674.
- 37 Guru, M. M.; Ali, M. A.; Punniyamurthy, T. *J. Org. Chem.* **2011**, *76*, 5295.
- 38 Saha, P.; Ramana, T.; Purkait, N.; Ali, M. A.; Paul, R.; Punniyamurthy, T. *J. Org. Chem.* **2009**, *74*, 8719.
- 39 Sluiter, J.; Christoffers, J. *Synlett* **2008**, *2009*, 63.

List of Publications

(副論文)

1. “Nickel-Catalyzed C–H Arylation of Azoles with Haloarenes: Scope, Mechanism, and Applications to the Synthesis of Bioactive Molecules”
Takuya Yamamoto, Kei Muto, Masato Komiyama, Jérôme Canivet, Junichiro Yamaguchi, Kenichiro Itami
Chem. Eur. J. **2011**, *17*, 10113–10122.
2. “Nickel-Catalyzed C–H/C–O Coupling of Azoles with Phenol Derivatives”
Kei Muto, Junichiro Yamaguchi, Kenichiro Itami
J. Am. Chem. Soc. **2012**, *134*, 169–172.
3. “C–H Alkenylation of Azoles with Enols and Esters by Nickel Catalysis”
Lingkui Meng, Yuko Kamada, Kei Muto, Junichiro Yamaguchi, Kenichiro Itami
Angew. Chem., Int. Ed. **2013**, *52*, 10048–10051.
4. “Isolation, Structure, and Reactivity of an Arylnickel(II) Pivalate Complex in Catalytic C–H/C–O Biaryl Coupling”
Kei Muto, Junichiro Yamaguchi, Aiwen Lei, Kenichiro Itami
J. Am. Chem. Soc. **2013**, *135*, 16384–16387.
5. “Key Mechanistic Features of Ni-Catalyzed C–H/C–O Biaryl Coupling of Azoles and Naphthalen-2-yl Pivalates”
Huiying Xu, Kei Muto, Junichiro Yamaguchi, Cunyuan Zhao, K. Itami, Djamaladdin G. Musaev
J. Am. Chem. Soc. **2014**, *136*, 14834–14844.
6. “Decarbonylative organoboron cross-coupling of esters by nickel catalysis”
Kei Muto, Junichiro Yamaguchi, Djamaladdin G. Musaev, Kenichiro Itami
Nat. Commun. **2015**, *6*, 7508.
7. “C–H Arylation and Alkenylation of Imidazoles with Nickel Catalyst”
Kei Muto, Taito Hatakeyama, Junichiro Yamaguchi, Kenichiro Itami, *To be*

submitted.

(参考論文)

1. “Decarbonylative C–H Coupling of Azoles and Aryl Esters: Unprecedented Nickel Catalysis and Application to the Synthesis of Muscoride A”
Kazuma Amaike, Kei Muto, Junichiro Yamaguchi, Kenichiro Itami
J. Am. Chem. Soc. **2012**, *134*, 13573–13576.
2. “Nickel-Catalyzed Direct Coupling of Heteroarenes”
Junichiro Yamaguchi, Kei Muto, Kazuma Amaike, Takuya Yamamoto, Kenichiro Itami
J. Synth. Org. Chem. Jpn. **2013**, *71*, 576–583.
3. 「ニッケル触媒を用いた新しいクロスカップリング反応とその応用」
山口潤一郎, 天池一真, 武藤慶, 伊丹健一郎
「触媒の設計・反応制御 事例集」株式会社 技術情報協会, **2013**, 624–645.
4. “Recent Progress in Nickel-Catalyzed Biaryl Coupling”
Junichiro Yamaguchi, Kei Muto, Kenichiro Itami
Eur. J. Org. Chem. **2013**, 19–30.
5. “Nickel-Catalyzed α -Arylation of Ketones with Phenol Derivatives”
Ryosuke Takise, Kei Muto, Junichiro Yamaguchi, Kenichiro Itami
Angew. Chem., Int. Ed. **2014**, *53*, 6791–6794.
6. “C–H Activation Generates Period-Shortening Molecules That Target Cryptochrome in the Mammalian Circadian Clock”
Tsuyoshi Oshima, Iori Yamanaka, Anupriya Kumar, Junichiro Yamaguchi, Taeko Nishiwaki-Ohkawa, Kei Muto, Rika Kawamura, Tsuyoshi Hirota, Kazuhiro Yagita, Stephan Irle, Steve A. Kay, Takashi Yoshimura, Kenichiro Itami
Angew. Chem., Int. Ed. **2015**, *54*, 7193–7197.